NUCAR - 2023

BOOK OF ABSTRACTS

16th Biennial DAE-BRNS Symposium on
NUCLEAR AND RADIOCHEMISTRY
(NUCAR-2023)

May 01-05, 2023

DAE Convention Centre, Anushaktinagar, Mumbai – 94

Editors

Bal Govind Vats,
Pratik Das
P. S. Ramanjaneyulu
S.C. Parida
S. Kannan

Organized by

Bhabha Atomic Research Centre (BARC), Mumbai
in association with
Indian Association of Nuclear Chemists and Allied Scientist
(IANCAS)

Sponsored by

Board of Research in Nuclear Sciences (BRNS)
Department of Atomic Energy (DAE), India

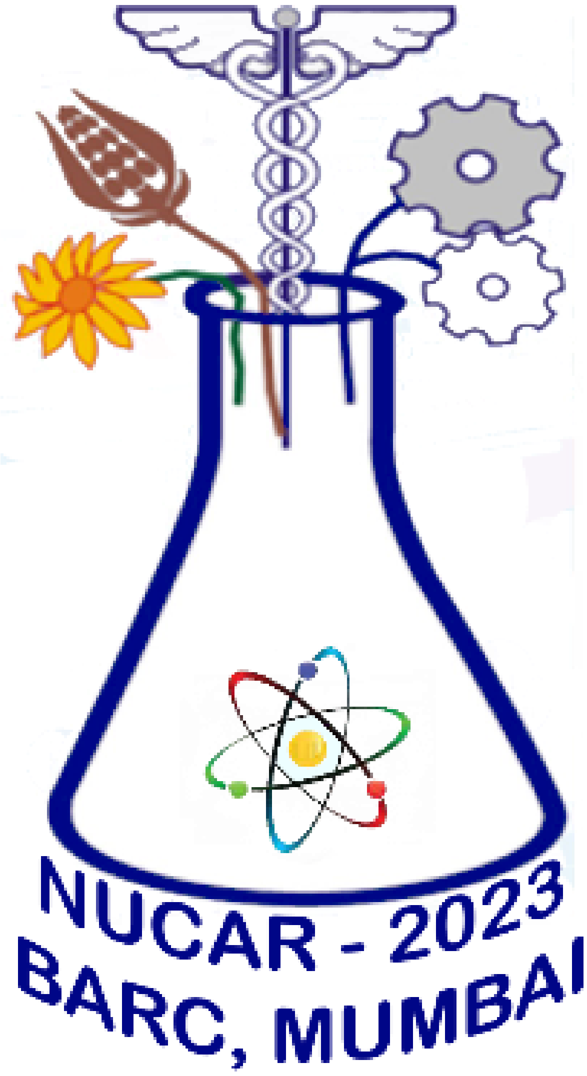
NUCAR - 2023
BARC, MUMBAI

सारांश पुस्तक

“नाभिकीय एवं रेडियोरासायनिकी” पर १६ वीं द्विवार्षिक डीएई – बीआरएनएस संगोष्ठी

(न्यूकार – २०२३)

१ – ५ मई, २०२३

डीएई सम्मेलन केंद्र
अणुशक्तिनगर, मुंबई – ४०००९४, भारत

संपादकगण
बाल गोविंद वत्स, प्रतीक दास, पी. एस. रामाञ्जनेयुलु, एस. सी. परिडा, एस. कन्नन

आयोजक
भाभा परमाणु अनुसंधान केंद्र (बीएआरसी), मुंबई

प्रायोजक
नाभिकीय विज्ञान अनुसंधान बोर्ड (बीआरएनएस)
परमाणु ऊर्जा विभाग (डीएई), भारत

16th Biennial DAE-BRNS Symposium

On

Nuclear and Radiochemistry

(NUCAR-2023)

May 01-05, 2023

DAE Convention Centre

Anushaktinagar, Mumbai-400094, India

Editors

Bal Govind Vats, Pratik Das, P. S. Ramanjaneyulu, S. C. Parida and S. Kannan

Organized by

Bhabha Atomic Research Centre (BARC), Mumbai

Sponsored by

Board of Research in Nuclear Sciences (BRNS)

Department of Atomic Energy (DAE), India

For further details contact:

Dr. P. S. Ramanjaneyulu
Convener, Organising Committee
DAE-BRNS Symposium on
Nuclear and Radiochemistry (NUCAR-2023)
Radioanalytical Division
Bhabha Atomic Research Centre
Trombay, Mumbai-400085, India
Email:psr@barc.gov.in

Printed by
Sheetal Stationary and Xerox
Asha Studio Coumpoud, Near R. K. Studio,
Sion Trombay Road, Chembur, Mumbai - 71
Contact : 9820835599, 9653643700
25202751, 67975232,
Email: ssxprint@gmail.com

Published by
Bhabha Atomic Research Centre
Department of Atomic Energy
Trombay, Mumbai-400085, India

Please Note:
The authors of the papers are alone responsible for
technical content of the papers and references cited therein

के. एन. व्यास
K. N. Vyas

भारत सरकार
Government of India

अध्यक्ष, परमाणु ऊर्जा आयोग
व
सचिव, परमाणु ऊर्जा विभाग
Chairman, Atomic Energy Commission
&
Secretary, Department of Atomic Energy

MESSAGE

I am pleased to know that the 16th DAE-BRNS Biennial Symposium on ''Nuclear and Radiochemistry (NUCAR -2023)" is being organized at BARC, Mumbai during 01-05, May, 2023. It is satisfying to learn that more than 350 delegates will be attending the symposium to present their recent research work in the area of nuclear and radiochemistry. This large participation shows the relevance of the symposium and the interest of the participating researchers. I expect that the participation of senior researchers from India and abroad will motivate the young researchers to carry out cutting-edge research in the area of Nuclear & Radiochemistry.

I am very impressed with role played by nuclear and radiochemistry in growth atomic energy in India including both power and non power applications of nuclear energy. I am glad to know that a half day seminar is being arranged on "Role of sciences in the progress of atomic energy in India" to commemorate the 75 years of formation of Atomic Energy Commission of India.

I am sure that the invited talks and contributory papers to be presented in NUCAR-2023 will generate new ideas among young faculty and research students. I appreciate the efforts of all members of NUCAR-2023 organizing team and I wish the symposium a grand success.

(K. N. Vyas)

अणुशक्तिभवन, छत्रपति शिवाजी महाराज मार्ग, मुंबई - 400 001, भारत • Anushakti Bhavan, Chhatrapati Shivaji Maharaj Marg, Mumbai - 400 001, India
दूरभाष/Phone:+(91) (22) 2202 2543 • फैक्स/Fax: +(91) (22) 2204 8476 / 2284 3888
ई-मेल/E-mail: chairman@dae.gov.in

डॉ. अजित कुमार मोहान्ती
Dr. Ajit Kumar Mohanty

भारत सरकार
Government of India

निदेशक, भाभा परमाणु अनुसंधान केंद्र
Director, Bhabha Atomic Research Centre
सदस्य, परमाणु ऊर्जा आयोग
Member, Atomic Energy Commission

MESSAGE

I am happy to know that Bhabha Atomic Research Centre is Organizing the 16th DAE-BRNS biennial symposium on *"Nuclear and Radiochemistry"* (NUCAR-2023) in association with Indian Association of Nuclear Chemists and Allied Scientists (IANCAS) during May 01-05, 2023 at DAE Convention Centre, Mumbai.

Nuclear and radiochemistry play a pivotal role in shaping the Indian Nuclear Power Programme over the years. The chemical quality control of nuclear materials in different stages of nuclear fuel cycle is the backbone of this development wherein various destructive and non-destructive methodologies were developed in-house. In the fuel development programme, it plays a key role in understanding the physico-chemical properties of fuel materials at reactor operating as well as transient conditions, optimizing the fabrication procedures of advanced vibro-compacted fuel pins, chemical quality control of optimized fuels during their fabrication and estimation of burn-up of highly irradiated nuclear fuels. Advanced separation processes are developed at BARC to separate minor actinides from high level waste solutions as part of the "partitioning & transmutation" strategy. Separation of useful fission products and activated radioisotopes has also been studied for their final applications in healthcare, hydrology and industry. Similarly, various advancements were made at this research centre for the development of nuclear probes for characterization of technologically important materials like thin films and estimation of radiation damage of nuclear structural materials and other energy materials.

To foster the growth in this important but restricted branch of science, NUCAR symposium is being organized biennially. This will provide a forum for discussion and sharing between scientists and researchers in terms of various aspects of nuclear and radiochemistry such as nuclear reactions & probes, chemistry & spectroscopy of actinides, reactor materials and fission products, chemistry of nuclear fuel cycle, radioanalytical chemistry, application of radioisotopes & radiation technology in healthcare, agriculture and industries, environmental radioactivity, nuclear instrumentation, nuclear safeguards & forensics etc.

Further, to commemorate the platinum jubilee year of formation of Atomic Energy Commission of India, a half day seminar on *"Role of sciences in the progress of atomic energy in India"* will be a special feature NUCAR 2023.

I am sure that the deliberations by eminent scientists and researchers from India and overseas as well as contributory papers to be presented during the symposium will benefit the participants in their future research endeavors.

I wish the conference a grand success.

Ajit Kumar Mohanty

19.04.2023

(Dr Ajit Kumar Mohanty)

भाभा परमाणु अनुसंधान केंद्र, ट्रॉम्बे, मुंबई- 400 085, भारत • Bhabha Atomic Research Centre, Trombay, Mumbai 400 085, India
दूरभाष/Phone:+(91) (22) 2550 5300, 2551 1910 • फैक्स/Fax: +(91) (22) 2559 2107, 2550 5151
ई-मेल/E-mail: ajitkm@barc.gov.in / director@barc.gov.in

प्रो. रवि भूषण ग्रोवर
एमिरिटस प्रोफेसर
Prof. R.B. Grover
Emeritus Professor

होमी भाभा राष्ट्रीय संस्थान
प्रशिक्षण विद्यालय परिसर, अणुशक्तिनगर, मुंबई-400 094, भारत

Homi Bhabha National Institute
Training School Complex, Anushaktinagar, Mumbai – 400 094, India
● Email: rbgrover@hbni.ac.in

I am happy to learn that DAE-BRNS sixteenth Biennial Symposium on ''Nuclear and Radiochemistry (NUCAR -2023)" is being organized at BARC, Mumbai during 01-05, May-2023. The scope of the symposium covers a wide range of topics like nuclear reactions & probes, chemistry & spectroscopy of actinides, reactor materials and fission products, the chemistry of nuclear fuel cycle, radio-analytical chemistry, application of radioisotopes & radiation technology in healthcare, agriculture and industries, environmental radioactivity, nuclear instrumentation, nuclear safeguards & forensics, etc. It is satisfying to note that the symposium has attracted large participation: about 360 contributory papers and about 30 invited talks.

The special half-day symposium, on the “Role of sciences in the progress of atomic energy in India” to celebrate the platinum jubilee year of the Indian Atomic Energy Commission, is an additional attraction of the symposium.

The Board of Research in Nuclear Sciences (BRNS) provides financial support for research in universities and institutions. Participation in this symposium will enable university researchers to interact with DAE counterparts and appreciate the research needs of the mission of DAE.

I wish the symposium all success.

RB Grover

14.04.2023

(R.B. Grover)
Chairman BRNS

Preface

The Sixteenth DAE-BRNS Biennial Symposium on Nuclear and Radiochemistry (NUCAR-2023) is organized by Bhabha Atomic Research Centre, Mumbai in association with Indian Association of Nuclear Chemists and Allied Scientists (IANCAS) at DAE convention Centre, Anushaktinagar, Mumbai. The aim of the symposium is to provide a common platform for exchanging and sharing the expertise in the domain of nuclear sciences among the active researchers, scientists and technologists in the field. The scope of NUCAR-2023 covers many important fields related to basic and applied research like nuclear reactions, chemistry of actinides and fission products, spectroscopy of actinides, environmental radioactivity and application of radioisotopes in healthcare and environment.

There is a prodigious response for NUCAR-2023 among researchers with more than 350 contributory papers from academic and research landscape of India. There are 31 invited talks by the eminent researchers of the fields form India and abroad as well as 34 oral presentations by young researchers. This abstract book contains all the invited papers and abstracts of contributory papers which are presented during the symposium.

Nuclear research is a frontrunner example of interdisciplinary science. All the major branches of sciences namely, physics, chemistry and biosciences contributed enormously for the advancement of atomic energy. To commemorate the platinum jubilee year of Indian Atomic energy commission, a special session is organized on the theme “Role of Basic Sciences in the Progress of Atomic Energy in India”. We are thankful to Dr. S. Kailash, Dr. K. L. Ramakumar and Dr. S. K. Apte for honoring our invitation to share their vast experience in this special session of NUCAR-2023.

We put on record our deep sense of gratitude to Shri K.N. Vyas, Chairman, Atomic Energy Commission and Secretary, Department of Atomic Energy and Dr. R. B. Grover, Chairman, Board of Research in Nuclear Sciences (BRNS), Department of Atomic Energy as the Patrons of NUCAR-2023. We are indebted to Dr. A. K. Mohanty, Director, Bhabha Atomic Research Centre, Mumbai for his support and advice as Chairman, National Advisory Committee of NUCAR-2023. We are grateful to BRNS for providing the financial support for organizing the symposium. We are thankful to all the members of National Advisory Committee and Symposium Organizing Committee for their constant guidance, support and encouragement. We highly appreciate Indian Association of Nuclear Chemists and Allied Scientists (IANCAS) for partnering in the organization of the symposium and sponsoring the prizes for best contributory papers. We are thankful to all Unit Heads, DAE, Group directors, Associate Directors and Heads of Divisions of BARC for their support.

We are highly obliged to all the members of technical committee whose thorough and timely reviewing of contributory papers helped us for rapid publishing of the abstract book. We are thankful to the members of local organizing committees whose tremendous support helped us for organizing the symposium successfully. We are also grateful to the session chairs, distinguished dignitaries, jury members and coordinators of technical sessions of NUCAR-2023. Our special thanks to Dr. Abhijit Saha, Shri Ashutosh Shrivastva, Shri Abhishek

Kumar Rai, Shri Shishu Kant Suman, Shri Manish Singh and Smt. Geeta Patkare for editing and compiling the abstract book with due diligence. We appreciate all the sponsors and exhibitors for their support to publish the Souvenir. We also thank technical staff of RC & IG for extending their help in successful organization of the symposium.

Editors

Patrons

Vyas K. N., Chairman, AEC
Grover R. B., Chairman, BRNS, DAE

National Advisory Committee

Mohanty A.K., Director BARC, Mumbai, **Chairman**
Ananthasivan K., Director, RPG, IGCAR, Kalpakkam
Asnani C. K., C&MD, UCIL, Jaduguda, Jharkhand
Aswal D. K., Director, HS&EG, BARC, Mumbai
Bhasin Vivek, Director, NFG, BARC, Mumbai
Dani U.,CE, NRB, BARC, Mumbai
Ghanty T., Director, BSG, BARC, Mumbai
Kapoor K, CE, NFC, Hyderabad
Karhadkar C. G., Director, RG, BARC, Mumbai
Manohar S., Director, NRG, BARC
Mukherjee P., CE, BRIT, Mumbai
Nakhe V. Shankar, Director, RRCAT, Indore
Nayak A.K., Head , NCPW, DAE Mumbai
Pathak B.C., CMD, NPCIL, Mumbai
Saravanan B., Director, AMDER, Hyderabad
Shenoy K. T., Director, ChEG, BARC, Mumbai
Singh D., CMD, IREL, Mumbai
Sivaraman N. Director, MC&MFCG, IGCAR, Kalpakkam
Som Sumit, Director, VECC, Kolkata
Srivastava J., Chairman and CE, HWB, Mumbai
Tewari R., MG ,BARC, Mumbai
Tyagi A. K., Director, CG, BARC, Mumbai
Venkatraman B., Director, IGCAR, Kalpakkam
Yusuf S. M., Director, PG, BARC, Mumbai
Kannan S., Director, RC&IG, BARC, Mumbai **Convener**
Mohapatra P. K., RCD, BARC, Mumbai **Co-Convener**

Symposium Organizing Committee

Kannan S., Director RC & IG, BARC **Chairman**
Mohapatra P.K., RCD, BARC **Co-Chairman**
Ramanjaneyulu P.S., RACD, BARC **Convener**
Adhikari S., SIRD, BARC,
Bagla Hemlata K., K C College, Mumbai
Bhardwaj Y.K., RTDD, BARC,
Chaudhury P., RSSD, BARC,
Chaudhury S., FCD, BARC,
Das Tapas, RPhD, BARC,
Ganesan R., MCD, IGCAR,
Gautam S., FTD, BARC,
Ghosh S., MF&PPD, IGCAR,
Jayaraman V., MCD, IGCAR,
Kulkarni M. S., HPD, BARC,
Kumar U., ITIS, BARC,
Mukhopadhyay S., ChED, BARC,
Pandey U., BRIT, Mumbai
Pant H. J., IRAD, BARC,
Parida S. C., PDD, BARC,
Prakash A., RMD, BARC,
Pujari P. K., RRF, BARC
Sapra B. K., RP&AD, BARC,
Saxena M. K., RACD, BARC,
Srivastava A., Punjab University, Chandigarh
Suresh A., FCD, IGCAR,
Venkatesan K.A., PRRR&DD, IGCAR,
Bal Govind Vats, FCD, BARC **Secretary**
Das Pratik, PDD BARC **Joint-Secretary**

Technical Committee

Parida S. C., PDD, BARC **Chairman**
Acharya R. V., IT IS, BARC
Agarwal C., RCD, BARC
Ankita Rao, RCD, BARC
Biswal J., IRAD, BARC
Chakravarty R., RPhD, BARC
Desigan N., RRDD, IGCAR
Dhara S., FCD, BARC
Guleria M., RPhD, BARC
Mishra N., RTDD, BARC
Mishra S., EMAD, BARC
Nayak A.K., NFC, DAE
Patra S., RCD, BARC
Pranaw Kumar, FCD, BARC
Reddy G. L. N., NCCCM, BARC
Sahu M., RACD, BARC
Sandeep P., EMAD, BARC
Sarkar A., FCD, BARC
Sharma M.K., FCD, BARC
Sharma S., RCD, BARC
Sudarshan K., RCD, BARC
Sumit Kumar, RACD, BARC
Surajit P., FRD, BARC
Swain K., ACD, BARC
Tirumalesh K., IRAD, BARC

NUCAR-2023 Secretariat

Abhijit Saha, RACD, BARC
Ashutosh Shrivastava, RCD, BARC
Abhishek Kumar Rai, PDD, BARC
Manish Singh, FCD, BARC
Shishu Kant Suman, RPhD, BARC
Geeta Patkare, FCD, BARC
Pratik Das, PDD, BARC **Joint Secreatary**
Bal Govind Vats, FCD, BARC **Secretary**

Exhibition Committee

Dr.K.Tirumalesh, IRAD, BARC **Chairman**
Dr. Manoj Mohapatra, RCD, BARC
Dr. Ram Avtar Jat, PDD, BARC
Dr.Viju Chirayil, RPhD, BARC
Dr. Arnab Sarkar, FCD, BARC
Dr. K. A. Dubey, RTDD, BARC
Shri. Rajesh V. Acharya, ITAS, BARC
Dr. Manjulata Sahoo, RACD, BARC

Local Organizing Committee:

Dr. K. Sudarshan, RCD, BARC **Chairman**

Registration Committee

Dr. Drishty Satpati, RPhD.,BARC **Convener**
Dr. Neetika Rawat, RCD, BARC
Smt. Jyotsna M Bhatt, RPhD, BARC
Dr. Shiny Suresh Kumar, RCD, BARC
Ms. Khushboo Kumari, RACD, BARC
Smt. Jayashree Gamare, FCD, BARC
Smt. Yogita Gawde, RCD, BARC

Hall Management Committee

Dr. Aishwarya S Kar, RACD, BARC **Convener**
Dr.Shikha Sharma, RCD, BARC
Dr.Akanksha Jain, RPhD, BARC
Dr.Ruma S Gupta, FCD, BARC
Dr.Jayashree Biswal, IRAD, BARC
Ms. Debarati Das, RCD, BARC
Dr. Sweety Mittal, RPhD, BARC

Transport Committee

Dr. Arnab Sarkar, FCD, BARC **Convener**
Dr.Sasi Bhushan, FCD, BARC
Mr. A.S. Yadav, RACD, BARC
Mr.Tushar Deshmukh, RCD, BARC

Technical Support Committee

Mr. Ghansyam Meena, RCD, BARC **Convener**
Mr. S.C. Vishwasrao, PDD, BARC
Mr. SibuSoren, RCD, BARC
Mr. Vishal S. Choughule, RCD, BARC

Catering Committee

Dr. S.A. Ansari, RCD, BARC **Convener**
Dr. Arvind Ambolikar, FCD, BARC
Mr. M. Phanindra , RACD, BARC
Mr. Lukman Ahamad, FCD, BARC
Mr. M. Sharath Babu, PDD, BARC
Mr. Amit S. Kulkarni, RACD, BARC

Accommodation Committee

Dr. Sandeep K. Sharma, RCD,BARC **Convener**
Dr. B.K. Nagar, RACD, BARC
Mr. Md. Sahiralam Khan, RPhD, BARC
Mr. Muhammed Shafeeq, FCD, BARC

Poster Presentation Management Committee

Dr. Manoj Mohapatra, RCD, BARC, **Convener**
Dr. Rohan Phatak, FCD, BARC
Dr.Kavitha Jaychandran, FCD, BARC
Shri. Yogendra Kumar, RPhD, BARC

CONTENT

Invited Talks

IT-1 **The nuclear phase diagram: critical point and spin polarization** 1

Singh Sushant K. and Alam Jane

IT-2 **Nanocosm and the nuclear chemist** 2

Ananthasivan K.

IT-3 **New biotechnologies for atomic energy programmes beyond crop improvement, food preservation and theranostics** 4

Apte Shree Kumar

IT-4 **Fusion and Plasma research in India: Status and future directions** 6

Chaturvedi Shashank

IT-5 **Computational and experimental methods to estimate burnup, cooling time, and reactor-type of irradiated nuclear fuel for nuclear forensics applications** 7

Chirayath Sunil S.

IT-6 **Novel synthesis of actinide halides: implications for the nuclear fuel cycle and nuclear forensics** 9

Victor Jason, Jang Harry, Louis-Jean James, Kerlin William, Poineau Frederic, Czerwinski Ken

IT-7 **Management of back end fuel cycle activities for power reactor by NRB** 10

Dani Umesh

IT-8 **Challenges in analysis of rare metals and rare earth elements in complex geological materials** 11

Durani Smeer

IT-9 **Role of physics in the progress of atomic energy in India** 12

Kailas S.

IT-10 **Development of methods for Carbon-14 specific activity determination, quantification of its release rates from PHWR nuclear power plant at Kaiga, excess activity in environmental biota and dose to the public** 14

Karunakara N.

IT-11 **High intensity (superconducting) proton accelerators for ADS** 16

Krishnagopal Srinivas

IT-12 **New radiopharmaceuticals: New insights into disease and therapy** 17

Lele Vikram

IT-13 **Recent advances in actinide-ligand multiple bonding** 18

Liddle Stephen T.

IT-14 **Advance nuclear fuels** 19

Mishra Sudhir

IT-15 **Selective dissolution of metal oxides in room temperature ionic liquids: A new strategy in separation science** 20

Mohapatra P. K.

IT-16 **Relevance of SMRs for a de-carbon energy scenario** 21

Nayak A. K.

IT-17 **Role of chemistry in the utilisation of atomic energy** 22

Ramakumar K. L.

IT-18 **Nuclear fuel complex-from past to present…fifty years of golden journey in indian nuclear power program** 23

Rao Y. Balaji

IT-19 **Distribution of Strontium-90 in soils affected by Fukushima Dai-ichi nuclear power station accident in the context of Cesium-137 contamination** 25

Sahoo Sarata Kumar

IT-20 **Thermodynamic modelling of the oxidation of *Ln*- and Pu-doped UO_2** 26

Vinograd Victor

Invited Short Presentations

ISP-1 **A systematic evolution towards the development of a comprehensive gamma scanning system for special nuclear materials assay** 27

Agarwal Chhavi

ISP-2 **Application of environmental radioactive isotopes (^{3}H and ^{14}C) in hydrological studies** 29

Chatterjee Sitangshu

ISP-3 **Positron Annihilation Spectroscopy: An excellent probe for observing changes in pore architecture during CO$_2$ adsorption in metal organic frameworks** 30

Mor Jaideep, Utpalla Pranav , Mukherjee Saurabh , Sharma Sandeep Kumar, Dutta Dhanadeep

ISP-4 **Radiolabeled porphyrins as theragnostic agents: Nuclear Medicine and PDT** 31

Guleria Mohini

ISP-5 **Identification and quantification of elemental and anionic impurities as forensic signature in isotopically natural uranium matrices** 32

Mishra Suchismita

ISP-6 **Separation of fission molly by pyrohydrolysis: an alternate approach** 34

Mishra V. G.

ISP-7 **Study of nuclear fission process using heavy ion induced nuclear reaction** 35

Pal Asim

ISP-8 **Advanced sample loading techniques for TIMS** 37

Paul Sumana

ISP-9 **Synchrotron beamline for study of radioactive materials** 38

Poswal H. K.

ISP-10 **Probing the depths: Ion beam analysis for material characterization** 39

Reddy G. L. N.

ISP-11 **Chemical Aspects of Advanced Nuclear Reactor** 40

Samui Pradeep

Contributory Abstracts

A-1 **Flexibility of mixed metal (Zn/Co) zeolitic imidazolate framework-8: an investigation using positron annihilation lifetime spectroscopy** 41

Mor J., Mukherjee S., Dutta D., Sharma S. K.

A-2 **Investigation of pore architecture in bimetallic zeolitic imidazolate framework-using variable energy positron spectroscopy (VEPS)** 42

Nelliyil R. B., Sharma S. K.

A-3 **Development of Dy^{3+} doped lithium magnesium borate glass system for thermoluminescence based neutron dosimetry applications** 43

Sen Meghnath, Shukla R., Mishra R. K., Pathak N., Sathian V., Chaudhury P., Tyagi A. K.

A-4 **Studies on vitrification of cerium oxide in sodium iron phosphate glass** 44

Vinod A. V., R. Jayashree, Jain Ashish, Joseph Kirti

A-5 **Electrodeposition of palladium nanoparticles from a deep eutectic solvent and its application to uranyl electrocatalysis and sensing** 45

Layek Arkaprava, Patil Sushil, Jayachandran Kavitha, Gupta Ruma

A-6 **Measurement of fast neutron induced (n, γ) reaction cross-section of ^{68}Zn in the energy range of 0.8 to 2 MeV** 46

Tawade N. S., Kumar S., Patra S.., Tripathi R., Datrik C. S., Pujari P. K., Thomas R. G., Mishra G., Kumar A., De S., Kumawat H.

A-7 **Activation cross sections of alpha induced reactions on 103Rh up to 40 MeV** 47

Raja Sk. Wasim, Acharya R.

A-8 **Study of fission product mass distributions in 12C+232Th reaction to investigate the role of shell closure** 48

Kumar Satyam, Patra Sabyasachi, Mhatre Amol, Kumar Ashwani, Ramachandran K., Tripathi Rahul

A-9 **Positron annihilation spectroscopic study of vacancy defects in aliovalent ion doped CeO_2 for technological applications** 49

Das D., Bandyopadhyay A., Gupta S. K., Sudarshan K.

A-10 **Understanding the defects in NIR emitting $SrGa_2O_4:Cr^{3+}$ using positron annhilation and luminescence spectroscopy** 50

Kambli Manish S., Balhara Annu, Gupta Santosh K., Sudarshan Kathi

A-11 **Synthesis, characterization and thermal studies of $[CH_3NH_3]Nd(SeO_4)_2 .3H_2O$** 51

Divekar S. K., Achary S. N.

A-12 **Investigating the local structure of silver in different chemical environments using TDPAC spectroscopy** 52

Kumar Ashwani, Patra Sabyasachi, Kumar Satyam, Tripathi Rahul

A-13 **Process intensification and optimization for sonocrystallisation of uranium peroxide** 53

Paik Shrishma, Satpati S. K., Singh D. K.

A-14 **Deep eutectic solvent based strippable thin films for decontamination of radioactive surface** 54

Patil Sushil M., Goswami Dibakar, Gupta Ruma

B-1 **Exploring fluorapatites for nuclear waste sequestration applications through natural analogue study** 55

Banerjee Rumu H., Alexander Rajath, Chaudhary Nishant, Sengupta Pranesh

B-2 **Nuclear waste disposal: Pyrochlore as a potential immobilization material** 56

Garg Rohini, Gulnar A. K., Ghosh Abhijit, Arya Ashok K.

B-3 **Integrated approach for chemical characterization of zirconium WDF and ZrO2 powders using ICP-OES** 57

Rao Y. Balaji, Gupta SNVMS , Nagendra Kumar P. V., Srivastava Dinesh

B-4 **Development of RF GD-OES technique as an analytical tool for chemical qualification of BWR and PHWR core components** 58

Rao Y. Balaji, Gupta SNVMS, Nagendra Kumar P. V., Srivastava Dinesh

B-5 **Corrosion inhibition efficiency of octadecylamine for incoloy 800 in presence of chloride ions** 59

Kuilya Subrata, Subramanian Veena, Bera S., Krishna Mohan T. V.

B-6 **Less hazardous & effective oxidant for solvent extraction of uranium in phosphoric acid solutions** 60

Sukumar S., Selvasundaravel R., Premchander, Murugesan P., Reston Joseph M., Mohan A., Ganesh S.

B-7 **Chemical qualification of zirconium based alloys using high resolution continuum-source atomic absorption spectrometer** 61

Rao Y. Balaji, Begum Zahida, Nagendra Kumar P. V., Srivastava Dinesh

B-8 **Development of a rapid method for chemical characterization of tin-tungsten ores** 62

Kumari Alpana, Krishnakumar M., Thomas Anitha Mary, Nandakishore S.

B-9 **Evaluation of the effect of Mg ions on corrosion properties of zircaloy-2 by plasma electrolytic oxidation (PEO) method** 63

Chandran Sinu, Subramanian Veena, H. Subramanian, Bera Santanu, Krishna Mohan T. V.

B-10 **Dissolution of divalent and trivalent metal ions from $M_xNi_{1-x}CrFeO_4$ (Mg & Zn) oxides in oxidising formulation** 64

Balaji V., Chandramohan P., Rajesh Puspalata, Bera Santanu, Krishna Mohan T. V.

B-11 **Phase relations in CeO2-substituted Gd2Ti2O7** 65

Nandi C., Bhattacharya S., Ajith D., Thorat K. Prakash A.

B-12 **Preliminary studies on preparation of UAl alloy by electro-reduction of UO_2-Al_2O_3 mixed oxide in LiCl-Li_2O melt** 66

Sanil N., Shakila L., Arunkumar V., Rajamadhavan R., Kumaresan R.

B-13 **Local structure and symmetry of Eu3+ in Y2Zr2O7 pyrochlore: A potential ceramic host for nuclear waste** 67

Parayil Reshmi Thekke, Gupta Santosh K., Patra G. D., Mohapatra M.

B-14 **Thermodynamic stability of Na_2MnF_5(s) using calorimetric technique** 68

Narang S., Aiswarya P. M., Dawar R., Mishra R.

B-15 **Thermal and spectroscopic studies of simulated actinide waste loaded niobium phosphate glass** 69

Senapati Abhiram, Barik Suvendu Kumar, Balakrishnan S., Madapu Kishore K., Jena Hrudananda

B-16 **High temperature mass spectrometric studies on U-Zr-Mn alloy** 70

Manikandan P., Manivannan A., Rao C. V. S Brahmananda, Joseph Kitheri

B-17 **Boron determination by time-resolved fluorescence spectrometry in uranium matrix** 71

Verma Poonam, Jeyakumar S.

B-18 **Assay of nitrogen content in nitrides of U-Zr using Kjeldahl-titrimetry** 72

Hemalatha V., Ushalakshmi K., Vithya J., Saha Debasish, Vijayalakshmi S., Jayaraman V.

B-19 **Study on isotopic effect in absorption of hydrogen on IPHWR pressure tube material** 73

Kumar Sunil, Ramanjaneyulu P. S., Kumar M. Phanindra, Kulkarni A. S., Nagar B. K., Saxena M. K.

B-20 **Thermodynamic characterization of $KMnF_3$(s) compound** 74

Dawar R., Narang S., Aiswarya P. M., Mishra R.

B-21 **Removal of organic template from magnetic porous silica a thermogravimatric analysis** 75

Karmakar Sanat, Pal Kuntal Kumar, Velavendan P. , Venkatesan K. A. , Ananthasivan K.

B-22 **Production of long-lived radionuclide Mn-53, Mn-54, Fe-55, Ni-59 and Co-60 via charged particle induced reaction inside fusion reactor environment** 76

Navita, Joshi G. C.

B-23 **Studies on hydrogen isotope preferential pickup by Zry-2 alloy** 77

Kumar Sunil, Ramanjaneyulu P. S., Kulkarni A. S., Kumar M. Phanindra, Saxena M. K.

B-24 **Uranium extraction with TiAP solvent in multistage annular centrifugal extractor** 78

Philip Kumar P., Balamurugan M., Ravi Jammu, Desigan N., Velavendan P., Rajeev R., Venkatesan K. A., Ananthasivan K.

B-25 **Effect of anions on formation of ferrite coatings on carbon steel by hydrothermal method** 79

Sumathi Suresh, Bera Santanu, Krishna Mohan T. V.

B-26 **Sr^{2+} sorption studies on serpentine minerals for potential Small Modular Reactors (SMR) spent fuel transport applications** 80

Prasher Meenu, Parab Harshala J., Sirvi R., Haria H., Kumar S. D., Sengupta P.

B-27 **Mutual Separation of Nb and Ta from aqueous HNO$_3$ stream using a task specific ionic liquid** 81

Goyal Priya, Sengupta Arijit, Mohapatra P. K.

B-28 **Preparation of Al-Co mixed hydroxide ion exchanger for removal of uranium from alkaline aqueous waste** 82

Kumar Ashok, Deb A. C., Gumber Nitin, Pai Rajesh V.

B-29 **Electrochemical Behaviour of LiF-CaF$_2$-UF$_4$ Molten Salt System** 83

Rai Abhshek Kumar, Sharma Manoj Kumar, Parida S. C.

C-1 **Application of chromatographic resin containing TAM-3-DGA for extraction of actinides from acidic feed** 84

Banerjee Piyali, Ansari S. A., Mohapatra P.K., Valsala T. P., Sathe D. B., Bhatt R. B., Verboom W.

C-2 **Thermo physical properties of sodium thorium phosphates** 85

Patkare Geeta, Shafeeq Muhammad, Keskar Meera

C-3 **Synthesis, characterization and evaluation of chitosan, graphene oxide nanocomposite towards uptake of Uranium** 86

Seshadri H., Mohapatra D. K.

C-4 **Local coordination and oxidation state of uranium in ZnGa$_2$O$_4$ spinel** 87

Chandra Shekhar D., Gupta Santosh K., Sudarshan K.

C-5 **Thorium (IV) ion assisted enhancement in up conversion fluorescence of Er^{3+} in YF_3** 88

Balhara Annu, Gupta Sonika, Acharya R., Gupta Santosh K.

C-6 **Amino based UiO-66 (Ce) for uranium adsorption from aqueous Solution** 89

Gumber Nitin, Pai Rajesh V.

C-7 **Insight into phase relation and cation ordering in U-RE-O system** 90

Shafeeq Muhammed, Nandi Chiranjit, Phatak Rohan

C-8 **On development of certified reference materials for trace metallic impurity analysis of Pu samples by ICP-OES** 91

Banerjee C., Mary G., Singh S. K., G. Sugilal

C-9 **Conformational preferences and interconversion barriers in trialkyl phosphate ligands** 92

Gopakumar G., Jayalakshmi S., Sachin Aditya Ramesh, Rao C. V. S. Brahmmananda

C-10 **Complexation of Np(V) with diglycolamide in an ionic liquid** 93

Ansari S. A., Gujar R. B., Mohapatra P. K.

C-11 **Enhancement of thermoluminescence property of LiMgPO4 by Tm doping: A DFT study** 94

Modak Brindaban

C-12 **Effect of interfering metal ions on the extraction and fluoroscence behavior of Eu(III) in a modifier based extraction system** 95

Rout Alok, Kumar S., Ramanathan N.

C-13 **Synthesis of novel covalent organic polymer (COP) for uranium removal from acid streams** 96

Yashwantrao Gauravi, Saha Satyajit, Kumar Shiny S., Rao Ankita

C-14 **Synthesis, characterization, and iodine adsorption studies in Th- based metal organic framework** 97

Sharma A., Vats B. G., Parida S. C.

C-15 **Cu^{2+} grafting in Th-Metal organic framework and its effect on iodine adsorption** 98

Sharma A., Vats B. G., Parida S. C.

C-16 **Sorption of plutonium from aqueous medium using nitrogen doped graphene nano walls** 99

Chaitanya V. Sri Datta, Manoj Kumar P. A., Mangamma G., Rao Srinivasa G., Kaushik C. P.

C-17 **Boosting energy transfer from defect to Eu^{3+} through U^{6+} doping in $MgAl_2O_4$ spinel** 100

Parayil Reshmi Thekke, Gupta Santosh K., Patra G. D., Mohapatra M.

C-18 **Trap level spectroscopic properties of uranium incorporated $LiZnPO_4$** 101

Patre Dinesh K., Reshmi T. P., Hemachandar V., Chattaraj Saparya, Mohapatra M., Ashokkumar P., Kolekar R. V.

C-19 **Complexation behaviour of thorium with phosphoryl ligands** 102

Sachin Aditya Ramesh, Gopakumar G., Sreenivasulu Balija, Rao C. V. S. Brahmmananda

C-20 **Understanding the bonding of Am(III) and Cm(III) ions with donor center modulated aza-crown based ligands** 103

Chattaraj Saparya, Bhattacharyya Arunasis

C-21 **Uranium extraction from acidic feed relevant to front-end applications with TOPO-menthol sorbed solid support** 104

Rao Ankita, Kumar Shiny S.

C-22 **Combination of branched DGA and aqueous soluble BTP (SO_3PhBTP) for Am^{3+}/Cm^{3+} separation** 105

Bhattacharyya A., Kanekar A. S., Mohapatra P. K.

C-23 **Nitridation & dissolution behaviour of U-Zr alloy with different wt % of Zr** 106

Bootharajan M., Sreenivasulu B., Sundararajan K., Rao C.V.S. Brahmananda, Jayaraman V.

C-24 **Extraction of Th(IV) using nitrilotriacetamide and N, N-dihexyl octanamide (DHOA)** 107

Karak Ananda, Mahanty B., Mohapatra P. K., Egberink E. J. M., Sathe D. B., Bhatt R. B., Valsala T. P., Huskens J., Verboom W.

C-25 **Complexation studies of thiazolidine-4-carboxylic acid with uranyl ion** 108

Sharma S., Dumpala R. M. R., Rawat N.

C-26 **Uranyl complexation with pyridine-2,6-diphosphonate: Combined spectroscopic, electrochemical and DFT studies** 109

Verma P. K., Mahanty B., Bhattacharyya A., Borisova N. E., Kalmykov S. N., Mohapatra P.K.

C-27 **Recovery and purification of uranium from analytical waste solution of quality control operation by precipitation method** 110

Kumar Shiny Suresh, Vats Balgovind, Rao Ankita, Rawat Neetika

C-28 **Hexa-valent uranium enabled forster resonance energy transfer (FRET) leading to fluorescence enhancement of Sm^{3+}** 111

Balhara Annu, Patra G. D., Gupta Santosh K.

C-29 **Solvent extraction studies with palladium from nitric acid medium employing phosphonate based ligands** 112

Sreenivasulu B., Sachin Aditya Ramesh, Gopakumar Gopinadhanpillai, Rao C. V. S. Brahmmananda

C-30 **Recovery of uranium from waste matrices by alicyclic hydrogen phosphonate in supercritical carbon dioxide medium** 113

Rajani P., Sreenivasulu B., Pitchaiah K. C., Rao C.V.S. Brahmananda, Sivaraman N.

C-31 **Solvent extraction studies for recovery of uranium from thiocyanate analytical waste using DAAP** 114

Sivaramakrishna B., Sreenivasulu B., Saipriya G., Rajani P., Rao G. S., Jawahar N.R., Rao C.V.S Brahmananda

C-32 **Thermodynamic complexation and decorporation efficiency of N-(-2-acetamido)iminodiacetic acid for Th(IV)** 115

Sharma S., Ali M., Kumar A., Rawat N.

C-33 **Complexation studies of U/La-α-alanine by IR, cyclic voltammetry and photoluminescence techniques** 116

Singh Ritu, Shrivastava Ashutosh, B. Annu, Mohapatra M.

C-34 **Extraction behaviour of Pu(IV) into synthesized DES (TBACL:DA):30% TBP** 117

Patil Prashant A., Sharathbabu, Pathak Sachin, Srivastava Ashutosh

C-35 **Diluent free solvent extraction of Pu(IV) from TOPO-DEHPA eutectic** 118

Sharathbabu, Pathak Sachin, Patil Prashant, Srivastava Ashutosh

C-36 **Investigating the feasibility of using N,N,N,N'-tetraoctyl diglycolamide-N,N-dioctyl hydroxyacetamide/n-dodecane for the minor actinide partitioning** 119

Parvathy N., Mishra Satyabrata, Prathibha T., Desigan N., Venkatesan K. A.

C-37 **Theoretical studies on tuning the selectivity of diglycolamide based ligands towards lanthanide-actinide separation** 120

Sengupta Somnath, Gopakumar G., Rao C. V .S. Brahmananda

C-38 **Speciation of Uranyl with varying pH in ethylene glycol eutectic media** 121

Pillai Jisha S., Srivastava Ashutosh, Ansari Seraj, Chaudhury S.

C-39 **ADU precipitation in presence of oxalate ion** 122

Prasad Arvind, Rekha V., Vijayan K. S., CH. U. Bhanu Prasad, Desigan N., Venkatesan K. A., Ananthasivan K.

C-40 **Simultaneous determination of uranium and free acidity in uranyl nitrate solution by chemometric method** 123

Kumar Mukesh, Suman Saurabh, Pugazhendi Prasad, Dhamodharan K., Venkatesan K. A., Ananthasivan K.

C-41 **Recovery of Pu from analytical waste solutions using dibutylbutyl phosphonate and diamylamyl phosphonate based solvents** 124

Bikash K. N., Rao Brahmaji J. S., Ashok Kumar G. V. S., Gopakumar G., Sreenivasulu B., Rao C. V. S. Brahmananda

C-42 **Development of magnetically separable Fe_3O_4-SiO_2@Pt catalyst for uranium reduction** 125

Pal Kuntal Kumar, Reddy Ramakrishna, Ananthasivan K., Velavendan P.

C-43 **Monitoring the preparation of pyrochemical salt (LiCl-KCl-UCl3) for bulk scale deposition of uranium using AAS and ICP-OES** 126

S. Annapoorani, Sriram S., Umamaheswari R., Suganthi, Suryakumari K., Revathy K., Aggarwal Sourabh, Vijayalakshmi S.

C-44 **Aqueous speciation of pentavalent uranium with heterobifunctional phosphonocarboxylates** 127

Srivastava Ashutosh, Dumpala Rama Mohan Rao, Rawat Neetika, Mohapatra P. K.

C-45 **Spectro-electrochemical studies of neptunium complex of N,N,N’,N’,N’’,N’’-hexa-n-octylnitrilotriacetamide (HONTA) in C_4mimNTf$_2$** 128

Srivastava A., Gujar R. B., Mahanty B., Mohapatra P. K., Verboom W.

C-46 **Development of ATF –studies on variation in grain size of doped urania microsphere prepared by sol-gel process** 129

Kanrar Buddhdev, Kumar Ashok, Deb A.C. , Pai Rajesh V.

D-1 **Optimization of process variables in solvent extraction separation of iron, cobalt and nickel from simulated PWR fuel crud solution** 130

Panda Pratyasha, Mishra Sujata

D-2 **Conversion of lanthanide (Sm, Pr and Nd) oxides to their chlorides in molten LiCl-KCl using $AlCl_3$ for pyrochemical reprocessing** 131

Samanta Nibedita, Maji S., Kumar Satendra, Jain Ashish

D-3 **Simulation of gaseous phase, liquid phase, and mass transfer reactions of iodine species in the containment under severe accident conditions** 132

V. Archana, Osmani Mohammad Saif

D-4 **Tracer technique to estimate the efficiency of radionuclide trap material in liquid sodium** 133

Manivannan A., Ravisankar P., Saravanan G., Sudha R., Joseph Kitheri

D-5 **Extraction studies on acidic intermediate level radioactive liquid waste (ILW) using composite solvent** 134

Saipriya G., Revathi P., Kutty Madhavan V. K., Rao G. Srinivasa, Jawahar N. R.

D-6 **Synthesis, characterization and thermophysical properties of multi lanthanide doped calcium fluorapatite** 135

Das Pratik, Vats Bal Govind, Shafeeq Muhammed, Parida S. C.

D-7 **Computational study of interaction of aqueous strontium nitrate with Kaolinite clay** 136

Goel Shelly, Singh Amrit Pal, Chopra Manish, Choudhury Niharendu,

D-8 **Enthalpy of formation of $RE_2(MoO_4)_3$[RE= La^{3+} and Sm^{3+}]** 137

Sahu Manjulata, Dawar Rimpi, Pandey Kanaklata, Saxena M. K.

D-9 **Study of proton induced activations in natural Fe and steel composites** 138

Paul Sabyasachi, Shanbhag A. A., Sharma S. C., Kulkarni M. S.

D-10 **Apparent enhancement in the mass transfer kinetics of Cs and Sr during microfluidic extraction/stripping conditions in nitric acid-CCD/PEG aqueous-organic pair** 139

Kumar Shekhar, Subba Rao R. V.

D-11 **Leaching behavior of technetium (99Tc) trapped in goethite and immobilized in CWP matrix** 140

Sah R. K., Mittal V. K., Valsala T. P., Sathe D. B., Bhatt R. B.

D-12 **Elucidating the corrosion effect of strontium on plant structural material** 141

Patra Kankan, Mittal V. K., Sahu Ashok Kumar, Valsala T. P., Sathe D. B., Bhatt R. B.

D-13 **Treatment feasibility of high active carbonate waste** 142

Sen Soumya, Sharma Gopal, Mittal V. K., Valsala T. P., Sathe D. B., Bhatt R. B.

D-14 **Performance evaluation of silver coated alumina catalyst for the removal of iodine species from aqueous streams** 143

Kumar Krishan, Seshadri H., Padhy Shrikant S., Mohapatra D. K.,

D-15 **Loss of metal ions and HDBP during acidification of hydrazine carbonate based waste stream resulted during lean organic treatment** 144

Mishra Satyabrata, Pankaj, Patra Chayan, Ghosh Debajyoti, Desigan N., Velavendan P., Venkatesan K. A., Ananthasivan K.

D-16 **Effect of assorted functional groups in highly stable zirconium based metal organic frame works on hydrogen adsorption under various pressures** 145

Sravani Venkata Vaddanam, Boothrajan M. Sreenivasul, Suresh A., Rao C.V. S. Brahmananda

D-17 **Recovery of calix-crown-6 from actual spent calix solution for efficient spent solvent management** 146

Nair Deepika, Gireesan Prema, Banerjee D, Mishra R. K., Dharashiokar D A, Kumar Sanjay, Manohar Smitha

D-18 **Nitric acid effect on oxalate destruction with and without catalyst** 147

Prasad Arvind, Vijayan K. .S, Desigan N., Venkatesan K. A., Ananthasivan K.

D-19 **Investigations on the extraction and aggregation behavior of Zr loaded dibutylbutyl phosphonate and diamylamyl phosphonate solvents** 148

Bikash K. N., Sushanthini G, Suneesh A. S., Sreenivasulu B., Rao C. V. S. Brahmmananda

D-20 **Extraction studies of Pd(II) by metal organic framework from aqueous medium** 149

Sengupta Somnath, Shrikala S. B., Sreenivasulu B., Rao Brahmananda C.V. S.

D-21 **A new composite of potassium cobalt hexacyanoferrate for sequestration of radio-cesium from contaminated water** 150

Sinharoy Prithwish, Yevale Pallavi, Banerjee Dayamoy, Kumar Sanjay, Manohar Smitha

D-22 **Characterization of ruthenium deposited silver disc: The core component of Ru-brachytherapy sources** 151

Sinharoy Prithwish, Joseph Annie, Banerjee Dayamoy, Kumar Sanjay, Manohar Smitha

D-23 **Metal retention behaviour of diluent degradation products** 152

Mishra Satyabrata, Ghosh Debojyoti, Rajesh Puspalata, Desigan N., Venkatesan K. A., Ananthasivan K.

D-24 **Vapour pressure measurements on Nd-Te system** 153

Kumar S. Shyam, Dhibojini V., Ganesan Rajesh

D-25 **Investigation on Gd-Te system by isopiestic method** 154

Patra Ranjan Chita, Kumar Shyam S, Samy R P Sowndharya, Ganesan Rajesh

D-26 **Thermodynamic studies on La - Te system** 155

Kumar Shyam S., Uvarani K., Ganesan Rajesh

D-27 **Studies on the extraction behaviour of Zr (IV) in HNO_3-TBP-HDBP/ n-dodecane system** 156

Sinha Pranay Kumar, Mishra Alok Kumar, Sampath M., Velavendan P., Venkatesan K. A., Ananthasivan K.

D-28 **Studies on chemisorption and physisorption capacity of iodine capture by silver zeolite 13x and Ag-Pb impregnated zeolite 13x for iodine trap application** 157

Sriram S., Annapoorani S., Mahalakshmi V., Vijayalakshmi S., Jayaraman V.

E-1 **Decay power measurements from P91, SS316L, SS304L and D9 steels using whole energy absorption spectrometer** 158

Pandikumar G., Subramanian D. V., Arul A. John, Haridas Adish, Raghupathy S.

E-2 **Synergistic aqueous biphasic separation of 90Nb from natural yttrium** 159

Mitra Sayantani, Naskar Nabanita, Lahiri Susanta, Chaudhuri Punarbasu

E-3 **HR GRS-HPGe as NDT method for quantification of uranium and U^{235} content in process stream samples from UO_2 fuel production facilities** 160

Rao Y. Balaji, Ray Vinod. K., Kumar P. V. Nagendra, Srivastava Dinesh

E-4 **Potentionmetric end point detection for destruction of oxalic acid using KMnO4 in oxalate supernatant-treatment** 161

Panja Suman, Rathore N. S., Gupta S. .K, Valsala T. P.

E-5 **Systematic investigation of inter-element effects during EDXRF measurements on mixed oxides of yttrium, aluminium and silicon** 162

Devi P. S. Remya, Chavan T. A., Sarma M., Swain K.K.

E-6 **Quantifying the loss in reactivity value of PFBR fuel due to Am-241 buildup over time employing differential perturbation** 163

Khan Bilal Hassan

E-7 **Determination of nitrogen and oxygen content in uranium metal using glove box adapted twin determinator system and related studies** 164

Raul Seema, Gaikwad Revati, Pandey Rakesh, Kumar Namrata, Raut D.R., Pandey Ashish, Kelkar Anoop, Valsala T. P., Sathe D.B., Bhatt R.B.

E-8 **Pulsed fast thermal neutron activation for characterization of coal** 165

Roy Tushar, Shukla Shefali, Kashyap Yogesh, Shukla Mayank, Singh Prashant, More M. R., Pant L. M.

E-9 **Quantification of Zr in simulated dissolver solution of U-Zr fuel by LIBS** 166

Maity U. K., Namitha J., Manoravi P.

E-10 **Survival probability of selenium - induced fusion reactions** 167

Anushree H.S., Sowmya N. , Manjunatha H. C.

E-11 **Tritium release from new ceramics of heavy elements** 168

Sowmya N., Manjunatha H. C., Sridhar K. N.

E-12 **Uncertainty analysis in estimation of radioactivity in the soil samples using gamma-ray spectrometry** 169

Arun B., Vijayalakshimi I., Viswanathan S., Menaka M., Subramanian V., Venkatraman B.

E-13 **Measurement of 144 Sm(p, γ) cross section using activation techniques for astrophysical p-process study** 170

Bar Tanmoy, Basak Dipali, Saha Sukhendu, Sahoo Lalit Kumar, Datta Jagannath, Dasgupta Sandipan, Basu Chinmay

E-14 **Estimation of fission product and other radioisotope activities and shielding requirement of storage bay of advanced water cooled reactor** 171

Suryanarayana P., Maheshwari N.K.

E-15 **Coulomb fission and coulomb time scales of superheavy nuclei Z=120** 172

Vasudha G. S., Sowmya N., Manjunatha H.C., Babu D. Prakash

E-16 **Bayesian neural networks for the evaluation of reaction cross-section of interest in nucleosynthesis studies** 173

Chakraborty Aparna, Sharma Aman, Kumar Ajay

E-17 **Exploring the neutron self-shielding factor of scattering-dominated activation foils** 174

Kavya S., Bagchi Subhrojit, Sunil Kumar D., Arul A. John

E-18 **Laser decontamination of SS304 and T91 clad material** 175

Bola Sankar D., Rahman M., Maity U. K., Manoravi P.

E-19 **Hydrogen diffusivity studies in niobium using neutron imaging** 176

Shukla Shefali, Roy Tushar, Kashyap Y.S., Singh Prashant, Shukla Mayank Singh R.N., L.M.Pant

E-20 **Decay power uncertainty estimation from nuclear reaction covariance data** 177

Pandikumar G., Arul A. John, Raghupathy S.

E-21 **Effect of aging in the performance of resin in reprocessing facility** 178

Sharma P. K., Banerjee P., Saini R., Kelkar A. Valsala T. P., Sathe D. B., R. B. Bhatt

E-22 **Radioactivity of francium** 179

Prabhavathi P. S., Sowmya N., Manjunatha H.C., Seenappa L.

E-23 **A re-assessment of 620 group SAND-II cross-section set based on IRDF-90** 180

Bhandari Deep, Deo Kapil, Samata Sudipta, Mallick Amod Kishore, Kumar Rajeev, Kannan Umasankari

E-24 **Study of entrance channel effect on shell-closure in fission dynamics for Rn212*** 181

Dubey Punit, Mishra Utkarsha, Kumar Ajay

E-25 **Decay power measurements from Na, Al, Sb and Cr using whole energy absorption spectrometer** 182

Pandikumar G., Subramanian D. V., Arul A. John, Haridas Adish, Raghupathy S.

E-26 **Understanding temporal evolution of diatomic rovibrational molecular spectra of BO molecule** 183

Mohan Anandhu, Banerjee Anannya, Sarkar Arnab

E-27 **Polyatomic molecular band and its temporal evaluation in a laser induced plasma: BO2 molecule** 184

Mohan Anandhu, Banerjee Anannya, Sarkar Arnab

E-28 **Wavelet analysis of autoradiography images** 185

Dixit Rajashree, Vrinda Devi K.V., Mukhopadhyay S. , Prakash Amrit

E-29 **Reverse-phase liquid chromatographic method for the measurement of uranium in process stream solutions from uranium extraction facility** 186

Rao Y. Balaji, Bano Shehanaz, Nagendra Kumar P. V., Srivastava Dinesh

E-30 **Quantitative estimation of microgram level of Pu in plutonium nitrate solution using controlled potential coulometry** 187

Guchhait S. R., Wagh P. J., Phadke M. P., Sankhe A., De V., Kelkar A., Valsala T. P., Sathe D. B., Bhatt R.B.

E-31 **Determination of trace level uranium content in mild steel wastes from uranium oxide plant at various stages of decontamination using LED based fluorescence spectrometer.** 188

Misra U.B., Rajendra B., Dutta M., Rao Y. Balaji, Chaube R. K, Kapoor K.

E-32 **Alpha induced gamma emission spectroscopy for determination of carbon in steel** 189

Reddy G. L. N., Sunitha Y., Sukumar A. A., Lakshmipathy D. V., Ramana J. V.

E-33 **Improving the sensitivity thermal ionization mass spectrometric analysis of thorium** 190

Goswami Preeti, Sasi Bhushan K., Paul Sumana, Jaison P. G.

E-34 **Studies on ion source chemistry of molybdenum** 191

Goswami Preeti, Sasi Bhushan K., Jaison P. G.

E-35 **Rapid screening technique for gross α and gross β estimation in aqueous samples during radiation emergency** 192

Bhade Sonali P.D., Sankhla Rajesh. Sawant Pramilla D.

E-36 **Electrochemical determination of thorium in aqueous medium** 193

Agarwal Rahul, Gamare Jayashree S., Rao Rama Mohana Dumpala, Sharma Manoj K.

E-37 **EPR dosimetric investigations of a tissue equivalent Li2B4O7 host for high dose applications** 194

V. Hemachandar, Chattaraj Saparya, Patre D. K., T. P. Reshmi, Mohapatra M., P. Ashok Kumar, Kolekar R. V.

E-38 **Study of degree of disequilibrium in jahaz uranium deposit, jhunjhunu district, rajasthan, India** 195

Sandilya M. K., Sharma L. K., Kishan B., Nayak A. R., Reddy B. R. M., Sharma S. K.

E-39 **Study of equilibrium status among uranium series radionuclides in ore samples** 196

Pant Amar D., Gupta Aashna, Dusane Chetan, Mishra Suchismita, Pillai Anilkumar S., A. Vinod Kumar

E-40 **Studies on alpha radiolysis of tri-butyl phosphate/n-dodecane system** 197

Mukhopadhyay Chandan, Mishra Satyabrata, Karthick R., Saha D., Sivakumar D., Dhamodharan K., Desigan N., Venkatesan K. A., and Ananthasivan K.

E-41 **Spectrophotometric determination of boron in boron doped Zr-Nb alloy employing methylene blue-BF4- complex** 198

Pandey K.L., Ramanjaneyulu P.S., Saxena M.K.

E-42 **Characterization of insoluble residue found in centrifuge extractor bowl** 199

Sivakumar D., Das Satya Narayan, Suganyadevi C. S., Kumar G. Santhosh, Dhamodharan K., Venkatesan K.A., Ananthasivan K.

E-43 **Extraction of U(VI) by phenoxy acetic acid modified zirconium phosphate** 200

Selvan B.Robert, Suneesh A.S., Amutha Suba M., Ramanathan N.

E-44 **Simultaneous removal of NOx and RuO4 from dissolver off gas stream of reprocessing plant** 201

Mukhopadhyay Chandan, Karthick R., Sivakumar D., Dhamodharan K., Venkatesan K.A., Ananthasivan K.

E-45 **Analytical estimation of 241Am in the irradiated U-Zr fuel** 202

Prathibha T., Suneesh A. S., Selvan B. Robert, Rout Alok, Amutha Suba M., Ramanathan N., Bola Sankar D., Rajeswari S., Rao J. S. Brahmaji, Kumar G. V. S. Ashok

E-46 **Dependence of resonance self-shielding factor on foil thickness** 203

Bagchi Subhrojit, Kumar D. Sunil, Arul A. John

E-47 **Optimizing the fusion reactions to synthesis Lr** 204

Rani L.Reddi, Sowmya N., Manjunatha H.C.

E-48 **Resolving isobaric interference and accurate quantification of cs and sr in dissolver solution by using isotopic dilution thermal ionisation mass spectrometry (ID-TIMS)** 205

Namitha J., Bera Suranjan, Joseph M., Sivaraman N.

E-49 **Deep eutectic solvent modified supported liquid membrane for actinide extraction** 206

Paul Sumana, Gupta Ruma

E-50 **Preliminary study on eye lens dose measurement during Ru-106 plaque making operation** 207

Sivakumar Susheela, Singh Sanjay, Banerjee D., Bhattacharya M., Bakshi A. K., Kumar M. K. Suresh, Kulkarni M. S.

E-51 **Determination of U(IV) concentration by ferric sulphate titration** 208

Aneesh T., Chandran Neeraja, Devi S. Sagunthala, Nair Bhavya S., Kumar D. Shravan, Mahildoss D. Jebaraj, Dhamodharan K., Venkatesan K. A., Ananthasivan K.

E-52 **Calculation of isotopic composition of boron using calibration-free LAMIS** 209

Banerjee Anannya, Mohan Anandhu, Sarkar Arnab

E-53 **Non-destructive assay of SNMs in samples having high gamma spectral interference** 210

Chaudhury Sanhita, Kumar Ashwani, Patra Sabyasachi, Tripathi Rahul

E-54 **Determination of Plutonium concentration in dissolver samples** 211

Pugazhendi S., Suman Saurabh, Kumar Mukesh, Rekha V., Sivakumar D., Dhamodharan K., Venkatesan K.A., Ananthasivan K.

E-55 **Method development for determination of Li isotopic abundance using LIMS** 212

Bapuji T., Bola Sankar D., Namitha J., Maity U. K., Manoravi P.

E-56 **Artificial neural network based direct non-destructive compositional analysis of (Th, U)O2 fuel pellets by x-ray fluorescence technique** 213

Kanrar B., Sanyal K., Pai R.V.

E-57 **Quality control of external particle induced gamma-ray emission (PIGE) method for quantification of low Z elements in cement samples** 214

Gupta Sonika, Samanta S. K., Acharya R.

E-58 **Chemical characterization of coal samples using ion beam analysis (iba) and instrumental neutron activation analysis (INAA) for coal quality: An intercomparison study** 215

Samanta S. K., Acharya R.

E-59 **Quantification of low Z elements and improvement of their detection limits in uranium matrix using external PIGE facility at FOTIA, BARC** 216

Raja Sk Wasim, Acharya R.

E-60 **Electro-refining of FBTR irradiated U-6Zr(Wt%) in hot cells** 217

Bolasankar D., Kalaiyarasu T., Karunakaran R., Rajeswari S., Pakhui Gurudas, Suganthi S., Suriyakumari K., Perumal Kakkum, Ganapathi A. S., Mariyappan S., Rajarajeswari S., Padmanaban R., Kumar Arul, Ravi N., Manoravi P., Kumaresan R., Venkatesh P., Suresh kumar V., Rao J. Prabhakar , Jayaraman V.

E-62 **Effect of temperature on the selectivity coefficient of a polymeric membrane sensor for Gd3+ detection** 218

Sharma D. B., Mahanty B., Mohapatra P. K., Verboom W.

E-62 **Chemical characterization of salt and deposit from the electro-refining of FBTR irradiated U-6Zr(Wt%) in hot cells** 219

Bolasankar D., Kalaiyarasu T., Karunakaran R., Rajeswari S., Pakhui, P. Manoravi Gurudas, Kumaresan R., Jayaraman V.

E-63 **Development of a process flow-sheet for the chemical separation and reconversion of plutonium and uranium in fast reactor fuel reprocessing** 220

Vijayan K. S., Prasad Arvind, Nair Akhilesh K., P. R. Dhanesh, CH.U Bhanu Prasad, Chokkalingam R. N., Rekha V., Desigan N., Venkatesan K. A., Ananthasivan K.

E-64 **Development of a chemically functionalized polystyrene for the bulk removal of yttrium from strontium** 221

Suba M. Amutha, Selvan B. Robert, Suneesh A. S., Ramanathan N.

E-65 **Assessment of potassium element concentration in vegetables using gamma spectrometry** 222

James Joshy P., Reji T.K., Joshi R.M., Vishnu M.S., Saradhi I. V.

E-66 **Elemental composition of soil samples collected from Uttarakhand state using X-ray fluorescence technique** 223

Tiwari M., Rathod T. D., Bhangare R. C., Sahu S. K., Pulhani V.

E-67 **BODIPY based fluorescent dosimeter for gamma radiation** 224

Choudhary Manoj K., Mula Soumyaditya

E-68 **Determination of 10B/11B in boric acid and B4C using LA-ICPMS** 225

Maity U. K., Bavya P., Ushalakshmi K., Manoravi P., Viajyalakshmi S.

E-69 **Determination of thorium at trace level in plutonium matrix by total reflection X-ray fluorescence spectrometry** 226

Dhara Sangita, Singh S. K.

E-70 **Studies on the elemental concentration determination in protein powder by instrumental neutron activation analysis (INAA)** 227

Sane Surekha U., Samanta S. K., Das Tapas

E-71 **Filament surface modifiers in thermal ionization mass spectrometry for Nd isotope ratio measurement** 228

Goswami Preeti, Sasi Bhushan K., Kumar Prana, Jaison P. G.

E-72 **Elemental analysis of ceramic insulation materials by INAA** 229

Rao J. S. Brahmaji, Raghunath T., Neelamegam M., Kumar G. V. S. Ashok, Ramakrishna V., Sundararajan K.

E-73 **Assessment of cement quality via rapid determination of Ca and Si in cement samples using NAA and PIGE methods** 230

Gupta Sonika, Samanta S. Acharya K., R.

E-74 **Utilization of pneumatic carrier facility of dhruva reactor for quality assurance of INAA by determining elements in CRMs through their short-lived activation products** 231

Gupta Sonika, Samanta S. K., Mestry Priya V., Acharya R.

E-75 **Determination of carbon in niobium by CPAA** 232

Sunitha Y., Reddy G.L.N., Sukumar A.A., Lakshmipathy D.V., Jayabun Sk., Ramana J.V.

E-76 **Determination of iodine in water by polarized energy dispersive X-ray fluorescence spectrophotometry: A comparison of Mo, Al_2O_3 and HOPG secondary targets** 233

Sunitha Y., Ramana J. V.

E-77 **Estimation of essential trace elements of baby food samples using pixe and comparison of results with EDXRF: Possible application of food forensics.** 234

George Reetta Sara, Datta Arpita, Sharma V., Acharya R.

E-78 **Neutron activation analysis using PCF dhruva reactor for the determination of trace rare earth elements (REEs) in bulk REE** 235

Gupta Sonika, Sharma V., Kumar Pranaw, Chaudhury S., Acharya R.

E-79 **Determination of hydrogen content and its possible buildup in the DDUO2 pellets using glove box adapted twin determinator system** 236

Raul Seema, Gaikwad Revati, Pandey Rakesh, Kumar Namrata, Raut D.R., Pandey Ashish, Kelkar Anoop, Valsala T. P., Sathe D. B., Bhatt R. B.

E-80 **Extraction of U (VI) by iminodiaceic acid functionalized mesoporous silica** 237

Selvan B. Robert, Suneesh A. S., Suba M. Amutha, Ramanathan N.

E-81 **Method for estimation of 99Tc activity content in low level liquid waste generated during Geltech (99Mo/99Tc) generator production at RPL, BRIT** 238

Chindarkar A. S., Sawant D. K., Chavan S. V., Sharma Ranjit, Sharma Abhishek K., Singh Balender, Thamke Ajay, Jaychandran N.

E-82 **Standardization of various parameters for the estimation of iodine by gas chromatography-electron capture detector (GC-ECD)** 239

Kumari A. Arul, Vithya J., Saha Debasish, Sundararajan K.

E-83 **Quantification of micronutrients in the baby food samples by INAA utilizing high flux reactor neutrons from dhruva reactor** 240

Datta Arpita, George Reetta Sara, Sharma V., Acharya R.

E-84 **Fission product 95Zr corrections for Zr analysis in U-Zr alloy samples by instrumental neutron activation analysis** 241

Rao J. S. Brahmaji, Kumar G. V. S. Ashok, Subramanian D. Venkata, Elumalai M., Sundararajan K.

E-85 **Fusion-fission and quasifission lifetimes of fusion reactions attempted to synthesis the SHE Z=120** 242

Manjunatha N., Sowmya N., Manjunatha H. C., Ganesh T.

E-86 **Non-destructive determination of uranium and plutonium in annular (U, Pu)O2 mixed oxide sintered pellets using matrix matched satnadard by WDXRF spectrometer** 243

Pandey A., Singh M., Meena D. L., Pradhan Lopamudra, Ranjan Aakash, Kelkar Anoop, Valsala T. P., Sathe D. B., Bhatt R. B.

E-87 **Utilization of nuclear analytical techniques (INAA and PIGE) towards preparation of in house sodalime glass reference material** 244

Sharma Vishal, Acharya R.

E-88 **Study on analytical parameters of TXRF Spectrometer-A tool for trace elemental analysis** 245

Manjunatha, Bennal A. S., Badiger N. M.

E-89 **Development of methodology for improvement of minimum detectable activity (MDA) for radioactive iodine and radioactive cobalt measurement in coolant water at KGS-3&4 using HPGe based gamma spectrometer** 246

Salunke G. S., D. Veerendra., Sunil G. K., Seshaiah M., Vinod Kumar B., Karunakara N., Nagaraja G. K.

E-90 **Theoretical modelling of proton induced ionisation cross-section of elements for their application in PIXE analysis of some indian medicinal plants** 247

Kaur Manpreet, Singh Amandeep

E-91 **Nondestructive determination of fuel-blanket gap in 1-m metal fuel pin** 248

Rao J. S. Brahmaji, Senthilvadivu R., Kumar G. V. S. Ashok, Ravisankar P., Padmanabhan R., Saisubalakshmi D., Sundararajan K.

E-92 **Determination of iron and chromium in bulk uranium matrix using energy dispersive x-ray fluorescence (EDXRF) technique** 249

Senthilvadivu R., Kumar G. V. S. Ashok, Sundararajan K.

E-93 **Establishing a nondestructive identification method for Pu samples with high 241Am content for nuclear reactor applications** 250

Kumar G. V. S. Ashok, Rao J. S. Brahmaji, Sundararajan K.

E-94 **Utilization of external PIGE and INAA methods for the radio-purity analysis of rock samples relevant for nuclear astrophysics** 251

Gupta Sonika, Mestry Priya V., Gamre Naresh, Thakare S. V., Rout P. C., Gupta A. K., Pradhan M.K., Acharya R.

E-95 **Application of PIGE and INAA using pneumatic carrier facility of dhruva research reactor for chemical characterization of agricultural soils from Punjab** 252

Dadwal Vaishali, Gupta Sonika, Sharma Vishal, Shikha Deep, Acharya R.

E-96 **Rapid estimation of uranium concentration in aqueous process solutions** 253

Kumar Shekhar

E-97 **Study of non-linear behaviour of photo-peak area in NaCl aqueous solutions using prompt gamma measurement** 254

Meena D., Gupta S. K., Meena P.

E-98 **Xe-induced fusion reactions to synthesize SHE Z=119** 255

Madhu S., Sowmya N., Manjunatha H.C., Seenappa L.

E-99 **Development of a cesium-specific solid phase adsorbent** 256

Selvan B. Robert, Suba M. Amutha, Suneesh A. S., Ramanathan N.

F-1 **Correlation of pendrin with 131iodine uptake in post-NAI treated thyroid cancer animal model** 257

Gholve C. S., Shete Y. H., Rakshit S., Basu S., Kulkarni S. P., Tyagi A. K.

F-2 **Effect of different doses of gamma radiation on the shelf life of chicken sausages in refrigerated storage** 258

Muppalla Shobita R., Gautam S.

F-3 **Cross section measurements of natMo(α,n)103Ru for production of Auger emitter for immunotherapy** 259

Upadhyay Mahima, Gandhi A., Sharma Aman, Choudhary Mahesh, Singh Namrata, Dasgupta S., Datta J., Kumar A.

F-4 **Semi-empirical systematics for the cross-sections of the (n,p), (n,α) and (n,2n) reactions at 145 MeV neutron energy** 260

Singh Namrata, Gandhi A., Sharma Aman, Choudhary Mahesh, Dubey Punit, Upadhyay Mahima, Kumar A.

F-5 **Excitation function analysis of α+95Mo reaction to produce medically relevant 97Ru up to 60 MeV** 261

Sagwal Malvika, Maiti Moumita

F-6 **Dual mode automated module for radiolabelling of 68Ga produced from both generator and medical cyclotron** 262

Nitin Yuva Raj, Nayak Shrinibas, Kumar Amit, Sharma B. K., Kulkarni Savita

F-7 **Total chemical synthesis PSMA-617: An API for prostate cancer endotherapeutic applications** 263

Kumar K. S. Ajish, Mathur Anupam

F-8 **Measurement of 109Ag(n,γ)110mAg reaction cross section in the incident neutron energy 05-16 MeV** 264

Upadhyay Mahima, Gandhi A., Sharma Aman, Choudhary Mahesh, Singh Namrata, Bamal Sumit, Hingu Akash, Mukherjee S., Mishra G., De Sukanya, Mitra A., Danu S. L., Sood Saurav, Prasad Sajin, Kumar Ajay, Thomas R. G., Kumar A.

F-9 **Standardization of an efficient method for the removal of toxic crown ether from process solution containing 89Sr radioisotope** 265

Vithya J., Saha Debasish, Kumari A. Arul, Sundararajan K.

F-10 **Production and radiochemical separation of 64Cu from enriched 68Zn target in 30 MeV cyclotron** 266

Chattopadhyay S., Ash S., Singha S., Barua L., Mahesh D. G., Das S. Saha, Madhusmita, Alam Md N., Kumar U., Roy S., Dhang P.

F-11 **Production and radiochemical separation of 68Ge from irradiated Ga-Ni alloy target in 30 MeV cyclotron** 267

Chattopadhyay S., Singha S., Ash S., Barua L., Mahesh D. G., Das S. Saha, Madhusmita, Alam Md N., Kumar U., Roy S., Dhang P.

F-12 **Preparation and supply of 90Sr/90Y large area check sources for the hand and foot contamination monitors** 268

Kumar Manoj, Gandhi Shyamala, Yadav Yugandhara Y., Saxena S. K.

F-13 **Selection of DNA aptamers against epidermal growth factor receptor-1 for tumor scintigraphy** 269

Kumar Chandan

F-14 **Study of alpha induced reactions for the production of 57Ni** 270

Singh Namrata, Gandhi A., Choudhary Mahesh, Sharma Aman, Upadhyay Mahima, Dubey Punit, Dubey Nitin, Mishra Utkarsh, Datta J., Dasgupta S., Kumar A.

F-15 **The detailed covariance analysis of natSn(α,x) nuclear reactions** 271

Choudhary Mahesh, Singh Namrata, Sharma Aman, Gandhi A., Upadhyay Mahima, Kumar A., Dasgupta S., Datta J .

F-16 **Application of nuclear imaging techniques in veterinary disease diagnosis for laboratory animals** 272

Shete Y., Bhatkar P., Rakshit S., Damle A., Tyagi A. K.

F-17 **Evaluation of differential cross section data of alpha induced reactions using Bayesian neural network** 273

Chatterjee Avika, Sharma Aman, Kumar Ajay

F-18 **Comparison of ZnS (Ag) scintillation detector-based contamination monitor and GM detector-based contamination monitor while handling 225Ac for radiopharmaceutical preparation** 274

Tervankar Shriram, Kamaldeep, Wanage Gaurav, Maletha Pravind, Bhoite Rahul, Basu Sandip, Sureshkumar M. K.

F-19 **Preparation and evaluation of a novel [177Lu]Lu-labeled antibody-drug conjugate for targeted radionuclidic therapy of non-Hodgkin lymphoma** 275

Kumar Naveen, Suman Shishu Kant, Guleria Mohini, Amirdhanayagam Jeyachitra, Mukherjee Archana, Das Tapas

F-20 **Study of the effect of electron beam irradiation on polyethylene /ethylene-octene copolymer blends** 276

Singh Manjeet, Agarwal Rohini, Chowdhury Subhendu Ray, Pant Jagat Harish

F-21 **Investigation on the effect of gamma radiation on structural and optical properties of Mg doped SnO2 nanoparticles** 277

Bisht Ruchi, Joshi G. C., Singh Pal Jagat

F-22 **Efficiency of gamma rays in developing mutants of bhagwa pomegranate and their stratification through ISSR marker** 278

Rawat Mandeep, Singh V. P., Joshi G. C., Verma S. K., Rai Ratna, Karki Kanchan

F-23 **Radiolytically synthesized photoluminescent silicon oxide nanomaterials: effect of doping and applications in Cr (6+) sensing** 279

Hari Abina, Guleria Apurav, Rath Madhab C., Adhikari Soumyakanti

F-24 **Radiation assisted modification of cellulose paper for application in paper based analytical devices (PADs)** 280

Rawat S., Misra N., Shelkar S. A., Kumar V.

F-25 **Application of the magnetizable cellulose particle in development of CRP radioimmunoassay** 281

Ghodke T. S., Kadwad V., Paradkar S. N., Karunakara N., Shenoy K. B.

F-26 **Synthesis of intrinsically radiolabelled gum arabic coated [169Yb]Yb2O3 hybrid nanoparticles for potential use in nanoscale brachytherapy** 282

Ghosh Sanchita, Patra Sourav, Gupta Santosh, Guleria Apurav, Chakraborty Avik, Chakraborty Sudipta, Chakravarty Rubel

F-27 **Gamma irradiation induced effect on structural, optical and elastic properties of nickel-cobalt ferrite** 283

Kholiya Deepak, Komal, Srivastava R. C., Joshi G. C., Joshi Chandra Shekhar

F-28 **Radiosynthesis of 99mTc-labeled albumin binder- cNGR peptide conjugate** 284

Vats Kusum, Sarma Haladhar D., Satpati Drishty

F-29 **Interaction of rhenium-188 labelled microspheres with primary hepatic cell-lines** 285

Aggarwal Aarti, Kaur Gurjeet, Jassal Ravjit Singh, Medhi Bikash, Mittal Bhagwant Rai, Shukla Jaya

F-30 **Improvement of anti-fouling properties of ethylene propylene diene elastomer (EPDM) by modifying surface properties** 286

Agarwal R., Chowdhury S. Ray, Pant H. J.

F-31 **Studies on the selective adsorption of strontium by surface modified $Fe_3O4-TiO_2$** 287

Patra Chayan, Pal Kuntal Kumar, Velavendan P., Venkatesan K. A., Ananthasivan K.

F-32 **Hydrophobic modification of jute fibre: reaction parameters optimization and structure-property analysis** 288

Jha A., Thite A., Chowdhury S. Ray, Pant H. J.

F-33 **Synthesis of scandium oxide microspheres by microfluidic route and their characterization** 289

Biswal Jayashree, Sen Nirvik, Goswami Sunil, Joseph Annie, Ananthanarayanan Arvind, Sharma V. K., Singh K. K., Pant H. J.

F-34 **Evaluation of corrosion rate of heat-treated carbon steel by using TLA method** 290

Biswal Jayashree, Mandal B. P., Sharma V. K., Pant H. J.

F-35 **Liquid-liquid extraction studies of Np(IV) using N,N,N',N'N'',N''-hexa-n- octylnitrilotriacetamide (HONTA) in C4mimNTf2** 291

Gujar R. B., Mahanty B., Mohapatra P. K., Verboom W.

F-36 **Freeze-dried 99mTc-HYNIC-PSMA kits for SPECT imaging of prostate cancer: Formulation and in vitro evaluation** 292

Mittal Sweety, Kumar Ajish, Chakraborty Avik, Damle Archana, Mallia Madhava B.

F-37 **Preparation of [^{64}Cu]Cu-NOTA complex as a renal PET imaging agent using 64Cu produced in direct activation route** 293

Patra Sourav, Jadhav Sachin, Chakraborty Avik, Rajeswari A., Shetty Priyalata, Vimalnath K. V., Chakravarty Rubel, Chakraborty Sudipta

F-38 **Recovery of radiochemically pure 106Ru from CORAL dissolver off gas scrubber** 294

Mukhopadhyay Chandan, Karthick R., Selvi T., Kumar G. Santhosh, Dhamodharan K., Venkatesan K. A., Ananthasivan K.

F-39 **Preparation of [2,5-14C]-tetrahydrofuran by catalytic cyclodehydration of 1,4-butanediol using tungsten-substituted-phosphoric acid** 295

Sahu R. K., Patil S. P., Kalgutkar D. B., Mathew K. M., Jayachandran N.

F-40 **An efficient synthesis of phenyl barbituric-[2-14C] acid** 296

Patil S. P., Kalgutkar D. B., Mathew K. M., Jayachandran N.

F-41 **Synthesis and radiolabelling of triple negative breast cancer targeting GE11 peptide analogue** 297

Jain Akanksha, Satpati Drishty

F-42 **Extension of shelflife through post harvest gamma radiation along with surface edible coating of litchi cv rose Scented** 298

Chandra Nikesh, Chand Satish, Srivastava Ranjan, Joshi G. C., Singh Omveer, Rawat Mandeep

F-43 **Understanding efficient sequestration of radioiodine using human hairs** 299

Sapkal Jyotsna A., Sorate Pankaj, Kolekar R. V.

F-44 **Reverse osmosis membrane based separation of solute containing Sr radioisotopes from bulk acidic solution** 300

Saha Debasish, Vithya J., Kumari A. Arul, Sundararajan K.

F-45 **On the optimization of the protocol for automated radiosynthesis of [^{68}Ga]Ga-pentixafor, [^{68}Ga]Ga-FAPI-4 and [^{68}Ga]Ga-dotatate in an EZ modular lab** 301

Menon Sreeja Raj, Mitra Arpit, Sahu Sudeep, Chakraborty Avik, Ray Mukti Kanta, Banerjee Sharmila

F-46 **Trastuzumab fragments labeled with Gallium-68 for PET imaging of HER-2 expression in cancers** 302

Suman Shishu Kant, Mukherjee Archana, Pandey Usha, Chakraborty Avik, Rakshit Sutapa, Tawate Megha, Sarma Haladhar Dev

F-47 **In-house developed freeze-dried kit of trastuzumab-DOTA: Efforts towards convenient clinical translation of [177Lu]Lu-trastuzumab** 303

Amirdhanayagam Jeyachitra, Guleria Mohini, Das Tapas

F-48 **Study of microwave irradiation induced expanded graphite: synthesis and characterization** 304

Bora Neetu, Joshi Deepika P.

F-49 **Application of radioactive ion chromatography system for medical radioisotopes production using FBTR** 305

Vithya J., Saha Debasish

F-50 **Preparation and evaluation of 175Yb produced by (n,γ) activation of indigenously produced isotopically enriched [174Yb]Yb(NO3)3 target** 306

Lohar Sharad P., Vimalnath K. V., Chakraborty Avik, Chakraborty Sudipta

F-51 **Elemental purification of indigenously produced isotopically enriched ytterbium precursor for radiopharmaceuticals** 307

Prabhala Anupama, Kumar Dheeraj, Mitra Arpit, Mathur Anupam, V. Manisha, Pandey Usha, Sethi Sanjay

F-52 **Materials development for laser isotope separation process to produce stable radiopharmaceutical precursors of ytterbium and samarium** 308

Alangi Nagaraj , Verma Mukesh K., Sethi Sanjay

G-1 **$Ce(OH)_4$-polymer (poly-ether-sulfone/chitosan) composite: Ru selective adsorbent in highly saline solution** 309

Selvakumar J., Kumari Anshul, Nishad Padala A., Bhaskarapillai Anupkumar, Srinivasan S., Jawahar N. R., Rufus A. L., Gayen J. K., Krishna Mohan T. V.

G-2 **Selective separation of lanthanides from high-level liquid waste using 2-ethylhexylphosphonic acid mono-2-ethyl-hexyl ester (HEH[EHP])-1,4-diisopropyl benzene (DIPB)** 310

Selvakumar J., Geetha N., Srinivasan S., Jawahar N. R., Gayen J. K.

G-3 **Determination of indoor and outdoor gamma dose rate in soils of leather industrial area of tirupattur district, tamil nadu, India** 311

Karthikayini S., Chandrasekaran A.

G-4 **Measurement of ambient gamma dose rate in urban areas of mumbai and its neighboring cities** 312

Shetty P. G., Swarnkar M., Takale R. A., Sahu S. K., Pulhani V.

G-5 **Scintillating polystyrene adsorptive membrane for alpha-beta particle discrimination** 313

Alset Utkarsh, Sodaye Suparna, Kulkarni Atul

G-6 **Assessment of gross alpha and gross beta activities in beach sediments along the northeast coast of tamil nadu, India** 314

Sathish V., Chandrasekaran A.

G-7 **Comparison of glass matrices used for containment of high-level radioactivity by Raman spectroscopy** 315

Prakash Amrita Dhara, Mittal V. K., Valsala T. P., Sathe D. B., Bhatt R. B.

G-8 **Study on the natural radionuclide (^{210}Po) level in the crustaceans and molluscan of muthupet mangrove ecosystem, tamil nadu, India.** 316

Raja P., Ravikumar S., Murugaiyan P., Krishnamoorthy R., Barkavi K.

G-9 **Synthesis and performance evaluation of copper-based hexacyanoferrate nanoparticles for the removal of cesium from aqueous streams** 317

Kumar Krishan, Padhy Shrikant S., Seshadri H.

G-10 **Determination of ^{238}U, ^{232}Th, and ^{40}K and the associated radiation hazards along the north chennai to pondicherry coastal area, India** 318

Sathish V., Chandrasekaran A.

G-11 **Natural background gamma radiation monitoring in kashmir valley using TLDs** 319

Swarnkar M., Shetty P. G., Takale R. A., Sahu S. K., Pulhani V.

G-12 **Estimation of effective radiation dose due to 222Rn in groundwater to the population of kodagu district, karnataka state, India** 320

Namitha S. N., Lavanya B. S. K, Hidayath Mohammed, Chandrashekara M. S.

G-13 **^{226}Ra and ^{222}Rn concentration in groundwater samples of chamarajanagar district, karnataka state, India.** 321

Lavanya B. S. K., Namitha S. N., Rani K. S. Pruthvi, Chandrashekara M. S.

G-14 **Transit time estimation of drying springs in uttarakhand region using environmental tritium concentration** 322

Chatterjee Sitangshu, Khati Vinod, Jaryal A., Mohokar H. V., Kamble S. N., Sinha U. K., Pant H. J.

G-15 **Synthesis of phosphoramide derivative functionalized Fe3O4 nanoparticles for separation of uranium** 323

Singhal Pallavi, Pulhani Vandana, Biswas Goutam

G-16 **Estimation of uranium distribution coefficient in soils collected from visakhapatnam DAE campus and role of groundwater chemistry** 324

Sandeep P., Maity Sukanta, Mishra Suchismita, Dusane C. B., Chaudhary Dilip Kumar, Balaram R. K., Savitri Padma P., Pillai Anilkumar S., Vinod Kumar A.

G-17 **Investigation on the parameters influencing the activity estimation of the natural radionuclides in the environmental samples** 325

Margret M., Chandrasekaran S., Srinivas C. V., Venkatraman B.

G-18 **Distribution of Indoor radon, thoron and progeny levels at three coastal areas of tamil nadu, India** 326

Nebin R. T. Asher, Chitra N., Bramha S. N., Briteena K. S., Chandrasekaran S., Yardily A., Wesley S. Godwin, Srinivas C. V., Venkatraman B.

G-19 **Analysis of natural background gamma radiation levels in and around coastline districts of tamil nadu, India** 327

Takale R. A., Shetty P. G., Swarnkar M., Sahu S. K., Pulhani V.

G-20 **A decade (2011-2020) of environmental monitoring of tritium and its committed effective dose assessment around rawatbhata rajasthan site** 328

Tiwari S. N., Gill Rajpal, Gocher A. K., Menaria Tejpal, Sisodia Mohit, Saradhi I. V., Vinod Kumar A.

G-21 **Estimation of atomic concentration ratio (137Cs/K) of cesium-137 and potassium in soil around kaiga** 329

Jain Sanyam, Joshi R. M., Vishnu M. S., Saradhi I. V.

G-22 **Distribution study of radium-226, polonium-210 and potassium-40 along with geochemical parameters in water samples of chittorgarh, rajasthan** 330

Menaria Tejpal, Rathore D. S., Tiwari S, N., Saradhi I. V., Vinod Kumar A.

G-23 **Evaluation of site-specific dry deposition velocity using 7Be at kakrapar site, gujarat.** 331

Jain Shilpa, Wagh S. S., Patra A. K., Saradhi I. V., Vinod Kumar A.

G-24 **Retention of radionuclides on vindhyan clays** 332

Kar Aishwarya Soumitra, Balan Priyanka, Das M. K., Jeyakumar S., Bajpai R. K.

G-25 **Role of organic matter on sorption of U in organic rich soil** 333

Maity Sukanta, Dusane C. B., Sandeep P., Mishra Suchismita, Chaudhary Dilip Kumar, Pillai Anilkumar S., Vinod Kumar A.

G-26 **Study of degree of disequilibrium in deeper levels of narwapahar uranium mine, singhbhum shear zone, jharkhand, India** 334

Gaur Diwakar, Sandilya M. K., Shrivastava H. B.

G-27 **Separation methodology for bulk elemental impurities in U rich geological matrix using tri(2-ethylhexyl) phosphate** 335

Singh Aditi, P. Sandeep, Mishra Suchismita, Maity Sukanta, Pillai Anilkumar S., Vinod Kumar A.

G-28 **Assessment of few heavy metals in vegetables from navi mumbai market** 336

Suresh Sugandhi, Suryavanshi Harshali S., Tiwari Mahesh, Pulhani Vandana A.

G-29 **Assessment of carbon-14 in wheat samples grown-up in the vicinity of NPP site narora** 337

Gautam Y. P., Kumar Deepak, Sharma A. K., Kumar Vineet, Kumar J., Saradhi I. V.

G-30 **Surface complexation of selenium oxyanions at the goethite-water interface: Validation through spectral signature of interfacial water** 338

Srabanee Snigdha, Bandyopadhyay Anisha, Kumar Sumit, Mondal J. A.

G-31 **Estimation of natural radioactivity in soil samples from uranium mining zone of Sikar, Rajasthan, India.** 339

Khyalia Bhupesh, Yadav Jyoti, Kumar Naresh, Singh Balvinder, Gautam Prikshit, Dalal Ranjeet

G-32 **Soil to plant transfer factors (Fv) of 40K for vegetables in the vicinity of IGCAR,** 340

Avaneesh R. U. K., Chandrasekaran S., Bramha S. N., Panigrahi S. N., Srinivas C. V., Ravi P. M., Karunakara N.

G-33 **Dietary intake of natural and anthropogenic radionuclides from the plant based dietary items cultivated around under construction NPP (GHAVP) site at gorakhpur, haryana** 341

Kumar Deepak, Gautam Y. P., Kumar S., Sharma A. K., Tripathi A. R., Saradhi I. V.

G-34 **Gas chromatographic separation of Krypton from air mixtures using a long molecular sieve column** 342

Krishnakumar P., Sureshkumar M. K., Bhatnagar Amit, Kulkarni M. S.

G-35 **Appraising the factors favouring uranium mobilization in alluvial and hard rock aquifers of rajasthan** 343

Pant Diksha, Keesari Tirumalesh, Roy Annadasankar, Sinha Uday Kumar, Pant Harish Jagat

G-36 **Evaluating sustainability of bhuj aquifer system, western india using nuclear dating techniques** 344

Roy Annadasankar, Sinha Uday Kumar, Hathi Bharatkumar G., Pant Diksha, Mohokar Hemant, Chatterjee Sitangshu, Pant Harish Jagat, Keesari Tirumalesh

G-37 **Estimation of natural radioactivity in soil samples from punjab, India** 345

Bhangare R. C., Tiwari M., Rathod T. D., Swarnkar M., Ajmal P. Y., Pillay R. H., Sahu S. K., Pulhani V.

G-38 **Natural Radioactivity levels and resulting annual effective dose to public around Kudankulam due to terrestrial radiation** 346

Selvi B. S., George Thomas, Rajan P. S., Vijayakumar B., Sarathi I. V.

G-39 **Risk assessment due to inhalation of radon in the environment of madikeri taluk, coorg district, karnataka state** 347

Prakash M. M.,Narayana Y., Kaliprasad C. S., B. N. Beena Ullala Mata, K. Ganesh Prasad

G-40 **Soil to rice transfer factor of 210Po in the local rice variety: a site-specific observation from the pot experiments** 348

Panigrahi S., Bramha S. N., Chandrasekaran S., Srinivas C. V., Venkatraman B.,

G-41 **Measurement and distribution of primordial radionuclides activities at three coastal areas of tamil nadu, India** 349

Nebin R. T. Asher, Bramha S. N., Chitra N., Briteena K. S., Chandrasekaran S., Yardily A., Wesley S. Godwin, Srinivas C. V., Venkatraman B.

G-42 **Geopolymer and cement as immobilization matrices in near surface disposal facility** 350

Khurana Sonali, Shrivastav Ritu M., Pal T. K., Sen S., Mittal V. K., Valsala T. P., Deokar U. V., Ganesh G., Kulkarni M. S., Sharma R., Jayan R. V., Bajpai R. K., Shivakumar Y. C. , Manohar S.

G-43 **Assessment of radioactivity levels and associated radiological hazards of urban soil from mumbai** 351

Kothai P., Sartandel Sangeeta J., Pulhani Vandana

G-44 **Studies on uptake of tritium by fish conducted by simulated experiment in an aquarium.** 352

Jha M. K., Patra A. K., Joshi C. P., Sudheeendran V., Baburajan A., Saradhi I. V., Vinodkumar A.

G-45 **Assessment of annual effective ingestion dose due to naturally occurring 40K through dietary intake at tarapur** 353

Pratibha, Sudheendran V., Gaikwad R. H., Baburajan A., Saradhi I. V., Vinod Kumar A.

G-46 **Study on distribution coefficient (Kd) of 137Cs in coastal sediment at tarapur** 354

Dalvi Sushant S., Shah C. A., Baburajan A., Saradhi I. V., Vinod Kumar A.

G-47 **X-ray photoelectron spectroscopy study on borosilicate glass-ceramics for nuclear waste immobilisation** 355

Pilania Ritu Kumari, Dube Charu Lata

G-48 **Polonium-210 and lead-210 in cigarette and beedi used by mangalore population, karnataka, India** 356

Kaliprasad C. S., Venunathan N., Prakash M. M., Narayana Y., B. N. Beena Ullala Mata, K. Ganesh Prasad

G-49 **Radiation protection during 46-Sc-radiotracer injection for sediment transport study at kolkata port, India** 357

Singh Pratap, Shreenivas V., G. Sunil, Sharma V. K., Kolekar R. V.

G-50 **Solid solubility of MoO3 in sodium borosilicate glasses for HLW vitrification** 358

Maity Sourav, Selvakumar J., Srinivasan S., Jena Hrudananda, Jawahar N. R.

G-51 **Measurements of indoor radon and thoron in dwellings of kasimpur thermal power plant uttar pradesh using twin chamber dosimeter cups with SSNTDs** 359

Mahur Ajay Kumar, Sharma Roshan Lal, Singh Hargyan

G-52 **EPR dosimetric properties of ‘Nd’ incorporated borate glasses: effect of sample composition** 360

Bhoir Seema, B. Rajeshwari, Singh Ritu, Mohapatra Manoj

G-53 **Natural radioactivity levels of coal combustion residues produced in Indian thermal power plants** 361

Dusane C. B., P. sandeep, Pant Amar, Maity Sukanta, Chaudhary D. K., Mishra S., Pillai Anilkumar S., Vinod Kumar A. Vinod

G-54 **Study of uranium and other toxic elements present in coal from jharia coalfield** 362

Srivastava A., Chauhan N., Jaswal N., Babbar N., Toor Amrit Pal, Farasat M., Goedert S., Scherer Ulrich W., Bol R.

G-55 **Estimation of 14C isoflux to the atmosphere: Impact on atmospheric Δ14CO2** 363

Yadav Sonali, Rout Sabyasachi, Murari Madav K., Sharma Rajveer, Chandrakar Amol, Pulhani Vandana, Vinod Kumar A.

G-56 **Activities of primordial radionuclides in the tobacco cultivated fields of dindigul and erode districts (tamil nadu, India)** 364

Periyasamy M., Christobher S., Athif P., Jishnu K., Mohamed H. E. Syed, Bukhari A. Sadiq

G-57 **Polymerization kinetics and rapid nuclear track detection properties of novel poly(disulfonyl diallyl carbonate) materials** 365

Shetgaonkar Abhijit D., Naik Diptesh G., Mandrekar Vinod K., Mascarenhas Adlete A., Nadkarni Vishnu S.

G-58 **Development of analytical methodology and study of C-14 release from gaseous effluents of KGS-3&4** 366

Salunke G. S., D. Veerendra, Sunil G.K., Seshaiah M., Vinod Kumar B., Bharat S., Nagaraja G.K., Karurnakara N.

G-59 **Activity concentration of 210Po and 210Pb in soil and water samples of tobacco cultivated fields of Dindigul and Erode districts (Tamil nadu, India)** 367

Christobher S., Periyasamy M., Athif P., Jishnu K., Mohamed H. E. Syed, Bukhari A. Sadiq

G-60 **Tight binding of Uranyl Ion in Rigid Coordination Environment in Non-Aqueous Medium** 368

Bhardwaj Deepa, Singh Jaideo

G-61 **Estimation of Radon-222 exhalation rate from soil surface in purulia district, west bengal, India** 369

Karmakar Subhradeep, Mukherjee Joydeep, Sutradhar Sushanta, Mitra Sayantan, Chowdhury Saheli, Barman Chiranjib, Mondal Sonjoy

G-62 **Study of Resuspension Factors of Radioactive Aerosols at Hotcell Facility** 370

Yadav S. A., Ghare P. T., Bhaktivinayagam A., Kaushik Vivek, Govalkar Atul , Rath D. P. , Pandit K. M., Ashok Kumar P. and Kulkarni M. S.

H-1 **Radiation shielding efficacy and structural properties of Bi_2O_6W nanomaterial** 371

Chandrika B. M., Ambika M. R., Manjunatha H. C., Seenappa L., Lourduraj A. J. Clement

H-2 **A thin film nano-composite scintillator for "in-field" uranium detection and assay in aqueous samples** 372

Patra Sabyasachi, Kumar Satyam, Mhatre Amol, Tripathi Rahul

H-3 **GANDA: A versatile python code for non-destructive nuclear forensics and assay of sealed radioactive samples using gamma-ray spectrometry** 373

Patra Sabyasachi, Kumar Satyam, Tripathi Rahul

H-4 **In-house fabricated gadolinium doped plastic scintillator for thermal neutron detection** 374

Bhakta S., Ajish J. K., Tyagi M., Sonu, Chauhan A. K., Kumar A.

H-5 **Methodology for non-destructive assay of heterogeneous special nuclear material (SNM) samples for nuclear forensic applications** 375

Patra Sabyasachi, Mani Agnes M., Kumar Satyam, Tripathi Rahul

H-6 **Non-destructive assay of LEU-Pu mixed solutions using high-resolution γ-ray spectrometry for nuclear forensic applications** 376

Patra Sabyasachi, Kumar Satyam, Tripathi Rahul

H-7 **Nondestructive assay of plutonium by lanthanum bromide detector** 377

Agarwal Chhavi, Gaur Monica, Mhatre Amol, Tripathi Rahul

H-8 **Machine learning based approach for identification of significant features for nuclear forensic analysis** 378

Bahadur Shuchita, Jose Jis Romal Sharma Mukesh Kumar

H-9 **Tellurite glass for high energy radiation shielding and effect of erbium on shielding properties** 379

Goswami Rabina ,Singh Virendra

H-10 **Assay and identification of plutonium of different grades present in sub-Becquerel level by fission track technique** 380

Mhatre Amol, Agarwal Chhavi, Tripathi Rahul

H-11 **Multifiller based polymer composites for shielding high energy ionising radiation** 381

Kuttukaran Sherry Shajan, Ambika M. R., Nagaiah N., Shashi Kumar S. K.

I-1 **Simulation of scintillator shape and geometry for fast timing applications** 382

Dhankar K., Hebbar K. R. Parthasarthy, Krishna K. R. Sathya, Shastry Karthik, Mukherjee S.

I-2 **Fabrication of experimental setup for qualification of pulsed eddy current sensor for creep measurement in molten metal environment** 383

Shyam T. V., Sharma Archana, Patankar V. H., Kaushik Ankur, Panda K. K., Basak A., Apraj S. K., Das Nirupam

I-3 **Development of liquid scintillation counter for alpha and beta counting** 384

Tawade n. S., Vishwasrao S. C., Sodaye S.

I-4 **Development of thermal neutron detector with excellent n/γ discrimination based on CsI:Tl scintillator** 385

Singh Shiv Govind, Sisodiya Durgesh, Patra Giri Dhari, Pitale Shreyas, Ghosh Manoranjan, Sen Shashwati, Pant L. M.

I-5 **Calibration of alpha spectroscopy based radon progeny monitor** 386

Rout R. P., Mishra R., Prajith R., Khan A. T., Sapra B. K.

I-6 **Single crystal growth of Tl doped sodium iodide (NaI:Tl) and in-house design, fabrication of gamma detector for field application** 387

Patra G. D., Singh S. G., Sonawane M., Gupta A., Romal J., Sharma M. K., Sen S.

I-7 **Comparison of counting efficiencies of shadow shield whole body monitor for paediatric BOMAB and reference computational phantoms** 388

Roy Rahul, Patni H. K., Singh P. K., Sawant P. D.

I-8 **Indigenous development of DC accelerator based compact sealed neutron generator** 389

Singh Prashant, Shukla Mayank, Roy Tushar, Kashyap Yogesh S., Shukla Shefali, More Mahendra, Ravi Baribaddala, Pant L. M.

I-9 **Track parameter of alpha particles with different energies in LR115 detector** 390

S. Jalaluddin, Mishra Rosaline, Rout R. P., Prajith Rama, Khan A. T., *Sapra B. K.*

I-10 **Tagged neutron system (TNS) with multiple gamma detector** 391

Bishnoi S., Jilju R., Patel T., Sarkar P. S., Pant L. M.

I-11 **Neutron spectrum unfolding: Effect of energy bin-width on the final solution spectrum and H*(10) values** 392

Tripathy S. P., Paul Sabyasachi, Sahoo G. S., Kulkarni M. S.

I-12 **Numerical estimation of efficiency of an over square LOAX HPGe detector for volume source** 393

Sharma Ram, Manohari M., Murugan S., Ganesh G., Kulkarani M. S.

I-13 **Application of two-dosimeter algorithms for dose estimation during hot cell refurbishment activities in a radiochemical plant** 394

Krishnakumar P., Jayan M. P., Bhatnagar Amit, Sureshkumar M. K.

I-14 **Effectiveness of lead apron for exposure control in mox fuel fabrication facility** 395

Dubla R. N., Pattanayak S., Jee Kanhaiya, Tibrewala S. K., Ganesh G., Kulkarni M. S.

I-15 **Study of LET and etching effect in PADC (CR-39) using FTIR spectroscopic analysis** 396

Sahoo G. S., Tripathy S. P., Paul Sabyasachi, Kulkarni M. S.

I-16 **Augmentation of hot cell facility of MC&MFCG for pyro-processing** 397

Bola Sankar D., Kalaiyarasu T., Karunakaran R., Rajeswari S., Padmanadan R., Kumar Arul, Masanam M., Mohanraj E., Ravi N., Manoravi P., Jayaraman V.

The nuclear phase diagram: critical point and spin polarization

*Sushant K. Singh and Jane Alam**
E-mail:jane@vecc.gov.in
Variable Energy Cyclotron Centre, 1/AF Bidhan Nagar, Kolkata- 700064, India

The nuclear phase diagram in temperature (T) and baryonic chemical potential (μ) plane reveals a rich and complex structure. While at high T and low μ (→ 0) the quark-hadron transition is a crossover, at low T and high μ the transition is of first order in nature. Therefore, it is expected that between the crossover and the first order transition there exists a criticl point in the $\mu - T$ plane where the first order transition ends and cross over begins. The CP can be realized experimentally by colliding nuclei at ultra-relativistic energies. The investigations of the CP and the spin polarization in QCD matter are two frontier areas of research. A connection between the CP and the spin polarization has been established recently by the present authors. To the best of our knowledge this is the first study on the effects of critical point on the spin polarization. We propose that the change in spin-polarization induced by the CP can be used to detect the CP.

Dr. Jane Alam is currently Head, Physics group, Variable Energy Cyclotron Centre. He did his post doc from Kyoto University and University of Tokyo during 1999-2001. He is expert in Nuclear Collisions at Relativistic Energies, Quark Gluon Plasma and Hadronic Matter at Non-Zero Temperature and Baryon Density. He got several prestigious awards like INSA Young Scientist Award (1995), DAE SRC Outstanding Research Investigator Award (2005), Homi Bhabha Science & Technology Award (2010), and Distinguished Faculty Award, Physical Sciences, Homi Bhabha National Institute (2015). He has published more than 190 publications in peer reviewed international journals.

Nanocosm and the Nuclear Chemist

K. Ananthasivan
*Reprocessing Group,*IGCAR, *Kalpakkam, INDIA 603102*
asivan@igcar.gov.in

Nanomaterials and nanostructured materials have become the main point of focus in materials chemistry as well as in many areas of industrial application owing to the interesting properties exhibited by them. Many of the ceramic materials including the oxides of actinides viz., UO_2, PuO_2 ,ThO_2 and a variety of other ceramics including B_4C, Y_2O_3, HfO_2 and yttria stabilized hafnia (YSH) are used in their microcrystalline form in the nuclear industry. Most of these are used as dense ceramic pellets and are manufactured through conventional powder metallurgical processes with a typical grain sizes of the order of a few hundred microns. However, of late, dense ceramic pellets having grains with a size of less than a micron (typically 100 to 200 nm) have attracted the attention of the nuclear technologists, owing to their superior high temperature physical properties. Studies carried out in the past on Light Water Reactor (LWR) (oxide) fuels with significant burn up had revealed that this fuel had undergone significant restructuring, and comprised nano pores and a nano grains at its rim. This feature was initially termed as the “rim structure” and later it was called as the “high burn-up structure” (HBS) [1]. Studies on HBS revealed that it possesses many advantageous features. Investigations on HBS analogue materials (partially stabilized zirconia doped with 4 mol% yttria by Spino et al.[2] revealed that the nanocrystalline material is a potential candidate material to be used in reactors which aim at a higher burn up as well as in inert matrix fuels. Nanostructured oxide foams and porous pellets also are relevant to advanced metal production viz., the direct oxide reduction (DOR) process [3]. The third application, which warrants the use of nanocrystalline oxides is the fabrication of chemically inert crucibles to be used in melting metallic uranium or alloys bearing uranium or plutonium.

To obtain highly dense monoliths from these powders with a nanocrystalline substructure, it is necessary that the sintering is carried out under such conditions that facilitate controlled grain growth. It is observed that the materials that comprise impurities and defects at the interface, as well as nanocrystalline materials exhibits abnormal grain growth [4]. Microstructure refinement can be done by optimizing the sintering curve profile by using sintering techniques viz., Rate Controlled Sintering, Two-Step Sintering and Spark Plasma Sintering. This paper describes some systematic studies carried out in our laboratory vis-à-vis those reported by others pertaining to the optimization of the sintering parameters for obtaining fine grained high density monoliths from nanocrystalline powders.

Acknowledgement**:** The author thanks Mr. D. Sanjay Kumar, Dr. S. Balakrishnan, Dr. N. Desigan and Shri Dasarath Maji for sharing the information of the recent research work carried out by them which are highlighted in this presentation.

References**:**

[1] J. Noirot, L. Desgranges, J. Lamontagne, Detailed characterizations of high burn-up structures in oxide fuels, J. Nucl. Mater. 372 (2008) 318-339.
[2] J. Spino, H. Santa Cruz, R. Jovani-Abril, R. Birtcher, C. Ferrero, Bulk-nanocrystalline oxide nuclear fuels – An innovative material option for increasing fission gas retention, plasticity and radiation-tolerance, J. Nucl. Mater. 422 (2012) 27-44.
[3] G.Z. Chen, D.J. Fray, T.W. Farthing, Direct electrochemical reduction of titanium dioxide to titanium in molten calcium chloride, Nature 407 (2000) 361-364.

[4] P.K. Kulriya, Tiankai Yao, Spencer Michael Scott, Sonal Nanda, Jie Lian, Influence of grain growth on the structural properties of the nanocrystalline Gd_2Ti_2O7, J. Nucl. Mater. 487 (2017) 373-379.

Dr. K. Ananthasivan is currently the Director of the Reprocesing Group, Indira Gandhi Centre for Atomic Research. His areas of interest include preparation and high temperature thermodynamics of advanced fuels for fast reactors, sol-gel processes and fast reactor fuel reprocessing. He is the reciepient of the Homi Bhabha National Science and Technology Award (2009), DAE Group achievement awards and H.J. Arnikar Best Thesis award (2003)

New Biotechnologies for Atomic Energy Programmes Beyond Crop Improvement, Food Preservation and Theranostics

Shree Kumar Apte
UM-DAE-Centre for Excellence in Basic Sciences, Vidyanagari, Mumbai-400098
Email : *aptesk@cbs.ac.in*

Biological Sciences have an important place in India's Atomic Energy Program. Effects of high background natural radiation on human populations living in Kerala coast, radiation-induced mutagenesis for crop improvement, use of radiations for food preservation and development of diagnostic/therapeutic nuclear medicines for a wide array of diseases have been major flagship programs of the biology-related research activities in BARC. These approaches demonstrating peaceful uses of nuclear energy, have not only given us products of immense societal benefit but also the much needed appropriate visibility. It is now time to think beyond these conventional approaches wherein biological processes and products have benefitted from use of radiations and radioisotopes. The instances where biology has helped develop novel nuclear science and technology have been somewhat rare, since they require unique organisms that can defy ill-effects of radiations or can live with hazardous materials (heavy metals and organic solvents) relevant to DAE's activities.

Deinococcus radiodurans, the world's most radiation-resistant bacterium, provided the first such opportunity to exploit microbes for application in high radiation environments. This together with discoveries of other microbes which can withstand toxic metals and tolerate and degrade organic solvents have led to the development of bioremediation technologies for heavy metals, such as uranium, cadmium and mercury, and organic solvents like tributyl phosphate (TBP) in radioactive aqueous nuclear waste. Marine cyanobacteria were developed which can sequester uranium from very low (3 ppb) concentrations of U available in sea-water. The same could also be used for removing U from RO-based desalination process or for removing traces of U in terrestrial contaminated water bodies. Recombinant DNA technology was employed for constructing *Deinococcus* strains that could bio-precipitate uranium (as phosphates) from both acidic and alkaline aqueous waste over a wide pH range (pH 5 to 10) in high radiation environment. A TBP-degrading bacterial strain was isolated from TBP storage site in BARC and characterised to reveal the hitherto unknown pathway of TBP degradation. The strain not only degraded TBP but also utilised the degradation products (butanol and phosphoric acid) for its own nutrition. Highlights of these approaches will be presented and future perspectives would be discussed.

Dr. S. K. Apte Joined DAE through 16th batch of BARC Training School in 1972. He was former Director, Bio-Science Group, & Head, Molecular Biology Division, BARC. He served as Emeritus Professor-HBNI (2014-2019), DST-J C Bose National Fellow (2009-2020), Raja Ramanna Fellow-DAE (2015-2018). Currently, he is Distinguished Professor, UM-DAE-Centre for Excellence in Basic Sciences (2018-continuing) Fellow, Indian National Science Academy, New Delhi; Indian Academy of Sciences, Bengaluru; National Academy of Science, Allahabad; National Academy of Agricultural Sciences, India; Maharashtra Academy of Sciences. He is recipient of several prestigious awards and fellowships like Prof. J.V. Bhat-Eureka Forbes Award - Excellence in Microbiology (1990); Young Scientist Award - Cyanobacterial Biotechnology (1996); Prof. K. S. Bilgrami Memorial Award - INSA (2006), Indian Nuclear Society Award (2006). Recipient IAEA Fellowship (1976-77); Nuffield Foundation Fellowship, U.K (1984); USAID Fellowship, USA (1988-89). He was India’s Representative at United Nation’s Scientific Committee on Effects of Atomic Radiations (UNSCEAR) (2014). He coordinated a DAE-sponsored multi-institutional project entitled “Thermal Ecological Studies” which assessed impact of thermal effluents from operating nuclear power plants on aquatic ecosystems (2000-2006). He was member of selection and evaluation Committees of INSA, DST, DBT, CSIR, ICAR and DAE and 6 research institutes in India. Currently he is engaged in teaching integrated 5-year M.Sc. programme and popularization of science and enhancing public awareness of science in India.

Fusion and Plasma Research in India: Status and Future Directions

Shashank Chaturvedi

Director, Institute for Plasma Research, Gandhinagar, India

*Email: director@ipr.res.in

The Institute for Plasma Research (IPR), Gandhinagar, is engaged in R&D aimed at the development of Nuclear Fusion as a long-term energy source, in the Societal applications of plasma technology, and in Directed Basic Research required for futuristic technologies. Fusion research itself includes the development and operation of nuclear fusion devices called tokamaks, participation as an equal partner in the international mega-project called ITER, and the indigenous development of Fusion Reactor Technologies that are essential for a self-reliant fusion programme. Another important vertical is the development & deployment of plasma technologies for Societal/Industrial benefit.

This talk will provide a brief overview of the above activities along with the Roadmap for the future.

Dr. Shashank Chaturvedi got his B.Tech. in Chemical Engineering from IIT Delhi, where he was awarded the Silver Medal for first rank in the Dept. He then got his Ph.D. in Chemical Engineering from Princeton University, USA. His PhD work involved the computational study of a novel Nuclear Fusion Reactor concept.

He was awarded the Homi Bhabha Science & Technology Award of DAE in 2005. He is a Fellow of the Indian National Academy of Engineering and Senior Professor in the Homi Bhabha National Institute (HBNI).

He has earlier served as Head, Computational Analysis Division in the Bhabha Atomic Research Centre (BARC), Visakhapatnam. He has been serving as Director of the Institute for Plasma Research, Gandhinagar, Gujarat, India, since August 2016.

His research interests include numerical modelling of pulsed-power & plasma systems, including Magneto-hydrodynamics, radiation-hydrodynamics, high-speed impact & shock waves, pulsed electromagnetics, High Performance Computing (HPC), Theoretical and experimental determination of materials properties (opacity, equation-of-state) under extreme conditions and automated processing of signals, voice, image & video data.

Computational and Experimental Methods to Estimate Burnup, Cooling Time, and Reactor-type of Irradiated Nuclear Fuel for Nuclear Forensics Applications

Sunil S. Chirayath [1, 2]
[1]*Department of Nuclear Engineering,*
[2]*Center for Nuclear Security Science and Policy Initiatives,*
Texas A&M University, College Station, TX-77843-3133, USA.
E-mail: sunilsc@tamu.edu

Technical nuclear forensics is one of the tools that can be used to deter nuclear terrorism and proliferation threats. Nuclear forensics techniques developed at Texas A&M University showed that ten intra-element nuclide ratios: ^{137}Cs/^{133}Cs, ^{154}Eu/^{153}Eu, ^{134}Cs/^{137}Cs, ^{135}Cs/^{137}Cs, ^{136}Ba/^{138}Ba, ^{150}Sm/^{149}Sm, ^{152}Sm/^{149}Sm, ^{240}Pu/^{239}Pu, ^{241}Pu/^{239}Pu, and ^{242}Pu/^{239}Pu can be utilized to estimate nuclear fuel burnup, cooling time, and rector-type of irradiation for the attribution of plutonium produced. Monte Carlo N-Particle code, MCNP6.2 was used to perform the neutronics simulations, which included fuel burnup simulations to build a database containing concentration of the aforementioned nuclides of interest that can be used to identify the characteristics of irradiated fuel. The isotopic information was stored as a function of fuel burnup and time since irradiation for each reactor-type simulated. The database was point validated using experimental neutron irradiations of uranium of various enrichments in research reactors. The point validations were possible by subjecting the irradiated uranium samples to radiochemical separations and performing nondestructive and destructive assays of nuclides. Using this point validated database, we were able to predict the characteristics of unknown irradiated nuclear reactor fuel samples in two different ways; one using a maximum likelihood statistical method and another using a combination of machine learning methods.

References

1. Osborn et al., “Nuclear Forensics Methodology for Reactor-Type Attribution of Chemically Separated Plutonium,” *Nucl. Tech.*, **201** (1), (2018).
2. Osborn et al., “Experimental Validation of a Nuclear Forensics Methodology for Source Reactor-Type Discrimination of Chemically Separated Plutonium,” *Nucl. Eng. & Tech.*, **51** (2), (2019).
3. O’Neal et al., “A Machine Learning Method for the Forensics Attribution of Separated Plutonium,” *Nucl. Sci. and Eng.* **196** (7) 811-823, (2022).
4. Martinson et al., “Nondestructive and Destructive Assay for Forensics Characterization of Weapons-grade Plutonium Produced in LEU Irradiated in a Thermal Neutron Spectrum,” *Annals of Nucl. Energy*, 183, Article No. 109645 (2023).

Prof. Chirayath is the Director of Texas A&M University (TAMU) Center for Nuclear Security Science and Policy Initiatives (NSSPI) since 2015 with a joint appointment of Associate Professor in the Department of Nuclear Engineering since 2017. He has a special appointment of an Associate Professor in the Tokyo Institute of Technology, Japan and as an Honorary Professor of Amity University, India. He has advised 16 postdoctoral research associates, graduated eight Ph.D. and over 30 M.S./M.E. students in the nuclear engineering. He has over 200 technical publications in peer reviewed journals (over 70) and conference proceedings (over

150). He is currently the Chair of Radiation Protection and Shielding Division of the American Nuclear Society (ANS), an executive committee (EC) member of the ANS Nuclear Nonproliferation Division, and an EC member of the Institute of Nuclear Materials Management (INMM). He is the first recipient of the INMM Education and Outreach Award. He is a recipient of the TAMU Association of Former Students Distinguished Achievement Award. His current research interests include advanced nuclear reactors, and nuclear security and safeguards. He was a scientific staff member of the Indian Atomic Energy Regulatory Board in Mumbai and Kalpakkam from 1991-2019. He was a Health Physics stipendiary trainee in the Bhabha Atomic Research Center (BARC) at Tarapur from 1990-1991.

Novel Synthesis of Actinide Halides: Implications for the Nuclear Fuel Cycle and Nuclear Forensics

Jason Victor, Harry Jang, James Louis-Jean, William Kerlin, Frederic Poineau, and Ken Czerwinski
Radiochemistry Program, University of Nevada Las Vegas 4505Maryland Parkway, Las Vegas, NV USA 89154-4009,czerwin2@unlv.nevada.edu

Actinide halides are strategic materials for the nuclear industry and important chemical precursors for actinide metal production and actinide inorganic synthesis . Actinide halides are currently used in the nuclear fuel cycle, envisaged as fuel in molten salt commercial reactors, and form the basis for the pyrochemical and pyroelectrochemical treatment of used nuclear fuel. Uranium fluorides have an important role in the existing fuel cycle. For metallic fuel, uranium tetrafluoride is a precursor to the formation of uranium metal. Both uranium fluoride and uranium chloride are proposed fuels in molten salt reactors. Plutonium fluoride share commonalities with the uranium species. This work will describe hydrothermal based synthesis of uranium halides and implications of the nuclear reactions within plutonium fluoride species.

Uranium microspheres are of interest due to their potential applications as targets for medical isotopes production, fuel for nuclear reactors and as standardized materials for nuclear forensics. Formation of uranium fluoride microspheres using an autoclave will be presented. This technique has been extended to the uranium chloride system. The resulting compounds are characterized by powder x-ray diffraction and scanning electron microscopy. The results demonstrate the formation of uranium halides species with applications to nuclear fuel and isotope production. Plutonium fluoride species can produce ^{22}Na from the ^{19}F(a,n)^{22}Na reaction. The synthesis of different plutonium species is described. The resulting gamma spectroscopy measurements of the compounds demonstrate the role of plutonium speciation in the formation of ^{22}Na. The analysis of the secondary nuclear reactions presents a new signature that can be used in the nuclear forensic evaluation of plutonium fluorides. This presentation provides a basis for expanding actinide halide synthesis and the potential development of novel nuclear forensic signatures.

Professor Ken Czerwinski was the first director of the Radiochemistry Ph.D. program at the University of Nevada, Las Vegas. He has worked in industry and consults for government and private entities. Professor Czerwinski has created multiple courses on radiochemistry and his experimental efforts focus on evaluating the chemical forms and molecular structure of compounds containing radioelements in liquid and solid phases. All research is tightly coupled to the education and training of students in the laboratory. He has received multiple grants from the DOE, NNSA, NSF, and industry during his academic career and has over 200 peer reviewed publications and patents.

Management of Back End Fuel Cycle Activities for Power Reactor by NRB

Umesh Dani
Nuclear Recycle Board, Mumbai
udani@barc.gov.in

The energy management strategy of India is to develop and utilise all types of energy resources to meet the demand for electricity. India’s long-term Nuclear power plan envisages a three-stage programme which will enable us to eventually utilise our large reserves of Thorium as reactor fuel. Reprocessing of spent fuel is an essential step in all the three stages of our indigenous Nuclear Power Programme. India has chosen a Close Fuel Cycle, taking into account the modest uranium resources in the country. The growth in the nuclear power generation capacity is hinged on the growth in the fast reactor programme, which depends on the reprocessing of the spent nuclear fuel from PHWRs, providing the initial charge of plutonium to few fast breeder reactors. For Speedy implementation of the reprocessing and associated waste management activities and for operation of large scale nuclear recycle plants, a separate entity viz. **Nuclear Recycle Board (NRB)** was constituted on 24th Sept 2009 in DAE. NRB, BARC is responsible for Back end fuel cycle activities of thermal & fast breeder power reactors. Nuclear Recycle Board is mandated to carry out following functions: Storage of spent fuel received from nuclear power stations; Reprocessing of spent fuels; Conditioning and confinement of high-level radioactive waste; Storage of radioactive wastes prior to final disposal; Fuel fabrication facilities. NRB is responsible for carrying out activities such as design, construction and commissioning of Nuclear Recycle plants and Infrastructure facilities located at various sites; Operation, maintenance and refurbishment of above plants and facilities; Providing waste management services to all units of DAE at Kalpakkam and Tarapur; fuel fabrication facilities for FBR programme. Talk presents strategy followed for reprocessing and waste treatment process. It showcases various operating facilities at Tarapur and Kalpakkam sites, its performance, challenges faced during its operation and maintenance, current status. Talk further gives an overview of two major on-going projects of NRB viz Integrated Nuclear Recycle Plant (INRP), Tarapur and Fast Reactor Fuel Cycle Facility (FRFCF), Kalpakkam.

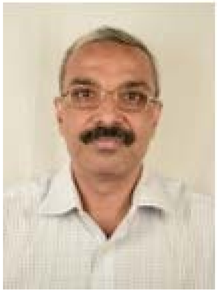

Shri Umesh Dani graduated from IIT, Delhi in Chemical Engineering and is Distinguished Scientist (DS) of DAE. He belongs to 31st Batch of BARC Training School. Presently, he is the Chief Executive, Nuclear Recycle Board. After completion of his training school course, he joined the Waste Management Division in the year 1988 and has donned various caps starting from Operation Supdt. of Radioactive Waste Management Facilities; Commissioning Supdt. of Integrated Nuclear Recycle Project; Project Manager, TNRPO; Dy Chief Executive, NRB; Director, GSO, Tarapur. He is having 34 years of work experience in Construction, Commissioning, Operation and Maintenance of Radioactive Waste Management facilities at NRB, Tarapur.He has to his credit fast track design, construction and commissioning of ILW treatment facility and achieved record processing of intermediate level waste. He has contributed significantly in various task forces and committees. He is a recipient of DAE Group Achievement Award in 2013 and Scientific & Technical Excellence Award in 2008. Apart from his excellence in the technical field he is an avid lover of sports and has played football, hockey and lawn tennis.

Challenges in analysis of rare metals and rare earth elements in complex geological materials

Smeer Durani
Chemistry Group, Atomic Minerals Directorate for Exploration and Research (AMD), DAE, Begumpet, Hyderabad, India
Email: headchem.amd@gov.in

Continental crust comprising igneous, metamorphic and sedimentary rocks is a store house of many economically important metals and their minerals. Analytical chemistry plays a major role at various stages of exploration, mining and beneficiation of these minerals. Each sample that the geoanalyst encounter is unique in nature and composition. The concentrations of elements vary widely from ppb to % ranges whereas the concomitant matrix also is not uniform. Rare metals (RM) such as U, Th, Li, Be, Nb, Ta, Zr, Hf etc are used directly as nuclear fuel or as their alloys for construction of nuclear reactor components. Rare earth (RE) elements (La-Lu, Y & Sc) are important for nuclear and allied industries. Both of these materials have strategic importance in ensuring the safety and energy security of our country.

Depending on the sample nature and concentration of elements being determined the decomposition procedures and analytical techniques are selected. It is also very important to analyse many of these metals at trace levels for geochemical understanding of the metallogeny. The analysis of Zircon mineral separated from rocks throws light to its genesis. The analysis of Hf in zirconium matrix is very important in quality control work of Zicaloy. REEs occur as a group and their values normalized with chondrites will indicate the depositional environment of a rock. The complete chemical characterization involves sample decomposition, separation and followed by determination of elements of interest using principally different techniques.

In this lecture various aspects of chemical characterization of RM & REEs in geological samples, mineral beneficiation products and nuclear industrial materials will be discussed. Evolution of sample decomposition techniques from conventional acid digestion-alkali fusion to most modern microwave digestion and green fusion methods; growth and development of separation methods from co-precipitation to solid phase micro extraction through solvent extraction and chromatography and advances in instrumental techniques from UV-VIS spectrophotometry to ICP-OES/MS for accurate determination of RM & REEs will be elucidated.

Dr Smeer Durani, Head, Chemistry Group of Atomic Minerals Directorate for Exploration and Research, Hyderabad joined the department after obtaining M.Phil and Ph. D. from University of Jammu. Dr. Durani has over three decades of experience in Chemical characterization of Geomaterials. As a team member he has worked in Killung Test Recovery Plant, Domiasiat a project for recovery of one ton of uranium. He has broad research interests from geomaterials to Nanomaterials. Dr. Durani is a recognized faculty member of HBNI, Mumbai. He has published over 50 articles in peer reviewed journals/seminars/symposia. He is also a life member of Indian Nuclear Society, Mumbai and has organised many seminars and conferences. Visited academic and research institutions of Germany as a part of DST nominated Indian delegation in 2013.

Role of Physics in the progress of Atomic Energy in India

S. Kailas
UM-DAE Centre for Excellence in Basic Sciences, Mumbai
Email: swaminathankailas305@gmail.com

When we are celebrating the 75 years of independence of our great country, it is interesting to note that Atomic Energy Commission of India will complete 75 years this year. Over the years the Department of Atomic Energy(DAE) has played a significant role in the development of India. In this context, it may be mentioned that Physics has occupied a pride of place in the growth of DAE since its inception.

Excellence and relevance to DAE have been the driving factors for physics inspired programmes. In the area of basic research, the investigations have a wide dynamic range in terms of size , energy and time scale covering particle physics to astrophysics. Investigation of matter at extremes -of temperature, pressure, and energy-density is a major area of frontier research. Indigenous development of state-of-the-art instrumentation has been a hallmark of physics inspired programmes from the beginning. Major facilities include the cyclotrons at Kolkatta, 14 MV Pelletron coupled to the super conducting LINAC, Folded Tandem Ion Accelerator(FOTIA) and Low Energy High Intensity Proton Accelerator (LEHIPA) at Mumbai; National neutron beam facility located at Mumbai Dhruva reactor ; nearly 25 Beam lines and experimental facilities at Indore synchrotrons; the Giant Metrewave Radio Telescope(GMRT) at Pune and Major Atmospheric Cerenkov Experiment (MACE) at Ladakh; Coupling external neutrons to sub-critical Uranium assembly- for Accelerator Driven System at Mumbai; contributions to ALICE and CMS detectors at CERN, Europe to name a few. Physicists have taken the lead in not only building most of these in India, but also operate the above national facilities for users.

The successful nuclear tests - Smiling Buddha and Operation Shakti at Pokhran- led by the physicists brought fame and name to India internationally. Physicists have contributed immensely to the 3 stage Indian Nuclear Power programme – Pressurised Heavy Water, fast breeder and 233U based reactors. The sustained nuclear data programme which is acclaimed by International Atomic Energy Agency(IAEA) is another important activity of the physicists. The physicists take care of the safety of operation of reactor, nuclear fuel and waste handling, accelerator facilities and also the humans working in these facilities. The contribution of physicists in development of mass spectrometers, gas sensors and crystals, neutron-based imaging, production of radioisotopes and non-destructive testing and evaluation, multilayer mirrors for neutron and synchrotron beam lines, laser and plasma-based techniques for not only DAE programmes but also society at large is noteworthy.

The physicists play an important role in the growth of human resources in the country by their organization/contributions in symposia, schools and workshops. It is needless to mention that many of these achievements have been possible as Physicists work in a team which included engineers and scientists from various disciplines. Multidisciplinary, multi-institutional and international collaborations have benefitted immensely the Physics inspired programs which in turn contributed to the progress of Atomic Energy in India.

Dr. Swaminathan Kailas, a graduate of Madras university and a trainee of the 14th batch of BARC training school, joined Nuclear Physics Division, BARC in 1971. He was awarded the Ph.D by Mumbai University and he has specialized in Accelerator based Nuclear Physics. He has more than 250 journal publications and has guided more than 10 students for Ph.D. He is a former Director, Physics Group, BARC. Currently he is INSA Senior Scientist at UM-DAE Centre for Excellence in Basic Sciences. He is a fellow of Indian Academy of Science, Indian National Science Academy, Tamilnadu Academy of Science and Maharashtra Academy of Science. He received the Sir.C.V.Raman memorial medal in Physical Sciences from the Indian Science Congress. He is a recipient of Life Time Achievement Award from Indian Society of Analytical Scientists. He is a former President of Indian Physics Association and editor of Physics News. He has edited special issues on Accelerator Driven System for Indian Nuclear Society, Atomic Energy in National Development for Science and Culture and Physics in the nuclear power programme for Indian Association of Nuclear Chemists and Allied Scientists.

Development of methods for Carbon-14 specific activity determination, quantification of its release rates from PHWR nuclear power plant at Kaiga, excess activity in environmental biota and dose to the public

Karunakara N.
Centre for Advanced Research in Environmental Radioactivity (CARER)
Mangalore University, Mangalagangotri -574 199, Mangalore, India.
e-mail : drkarunakara@gmail.com

Carbon-14 (half-life=5730±40 y, maximum beta energy=156.5 keV) is produced naturally in the atmosphere at a rate of 1.54×10^{15} Bq y^{-1} through $^{14}N(n, p)^{14}C$ reaction due to the interaction of cosmic rays. The ^{14}C thus produced is immediately oxidized to CO_2 species and enters the biological and geochemical carbon cycles. Through the photosynthesis process, it gets incorporated into the plant biota and enters the food chain, and thus a uniform and equilibrium distribution of this radioisotope are attained in the atmosphere and biosphere. The specific activity of naturally produced ^{14}C in atmospheric CO_2 was determined to be 226 ± 1 Bq kg^{-1}C or 100 pMC (percent of modern carbon) with 1950 as the reference year. The effective radiation dose to an adult human individual due to natural ^{14}C is quantified to be ~ 12 μSv y^{-1}.

Testing nuclear weapons in the atmosphere in the 1950s and 1960s released ~ 2.2×10^{17} Bq of ^{14}C to the environment. This increased the atmospheric ^{14}C specific activity significantly, and in 1963 it was about twice the natural activity in the northern hemisphere. Thereafter it steadily decreased due to (i) mixing with the biosphere and absorption in oceans and (ii) an increase in the input of ^{14}C depleted carbon to the environment from the combustion of fossil fuels. ^{14}C is also released into the atmosphere through gaseous discharges in oxidized (mainly CO_2 species) and reduced (CH_4 species) forms during the routine operation of nuclear power plants (NPPs) and nuclear fuel reprocessing plants.

Considering the biological importance of ^{14}C in the organism and its long half-life, significant importance is given to monitoring its activity in the region around the NPPs. The Centre for Advanced Research in Environmental Radioactivity (CARER), Mangalore University conducted the first systematic study on ^{14}C specific activity measurements in the vicinity of NPP in India. Through this study methods for the determination of (i) ^{14}C activity in ambient air, terrestrial and aquatic biota samples, and (ii) gaseous effluents were developed. Significant improvements over the routine method designed for analysis of samples with specific activity well above ambient ^{14}C level were implemented so that a commercially available tube furnace batch combustion system can be conveniently used to determine the ^{14}C specific activity in the environmental matrices. The MDA achieved in this study (13 Bq kg^{-1}C for a counting time of 300 min and 7 Bq kg^{-1}C for 1000 min counting, at 2σ) is an improvement over the previously reported methods. Also, a secondary ^{14}C reference material, which is A truly representative matrix for the plant species of the tropical regions, has been developed for quality assurance programmes.

The ^{14}C release rates in oxide and reduced forms through gaseous effluents from the Pressurised Heavy Water Reactor (PHWR) NPP at Kaiga were quantified in a study extended over 5 years. A large database on excess ^{14}C activity in terrestrial, aquatic and atmospheric environmental matrices of Kaiga NPP was established. The following are the important findings:

- The normalized release rate of ^{14}C, through gaseous effluents from the Kaiga NPP, for the four-year monitoring period of 2017-2020, had a geometric mean value of 0.12 TBq $GW(e)^{-1}$ a^{-1} (GSD=7.4), and the arithmetic mean with associated standard deviation was 0.75 ± 1.47 TBq $GW(e)^{-1}$ a^{-1}.
- The relative percentage contribution of reduced form (CH_4) of ^{14}C species was less than 1.27 % of the total release.
- The maximum excess ^{14}C activity recorded in terrestrial biota in the vicinity of Kaiga NPP was 44 Bq $kg^{-1}C$ (19 pMC).
- The maximum excess ^{14}C activity values in the atmospheric air in the vicinity of the NPP were 65 Bq $kg^{-1}C$ (29 pMC) and 222 Bq $kg^{-1}C$ (98 pMC) for the years 2019 and 2020 respectively.
- Statistical tests on the ^{14}C specific activity dataset for 2.3-5, 5-10, and 10-20 km radial zones confirmed that the impact of the operation of the NPP on the environment beyond 5 km is minimal.
- The ingestion dose to the population in the 2.3-5 km radius zone, attributable to the release of ^{14}C from the NPP, was 0.75 µSv y^{-1}.

The details of these studies are presented in this talk.

Professor Karuankara Naregundi is heading the Centre for Advanced Research in Environmental Radioactivity (CARER), Mangalore University and Centre for Application of Radiation and Radioisotopes Technology (CARRT), Mangalore University, Mangalagangothri-574199, Mangalore, India. He is responsible for the establishment of CARER as a National Facility through funding from the Board of Research in Nuclear Sciences, Govt. of India. He has authored 130 research publications in journals and has ongoing research collaborations with leading scientific institutions in India and abroad. He served as Editor of the special issue of the Journal of Environmental Radioactivity, Elsevier (Volume 138, 2014). He is the editorial board member for the Journal of Environmental Radioactivity. He is the recipient of the Sir C V Raman Award from The State Council for Science and Technology, Govt. of Karnataka (in the year 2017) and Dr A K Ganguly Award (in the year 2012) from the Indian Association for Radiation Protection (IARP). He is a member of the International Steering Committee to organise the International Conferences series on Polonium and radioactive Pb isotopes in the environment. He has served as an expert member in the IAEA missions to member countries.

High Intensity (Superconducting) Proton Accelerators for ADS

Srinivas Krishnagopal
HIPL, IADD, BARC , Mumbai
Email: krishnas@barc.gov.in

Accelerator Driven Systems (ADS) are sub-critical reactors driven by high intensity proton accelerators. At BARC, the first step has been taken in the form of the normal-conducting Low Energy High Intensity Proton Accelerator (LEHIPA), which is a 20 MeV front-end of an ADS accelerator, which is presently being commissioned. To go to higher energy, one has to switch to superconducting technology. To enable this, DAE is involved in the Indian Institutions and Fermilab Collaboration (IIFC) in developing an 800 MeV superconducting accelerator, PIP-II, at Fermilab, USA, as part of an international collaboration. In addition, BARC is also planning for the next step in the ADS roadmap, in terms of Phase 1 of the Medium Energy High Intensity Proton Accelerator (MEHIPA) that will be a 40 MeV, high intensity, superconducting proton accelerator proposed to be located at BARC Facilities, Vizag. This talk will cover all these three projects.

Srinivas Krishnagopal completed his Ph.D. in accelerator physics from Cornell University, in 1990, working on accelerator theory. From 1990-92 he worked at the Lawrence Berkeley Laboratory on free-electron laser theory. This included a study of resonator stability, and new concepts such as the multi-cavity FEL. He returned to India in 1993, and joined the Centre for Advanced Technology. Initially he worked on accelerator theory. Later, he took up the challenge of technology development and built up a group that has indigenously developed a Plane-Wave Transformer linac and undulators for the free-electron lasers, and are working on photoinjectors for short wavelength FELs. He moved to the Bhabha Atomic Research Centre in 2008, where he is presently Director (N), MRG, to work on the development of high intensity proton accelerators for Accelerator Driven Reactor Systems. Dr. Krishnagopal was awarded the N.S. Sathyamurthy Young Scientist Award of the Indian Physics Association in 1996; he was elected Member of the National Academy of Sciences, Allahabad, India, in 1998; he was awarded the Outstanding Research Investigator Award of the Science Research Council of the Department of Atomic Energy in 2005; and in 2022 he was elected Fellow of the American Physical Society

New radiopharmaceuticals: New insights into disease and therapy

Dr. Vikram Lele
Jaslok Hospital, Mumbai
Email: vikram.lele@gmail.com

Dr. Vikram R. Lele is Director, Department of Nuclear Medicine & PET-CT at the Jaslok Hospital & Research Centre, Mumbai, India. He did MD (medicine) in 1986 with 2 gold medals, followed by DRM and DNB (nuclear medicine). He got further training in Nuclear Medicine at the Johns Hopkins Medical institutions, USA and in Germany. He is examiner for DRM in Nuclear Medicine for Mumbai University and a teacher in the national Board of examinations (DNB) for Nuclear Medicine. He was on the editorial board of the European Journal of Nuclear Medicine and Molecular imaging (EJNMMI) and the Indian Journal of Nuclear Medicine. He is past President of Association of Nuclear medicine Physicians of India (ANMPI) ,Nuclear cardiological Society of India (NCSI) and Western Chapter of Society of Nuclear medicine India. He has delivered several invited lectures and orations at national and international conferences in Nuclear Medicine and is author of over 38 publications and text book chapters in Nuclear Medicine in API textbook of Medicine, textbook of orthopaedics, among others. He was on the SARCAR committee of the Atomic Energy Regulatory Board (AERB) of Govt. of India. He has pioneered several new tests and therapies in Nuclear Medicine in India.

Recent Advances in Actinide-Ligand Multiple Bonding

Stephen T. Liddle[1]
[1]*Department of Chemistry and Centre for Radiochemistry Research, The University of Manchester, Oxford Road, Manchester, M13 9PL, UK*
*Email: steve.liddle@manchester.ac.uk

A central aim of synthetic f-block chemistry is to quantify the extent and nature of covalency in the bonding of these ions [1]. When considering ways to achieve this aim, studying early actinide-ligand multiple bonding is an attractive place to start because such linkages tend to, by definition, exhibit appreciable amounts of covalency and thus they are amenable to being probed using a wide range of structural, spectroscopic, magnetic, and quantum chemical calculation techniques. Additionally, whilst of interest in their own right, early actinide-ligand multiple bonds can provide a baseline for comparisons to transuranium and lanthanide analogues; this will in turn provide a rounded picture and understanding of these ions overall, enabling contextualization of their bonding with respect to the d-transition metals as well. This talk will describe some of our research in this area, specifically: (i) our terminal uranium-nitride work [2-7], where most importantly the above approach has enabled quantification of the covalency of this benchmark linkage; and (ii) extension of this approach to include neptunium-oxo, -imido, and carbene complexes [8,9], which has revealed some fundamental similarities and differences between the behaviour of uranium and neptunium.

References

1. Liddle, *Angew. Chem. Int. Ed.*, ***54***, 8604 (2015).
2. Liddle et al., *Science*, ***337***, 717 (2012).
3. Liddle et al., *Nat. Chem.*, ***5***, 482 (2013).
4. Liddle et al., *Nat. Commun.*, ***7***, 13773 (2016).
5. Liddle et al., *Nat. Commun.*, ***11***, 337 (2020).
6. Liddle et al., *Nat. Commun.*, ***12***, 4832 (2021).
7. Liddle et al., *Nat. Commun*, ***12***, 5649 (2021).
8. Liddle et al., *Nat. Chem.*, ***14***, 342 (2022).
9. Liddle et al., *J. Am. Chem. Soc.*, ***144***, 9764 (2022).

Prof. Liddle is head of Inorganic Chemistry and Co-Director of the Centre for Radiochemistry Research at The University of Manchester. He is a Fellow of the Royal Society of Chemistry, Fellow of the Royal Society of Edinburgh, and Vice President of the European Rare Earth and Actinide Society. His work has been recognised by a number of national and international society prizes, and he has published over 200 research articles, reviews, books, book chapters, and other articles.

Advance Nuclear Fuels

Sudhir Mishra[1], Vivek Bhasin[2]
[1]Integrated Fuel Fabrication Facility, [2]Nuclear Fuels Group
Bhabha Atomic Research Centre
Mumbai-400085
Email: sudhir@barc.gov.in

Fuel is the heart of nuclear reactor. Energy is produced by interaction of neutrons with fuel material which is subsequently utilised to produce steam to run turbine and produce electricity. Different forms of fuels are being used in various reactors all over the world. These fuels can be categorised into oxide, non-oxide, metallic and dispersion types. A fuel should have attributes like easy fabricability, efficient use in reactor and amenable to established reprocessing process. The first thermal and fast power reactors were loaded with Uranium based metallic fuel. Later on in 50s and 60s, other type of nuclear fuels e.g. oxides, carbides, nitrides and silicides were investigated. The technical and economic advantages of oxide fuels over other fuels led to its global use in nuclear power plants with thermal and fast reactors. However for research reactors, U/U based metallic fuel and fuel with dispersion of fissile uranium compound in the metal matrix were used from beginning. In fast reactor because of neutronic requirement, fuel with high fissile material density is used and high power density of the reactor core, also demands high thermal conductivity of the fuel. The advantage of oxide/mixed Oxide (MOX) fuel therefore is not so attractive with regards to its use in fast reactor. The non-oxide fuels like carbides, nitrides, U-Pu based metallic fuels have distinct advantage over oxide fuels for fast reactor use. After the accident at Fukushima Daiichi Nuclear plant in Japan, world wise focus is towards development of accident tolerant fuels and claddings. Accident tolerant fuel is supposed to keep integrity of fuel element for a long time without Zr-steam reaction stimulating hydrogen release. In India development work towards fabrication of advance fuels like U-Pu metallic fuel, CERMET fuel for fast reactor is being pursued. Also new U_3Si_2 dispersion fuel for research reactor is being fabricated and used in APSARA-U reactor. This presentation discusses the development and fabrication aspects of different types of fuels being used in Indian reactors.

Dr. Sudhir Mishra joined BARC after completeing 34th batch of training school BARC Mumbai. He is currently Head, Integrated Fuel Fabrication Facility (IF3) BARC, Mumbai. He is an expert in fabrication and development of nuclear fuels for thermal and fast reactors. He received DAE Scientific and Technical Excellence Award and Group achievement awards.

Selective Dissolution of Metal Oxides in Room Temperature Ionic Liquids: A New Strategy in Separation Science

P.K. Mohapatra
Radiochemistry Division, Bhabha Atomic Research Center, Trombay, Mumbai- 400 085
Email: mpatra@barc.gov.in

Room temperature ionic liquids (RTILs) are a class of benign neoteric diluents which are suggested to be the next generation diluents for spent fuel reprocessing [1]. However, with the prospects of electro winning of the extracted metal ions, due to the wide electrochemical window prevalent in RTILs, it is proposed to opt for a non-aqueous method of reprocessing akin to the pyrochemical process. However, for this purpose, one would like to have the direct dissolution of the spent fuel oxide using the RTILs. On the contrary, the dissolution of metal oxides in RTILs is a challenging issue due to the high viscosity of the diluents [2].

We have carried out the dissolution of UO_3 using HD2EHP (di-2-ethylhexyl phosphoric acid) in C_8mim.NTf_2, an RTIL. Interestingly, while the dissolution of UO_3 was facile, that of UO_2 and U_3O_8 was not feasible. Furthermore, a phase splitting after a certain metal ion loading has resulted in the pre-concentration of the U-HD2EHP complex [3]. In a separate study, Eu-oxide (Eu_2O_3) was preferentially dissolved as compared to the Am-oxide (AmO_2) with very high efficiency suggesting possibility of Ln-An separation using the RTIL based solvent containing a beta-diketone [4]. Both these case studies suggest rather facile dissolution of the trivalent metal ion and it was inferred that the dissolution of MO_2 was really hard. This lecture will bring out the basic problem areas in the dissolution of metal oxides in RTILs and there will be discussion on the mechanism of dissolution.

References

1. X. Sun, H. Luo and S. Dai, *Chem. Rev*., 2012, 112, 2100–2128.
2. B.N. Mahanty and P.K. Mohapatra, *Sep. Sci. Technol*., 2022, 57, 2792–2823.
3. P.K. Verma, B.N. Mahanty, S.M. Ali and P.K. Mohapatra, *Inorg. Chem*. 2021, 60, 10147−10157.
4. P.K. Verma, B.N. Mahanty, A. Sengupta, P.K. Mohapatra, R. Kumar, D. Bhattachayya, S.N. Jha and S.M. Ali, *Inorg. Chem.* 2023, 62, 87−97.

Dr. P. K. Mohapatra joined Radiochemistry Division, BARC, Mumbai in 1987. He did his Ph.D. from University of Bombay in 1994 and did postdoctoral research in University of Mainz, Germany (1999-2000) under Alexander von Humboldt fellowship. His research interests include complexation of actinides and separation of actinides and fission products using novel extractants. He is a fellow of National academy of Sciences, Allahabad. Dr. Mohapatra is an Associate Editor of Separation Science and Technology and one of the editors of Radiochimica Acta. Currently He is associate director of Radiochemistry and Isotope Group and Head, Radiochemistry Division. He has over 400 publications in peer reviewed international journals with over 8000 citations.

Relevance of SMRs for a De-carbon Energy Scenario

A.K. Nayak
Head, Nuclear Control & Planning Wing, DAE, Mumbai
Email: arun.nayak@dae.gov.in

Energy is one of the most critical requirements for the development of a nation. Of course, India, at present is one amongst the top producers and consumers of energy globally, however, our per capita energy consumption is still very low. We are a developing nation, with an ambitious GDP growth rate which would require significant demand in energy in domestic, transport, industries, infrastructure, etc for a growing population. Today, the country's energy supply is primarily driven by carbon based sources. The international pledge to reduce the global warming due to emission of carbon dioxide gases, would require replacement of carbon based energy sources with clean and green energy sources very soon.
This talk would focus on energy demand of India by 2050, contributions from renewable and requirements of nuclear to meet the low carbon energy budget of India. SMRs are being developed globally as new frontiers in nuclear reactor technology for enhanced safety, economics, accelerated capacity building, and particularly their role in replacement of retired coal plants. Relevance of SMRs for Indian energy sector will be presented. Apart from electricity production, the energy sector would require green hydrogen and high temperature carrying fluids for industry requirements. This talk would also present role of SMRs for low carbon hydrogen production and desalination.

Dr. A. K. Nayak is Head, Nuclear Control & Planning Wing, Department of Atomic Energy, Mumbai. He is a renowned expert in the field of advanced nuclear reactor design, nuclear safety, security & safeguards, nuclear policy & planning. He is an associate Editor of ASME Journal of Nuclear Engineering and Radiation Science, Journal of Computational Thermal Science, Member of Editorial Board of Frontiers of Energy. He is recipient of several awards and has written 4 books and published more than 500 research papers in academic journals and conferences. He is a Fellow of Indian National Academy of Engineering and Maharashtra Academy of Science.

Role of Chemistry in the Utilisation of Atomic Energy

K.L. Ramakumar
Email: Karanam.ramakumar@gmail.com

The development of atomic energy has been unique from a chemical point of view. Chemistry played an important role in the development of radioactivity and nuclear physics since the discovery of radium by Madame Curie. Its stellar role was exemplified in the discovery of nuclear fission and then in Manhattan Project during the successful commissioning of the world's first nuclear reactor Chicago pile-1. Atomic energy can be divided into the following broad fields, from the chemical point of view, viz., raw materials; production of fuel elements and other special reactor materials; reactor chemistry; chemical processing of irradiated materials; disposal and utilization of radioactive waste materials.

India had foreseen the potential for the peaceful utilization of atomic energy at a time when the pioneering activities in this field were geared essentially for military use. Chemistry programme began in the formative years of the Department of Atomic Energy during 1958s. India had consciously avoided softer options and chosen the slower and harder path of a programme aimed at self-reliance which, in all these years paid substantial dividends. India thus reaped rich dividends in the application of chemistry in diverse fields of atomic energy not only in developing nuclear energy for electricity generation but also in other areas as well that include water resources management, industrial applications, radiopharmaceuticals, environmental applications. This talk is aimed at giving glimpses of chemistry applications in Indian atomic energy programme on the momentous occasion of Amrit Mahotsav celebrations of India's Independence and the establishment of Indian atomic energy commission.

Dr. K.L. Ramakumar has superannuated from the Department of Atomic Energy (DAE), Government of India in 2016 after serving the Department for more than 40 years in different capacities. Before superannuation he was Head, Nuclear Controls & Planning Wing (NCPW) in DAE and also Director, Radiochemistry & Isotope Group in Bhabha Atomic Research Centre, Mumbai. In addition to his scientific and technical publications which are more than 500, Dr. Ramakumar also has publications on policy related topics including nuclear safeguards as a powerful tool for ensuring nuclear safety and security, nuclear forensics, nuclear security: National requirements in the context of global governance. In 2007, 2019 and 2021, he co-organised a three-week course on Nuclear Law under the auspices of Homi Bhabha National Institute. He was member of The Standing Advisory Group on Safeguards Implementation (SAGSI), IAEA from 2011-2016 and from 2016 is serving as member of Advisory Group on Nuclear Security (ADSEC), IAEA. He participated in the High-Level Fissile Material Cut-Off Treaty Experts Preparatory Group meeting and Group of Government Experts meeting on role of verification in advancing nuclear disarmament held in Geneva, as advisor from India. Dr. Ramakumar provides technical expertise in the areas of nuclear safeguards, nuclear security, fissile material cut-off treaty and nuclear disarmament, as required, to the relevant agencies of the Government of India.

Nuclear Fuel Complex-from Past to Present...
Fifty Years of Golden Journey in Indian Nuclear Power Program

*Y. Balaji Rao*and Komal Kapoor*
Nuclear Fuel Complex, Hyderabad-500062, Telangana, India
Email:ybr@nfc.gov.in

Nuclear Fuel Complex (NFC), a major industrial arm of the DAE, was conceived in middle 1960s by Dr. Homi J Bhabha, the father of Indian Nuclear Power Program (INPP). It came into existence formally in 1971 at Hyderabad. NFC is engaged in manufacturing and supply of Fuel sub-assemblies and other reactor core structural components to India's Pressurized Heavy Water Reactors (PHWR), Boiling Water Reactors (BWR) as well as Fast Breeder Reactors (FBR). After conceptualization of NFC during 1960s, a pilot plant was established in 1961 to produce nuclear grade natural UO_2 powder and pellets. Further, the half core of first PHWR (RAPS-I) was fabricated at Atomic Fuel Division (AFD), Trombay. The rich experience gained during this time has enabled DAE to embark upon commercial production of nuclear fuel and thus, NFC had come into existence with a production capacity of 100 Te of PHWR fuel and 24 Te of BWR fuel in 1972 at Hyderabad. The first 19 element PHWR fuel bundle with wire wrapped spacers was produced in NFC on 8th June 1973 with the available indigenous technologies and assistance from Russia & Canada. Presently, NFC has got the capacity to produce 1500MT of PHWR fuel, 25 Lakhs of fuel clad tubes and 1 lakh fuel bundles per annum with adaptation & implementation of innovative and break-through technologies into manufacturing and inspection & testing methodologies.

As an ISO 9001, 14001 and 45001 certified organization, NFC adheres to all the three ISO standards during manufacturing & supply processes. Natural UO_2 and enriched UO_2 in the form of pellets are being used as fuel in PHWR and BWR respectively. Where-as core components includes zirconium based alloys (Zircaloys) such as Zr-4 alloy and Zr-2 alloy as fuel clad materials for PHWR & BWR respectively and Zr-Nb alloy is being used for pressure tube manufacturing. It's important contributions to fast breeder reactor (FBR) programme is fabrication of high temperature and high burn-up compatible advanced stainless steel structural materials. Nuclear grade natural Uranium Dioxide (UO_2) pellets are produced at NFC by converting variety of raw materials using a well-established chemical conversion processes to get sinterable UO_2 powder followed by its granulation, pre-compaction and high temperature sintering. Similarly, several core structural components like fuel clad tubes, calandria tubes, pressure tubes, grid spacers etc., are being fabricated through fabrication route involving VAR melting, machining, extrusion/forging, pilgering etc.,. Finally, fuel sub-assemblies are made by encapsulating UO_2 pellets into zirconium alloy fuel tubes. The desired specifications are achieved by having a strict vigil on process conditions at each stage of manufacturing process as an integral part of QA/QC program. The production of nuclear grade materials with acceptable quality involves mastery of many diverse technologies in the fields of mechanical, chemical, metallurgical processes and testing methodologies. Besides this, NFC also manufactures different reactor components using special alloys including special steels for strategic application and also produces high purity materials of 5N & 6N purity for electronic & tool applications. Apart from principal customer NPCIL, the list includes DRDO, ISRO, HAL, BHAVINI, IGCAR, BARC, RRCAT etc.

NFC stands as a testimony to "Atmanirbhar Bharat" mission of the country in indigenous design and development of nuclear materials as well as special materials. During its 50 years of journey, NFC has attained complete self-reliance in the manufacture & supply of fuel and core components for PHWRs and BWRs operating in the country. With comprehensive nuclear fuel manufacturing cycle under its belt, NFC is the only organization in the world to have capabilities to process uranium and zirconium streams from ore to core, all under one roof.

Shri Y. Balaji Rao is currently working as General Manager at NFC and has got more than three decades of experience in Chemical Characterization of Nuclear Materials like Uranium, zirconium & zirconium based alloys and different grades of steels and received several DAE Group Achievement Awards.

Distribution of Strontium-90 in soils affected by Fukushima Dai-ichi nuclear power station accident in the context of Cesium-137 contamination

Sarata Kumar Sahoo[1] *, *Norbert Kavasi*[1,2]

[1]*Department of Radioecology and Fukushima Project, National Institute of Radiological Sciences, National Institutes for Quantum Sciences and Technology, 4-9-1 Anagawa, Inage-ku, Chiba 263-8555, Japan*

[2]*Laboratory for Radiochemistry, Department of Environmental Sciences, Jožef Stefan Institute, 39 Jamova, Ljubljana 1000, Slovenia*

*Email: sahoo.sarata@qst.go.jp

^{90}Sr is an artificial pure beta emitting radionuclide that has been released into the environment through nuclear accidents and nuclear weapon tests. Due to its relatively long half-life (28.9 years) and bio-chemical similarities to Ca, there is a risk of internal radiation dose increment for living beings. The database for ^{90}Sr released by the Fukushima Daiichi Nuclear Power Plant (FDNPS) accident is quite limited compared to ^{137}Cs. In this work, ^{90}Sr and ^{137}Cs activity concentrations were determined with radiometric methods in soil samples (soil, litter, rain gutter deposit, and roadside sediment samples) collected from the Fukushima exclusion zone (1,2). This work focuses to uncover the details of ^{90}Sr deposition and migration in the context of ^{137}Cs occurrence, as ^{137}Cs and ^{134}Cs are the dominant contaminants and ^{134}Cs unquestionably indicates its FDNPS accident origin due to its shorter half-life (2.1 years). A moderate positive correlation was revealed between ^{90}Sr and ^{137}Cs and higher mobility of the ^{90}Sr was confirmed in Japanese soil. The activity ratio of for ^{90}Sr/^{137}Cs was in the range of 5.0×10^{-5} to 5.0×10^{-4} with a median of 1.2×10^{-4}. From the activity ratio values it was concluded that the ^{90}Sr released to the atmosphere was only around 0.001-0.01 PBq which is negligible compared to the Chernobyl accident (~10 PBq) or other nuclear accident contaminations. From the standpoints of radioecology and radiation safety, ^{137}Cs remains the primary pollutant of the FDNPP accident.

References

1. Sahoo et al., *Scientific Reports*,***6***,*23925* (2016).
2. Kavasi et al., *Env. Pollution*, ***326***, 121487 *(*2023).

Dr. Sahoo is currently working as Senior Expert in the Fukushima Environmental Research Project, National Institute of Radiological Sciences, Chiba, Japan as well as Adjunct Professor, Tokyo Metropolitan University, Arakawa campus, Tokyo. He has been awarded Eminent Mass Spectrometry-Award, Indian Mass Spectrometry Society in year 2019 and RADNET Eminent Research Award, National Radon Network Society, India in year 2023.

Thermodynamic modelling of the oxidation of *Ln*- and Pu-doped UO_2

Victor Vinograd[1,*], Andrey Bukaemskiy[1], Guido Deissmann[1] and Giuseppe Modolo[1]
[1] *Forschungszentrum Jülich GmbH, Institute of Energy and Climate Research – Nuclear Waste Management (IEK-6), 52428 Jülich, Germany*
*Email: v.vinograd@fz-juelich.de

Recent research shows that fission products and actinides contained in UO_2-based spent nuclear fuel significantly enhance its resistivity to oxidation in air and to oxidative dissolution in aqueous media relative to pure UO_2 [1-3]. Mechanisms of these retardation effects are not yet fully understood. Here we develop thermodynamic models of the oxidation of *Ln*- and Pu-doped UO_2 solid solutions in air referring to measured data on the oxygen partial pressure at equilibrium. The key result of this modelling is the demonstration of a strong partitioning of *Ln* or Pu between MO_2, M_4O_9 and M_3O_8 phases. Particularly, the cubic phases tend to be enriched in *Ln* or Pu, while the M_3O_8 phase tends to have the smallest fraction of an impurity component. The achievement of a large O/M ratio at thermodynamic equilibrium requires this fractionation to be completed. Consequently, the slow diffusion of *Ln* or Pu within any of the relevant phases may be the cause of the enhanced resistance to oxidation.

References:
[1] C. Jégou et al., *J. Nucl. Mater.*, **405** (2010) 235.
[2] A. Casella et al., *J. Nucl. Mater.*, **476** (2016) 45.
[3] V. Kerleguer et al., *J. Nucl. Mater.*, **529** (2020) 151920.

Dr. Victor Vinograd is currently a research scientiest at Research Centrum Jülich, Institute of Energy and Climate Research (IEK-6). He is expert in thermodynamics of solid solutions related to actinides.

A Systematic Evolution towards the Development of a Comprehensive Gamma Scanning System for Special Nuclear Materials Assay

Chhavi Agarwal

Radiochemistry Division, Bhabha Atomic Research Centre, Trombay, Mumbai-400085
Chemical Sciences, Homi Bhabha National Institute, Mumbai-400094
Email: cagarwal@barc.gov.in

Nondestructive assay based on gamma ray spectrometry is extensively used in nuclear fuel cycle, nuclear safeguards and for the categorization of nuclear waste. The technique is challenging due to the diverse nature of samples that are encountered. This includes voluminous, inhomogeneous samples having varied sizes and shapes. Segmented gamma-ray scanning (SGS) is the most common and versatile technique for the assay of such samples [1] and has been successfully applied to voluminous samples of different configurations ranging from small vials to 200 L drums. This technique accounts for the variation of matrix materials in different segments but assumes both the source and matrix to be homogeneously distributed in each segment. However, due to the lower efficiency of a collimated detector, the SGS scan of a low activity sample may sometimes take a day or even more. For relatively uniform matrix and radioactivity distribution, the throughput of assay can be significantly improved by using open detector geometry. Also, the SGS technique traditionally requires a calibration standard which may not always be a true representative of the sample. To deal with it, a non-conventional Absolute Segmented Gamma Scanning (ASGS) methodology using a standard point source has been developed [2]. A major limitation of SGS is the presence of lumps of gamma ray emitting nuclides which has high self-attenuation, which may result in significant underestimation of the assay results. An alternate single pass absolute efficiency approach following the principle of infinite energy extrapolation of apparent mass has been developed for the assay of waste drums containing Pu lumps [3]. For situations where the radionuclide source distribution as well as matrix distribution is significantly heterogeneous, SGS and the open detector technique may lead to large errors [4]. Another advanced NDA technique to assay radioactive waste is tomographic gamma scanning (TGS) which is capable of assaying radionuclide content in heterogeneous media with medium and high density and is widely used to assay the location and quantity of radioisotopes in the container. The TGS combines transmission and emission reconstructive tomography techniques in an effort to improve the accuracy of the measurement and relies on the image reconstruction techniques to yield a coarse 3-D radionuclide and matrix density distributions, with a typical spatial resolution of 5-6 cm [4]. Among the limitations of the TGS technique are the statistical fluctuations in the transmission and emission data, which eventually results in long measurement times.

The presentation will highlight the studies carried in our division that lead to a systematic evolution of the measurement systems for the assay of special nuclear materials in voluminous samples.

References

[1] E.R. Martin et al., Los Alamos National Laboratory report, LA-7059 (1977).
[2] S. Patra, C. Agarwal, and S. Chaudhury, Applied Radiation and Isotopes, 144 (2019) 80–86.
[3] S. Patra and C. Agarwal, Applied Radiation and Isotopes, 153 (2019) 108827.
[4] R.J. Estep et al., Los Alamos National Laboratory report, LA-UR-93-1637 (1993).

Dr. Chhavi Agarwal joined Bhabha Atomic Research Centre in 2004 after graduating from the OCES-47th batch of BARC Training School. She completed her M.Sc. (Chemistry) from Delhi University in 2003 and obtained Ph.D. (Chemical Science) from Homi Bhabha National Institute in the year 2011. She has been awarded Endeavour Postdoctoral Research Fellowship of Australian Government for carrying out research at Melbourne University for four months. She has also worked at Universitat Duisburg-Essen under INSA-DFG bilateral exchange program for three months to carry out research work on synthesis and permeability studies on stimuli responsive membranes. She has been awarded H.J. Arnikar Best thesis award by Indian Association of Nuclear and Allied Chemists for her thesis work. Her expertise includes non-destructive assay of nuclear materials and on physico-chemical studies on ion-exchange membranes and polymer gels. She has published >50 international journal publications.

Application of environmental radioactive isotopes (^{3}H and ^{14}C) in hydrological studies

Sitangshu Chatterjee

Isotope and Radiation Application Division, BARC, Mumbai
Email: sitanshu@barc.gov.in

Tritium (^{3}H) and carbon-14 are the two most important environmental radioactive isotopes that are often used in hydrological studies to estimate the transit time (age) as well as dynamics of the water. Tritium (half-life = 12.43 years) is generally used to act as a qualitative indicator for the groundwater residence time. In most of the cases, environmental tritium data suggests whether the groundwater is modern or old or a mixture of both. Samples containing tritium values greater than 1.0 TU indicate modern recharge or a mixture of old and modern water whereas values less than 1.0 TU typically indicate recharge prior to 1951. Using tritium, we can date water up to ~50 years of age. However, if the time series data of tritium concentration is available, quantitative estimation of groundwater ages can also be made out using lumped parameter models (LPMs). On the other hand, C-14, a radioactive isotope of carbon has half-life of 5730 years and is useful to date groundwater up to 40,000 years old. ^{14}C dating technique is generally employed to estimate the residence time of those groundwater samples which do not contain significant amount of modern recharge (i.e. negligible tritium concentration). Water having low C-14 content is very vital from the sustainable viewpoint. These waters should be judiciously used. In this talk, I will elucidate how both these isotopes are used to have an idea about the age of water.

Dr. Sitangshu Chatterjee obtained his M.Sc. Degree in Chemistry from IIT-Kanpur in 2012 and joined Isotope Hydrology Section, Bhabha Atomic Research Centre, Mumbai in 2013 after graduating from the 56th Batch of BARC training school. He obtained his Ph.D. degree in Chemistry from Homi Bhabha National Institute (HBNI) Mumbai in 2021. Dr. Chatterjee is working in the field of sustainable management of water resources using isotopic techniques. He is involved in the mass spectrometric determination of various stable isotopes and their applications in delineating various hydrological processes such as geochemical evolution, aquifer-aquifer interconnection, geothermal systems, transit time modelling etc. He is the recipient of the “DAE Young Scientist Award-2020” as well as “DAE Group Achievement Award-2017”. He has 18 publications in international journals. He is a member of International Association of Geochemistry (IAGC).

Positron Annihilation Spectroscopy: an excellent probe for observing changes in pore architecture during CO_2 adsorption in metal organic frameworks

Jaideep Mor[1], *Pranav Utpalla*[1, 2], *Saurabh Mukherjee*[1], *Sandeep Kumar Sharma*[1, 2] *and Dhanadeep Dutta*[1, 2]

[1]*Radiochemistry Division, Bhabha Atomic Research Centre, Trombay, Mumbai - 400085,*

[2]*Homi Bhabha National Institute, Anushaktinagar, Mumbai-400094*

deep@barc.gov.in

Abstract

Metal Organic Frameworks (*MOF*s) are highly porous crystalline materials having extraordinarily high specific surface area formed from the self-assembled metals or metal-oxide clusters and organic ligands (linkers). Zeolitic Imidazolate Frameworks (*ZIF*s) are a special class of *MOF*s comprised of imidazolate linkers and metal ions having structures similar to zeolites. The flexible nature of *ZIF*'s structure assures its use as an efficient gas storage material at high pressure. Using positron annihilation lifetime spectroscopy (PALS) it is observed that the pore volume in some representative flexible *ZIF*s (namely, *ZIF*-8, *ZIF*-67, and *ZIF*-7) expands during CO_2 gas adsorption at high pressure (up to ~60 kg cm^{-2}). The linker rotation as well as reversible phase transformation of the framework may cause the enhancement of the pore volume at high pressure. The details of the changes in pore architecture of *ZIF*s during CO_2 gas adsorption as observed through PALS will be discussed.

Dr. Dhanadeep Dutta is currently working at Radiochemistry Division, BARC, Mumbai as a Scientific Officer. His research interest includes positron annihilation spectroscopy in nano-porous materials. He is the recipient of "Max-Planck-India Fellowship" from the Max-Planck Society, Germany for the years 2006-09. He is the author of more than 70 articles published in the leading International Journals.

Radiolabeled porphyrins as theragnostic agents: Nuclear Medicine and PDT

Mohini Guleria[1, 2]

[1]*Radiopharmaceuticals Division, Bhabha Atomic Research Centre, Trombay, Mumbai-400085*

[2]*Homi Bhabha National Institute, Anushaktinagar, Mumbai-400094*

E-mail: mohini@barc.gov.in

Porphyrins have long been known for their inherent ability towards exhibiting localization in neoplastic tissues. Hence, radiolabeled porphyrins could be utilized for delivery of radionuclides (diagnostic as well as therapeutic) at the site of tumorous lesions. Such radiolabeled porphyrin complexes could find utility for nuclear imaging as well as radionuclidic therapy of tumors. Compatibility of porphyrin core size with ionic radii of variety of radiometal ions make it feasible to carry out radiolabeling of porphyrin derivatives in the central cavity following an 'integrated approach of radiometal complexation. Additionally, radiolabeling with radionuclides having ionic radii mismatch with that of porphyrin core could be performed at the peripheral position of porphyrin using external chelating moieties called as bi-functional chelating agents (BFCAs). Apart from aforementioned properties, the porphyrin molecules exhibit another feature which make them suitable for applications in another modality known as photodynamic therapy (PDT). Photodynamic therapy utilizes effects of light for expediating the therapeutic efficacy and this approach has showcased the potential for clinical management of certain type of cancers. Porphyrins act as excellent photosensitizers which upon light excitation lead to the generation of reactive oxygen species (ROS) which in turn initiate a cascade of bio-chemical reactions leading to cell death. The short talk will comprise a brief overview of the work carried out by the speaker in the field of development of porphyrin derivatives, radiolabeled with a variety of radionuclides viz. ^{68}Ga, ^{99m}Tc, ^{90}Y and ^{177}Lu, prepared using both 'integrated and BFCA approach' as well as evaluation of their potential in *in-vitro* and *in-vivo* models. The talk will also cover the studies carried out towards evaluation of the in-house synthesized porphyrin derivatives (in non-radiolabeled form) for photo-cytotoxic effects in different cancer cell lines.

Dr. (Smt.) Mohini Guleria joined BARC from 52nd batch of Training School. Her research work includes syntheses and functionalization of tumor avid bio-molecules including porphyrins and antibodies. She has experience in radio-metal complexation of functionally modified ligands using various radionuclides bearing nuclear diagnostic and therapeutic importance as well as their evaluation in animal models. Dr. Guleria has published about 28 articles in peer-reviewed international journals and was also awarded with DAE-Young Applied Scientist Award in 2017.

Identification and quantification of elemental and anionic impurities as forensic signature in isotopically natural uranium matrices

Suchismita Mishra
Environmental Monitoring and Assessment Division, Health Safety and Environment Group,
Bhabha Atomic Research Centre, Mumbai-400085, India
**Email:suchim@barc.gov.in*

Nuclear forensics supports the criminal investigation involving nuclear and radioactive materials. It involves the identification and quantification of different signatures in the intercepted nuclear material. Examples of such signatures are trace elemental and anionic impurities present in the bulk matrix, isotopic composition, age etc. of the nuclear material. These signatures provide clues for identification of origin, intended use or process history of the material. Effective forensic investigation relies on the identification and accurate and precise determination of these signatures. In this present work, isotopically natural uranium materials, e.g, uranium ore with different geological and geographical origin and uranium ore concentrate (UOC) or yellow cake samples produced from the corresponding ore samples are investigated, for identification and evaluation of elemental and anionic impurities for forensic purposes. The formation of U-ore deposits occurs under a large range of conditions including temperature and source (elemental availability). That’s why variations in their major and trace element compositions and anionic signatures are expected. The impurity profile (pattern or ratio) of some specific elements or anions observed in UOC can imitate U ore, the precursor material, owing to chemical or physical inertness of the impurity during production process. A significant variation in some elements and anions can also be observed in UOC samples considering the huge variation in the original U ore mineralogy and metallurgical processing of the ore. This variation can help in distinguishing the origin of the material.

For elemental and anionic impurity analysis in uranium rich materials, inductively coupled plasma mass spectrometer (ICPMS) and ion chromatograph are mainly used. The various challenges with respect to homogenisation, complete dissolution, separation and analysis for the precise measurement of elemental and anionic impurities in uranium bearing materials is addressed in the present study. For complete dissolution of bulk geological matrices with different mineralogy, both microwave digestion and electric fusion techniques are used independently or in combination. For separation and preconcentration of desired elements from the bulk matrix, different techniques like ion exchange or/and extraction chromatography and solvent extraction are used as and when required. Similarly, for extraction of anions both water leaching and pyro hydrolysis method are used. For quality assurance of the method and data different approaches like blank control, duplicate analysis, spike recovery, analysis of standard reference materials, cross checking with different instrumental techniques etc. are carried out. Statistical approach, like multiple regression methods, majorly principal component analysis (PCA) has been applied for data segregation in order to identify the different group of elements or anions associated with particular uranium material for origin assessment.

For example, chondrite-normalized rare earth element (CN-REE) pattern was found to be a very good signature for forensic application. Fig.1 shows the CN-REE pattern for U ore samples with different geological formation.

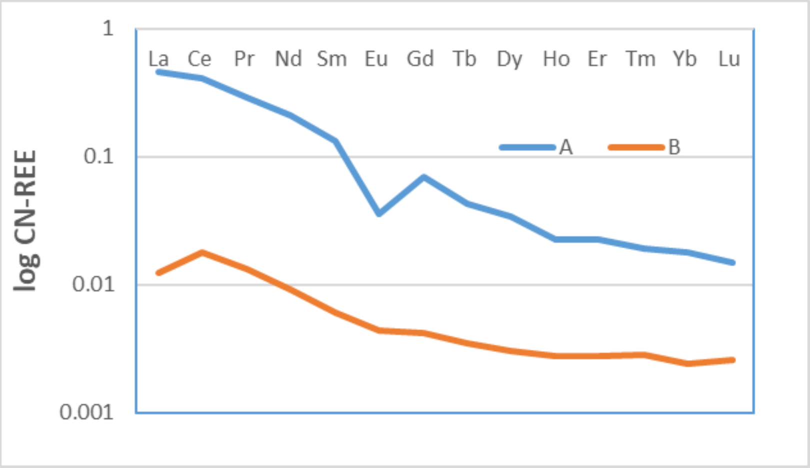

Figure 1. CN-REE pattern in bulk uranium ore samples from two different type uranium deposits (A: Granitic related vein type from Shinghbhum, Jharkhand (average of 160 samples) and B: Carbonate host rock from Tummallapalli, Andhra Pradesh (average of 60 samples).

Dr. Suchismita Mishra obtained her M. Sc. in Chemistry from Utkal University, Odisha in 1997. And then after graduating from 41st Batch of Training School, BARC, in chemistry discipline joined Environmental Assessment Division in 1998 and subsequently in Environmental Monitoring and Assessment Division in 2019. After her Ph.D. from the University of Mumbai in 2009, she carried out her postdoctoral research at National Institute of Radiological Sciences (NIRS) Chiba, Japan during 2011-2013 through JSPS (Japan Society for Promotional Science) fellowship. Dr S. Mishra has expertise in environmental analytical chemistry mainly in analysis of stable elements and radionuclides at trace and ultra-trace level using different spectroscopic and radio analytical techniques. She has carried out extensive work on sorption behavior of natural radionuclides and fission products in geological matrices for contaminant transport around uranium tailings and Fukushima nuclear power plant accidental site. Currently involved, in the development of analytical capability for nuclear forensic studies for nuclear/radiation emergency preparedness. Dr. Mishra has several quality research publications in international journals to her credit.

Separation of fission molly by pyrohydrolysis: an alternate approach

V. G. Mishra
Radioanalytical Chemistry Division, Bhabha Atomic research Centre, Mumbai 400085
E-mail: vgmishra@barc.gov.in

In reactor ^{99}Mo can be produced by nuclear reactions like either by ^{98}Mo (n, γ) ^{99}Mo or ^{235}U (n, fission) ^{99}Mo. During fission of the ^{235}U, fission product ^{99}Mo is generated with yield of ~ 6.1%. Further the specific activity of the ^{99}Mo which is generated through fission reaction is higher than ^{98}Mo (n, γ) ^{99}Mo. Once a uranium containing target is irradiated in the reactor ^{99}Mo has to be separated from the target material at the earliest to get maximum activity, employing suitable procedure. Mainly two dissolution based procedures are followed which are called Alkali method and Acidic methods based on the dissolution medium used. After dissolution, several steps of separations and purifications employing variety of reagents are followed in both the methods to get ^{99}Mo of desired purity. Owing to the associated non-proliferation benefits, the use of LEU fuels and target materials for production of radiopharmaceuticals are being considered. However the LEU targets are associated with few important challenges: (i) ^{99}Mo efficiency is reduced due to low ^{235}U fraction (ii) generation of radioactive liquid waste solutions is significantly higher. In addition, dissolution of some LEU materials such as U_3Si_2 (having higher U density) is difficult and requires aggressive conditions for dissolution. To overcome these problems, new approaches for separation of ^{99}Mo from the irradiated targets are highly recommendable.

In the background of the existing procedures where target matrix is dissolved and then ^{99}Mo is separated using series of complex chemical steps, there is also a scope of developing procedures by converting ^{99}Mo to its volatile form and separating it directly from the solid matrix employing pyrohydrolysis. We explored pyrohydrolysis to understand the feasibility of separating ^{99}Mo directly from solid target matrices by converting Mo into its volatile form. Fig.1 shows a pictorial representation of a pyrohydrolysis set up. The analytes extracted from the matrices are trapped in a suitable solution and then quantified using ion chromatography and HPGe. The recovery of Mo from U matrix was optimized using un-irradiated U matrices with known Mo. The finalised pyrohydrolysis procedure was subjected to irradiated U_3Si_2 (containing natural U) at lab scale. The recovery of ^{99}Mo was observed to be better than 90%. However in addition to ^{99}Mo other volatile radioisotopes of I, Te and Ru were also separated during the pyrohydrolysis. On the other hand isotopes of Np, Zr, Nb, Ce, Ba and La were below the detection limit in the distillate. The pyrohydrolytic separation was associated with the advantages of (i) matrix free clean distillate; (ii) the only reagent used during trapping was a 15 mM NaOH. Further, required radiochemical purity of ^{99}Mo for its application as radiopharmaceuticals was achieved employing ion-chromatographic separation at lab scale. Moreover, the present process produced lower radioactive waste volume as the target matrix remained in the solid form. Further studies have to be carried out to scale up target matrices (with more amount of target material and irradiation time).

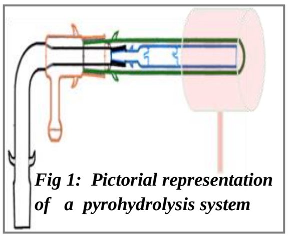

Fig 1: Pictorial representation of a pyrohydrolysis system

Dr. V. G. Mishra joined Radioanalytical Chemistry Division in 2008 after graduating from 51st batch of BARC Training School. He is involved in development of CQC methods for various kinds of nuclear materials using pyrohydrolysis and ion chromatography. His research interest includes studies on separation of various species using ion chromatography and separation using pyrohydrolysis with a view to explore the mechanism involved during separation.

Study of nuclear fission process using heavy ion induced nuclear reaction

A. Pal
Nuclear Physics Division, *Bhabha Atomic Research Centre, Mumbai , India*
Email: asimpal@barc.gov.in

Nuclear fission is a very complex process in which a heavy nucleus undergoes shape changes and breaks into nearly two symmetric fragments. It has many societal applications like nuclear power productions, productions of radioisotopes for medical treatments etc.. Although, the discovery of the process was made using radio-chemical analysis for the first time almost 85 years back, now-a-days the process is often studied using heavy ion induced reactions aiming to resolve many puzzling features observed in nuclear fission process. In modern times, the study of nuclear fission process becomes relevant in the context of synthesizing new high Z elements in the laboratory and extending the periodic table of elements. While fusing two heavy nuclides in order to produce high Z elements, the compound nuclear fission process and a pre-equilibrium fission process are the main culprits for inhibiting the formation of super-heavy-elements. Therefore it is very important to choose suitable colliding partners and colliding energy so that those competing processes become minimized and SHE formation becomes feasible. Therefore, considering the above facts, a thorough knowledge of nuclear fission and pre-equilibrium fission processes are of utmost importance.

We explore the avenues of nuclear fission process using heavy ion induced nuclear reactions at BARC-TIFR Pelletron-Linac facility, Mumbai. Using the heavy ion beam like ^{11}B,^{12}C,^{16}O,^{19}F etc. delivered by the said facility and actinide targets we form a compound nucleus by fusion reactions and measure the fission fragment mass and total kinetic energy (TKE) distributions with the help of position sensitive multi-wire proportional counters (MWPC) developed in-house [1]. Using this setup, we attempted to address the key question:``Upto how much excitation energy shell effect (the main reason for the production of asymmetric fragments in the fission of actinides) persists in the process of nuclear fission?" We found that the shell effect can persist upto very high (~70 MeV) excitation energy, mainly due to the role of multi-chance fission [2]. In another work we have populated a neutron rich compound nucleus ^{257}Md by $^{19}F+^{238}U$ reaction and observed that a high TKE mode exists at excitation energies beyond 40 MeV which challenges the existing theories on nuclear fission [3]. Now another facet of heavy ion induced fission, known as pre-equilibrium fission has been explored by comparing the measured mass-distributions data and theoretical model calculations, we have successfully extracted the contribution from pre-equilibrium process for the presently measured data and data available in literature. From the systematic evidence we show for the first time that the pre-equilibrium process is governed by the shell effect. Further, using the same systematic we have prescribed one formula for estimating the probability for pre-equilibrium fission, a key process for inhibiting the formation of super-heavy elements [4].

References:

[1] A. Pal et.al., *JINST*, **15** (2020) P02008.
[2] S. Santra, A. Pal et.al., *Phys. Rev. C (under review).*
[3] A. Pal et.al., *Phys. Rev. C,* **104** (2021) L031602.
[4] A. Pal et. al., *arxiv:2211.15134* (2022)

Dr. Asim Pal completed B.Sc. (Hons.) in Physics from Jadavpur University, Kolkata and M.Sc. in Physics from Indian Institute of Technology Kharagpur. After that he joined BARC Training School as Trainee Scientific Officer in the year 2011. After successful completion of the one year training program, he joined Nuclear Physics Division, Bhabha Atomic Research Centre. Since then he continues working there in the field of nuclear reaction. He obtained his Ph.D. from Homi Bhabha National Institute in the year 2019 for his thesis work “Study of fission reactions involving weakly bound projectiles”. His research interests include studies of nuclear fusion-fission reactions, nuclear reaction relevant to nuclear astrophysics and super-heavy element synthesis. He has also indigenously developed a few gas detectors and array of silicon strip detectors, which have high impact in improving the charged particle detection system at BARC-TIFR Accelerator facility, Mumbai. He has published more than 40 papers in reputed international journals and more than 75 conference papers.

Advanced Sample Loading Techniques for TIMS

Sumana Paul
Fuel Chemistry Division, Bhabha Atomic Research Centre, Mumbai 400 094
Email: sumana@barc.gov.in

Isotope analysis of actinides is important for nuclear safeguards and nuclear forensics, which requires suitable analytical methodologies with high sensitivity, accuracy, and precision. Thermal ionization mass spectrometry (TIMS) is one of the most powerful techniques available for isotopic measurement with very high precision and accuracy [1] – although TIMS usually suffers from its relatively low sensitivity in ultratrace measurements, particularly for actinides. For example, the ionization efficiency of TIMS for uranium with a double filament setup is typically <0.05%. Such poor ionization efficiency limits the accuracy and precision of actinide isotopic analysis, since actinides are usually present at ppb or sub-ppb level concentrations in the environmental samples as well as the swipe samples available for nuclear forensic and safeguards. Also, TIMS involves elaborate sample pre-treatment and manipulation steps to eliminate the undesirable matrix and subsequent manual loading of small volumes of purified aqueous samples on a filament for thermal ionization. This is cumbersome, particularly for the handling of radioactive samples like uranium and plutonium. The conventional loading method of actinides as acidic solution produces more volatile oxide ions, apart from the elemental ions, during TIMS analysis which further degrades the analysis performance. In order to improve ionization efficiency of the actinides in TIMS, graphite/carbon based additives are employed as filament surface modifiers that can serve as reducing agents and suppress the formation of undesirable oxide ions, thereby increasing the ionization efficiency. In recent times, Thermal Ion Cavity (TIC) and Porous Ion Emitters (PIE) have also emerged as yet another promising substrate for loading of actinides in TIMS. However, the carbon additives/TIC/PIEs etc. serve as mere filament modifiers, and the requirement for sample pre-treatment and chemical separation to get the analyte in the purest possible form still persists. An alternative approach could be pre-concentration of the analyte on a suitable solid phase substrate that can be directly loaded on Re filament for TIMS analysis. In our lab, we have developed and reported various polymeric substrates e.g. gel, resin, membrane etc. for the single step matrix elimination and source preparation for the loading of U and Pu, selectively pre-concentrated from a variety of environmental and nuclear fuel reprocessing samples [2]. This short lecture focuses on some recently developed supported liquid membranes that has significantly improved the sensitivity of isotopic measurements of U and Pu by TIMS, with particular emphasis on the measurement of low abundant ^{234}U and ^{238}Pu isotopes.

References

[1] N. Vajda, C.K. Kim, Anal. Chem. 83 (2011) 4688−4719.
[2] S. Paul, K.S. Bhushan, P. Goswami, Anal. Chem. 91 (2019) 14383.

Dr. Sumana Paul is currently serving in Fuel Chemistry Division of Bhabha Atomic Research Centre, after graduating from 51st batch of Training School. She received her PhD degree in Chemical Sciences from Homi Bhabha National Institute in the year 2016 for her work in polyemeric substrate based analytical techniques for actinide assay. Her field of specialization includes development of novel polymeric materials for the separation of actinides from complex matrices. She is the recipient of IANCAS-Prof H.J. Arnikar Best PhD Thesis Award and DAE Young Scientist Award. She has, to her credit, more than 55 publications in various peer-reviewed journals and conferences.

Synchrotron Beamline for Study of Radioactive materials

H. K. Poswal

Email: himanshu@barc.gov.in

High Pressure & Synchrotron Radiation Physics Division, Physics Group, BARC

The Multi Investigation of Radioactive Actinides (MIRA) beamline, specifically designed for the study of radioactive materials, is being developed at Indus-2 synchrotron source at RRCAT, Indore. The beamline will provide a unique opportunity to investigate the structural and chemical properties of these materials using X-Ray Diffraction (XRD), X-Ray Absorption (XAS) (Near Edge X-ray Absorption and Extended X-Ray Absorption Fine Structure), and X-Ray Fluorescence (XRF) techniques. These techniques offer a non-destructive means of studying the materials, allowing researchers to gain insights into their behaviour and properties without compromising their integrity. The beamline will be helpful in making significant advances in our understanding of radioactive materials and their potential applications in a variety of fields, including materials science, nuclear energy, and medicine. In this presentation, salient features and capability of the upcoming MIRA beamline will be presented.

Dr. Himanshu Kumar Poswal secured first rank in his post graduate course in physics from BARC training school in the year 2002. After finishing the course, he joined high-pressure physics division, BARC. Since then he is working in the field of high pressure. He obtained his Ph. D degree from HBNI, Mumbai in 2014. Dr. Poswal has actively participated in the development of beamlines viz. ECXRD beamline (BL-11) and protein crystallography beamline (BL-21) at Indus-2 synchrotron radiation source. His research interests include structural investigations of materials under extreme conditions using first principles simulations and experimental techniques.

Probing the Depths: Ion Beam Analysis for Material Characterization

G. L. N. Reddy
National Center for Compositional Characterisation of Materials (NCCCM),
Bhabha Atomic Research Centre (BARC), Hyderabad, India-500062
glnreddy@barc.gov.in

Ion Beam Analysis (IBA) plays a crucial role in non-destructive depth profiling of elements in the surface regions of materials. Narrow resonance profiling (NRP), a variant of nuclear reaction analysis (NRA), is bestowed with selectivity, sensitivity and high depth resolution. It exploits narrow resonances in the excitation function of a nuclear reaction and invokes the concept of stopping power for non-destructive depth profile measurements. A resonance in a nuclear reaction is characterized by resonance energy E_R, cross section σ_R, and resonance width Γ_R. Each of these parameters plays a vital role in depth profiling measurements. Ideally a resonance should be strong, narrow and well isolated to facilitate sensitive and high depth resolution measurements and to probe larger depths in the sample. Further, the off resonance cross sections should be as low as possible and there should be no interferences from competing nuclear reactions. Nuclear resonance reaction analysis is carried out by impinging the target material with projectiles of energy E less than E_R and subsequently increasing beyond E_R in regular energy intervals. Upon reaching the resonance energy E_R in the target material the characteristic charged particles or γ-rays emitted, are detected for depth distribution studies.

In the present talk some of the nuclear resonance reaction (NRRA) methodologies (see the table) that have been standardised / developed in our laboratory will been presented. The NRRA methodologies thus developed have been employed for the characterisation of materials for technological, industrial, strategic and energy applications.

Dr. G. N. Reddy did his post-graduation in Physics from Osmania University and M.Phil from University of Hyderabad. He joined the BARC in the year 1998 after his successful stint as trainee in 41^{st} Batch BARC Training School. He acquired Ph.D in Physics from Osmania University in the year 2012. He is associated with Tandetron since 2003. He has been working in the field of Ion beam analysis for carrying out compositional analysis of variety of materials. He is involved in various R&D activities related to the development of thin films for hydrogen storage applications. He has about 61 publications in various journals and conferences.

Chemical Aspects of Advanced Nuclear Reactor

Pradeep Samui
Product Development Division
Bhabha Atomic Research Centre, Trombay, Mumbai – 4000 085
Email: psamui@barc.gov.in

For efficient utilization of nuclear resources and production of least radioactive wastes, Generations IV (G-IV) reactors designs have been proposed [1]. The characteristics of these reactors include: inherent or passive safety features, simplified or modular designs, high-temperature stability, fast neutron spectrums, and "closed" fuel cycles. To achieve these goals, a non-classical reactor systems is considered in Gen IV reactor system for energy production: Molten salt Reactor (MSR) along with other classical five reactor concepts which are based on solid nuclear fuel cooled by a gas or a liquid, viz, i) Gas-Cooled Fast Reactor (GFR); ii) Lead-Cooled Fast Reactor (LFR); iii) Sodium-Cooled Fast Reactor (SFR); iv)) Supercritical Water-Cooled Reactor (SCWR); v) Very High Temperature Reactor (VHTR). The successful deployment of advanced nuclear systems demands the development of new materials and chemical processes under extreme conditions of radiation, temperature, and corrosive environments. As a part of this studies, choice fuel salt and their melting point, compatibility with structural materials, fission product interaction, choice of coolant composition, the chemical aspect of MSR will be discussed in this paper.

In Indian scenario, Accelerator-driven sub-critical reactor systems (ADS) address the two important concerns like transmutation of long-lived components of the spent fuel and nuclear energy generation utilizing thorium as fuel. The chemistry of LBE is a critical issue for its use as liquid spallation target and coolant for ADS. The corrosion by liquid metals/alloys can change the microstructure, composition, and surface morphology of the structural materials, which in turn affects the mechanical and physical properties of the structural materials, etc. leading to system failure. Studies of chemistry of liquid metal corrosion will be discussed in this studies.

References:

1) "A Technology Roadmap for Generation IV Nuclear Energy Systems", The U.S. DOE Nuclear Energy Research Advisory Committee and the Generation IV International Forum, 39, 2002.

2) Accelerator Driven Systems; Energy Generation and transmutation of nuclear waste – Status Report; IAEA – TECDOC-985 (November 1997).

Dr. Pradeep Samui joined BARC training school (IGCAR campus) in 2007 (51st batch) after completing his M.Sc. from Burdwan University, West Bengal. After completing one year orientation course in nuclear science and engineering from BARC training school, he joined Product Development Division, BARC in 2008. He is recipient of Homi Bhabha Award for overall topper of his batch. He obtained his PhD in Chemical Science from Homi Bhabha National Institute in 2018. He has been actively involved in studies related to determination of thermodynamic parameters of various alloys and oxide system. He is also investigated the interaction of Pb/Bi with structural materials and fuel in off normal condition for application in ADS system. He is a recipient of various awards like Homi Bhabha Prize (2008), DAE-Special Contribution Award (2016), Gurdip Singh Best thesis award (2020) by Indian Thermal Analysis Society**.** He has more than 20 publications in his credit.

Flexibility of Mixed Metal(Zn/Co) Zeolitic Imidazolate Framework-8: An Investigation Using Positron Annihilation Lifetime Spectroscopy

J. Mor[1], S. Mukherjee[1],D. Dutta[1,2] and S. K. Sharma[1,2§]

[1]*Radiochemistry Division, Bhabha Atomic Research Centre, Mumbai – 400 085, India*
[2]*Homi Bhabha National Institute, Anushaktinagar, Mumbai – 400 094, India*
[§] Email: skumars@barc.gov.in

Zeolitic Imidazolate Framework (ZIF) are porous crystalline materials with tetrahedral networks that resemble those of zeolites [1]. Due to high thermo-chemical stability andporosity, ZIFs have many applications in gas storageand separation [2].The gas separation efficiency is limited due to the flexibility of theirframeworks leading to diffusion of larger size molecules under applied pressure through the pore network.This phenomenon is termed as '*gate-opening*'. Understanding the flexibility of ZIFs at microscopic level is of significant interest because it can explain the various novel properties of ZIFs.

Positron annihilation lifetime spectroscopy (PALS) has been shown to be highly efficient in probing defects, pore architecture during gas sorption in microporous coordination polymers (MCPs) and CO_2 exposed zeolites.In the present study, *in-situ* PALS measurements under different gas pressures have been carried out to investigate the gas pressure induced modifications in pore architecture and flexibility of mixed metal (Co/Zn) ZIF-8.

Mixed metal ZIF($Zn_{0.4}Co_{0.6}$-ZIF-8) has been synthesized using metal precursor and respective ligands at room temperature. The phase purity, chemical bonding and morphology of theframework have been characterized using XRD, FTIR and SEM.

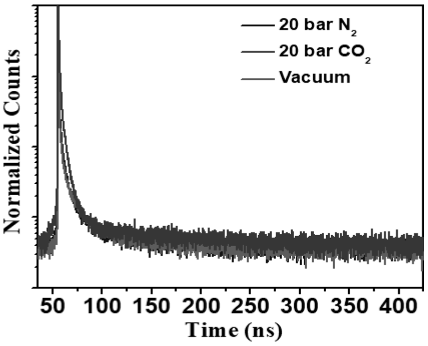

Fig. 1: Typical PALS spectra for $Zn_{0.4}Co_{0.6}$-ZIF-8 in vacuum (~10^{-3} mbar) andunder 20 bar pressure of CO_2&N_2.

Upon applying CO_2, $N_2$and Ar pressures, differences in PALS spectra (Fig. 1) of $Zn_{0.4}Co_{0.6}$-ZIF-8w.r.t. its vacuum state show the changes in its pore architecture. Gas pressure dependent *ortho*-positronium (*o*-Ps) annihilation parameters confirm that flexibility as well as pore architecture of the studied ZIF depends on the gas-framework interaction. The present study also confirms that *o*-Ps is an efficient probe to investigate the pore site specific open volume evolution during gas adsorptions in ZIFs having non-uniform pore network, which is required for complete understanding of '*gate-opening*' phenomenon in flexible ZIFs at microscopic level.

References:
[1] K.S. Park et.al., *Proc. Nat. Acad.Sci.*, U.S.A. **103** (2006) 10186.
[2] B. Chen et.al., *J. Mater. Chem. A*, **2** (2014) 16811.
[3] J. Hou.et.al.,*Angew. Chem., Int. Ed.*, **55** (2016) 3947.

Investigation of Pore Architecture in Bimetallic ZeoliticImidazolate Framework– Using Variable Energy Positron Spectroscopy (VEPS)

R.B. Nelliyil[1, 2], S.K. Sharma[1, 2 §]

[1]Homi Bhabha National Institute, Mumbai – 400 094, India
[2]Radiochemistry Division, Bhabha Atomic Research Centre, Mumbai – 400 085, India
[§] Email: skumars@barc.gov.in

Zeoliticimidazolate frameworks (ZIFs) are a class of nanoporous crystalline metal−organic frameworks (MOFs) having zeolitictopology [1]. ZIFs have gained significant attention in various fields like gas separation and gas storage because of their rich structural and topological varieties due to flexibility in the choice of metals and bridging ligands along with properties such as tunable porosity, structural flexibility, high thermal, mechanical, and chemical stability. In case of gas separation, ZIFs based membranes are found to be more energy efficient than the conventional processes currently used in the industries [2]. ZIF-8 and ZIF-67 membranes assembled from Zn^{2+} and Co^{2+} with the 2- methylimidazole (2-mIm) organic linker respectively with the same sodalite topology are extensively studied for their gas separation capabilities.The unsatisfactory separation performance observes in case of ZIF-67 and ZIF-8membranes arises from the poor grain boundary structure andframework flexibility respectively [3].So to obtain the optimal separation performance, the perfect balance between the grain boundary structure and the framework flexibility is necessary which can be achieved by the slow crystallization kinetics of ZIF-8,results inbetter grain boundary structureand flexibility reduction by incorporation of Co^{2+} in ZIF-8 framework result in more rigid structure because of the strong Co-N bond [3].

To exploit this concept, we prepared a series of Bimetallic ZIFfilmsZn$_{(100-x)}$ Co$_x$ (x is the molar percentage of Co in the films)in one step fast current driven synthesis (FCDS) method by introducing Zn^{2+}andCo^{2+} into the 2-mIm solution. The phase purity and chemical bonding of the bimetallic ZIF films have been established using XRD and FTIR spectroscopy. Mixed metal ZIF films studied using Variable energy positron spectroscopy(Fig 1.) confirms the modifications in pore interconnectivity and crystal packing as compared to single metal films (ZIF-8 and ZIF-67). Changes in the S-parameter confirms that grain boundary structure is significantly improved in case of bimetallic films.

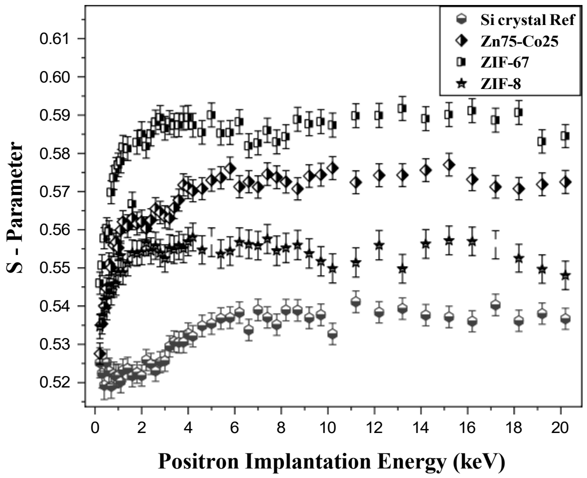

Fig.-1 S-parameter as a function of positron implantation energy for Bimetallic ZIF layer deposited on silicon

References:

[1] O. M. Yaghi et al., *Nature* **402** (1999) 276-279.
[2] P. Utpalla et al., *J. Solid State Chem*. **316** (2022) 123-601.
[3] H. Wang et al., *JACS*, **142** (2020) 9582-9586.

Development of Dy^{3+} doped lithium magnesium borate glass system for thermoluminescence based neutron dosimetry applications

Meghnath Sen[1,5,§], R. Shukla[2], R. K. Mishra[3], N. Pathak[4], V. Sathian[1], P. Chaudhury[1], A. K. Tyagi[2,5]

[1]*Radiation Safety Systems Division;* [2]*Chemistry Division;* [3]*Waste Management Division;*
[4]*Radio Chemistry Division, Bhabha Atomic Research Centre, Mumbai, 400085*
[5]*Homi Bhabha National Institute, Anushakti Nagar, Mumbai 400094*
[§] Email: meghms@barc.gov.in; Phone 022-2559-0948

In the field of nuclear power plants and related installations, personnel dosimetry specifically for neutron radiation is extremely important because of its higher Relative Biological Effectiveness (RBE) as compared to beta and gamma radiations. Currently, personnel neutron dosimetry is carried out using SSNTD based imported CR-39 detector which is mainly sensitive for fast neutrons (>100 KeV). Neutron sensitive thermoluminescence (TL) based materials have great potential to provide dosimetric response for slow neutrons (<100 KeV) [1,2]. However, number of reported articles in this field is significantly less. In view of the above, the present paper reports the development of Dy^{3+} doped lithium magnesium borate (LMB) glass as a slow neutron sensitive TL material for dosimetry applications.

The synthesis of the LMB: Dy^{3+} glass was carried out by melt quenching technique where the starting chemicals used were lithium carbonate (Li_2CO_3, 99.99%, sigma aldrich), magnesium oxide (MgO, ≥99%, sigma aldrich), boric acid (H_3BO_3, AR grade) and dysprosium oxide (Dy_2O_3, 99.9%), respectively. X-ray Diffraction (XRD) pattern as depicted in **Fig. 1a** showed the presence of two broad humps instead of sharp peaks which confirmed the amorphous nature the synthesized materials. Fig. 1b depicts the photoluminescence (PL) spectra which clearly exhibits three well resolved peaks situating at 482, 578 and 666 nm corresponding to the $^4F_{9/2} \rightarrow {}^6H_{15/2}$, $^4F_{9/2} \rightarrow {}^6H_{13/2}$ and $^4F_{9/2} \rightarrow {}^6H_{11/2}$ transitions, respectively. These characteristic peaks confirmed the presence of Dy^{3+}. In order to characterize the TL response, the material was irradiated (dose equivalent ~20 mSv) with thermal neutrons using the Standard Thermal Assembly in Graphite facility, a primary standard for thermal neutron fluence rate present at RSSD, BARC [3]. Fig. 1c depicts the observed TL glow curve pattern of the developed LMB: Dy^{3+} glass where a single peak (maxima lies at ~452 K) was observed which is highly desirable for dosimetry applications.

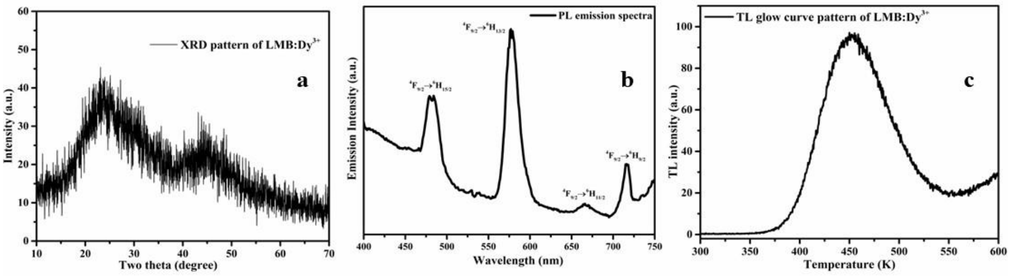

Fig. 1 (a) XRD pattern (b) PL spectra and (c) neutron irradiated TL glow curve of LMB: Dy^{3+} glass

Acknowledgements: The author expresses sincere thanks to Dr. D. K. Aswal, Director, HS&EG for his constant support and motivation for carrying out the research works.

References:
[1] M. Sen et al., *Ceram. Int.*, 46 (2020) 20236.
[2] M. Sen et al., *Mater. Adv.*, 2 (2021) 3405.
[3] A. Kannan et al., *BARC external report*, BARCBARC/I992/E/O48.

Studies on vitrification of cerium oxide in sodium iron phosphate glass

A.V.Vinod[1,2], R.Jayashree[1], Ashish jain[§1,2] and Kitheri Joseph

[1]*MFRG, Materials Chemistry and Metal fuel Cycle Group, Kalpakkam, India*
[2]*HomiBhabha National Institute, Anushaktinagar, Mumbai 400094, India*
[§] Email: ashish@igcar.gov.in

Homogeneoussodium iron phosphate glass (NaIPG) doped with cerium oxide (100-x)NaIPG -xCeO_2 (x=2.5mole%) was prepared by melt quench method. The crystallographic nature, thermophysical properties were studied using x-ray diffraction (XRD), differential thermal analysis (DTA) and by dilatometry. The change in structural connectivity in the CeO_2 doped glass was analyzed using Raman spectroscopy and compared with that of undoped Iron Phosphate Glass. Iron phosphate glass (IPG) is developed as an alternate host matrix for vitrification of high levelwaste. IPG with nominal composition of Fe/P=0.67 is widely studied owing to its excellent chemical durability. In case of NaIPG, the presence of Na_2O increases the basicity of the glass and increases the Fe^{3+}/Fe ratio, a desirable property in IPG. It is proposed to immobilize nuclear waste rich in lanthanides into the NaIPG matrix. Accordingly, the present study describes the immobilization of CeO_2 in NaIPG and its characterization.

Experimental

The composition of NaIPG is fixed by maintaining the ratio of Fe/P=0.67. The glass with compositions (100-x)NaIPG-xCeO_2 (x=2.5mole %) (henceforth labelled as NaIPGCe)was prepared from the precursor salts, calcined at 873K and melted and air quenched at 1423K into a graphite mould. The quenched solid was characterized for crystallographic nature, thermal expansion and glass transition temperature (T_g) utilizing XRD, push rod dilatometry and differential thermal analyser respectively. Raman spectroscopy (range:400 to 2000 cm^{-1}) was used to evaluate the network connectivity of NaIPGCe and compared with that of undoped IPG.

Results and discussion

Non-crystalline nature (inset of Fig. 1) of the quenched sample was confirmed by XRD technique. The T_g of NaIPGCewas776 K compared to the reported value of 783 K forUn-doped IPG. Although addition of $CeO_2$is expected to increase the T_g, presence of Na_2O surpasses the effect of CeO_2leading to reduction in T_g compared to undoped IPG. This is due to increase in NBO (Non-bridging oxygen). Thermal expansion of NaIPGCe is higher than that of undoped IPG (Fig. 1) indicating the effect of presence of alkali oxide, i.e., Na_2O. The Raman spectrum (Fig. 2) shows the presence of pyro (Q^1), meta (Q^2) and ortho (Q^0) linkages in the glass networksimilar to that of undoped IPG. However, the redshift of the various bands clearly indicates the effect of reduction of network connectivity due to the presence of modifier (Na_2O). However, the primary glass network units are of Q^1type, indicating the major linkages in NaIPGCe as pyro phosphate linkage.

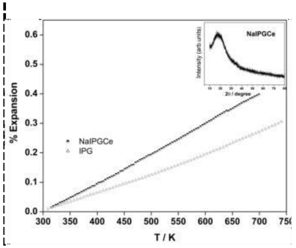

Fig 1 Thermal expansion of IPG and NaIPGCe, inset XRD of NaIPGCe

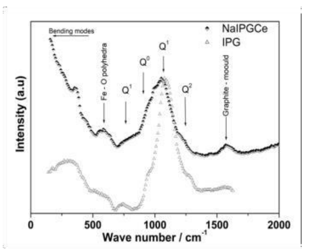

Fig.2 Raman spectra of IPG and NaIPGCe

Conclusion

Based on the available data on NaIPGCe, NaIPG can be considered as a promising matrix for the immobilization of waste rich in lanthanide, i.e., CeO_2. Effect of doping on the chemical durability and specific heat of NaIPGCe are under progress.

Electrodeposition of Palladium Nanoparticles from a Deep Eutectic Solvent and its Application to Uranyl Electrocatalysis and Sensing

Arkaprava Layek, Sushil Patil, Kavitha Jayachandran and Ruma Gupta[§]

Fuel Chemistry Division, Bhabha Atomic Research Centre, Mumbai 400094
[§] Email: rumac@barc.gov.in

Chemical and electrochemical methods have been reported to synthesize the metal nanoparticles. The chemical methods are generally time-consuming, multistep processes that require the use of both reducing agents and stabilizing molecules. In contrast, the electrochemical methods allow the nanostructures to be grown directly onto the final support in just one step, without the need for reducing and stabilizing agents or further sample preparation, thereby improving the electron pathway within the substrate, nanostructure and environment. Deep eutectic solvents (DESs) are a new generation of green solvents and have wide applications in nanoparticle synthesis, electrochemistry, and biochemistry owing to their remarkable physicochemical properties different from ionic liquids [1]. We electrochemically synthesized palladium nanoparticles (PdNPs) utilizing a Pd salt on a gold (Au) electrode from a deep eutectic solvent formed by mixing choline chloride and urea at room temperature. PdNPs has emerged as an effective surface modifier for working electrodes in electrocatalysis and electroanalysis. However, the aqueous electrochemistry of the actinides on PdNPs is still unexplored. In this work, the aqueous electrochemistry of the redox couple $[U^{VI}O_2(CO_3)_3]^{4-}$/$[U^{V}O_2(CO_3)_3]^{5-}$ was systematically investigated on a PdNPs/Au electrode in saturated Na_2CO_3 solution. It is known that the aqueous solution of UO_2^+ is very unstable as U(V) disproportionates to U(VI) and U(IV). The disproportionation reaction is catalyzed in the presence of acids. The carbonate forms a strong complex with uranium in the alkaline solution and thus stabilizes U(V) in aqueous solution. Due to long-term transport in the geosphere, CO_3^{2-} is abundant in groundwater. Therefore, it would be of interest to develop an efficient electrochemical sensor to detect uranium carbonate complexes migrating through the environment. In this direction, we have studied the electrochemistry of the U(VI)/U(V) redox couple on PdNPs in saturated Na_2CO_3 solution. The results showed that PdNPs can catalyze the redox chemistry of the U(VI)/U(V) redox couple by reducing both cathodic and anodic overpotentials upto 50 mVcompared to a bare Au electrode.

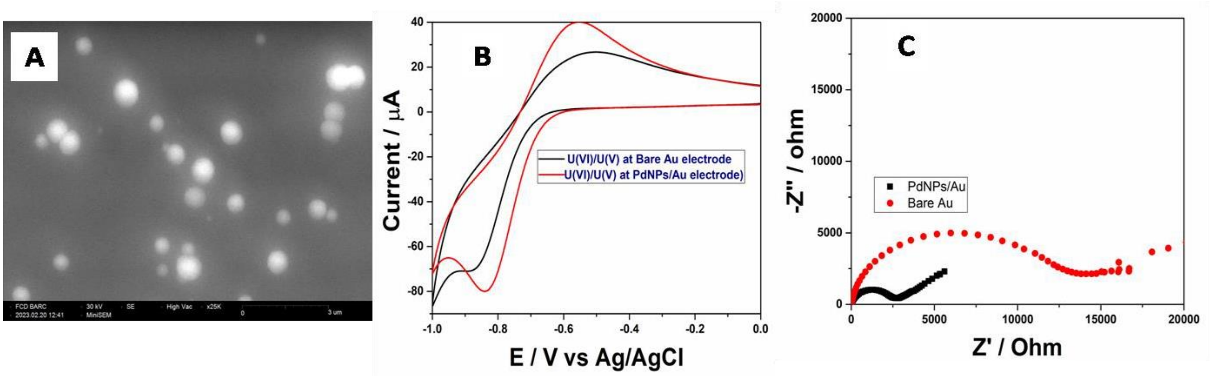

Fig. 1: (A) SEM image of Pd NPs (B) CV of uranyl system at bare and PdNPs/Au electrode (C) Nyquist plot at bare and PdNPs/Au electrode in uranyl carbonate solution.

References:
[1]Gupta, R.; Vats, B.; Pandey, A. K.; Sharma, M. K.; Sahu, P.; Yadav, A. K.; Ali, S. M.; Kannan, S. *J. Phy.Chem. 2020, 124, 181-189.*

Measurement of fast neutron induced (n,γ) reaction cross-section of ^{68}Zn in the energy range of 0.8 to 2 MeV

N. S. Tawade[1,4§], S. Kumar[1], S. Patra[1,4], R. Tripathi[1,4], C. S. Datrik[2], P. K. Pujari[1,4]
R. G. Thomas[3,4], G. Mishra[3,4], A. Kumar[3], S. De[3,4] and H. Kumawat[3,4]

[1]Radiochemistry Division, [2]Product Development Division, [3]Nuclear Physics Division,
Bhabha Atomic Research Centre, Mumbai - 400085, INDIA
[4]Homi Bhabha National Institute, Anushaktinagar, Mumbai-400094, INDIA
[§] Email: nstawade@barc.gov.in

In the conventional reactor systems such as pressurized water reactors, Zn is used to inject in primary system, worldwide, to avoid activity deposition in coolant channels resulting in dose build-up [1]. It may also find applications in advanced nuclear reactors based on fast neutrons for which neutron energy peaks in the energy region of ~1-2 MeV for which very limited data is available on (n,γ) reaction cross-section. Further, it is important to measure more and more data for fast neutron induced reactions to better constrain the parameters of theoretical models as well as to improve the nuclear data evaluation. In the present study, the (n,γ) reaction cross-section for the element ^{68}Zn was measured by neutron activation technique in the neutron energy region of ~0.8 to 2.0 MeV A newly established natural strontium (^{nat}Sr) neutron flux monitor [2] was used by considering effective combined reaction cross-section for ^{86}Sr(n,γ)^{87}Sr^{m} and ^{87}Sr(n,n')^{87}Sr^{m} reactions. The theoretical (n,γ) reaction cross-sections were calculated using TALYS 1.8.

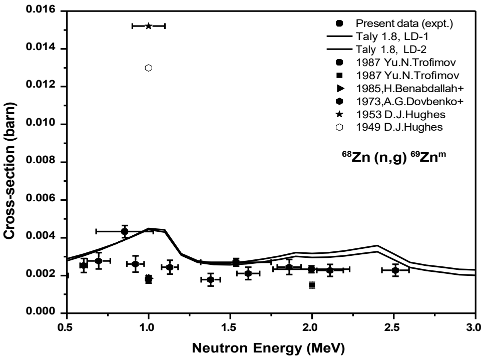

Fig. 1:Plot of cross-sections Vs neutron energy for^{68}Zn(n,γ)^{69}Zn^{m} reaction

Thus, (n,γ) reaction cross-section of Zn element is important in calculation of the activity build up due to this element, during reactor running time. The available data in literature based on the previous measurements by different groups were carried out using GM counter, NaI(Tl) detector and proportional counter. In the present study, high resolution gamma-ray spectrometry using high purity germanium [HPGe] detector has been used to measure the activity.

The pellets of mixture of sample and monitor were irradiated by quasi-mono energetic fast neutron beam, generated by ^{7}Li(p,n)^{7}Be reaction at FOTIA, Bhabha Atomic Research Centre, Mumbai, India. The activity of activation products was measured by off-line gamma ray spectrometry.An in-houseMonte-Carlo code was used to simulate neutron energy spectrum corresponding to proton energy. The measured cross-sections at three neutron energies have been plotted in Fig.1. The uncertainty in the cross-section data has been measured using covariance matrix calculation.The present data with improved uncertainty and covariance analysis enhances the cross-section data base for better constraining the evaluated data and theoretical models.

Acknowledgements: Authors thank the staff of FOTIA, BARC, Mumbai, India.

References:

[1] D. H. Hur, Kyeong-Su Kim, Hee-Sang Shim, J. Choi and K. M. Song, Materials, **13** (2020), 4317.
[2] N.S. Tawade, R. Tripathi, et.al, *15th DAE BRNS Symposium NUCAR-2021,*Mumbai,(2022)40.

Activation cross sections of alpha induced reactions on ^{103}Rh up to 40 MeV

Sk Wasim Raja[1,3§], R. Acharya[2,3]

[1] *RCD (BARC), Variable Energy Cyclotron Centre, Kolkata-700064, India*
[2] *Radiochemistry Division, Bhabha Atomic Research Centre, Mumbai-400085, India*
[3] *Homi Bhabha National Institute, Anushaktinagar, Mumbai-400094, India*
[§]Email: sw.raja@vecc.gov.in

Activation cross sections of ^{103}Rh(α,xn)$^{107-n}$Ag (n=1-4) were measured from their respective threshold up to 40 MeV using alpha beams from RT cyclotron at VECC, Kolkata. The produced radioisotopes have importance in medicine and technology [1]. The experimentally measured cross section data are useful for optimized production of the radioisotopes of interest, understanding nuclear reaction mechanisms and to test nuclear reaction model codes.

Standard stacked foil irradiation followed by measurement of gamma activity using HPGe detector based high resolution gamma ray spectrometry has been performed [2]. Two stacked foils each consisting of four natural Rh targets (thickness 6 µm) were irradiated for 40 minutes with initial alpha beams of energies 28 and 40 MeV, respectively and beam current ~100 nA. Natural Cu foils (15 µm thickness) were used to monitor the beam intensity. After each target, one Al (18 µm thick) catcher foil was kept. After the irradiation, each target foil along with the catcher foil were individually separated and counted using 50% HPGe detector after providing sufficient cooling time. Energy on the target foils in the stack was calculated using SRIM 2013.

^{106m}Ag ($T_{1/2}$ = 8.5 d), ^{105g}Ag ($T_{1/2}$ = 41.2 d) ^{104g}Ag ($T_{1/2}$ = 69.2 minutes), ^{103g}Ag ($T_{1/2}$ = 1.1 h), ^{102g}Rh ($T_{1/2}$ = 206 d), ^{101m}Rh ($T_{1/2}$ = 4.34 d) and ^{100}Rh ($T_{1/2}$ = 20.8 h) radionuclides were identified in the measured spectra. Cross sections were calculated using standard activation equation [3] from the measured peak area. Each target was measured several times and interference free high intensity gamma rays were used for cross section calculation. Thick target yield of the medicinally important radioisotopes will be calculated from the measured cross section data and stopping power of natural Rh using SRIM 2013. The obtained results will be compared with the available literature data, theoretical data from TENDL-2021 nuclear data library as well as using theoretical code TALYS-1.96.

Acknowledgements: Dr. S. Kannan, Director, RC&IG, BARC and Dr. P. K. Mohapatra, Head, RCD, BARC are acknowledged for their constant support for this work. VECC RT cyclotron operation crew are acknowledged for their help during the irradiation. We thank our colleagues at RCD, VECC for their help during the experiment.

References:
[1] M. S. Gadkari and N. L. Singh, *Pramana-J of Phys*, **62(5)** (2004) 1059.
[2] Sk Wasim Raja, S. Dey Chaudhuri, D. Banerjee, R. Acharya and P. K. Pujari, *Nucl. Phys. A,* **1015** (2021) 122309.
[3] S.W. Raja, R. Acharya and S. Dey Chaudhuri, *Eur. Phy. J. A*, **58** (2022) 259.

Study of fission product mass distributions in ^{12}C+^{232}Th reaction to investigate the role of shell closure

Satyam Kumar[1,§], Sabyasachi Patra[1], Amol Mhatre, Ashwani Kumar[1], K. Ramachandran[2]
and Rahul Tripathi[1,3]

[1] *Radiochemistry Division, Bhabha Atomic Research Centre, Mumbai – 400 085, India*
[2] *Nuclear Physics Division, Bhabha Atomic Research Centre, Mumbai – 400 085, India*
[3] *Homi Bhabha National Institute, Mumbai – 400 094, India*
§ Email: ksatyam@barc.gov.in

The investigation of the role of neutron and proton shell closure as well as the effect of excitation energy in governing the fission process have gained significant attention in the recent past in view of the observation of the dominant role of proton shells [1]. The availability of the GEF code which attributes asymmetry in the mass distribution in the actinide region to proton shells Z~52 and 55 [2], can help to investigate the role of shell closure by comparing the experimental and theoretical results on the mass distribution. Measurement of mass distribution of ^{12}C+^{232}Th reaction by Manohar *et al.* at beam energy of 79 MeV showed a symmetric mass distribution [3] while that by Ramaswami *et al.* at beam energy of 72 MeV showed a significant deviation from symmetry, though the mass distribution was fitted to a single Gaussian assuming symmetric fission [4]. In the present study, experiment was carried at BARC-TIFR Pelletron-LINAC facility using recoil catcher technique followed by offline gamma-ray spectrometry to measure fission product yields in ^{12}C+^{232}Th reaction in order to investigate the contribution from symmetric and asymmetric fission. The ^{232}Th target (~2 mg/cm^2) was placed between two Al catcher foils (~6.75 mg/cm^2) and irradiated with ^{12}C beam of 80 MeV energy (~22 hours). The actual beam energy at the target, as estimated by comparing the measured fission cross section data with the literature [5], was 63.8 MeV and was within 2% of that calculated by the beam energy loss in backward catcher foil using the code SRIM [6]. The gamma-ray activity of the fission products was used to obtain their yields which were subsequently corrected for the charge distribution to obtain mass yields. As seen from Fig. 1, the obtained mass yield distribution is flat-top having significant asymmetric fission contribution (mainly from S2 mode corresponding to Z~55) as evident form comparison with GEF calculations. A systematic study of the contribution from different fission modes along with comparison with GEF calculations for different fissioning systems will help in connecting the role of various shells in different mass regions and will also confirm the dominance of proton shells.

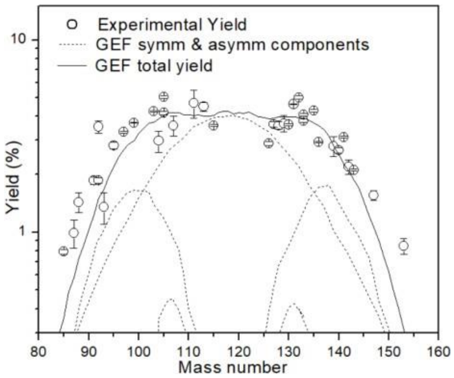

Fig. 1: Mass yield distribution curve of ^{12}C+^{232}Th reaction at E_{lab} = 63.8 MeV.

References:
[1] G. Scamps et al., Nature, **564** (2018) 382.
[2] K.-H. Schmidt et al., Nucl. Data Sheets **131**, (2016) 107.
[3] S. B. Manohar et al., Radiochim. Acta., **56** (1992) 69.
[4] A. Ramaswami et al., J. Radioanal. Nucl. Chem., **246** (2000) 225.
[5] A. Karnik et al., Z. Phys. A., **351** (1995) 195.
[6] J.F. Ziegler et al., TRIM code, SRIM-2013.

Positron Annihilation Spectroscopic Study of vacancy defects in aliovalent ion doped CeO_2 for technological applications

D. Das[1,2], A. Bandyopadhyay[2] , S.K. Gupta[1,2] and K. Sudarshan[1,2, §]

[1] *Radiochemistry Division, Bhabha Atomic Research Centre, Mumbai, India*
[2] *Homi Bhabha National Institute, Ansuhaktinagar, Mumbai, India*
[§] Email: kathis@barc.gov.in

Defect engineering in CeO_2 has received paramount attention of the researchers by virtue of its diverse technological applications encompassing the areas like catalysis, sensors, energy storage, optoelectronics etc [1, 2]. The multifunctional behavior of ceria is primarily governed by the concentration of oxygen vacancies and Ce^{3+}/Ce^{4+} ratio. In our previous studies we have extensively investigated the effect of the size of the dopants on the evolved oxygen vacancies in aliovalent ion doped ceria [3, 4]. In this present work our aim is to understand the other subtle factors apart from charge compensation influencing the evolution of vacancies keeping the total concentration of trivalent dopant ions fixed as well as to tune the lattice relaxation by the judicious choice of dopants of suitable size. In this regard, CeO_2 doped with varied relative concentrations of Sc^{3+} (smaller than Ce^{4+}) and La^{3+} (larger than Ce^{4+}) and codoped with a fixed amount of Eu^{3+} have been synthesized and Positron Annihilation Lifetime Spectroscopy (PALS) along with other complementary techniques were employed to investigate the evolution of defect.

The ceria samples were synthesized by gel-combustion route, followed by calcinations at 500 °C and annealing at 800 °C for four hours and the annealed samples were characterized by powder XRD technique. The crystallite size along with lattice strain was determined from the acquired XRD patterns using Williamson-Hall approach. Rietveld refinement analysis of the patterns was further carried to quantify the changes in the lattice parameters of the doped samples. PALS results showed creation of more oxygen vacancy with higher La fraction as reflected from the variation of the shorter lifetime component τ_1. Photoluminescence (PL) measurements were carried out to get complementary information about the distribution of the vacancies around the dopants using the hypersensitive EDT transition of Eu^{3+} as a probe. Further studies are planned to correlate the effect of the evolved oxygen vacancies as well as their distribution with the catalytic activity of the material.

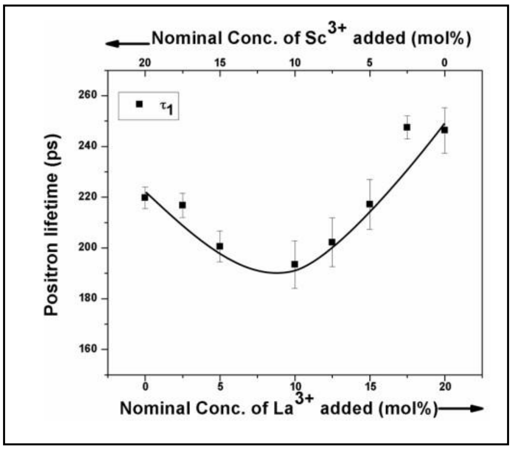

Fig. 1: Variation of positron lifetime component τ_1 with the relative conc. of the dopants. The line shown is eye guide only.

References:
[1] H.J. Kim et al., *ACS Catal.* **10, 24** (2020) 14877.
[2] L. Ma et al., *Appl. Mater. Today*., **22** (2021)100946.
[3] D. Das et al., *Dalton Trans.*, **50** (2021) 17378.
[4] D. Das et al., *Dalton Trans.*, **51** (2022) 18572.

Understanding the Defects in NIR Emitting $SrGa_2O_4:Cr^{3+}$ using Positron Annhilation and Luminescence Spectroscopy

Manish S. Kambli[1,2], Annu Balhara,[2,3], Santosh K.Gupta[2,3], Kathi Sudarshan,[2,3§]

[1]*KJ Somaiya College of Science and Commerce, Vidyavihar, Mumbai-400086*
[2]*Radiochemistry Division, Bhabha Atomic Research Centre, Mumbai-400085*
[3]*Homi Bhabha National Institute, Anushakti Nagar, Mumbai-400094*
[§] Email: kathis@barc.gov.in

Generally, lanthanide ions are commonly regarded as main activators to engineer the luminescence properties of the commercial photo and persistent luminescent materials. On the contrary, effective 3d transition-metal ion-doped materials, especially with a near infrared emission and suitable decay time, have not been reported so far. Due to the advantages like deep penetrability of near infra-red (NIR) emissions, the phosphors emitting in this region have attracted enormous interest especially for biological imaging applications [1]. Furthermore, the sensitivity of the rare earth price to the global consumption amount greatly limits their applications. Therefore, finding an efficient and rare earth-ion-free new NIR-emitting phosphor has been an important and long-standing issue. Among the gallate compunds, $SrGa_2O_4$ attracted attention as aself-luminescing material, with the afterglow duration time of about 3 min, implying that some trap levels already existing in the host have the capability to delay the emission as well as excellent host to dopants in giving further tuning in the emission and lifetime.[2]

Thus, it is feasible to achieve the both PL and persistent luminescence (PerL) phenomenon in $SrGa_2O_4$ doped by Cr^{3+}, which is not verified, and the relevant luminescence properties have not been reported before. But as a result of aliovalent substitution of Cr^{3+} ion at Sr^{2+} site charge compensating defects are expected to be formed which will drastically affect the PL and PerL properties of the $SrGa_2O_4:Cr^{3+}$.In the present study, phase pure Cr3+ doped samples were prepared by solid state method and phase purity was confirmed by powder XRD patterns (***Figure 1***). In this compound, GaO_4 tetrahedra connect with each other through the vertex-sharing O^{2-}. The Sr^{2+} ions locate in the interstitials of GaO_4 tetrahedra with two different sites, namely eightfold- and sevenfold-coordinated Sr1 and Sr2 sites. PL spectroscopy showed emission in near infrared region endowed by due to its $^2E \rightarrow {}^4A_2$ transition in an octahedral (Oh) crystal field.. Positron annihilation lifetime (PALS) confirmed the increase in lifetime upon Cr^{3+} doping in Sr^{2+} sites. Alkali codoping for removal of charge compensating defects is attempted. The results of positron lifetimes to understand the defects and their correlation with PL will be discussed.

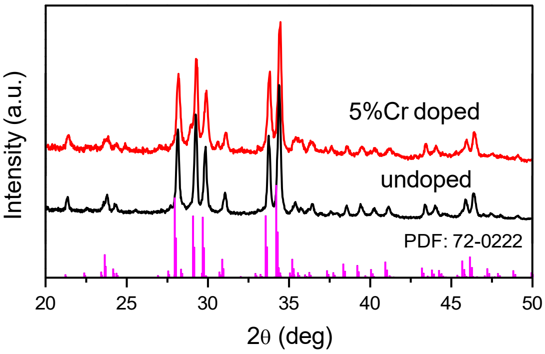

Figure 1: XRD pattern of undoped and Cr^{3+} doped $SrGa_2O_4$

References:
[1] S.K. Gupta *et al. Phys. Chem. Chem. Phys.***420** (2020)213405
[2] C. Wang*et al. Chem. Mater.,***34**(2022) 10068–10076

Synthesis, Characterization And Thermal Studies of $[CH_3NH_3]Nd(SeO_4)_2 .3H_2O$

S. K. Divekar [1, §] and S. N. Achary[2]

[1]Ramniranjan Jhunjhunwala College of Arts Science and Commerce, Ghatkopar, Mumbai, 400086, India, Mob: 9769299520 Fax No.+91 22 25150957
[2]Chemistry Division, Bhabha Atomic Research Centre, Mumbai 400085, India
[§] Email: sandesh.sarvesh@gmail.com

Abstract: Hybrid materials containing organic and inorganic moieties bear significant research attentions due to the scope to design new porous and dimension-controlled crystal structures and materials for potential for applications in separation and purification of ionic and molecular species [1,2]. Such porous three-dimensional materials can be achieved with varieties of ions including rare-earth and actinide ions as well as organic amines. The crystal structure of such materials not only depends on the nature and dimension of organic ions but also on the ionic radii of the rare earth or actinide ions. The structure and stability of the complex or hybrid compounds govern their scope of application, and hence studies have been taken up to develop new hybrid molecules using aliphatic amines, and to correlate their structure and stabilities with nature and dimension of organic amines. Herein we describe the crystal structure and thermal stabilities of a hydrated double selenate of monomethylammonium and rare earth ion as $[CH_3NH_3]Nd(SeO_4)_2.3H_2O$. The crystal structure of was obtained from single crystal X-ray diffraction and revealed a monoclinic lattice ($P2_1$) with unit cell parameters as: a = 6.7624(4) Å, b = 8.7727(6) Å, c = 9.7265(6) Å and β = 95.421(2)°, V = 574.44(6) Å^3, Z = 2. The structure is built as 3-D architecture with channel structures from NdO_9 and SeO_4 units. Typical connections of these units are shown in Figure 1. Each NdO_9 polyhedron is connected to four selenate tetrahedra sharing total six oxygen atoms (two edge and two corners) and that extends to a three-dimensional architecture. The compound decomposes sequentially by losing water, SeO_2 and organic components leaving oxides of rare-earth ions.

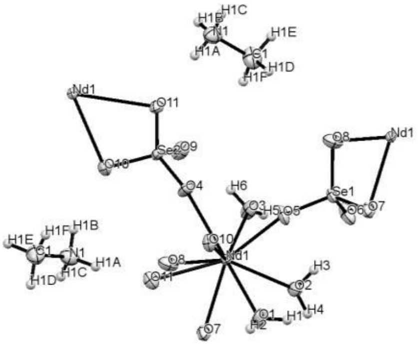

Figure [1] Schematic of 3D Nd-selenate architecture incorporating $[CH_3NH_3]^+$

Acknowledgements: Dr. Sandesh Krishnakant Divekar is thankful to Ramnirnajan Jhunjhunwala College for providing the financial assistance and supporting this work through the seed grant project (Ref: 887 dated 13th December 2021).

References:
[1] C. N. R. Rao, J. N. Behera and Meenakshi Dan, Chem. Soc. Rev., 35 (2006) 375.
[2] N. Budantseva, G. Andreev, M. Sokolova and A. Fedoseev, *Inorg. Chem.*, **60** (2021) 18406.

Investigating the local structure of silver in different chemical environments using TDPAC spectroscopy

Ashwani Kumar[§], Sabyasachi Patra, Satyam kumar, Rahul Tripathi

Radiochemistry division, BARC, Mumbai-400085
[§] Email: kashwani@barc.gov.in

Nanomaterials have been the topic of notable research for various applications due to its different properties than exhibited by bulk materials. To find suitable structure-property correlations of different nanostructures, understanding their local electronic structure is important. Time differential perturbed angular correlation (TDPAC) is a potential spectroscopic technique used to investigate the local structures of different materials [1].

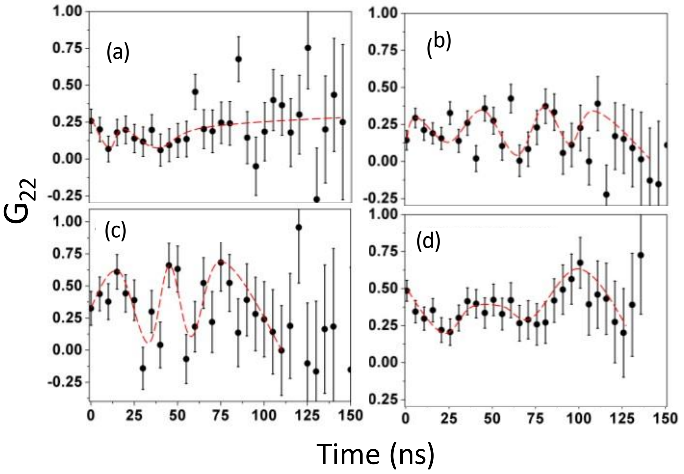

Fig. 1. TDPAC spectra of Ag^+ ions in Nafion (a), after reduction with citrate in Nafion (b), after reduction with $NaBH_4$ in Nafion (c) and Ag^+ ions reduced with $NaBH_4$ in bulk (d). The red dashed lines are eye guide only.

In this work, the local structure of silver, hosted in Nafion-117 membrane as Ag^+ ions and after *in-situ* chemical reduction with $NaBH_4$ and tri-sodium citrate [2] was studied using ^{111}Ag ($t_{1/2}$ = 7.5 d) as TDPAC probe and compared with the BH_4^- reduced silver precipitate at bulk. The ^{111}Ag probe was prepared by nuclear reaction: $^{110}Pd(n, \gamma)^{111}Pd(\beta^-)^{111}Ag$ by irradiating ^{nat}Pd metal powder at Dhruva reactor. Separation of ^{111}Ag from the irradiated ^{nat}Pd was carried out following the protocol of Khalid *et. al.* [3]. TDPAC spectra of the as prepared samples were acquired to investigate the change in local structure of silver as ions and in the reduced Ag^0 form in Nafion-117 membrane (see Fig. 1). It can be seen that, the TDPAC response of silver in Nafion-117 membrane before and after chemical reduction is noticeably different. The amplitude of oscillations in case of the reduced silver (Fig. 1b & c) is higher compared to Ag^+ ions (Fig. 1a), suggesting the formation of silver nanoparticles in the membrane as a result of chemical reduction. The amplitude is highest in case of the BH_4^- reduced sample, suggesting smaller particle size in case of the BH_4^- reduction compared to the citrate reduction. The presence of oscillations in the TDPAC response of the BH_4^- reduced silver in bulk (Fig. 1d) points to the formation of nano-silver even in absence of Nafion, suggesting the role of BH_4^- ions as capping agent in addition to its reducing properties. The lesser oscillation amplitude suggests larger NPs compared to that in Nafion. The results of the present study open up the possibility of using *in-situ* TDPAC spectroscopy to explore the structure-property relations of nanomaterials.

Acknowledgement: Authors are thankful to Dr. A. Mhatre for his support during the work.

References:

1. J. Schell et. al. Crystals 9 (2011), 611
2. S. Patra et. al. Langmuir 30:9 (2014), 2460.
3. M. Khalid et. al. Appl. Rad. Isot. 52:1 (2000), 19.

Process intensification and optimization for sonocrystallisation of uranium peroxide

Shrishma Paik[1,3], S K Satpati[1,3], D K Singh[2,3]

[1]Uranium Extraction Division, Materials Group, Bhabha Atomic Research Centre
[2]MP&CED, Materials Group, Bhabha Atomic Research Centre
[3]Homi Bhabha National Institute (HBNI), Anushakti Nagar, Mumbai 400 094, India
Email: shrishma@barc.gov.in

Ultrasonic processing is an emerging technology which has been generally shown to improve the crystallization process of a number of chemical compounds, mainly improving control over the crystal properties and recovery. Application of ultrasound or sonochemical technique is one of the techniques which can intensify the crystallization event to a large extent by the impact of its cavitational process imparting micromixing, enhanced mass transfer and the effect of additional spontaneous nucleation [1, 2]. Here, study was carried out for establishing important process parameters namely uranium conc. and temperature for ultrasonic precipitation compared to conventional methods in laboratory scale with a ultrasound horn at 35 KHz. Uranyl nitrate with 30% hydrogen peroxide was used for the reaction in 1 litre scale. No appreciable differences in the phases have been found from the XRD study. However, a more homogeneous, regular and smooth crystalline appearance is observed in sonochemical precipitation route compared to conventional route under SEM study at 100 g/L uranium with 60◦C temperature. The crystal shape is rhombohedra with a spherical aggregation in comparison to needle shaped crystals in conventional route. Significant improvement is also seen in specific surface area and tap density of the prepared powder in sononchemical route. The powders obtained from this novel technique are having recovery more than 99.9% w.r.t. uranium. The purity of the synthesized powder also meets the specification of nuclear grade quality. Overall, the sonochemical method of precipitation of uranium peroxide is a fast, simple, convenient and intensifying technique imparting appreciable morphology and physical characteristics over the conventional precipitation process.

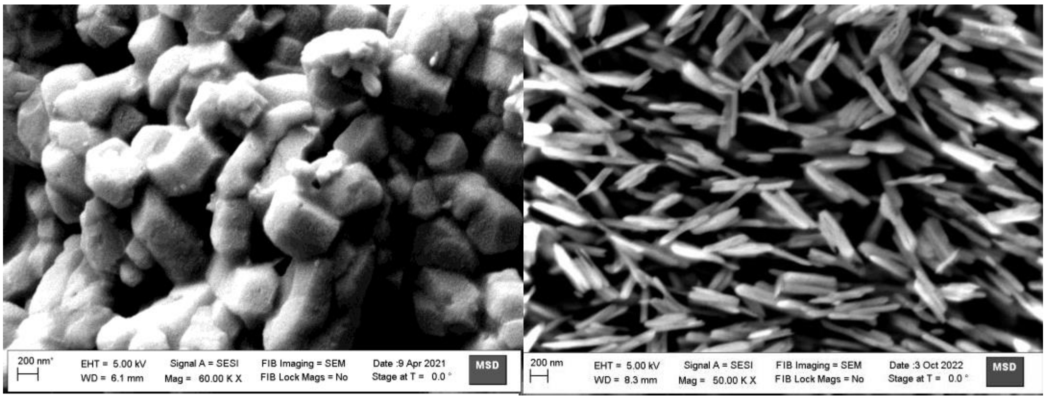

Fig 1: SEM pictures of Uranium peroxide in sonochemical(left) and conventional route(right)

References

1. Ruecroft, G., Hipkiss, D., Ly, T., Maxted, N., Cains, P.W., 2005. Sonocrystallization: The use of ultrasound for improved industrial crystallization. Org. Process Res. Dev. 9, 923–932.
2. Li, Hong, Li, Hairong, Guo, Z., Liu, Y., 2006. The application of power ultrasound to reaction crystallization. Ultrason. Sonochem. 13, 359–363.

Deep Eutectic Solvent based strippable thin films for decontamination of radioactive surface

Sushil M Patil[1,3], Dibakar Goswami[2,3] and Ruma Gupta[§1,3]

1Fuel Chemistry Division, [2]BioOrganic Division, Bhabha Atomic Research Centre, Trombay,
Mumbai-400085, India,
3Homi Bhabha National Institute, Mumbai 400094, India
[§] Email: rumac@barc.gov.in, 25590642

Deep eutectic solvents (DES) are constantly finding applications in a variety of fields such as analytical chemistry, electrochemistry, metal oxide dissolution, catalysis, carbon dioxide absorption, separation science and other synthetic chemistry over the past decade due to their ionic nature and unusual solvent properties [1]. Here, we synthesized a DES based on heptyltriphenylphosphonium bromide as a hydrogen bond acceptor and decanoic acid (DA) as a hydrogen bond donor [2]. This DES showed the potential to efficiently complex highly toxic radionuclides. Therefore, we propose a thin film based on poly vinyl alcohol (PVA) gel with DES (20%) as a decontamination agent. The decontamination studies were conducted in a fume hood on a radioactive stainless steel surface having loose activity. The PVA-DES gel was brushed onto the active stainless steel surface, allowed to dry and pulled out after 24 hours. Activity was measured before and after thin film application and the results are tabulated below (Table 1). The results show that the peelable thin film is highly effective for decontamination of surfaces contaminated with all types of radionuclides. We believe this work is a way forward to establishing a simple and efficient method based on peelable film for applications in the nuclear and other chemical industries.

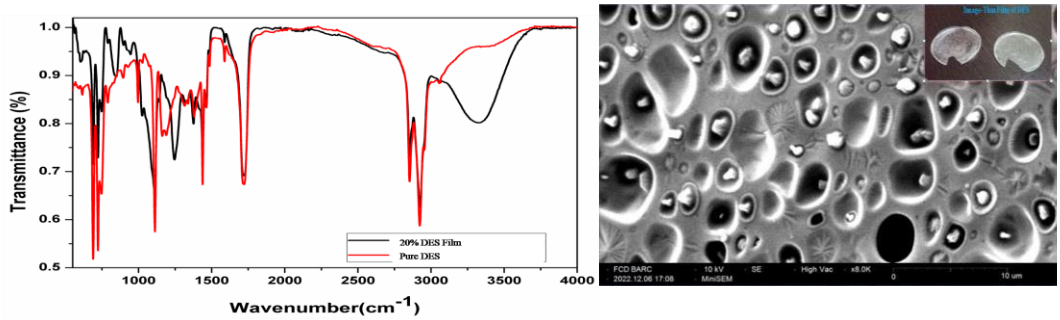

Figure 1 : a) FTIR comparison of pure DES and thin film formed b) SEM image of thin film

Active surface	Counts (cpm)		
	Before decontamination	After decontamination	% Decontamination
Stainless Steel surface 1	650	2	>99%
Stainless Steel surface 2	547	10	99%
PVC floor	766	8	99%

Table 1: Activity evaluation of different surfaces

References:
[1] Clarke, C.J. et al., *ACS Chemical reviews*, **118**(2) (2018) p. 747-800.
[2] Patil, S.M., Gupta R, *ACS Appl. Electron. Mater.*, **61**(32) (2022) p. 12599-12609.

Exploring Fluorapatites for Nuclear Waste Sequestration Applications Through Natural Analogue Study

Rumu H. Banerjee[1,§], Rajath Alexander[2], Nishant Chaudhary[3,4], Pranesh Sengupta[1,4]

[1]*Materials Science Division,* [2]*Glass and Advanced Materials Division,* [3]*Accelerator and Pulse Power Division, Bhabha Atomic Research Centre, Mumbai, India-400 085*
[4]*Homi Bhabha National Institute Mumbai, India – 400 094*
[§] Email: rumu@barc.gov.in

Development of Molten Salt Breeder Reactor (MSBR) for thorium utilization as a part of the upcoming Small Modular Reactor (SMR) initiative is being pursued by India. Materials Group, BARC has been actively involved to address the various materials-based issues associated with the MSBR-SMR based nuclear fuel cycle including studies on the long-term performance assessment of potential wasteforms to host nuclear waste. Owing to the choice of fluoride-based fuel salt and higher operating temperatures in MSR, the high-level waste generated will be significantly different from those generated in the conventional power reactors. Among the suitable alternatives, apatite class of materials [$Ca_{10}(PO_4)_6F_2$] have emerged as potential host matrices for the molten salt reactor waste management [1]. These waste forms must exhibit stability under irradiation and various physio-chemical processes in geological repository conditions for million years. The study of such long-term performance assessment cannot be studied using synthetic samples and hence natural analogue study was undertaken.

In the present study, naturally occurring fluorapatites were collected from Beldih, West Bengal. The apatites were subjected to petrographic examination after separating grains, mounting on glass slides and polishing. The petrography revealed a rim and core region in the apatite grains. Elemental analyses reveal presence of FeO, MnO, Nd_2O_3 and Pr_2O_3 in the apatite grains. The XRD patterns also match well with the fluorapatite peaks from database indicating that the rare earths and other elements are well accommodated in the lattice sites. This indicates the stability of fluorapatites over geological periods of time in retaining the rare earth/transition elements. Raman spectroscopic investigations revealed bands in the 967 cm^{-1} attributable to the symmetric stretching frequencies of (PO_4^{3-}). Furthermore, the bands located in (500–600) cm^{-1} region were ascribed to the anti-symmetric and symmetric O–P–O bending modes.

In addition, the specimens were irradiated using 10 MeV electron beam at Electron Beam Centre, Kharghar upto dose of 20 MGy. The effects of irradiation on the vibrational and structural properties of the apatites will be discussed in detail.

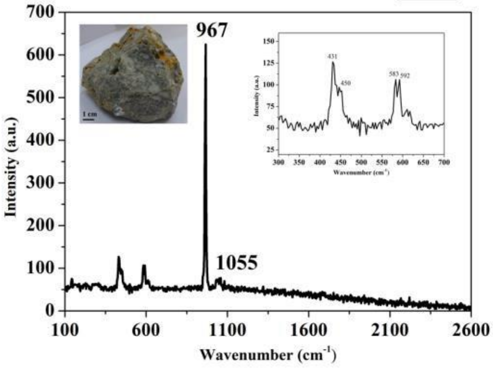

Fig. 1: Raman Analyses of Beldih Apatites.

References:

[1] Pranesh Sengupta, *Journal of Hazardous Materials*, 235–236 **(2012)** 17-28.

Nuclear waste disposal-: Pyrochlore as a potential immobilization material

Rohini Garg[§], A. K. Gulnar, Abhijit Ghosh and Ashok K. Arya

Glass and Advanced Materials Division
Bhabha Atomic Research Center, Mumbai, India, 400085
[§] Email: rohinig@barc.gov.in

India uses the policy of 'closed fuel cycle' which implies reprocessing of spent nuclear fuel thereby recycling the Uranium (U) and Plutonium (Pu) extracted from the spent fuel. Reprocessing leads to generation of highly radioactive liquid wastes (HLW) (consists of U, Pu, fission products and minor actinides) that needs to contained for periods ranging from few years to thousands of years [1]. Though, glasses have been considered as promising host materials for fixation of various radionuclides, the low solubility of minor actinides in glass matrix as well as possibility of devitrification due to self-heating by stored activity and subsequent variation in structure or microstructure pose a concern for their long duration usage. There is always a need to find new and safer materials having phases that are radiation resistant for waste disposal.

In order to develop, incorporate and thus immobilize nuclear waste, pyrochlore ($A_2B_2O_7$) structure type material has been extensively investigated as they can accommodate larger proportion of minor actinide ions owing to its cation, anion deficient fluorite structure and have higher stability under high radiation field [2]. To evaluate the role of A and B cation of pyrochlore structure ($A_2B_2O_7$) with the radiation stability a number of rare-earth based materials have been synthesized such as $Gd_2Ti_2O_7$, $Gd_2Zr_2O_7$ and $Gd_2Hf_2O_7$. These ceramic pellets have been irradiated with 75 Mev $_{35}Cl^{+7}$ ion with 60 nAmp with fluence of ~ 10^{15}ions/cm^2/sec at room temperature at Pelletron, TIFR. Their structural phase transition with irradiation was studied using XRD and Raman spectroscopy. Synchrotron diffraction (RRCAT, Indore) and Raman spectroscopy exhibits complete amorphization of Gadolinium Titanate ($Gd_2Ti_2O_7$) whereas in the case of Gadolinium Zirconate ($Gd_2Zr_2O_7$) the pyrochlore structure retains its crystallinity and transformed to a disordered fluorite structure.

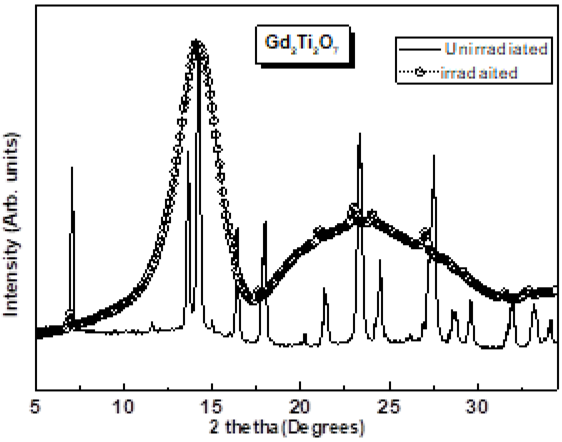

Fig. 1: XRD of unirradiated and irradiated $Gd_2Ti_2O_7$.

Acknowledgements: Authors would like to thank Shri Rajath Alexander for helping in carrying out the Raman spectroscopy for all the irradiated and unirradiated sample. The technical assistance by Shri V. Srihari for synchrotron data collection for irradiated samples is highly acknowledged.

References:
[1] P. K. Wattal, *Progress in nuclear energy* **101** (2017) 133.
[2] R. C. Ewing, W. J. Weber and J. Lian, *J. Appl. Phys.,* **95** (2004) 5949.

Integrated approach for chemical characterization of Zirconium WDF and ZrO_2 powders using ICP-OES

Y. Balaji Rao[1§], SNVMS Gupta[1], P.V. Nagendra Kumar [2], Dinesh Srivastava[1]

[1 & §] Nuclear Fuel Complex, Dept. of Atomic Energy, ECIL post, Hyderabad- 500062, India
2Asst Professor, Dept of Chemistry, GITAM University, Hyderabad-502329, India
[§] Email: ybr4793@gmail.com / ybr@nfc.gov.in

Reactor Grade Zirconium Oxide (RG-ZrO_2), which is the starting material for production of Reactor Grade Zirconium (RG Zr) metal, is being produced from Zirconium Washed and Dried Frit (Zr-WDF) powder by following the well established chemical conversion process in Nuclear Fuel Complex (NFC). Zr-WDF is obtained from zircon sand (also known as beach sands). Various grades of zirconium alloys (Zircaloys) are being manufactured from RG-Zr metal after the addition of specified quantities of alloying elements. Zircaloys are being used as structural materials in PHWRs and BWRs. In the above chemical conversion processes, all undesired elements including Rare Earth Elements (REEs) present in beach sands [1] find their way into process streams of RG-ZrO_2 production and further down to RG Zirconium metal and then to Zircaloys. In view of the detrimental effect of impurities on final products of Zircaloys, stringent specifications have been laid down for Zr-WDF and ZrO_2 powders to get desired quality of RG- Zr metal. Therefore, it has become mandatory to monitor different parameters like ZrO_2, Al, B, Ca, Co, Cr, Cu, Fe, Hf, Mg, Mn, Mo, Ni, Pb, Sn, Ti, V, Na, Si, REEs, sulfate on regular basis in Zr-WDF and ZrO_2 powders as part of QA/QC program. Several methods are cited in the literature for estimation of these parameters [2-4] and are being practiced for qualifying both Zr-WDF and RG-ZrO_2. It is preferred to have a single method/technique to cater to a high analytical load as seen in QC Lab attached to manufacturing industry. This development will lead to an increase in through-put and also minimizes the analytical waste generated. In view of this important requirement, a successful effort has been made to integrate the analytical methodology for the analysis of Zr-WDF and RG-ZrO_2 using Inductively Coupled Plasma Optical Emission Spectrometer (ICP-OES). The developed method has resulted in giving quick analytical feed-back to the production plants for downstream processing and reduced the waste for disposal. For the development of method, studies have been carried-out on comparison of presence of matrix on the determination of analytes, removal of matrix using different solvents, selection of interference free & sensitive wave-lengths, calibration such as internal standard & standard addition calibrations and on several instrumental parameters like RF power, plasma gas flow, nebulizer gas flow, height of viewing zone of plasma, nitrogen purging etc., and are discussed in the paper. Recovery study has been carried out for all the elements. It is seen that all the calibration curves are found to be linear with co-relation coefficient greater than 0.99. A % RSD of less than 1% obtained for Zr and less than 3% obtained for other elements.

References:

1. A.V Murali, et.al. *Geochimica et Cosmochimica Acta.* Vol. **47** pp 2047-2052; **1983**
2. T.S Krishnan; Technical note on 'Analytical Quality control in the production of nuclear grade zirconium and its alloys'; Presented in symposium on 'Recent developments in Non ferrous metals technology'; Dec 4-7, **1968**, NML, Jamshedpur;
3. Beata Zawisza, et.al. J. Anal. At. Spectrom., **2011**, **26**, 2373
4. Velmer A. Fassel, et.al. *Anal. Chem.* volume **27**, NO. 6**,** June **1955**

Development of RF GD-OES technique as an analytical tool for chemical qualification of BWR and PHWR core components

Y. Balaji Rao[1§], SNVMS Gupta[1], P.V. Nagendra Kumar[2], Dinesh Srivastava[1]

[1 & §] *Nuclear Fuel Complex, Dept. of Atomic Energy, ECIL post, Hyderabad- 500062, India*
[2]*Asst Professor, Dept of Chemistry, GITAM University, Hyderabad-502329, India*
[§] Email: ybr4793@gmail.com / ybr@nfc.gov.in

Zirconium alloys are widely used for manufacturing of various reactor core components such as fuel clad, calandria tubes etc. employed in BWRs and PHWRs due to their optimum mechanical properties, corrosion resistance to high temperature aqueous environments, low neutron absorption cross section and resistance to radiation damage [1]. Series of Zirconium alloys (also known as Zircaloys) viz; Zr-Sn, Zr-Nb; Zr-Sn-Nb have been developed for this purpose. Among them Zr-2 (Zr-1.2-1.7 %Sn, 0.07-0.2 %Fe, 0.05-0.15 %Cr, 0.03-0.08 % Ni) and Zr-4 (Zr-1.2-1.7 %Sn, 0.18-0.24 %Fe, 0.07-0.13 %Cr) are the important alloys of Zr-Sn series. In order to get the optimum behaviour of Zircaloy products under the reactor conditions, it is essential to monitor the content of alloying elements and critical impurities in the alloy as part of QA/QC program [2]. Several techniques like ICP-AES, AAS [3], and SS-OES techniques are being used for chemical characterization of Zircaloy materials. In view of limitations of these techniques, successful attempt has been made to develop an analytical method to analyse directly zircaloy solid samples for alloying elements such as Sn, Fe, Cr, Ni and impurities like Al, Cu, Mn, Mo, Nb, Si, Ti using Radio Frequency Glow Discharge Optical Emission Spectrometer (RF GD-OES). The developed RF GD-OES method plays an important role as an analytical tool in qualifying very high analytical load which includes process intermediates, final products on regular basis as seen in any laboratory attached to a manufacturing industry. Further to this, the developed method has eliminated the generation of liquid analytical waste completely, which otherwise is laborious to dispose. Important instrumental conditions like forward RF power, plasma gas pressure, integration time, pre-integration time are optimized and discussed in the paper. The instrument has been calibrated with Certified Reference Materials (CRMs) prior to the analysis. The calibration curves for all the elements are found to be linear with co-relation coefficient (R^2) ≥ 0.99. Statistical analysis has been carried out for comparing GD-OES method with ICP-OES, AAS, SS-OES for its validation and discussed in the paper. A precision of less than 3% RSD is obtained in the developed method.

References:

[1] Technical note on ‘Analytical Quality control in the production of nuclear grade zirconium and its alloys’, T.S Krishnan; Symposium on ‘Recent developments in Non ferrous metals technology’; Dec 4-7, 1968, NML, Jamshedpur;
[2] Impurities and their effect on the structure and properties of Zirconium parts in Nuclear Reactors; Atomic Energy, Vol. 105, No. 5, 2008
[3] Techniques for chemical characterization of Zirconium and its alloys, K.V.Iyer et al, Proceedings of the symposium Zirconium-2002 (ZIRC-2002), September 11-13, 2002, BARC, Mumbai.

Corrosion Inhibition Efficiency of Octadecylamine for Incoloy 800 in Presence of Chloride ions

Subrata Kuilya, Veena Subramanian§, S. Bera, T. V. Krishna Mohan

Water and Steam Chemistry Division
BARC Facilities, Kalpakkam, 603 102
§ Email: veena@igcar.gov.in

In Indian pressurized heavy water reactor (PHWR), Incoloy 800 is the steam generator tube material. At present, all volatile treatment (AVT) using amines like ethanolamine (ETA) is in practice to protect the structural materials in the secondary side during operation [1]. Recently there is an increased interest in addition of film forming amines (FFAs) along with AVT as they are known to reduce the corrosion of materials to extremely low values by forming a hydrophobic barrier [2]. In this study, inhibitive effects of one of the widely used FFAs viz. octadecylamine (ODA) on the corrosion of Incoloy in presence of high concentration of chloride is evaluated by using potentiodynamic anodic polarization (PDAP) technique. The study is aimed at developing and optimizing the layup strategies for long term outages in power plants. Hence, experiments were carried out at lower temperatures (75 °C). ETA was kept constant at 6 ppm; the concentrations of ODA used were 0 ppm, 6 ppm, 12 ppm, 24 ppm and 50 ppm. The PDAP curve in Figure 1(a) suggests pitting tendency for Incoloy in presence of 50 ppm Cl^- under aerated conditions. However, ODA in adequate quantities (18 ppm) was found to inhibit pitting on Incoloy as evident by the increase in pitting potential of Incoloy on addition of ~ 18 ppm ODA to the system both in presence of 50 ppm Cl^- and 5800 ppm Cl^- (see Figure 1(b)). The results suggest that the corrosion inhibition presumably depends upon an optimum thickness of layers made by the adsorbed ODA molecule. Increase in ODA concentration would result in the thickness of the film to exceed the optimum value and thus it will peel off leading to an increase in corrosion rate. Variation in pitting potential shows the role of ODA, in aiding repassivation of the film in case of pitting corrosion, in addition to inhibiting uniform corrosion. Figure 1(c) shows the rates of uniform corrosion estimated by doing Tafel analysis and in the inset, inhibition efficiency (IE) of ODA that was calculated by normalizing the values to that of exposure to only ETA is given. IE was observed to be ~40-50% when ODA was in the range of 12-18 ppm.

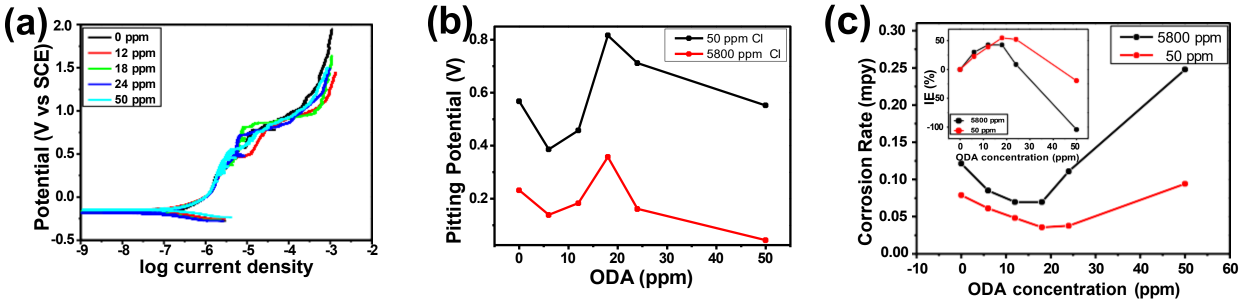

Figure 1. (a) Potentiodynamic polarization curves for Incoloy 800 exposed to ETA containing ODA of varying concentrations of ODA+50 ppm Cl^- and estimated (b) pitting potential, and (c) corrosion rates and inhibition efficiency with ODA concentration(in inset).

References:

[1] Nordmann F, Fiquet JM.. Nucl Eng Des. 1996;160:193
[2] Fandrich J, Stiepani C, Ramminger U. AWC. 2019;1

Less hazardous and effective oxidant for solvent extraction of Uranium in Phosphoric acid solutions

S.Sukumar[1§], R.Selvasundaravel[1], Premchander[1], P.Murugesan[1], M.Joseph Reston[1], A.Mohan[1]& S.Ganesh[1]

[1]*Heavy water plant, Tuticorin 628 007. Tamil nadu, India.*
Heavy water Board, Department of Atomic Energy.
[§] Email: sukumar@tut.hwb.gov.in

Phosphoric acid is one of the secondary sources of uranium which provides significant contribution for the demand of uranium. The solvent extraction procedure has been normally employed for recovery of uranium from phosphoric acid. D_2EPHA with TOPO mixture in Hydrocarbon diluents has been used as a solvent. Before the solvent extraction, uranium valence conditioning may be done bypassing air/O_2 and finishing with H_2O_2addition.[1]Oxidation reduction potential (ORP) of the acid should be >500 mV which is the suitable for solvent extraction.[2]In the valence conditioning process, pre-treated phosphoric acid is conditioned for uranium valence states from +4 to +6 which is indicated by ORP values. On consideration to the hazardous nature of H_2O_2 and instability of ORP with the time, an effective and less hazardous oxidant is being need of the hour. In this juncture, fluoride ion which is always present with wet phosphoric acidmay stabilise the fourth valence state of uranium (U^{4+}) which is highly unstable in aqueous solutions. Hence, if we remove fluoride ion availability by complex formation with suitable metal ion, U^{4+} ion will automatically will oxidise to U^{6+} state (as UO_2^{2+} ion). Taking this point in to consideration, Al^{3+} ion which is forming strong complexes with fluoride ion was chosen and further study was carried out. In this study, Pre-treated phosphoric acid was added with different amounts of $Al(NO_3)_3$ solutions. ORP measured at different times. The results are given in Table 1.

Table 1. Effect on ORP value in phosphoric acid by aluminium nitrate addition

Volume of $Al(NO_3)_3$ (1.78 M) solution added per 100mL of phosphoric acid	**ORP value in mV**					
	Immediate	**After 5 hours**	**After 10 hours**	**After 24 hours**	**After 48 hours**	**After 120 hours**
0.5mL	290	300	316	315	310	310
1.0mL	292	300	720	700	690	690
2.0mL	293	740	720	700	710	710
3.0mL	291	780	755	710	715	715
4.0mL	295	790	760	710	736	735
5.0mL	300	790	760	725	736	735

Feed phosphoric acid: P_2O_5≈ 37.2% – 40.0%; Fluoride ion≈ 23 g/L

From the values of Table 1, 1.0 mL of the aluminium nitrate solution is enough per 100 mL of phosphoric acid. After optimizing the Al^{3+} ion concentration (480 mg/L) in phosphoric acid for allowable ORP value after 10 hours, the extraction and stripping efficiencies were tested. From the results obtained, ithas shown that aluminium nitrate valence conditioning was effective in extraction of uranium in cycle I and cycle II.

Reference:

[1] D.K.Singh, et al. (2016), Solvent Extraction and Ion Exchange, 34:3, 201-225.
[2] A. Davister, J.Martin. IAEA-TECDOC-533, pp.37-44.

Chemical qualification of Zirconium based alloys using High Resolution Continuum-source Atomic Absorption Spectrometer

Y. Balaji Rao[1§], Zahida Begum [1], P.V. Nagendra Kumar [2], Dinesh Srivastava[1]

[1 & §] Nuclear Fuel Complex, Dept. of Atomic Energy, ECIL post, Hyderabad- 500062, India
[2]Asst Professor, Dept of Chemistry, GITAM University, Hyderabad-502329, India
[§] Email: ybr4793@gmail.com / ybr@nfc.gov.in

Owing to their low neutron absorption cross section and good mechanical & corrosion resistance properties, zirconium based alloys such as Zirconium alloy-2(zircaloys-2/Zr-2), Zirconium alloy-4(zircaloys-4/Zr-4) and Zirconium-Niobium alloys (Zr-Nb alloy) are preferred as structural material for PHWRs and BWRs operating in India. Several core structural components like fuel clad tubes, calandria tubes, pressure tubes, grid spacers etc., are being fabricated in Nuclear Fuel Complex (NFC). Stringent specifications, especially for alloying elements, are laid-down for these materials for obtaining optimal performance of these structural components under reactor operating conditions and are maintained throughout the fabrication process. The fabrication process involves several steps which includes melting of reactor grade zirconium metal after the addition of requisite quantities of alloying elements like Fe, Cr, Sn, Ni, Nb. And, chemical quality checks are being done from starting materials to intermediates from different stages of melting to final products for ensuring conformance to specifications as part of QA/QC program.

In view of this mandatory requirement, a successful effort has been made to develop an analytical method for chemical qualification of zircaloys-2/Zr-2, zircaloys-4/Zr-4, Zr-Nb alloys from different stages of production process using High Resolution Continuum-source Atomic Absorption Spectrometer (HR CS-AAS) [1]. In the present study, Fe, Cr, Sn, Ni, alloying elements are determined in above mentioned materials for the first time using HR CS-AAS. The present study includes various approaches adopted for measurements, change in signal to noise ratio of element of interest because of continuum-source, effect of matrix element on intensity of analyte signal, optimization of flame & burner conditions, factors affecting the detection limits, precession & accuracy etc.,. Further to this, the results obtained using HR CS-AAS are compared with the results obtained by conventional line source AAS. For this purpose, samples are dissolved in mixture of HF-HNO_3 media and a stock solution of 50gpl of zirconium concentration has been prepared for the study. The matrix effect has been studied on individual element absorbance by maintaining zirconium concentrations ranging from 0.5-10 g/l. All the measurements are performed with the calibration plots obtained from matrix matching standards in place of aqueous standards due to matrix influence. ContrAA 800 Analytik Jena (Analytik Jena, Germany) with High Resolution Continuum Source AAS (HR-CS AAS) and with a 300W xenon short arc lamp (XBO 301, GLE, Berlin, Germany) as a source and CCD detector with argon (99.99%) as a purge gas was employed for the above studies. Also, AAS Vario-6 Analytik Jena (Analytik Jena, Germany) with hollow cathode lamps as line source and PMT detector was used for comparison studies.

References:
[1] Bernhard Welza etal. *J. Braz. Chem. Soc.,* Vol. 14, No. 2, 220-229, 2003.

Development of a Rapid Method for Chemical Characterization of Tin-Tungsten Ores

Alpana Kumari, M. Krishnakumar[§], Anitha Mary Thomas and S. Nandakishore

Chemistry Laboratory, Atomic Minerals Directorate for Exploration and Research,
Department of Atomic Energy, Nagarbhavi, Bengaluru, India
[§] Email: krishnakumar.amd@gov.in,

During the mineral exploration for strategic Tin-Tungsten minerals, a large number of geological samples are to be chemically characterized for their major, minor and trace constituents. Tin mineral, Cassiterite and Tungsten minerals Wolframite (Fe, MnWO4) and ferberite ($FeWO_4$) are resistant to acid attack [1] and demand NaF/KHF_2 or $KHSO_4$ fusion for complete dissolution, a pre-requisite for ICP-OES/ AAS analysis. An effective, rapid, economic and green sample dissolution method for Tin-Tungsten ores using molten ammonium bifluoride (ABF) [2, 3] is described here.

Methodology: The ore (0.2g), finely ground to 75µm size, was digested for 2 hours at 200^{o}C, with 2g of ABF in a platinum crucible. The melt was further heated at 300^{o}C for 30 minutes. The residue was treated with 2mL HCl for complete dissolution and made up to desired volume. The analytical results obtained for Na and K using Flame photometer (Systronics, India), Li and Rb using Flame-AAS (SavantAA, GBC, Australia) and Fe, Ti, Sn, W, Mn, Nb, Ta, Ti and Ca using ICP-OES (Ultima Expert, HJY France) are given below.

Sample		**W**	**Sn**	**Li**	**Rb**	**Nb**	**Ta**	**MnO**	**Fe_2O_3**	**CaO**	**Na_2O**	**K_2O**	**TiO_2**
		ppm						%					
AMD-1		300	147	235	208	101	60	0.28	4.80	7.97	3.66	0.31	0.33
AMD-2		1067	23	58	176	45	23	0.06	2.54	0.29	4.01	1.09	0.03
CGL 126	**CV**	88	126	37	641	1700	123	0.06	3.38	2.03	3.46	3.70	0.31
	OV	<20	124	34	510	1715	134	0.08	3.27	2.00	3.48	3.89	0.29
BH-1	**CV**	4220	-	-	-	-	-	0.26	4.57	0.50	0.13	2.04	0.67
	OV	4010	25	97	336	228	<10	0.34	4.42	0.48	0.10	2.06	0.65

CGL 126: *Rare earth ore, Mongolia;* ***BH-1****, Wolframite ore, CANMET, Canada*

Results and Discussions: Results obtained for samples agreed well with those obtained using established NaF/KHF_2 fusion method. The obtained values (OV) are in close agreement with the Certified values (CV) in reference materials (CRMs). A few advantages of the proposed method is that the reagent, ABF, is completely removed while the sample is digested. A single solution containing all the desired elements including refractory elements is obtained. As the fusion/ digestion is done at 300^{o}C, the method is energy efficient. No matrix elements are added during the digestion and therefore, Na & K can also be analysed. The reproducibility of the method is found to be better than 95% in samples and the CRM analyzed. Therefore, the proposed sample digestion method for determination of major, minor and trace elements in tin-tungsten ores is rapid, safe, green and equipment-friendly compared to the acid-digestion-fusion route.

Acknowledgements: Authors wish to thank Regional Director, SR for encouragement and support and Director, AMD for granting approval for presentation of this work in the seminar.

References:
[1] S C Srivastava et.al., Bull.Mater. Sci., vol 19 (1996) 331.
[2] M. J. O'Harra et.al., Chemical Geology, 466 (2017), 341.
[3] C. Chang et.al., Geo-standards and Geo analytical Research, 46, 1 (2022), 21

Evaluation of the Effect of Mg Ions on Corrosion Properties of Zircaloy-2 by Plasma Electrolytic Oxidation (PEO) Method

Sinu Chandran, Veena Subramanian[§], Subramanian H, Santanu Bera, TV Krishna Mohan

Water and Steam Chemistry Division
BARC Facilities, Kalpakkam, Tamilnadu, INDIA
[§] Email: veena@igcar.gov.in

Structural material corrosion, generation of activated corrosion products, and their deposition on the out of core surfaces are the problems associated with nuclear reactors. Boiling Water Reactor (BWR)/ Pressurized Water Reactor (PWR) experience shows that the addition of ppb levels of zinc ions to the coolant circuits can effectively control the corrosion/activity deposition on Stainless Steel (SS) surfaces. The promising effect of Mg ions to reduce the corrosion of Carbon Steel (CS) under Pressurized Heavy Water Reactor (PHWR) water chemistry conditions has been reported in the literature [1, 2]. The aim of this study is to understand the effect of Mg ions on the corrosion behavior of the reactor core materials like Zircaloy-2 under reactor water chemistry conditions. Plasma Electrolytic Oxidation (PEO) technique was used to produce oxide films on Zircaloy-2 surfaces on a shorter timescale in de-aerated borate buffer solution (pH- 9.8) at ambient temperatures in the presence and absence of magnesium ions. Three DC voltages, viz; 300, 400, and 500 V for 30 seconds were applied to the specimen and resultant oxides were characterized by SEM/EDAX, GIXRD, LRS, and electrochemical techniques. The Mg-modified oxide films were found to be thinner as revealed in the cross-sectional SEM image of PEO film formed on Zircaloy-2 corresponding to 400 V (Fig. 1), and had higher volume fraction of t-ZrO_2. Electrochemical studies indicated that Mg doped oxide films resist corrosion better compared to their without-Mg counterpart by having a higher charge transfer resistance, lower passive current density, and lower defect densities. Thus Mg incorporation was observed to have beneficial effect on Zircaloy corrosion.

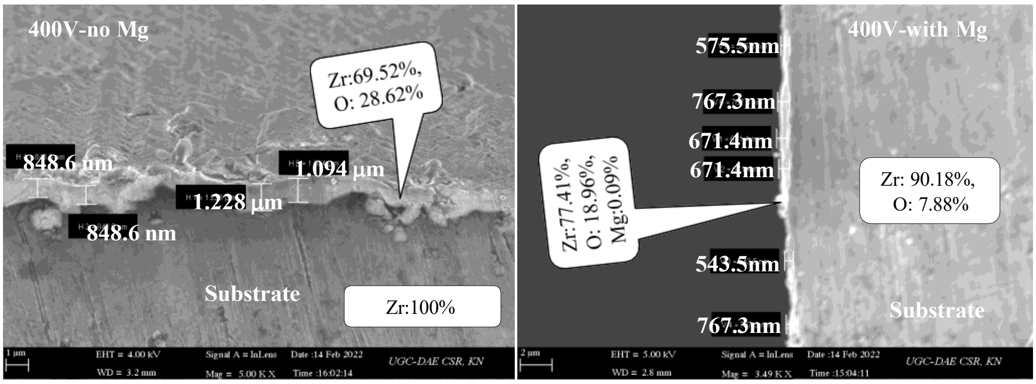

Fig. 1: Cross- sectional SEM images of PEO films formed on ZIrcaloy-2 at 400 V for 30 seconds in borate buffer medium.

References:
[1] H. Subramanian et al., Corrosion Science **70** (2013) 127
[2] S. Velmurugan et al., Journal of Nuclear Science and Technology (Tokyo) **33** (1996) 641

Dissolution of divalent and trivalent metal ions from $M_xNi_{1-x}CrFeO_4$ (Mg & Zn) Oxides in Oxidising formulation

V. Balaji[§], P. Chandramohan, Puspalata Rajesh, Santanu Bera & T.V. Krishna Mohan

Water & Steam Chemistry Division, BARC Facilities, Kalpakkam
[§] E-mail: balajiv@igcar.gov.in

Nickel-chromium ferrites are one among the corrosion products formed in the heat transport circuits depending on the water chemistry and alloy combinations in Boiling Water Reactors (BWRs). These oxides generate radiation field build-up through neutron activation causing Man-rem problem. Addition of Zn/Mg has been normal practice to control the radiation fields. Addition of these divalent metal ions reduce the general corrosion of structural materials by forming a thinner non-stoichiometric passive oxide film of Zn/Mg Ni-Cr ferrites by incorporation of Zn or Mg in to the lattice of Ni-Cr ferrites which castoffs the inclusion of cobalt activity in to the oxide film by preoccupying the tetragonal and octahedral void sites [1]. These modified Ni-Cr ferrites can affect the overall chemical decontamination process due to their structural modification. Hence, simulated oxides of Mg^{2+} / Zn^{2+} substituted Cr containing nickel-ferrites of varying compositions were synthesized by sol-gel combustion method, characterized by XRD, LRS and FE-SEM and their dissolution studies were carried out to understand the dissolution kinetics in oxidising step using permanganic acid in comparison to Ni-Cr ferrites [2].

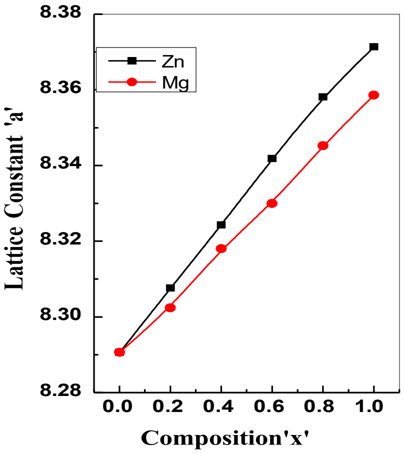

Fig. 1: Lattice parameters change in $M_xNi_{1-x}CrFeO_4$ [M = Zn/Mg, x = 0-1]

The XRD & LRS indicated that the synthesized oxides have a single-phase spinel structure. The lattice parameters were found to increase upon substitution of Zn^{2+} and Mg^{2+} in $NiCrFeO_4$ oxide (Fig 1) and the increase is higher in the case of Zn. Optical Diffuse Reflectance Spectra (DRS) were recorded to calculate band gap energy. The band gap values increased from 1.48 eV to 1.88 eV in $M_xNi_{1-x}CrFeO_4$ (M= Zn). The band gap is also related to crystallite size which can affect the dissolution rates during decontamination process. Release of divalent metal ions Zn, Mg, Ni was observed along with Cr during dissolution in 3.0 mM $HMnO_4$ at 90 ºC. The rate coefficients were evaluated by using both inverse cubic rate (ICR) law (applicable for uniform spherical particles) and general kinetic equation (GKE) (applicable for poly-dispersed particles). Both the models showed similar trend of increase in the rate constants. The dissolution rate constant for Cr changed from 5.38×10^{-4} (for $NiCrFeO_4$) to 2.23×10^{-3} and 6.12×10^{-4} min^{-1} for $MgCrFeO_4$ and $ZnCrFeO_4$, respectively. Maximum dissolution rate of 7.90×10^{-4} and 2.51×10^{-3} min^{-1} was observed by ICR model for $Zn_{0.6}Ni_{0.4}CrFeO_4$ and $Mg_{0.6}Ni_{0.4}CrFeO_4$, respectively. Higher Cr release was observed in Mg substituted Cr containing nickel ferrites as compared to their Zn substituted counterparts which indicated facilitation of dissolution on substitution.

References:

[1] D. H. Lister and G. Venkateswaran, *Nuclear Technology*, **125** (1999) 316.
[2] V.Balaji et al., *Progress in nuclear energy,* **104**, (2018) 136.

Phase relations in CeO_2–substituted $Gd_2Ti_2O_7$

C. Nandi, S. Bhattacharya, D. Ajith, K. Thorat and A. Prakash[§]

Radiometallurgy Division, Bhabha Atomic Research Centre, Mumbai-400 085, India
[§]Email: amritp@barc.gov.in

Pyrochlores which can host the troublesome actinides like plutonium (Pu) and minor actinides (MAs) in their crystalline structure have been proposed as an alternative option, apart from borosilicate glasses, for immobilization of actinide wastes [1]. Infact, these oxide-based matrices are superior in terms of chemical durability and waste loading capability than glass waste forms. In the present study, $Gd_2Ti_2O_7$ pyrochlore has been explored as the host matrix for plutonium incorporation by investigating $(Gd_{1-x}Ce_x)_2Ti_2O_{7+\delta}$ samples exploiting CeO_2 as a surrogate for PuO_2.

To investigate the phase relation upon Ce-substitution at the Gd-site of $Gd_2Ti_2O_7$ pyrochlore, $(Gd_{1-x}Ce_x)_2Ti_2O_{7+\delta}$ ($0 \leq x \leq 0.3$, $\delta \geq 0$) samples have been synthesized by a solid-state route under oxidizing conditions at 1773 K and characterized by X-ray diffraction.

$Gd_2Ti_2O_7$ exhibits the presence of super-lattice reflections (marked by asterisks (*) in Fig. 1(a)) in addition to fluorite-type reflections confirming its pyrochlore structure. XRD pattern for nominal compositions with x = 0.1 resembles the parent $Gd_2Ti_2O_7$ phase indicating the retention of the pyrochlore-type phase. Further substitution of Gd^{3+} by Ce^{4+} (x = 0.2) exhibits emergence of F-type CeO_2 phase along with predominant pyrochlore-type phase. The onset of bi-phasicity at this nominal composition has been clearly depicted in Fig. 1(b). The figure also shows increasing amount of CeO_2 phase with increasing x values. The phase relation is therefore biphasic and consists of F-type CeO_2 and pyrochlore-type phases at $x \geq 0.2$.

XRD studies reveal that cerium forms a solid solution in oxidizing condition retaining the pyrochlore-type phase only till $x \leq 0.1$ and an additional fluorite-type CeO_2 phase appear along with the existing pyrochlore-type phase at $0.2 \leq x \leq 0.3$.

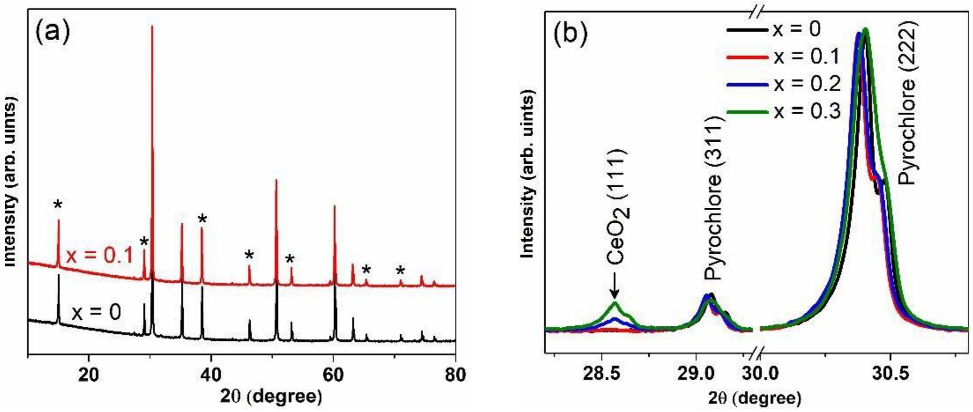

Fig.1: (a) XRD patterns for $(Gd_{1-x}Ce_x)_2Ti_2O_{7+\delta}$ samples, P-type reflections are marked by asterisks; (b) enlarged view of (111) peak of CeO_2 showing its variation w.r.t (222) peak of pyrochlore with increasing x values.

References:

[1] C. Nandi et. al., J. Nucl. Mater. 556 **(2021)** 153208

Preliminary studies on preparation of U-Al alloy by electro-reduction of UO_2-Al_2O_3 mixed oxide in LiCl-Li_2O melt

N.Sanil[1,§], L.Shakila[1], V.Arunkumar[1], Raja Madhavan[1] and R.Kumaresan[1]

Metal Fuel and Pyroprocessing Division,
Materials Chemistry & Metal Fuel Cycle Group
IGCAR, Kalpakkam, India
§ Email: sanil@igcar.gov.in

Uranium–aluminium alloys have widespread application in nuclear industry. The alloy has been used as nuclear fuel elements in nuclear research reactors and as target for preparation of medical radio-isotopes [1]. KAMINI research reactor in IGCAR uses ^{233}U (20%)–Al alloy plates with Al clad as the fuel [2]. UAl_2 is also considered for rod type fuel elements because of its high thermal conductivity and high melting point. Generally these alloys are prepared by induction or arc melting or by solid state reactions all of which are multi-step processes and needs specialised equipment operating at very high temperature and vacuum.

Herein, we report the feasibility of preparation of U-Al alloy in a single step employing Direct Oxide Electro Reduction (DOER) method. Initially, cyclic voltammetry studies were performed using metallic cavity electrode to find the reduction steps involved during electro-deoxidation. Cyclic voltammogram of UO_2-Al_2O_3 recorded in LiCl melt at 630°C is shown in Fig. 1. The cathodic peak at – 2.16 V (A,B) against Ni|NiO was assigned to the reduction of both UO_2 and Al_2O_3. The feasibility of preparation of U-Al alloy was attempted by electro-lithiothermic reduction of UO_2-Al_2O_3 composite in LiCl-Li_2O molten salt. The composition of UO_2 and Al_2O_3 used in this study corresponded to the metal molar ratio of 1:3 (U:Al). Constant current electrolysis was performed on a sintered composite pellet configured as the cathode using platinum anode in LiCl-0.5wt% Li_2O melt at 630 °C. At this condition, UO_2-Al_2O_3 composite reacted with in-situ electro-generated lithium and converted into alloy. Fig. 2 shows the XRD pattern and photograph (inset) of the pellet before and after electrolysis. The XRD analysis of the product showed the formation of UAl_2 intermetallic and U metal instead of UAl_3. This could be attributed to the loss of Al in the melt during electrolysis.

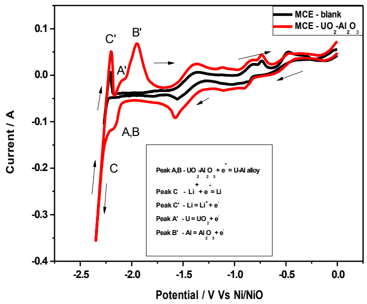

Fig. 1 CV of UO_2-Al_2O_3 powder in LiCl-Li_2O melt at 630 °C

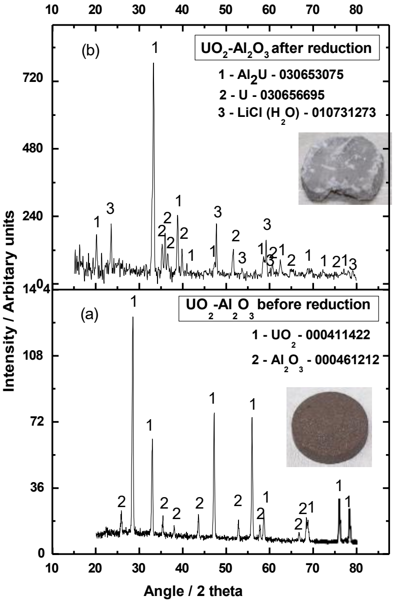

Fig. 2 XRD of pellet (a) before (b) after reduction (inset: photo of pellet before and after

References:
1. G.L.C.R. Counturiba et al. Jrl. of Nuc. Mat., 509 (2018) 465-477.
2. S.Usha et al, Nuc. Eng. and Design 236 (2006) 872–880.

Local structure and Symmetry of Eu^{3+} in $Y_2Zr_2O_7$ Pyrochlore: A Potential Ceramic Host for Nuclear Waste

Reshmi Thekke Parayil [1,2], Santosh K.Gupta[1,2*], G.D. Patra,[3] and M. Mohapatra[1,2,#]

[1] *Homi Bhabha National Institute, Anushakti Nagar, Mumbai-400094*
[2] *Radiochemistry Division, Bhabha Atomic Research Centre, Mumbai-400085*
[3] *Technical Physics Division, Bhabha Atomic Research Centre, Mumbai-400085*
[§] Email: [*] santoshg@barc.gov.in (SKG) and [#]manojm@barc.gov.in (MM)

The environmental issues associated with the development of nuclear power are of great concern due to the high radiotoxicity of used fuels. Minor actinides (Am, Cm) are the predominant remaining long-term, radiotoxic elements after recycling uranium and plutonium by the PUREX (plutonium and uranium extraction) process, which will pose potential long-term risk to the environment.**[1]** Due to the radiological issues surrounding the use of Am, the lanthanide europium has commonly been used as a surrogate, given that these 4f and 5f ions generally display similar chemistry and the eight coordinate ionic radii are comparable (Eu(iii) = 107 pm; Am(iii) = 109 pm).**[2]** In case of $A_2B_2O_7$-type oxides, excess radiation is dissipated in the form of cation antisite defect (A_B+B_A) and anion Frenkel pairs ($V_O + O_i$) and are considered excellent host for immobilization of nuclear waste. Photoluminescence (PL) is used to probe the local site, structure and symmetry of Eu^{3+} ion in $Y_2Zr_2O_7$ (YZO) pyrochlore. ***Figure 1a*** shows the emission spectra of as prepared and high temperature annealed YZO: 1%Eu^{3+} samples. PL spectra in ***Figure 1a*** consisted of 5 main features located at 579, 593, 611, 653 and 710 nm and they are ascribed to $^5D_0\rightarrow{}^7F_0$ (00), $^5D_0\rightarrow{}^7F_1$ (01), $^5D_0\rightarrow{}^7F_2$ (02), $^5D_0\rightarrow{}^7F_3$ (03) and $^5D_0\rightarrow{}^7F_4$ (04), transitions of Eu^{3+}. Among these 02 is hypersensitive electric dipole (h-EDT) and 01 is magnetic dipole transitions (MDT). The fact that 02 intensity is > than 01 clearly suggested that Eu^{3+} is occupying site low symmetry. And with no of stark components as 1 and 3 respectively for 00 and 01 transitions local point group symmetry of Eu^{3+} ion in YZO is orthorhombic and point group is C_{2v}. The reduction from original cubic and D_{3d} is endowed to size and charge induced strain and creation of charge compensating defects. Dual PL lifetime suggested that Eu^{3+} occupies both Y^{3+} and Hf^{4+} site with later favouring creating of V_O. With increase in temperature; emission intensity monotonically increases as can be seen from the ***Figure 1b*** due to reduction in surface defects induced lowering of non-radiative channels. All these data would be quite useful to simulate the behavior of Am^{3+} in pyrochlore matrix.

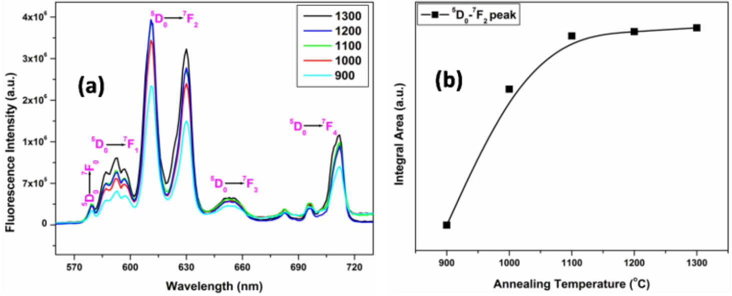

Figure 1: (a) Fluorescence spectra of $Y_2Zr_2O_7$:Eu^{3+} pyrochlore annealed at different temperature and (b) Variation in emission intensity as function of temperature.

References:
[1] C. Xiao *et al.*, *J. Am. Chem. Soc.* 2017, 139 (2017)16494
[2] S. Bishwas *et al. Dalton Trans.*, **45** (2016) 6383

Thermodynamic stability of Na_2MnF_5(s) using calorimetric technique

S. Narang[1], P. M. Aiswarya[2], R. Dawar[1,2,§] and R. Mishra[1,2]

[1] *Chemistry Division, Bhabha Atomic Research Centre, Trombay*
[2] *Homi Bhabha National Institute, Anushaktinagar, Mumbai*
[§] Email: rimpid@barc.gov.in

The Molten Salt Breeder Reactor (MSBR) is a class of generation IV nuclear reactor, where the proposed fuel, in the form of molten salt, will be circulated through the heat exchangers. NaF is the component of secondary coolant salt (FLiNaK) and of proposed alternative fuel salt for MSBR. Mn is structural material (Ti modified Hastelloy) component which can interact with NaF at high temperatures to form Na_2MnF_5(s). Coolant salt FLiNaK is in direct contact with structural material at temperature varying from 723K to 873K. Hence, there is a possibility of formation of Na_2MnF_5(s) during reactor operation. Also, Na_2MnF_5(s) shows superior electrochemical properties which leads to its application as positive electrode material for Na ion battery [1]. In the present work, we report enthalpy of formation of ternary fluoride, Na_2MnF_5(s).

The synthesis of Na_2MnF_5(s) was carried out by dissolving Mn_2O_3(s) and NaF(s) in aq. HF with vigorous stirring. The precursor solution was then stirred mildly for 6 h at room temperature. Pink solid was gradually precipitated from the solution. This solid was washed with ethanol 3-4 times and then finally dried at 343K. The phase purity of the compound was confirmed using powder X-ray diffraction (XRD) technique. The obtained XRD pattern (Fig. 1) matches with the reported PCPDF pattern (#78-0331). Enthalpy of formation of the compound at 298K was determined by measuring its molar enthalpy of dissolution and also its binary constituents NaF(s) and MnF_3(s) at room temperature in 150 ml of 3 M HCl as a calorimetric solvent. For this measurement, room temperature isoperibol solution calorimeter was used whose energy equivalent was determined before and after each measurement by performing in-situ electrical calibration. The chemical calibration of the calorimeter was carried out by measuring the dissolution enthalpy of KCl (s) in 100 mL of distilled water. The exact procedure has been described in Ref. [2]. The average enthalpy of dissolution of NaF(s), MnF_3(s) and Na_2MnF_5(s) was found to be 14.57 ± 0.16,-17.36 ± 0.09 and 108.76 ± 0.26 kJ mol^{-1}, respectively. The enthalpy of dissolution values along with literature values of standard molar enthalpies of formation of NaF (s) and MnF_3 (s) have been used to derive the standard molar enthalpy of formation of Na_2MnF_5(s) at 298 K employing a suitable thermochemical cycle. The value of standard molar enthalpy of formation $(\Delta_f H^\circ_{298K})$ of Na_2MnF_5(s) was found to be -2318.84 ± 1.40 kJ mol^{-1}.

References:

[1] J. N. Avendaño et. al., *Solid State Ionics*, **278** (2015) 106–113.
[2] V.T. Athavale, M. Sundaresan, *Ind. J. Chem.*, **7** (1969) 386-391.

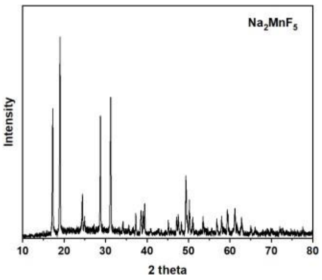

Fig. 1 Powder XRD pattern of Na_2MnF_5(s)

Thermal and spectroscopic studies of simulated actinide waste loaded niobium phosphate glass

Abhiram Senapati[1, 2], Suvendu Kumar Barik[1, 2], S. Balakrishnan[1], Kishore K. Madapu[3], Hrudananda Jena[1, 2§]

[1]*MC & MFCG, Indira Gandhi Centre for Atomic Research, Kalpakkam 603102, India*
[2]*Homi Bhabha National Institute, Anushaktinagar, Mumbai 400094, India*
[3]*MSG, Indira Gandhi Centre for Atomic Research, Kalpakkam 603102, India*
[§] Email: hnje@igcar.gov.in, balakrish@igcar.gov.in

Phosphate glasses have been investigated extensively as waste matrix for immobilizing high level nuclear waste because of their low processing temperature and high waste loading capacity [1]. The long-lived actinides such as Np, Pu, Am and Cm bearing radioactive wastes generated from the reprocessing of spent nuclear fuel requires long term storage in an inert matrix. In present work, Ce^{+4} ion used as nonradioactive simulant for Pu^{+4} and Np^{+4} ion to understand its influence on the structural and thermal properties of the niobium phosphate glass. Niobium phosphate glasses in system of $(100-x)(40Na_2O-20Nb_2O_5-40P_2O_5)-xCeO_2$ (x = 0, 1, 3, 5 and 8 mol. %), denoted as Ce0-Ce8 were prepared by melt-quenching method and are characterized by XRD, DSC, FTIR and Raman spectroscopy.

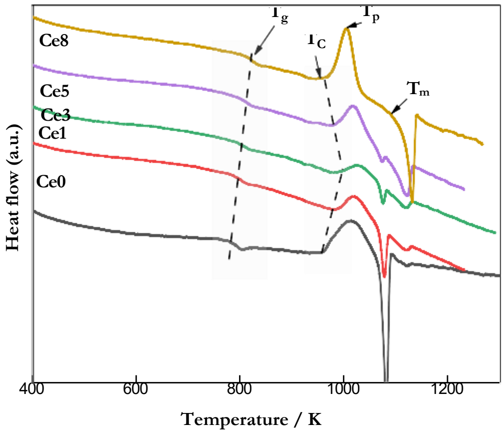

Fig.1 DSC thermograms of CeO_2 doped niobium phosphate glasses

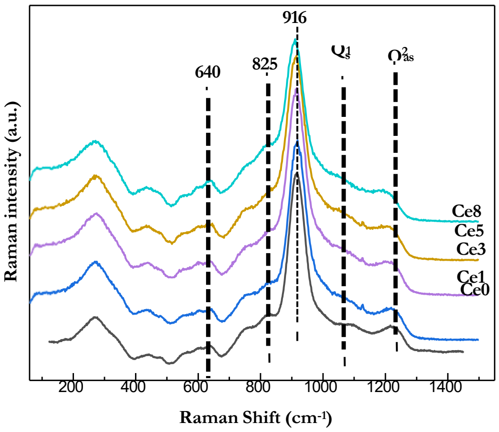

Fig.2 Raman spectra of CeO_2 bearing niobium phosphate glasses

All these synthesized glasses are X-ray amorphous. From DSC thermograms, the glass transition temperatures (T_g) are found to increase with increase in CeO_2 content in the glass (Fig.1). The thermal stability (T_c-T_g) value which indicates the delay of nucleation is increasing with CeO_2 content up to 3%, then decreases with its higher incorporation into the glass. From the Raman spectra of these glasses (Fig.2), the Raman shift nearly at 916 cm^{-1} is assigned for the short Nb–O bonding in isolated NbO_6 octahedra and at about 825 cm^{-1} is assigned to the NbO_6 octahedra linked into chains. The band nearly at 640 cm^{-1} is attributed to the Nb–O stretching mode of corner shared NbO_6 octahedra [2]. Hence, it can be summarized that niobium is present in octahedral sites within metaphosphate and pyrophosphate structural units and by adding ceria does not significantly influence the glass network of this niobium phosphate glass system.

References:
[1] S.V. Stefanovsky et. al., *Ceramics International*, 45 (2019) 9331-9338.
[2] A. Senapati et. al., *Journal of Thermal Analysis and Calorimetry*, 148 (2023) 355-369.

High temperature mass spectrometric studies on U-Zr-Mn alloy

P. Manikandan§,1, A.Manivannan[1], C.V.S. Brahmananda Rao[1], Kitheri Joseph[1]

Materials Chemistry & Metal Fuel Cycle Group, IGCAR, Kalpakkam
§ Email: manikandan@igcar.gov.in

In India, U-Pu-Zr is considered as candidate fuel for future fast reactor and appreciable amount of americium (Am) builds up in the fuel by beta decay of ^{241}Pu. In order to simulate the loss of Am during fabrication of U-Pu-Zr fuel by injection casting mode, Mn is taken as surrogate of Am due to its similar vapour pressure [1]. In the present study, vaporisation behaviour of U-6Zr-5Mn (wt.%) was studied using Knudsen Effusion Mass Spectrometry (KEMS). Homogeneous alloy was prepared by arc melting under inert atmosphere, sealed in a quartz tube under vacuum and annealed at 823 K for 72 hours. Two lots of samples (each lot: 400- 500 mg) were used in the experiments. KEMS consists of two chambers stacked one over another [2]. The bottom chamber houses electron bombardment (EB) furnace whereas the top chamber accommodates Quadrupole mass spectrometer (QMS). The samples were taken in an yttria Knudsen Cell having an orifice of 0.5 mm in diameter at the center of its lid and placed into tantalum outer cup. Temperature of tantalum outer cup placed at the top of EB furnace was measured by focusing a disappearing filament pyrometer to a black body hole at the bottom of the cup. The equilibrium vapour effusing from the cell was ionised in the ion source using energetic electrons (30 eV). The ions formed were mass analysed by QMS and detected by secondary electron multiplier (SEM) operating in pulse counting mode.

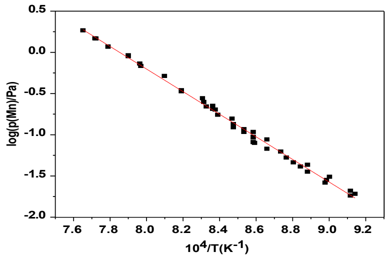

Fig 1: Plot of log(p(Mn)/Pa vs 1/T over U-Zr-Mn alloy

Mn^+ was the only ionic species observed in the mass spectrum of equilibrium vapour over the sample and identified from the mass number of the peak. Appearance energy deduced from ionisation efficiency (IE) curve recorded at m/z of 55 was found to match with the first ionisation energy of Mn(g) indicating Mn(g) as the neutral precursor of Mn^+. The temperature dependence of intensity of $^{55}Mn^+$ (five runs: 3 runs over lot 1 and 2 runs over lot 2) was carried out over two lots of sample in the temperature range 1094-1307 K. The intensity of Mn^+ was converted to partial pressure of Mn(g) [p(Mn)] by using pressure calibration constant derived from the experiments over pure Ag. The recommended partial pressure temperature (p-T) relation, which was obtained by fitting p(Mn) data from all the runs against the temperature, is $\log (p(Mn)/pa) = - (13711 \pm 135)/T + (10.77 \pm 0.11)$. The plot is shown in Fig 1. a(Mn) in the alloy at 1201 K ($x_{Mn} = 0.17$), which was calculated from p-T relation, is 0.42 indicating positive deviation from ideality since γ_{Mn} (activity co-efficient) > 1).

From the slope of individual runs, the enthalpy of vaporisation of Mn(g) over the alloy was deduced. The mean enthalpy of vaporisation was deduced by averaging individual values and is 260.1 ± 6.0 $kJ.mol^{-1}$ at 1201 K against 271.3 $kJ. mol^{-1}$ for pure manganese.

Acknowledgment: The authors thank P. Ravisankar and G. Saravanan for alloy preparation.

References:

1. Jong-Hwan Kim, et al. Advances in Materials Science and Engineering, 2015, 8 pages
2. D. Darwin Albert Raj, R. Viswanathan, P. Manikandan, ECS Trans. 46 (1) (2013) 77

Boron Determination by Time-Resolved Fluorescence Spectrometry in Uranium Matrix

Poonam Verma§ and S. Jeyakumar

Radioanalytical Chemistry Division, Bhabha Atomic Research Centre,Mumbai 400085
§ Email: poonamv@barc.gov.in

Boron plays a crucial role in the nuclear power industry because of its high neutron absorption cross-section. Hence, specification forB in nuclear fuels is very stringent. B complexes with fluorophore chromotropic acid (4,5-dihydroxynaphthalene-2,7- disulfonic acid) to formboron-chromotropic acid complex which is a measure of B concentration [1].However, fluorescence spectra of excess chromotropic acid present in the solution overlaps with that of the complex (*cf.* Figure 1). Interference from excess ligand could be eliminated by either quenching the ligand fluorescence or physically separating the ligand [2].

Present work discusses spectroscopic elimination of interfering ligand fluorescence employing time resolved fluorescence technique. The fluorescence lifetime of chromotropic acid is about 1.92 ns, whereas, for boron-chromotrope complex, lifetime is 7.13 ns. For each addition of B in chromotropic acid, fluorescence lifetime of solution was measured for the entire spectral range. Decay associated spectra (DAS) of the species present in the solution was then plotted from the measured lifetimes [3]. DAS of boron-chromotrope represents B concentration (*cf.* Figure 2). Calibration plot is linear between 5-100 ng mL^{-1} with r^2 better than 0.998. LOD is 2 ppb. Precision is better than 5% at 10 ppb level. Boron in U_3O_8 powder samples was determined after separating the matrix cations from the dissolved sample solutions by cation exchange resin cartridge. Recovery of B (25 ppb) fromthe spiked U_3O_8 powder samples was better than 94%. For validating the developed method, B was also analyzed by alternate synchronous derivative fluorimetric method and the results agreed within 8%.Developed methodis sensitivewith negligible background fluorescence.

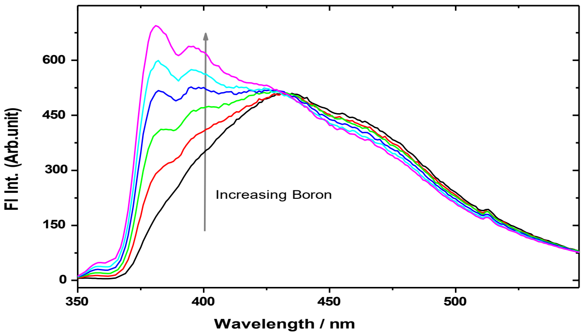

Fig. 1: Steady-State spectra of Chromotropic acid and B-Chromotropic acid complex

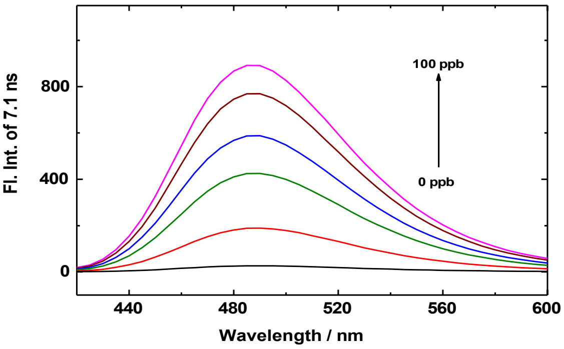

Fig. 2: Decay associated spectra of boron-chromotropic complex of 7.13 ns lifetime

References

[1] P. Verma, S. S. Kumar, R. M. Sawant, B. S. Tomar, K. L. Ramakumar, *J. Luminescence*, **153** (2014) 162.

[2] A.Economou,D.G.Themelis,H.Bikou,P.D.Tzanavaras,P.G.Rigas,*Anal.Chim.Acta* **510**(2004)219.

[3] J. R. Lakowicz, Principle of Fluorescence Spectroscopy, 3rd ed.; Spinger: New York, 2006.

Assay of nitrogen content in nitrides of U-Zr alloy using Kjeldahl Titrimetry

V. Hemalatha, K. Ushalakshmi, J. Vithya, Debasish Saha, S. Vijayalakshmi[§] & V. Jayaraman

Analytical Chemistry & Spectroscopy Division, MC&MFCG, IGCAR, Kalpakkam
[§] Email: sviji@igcar.gov.in

Nitrogen determination in nuclear materials is important at trace levels towards their quality control. Kjeldahl method has been reported to determine the nitrogen content in uranium [1]. In fast reactors, use of metallic fuels is recommended owing to their major advantage of lower doubling time. Determination of nitrogen by Kjeldahl-IC method has been carried out in uranium samples from pyroprocess method [2]. Aqueous reprocessing of metallic fuel has been reported which demands the conversion of metallic fuel to suitable form such as nitride. In this study, Kjeldahl-titrimetry was standardized for the determination of nitrogen in the nitride of U-6%Zr alloy.

Standardisation of Kjeldahl method for the determination of nitrogen in nitrides of U-Zr:

This method involves dissolution of material in Kjeldahl's flask to convert its nitrogen content to ammonium form which is subsequently distilled as ammonia under basic condition and collected in hydrochloric acid medium. Determination of nitrogen in U-6% Zr alloy matrix was standardized by spiking ammonium chloride (1.5g) to the mixed standard solutions of U and Zr. The decrease in the hydrochloric acid concentration due to the passage of ammonia was estimated by titration with NaOH using methyl orange indicator. The recovery in the measurement of ammonium by titrimetry was found to be 98% with the precision of 0.3%

Analysis of samples: Nitrides of U-6% Zr (132 mg) was heated with 15 mL of H2SO4 and 5 mL of HF for 6 hr to get complete dissolution. 20% NaOH solution was added to this solution to facilitate distillation of ammonia. The evolved ammonia was collected in hydrochloric acid solution and subsequently titrated with NaOH. The measured nitrogen content in the nitride is given in Table 1. After the completion of experiment, standard addition study was carried out to the sample solution i.e. known amount of ammonium chloride (1.5g) was added and Kjeldhal experiment was carried out. Results of titrimetry indicated the complete recovery of ammonia. Accuracy of the method was established by the analysis of aluminium nitride which contains nitrogen in percentage level. Measured value of nitrogen in AlN is given in Table 1. The excellent agreement of measured value with the actual value of 34.14% confirmed the accuracy of this method.

Table 1. Results of Kjeldahl-Titrimetry

Sample	Nitrogen conc.%
Nitride (U-6%Zr)	4.2
AlN	34.3

Conclusion: Kjeldahl –titrimetry was standardized for the determination of nitrogen content in U-Zr nitride and was applied to analysis of samples

Acknowledgements: Authors wish to acknowledge Dr. M. Bootharajan and Dr. K. Sundararajan for providing the samples for analysis and Dr. N. Sivaraman, Director, MC&MFCG, IGCCAR for his support and encouragement.

References:
1. BARC Report 2006/024
2. E13-Webinar, Proceedings of the ninth DAE-BRNS Biennial symposium (webinar) on emerging trends in separation science and technology, SESTEC 2020

Study on Isotopic Effect in Absorption of Hydrogen on IPHWR Pressure Tube Material

Sunil Kumar[1, 2], P.S. Ramanjaneyulu[1, 2§], Taslim Ali[2], M. Phanindra Kumar[1], A.S. Kulkarni[1], B.K. Nagar[1], M.K. Saxena[1]

[1]*Radioanalytical Chemistry Division, B.A.R.C., Mumbai-85.*
[2]*Homi Bhabha National Inististute, Anushaktinagar, Mumbai-94*
[§]Email: psr@barc.gov.in

Hydrogen embrittlement limits the life of zirconium based pressure tube materials of nuclear reactors. For efficient and safe operation of nuclear power reactors, ageing management i.e. regular monitoring and inspection of these pressure tubes is essential. As a part of lifetime management of pressure tubes, slivering of samples are being carried out periodically without spoiling their physical integrity. These sliver samples are being analyzed for hydrogen (H) and deuterium (D) content in our laboratory. It was observed that H content was always much higher than D content even though H content in newly fabricated pressure tubes was maintained as less than 5 ppmw and nuclear grade D_2O (D isotopic purity ≥ 98.6%) is being used as a coolant in IPHWRs. In addition, the operators have taken enough care to avoid H pick-up during slivering of the samples. This clearly shows that excess H content observed in the sliver samples was picked up by pressure tube material during their operation in the reactor. According to the well accepted mechanism about H/D pick-up by Zr based material, nascent H/D generated due to reduction of H^+/D^+ at metal and metal oxide interface gets partially absorbed by the base materials [1]. With this in view, earlier studies were carried out on isotopic effect on electrochemical charging of H/D on the surface of a cathode, Zr-2.5%Nb alloy, with varying isotopic composition of electrolyte as O.4 N H_2SO_4 in H_2O & D_2O. It was observed that, H was preferentially absorbed on Zr-2.5%Nb alloy by about 5 to 7 times more than D [2]. The observed H preferentiality was mainly influenced by two factors namely reduction of H^+/D^+ on cathode surface and adsorption and then absorption of necesant H/D on cathode surface. The aim of present studies is estimation of H preferentiality in adsorption and then absorption of H & D on IPHWR pressure tube material Zr-2.5% Nb alloy. For this purpose, a well-polished virgin IPHWR pressure tube material, Zr-2.5%Nb alloy was taken in a quartz reaction tube and connected to hot vacuum extraction-quadrupole mass spectrometer (HVE-QMS) system. The H content present in the sample was completely removed by de-gassing at 1323 K under the vacuum of better than 10^{-3} Pa. Gas mixture of H_2 and D_2 were prepared with known isotopic composition employing pure H_2 and D_2 gases. This gas mixture was taken into a quartz reaction chamber where de-hydrogenated sample piece was present. After isolation of quartz reaction tube, temperature was raised to 533 K and maintained for two hours for charging of H/D on alloy. After temperature was brought down to room temperature, evacuated the remaining gases present in the tube, ratio of mole fraction of absorbed H and D was determined employing HVE-QMS technique. Hydrogen preferentiality factor was determined from the ratio of mole faction of H and D absorbed and the gas used for charging. It was found to be in the range from 1.5 to 6.0. It clearly shows that H preferentially absorb on Zr-2.5% Nb alloy surface over D. The variation in preferentiality may be due to variation in surface characteristics of Zr-2.5% Nb alloy pieces used for experiment. Further studies have to be carried out for better understanding this variation.

References:

1. B.Cox, Journal of Nuclear Materials, 264 (1999) 283-294.
2. Sunil Kumar et. al., Abstract No. B20, Proceedings of NUCAR-2021.

Thermodynamic characterization of $KMnF_3$(s) compound

R. Dawar[1,2], S. Narang[1], P. M. Aiswarya[2] and R. Mishra[1,2,§]

[1]*Chemistry Division, Bhabha Atomic Research Centre, Trombay*
[2]*HomiBhabha National Institute, Anushaktinagar, Mumbai*
[§] Email: mishrar@barc.gov.in

In recent years there is revival of interest on MSBR research programme in India for the effective utilization of large thorium reserves [1]. Proposed secondary coolant for IMSBR (Indian Molten Salt Breeder Reactor) is eutectic mixture of LiF, NaF and KF in mole ratio 46.5:11.5:42 respectively. During reactor operating conditions, there is possibility of formation of $KMnF_3$(s) compound due to interaction between FLiNaK and structural material (Ti modified Hastelloy-N). Hence, in the present work standard molar enthalpy of formation of this compound has been determined. Also, perovskite-structured $KMnF_3$(s) has been identified as one of the good supporters for lanthanide up-conversion emission [2].

In the present study, $KMnF_3$(s) was synthesized using co-precipitation method. Powder X-ray diffraction (XRD) techniquewas used to confirm the phase purity of the solid product obtained. The obtained XRD pattern matches well with the reported pattern (PCPDF#84-0441). An isoperibol solution calorimeter, maintained at 298 K was used to determine the standard molar enthalpy of formation $(\Delta_f H^\circ_{298K})$ of the compound $KMnF_3$(s). First, the molar enthalpy of dissolution of the compound and its binary constituents KF(s) and MnF_2(s) at room temperature in 150 ml of 3 M HCl as a calorimetric solvent was measured. The dissolution of KF(s) and MnF_2(s) is exothermic while that of the compound $KMnF_3$(s) is endothermic as indicated by the electric signal recorded as the function of the time. The average enthalpy of dissolution of KF(s), MnF_2(s) and $KMnF_3$(s) was foundto be -10.28 ± 0.17, -2.51 ± 0.12 and20.95 ± 0.54kJ mol^{-1}, respectively. Employing a suitable thermochemical cycle (Table 1), standard molar enthalpy of formation of the compound $KMnF_3$(s) was derived using the enthalpy of dissolution values along with literature values of standard molar enthalpies of formation of KF (s) and MnF_2 (s).Standard molar enthalpy of formation $(\Delta_f H^\circ_{298K})$of $KMnF_3$(s) at 298 K was found to be -1451.70 ± 1.18 kJ mol^{-1}.

Table 1: Thermochemical cycle for derivation of standard molar enthalpy of formation of $KMnF_3$ (s) at 298K

Reaction	**ΔH(kJ mol^{-1})**
$KF(s) + HCl(sln) = KCl(sln) + HF(sln)$	ΔH_1= -10.28 ± 0.17
$MnF_2(s) + 2\,HCl(sln) = MnCl_2(sln) + 2\,HF(sln)$	ΔH_2= -2.51 ± 0.12
$KMnF_3(s) + 3\,HCl(sln) = KCl(sln) + MnCl_2(sln) + 3\,HF(sln)$	ΔH_3 = 20.95 ± 0.54
$K(s) + 0.5\,F_2(g) = KF(s)$	ΔH_4 = -568.61 ± 0.57
$Mn(s) + F_2(g) = MnF_2(s)$	ΔH_5 = -849.35 ± 0.85
$K(s) + Mn(s) + 1.5\,F_2(g) = KMnF_3(s)$	

References:
[1] S. Delpech et al., *J Fluorine Chem*. **11** (2009) 130.
[2] J. Wang et.al.,*Angew. Chem.*, **50** (2011) 10369.

Removal of Organic Template from Magnetic Porous Silica A Thermogravimatric Analysis

Sanat Karmakar, Kuntal Kumar Pal, P Velavendan§, K A Venkatesan, and K Ananthasivan

Process Radiochemistry Reprocessing R&D Division, Reprocessing Group
IGCAR, Kalpakkam, Tamil Nadu – 603102
§ Email: velp@igcar.gov.in

In the PUREX process, uranous nitrate (U(IV)) is employed for the conversion of Pu(IV) to Pu(III). Large quantities of U(IV) is required for Pu(IV) reduction due to presence of higher concentration of plutonium in the feed solution during reprocessing of fast reactor fuel. A number of methods have been referred in literature for the preparation of U(IV). These methods involve the reduction of U(VI) to U(IV) by suitable catalytic process. Platinum group metal impregnated silica catalyst has been reported for the reduction of U(VI) to U(IV) by many researchers. To facilitate the easy separation after the usage of catalyst from solution, magnetic silica catalyst was synthesized by encapsulating silica over Fe_3O_4 nano particles. For excellent metal loading capacity porous silica was synthesized with the help of hexadecyltrimethylammonium bromide (CTAB) as template material. Various techniques are available for the removal of template from porous silica [1]. Fe_3O_4-SiO_2-CTAB was treated with 50% H_2 at 300 °C for 15 hours to remove the CTAB template. To understand the CTAB removal efficiency, a thermogravimetric analysis was performed with virgin CTAB, porous silica-CTAB, Fe_3O_4-SiO_2-CTAB, H_2 treated porous silica-CTAB and H_2 treated Fe_3O_4-SiO_2-CTAB.

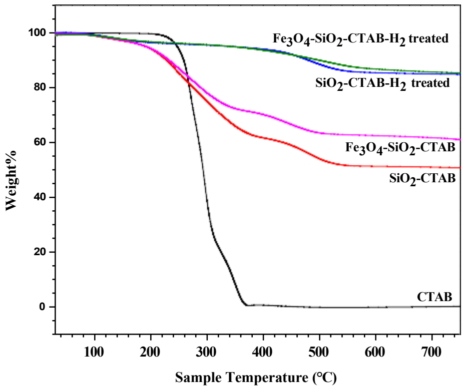

Fig. 1: TGA plot of virgin CTAB, CTAB-modified silica, CTAB modified magnetic silica and H_2 treated modified silica in 20ml/min UHP N2 flow at 10 °C/min heating ramp.

Fig. 1 shows the TGA plot in UHP nitrogen atmosphere of virgin CTAB, CTAB-modified silica, CTAB modified magnetic silica and H_2 treated modified silica. Virgin CTAB decomposes in two steps before 375 °C with no residue. Untreated porous silica-CTAB shows 49% weight loss before 550 °C due to CTAB decomposition concludes 49% CTAB load on silica. 49% CTAB loaded silica was treated with H_2 and TG shows only 14% weight loss before 550 °C. Thus CTAB load was decreased by 35% from 46% after H2 treatment which concluded that 71% of template was removed from porous silica-CTAB by H_2 treatment technique. In a similar way 65% CTAB removal efficiency was observed in case of magnetic porous silica CTAB catalyst material by H_2 treatment technique.

Acknowledgement: S. Prakash, Process Radiochemistry Reprocessing R&D Division, Reprocessing Group.

References:
[1] H. Ghaedi and M. Zhao, *Energy Fuels*, **36** (2022) 2424.

Production of long-lived radionuclide^{53}Mn, ^{54}Mn, ^{55}Fe, ^{59}Ni and ^{60}Co via charged particle induced reaction inside fusion reactor environment

Navita[1] and G. C. Joshi[2§]

[1]*Department of Physics,*[2] *Radiations And Isotopic Tracers Laboratory(RITL)*
G.B.Pant University of Ag. & Tech., Pantnagar, Uttarakhand, 263145, India
[§]Email: gc.joshi@gbpuat-cbsh.ac.in

Nowadays, the requirement of energy is going to increase day by day. Nuclear Fusion is one of the best ways to produce energy in large amount with no CO_2 or SO_2 emission [1]. In fact, nuclear fusion has a great potential for future power generation due to the large amount and accessibility of its raw materials [2]. The advancement of fusion reactor depends on improvement of plasma facing material and structural material. One of the main objectives of fusion energy research is to evaluate the production of radionuclide inside fusion reactor which may lead to change the property of original material as well as become cause of radiological hazards. There are lots of experimental nuclear data for neutron induced reactions but for charged particle induced reactions, experimental nuclear data is scarce and discordant. In recent time, it was pointed out that not only neutrons but charged particles are also responsible for the production of radioactive nuclides in fusion reactor environment. ^{53}Mn ($t_{1/2}$= 3.74×10^{6}yrs), ^{54}Mn ($t_{1/2}$= 312.20 days), ^{55}Fe ($t_{1/2}$=2.73yrs), ^{59}Ni ($t_{1/2}$= 7.6×10^{4} yrs.), and ^{60}Co ($t_{1/2}$=5.2714 yrs) are some radionuclide of interest which may produce through charge particle induced reaction.

This investigation evaluates the production cross-section of ^{53}Mn, ^{54}Mn, ^{55}Fe, ^{59}Ni and ^{60}Co radionuclide via charged particle induced reaction and the contribution to the total reaction cross-section due to various reaction mechanisms i.e. compound, pre-equilibrium and direct reaction by TALYS-1.9 using different nuclear level density models. All the major pathways via charge particle induced reactions inside the fusion reactor have also been studied.

From this study, it has been observed that the participation of direct reaction and pre-equilibrium reaction to the total reaction cross-section is sort of minimal compared of compound reaction and the contribution of charge particle induced reactions is quite high for the production of ^{53}Mn, ^{54}Mn, ^{55}Fe, ^{59}Ni and ^{60}Co. Any reaction channel either neutron induced or charged particle induced (p, α, d) reactions can breed radio-nuclides during reactor operation. Inclusion of the charged particle inventory in the activation code would be able to complete the real activation scenario.

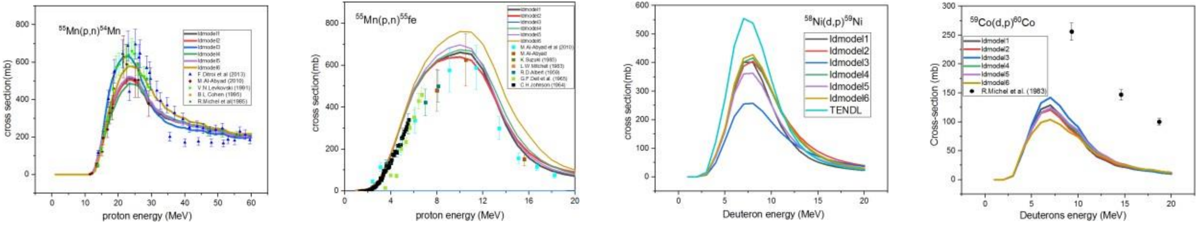

Fig.1 : Excitation function of reaction ^{55}Mn(p,n)^{54}Mn, ^{55}Mn(p,n)^{55}Fe, ^{56}Ni(d,p) ^{59}Ni and ^{59}Co(d,p) ^{60}Co

References:

[1] M. Yiğit., and M. E. Korkmaz, J. Modern Physics Letters A (2018), p1850155(1).
[2] Tejado, E. *et.al.,* J. Nucl. Mat., 467 (2015) p949.

Studies on Hydrogen Isotope preferential pickup by Zry-2 alloy

Sunil Kumar[1, 2], P.S. Ramanjaneyulu[1, 2§], A.S. Kulkarni[1, 2],
M. Phanindra Kumar[1], M.K. Saxena[1]

[1] *Radioanalytical Chemistry Division, B.A.R.C., Mumbai-85.*
[2] *Homi Bhabha National Inististute, Anushaktinagar, Mumbai-94*
[§] Email: psr@barc.gov.in

Hydrogen embrittlement deteriorates the mechanical properties of the Zirconium based alloys which are being used as structural materials for water cooled nuclear reactors. These alloys interact with surrounding environment at adverse reactor operating conditions. D_2O is used as coolant in IPHWR reactors. Protective oxide layer is being maintained on the surface of these alloys during fabrication to avoid direct interaction with coolant in their application in the reactor. However, due to extreme conditions of operation, fine cracks in the oxide layer appear after certain time of operation and this creates path for interaction of coolant with pressure tube or clad material. This leads to H/D pick up by these materials and cause hydrogen embrittlement. Different mechanisms have been proposed for hydrogen pickup by Zr based materials at nuclear reactor operating conditions. The well accepted mechanism for H pick-up says that nascent H/D generated due to reduction of H^+/D^+ at metal to metal oxide interface is partially absorbed by this material [1]. Isotopic effect on H/D pick-up by Zr based materials has to be studied for better ageing management of pressure tubes of IPHWRs. Previously, studies have been carried out in our laboratory about isotopic effect on pickup of hydrogen by Zr-2.5%Nb which is being used as pressure tube material in IPHWRs [2]. It was observed that H preferentially absorb over D on Zr-2.5% Nb alloy its preferentiality is in the range of 5-7. Previously zircaloy-2 was used as a pressure tube material and it was replaced with Zr-2.5%Nb alloy. In order to comparison of isotopic effect on absorption of hydrogen among these two alloys, present studies have been carried out isotopic effect on H/D pick-up by zircaloy-2 material. To generate nascent H/ D on the surface of Zry-2, electrolytic cell was made with Zircaloy-2 as a cathode, helical shape platinum wire as an anode and 0.4 N H_2SO_4 in known composition of H_2O & D_2O as an electrolyte. Electrolyte was maintained at about 325 K and 4.0 V of potential applied to the cell to enhance reduction kinetics. These conditions were maintained continuously for 100 hours. At each composition of H_2O & D_2O, fresh zry-2 piece was taken as a cathode. H/D generated in this process partially adsorbs and then absorbed by zry-2 material. Absorbed H/D content on Zry-2 was determined employing hot vacuum extraction-quadrupole mass spectrometer (HVE-QMS) technique. After subtraction of background hydrogen content from the observed hydrogen content, plot was constructed between $(X_{(H, M)}/ X_{(D, M)})/(X_{(H, S)}/ X_{(D, S)})$ versus $(X_{(H, S)}/ X_{(D, S)})$ (M=material, S=solution). The plot is shown in the figure. From the plot we can see that hydrogen is preferentially picked up by Zry-2 material over deuterium. Preferentiality factor was found in the range of 2-3 and it is significantly varies with Zr-2.5% Nb alloy. This difference in preferentiality may be due to variation in the microstructure or constituents of the alloy. Further studies are in progress to understand these phenomena.

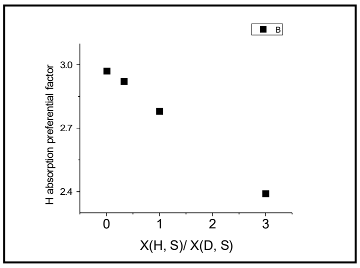

References:

1. B. Cox, Journal of Nuclear Materials, 270 (1999) 134-146
2. Sunil Kumar et. al., Abstract No. B20, Proceedings of NUCAR-2021.

Uranium extraction with TiAP solvent in Multistage Annular Centrifugal Extractor

P. Philip Kumar[1], M. Balamurugan[1], Jammu Ravi[1], N. Desigan, P. Velavendan[1], R. Rajeev[1]
and K.A. Venkatesan[1,§] K Ananthasivan

[1]*PRCRRD, Reprocessing Group, IGCAR, Kalpakkam*
§ Email: kavenkat@igcar.gov.in

PUREX process has been widely employed in nuclear reprocessing industries for more than six decades to separate U and Pu from the spent nuclear fuel. Even though, the solution of 1.1 M TBP in n-dodecane or NPH is regarded as workhorse of PUREX process, it has some limitations, such as (i) third phase formation, (ii) aqueous solubility, and (iii) chemical and radiation degradation, etc. The above limitations pose a number of problems in the fast reactor fuel reprocessing. To overcome the above limitations, alternate solvents were developed. Among the various solvent, tri-iso-amylphosphate (TiAP) is found to be the most promising solvent for fast reactor fuel reprocessing applications. The main advantages of TiAP are low aqueous solubility and the higher third phase formation limits.

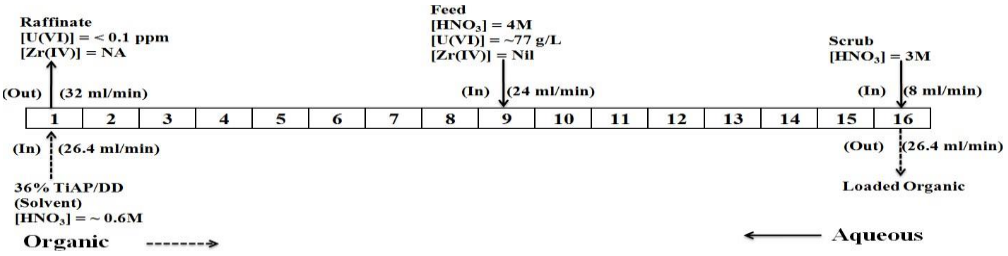

Fig. 1 The aqueous and organic flow rates with U conc. and its feed location during extraction run in 16 stages 25 mm ACE setup

The centrifugal extractors have been employed as contactors for fast reactor fuel reprocessing. It has several advantages compared to conventional pulse columns, such as: (i) low residence time, (ii) high throughput, and (iii) compact size (low footprint) etc. In this work, the performance of both TiAP and ACE has been validated by conducting uranium extraction runs in 16 stages ACE. Experimental feed condition and flow rates are shown in the Fig. 1. Uranium concentration profiles with respect to ACE stages were compared with mixer settler runs reported in literature. The comparison revealed that the uranium concentration profiles in a 16 stages ACE was quite similar to the literature reported data. Uranium concentration profile w.r.t to ACE stage is shown in the Fig. 2. From extraction results, it was concluded that four stages were required to complete the uranium extraction.

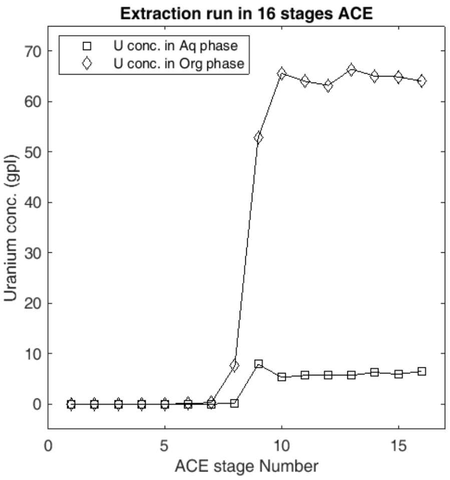

Fig. 2 Uranium concentration in 16 stages ACE

References:
[1] B. Sreenivasulu et.al., *Solvent Extraction and Ion Exchange,* **34 (5)** (2016)422.

Effect of anions on formation of ferrite coatings on carbon steel by hydrothermal method

Sumathi Suresh[§], Santanu Bera and T.V. Krishna Mohan

Water and Steam Chemistry Division, BARCF, Kalpakkam, Tamil Nadu, India
[§]Email: sumathi@igcar.gov.in

Metal ion passivation method is used to modify the oxide films to control the corrosion of carbon steel (CS), out of core structural material in primary heat transport system of Pressurized Heavy Water Reactors [1]. The extent of passivation depends on the metal ion concentration and type of anions present like hydroxyl (OH^-), sulphate (SO_4^{2-}), nitrate (NO_3^{2-}) and acetate (CH_3COO^-). In this work, ferrite coatings were formed on CS by hydrothermal method in lithium hydroxide (LiOH) in presence of Zn^{2+} and Ni^{2+} ions containing anions SO_4^{2-}, NO_3^{2-} and CH_3COO^- at 250°C exposed for 240 hours. The effects of SO_4^{2-}, NO_3^{2-} and CH_3COO^- anions on the microstructure of the coatings and corrosion behaviour of CS were studied by FESEM and electrochemical techniques. The Potentiodynamic anodic polarization (PDAP) plots were obtained at 28°C in LiOH medium by polarizing CS from -0.4 V to +1.2 V with respect to open circuit potential at a scan rate of 0.5mV/s. The formation of ferrite films on CS was confirmed by GIXRD. Table 1 shows the thickness of ferrite films estimated by Clarke's method. The film thickness obtained in presence of acetate ions was less than magnetite film (absence of Zn^{2+} and Ni^{2+} ions) and films obtained in presence of sulphate and nitrate. FE-SEM images in Fig.1 (a-c) show that the CS surface is uniformly covered with octahedron shaped particulates of bigger sizes in presence of nitrate and sulphate anions and smaller particles in case of acetate anions. In Fig.1 (d) PDAP plots from coated CS are compared. In general, the OCP for all ferrite films shifted to noble side (-0.262 to -0.403V vs. SCE) compared to unexposed CS (-0.495V vs. SCE).

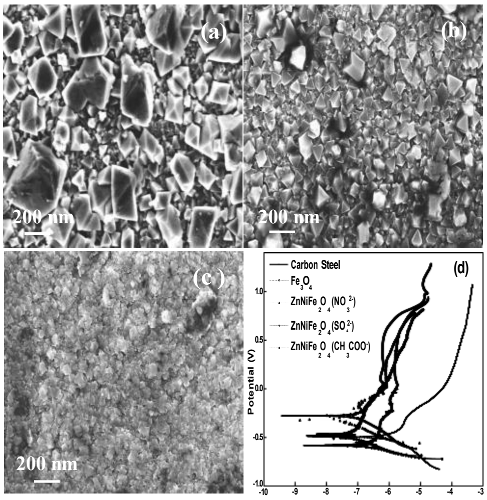

Fig 1: FE-SEM of $ZnNiFe_2O_4$ in (a) nitrate, (b)sulphate (c)acetate (d) PDAP of $ZnNiFe_2O_4$

An active to passive transition was observed in all the cases due to the formation of ferric hydroxide film at anodic potentials and the passive region was broader. At higher anodic potentials, passive current was slightly higher in presence of acetate, nitrate and sulphate anions compared to magnetite but lower than the passive current of CS. The morphology was different in presence of different anions as observed by FE-SEM. The corrosion protection offered by ferrite films formed on CS in presence of acetate was highest followed by the order : Fe_3O_4 < Sulphate < Nitrate ≅ Acetate. It is inferred that ferrite films formed in presence of acetate ions are more adherent and compact compared to magnetite and those formed in nitrate and sulphate anions.

Table 1 (Clarke's method)	Thickness (μm)
Fe_3O_4 (OH^-)	0.55
$ZnNiFe_2O_4$ (NO_3^{2-})	0.63
$ZnNiFe_2O_4$ (SO_4^{2-})	0.44
$ZnNiFe_2O_4$ (CH_3COO^-)	0.10

References:
[1] Choi J.S. et.al.; *Natural Science*, **5** (2013) 173.

Sr^{2+} sorption studies on serpentine minerals for potential Small Modular Reactors (SMR) spent fuel transport applications

Meenu Prasher[1,§], Harshala J. Parab[2], R. Sirvi[3] , H. Haria[4] , S. D. Kumar[2,5] and P. Sengupta[1,5]

[1] *Materials Science Division, Bhabha Atomic Research Centre, Mumbai, India-40085*
[2] *Analytical Chemistry Division, Bhabha Atomic Research Centre, Mumbai, India-40085*
[3]*Department of Petroleum Engineering, P. D. E. University, Gandhinagar, India-382421*
[4]*K. J. Somaiya College of Science and Commerce, Mumbai, India-400077*
[5] *Homi Bhabha National Institute, Anushaktinagar, Mumbai-400094*
[§] Email: meenu@barc.gov.in

Strontium-90 ($t_{1/2}$=28.6 years) is one of the primary fission product and is a major concern for safe management of nuclear waste due to its high yield and negative biological effects. Small Modular Reactors (SMRs) are advanced nuclear reactors that have power capacity up to 300 MWe, are small in size and modular. The SMR designs consider compact reactor cores due to which high concentration of fissile nuclei and neutron radiation is expected from their spent fuels. Magnesium silicate minerals are proposed as filler material in spent nuclear fuel storage casks due to their high sorption capacity for radionuclides [1, 2]. Serpentine ($Mg_3Si_2O_5(OH)_4$) is a naturally occurring hydrated magnesium silicate mineral [3] consisting of 1:1 silica tetrahedral (T-sheet) and Magnesium Octahedral (O-sheet) with inter layer spacing of ~7Å. It occurs in three polymorphs: Lizardite, Antigorite and Chrysotile. Although few studies on heavy metal sorption in serpentine [4, 5] are available in literature, reports on Sr^{2+} sorption in serpentine are scarce. Here, we report sorption of non-radioactive Sr^{2+} ions on thermally treated Antigorite-rich polymorph to explore the influence of thermal activation of the T- and O-sheets on its adsorption capability. Batch sorption experiments were conducted using five mineral samples (as sorbents) thermally-treated at different temperatures from 450°C-1100°C for 24 hours each under ambient conditions. 0.1 g of each sorbent was kept in contact with 25 mL of 500 mg L^{-1} of Sr^{2+} solution for 60 h in triplicate followed by separation of the sorbent using centrifugation. The residual concentration of Sr^{2+} ions in supernatant solution was determined using XRF analysis performed at room temperature using a Xenemetrix Genius IF EX-2600 spectrometer in the air atmosphere. The optimised conditions for the analysis are: emission current = 1200 μA, applied voltage = 35 kV, Mo-secondary target and counting time = 100 s. The X-ray diffraction analysis revealed the structural transformation of serpentine to forsterite upon thermal treatment which led to significant modification in the Sr^{2+} sorption capacity (shown in Fig. 1). Together, these results will give a better understanding into the mechanism of Sr^{2+} sorption in serpentine minerals.

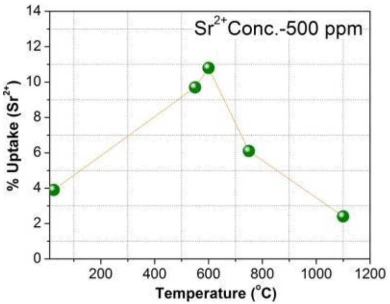

Fig. 1: % uptake of Sr^{2+} ions on the thermally activated serpentine as a function of thermal treatment temperature.

References:
[1] F. Z. El Amarani et. al.; Applied Geochemistry 17 (2002) 399–408
[2] M. Rovira, et. al.; Radiochim. Acta 88 (2000) 665–671
[3] Deschamps et. al.; Lithos (2013) 96-127.
[4] Chun-Yan Cao, et. al.; Journal of Hazardous Materials 329 (2017) 222-229.
[5] Z. Li, P. Huang et. al.; Chemosphere 258 (2020) 127275.

Mutual Separation of Nb and Ta from aqueous HNO_3 stream using a task specific ionic liquid

Priya Goyal, Arijit Sengupta[§], P.K. Mohapatra
Radiochemistry Division, Bhabha Atomic Research Centre, Mumbai - 400 085
[§] *Email: arijitbarc@gmail.com*

Ionic liquid has worldwide been considered as potential 'green' alternatives to volatile organic compounds [1]. The similar size and speciation of Nb and Ta lead to similar chemistry resulting their mutual separations very difficult. However, both these elements have very different physical and nuclear properties. Nb finds application in the production of high refractive index lenses, dielectric materials, capacitors and surface acoustic wave filters. Due to very low neutron absorption cross section for thermal neutrons, Nb is used in combination with Zr for nuclear cladding materials. However, Ta mostly being accompanied with Nb, exhibited 20 times high neutron absorption cross section than Nb. Ta can be used as control rod in nuclear reactors. Therefore, an efficient method for Nb and Ta separation is the need of the hour. To our knowledge, ionic liquid based separation methods are not reported for this purpose. A Task Specific Ionic Liquid (TSIL), i.e., trihexyl tetra ethyl phosphonium bis 2,4,4 trimethyl phenyl phosphinate has been used in this study. In view of the very high viscosity of the TSIL, two ionic liquids ($C_4mimNTf_2$ and $C_8mimNTf_2$) were utilized for dilution purpose. Fig. 1(a) is showing the D values for Nb and Ta as a function of aqueous feed HNO_3 concentration. The D values for Nb were found to be greater than that of Ta in solutions in both the ionic liquids. The D values for both the metal ions were found to decrease with increasing feed acidity indicating the predominance of a cation exchange mechanism. The maximum separation factor achieved in $C_4mimNTf_2$ was found to be ~ 33 at 2 M HNO_3, while that for $C_8mimNTf_2$ was ~47 at 2 M HNO_3. The slope ratio method was used for estimating the metal ligand stoichiometry [Fig.1 (b)]. The Nb and ta were found to form 1:2 and 1:1 complex in $C_4mimNTf_2$, whereas only 1:1 metal-ligand complexes were formed in $C_8mimNTf_2$.

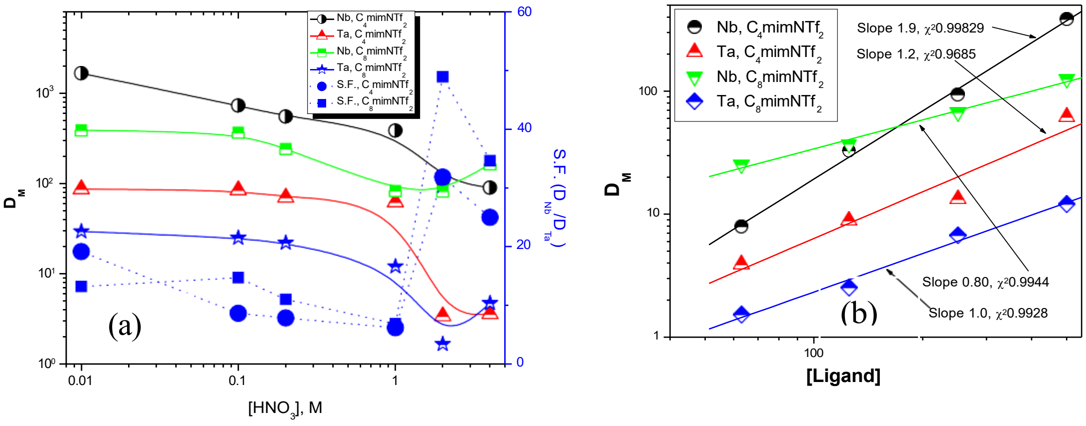

Fig. 1: (a) Variation in D_{Nb} and D_{Ta} and Separation Factor as a function of HNO_3 concentration in aqueous phase; (b) The variation in logD values as a function of ligand concentration in ionic liquid phase.

References:
[1] Z Lei, B Chen, Y-M Koo, D R. MacFarlane, Chem. Rev. 2017, 117, 10, 6633–6635.

Preparation of Al-Co mixed hydroxide ion exchanger for removal of uranium from alkaline aqueous waste

Ashok Kumar, A. C. Deb, Nitin Gumber, Rajesh V Pai
Fuel Chemistry Division, Bhabha Atomic Research Centre, Trombay, Mumbai – 400 085
E-mail: ashkumar@barc.gov.in

Inorganic ion exchanger is considered superior due to its thermal and radiation stability and non-swelling nature in water. Double hydroxides are widely known form of inorganic ion exchanger for removal of anionic species from the aqueous stream. Co-precipitation route is one of the preferred processes for preparation of double hydroxides. With suitable experimental conditions, Layered Double Hydroxide (LDH) [1] can be produced with improved anion exchange characteristics. LDH are complex hydrous oxide with an interlayer space capable of hosting an additional amount of anionic particles. A combination of M^{2+} (Fe(II), Co(II), Zn, Mn(II) etc.) and M^{3+} (Al, Fe(III) etc.) metals ions have been used for synthesis of LDH. In one of method urea decomposition has been used as precipitation material [2]. In another study, dilute Hexamethylenetetramine (HMTA) [3] have been employed for preparation of Fe-Co LDH. However these two experimental procedures have some limitations namely, difficulty in producing bulk product and the material being in powder form are not suitable for setting up an ion exchange column for removal of uranium from the alkaline solution.

The present study was undertaken to synthesize Al-Co double hydroxide by internal gelation process [4] and to investigate its use in removal of uranium from the alkaline solution. 3M solution, each of aluminium nitrate, cobalt nitrate and mixture of HMTA and urea were prepared separately. $(Al_{0.9}Co_{0.1})O_{2+x}$ microspheres were prepared by internal gelation process using feed composition, [M] =1.25 M and [HMTA+urea] = 1.74 M. Microspheres were washed and dried at 100ºC. About 10 gram of dried mass of mixed hydroxide was taken a column and uranium containing alkaline solution was passed through it at a flow rate of 20ml per hour. 5 ml fractions of the effluent were collected separately and assayed for uranium content spectrophotometrically using arsenazo (III) as colour forming agent [5]. Absorbance at 655 nm was recorded using the Cary-500-SCAN-UV-VIS NIR spectrophotometer. Content of uranium in the alkaline solution was 50 ppm. No uranium was detected in the column effluent after collection of initial four fractions each of 5ml. Amount of uranium held on the exchanger was calculated to be 1000µg without any breakthrough. The result showed that Al-Co mixed hydroxide produced by internal gelation process exhibit absorption of anionic polymeric species of uranium present in the alkaline waste solution.

Reference

1. Clearfield A. Solvent Extr Ion Exch 18 (2000) 655.
2. Costantino U, Marmottini F, Nocchetti M, Vivani M. Eur J Inorg Chem 10 (1998) 1439.
3.Ma R, Liang J, Takada K, Sasaki T. J Am Chem Soc 133 (2011) 613.
4. P. A. Haas, J. M. Bagovich, A. D. Ryon and J. S. Vavruska, Ind. Eng. Chem. Prod. Dev. 19 (1980) 459.
5. S. B. Savvin, Talanta, 8 (1961) 673.

Electrochemical Behaviour of LiF-CaF$_2$-UF$_4$ Molten Salt System

Abhishek Kumar Rai*[a,c], Manoj Kumar Sharma[b,c], S.C. Parida[a,c]
[a]*Product Development Division, Bhabha Atomic Research Centre, Mumbai-400 085, India*
[b]*Fuel Chemistry Division, Bhabha Atomic Research Centre, Mumbai-400 085, India*
[c]*Homi Bhabha National Institute, Mumbai-400 094, India*
**E-mail: abhirai@barc.gov.in, Tel. No.: +91 22 2559 4593*

Electrochemical separation is one of the promising techniques for the pyro-processing of spent fuel of molten salt reactors. For the optimization of this reprocessing method, the precise knowledge of different electrochemical as well as solubility parameters for U(IV) and U(III) species in the molten salt mixture are of prime importance. In the present work, the apparent reduction potentials, diffusion coefficients, etc. for U(IV) and U(III) species in molten mixture of 70 mol% LiF – 8 mol% CaF$_2$ – 22 mol% UF$_4$, the proposed fuel salt for *IMSR*.

The salt mixture was prepared in an inert atmosphere furnace by heating the intimate mixture of pre-purified LiF, CaF$_2$, and UF$_4$ in the required ratio with a little amount of NH$_4$HF$_2$ up to 1123 K. Metrohm PGSTAT302N was used for CV, SWV and CP studies of the mentioned system. For sake of representation, cyclic voltammogram (CV) of this system at 300 mV/s at 1023 K is shown in Fig. 1.

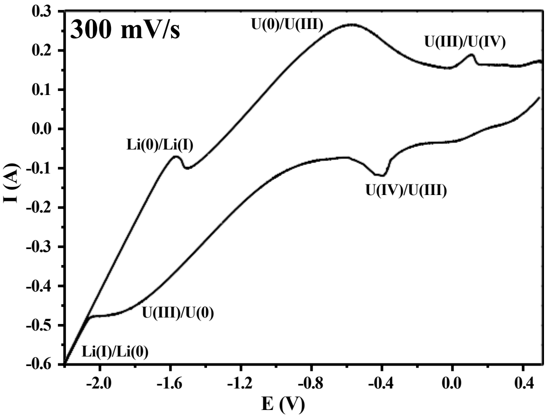

Fig .1: CV of 70 mol% LiF – 8 mol% CaF$_2$ – 22 mol% UF$_4$ at 1023 K

Diffusion coefficients of U(IV) and U(III) species in LiF-CaF$_2$ melt were calculated from the slope of the linear plot of reduction peak current vs. square root of scan rate. The diffusion coefficients of U(IV) and U(III) species at 1023 K were found to be 9.5×10^{-6} cm^2/s and 6.5×10^{-6} cm^2/s, respectively which are less than half of the values reported by Nourry et al. [1]. The reason for the significant difference in the values may be attributed to the much higher concentration of UF$_4$ taken in the present work as compared to the literature [1]. Also, lower diffusion coefficient of U(IV) species as compared to that of U(III) species is due to higher charge density in the former case.

The U(IV) to U(III) and U(III) to U(0) reduction potentials are used to calculate the activity and activity coefficients of U(IV) and U(III) species in this mixture at 1023 K, which will be further used to deduce partial molar thermodynamic properties of these species.

References:

1. C. Nourry, et al., J. Nuc. Mat., 430 (**2012**) 58–63.

Application of Chromatographic Resin Containing TAM-3-DGA for Extraction of Actinides from Acidic Feed

Piyali Banerjee,[1,2,] § S.A. Ansari,[2,3] P.K. Mohapatra,[2,3]
T.P. Valsala,[1] D.B. Sathe,[1] R.B. Bhatt,[1]and W. Verboom[4]

[1]*Nuclear Recycles Board, INRPO, BARC, Tarapur, Maharashtra – 401 502, India*
[2]*Homi Bhabha National Institute, Anushakti Nagar, Mumbai – 400094, India*
[3]*Radiochemistry Division, Bhabha Atomic Research Centre, Mumbai – 400 085, India*
[4]*Laboratory of Molecular Nanofabrication, MESA+ Institute for Nanotechnology,*
University of Twente, P.O. Box 217, 7500 AE Enschede, The Netherlands
§ E-mail: piyalib@barc.gov.in

Treatment of plutonium bearing waste generated in the analytical laboratories is an important activity of the liquid radioactive waste management. If plutonium along and other actinides are recovered from the waste, theradioactive waste management becomes facile. Conventional diglycolamide (DGA) ligands such as TODGA and T2EHDGA have been extensively studied for separation of lanthanides and actinide from liquid nuclear waste [1]. However, recent studies have shown that the tripodal DGA ligands are more efficient for actinides as compared to conventional TODGA and T2EHDGA lignads [2].

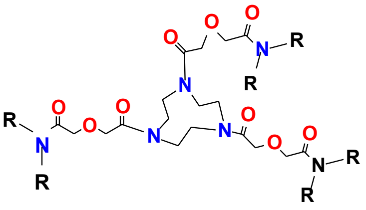

Fig. 1. TAM-3-DGA

In the series of tripodal DGA ligands, a unique ligand was synthesized, where 3 DGA moieties were chemically grafted on a triaza-9-crown-3 scaffold (termed as TAM-3-DGA, Fig. 1). Solvent extraction studies with TAM-3-DGA ligand gave encouraging results for the separation of actinides yeided very encouraging results [3]. In order to utilize the efficacy of TAM-3-DGA ligand in an alternate separation method, an extraction chromatographic resin was prepared using this ligand for the separtion of actinides.The ligand loading on the resin was 11% (w/w) that corresponded to 97µmol/g of resin.

The distribution coefficient (*K_d*) of trivalent and tetravalent actinides (Eu^{3+}, Am^{3+}, Np^{4+}, Pu^{4+} and UO_2^{2+}) on the resin werevery large (>1 x 10^4) in the acid range of 2 – 6 M HNO_3 (Fig. 2). On the other hand, hexavalent uranyl ion was poorly sorbed, giving a very good separation factor for trivalent and tetravalent actinides over uranium.The resin capacity was 13.9±0.3 mg of Eu^{3+} (as a surrogate for Am^{3+}) and 11.7±0.4 mg of Pu^{4+} per g of the resin, corresponding to the formation of a 1:1 metal/ligand complex for Eu^{3+} and 1:2 metal/ligand complex for Pu^{4+} ions. The sorbed Eu^{3+} and Pu^{4+} ions from the resin could be efficiently desorbed with 0.1 M HEDTA and 0.5 M oxalic acid respectively. The feasibility of using this material for actinide separation was successfully tested in column mode with encouraging results. The column loading of $Pu^{4+}$was ~80% of the static equilibrium value with a narrow elution profile.

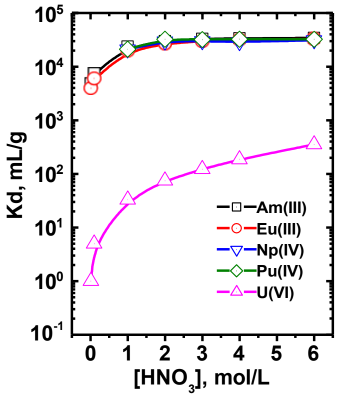

Fig. 2. Variation ofK$_d$ with acidity

References:

1. S.A. Ansari, *et. al.*, ***Chem. Rev.***112 (**2012**)1751-1772.
2. A. Leoncini, *et. al.*, ***Chem. Soc. Rev.*** 46 (**2017**) 7229-7273.
3. A. Bhattacharyya, *et. al.,**Inorg. Chem.***57 (**2018**) 12987–12998

Thermo physical properties of sodium thorium phosphates

Geeta Patkare, Muhammad Shafeeq, Meera Keskar§

Fuel Chemistry Division, Bhabha Atomic Research Centre, Mumbai, India 400085
§ Email address : mskeskar@barc.gov.in

Structures of numerous phosphates, an alternative ceramic host matrices for immobilization of high level radioactive waste, are reported [1,2] but less data is available on their thermal properties. Here, thermal expansion and heat capacities of $Na_2Th(PO_4)_2$ (1) and $NaTh_2(PO_4)_3$ (2) are calculated using HT-XRD and DSC techniques. Compounds were synthesized by solid state route reacting Na_2CO_3, ThO_2 and ADHP in desired molar proportion up to 1173 K. Powder X-ray diffraction confirmed formation of desired phases. To calculate thermal expansion coefficients, high temperature XRD data of (1) and (2) was collected in air from 298-1173 K. No additional peaks in XRD confirmed thermal and structural stability of them. Plots of cell volume against the temperature for the compounds are shown in Fig. 1. Thermal expansion coefficients (TEC)s of the compounds were calculated using relation

$$\alpha_a=\left(\frac{\delta_{aT}}{\delta_T}\right)\times\left(\frac{1}{a_{298}}\right)$$

where $(\delta a_T/\delta_T)$ is temperature derivative of (LP/Vol.) and a_{298} is value at 298 K. Both compounds show positive thermal expansion and their average expansion coefficients are given in Table 1. Heat capacities (C_p) of (1) and (2) were measured between 300 to 863 K using DSC. Typical three step method was used to calculate molar heat capacities which are plotted against the temperature (Fig. 2). The plots were fitted as a function of temp. (K) in the form

$$C_p=A+BT+\frac{C}{T^2}$$

Values of constants are given in Table 1 and fitted curves are shown in Fig. 2 (solid lines).

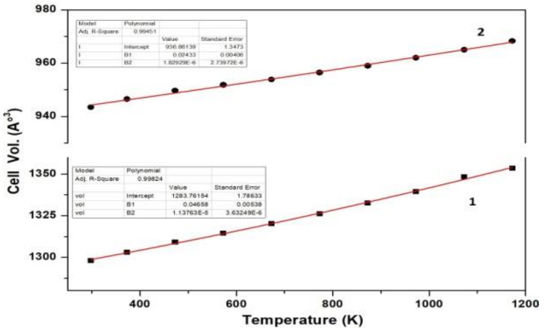

Fig. 1. % volume expansion vs temp (K)

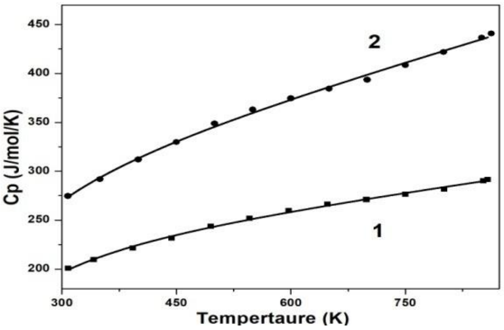

Fig. 2. Cp vs temp (K)

Table 1. Average TECs and C_P data for (1) and (2)

Comp.	Average TEC [$\times 10^{-6}$] K^{-1}				$Cp = A + BT + C/T^2$ ($J K^{-1} mol^{-1}$)		
	α_a	α_b	α_c	$\alpha_{vol.}$	A	B	$C\times 10^5$
(1)	21.46	7.46	18.25	43.04	206.153	0.104	-3.69356
(2)	11.05	6.52	13.7	29.11	252.04	0.222	-4.44020

References

[1] S.V. Krivovichev, P.C. Burns, I.G. Tananaev (Eds.), Structural Chemistry of Inorganic Actinide Compounds, Elsevier (2007).
[2] S. Neumeier et al. Radiochim. Acta 105 (2017) 961.

Synthesis, Characterization and evaluation of Chitosan-Graphene oxide nanocomposite towards uptake of Uranium

H. Seshadri[1§], D.K.Mohapatra[1]

[1] Safety Research Institute, AERB, Kalpakkam India
[§] Email: sesh@igcar.gov.in

The treatment and recovery of uranium from lean streams during uranium ore processing and recovery of uranium from effluents from fabrication and reprocessing operations is quite challenging. Although Graphene Oxide (GO) is a known adsorbent for metal ions, its efficiency can be further improved by combining it with Chitosan (CTS), a biopolymer wherein chitosan can undergo an amidation reaction with the carboxyl groups of graphene oxide to form well dispersed Chitosan-Graphene Oxide composite (CTS-GO) composite. In this work, CTS-GO composite was synthesized in-house by crosslinking chitosan and graphene oxide using modified Hummer‘s method to yield fr mework m teri l [1]. The synthesized composite was characterized using XRD and SEM to assess the structure and morphology of the composite. The adsorbent was evaluated for the uranium adsorption studies by equilibrating 25mg/L uranium solution with 25mg composite for 120 minutes. Experiments were repeated by varying the catalyst dosage as well as by varying the pH. Uranium concentration was estimated using spectrophotometric route using Arsenazo (III).

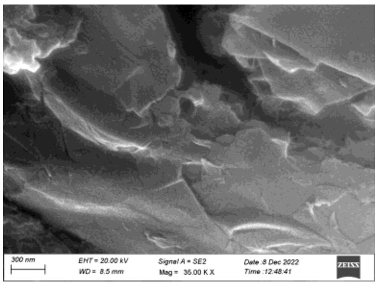

Fig.1 SEM Micrograph of GO-CTS nanocomposite

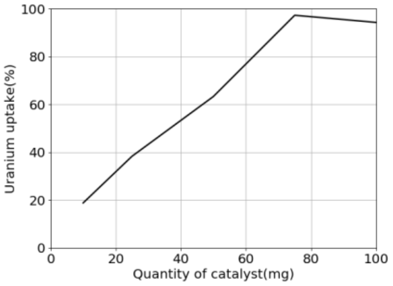

Fig.2 Influence of catalyst dosage on the uptake of uranium

It was observed that the addition of GO alters the crystallinity of chitosan which is a desirable feature for the improvement of the tensile properties of the polymer. The SEM image of GO-CTS showed agglomerates consisting of several smoother layers indicating that more chitosan has got attached to the GO in the composite (Fig.1). Uranium adsorption studies indicate that more than 97% of uranium un uranyl nitrate solution could be removed at pH 4. On increasing the catalyst dosage, the uranium adsorption has also increased till 75mg/L (Fig.2). Further, the influence of pH towards the removal of uranium was found to follow the order acidic < neutral< alkaline indicating the electrostatic interaction between the catalyst and uranium at lower pH ranges although significant removal was observed in all the pH ranges. Results of this study show that the synthesized chitosan-graphene oxide composite can effectively remove uranium from effluents arising from different process streams.

References:

[1] W. S. Hummers, R. E. Offerman, *Journal of American Chemical Society, 80*(1958), 1339.

Local Coordination and Oxidation state of Uranium in $ZnGa_2O_4$ Spinel

D. Chandra Shekhar [1]§, Santosh K.Gupta[2, 3], and K. Sudarshan[2,3,#]

[1]Product Development Division, Bhabha Atomic Research Centre, Mumbai-400085
[2]Homi Bhabha National Institute, Anushakti Nagar, Mumbai-400094
[3]Radiochemistry Division, Bhabha Atomic Research Centre, Mumbai-400085

§Email: datrikcs@barc.gov.in

The spectra of Actinides are similar to those of lanthanides but are more complicated because of the various reasons [1]. These includes Russell–Saunders coupling scheme is inefficient in heavier actinides, 5_f‘ electrons have greater penetrating effect and come closer to the nucleus and improper shielding of 5_f‘ electrons from the surrounding chemical environment leads to ligands effects. Since 5_f‘, 6_d‘ and 7_s‘ electrons have comparable energies, the electronic configuration of the element in a given oxidation state in solution depends on the ligand. This property is known as ligand effect. This is not shown by lanthanides. The f—f transitions in actinides are about 10 times more intense and the ligand field effect is about 2 to 5 times stronger than in other lanthanides. Methods to measure uranium content and its speciation are important in a wide range of fields including nuclear fuel production, nuclear forensics, and nuclear waste remediation. The actinide element U can exist in different oxidation states, such as U (III), U (IV), U (V) and U (VI)[2]. Each oxidation state has a characteristic optical spectroscopic fingerprint [3]. Hexavalent Uranium depending on the synthesis conditions can have different molecular structure leading to UO_4^{2-}, UO_6^{6-} or UO_2^{2+} species [4]. The environmental impact of any metals ion depends on its concentration and more precisely its speciation. AB_2O_4 based spinel matrix are considered potential host for radioactive waste immobilization and transmutation of actinides. Through the present work we have made an attempt to identify the oxidation state and coordination geometry by incorporating uranium in $ZnGa_2O_4$ and studying them by time resolved photoluminescence spectroscopy. ***Figure 1*** shows the PL emission spectra of $ZnGa_2O_4$:U (5.0 mol %) under 254 nm excitation. The spectra displayed a broad band peaking around 500 nm in the green spectral domain. The same has been ascribed to ligand to metal charge transfer involving bonding oxygen orbital (Πu, Πg, Ωg, Ωu) to non bonding 5f and 5fΦ orbitals of uranium ion. This is peculiar of hexavalent uranium ion stabilizing a octahedral uranate UO_6^{6-} ion. The excitation peak at 254 nm corresponds to oxygen to uranium charge transfer.

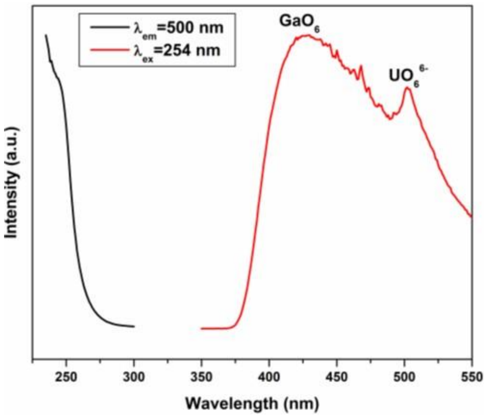

Figure 1: Fluorescence spectra of $ZnGa_2O_4$: U(5.0 mol %) under 254 nm excitation and 500 nm emission.

References:
[1] S.K. Gupta, et. al., Coord. Chem. Rev., 420, 213405 (2020).
[2] Leinders et al., *Inorg. Chem*. 2020, **59**, 4576–4587.
[3] Soldatov et al., *J. Solid State Chem*., 2007, **180**, 54-61.
[4] Abdou et al., *Mater. Chem. Front*., 2018,**2**, 2201-2211.

Thorium (IV) Ion Assisted Enhancement in Upconversion Fluorescence of Er^{3+} in YF$_3$

Annu Balhara[1,2], Sonika Gupta,[1,2], R. Acharya, Santosh K.Gupta[1,2]§

[1]Radiochemistry Division, Bhabha Atomic Research Centre, Mumbai-400085
[2]Homi Bhabha National Institute, Anushakti Nagar, Mumbai-400094

§Email:santoshg@barc.gov.in (SKG)

The lanthanide dopedupconversion (UC) phosphors have been gaining significant research interests owing to their diverse biomedical applications due to use of NIR excitations that have low photo-toxicity, less tissue damage and low autofluorescence. Hence, utilization of UC phosphors outperforms the traditional downconversion (DC) phosphors as the NIR excitation falling in the biological transparency region (~ 650-1700 nm) results in higher spatial resolution, deeper penetration, and high photostability. The UCemissions of Er^{3+}/Yb^{3+} doped phosphors have been well reported, but the problem of low UC emission output is the major hindrance in their real applications as bio-probes and further strategies to improve UC.The inclusion of non-luminous centers in host lattice is one of the promising strategies as the aliovalent dopant ion could result in alteration of defects and symmetry around the Er^{3+} ions which is very effective in enhancing the UCL. YF$_3$ is a potential host due to wide band gap and low phonon energy is useful in preventing large non-radiative losses. In this work, we have developed a YF$_3$:Er^{3+}, Yb^{3+}, Th^{4+} UCphosphor with different codoping concentrations of Th^{4+} ions wherein the presence of Th^{4+}and it's composition is well established using neutron activation analysis (NAA). In our case, we achieved strong green and red emissions at 540 and 646 nm under 980 nm excitations, that could be ascribed to $^2H_{11/2} \rightarrow {}^4I_{15/2}$, and $^4H_{9/2} \rightarrow {}^4I_{15/2}$, respectively (***Fig 1a***). The effect of codopingTh^{4+} ions is demonstrated by ***Fig 1b***and the enhancement in green and red UC emissions by 3 and 3.67 times was observed by codoping of 2 mol% Th^{4+} ions in YF$_3$:Er^{3+}, Yb^{3+} system. Interestingly, color tunability is achievable on changing Th^{4+} ions codoping concentrations and laser power. In addition, role of Th^{4+} ions have been investigated using positron annihilation lifetime spectroscopy (PALS). The observed results provide evidence for the potential of YF$_3$:Er^{3+}, Yb^{3+}, Th^{4+} UC phosphor for bioimaging, therapeutic and biosensing applications.

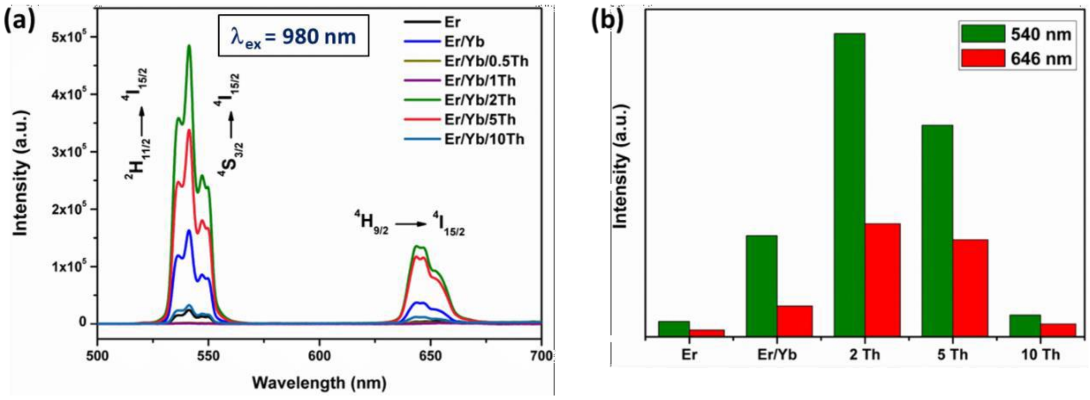

Figure 1: (a) Visible UC Emission spectra of YF$_3$:0.02Er and YF$_3$:0.02Er^{3+}, 0.2Yb^{3+}, xTh^{4+} (x = 0.5, 1, 2, 5 and 10 mol %),and (b) Variation of green and red UC emission

References:
[1] S.K. Gupta *et al.Coord. Chem. Rev.* **420** (2020)213405
[2] Thi Tuyen Ngo, *et al.ACS Appl. Mater. Interfaces,***13** (2021) 25 30051–30060.

Amino Based UiO-66 (Ce) for Uranium Adsorption from Aqueous Solution

Nitin Gumber[1, 2] and Rajesh V. Pai[1, 2, #]

[1] Fuel Chemistry Division, Bhabha Atomic Research Centre, Mumbai
[2] Homi Bhabha National Institute, Anushaktinagar, Mumbai
[#] Corresponding author email: rajeshvp@barc.gov.in

Metal Organic Frameworks (MOFs) built from organic ligands and metal ion clusters have recently shown applications in diverse fields like catalysis, drug delivery, separation etc [1]. These exhibit favorable characteristics like high surface area and pore volume for the sequestration of metal ions from aqueous solutions. In case of nuclear industry, for the sustainable power production, a secure source is uranium is required. The presence of uranium in sea water and other aqueous streams around the world constitutes ~ 4.5 billion tons which could be explored and extracted.

UiO-66 (Ce)-NH_2 MOF was synthesized at room temperature using aminoterepthalic acid as the linker and Ce (IV) as the metal ion along with small amount of HCl which acts a modulator. The MOF synthesized was characterized using different techniques like XRD, FT-IR, SEM, TGA etc. XRD pattern of synthesized MOF matches well with the simulated pattern of UiO-66 (Ce) exhibiting no effect of amino group on crystal structure as shown in Fig 1. The morphological analysis using SEM showed MOF to be spherical in nature.

The synthesized MOF was utilized for uranium remediation from aqueous media by varying the pH from 2-9 and the amount of uranium adsorbed at different pH is shown in Fig. 2. Further, adsorption kinetic studies were carried out. The adsorption studies showed that adsorption equilibrium could be attained by ~ 240 minutes. Maximum adsorption capacity ~ 330 mg/g was achieved as per the Langmuir adsorption isotherm which is in close agreement to the adsorption capacity obtained experimentally. In future studies related to selectivity and reusability would be carried out.

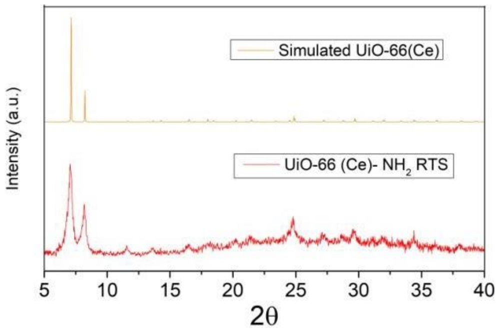

Fig. 1. XRD pattern of simulated UiO-66 (Ce) and synthesized UiO-66 (Ce)-NH_2

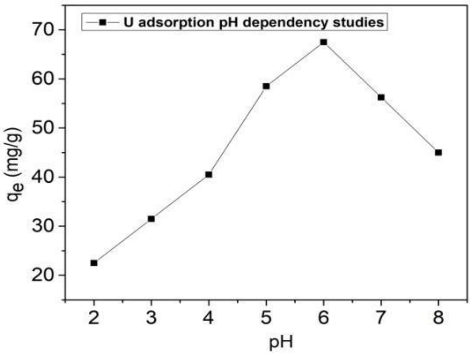

Fig. 2. Effect of pH on U adsorption at UiO-66 (Ce)-NH_2

References:

[1] Y. Li, G. Wen et.al., *Chem. Commun*., **58**, 2022,11488.

Insight into phase relation and cation ordering in U-RE-O system

Shafeeq Muhammed[1], Chiranjit Nandi[2], Rohan Phatak[1,§]

[1] *Fuel Chemistry Division, Bhabha Atomic Research Centre, Mumbai-85, India*
[2] *Radiometallurgy Division, Bhabha Atomic Research Centre, Mumbai-85, India*
[§] Email: raphatak@barc.gov.in

All over the world, Uranium dioxide and MOX fuels are the most widely accepted nuclear fuel forms in BWR, PHWR and FBR nuclear reactors. Aliovalent substitution in UO_2 matrix has been studied exhaustively and still continued for its variety of applications related to advanced nuclear fuels with improved properties and also as an inert matrix fuel. The resistance to oxidation and stabilization of cubic Fluorite phase (FCC) in rare-earth (RE) substituted UO_2 is still not well understood and many models have been predicted in literature [1 and literature therein].

In this study, La^{3+} and Nd^{3+} substituted uranium dioxide samples are investigated to understand the phase relations under reducing and oxidizing environment. Samples $(U_{1-y}RE_y)O_{2\pm x}$ for (RE=La and Nd, y=0.1 to 0.9) were synthesized by gel combustion method and were reduced in Ar+8% H_2 gas up to 1700°C for more than 10hr. Part of these reduced samples were subjected to oxidation in air at 1250°C for 10hrs and 160hrs. The lattice parameters O/M determination is done by measuring O/U of the samples using UV-Visible spectrometry. Lattice parameters (LP) of FCC phase were determined by Rietveld refinement of XRD pattern. For reduced samples pure FCC phase is observed for $0<y<0.8$ for La-samples and $0<y<0.7$ for Nd-samples, respectively. In case of $U_{0.2}Nd_{0.8}O_{2-x}$ sample, additional cubic Y_2O_3 type phase (C-type, where cation has 6-coordination) is observed along with FCC phase. Fig. 1 (a) and (b) show observed lattice parameters for La and Nd samples respectively along with the calculated LP using equation, LP 4/√3 (Rc Ro), where Rc is effective ionic radius of cation (considering composition, co-ordination and cation charge) and Ro is ionic radii of oxygen.

As observed from the figure, the LP for La samples lies close to the calculated LP for U^{4+} in 8 co-ordination and La^{3+} in 7 co-ordinations denoted as U8La7. The same notion cannot be extrapolated to Nd samples, where it can be seen that the observed LP are much smaller compared with calculated LP for U8Nd7 configuration. The smaller observed LP can be explained if partial contribution from U8Nd6 configuration is considered. These observations imply why there is C-type phase segregation for $U_{0.2}Nd_{0.8}O_{2-x}$ composition and the same is not seen for La counterpart. As the contribution from U8Nd6 increases and at a composition y=0.8, the C-type phase (with 6-coordinatinated cation) segregation occurs to attain thermodynamic equilibrium. The method of comparing the calculated LP and observed LP in oxidized samples also predicts why the charge ordering takes place between RE and U for samples close to composition y=0.6 when annealed for long hours.

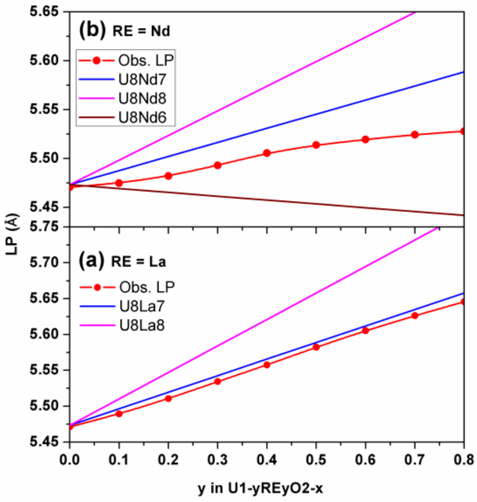

Fig. 1: Variation of observed and calculated LP for $U_{1-y}RE_yO_{2-x}$ system with conc. of RE.

References:
[1] Victor L. Vinograd et.al., *Front. Chem*, **9** (2021) 705024.

On Development of Certified Reference Materials for Trace Metallic Impurity Analysis of Pu Samples by ICP-OES

C. Banerjee[1,§], Mary G[1] , S. K. Singh[1] and G. Sugilal[1]

[1]*Fuel Reprocessing Division, Bhabha Atomic Research Centre, Mumbai-400085, India*
§ Email: chayan@barc.gov.in

Trace metallic impurities need to be analysed in various matrices of plutonium samples with very high confidence levels owing to the stringent requirements of –nuclear grade purity‖. Matrix matched Certified Reference Materials (CRM) are routinely used in the assessment of the quality of any acquired analytical data as a standard procedure for both quality control and method validation, but these are almost unavailable for applications in the nuclear domain due to various international restrictions requiring the countries analysing radioactive samples to indigenously develop their own CRM for different matrices. In view of this, Inter-Laboratory Comparison (ILC) exercises for precision and accuracy are carried out between various laboratories routinely analysing these samples. For ILC of Pu samples, it was decided that known matrix matched solutions of plutonium, with known additions of trace metallic impurities, should be prepared and then analysed by various relevant laboratories in India. Such matrix matched Pu samples are prepared and treated following approved standard procedures [1] and analysed by Inductively Coupled Plasma-Optical Emission Spectroscopy (ICP-OES) yielding excellent results [Table 1]. These matrix matched Pu standards, prepared and analysed by this methodology, after validation through ILC, can be designated as CRM for Pu samples. These indigenous CRM can be used for routine analysis at plant level overcoming the unavailability of international CRM for Pu.

Table 1: ICP-OES analysis of Pu samples (All values are in μg g^{-1} on PuO$_2$ basis, relative standard deviation is in the range of ±1-5 % for each element)

Element	Det. limit (in 10 g/L Pu)	Sample 1	Sample 2	Sample 3	Sample 4	Sample 5
Al	0.5	105.0	55.1	126.0	135.0	84.5
B	2.0	<2.0	< 2.0	< 2.0	< 2.0	< 2.0
Be	0.1	<1.0	< 1.0	< 1.0	< 1.0	< 1.0
Ca	1.0	265.0	227.0	376.0	297.0	275.0
Cd	1.0	< 1.0	<1.0	<1.0	<1.0	<1.0
Cr	1.0	36.3	23.2	40.6	18.4	35.9
Cu	0.5	18.5	7.6	20.4	28.1	15.4
Fe	0.4	245.0	124.0	243.0	127.0	223.0
Mg	0.4	62.3	76.1	82.5	38.0	76.6
Mn	0.5	9.1	8.3	7.6	7.4	8.6
Mo	0.5	26.9	6.4	13.3	27.6	20.4
Ni	0.5	395.0	72.0	192.0	20.3	225.0
Pb	1.0	21.9	21.2	30.2	10.6	30.8
Si	2.0	66.0	286.0	159.0	450.0	750.0
Zn	2.0	551.0	340.0	558.0	372.0	480.0

Reference:
[1] A. B. Patwardhan, M. V. Joshi, V. T. Kulkarni, K. Radhakrishnan, S. Sumathi and M. Jacob, BARC/1993/**E**/027.

Conformational Preferences and Interconversion Barriers in Trialkyl Phosphate Ligands

G. Gopakumar[1,2§], S. Jayalakshmi,[1] Aditya Ramesh Sachin,[2] and C. V. S. Brahmmananda Rao[1,2]

[1] *Indira Gandhi Centre for Atomic Research, Kalpakkam – 603102, Tamil Nadu, India.*
[2] *Homi Bhabha National Institute, IGCAR Campus, Kalpakkam – 603102, Tamil Nadu, India.*
[§] Email: gopakumar@igcar.gov.in

Nuclear fuel reprocessing and waste management are two important processes in closing the fuel cycle.[1,2] Solvent extraction is the key method of separating actinides during this step, where the Tri-*n*-butyl phosphate (TBP) ligand is used as an extractant. The remarkable ability of TBP to extract uranium and plutonium from the nitric acid medium, together with its exceptional stripping behaviour at lower acid concentrations, makes it an excellent solvent in reprocessing industry with unique characteristics.[3] The extraction mechanism is stepwise and is presumed primarily controlled by the coordination of the phosphoryl oxygen with actinide metal ions. In this regard, theoretical studies provide additional insights into the nature of metal–ligand interactions,[4,5] which often require an accurate characterization of ground state geometries of the ligand and corresponding metal complexes. The number of structures needed to scan the entire conformational landscape of ligands and metal complexes is enormous.[6] On the other hand, the existence of several low-energy conformers and a very small energy difference between them indicate that the C-C single bond rotations in alkyl groups are energetically viable processes under ambient conditions. This further indicated the possibility of dynamic equilibrium in the system, allowing interconversions of several low-energy conformers. Consequently, several low-energy conformers can coexist, most of which can ideally bind the metal nitrate unit to form complexes. In this context, density functional theory (DFT) calculations are applied to explore the conformational preferences and interconversion barriers of various tri-alkyl phosphate ligands and metal complexes. Our calculations indicated that the free energy barrier for rotations of the C-C bonds near the P=O group is more significant than that of the other C-C bonds in the system. Nevertheless, all the calculated rotational free energy barriers in phosphate ligands are energetically lower-lying, indicating the possibility of interconversion of these conformers under ambient conditions.

Acknowledgements: The authors gratefully acknowledge the computing time on IVY–Cluster, the High–Performance Computing facility at IGCAR, India.

References:

[1] D. D. Sood, S. K. Patil, *J. Radioanal. Nucl. Chem.*, **203** (1996) 547.
[2] C. F. Coleman, R. E. Leuze, J. Tenn. Acad. Sci., **53** (1978) 102.
[3] W. W. Schulz, J. D. Navratil, *Science and Technology of Tributyl Phosphate vol I: Synthesis, Properties, Reactions, and Analysis.* CRC Press, United States, 1984.
[4] L. E. Roy, N. J. Bridges, L. R. Martin, *Dalton Trans.*, **42** (2013) 2636.
[5] D. Raychaudhuri, G. Gopakumar, N. Sivaraman, C. V. S. Brahmmananda Rao, *J. Phys. Chem. A.*, **124** (2020) 7805.
[6] N. Ramanathan, *Matrix Isolation Infrared and ab initio Studies on the Conformations and Reactions of Selected Organophosphorus Esters*, Ph.D. Thesis, Materials Chemistry Division, Chemistry Group, IGCAR, Kalpakkam, India, 2013.

Complexation of Np(V) with Diglycolamide in an Ionic Liquid

S.A. Ansari [§], R.B. Gujar and P.K. Mohapatra

Radiochemistry Division, Bhabha Atomic Research Centre, Mumbai – 400 085, India
§ E-mail: ansaris@barc.gov.in

In the recent past, roomtemperature ionic liquids (IL) have gained the status of *–design‖* solvents, where the properties of the solvent can be tailored through the judicious choice of their cationic and anionic components [1]. The separation studies in ILs have shown unusually high extractability for metal ions, several orders of magnitude higher than those observed in molecular solvent like dodecane. The nature of bonding between the metal ions and the ligands in ILs is, however, not clearly understood.

Recent studies have shown that the complexes of $UO_2^{2+}$with TMDGA (N,*N,N',N'*-tetramethyl diglycolamide) formed in IL phase ($C_4mim{\cdot}Tf_2N$) are several times stronger than those formed in the aqueous medium. The complexes formed in IL medium were exothermic vis-à-vis endothermic in the aqueous medium. This feature indicates that the solvation of UO_2^{2+} ions in IL and water medium is different. However, the final complex formed either in IL or water medium was exactly same as seen on the solid UO_2^{2+}/TMDGA complex [2]. Looking at these features, it was of our interest to study the complexation behaviour of NpO_2^+ ion with TMDGA in IL, and compare its complexation features with those observed in aqueous medium.

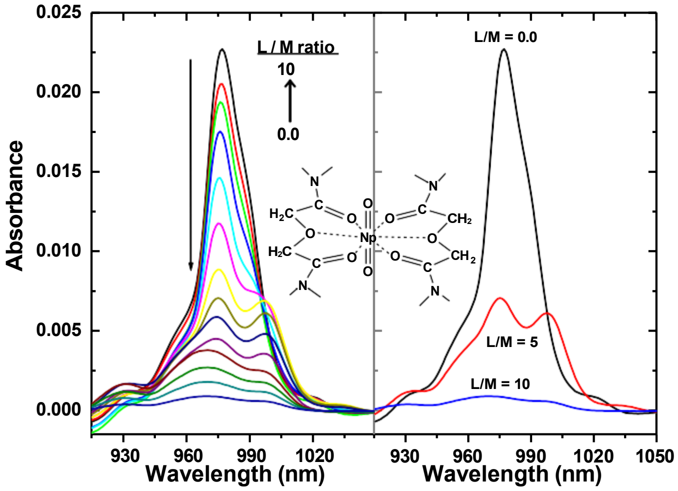

Fig. 1. Spectrophotometric titration of $NpO_2(Tf_2N)$ with TMDGA. Cuvette: 0.0224 mM $NpO_2(Tf_2N)$; Titrant: = 55 mM TMDGA, Medium: $C_4mim.Tf_2N$

As shown in Fig. 1, dioxo-cation of NpO_2^+ shows a strong absorption band at 977 nm, with an epsilon value of 980L/mole/cm. Addition of TMDGA ligand resulted in the formation of $(NpO_2L)^+$ complex (1:1 complex) and a new absorption band appeared by splitting the main peak at 997 nm. It is well known that the absorption spectra of NpO_2^+ arises due to break in the centre of symmetry around the central Np atom in he $[NpO_2(H_2O)_5]^+$ complex. The first complex of NpO_2^+/DGA is formed by replacing the 3 H_2O molecules from the primary coordinationsphere of the central Np atom, and the overall complex remains unsymmetrical, and shows absorption. Further addition of ligand results in the formation of a centrosymmetric $(NpO_2L_2)^+$ complex (1:2 complex), which has no absorption spectra. The stability constants (logβ) were calculated to be 3.82±0.11 and 6.58±0.24 for ML_1 and ML_2 complexes vis-à-vis 1.37 and 2.47 obtained in aqueous medium, respectively. The nature of the complex was found to be identical in both the medium, IL and water medium.

References:

1. X. Sun, H. Luo and S. Dai, ***Chem. Rev.***, 112 (2012) 2100.
2. S.A. Ansari, et. al., ***New J. Chem.***, 46 (**2022**) 950.

Enhancement of Thermoluminescence Property of $LiMgPO_4$ by Tm Doping: A DFT Study

Brindaban Modak [§]
Theoretical Chemistry Section, Chemistry Division, Bhabha Atomic Research Centre,
Mumbai 400 085, India
[§] Email: bmodak@barc.gov.in

Abstract: $LiMgPO_4$ doped with rare-earth elements has become a material of choice for dosimetric applications [1]. To obtain a material with enhanced properties, the knowledge on the nature of defects in doped $LiMgPO_4$ is of much importance. The thermoluminescence (TL)/optically stimulated luminescence (OSL) signal originates from the recombination centres /luminescence centres existing deep in the forbidden band gap, and the whole process depends on the electronic structure of the material. Present study aims to investigate geometry and electronic structure of $LiMgPO_4$ doped with Tm using density functional theory (DFT).

Computational Section: All the calculations have been carried out using the VASP electronic structure code [2]. A k-point set of 6×6×6 is found to be sufficient for the relaxation step. Perdew-Burke-Ernzerhof (PBE) functional under generalized gradient approximation (GGA) has been chosen during the geometry optimization procedure. For electronic structure calculations, PBE0 hybrid functional has been employed to overcome the limitation of standard density functional [3].

Results and Discussion: The calculated band gap for $LiMgPO_4$ using PBE0 is found to be 8.12 eV and direct in nature, which is very close to the experimentally reported value (8.20 eV). Fig. 1 shows densities of states (DOS) for Tm doped $LiMgPO_4$. Tm introduces discrete partially occupied impurity states at energy at the mid gap region. Thus, the total gap divides into three energy regions, 3.92 , 1.02, and 1.15 eV. Analysis of PDOS indicates that the impurity states at the mid gap region are mainly contributed by Tm 4f states. The localized impurity states can serve as trap centers for electrons and hole or acts as recombination centers. Thus, present study reveals that the presence of the trap states is attributed to enhanced thermoluminescence property of Tm-doped LiMgPO4.

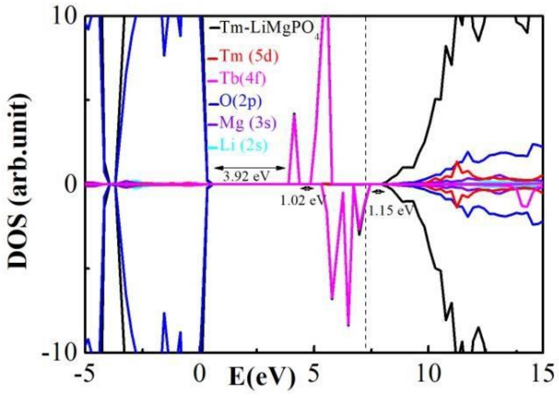

Fig.1: Density of states for Tm-doped $LiMgPO_4$

Acknowledgements: Author thank Prof. A. K. Tyagi, and Prof. T. Bandyopadhyay for their valuable discussions.

References

[1] D. G. Kellerman, M. O. Kalinkin, D. A. Akulov, R. M. Abashev, V. G. Zubkov, A. I. Surdo, N. I. Medvedeva and M. V. Kuznetsov. *J. Mater. Chem. C*, 2021, 9, 11272
[2] G. Kresse and D. Joubert, *Phys. Rev. B*, 1999, 59, 1758.
[3] P. Modak, and B. Modak, *Phys. Chem. Chem. Phys.*, 22, 16244 (2020)

Effect of interfering metal ions on the Extraction and Fluoroscence behavior of Eu(III) in a Modifier based Extraction System

Alok Rout[1,§], S. Kumar[1,2], N. Ramanathan[1,2]

[1]*Materials Chemistry & Metal Fuel Cycle Group, Indira Gandhi Centre for Atomic Research, Kalpakkam 603 102, India*
[2]*HomiBhabha National Institute, Indira Gandhi Centre for Atomic Research, Kalpakkam 603102, India*
[§] Email: alokrout@igcar.gov.in

The role of interfering metal ions in the extraction and coordination process of Eu(III) ion in a modifier based extraction system was explored by combined extraction and fluorescence spectroscopy study. A DGA ligand: *N,N,N',N'* tetra(ethylhexyl)diglycolamide(T2EHDGA) along with tri-*n*-butylphosphate (TBP) as the phase modifier in *n*-dodecane (*n*-DD) medium was employed for the study [1]. The extraction behavior of Eu(III) by (0.1 M T2EHDGA + 1.1 M TBP)/ *n*-DD phase was compared in the presence or absence of Zr(IV) which is a major troublesome metal ion present in HLLW (High Level Liquid Waste) solution during Ln(III)/An(III) partitioning (Figure 1). It was observed that the extraction and hence loading of Eu(III) was less in presence of a fixed concentration of Zr(IV) as compared to that in the absence of Zr(IV) in the feed phase. In contrast to this observation, the luminescence intensity of the extracted Eu(III) was found to be higher in presence of Zr(IV) (Figure 2). This certainly indicates the sensitization effect of Zr(IV) that essentially helps in enhancing the peak intensity of Eu(III) luminescence. However, the presence of another important fission product metal ion such as Pd(II) reduced the emission intensity of Eu(III) with noisy baseline due to severe quenching effect of the former. The systematic variations in some of the important experimental parameters have been furnished to draw out the precise role of these interfering metal ions on the coordination behavior of Eu(III) and the results would be presented in the conference.

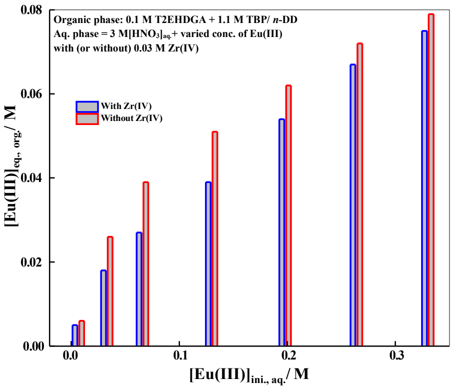

Figure 1. Variation in Eu(III) equilibrium concentration in organic phase as a function of initial feed Eu(III) concentration.

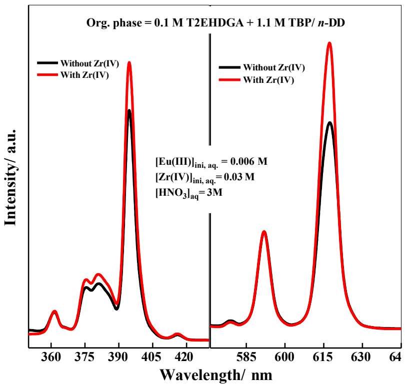

Figure 2. Excitation (A) and emission (B) spectra of Eu(III) in organic phase after extraction.

Acknowledgements: The authors sincerely thank Dr. A. Suresh, Head, Fuel Chemistry Division for his keen interest in this work.

References: [1] Alok Rout, S. Kumar and N. Ramanathan, *ChemistrySelect* 7**(2022)** e20220279.

Synthesis of Novel Covalent Organic Polymer (COP) for Uranium Removal from Acid Streams

Gauravi Yashwantrao[1], Satyajit Saha[1], Shiny S. Kumar[2] and Ankita Rao[2, §]

[1]*Department of Speciality Chemicals Technology, ICT Mumbai, Maharashtra, India*
[2] *Radiochemistry Division, BARC, Mumbai, India, Country*
[§] Email: ankita@barc.gov.in

Devising sustainable actinide separation strategies form the cornerstone for global acceptance of nuclear energy. While search for adsorbents for actinides is ever important, the removal of actinides from waste streams of nuclear fuel cycle activities are challenging task owing to the harsh radiochemical conditions as well as the co-existence of multiple metal ions in the aqueous stream. The studies for Covalent Organic Polymers (COPs) pertaining to the area have been limited to U removal from sea water and low pH solutions.[1] Unlike Metal Organic Frameworks (MOFs), COPs offer an excellent platform as they are metal free and can be made incinerable with respect to CHON principle.[2] Also, the strong covalent bonds in COPs endow them with desirable stability under various harsh conditions and are easy to engineer according to the targeted task.

Herein, we present the preliminary studies with COP (Fig.1) which has been designed with amide functionality appended to the polymer backbone which acts as a potential site for the capture of uranium. COP‘s containing aromatic backbone are envisaged to have enhanced radiochemical stability. The COP has been synthesised and characterised by IR spectroscopy, solid state NMR and porosity was determined by the BET surface area analysis.

Periodic acid stability has been examined at 4 M HNO_3 medium for 7 days (confirmed by IR spectra). Batch sorption studies were carried out wherein uranium extraction was found to be 84 % (2 hrs. equilibration, 4 M HNO_3). The encouraging stability in acidic environments and performance for U uptake make the newly developed COP an attractive candidate for uranium removal from acid waste streams. Further studies are in progress.

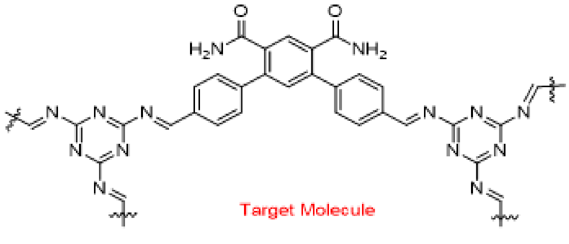

Figure 1. Designed Covalent Organic Polymer (COP) used for the Uranium removal from the acid streams.

Acknowledgements: SS acknowledges SERB (CRG/2022/000579) and DST-PURSE for the funding. AR is thankful to Dr. Neetika Rawat, Head, IICS and Dr. P. K. Mohapatra, Head, RCD for their support and encouragement.

References:

[1] Z. D. Li, H. Q. Zhang, X. H. Xiong, F. Luo, J. *Solid State Chem.*, **2019**, *277*, 484.
[2] N. B. McKeown, P. M. Budd, *Chem. Soc. Rev.*, **2006,** *35*, 675.

Synthesis, Characterization and Iodine Adsorption Studies in Th-based Metal Organic Framework

A. Sharma[1,3], B. G. Vats[2, 3§], S. C. Parida[1,3]

[1]*Product Development Division, Bhabha Atomic Research Centre, Mumbai 400085, India*
[2]*Fuel chemistry Division, Bhabha Atomic Research Centre, Mumbai 400085, India*
[3]*Homi Bhabha National Institute, Bhabha Atomic Research Centre, Mumbai 400085, India*
Telephone- +91-22-25599079
[§]Email: bgvats@barc.gov.in

Nuclear energy is a green and sustainable energy source to meet the ever increasing global energy demand. With increasing production of nuclear energy, nuclear waste also tends to increase in near future. Radioactive gaseous waste like I-129, Kr-85, Tc etc. which accumulates in atmosphere due to their longer half life needs to be captured during reprocessing of spent nuclear fuel. Researchers have studied various solid porous materials like activated charcoal, zeolites, macroreticular resins etc. for their intended gas sorption applications [1]. However, their poor iodine retention and absorption capacity limits their practical applicability. In recent years, Metal Organic Frameworks (MOFs) has emerged as a new class of porous material with tunable porosity, favorable adsorption kinetics and uniform pore architecture which make them promising materials for gas adsorption.

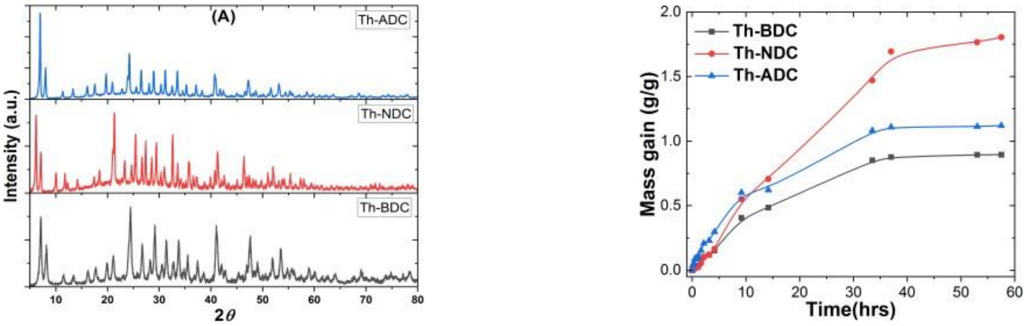

(a) **(b)**

Fig.1: (a) XRD patterns of synthesized MOFs. (b) Iodine adsorption curves of the investigated MOFs.

We have synthesized three thorium based UiO-66 series MOFs with $Th_6(\mu_3\text{-}O)_4(\mu_3\text{-}OH)_4$ cluster and organic linkers, namely, 1,4-benzenedicarboxylic acid (BDC), 1,5-napthalenedicarboxylic acid (NDC) and 9,10-antharcenedicarboxylic acid (ADC) by solvothermal reaction at 120°C in DMF-water solvent. Then synthesized MOFs were characterized employing powder X-ray Diffraction (XRD) (Fig. 1 (a)), Infrared (IR) spectroscopy and surface area measurement. These MOFs were then studied for vapor phase iodine absorption. The iodine adsorption kinetics of Th-BDC, Th-NDC and Th-ADC has been shown in Fig. 1(b). Only after 30 hours the equilibrium is reached. The iodine absorption capacity follows the trend Th-NDC>Th-ADC>Th-BDC. This trend is a combined effect of surface area, pore volume and electron density around the pore in this series of MOFs.

Reference:

1. X. Zhang, J. Maddock, T. M. Nenoff, M. A. Denecke, S. Yang and M. Schröder *Chem. Soc. Rev.*, **51** (2022) 3243-3262.

Cu^{2+} Grafting in Th-Metal Organic Framework and its Effect on Iodine Adsorption

A. Sharma[1, 3], B. G. Vats[2, 3 §], S. C. Parida[1, 3]

[1]*Product Development Division, Bhabha Atomic Research Centre, Mumbai 400085, India*
[2]*Fuel chemistry Division, Bhabha Atomic Research Centre, Mumbai 400085, India*
[3]*Homi Bhabha National Institute, Bhabha Atomic Research Centre, Mumbai 400085, India*
Telephone-+91-22-25594080, +91-22-25599079
[§] Email: bgvats@barc.gov.in

Metal organic frameworks (MOFs) have emerged as promising materials for gas adsorption mechanism due to their relatively high specific surface area (SSA), tailorable pore architecture and tunable chemistry. In this direction, UiO-66 type MOF are found to be relatively more stable. Amongst these, Thorium based MOFs have emerged as a unique subclass due to their variable coordination numbers and availability of variety of frontier orbital for bonding. Moreover less hydrolysis of Th^{4+} as compared to Zr^{4+} and Hf^{4+} make thorium based MOF easy to synthesize. Metal grafting on MOF pore recently exploited for applications like catalysis and photoluminescence applications but the gas sorption studies are rarely investigated.

We have synthesized thorium based UiO-67 MOF (Th-BiPy) with $Th_6(\mu_3\text{-}O)_4(\mu_3\text{-}OH)_4$ cluster nd 2, 2‘-bipyridine-5, 5‘-dicarboxylic acid (BiPy) as organic linker by solvothermal reaction at 120°C in DMF-water solvent and used AcOH as moderator. Thereafter, Cu^{2+} metal was grafted to synthesized Th-BiPy MOF by taking 50 mg of MOF and dispersing it in 20ml of 10 mmol $CuCl_2$ solution in DMF and left for 48 hrs for Cu^{2+} grafting on bipyridyl units of MOF. Th-BiPy and Th-BiPy/Cu MOFs were characterized employing powder X-ray diffraction (XRD) and Infrared (IR) spectroscopy.

(a) (b)

Fig.1: (a) XRD patterns of synthesized MOF. (b) Iodine adsorption curves of the investigated MOFs.

XRD patterns of synthesized MOFs are shown in fig. 1(a) and are in good agreement with the literature, confirming the formation of MOFs. XRF studies of Th-BiPy/Cu MOF has shown that the relative concentration of Th:Cu is near to 1:1 which signifies that the Cu^{2+} ion has grafted in all the bipyridyl moieties of the parent MOF. The calculated BET surface area and pore volume of Th-BiPy MOF was found to be 409.32 m^2/g and 0.23 cm^3/g respectively. From the Iodine adsorption studies, it can be seen that the iodine adsorption capacity of metal grafted MOF has decreased to around 1/3 of the parent MOF (Fig. 1(b)) which can be attributed to the fact that Cu^{2+} ion has also occupied the pores of host MOF which results in lesser surface area for the guest Iodine atoms.

References:

[1] Z. Li, X. Guo, J. Qiu, H. Lu, J. Wang and J. Lin; *Dalton Trans.*, **51** (2022) 7376-7389.

Sorption Of Plutonium From Aqueous Medium Using Nitrogen Doped Graphene Nano Walls

V. Sri Datta Chaitanya[1,2 §], P. A. Manojkumar[3§], G. Mangamma[3], G. Srinivasa Rao[1],
C. P. Kaushik[2,4]

1. Nuclear Recycle Board, Bhabha Atomic Research Centre Facilities, Kalpakkam, Tamilnadu, India
2. Homi Bhabha National Institute, Mumbai, India
3. Indira Gandhi Centre for Atomic Research, Kalpakkam, Tamilnadu, India
4. Bhabha Atomic Research Centre, Mumbai, India
[§] Email: vsdchaitanya@igcar.gov.in, manoj@igcar.gov.in

Recovery of trace amounts of actinides from aqueous raffinate streams is an important aspect of nuclear waste management. Alpha emitting radionuclides such as plutonium was given special attention due to their radiotoxicity. Though several methods are suggested to recover trace levels plutonium from aqueous streams, sorption is proved to be the effective methodology to achieve good decontamination factor [1]. Owing to large surface area and active sites, graphene-based materials have been emerged as an excellent choice for actinides (Cerium) sorption [2]. Cerium is considered as a surrogate of plutonium for chemical studies [3] and hence, the sorption studies have been extended to plutonium.

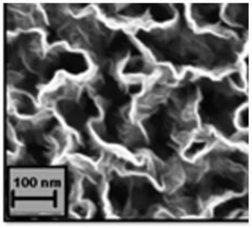

Fig.1 SEM image of NGNWs

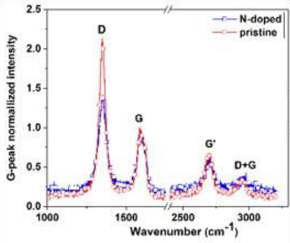

Fig. 2 Raman spectra of GNWs and N-GNWs

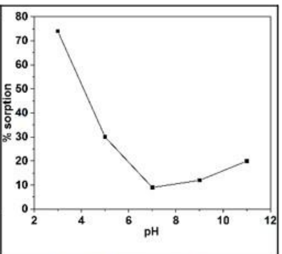

Fig. 3 Percentage sorption

In the present study, nitrogen doped graphene nano walls (NGNWs) were synthesized on carbon fibre paper substrate using plasma enhanced chemical vapour deposition [4]. The FESEM image shows the large surface area and corrugated nature of graphene nanowalls (Fig.1). The Raman peaks confirm defective and nano nature of sp^2 bonded GNWs (Fig.2). The NGNWs, 10 x10 (mm) size were dropped to an aqueous solution of Pu (IV) (0.1-1 ppm) and gently agitated for 30 minutes. The residual solution was analysed by alpha radiometry and compared with the pristine solution. Fig. 3 shows the acidic nature of the solution enhances the sorption and more than 75% sorption was observed at pH below 3. The effect of the complexing ligand on the sorption was modelled using Visual Minteq 3.1 and it is found that the cationic hydroxyl species of plutonium are responsible for improved sorption. The study shows excellent sorption capability of NGNWs for the separation of trace levels of Pu from aqueous solutions.

Acknowledgement: The authors acknowledge the consistent support and encouragement given by NRB management

References:

1. Imran ali, *Chem.Rev.***112** (2012) 5073
2. V S D Chaitanya, P.A. Manojkumar, et.al., *Abstracts of 75th annual theme meeting,* pp. 282., *Indian Institute of Metals (2021), Jamshedpur, India.*
3. R. Marsac, *Dalton Trans.* **46** (2017) 13553
4. P. A. Manojkumar, et.al., *Diam. Relat. Mater.* **97** (2019) 107452

Boosting Energy Transfer from Defect to Eu^{3+} Through U^{6+} Doping in $MgAl_2O_4$ Spinel

Reshmi Thekke Parayil [1,2], Santosh K.Gupta[1,2§], G.D. Patra,[3] and M. Mohapatra[1,2, §]

[1] Homi Bhabha National Institute, Anushakti Nagar, Mumbai-400094
[2] Radiochemistry Division, Bhabha Atomic Research Centre, Mumbai-400085
[3] Technical Physics Division, Bhabha Atomic Research Centre, Mumbai-400085

[§] Email: santoshg@barc.gov.in and manojm@barc.gov.in

Commercial White LEDs-based on yellow phosphor $Y_3Al_5O_{12}:Ce^{3+}$ ($YAG:Ce^{3+}$) excited by blue InGaN chip. However, the lack of red spectral component leads to poor colour rendering index (CRI, $R_a < 80$) and high correlated colour temperature (CCT > 4500 K). These issues can be solved by using Eu^{3+} doped red emitting phosphor. **[1]**

Trivalent lanthanide ions show unique optical properties due to their narrow emission, high color purity, high excited-state lifetimes, high photo stability, and large Stokes shift. **[1]** Due to the forbidden nature of ***f→f*** transition there is a need for the sensitizer which enhances the emission by the energy transfer mechanism. Here we are utilizing the UO_2^{2+} co-doping with Eu^{3+} in $MgAl_2O_4$ host matrix owing to better energy mismatch. $^5D_0$ emissive levels have the value of 17800 cm^{-1} which is close to the emissive state of UO_2^{2+}; with the value of 19200 cm^{-1}.**[2]** The $MgAl_2O_4$:1%U+x%Eu (x=1, 2, 5, 10) spinel has been synthesized by solid state reaction route in which MgO, Al_2O_3, Eu_2O_3 and U_3O_8 is used as the precursors. ***Figure 1a*** shows the emission spectra of as prepared combustion synthesized $MgAl_2O_4$:1%U+x%Eu (x=1, 2, 5, and 10) spinel. From the emission spectra; it can be clearly seen that uranium stabilizes as U^{6+} ions as UO_6^{6-}. Furthermore it is observed that with increase in the concentration of Eu the intensity uranyl emission has been diminished whereas the emission of Eu is enhanced, which is a sign of energy transfer from U^{6+} to Eu^{3+}. The emission intensity increased up to a 5.0 mol % Eu^{3+} doping and then decreased due to concentration quenching. ***Figure 1b*** represents the emission spectra of $MgAl_2O_4$:1U+1Eu annealed at 800^0C. Here the uranium coordination changes from UO_6^{6-} to UO_2^{2+} which can be seen from the spectral features displaying equidistant vibronic coupling regular at 827 cm^{-1}.

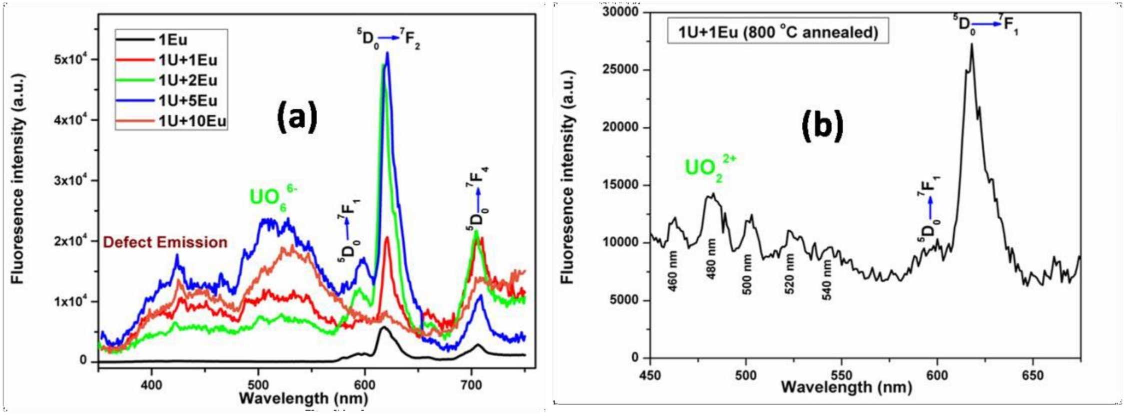

Figure 1: Emission spectra of (a) as prepared $MgAl_2O_4$:1%U+x%Eu (x=1, 2, 5, and 10) spinel and (b) 800 °C annealed $MgAl_2O_4$:1%U+1%Eu

References:
[1] S.K. Gupta, P.K. Pujari and R.M. Kadam, *Coord. Chem. Rev.* **420** (2020) 213405
[2] Reshmi Thekke Parayil *et al. ACS Appl. Opt. Mater.* **1** (2023) 179

Trap level spectroscopic properties of Uranium incorporated $LiZnPO_4$

Dinesh K. Patre[1, §], Reshmi T. P.[2], Hemachandar V.[1], Saparya Chattaraj[1], Mohapatra M.[2,3], Ashokkumar P.[1], and Kolekar R. V.[1]

[1]Health Physics Division, [2]Homi Bhabha National Institute, [3]Radiochemistry Division,
Bhabha Atomic Research Centre, Trombay, Mumbai 400085
[§] Email: dpatre@barc.gov.in

Trap level spectroscopic properties such as activation energy (Ea) and frequency factor (s) play important roles in the thermoluminescence (TL) process. This in turn dictates the dosimetric behaviour of a phosphor material. Recently, phosphate based inorganic phosphors have been demonstrated to give excellent results in terms of TL dosimetry [1]. In Particular, $LiZnPO_4$ (LZP) based phosphors have been reported to be excellent hosts not only for TL but also for other applications [2]. In this work, we report the photo luminescence (PL) and TL properties of uranium incorporated LZP synthesized via a solid state reaction route using stoichiometric amounts of Li_2CO_3, ZnO, $(NH_4)_2H_2PO_4$ and U_3O_8. XRD studies were done on a Proto tabletop instrument to confirm the phase purity of the material. PL investigations were done on an Edinburgh F 900 Fluorescence spectrometer and the TL glow curves were recorded using a Nucleonix unit.

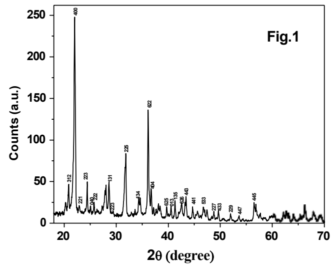

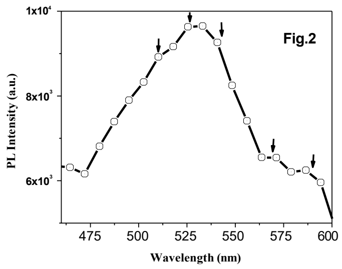

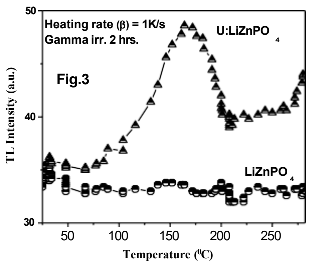

Fig 1. XRD patterns of U doped LZP ceramics sintered at 900^0C for 5 hrs, Fig 2. PL emission spectrum of (1 mol%) U:LZP, Fig.3.TL glow curve of U doped $LiZnPO_4$ and blank

Figure 1 shows the powder XRD patterns of (1mol %) U:LZP which suggested the formation of a single phase compound without any impurity phase. The observed patterns matched with the standard ICDD file no-65764. The emission spectra for the system with λ_{ex}=242 nm (Fig. 2) is characterized by peaks at 502, 524, 547, 569 and 597 nm. These features suggested that in this phosphate system, uranium is stabilized as the octahedral uranate (UO_6^{6-}) ion. The TL data for the irradiated system (2kGy) is given in figure 3 that showed a glow peak at 170^0C. The trap parameters associated with this peak were evaluated to be Ea=0.93 eV and s=$6.4x10^8$ s^{-1} by adopting standard peak shape method. The structural features of the glow curve suggested a second order kinetics for the destruction of the radical with a higher probability for retrapping. The activation energy values indicated formation of deep trap sites for the radical ion. These results indicated that the material has enough potential to act as a TL dosimetric material.

Acknowledgements: Authors extend their gratitude to Dr. M. S. Kulkarni, Head, HPD and Dr. P. K. Mohapatra, Head, RCD for their support and encouragement.

Reference

1. T. S. Chan, R. S. Liu, I. Baginskiy, N. Bagkar, and B. M. Cheng, Journal of The Electrochemical Society, 155 (10) J284-J286 (2008)
2. C. C. Xia, D. H. Jiang, G. H. Chen, Y. Luo, B. Li, C. L. Yuan, C. R. Zhou J Mater Sci: Mater Electron (2017) 28:12026–12031

Complexation Behaviour of Thorium with Phosphoryl Ligands

Aditya Ramesh Sachin[1,2], G. Gopakumar[1,2,§], Balija Sreenivasulu[1] and C V S Brahmananda Rao[1,2]

[1] *Fuel Chemistry Division, MC&MFCG, IGCAR, Kalpakkam – 603102*
[2] *Homi Bhabha National Institute, IGCAR, Kalpakkam - 603102*
[§] Email: gopakumar@igcar.gov.in

Thorium plays a crucial role in the Indian nuclear power program. Thorium is extracted *via* solvent extraction from its most important ore, *viz.* monazite.[1] During this step, tri-*n*-butyl phosphate (TBP) is used as the extractant, which possess several limitations, such as higher aqueous solubility (0.4 g/L), third-phase formation, etc. Search for an alternative to TBP is a long-standing research problem. Experimentally this task is achieved by systematically modifying the ligands. On the other hand, understanding the electronic structure and properties of molecular systems, by applying quantum chemical methods, will be highly useful in fine-tuning the properties of TBP. The insights derived from such calculations will be useful in shortlisting potential ligands for experimental studies. In this context, we have performed quantum chemical computations on the various phosphoryl oxygen donor ligands such as TBP, TBPO, CMPO, HBPA and their complexes with Th(IV) nitrate. The lowest energy geometries were identified, and complexation energies were evaluated by applying density functional theory (DFT) calculations. The computed complexation energies were subsequently decomposed into various stabilizing and destabilizing components. ORCA 4.2.1 [2] and ADF 2016 [3] program packages were used to perform these computations.

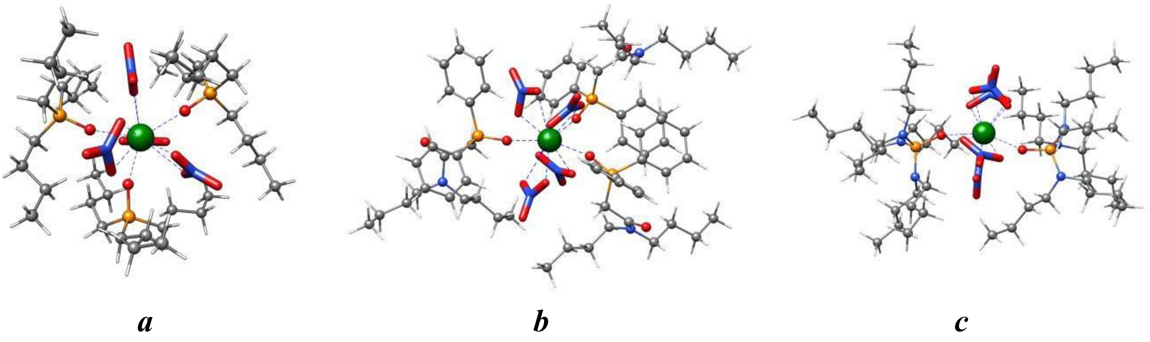

Figure 1. The lowest energy geometries of (*a*) $Th(NO_3)_4.3TBPO$, (*b*) $Th(NO_3)_4.3CMPO$ and (*c*) $Th(NO_3)_4.2HBPA$. Color code: Green is thorium, red is oxygen, orange is phosphorus, grey is carbon, and white is hydrogen.

References:

1. Schulz, Wallace W.. "Thorium processing". *Encyclopedia Britannica*, 26 May. 2022, https://www.britannica.com/technology/thorium-processing. Accessed 27 February 2023.
2. Neese, F. ―Software update: the ORCA program system, version 4.0‖ *Wiley Interdisciplinary Reviews: Computational Molecular Science*, 2017, Vol. 8, Issue 1, p. e1327.
3. Theoretical Chemistry; SCM. ADF 2016; Vrije Universiteit: Amsterdam, The Netherlands, 2016; http://www.Scm.Com/.

Understanding the bonding of Am(III) and Cm(III) ions with donor center modulated aza-crown based ligands

Saparya Chattaraj[1,3] and Arunasis Bhattacharyya[2,3§]

[1] *Health Physics Division, Bhabha Atomic Research Center, Mumbai, India*
[2] *Radiochemistry Division, Bhabha Atomic Research Center, Mumbai, India*
[3] *Homi Bhabha National Institute, Mumbai, India*
[§] Email: arun12@barc.gov.in

Effective transmutation of Am necessitates the mutual separation of Am and Cm, which is one of the most challenging task because of their close ionic potential. The knowledge about the bonding characteristics of these chemically similar trivalent ions is a prerequisite for designing selective ligands for their mutual separation. A detailed computational study was, therefore, carried out on the interaction of trivalent Am(III) and Cm(III) ions with N,N′- bis[(6-carboxy-2-pyridyl)methyl]-1,10-diaza-18-crown-6 (0SL) and another ligand where the ‗O‘s in the aza-crown moiety of N,N′- bis[(6-carboxy-2-pyridyl)methyl]-1,10-diaza-18-crown-6 [named 4SL] are replaced by soft donor ‗S‘.

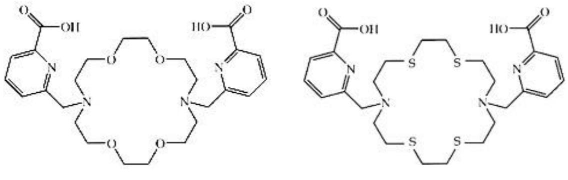
0SL **4SL**

Fig. 1: Representation of the ligands considered.

Geometry optimisation for all the systems was performed using BP86 functional where def-TZVPP basis sets were used for Am (f^6) & Cm (f^7) and def2-TZVP for the rest of the atoms. The bond parameters were benchmarked with the data in [1]. Single point calculations were done at B3LYP/TZ2P level incorporating scalar zeroth-order regular approximation (ZORA) to account for the relativistic effect of the heavy ions and the COSMO model for accounting the solvent effect. Higher SOMO-LUMO energy gaps of the Cm complexes, indicated their lower reactivity. Energy decomposition analysis showed that electrostatic interactions have the predominant contribution to the bonding energies. Upon probing the subtle orbital contribution, it was noted that its magnitude is highest for the Am-4SL complex. Wiberg bond indices and delocalisation indices were higher for Am-L systems than Cm-L, which clearly indicates the higher Am(III) selectivity of 4SL as compared to 0SL Natural population and bond orbital analyses indicated, ligand to metal charge transfer to be the highest for Am-4SL, followed by Cm-4SL, Am-0SL and Cm-0SL. Predominant mode of orbital interaction for these systems is through metal d-orbitals with donor p-orbitals. f- orbital participation in the Cm complexes is much lower in comparison to that of the Am complexes due to the half-filled nature of the metal orbital.

Acknowledgements: Authors extend their gratitude to Dr. Ashokkumar P., Shri R. V. Kolekar, Dr. M. S. Kulkarni and Dr. P. K. Mohapatra for their support and encouragement.

Reference:
[1] M. P. Jensen et al, *Inorg. Chem.*, **53**(2014) 6003

Uranium extraction from acidic feed relevant to front-end applications with TOPO-menthol sorbed solid support

Ankita Rao, [§], Shiny S. Kumar

Radiochemistry Division, Bhabha Atomic Research Centre, Trombay, Mumbai – 400 085

[§]E-mail: ankita@barc.gov.in

Natural uranium, containing 0.7 % of fissile ^{235}U, is a precious resource that fuels nuclear power plants. Phosphate based extractants have conventionally played a crucial role for extraction and purification of uranium by liquid-liquid extraction. Solid phase extraction (SPE) is an acknowledged resort to minimize extractant and volatile organic diluent inventory and enhance ease of operation. SPE also cuts down high viscosity and density related hindrances with eutectic solvent associated with bulk liquid-liquid extraction. With an aim to develop separation scheme for uranium uptake from acid medium, tri-octyl phosphine oxide (TOPO) – menthol (1:2) based eutectic solvent was sorbed onto Chromosorb W solid support. Chromosorb W is a commercially available diatomaceous silica based solid support known for its radiochemical stability. TOPO is a popular organophosphorus extractant for actinides and functions as a hydrogen bond acceptor while menthol was chosen as the hydrogen bond donor as it is endowed with advantageous properties of biodegradability and hydrophobicity. Batch sorption studies of U(VI) from nitric acid medium were carried out showing attainment of equilibrium at 60 min., following a pseudo second order rate equation, Langmuir adsorption isotherm and a static capacity of 19 mg g^{-1}. Effect of nitric acid molarity on U uptake was studied and extraction was found to increase with acid molarity indicating solvating mechanism of extraction (k_D = 1240, 4 M HNO_3). Crude yellow cake matrices, sodium diuranate (SDU), magnesium diuranate (MDU) and heat-treated uranium peroxide (HTUP) were digested in nitric acid. The results of U uptake by SPE are depicted in Table 1. Recyclability was established and stripping was effective with 0.5 M HNO_3. Selectivity of U uptake w.r.t. other impurities is being examined.

Table 1. Uranium distribution co-efficient, k_D with TOPO-menthol sorbed on Chromosorb W

Matrix	U content (%)	U k_D
SDU	49	854
MDU	57	947
HTUP	73	1020

(Results are average of duplicate runs; Eqm. Time 2 hrs.; 4 M HNO_3 medium)

Acknowledgement:
Authors acknowledge the support and encouragement from Dr. Neetika Rawat, Head, IICS and Dr. P. K. Mohapatra, Head, RCD.

References:

[1] A. Abbott, G. Capper, D.L. Davies, R.K. Rasheed, V. Tambyrajah, *Chem. Commun.* (2003) 70.
[2] Y.S. Asci, M. Lalikoglu, *Ind. Eng. Chem. Res.* (2021) 1356.

Combination of branched DGA and aqueous soluble BTP (SO_3PhBTP) for Am^{3+}/Cm^{3+} separation

A. Bhattacharyya[§], A.S. Kanekar and P.K. Mohapatra[§]

Radiochemistry Division, BARC, Trombay, Mumbai, India
[§] Email: arun12@barc.gov.in; mpatra@barc.gov.in

Separation of Am^{3+} and Cm^{3+} is the most challenging step in the back end of the nuclear fuel cycle owing to their very close chemical behavior. Their separation is, however, crutial for the safe management of the nuclear waste because of the vast difference in their major isotopes present in the nuclear waste [1]. Significant amount of research is being directed towards the development of the process for their mutual separation. In our previous study we observed that the selectivity of TODGA for Am^{3+} over Cm^{3+} enhanced in presence of aqueous soluble BTP derivative [2]. It will, therefore, be of interest to evaluate the branched DGA derivative (T2EHDGA) for the sedlective extraction of Am^{3+} over Cm^{3+} in presence of aqueous soluble BTP as T2EHDGA is inherently more selective towards Am^{3+} over Cm^{3+}. In the present work, therefore, separation studies of Am^{3+} and Cm^{3+} were performed using T2EHDGA in the organic phase and SO3PhBTP in the aqueous phase of different nitric acid concentration. Diluent variation studies showed highest separation factor (S.F.) in the solvesso100 medium (Fig. 1). However, considering the D_{Am} value and process suitability, *n*-dodecane was chosen for further studies. Higher slope in the T2EHDGA concentration variation experiment in case of Am^{3+} as compared to that in case of Cm^{3+} (Fig. 2) suggests the preference of T2EHDGA for Am^{3+} and SO_3PhBTP for Cm^{3+}.

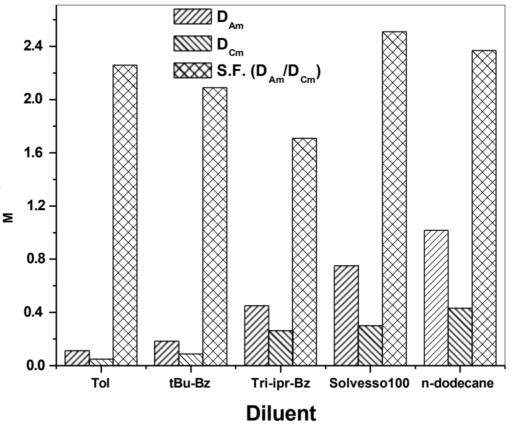

Fig. 1: Effect of the extraction of Am^{3+} and Cm^{3+} on the concentration of T2EHDGA in n-dodecane; Aq. Phase: 0.007 M SO_3PhBTP in 1.5 M HNO_3.

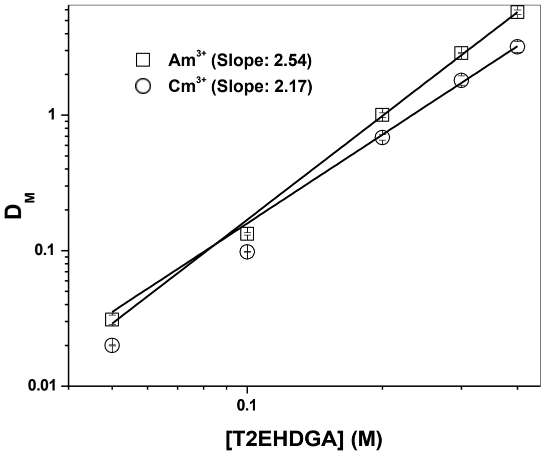

Fig. 2: Effect of the extraction of Am^{3+} and Cm^{3+} on the concentration of T2EHDGA in n-dodecane; Aq. Phase: 0.007 M SO_3PhBTP in 1.5 M HNO_3.

References:
[1] S. Pillon, J. Somers, S. Grandjean, J. Lacquement, *J. Nucl.Mat.*, **320** (2003) 36.
[2] A. Bhattacharyya, S.A. Ansari, N.S. Karthikeyan, C. Ravichandran, B. Venkatachalapathy, T.S. Rao, H. Seshadri, P.K. Mohapatra, , *Dalton Trans.* **50** (2021) 7783.

Nitridation & dissolution behaviour of U-Zr alloy with different wt % of Zr

M. Bootharajan*, B. Sreenivasulu, K. Sundararajan, C.V.S. Brahmananda Rao, V. Jayaraman
Materials Chemistry and Metal Fuel Cycle Group
Indira Gandhi Centre for Atomic Research,
Kalpakkam-603102, India
(*mbrajan@igcar.gov.in)

In the fast breeder reactor (FBR) metal (U-Pu-Zr) alloy fuel is preferred over (U-Pu) oxide or carbide fuel, owing to the safety, thermal conductivity, fissile atom density, higher breeding capacity and lower doubling time. A pyro-reprocessing is the best suitable method for reprocessing the metallic fuel. An alternate method is aqueous reprocessing (PUREX) which involves, the conversion of metallic fuel into respective oxides or nitrides followed by dissolution [1]. This study is aimed to determine the effect of Zr (10-50 wt%) addition in U-Zr metallic alloys on nitridation and its dissolution behaviour. Initially the U-Zr_x(x=10-50 wt%) with varying Zr composition was prepared by arc melting method. A linearity was achieved for different concentration of uranium as prepared alloys by measuring gamma energy of uranium at 1000 keV by gamma spectrometry. The XRD analysis was carried out for the U-Zr_x(x=10-50 wt%) and compared with pure uranium and zirconium. The metallic nitrides can be converted by two methods 1) Direct Nitridation 2) Hydridation followed by Nitridation [2]. Initially, U-10wt%Zr was converted into hydrides at 400-500°C using hydrogen getters followed by de-hydriding at 700°C. Nitridation was initiated in N_2 atmosphere at 400°C. To ensure the complete reaction the temperature was gradually raised up to 1100°C with rate of 10-12°C/min. After nitridation, for the complete conversion of nitrides, the samples were heated at 1000°C under vacuum. The formation of nitride was confirmed by comparing the XRD pattern with standard JCPDF as shown in Fig. 1. Further, similar procedure was adopted for nitridation of 20 and 30 wt% of Zr in U-Zr alloys. The nitridation was found to be difficult owing to poor kinetics due to high Zr content (40 & 50 wt % of Zr in U-Zr) and demands high temperature >1100°C to carry out nitridation. Furthermore, the metallic nitrides were dissolved in nitric acid by refluxing in 12 M HNO_3 at 120°C for 8h. The dissolution of U was found to be > 99.9% in all the cases and the dissolution of Zr decreases with increase in Zr content in U-Zr alloys (Table 1). These studies will be useful for the development of flow sheets for the aqueous reprocessing of metallic fuels by nitridation route.

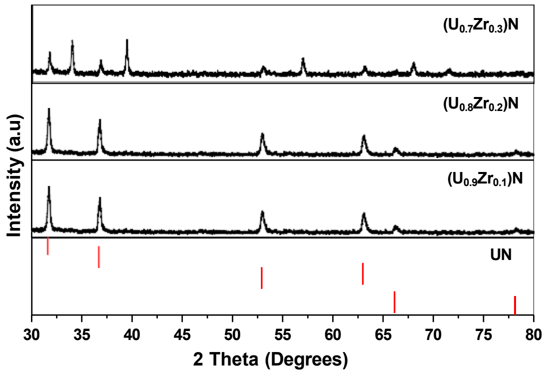

Fig. 1 XRD pattern of UN, $(U_{0.9}Zr_{0.1})N$ $(U_{0.8}Zr_{0.2})N$ and $(U_{0.7}Zr_{0.3})N$

Table: 1 Disoolution results of uranium and zirconium

Compositions of U-Zr alloys	**Preparation of Nitrides**	**Dissolution (%)**	
		U	**Zr**
U-10%Zr	Hydridation & nitridation at 600 °C & 1050°C respectively	>99	89
U-20%Zr		>99	63
U-30%Zr		>99	24
U-40%Zr	Hydridation and nitridation is difficult and kinetics is very slow	Dissolution was not preformed since nitrides were not prepared	
U-50%Zr			

References:

1. B. Sreenivasulu, et al. Solvent Extr. and Ion Exch. 34.5 (2016).
2. Hadi Suwarno Advanced Materials Research. 789 (2013) 360-366

Extraction of Th(IV) using nitrilotriacetamide and N,N-dihexyl octanamide (DHOA)

Ananda Karak,[1,2,] B. Mahanty,[2,3] P. K. Mohapatra,[2,3,§] R. J.M. Egberink,[4] D. B. Sathe,[1] R. B. Bhatt,[1] T. P. Valsala,[1] J. Huskens[4] and W. Verboom[4]

[1] *INRPO, FF, NRB, BARC, Tarapur,* [2]*HBNI, Anushakti Nagar, Mumbai-400094,* [3]*RCD, BARC, Mumbai-400085,* [4]*Laboratory of Molecular Nano fabrication, Department of Molecules & Materials, MESA+ Institute for Nanotechnology, University of Twente, P.O. Box 217, 7500 AE Enschede, The Netherlands*
[§] Email: mpatra@barc.gov.in

Liquid-liquid extraction plays an important role to separate the metal ion of interest from a mixture of ions. Different *N*-pivot tripodal amides were reported for their metal ion extraction ability/selectivity in the presence of only *n*-dodecane or *n*-dodecane + isodecanol mixture[1,2] at different feed nitric acid concentrations. These *N*-pivot tripodal amides have the tendency of third phase formation at higher nitric acid concentrations and metal ion loading conditions [1]. The third phase formation can be avoided by using a suitable phase modifier. *N, N*-dihexyl octanamide (DHOA) is a known phase modifier for the extraction of trivalent actinides using diglycolamide extractants[3]. In this work, two *N*-pivot tripodal amides, viz. *N,N,N',N',N",N"*-hexa-*n*-hexylnitrilotriacetamide (HHNTA) and *N,N,N',N',N",N"*-hexa-*n*-octylnitrilotriacetamide (HONTA) (Fig. 1) were investigated to understand the extraction behaviour of Th(IV) in the presence of DHOA in nitric acid solution.

From our earlier study [1], it was seen that 0.1 M HHNTA in *n*-dodecane formed third phase at 0.1 M HNO_3 which could be prevented up to 3 M HNO_3 by using 10% isodecanol in *n*-dodecane . In the present study, 10% DHOA was used to prevent third phase formation up to 6 M HNO_3 indicating better extraction behaviour of the ligand in the presence of DHOA. On the other hand, 0.1 M HONTA in *n*-dodecane alone formed third phase at above 10 M HNO_3, however in presence of 10% DHOA as the phase modifier it was found to be formed at 8 M HNO_3 (Fig 2). This different behaviour of DHOA towards two NTAamides is an interesting observation and needs further investigation. The extraction of Th(IV) in 10% DHOA in *n*-dodecane was found to be negiligible whereas in the presence of HHNTA and HONTA solutions containing 10% DHOA showed the trend as HHNTA>HONTA (Table 1). The Th(IV) loading was studied with 0.1 M HHNTA in 10% DHOA in *n*-dodecane at 3 M HNO_3 which indicated third phase formation and the limiting organic concentration (LOC) of Th(IV) was found to be 0.06 M. The metal-ligand stoichiometry was found to be 1:2 with HHNTA.

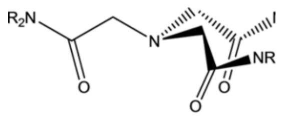

$R=C_6H_{13}$, HHNTA
$R=C_8H_{17}$, HONTA

Fig 1: HONTA/HHNTA

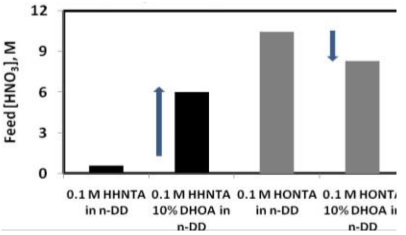

Fig 2: Nitric acid conc. for third phase

Table 1: $D_{Th(IV)}$ values using different solvent systems

[Ligand]	$D_{Th(IV)}$
10% DHOA in *n*-DD	**0.017**
0.1 M HONTA in *n*-DD	**38.0**
0.1 M HONTA + 10% DHOA in *n*-DD	**22.2**
0.1 M HHNTA + 10% DHOA in *n*-DD	**42.0**

References

1. Karak et.al., Solvent Extr. Ion Exch. **40** (2021) 1
2. Karak et.al., Sep.Puri.Technol. **279** (2021)119584
3. Swami et.al., Solvent Extr. Ion Exch. **37** (2019) 500–517

Complexation Studies of Thiazolidine-4-carboxylic acid with Uranyl ion

S. Sharma[1,§], R.M.R. Dumpala[1] and N. Rawat[1,§]

[1] *Radiochemistry Division, Bhabha Atomic Research Centre, Trombay, Mumbai, India-400 085*
[§] Email: sshikha@barc.gov.in

Thiazolidine-4-carboxylic acid (Thia4ca) has been clinically used for about 20 year specially in the treatment of liver diseases and related gastrointestinal disturbances [1]. It's derivatives are used as activator in horticultural crops, industrial crops, tropical crops and fruit trees [2]. This confirms the presence of thia4ca in the human body as well as in the environment. The complexation study of thia4ca with actinides and lathanides is important for environmnental point of view as well as the ligands can be checked for their performance as an actinide decorporating agent in human body.

As the ligand thia4ca is acidic in nature and has replaceable hydrogens therefore the complexation reactions are accompanied with replacement of acidic protons. Protonation studies are prerequisite to understand the complexation of thiazolidine carboxylic acids with actinides. Thia4ca showed two protonations in the given experimental conditions. The log K_{P1} and log K_{P2} are 6.22 and 1.50 respectively. Potentiometric titrations were carried out to know the speciation and stability constant values for the uranyl-thia4ca complex species formed during the course of reaction. The thia4ca forms ML_1, ML_2 and ML_3 type of complexes with uranyl with log K values 4.19, 3.3, 2.56 respectively. The log K_{ML} values were further validated with UV-Visible spectrophotometric method. The log K values obtained from UV-Visible spectroscopy are very near to the values obtained from potentiometry *i.e.* 4.04, 3.19, 2.62 (for ML_1, ML_2 and ML_3). The calorimetry studies gave information about the heat changes during complexation. Formation of all the three complexes are exothermic in nature and complexation is driven by both enthalpy and entropy. The density functional theoretical calculations were carried out to understand the complexation at molecular level. The theoretical findings are in line with the obtained experimental results and provided information about the mode of binding, bond distances and partial charges over atoms of interest. Biological experiments using human erythrocytes and whole blood is in process to know the cytocompatibility and decorporation ability of thia4ca for uranium.

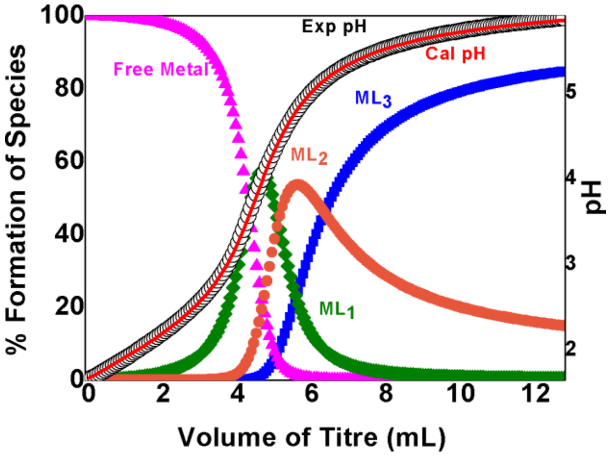

Fig. 1 Experimental and fitted potentiometric data for titration of UO_2(VI) and thia4ca

References:

[1] H. U. Weber, J. F. Fleming and J. Miquel, *Archives of Gerontology and Geriatrics*, 1 (1982) 299.

[2] D.D. Chauhan, T.M. Pancha, A.V. Pate, J.V. Pate and M. Thomas, *International Journal of Chemical Sciences and Technology*, 1 (2016) 14.

Uranyl complexation with pyridine-2,6-diphosphonate: Combined spectroscopic, electrochemical and DFT studies

P.K. Verma[1,§], B. Mahanty[1], A. Bhattacharyya[1], N.E. Borisova[2], S.N.Kalmykov[2],and P.K. Mohapatra[1]
[1]*Radiochemistry Division, BARC, Trombay, Mumbai, India,* [2]*Lomonosov Moscow State University, Moscow, Russia*;
[§]Email: parveen@barc.gov.in

Understanding the complexation of uranyl ion with pyridine based multidentate ligand is of importance as the complexes of these ligands showed enhanced stability of the pentavalent uranyl ion[1]. Complexation studies of U(VI) ion is, therefore, carried out with pyridine-2,6-diphosphonate[2] employing UV-Vis absorption, photoluminescence spectroscopy , electrochemical technique and DFT calculations. The photoluminescence spectra of U(VI) complexes at different metal to ligand ratio was recorded. The excitation spectra at different metal to ligand ratio look very different suggesting formation of different U(VI)-L species. The decay lifetime spectra suggested formation of two species (ML and ML_2) at U(VI) to L ratio 1:5, whereas ML and U(VI)-hydroxo was seen at U(VI) to L ratio of 1:2 and 1:1. The decay lifetime of 143±7, 67±5 and 22±3µs was observed for ML_2, ML and U(VI)-hydroxo species.To the best of our knowledge, such a high decay lifetime for U(VI) complex in solution is not reported. The present lignad also shows very high lifetime for Eu(III) ion[2]. DFT studies on the U(VI) and U(V) complexes of both the 1:1 and 1:2 stoichiometries (Fig. 1(b)) suggested the shortening of the _U-O‘ bond lengths with the phosphonate groups when U(V) was replaced with U(VI) whereas the _U-N‘ bond length was found to be shorter in case of U(V) complex as compared to that in case of U(VI) which indicates the reason for the stability of the U(V) ion using pyridine based ligands. Cyclic voltametric studies also indicated presence of different U(VI)-L species at different ML ratio.

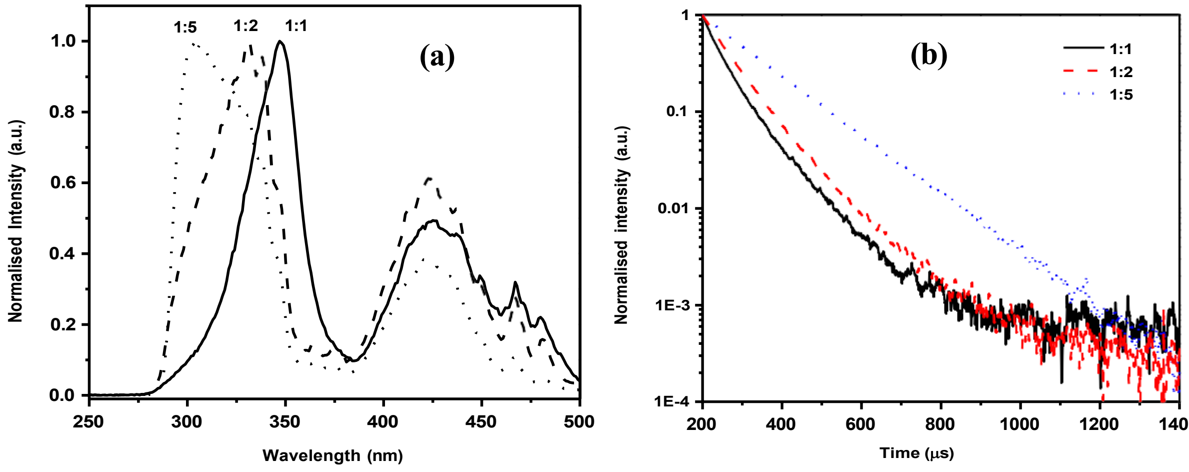

Fig.1 : (a) Excitation spectra of U(VI) complexes; and its (b) decay profile at different metal to ligand ratio; pH : 10.2 ±0.1.

References

[1] R. Agarwal, R. M. R. Dumpala, M. K. Sharma, A. K. Yadav, T. K. Ghosh, *Dalton Trans.* **50 (**2021**),** 1486.

[2] A. Bhattacharyya, S. A. Ansari, P. I. Matveev, G. G. Zakirova, N. E. Borisova, V. G. Petrov, T. Sumyanova, P. K. Verma, S. N. Kalmykov, P. K. Mohapatra, *Dalton Trans.* **48** (2019), 16279.

Recovery and purification of uranium from analytical waste solution of quality control operation by precipitation method

Shiny Suresh Kumar[1,§], Balgovind Vats[2], Ankita Rao[1] and Neetika Rawat[1]

[1] *Radiochemistry Division, BARC, Mumbai, India*
[2] *Fuel chemistry Division,BARC, Mumbai, India*
[§] Email: shiny@barc.gov.in

Chemical quality control is being carried out in all stages of fuel fabrication. The chemical quality control (CQC) of bulk elements in nuclear fuels are carried out by destructive methods. Uranium content in uranium based fuel samples were determined by redox titrimetry, employing Ti(III) reduction method. This generates uranium analytical waste solution containing metal ions Ti(III), Fe(III) and Cr(VI). Magnesium diuranate (MDU) is an intermediate product in uranium fuel fabrication. Determination of U in MDU by Ti(III) reduction method resulted in the accumulation of analytical waste. The ligand N,N′-bis-(N″,N″-diethyl carbamoyl) piperazine (BDECP) (Fig. 1) is reported for selective precipitation of hexavalent actinyl UO_2^{2+} and PuO_2^{2+} ions from aqueous nitric acid medium. Owing to its high selectivity for uranium in presence of other metal ions, the same ligand was employed for the selective precipitation of uranium from analytical waste solution. The MDU analytical waste solution assayed for U concentration by biamperometric method. The acidity of the solution was found to be 1M. Weighed amount of BDECP in the mole ratio 3 times than that of U concentration was mixed with uranium analytical waste solution and allowed to precipitate overnight.

The colourless supernatant itself was the clear indication of quantitative precipitation of U and the same was confirmed by U determination by biamperometric method as U concentration obtained below detectable limit in the supernatant. The yellow precipitate was washed with 1 M sulphuric acid to remove impurities and heated to 450 ^{0}C to convert U_3O_8 and the same was confirmed by powder XRD method (Fig.2).

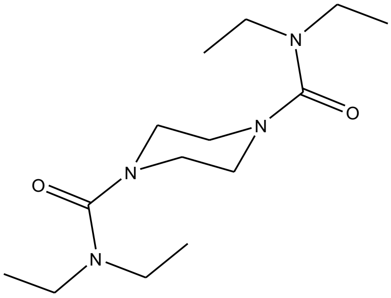

Fig. 1: Structure of N,N′-bis(N″,N″-diethylcarbamoyl)piperazine (BDECP)

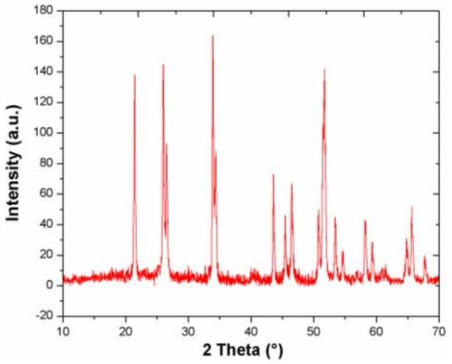

Fig. 2: Powder XRD patterns of U_3O_8

References:

1. BalGovind Vats, Arunasis Bhattacharyya, KaushikSanyal, Mukesh Kumar, Jayashree SugatGamare, and S. KannanPiperazinyl-Based Diamide Ligand for Selective Precipitation of Actinyl (UO_2^{2+}/PuO_2^{2+}) Ions with Fast Kinetics, *Inorganic chemistry* 60(2021) 17529.
2. Xavier, M., et al., Determination of uranium in the presence of iron and plutonium by Ti (III) reduction and biamperometric titration. *Journal of radioanalytical and nuclear chemistry,* 148(2),(1991)251.

Hexa-valent Uranium Enabled Forster Resonance Energy Transfer (FRET) Leading to Fluorescence Enhancement of Sm^{3+}

Annu Balhara[1,2], G.D. Patra,[3]Santosh K.Gupta[1,2§]

[1]*Radiochemistry Division, Bhabha Atomic Research Centre, Mumbai-400085*
[2]*Homi Bhabha National Institute, Anushakti Nagar, Mumbai-400094*
[3]*Technical Physics Division, Bhabha Atomic Research Centre, Mumbai-400085*
[§]Email:santoshg@barc.gov.in

The entire globe is facing an intensive energy crunch owing to exponential growth in population, rapid rise in industrialization and depletion of fossil fuel reserves. In the last decade or so the energy demand for lighting and electrification has increased manifolds as well. In this context there has been a lot of focus vested by the scientific community in developing efficient light emitting materials with multifunctionality. But most of photoluminescent phosphors (PLPs) requires lanthanide ion doping to achieve the same. **[1]** Because of the intrinsic issue associated with low absorption coefficient of Ln^{3+} ion; desirable level of success is yet to be achieved and this triggers the use of sensitizer for improving the luminescence of lanthanide doped PLPs. **[2]** Till now the extensively used sensitizer particularly for Sm^{3+} are Bi^{3+}, Al^{3+}, Pb^{2+}, Mn^{2+} which doesn't yield desired result owing to energy mismatch. The problem with use of another lanthanide ion such as Gd^{3+} and Tb^{3+} leads to low absorption of near UV light and with Ce^{3+} ion the fluorescence quenching happens owing to the presence of Ce^{4+} ion. Here in this work we have utilized U^{6+} (5f ion) to sensitize Sm^{3+} ion (4f ion) doped in low phonon $Li_2B_4O_7$ (LTB) host and achieve efficient energy transfer (ET) from $U^{6+}\rightarrow Sm^{3+}$ leading significant enhancement in emission intensity. This material could further be explored for designing color tunable phosphors and optical sensors for uranyl ions. In this work, we have developed a LTB: Sm^{3+}, U^{6+} phosphor with different doping concentrations of Sm^{3+} ions. Owing to efficient $UO_2^{2+}\rightarrow Sm^{3+}$ FRET remarkable enhancement in Sm^{3+} emission was achieved (***Figure 1***) upto 0.5 % doping and beyond that concentration quenching leads to reduction in the same. Because of the different extent of $UO_2^{2+}\rightarrow Sm^{3+}$ energy transfer at different europium ion concentration; color tunable emission could be achieved. Here, we could also present the feasibility for sensing uranyl (VI) ions through the exploration of a unique FRET to samarium (III) using selective excitation of near UV 330 nm photons.

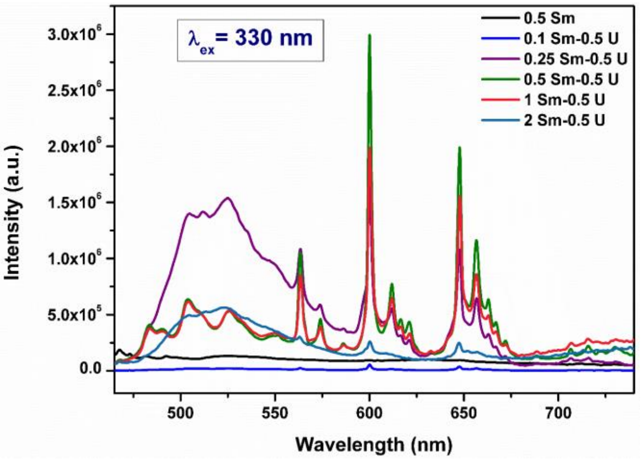

Fig. 1: Emission spectra of LTB: 0.5%U,x%Sm(x=0.1-2) under 330 nm excitation

References:
[1] S.K. Gupta, *et al.Coord. Chem. Rev.* **420** (2020)213405
[2] Reshmi T.P. et al., *ACS Appl. Opt. Mater,***1** (2023) 179-192.

Solvent Extraction Studies with Palladium from Nitric Acid Medium Employing Phosphonate Based Ligands

B. Sreenivasulu,[1, §] Aditya Ramesh Sachin[1,2], Gopinadhanpillai Gopakumar[1],
C.V.S. Brahmmananda Rao,[1]
[1] *Fuel Chemistry Division, MC&MFCG, IGCAR, Kalpakkam – 603102*
[§] Email: bsrinu@igcar.gov.in

The demand for Palladium has increased due to various applications in many industries. Due to the limited availability of Pd in the earth‘s crust, there is a need to search for alternative sources of Pd. Spent nuclear fuel, which arises from power reactors, is one of the sources with a significant amount of palladium along with other fission products and actinides. It is important to recover Pd from high-level waste (HLW). Several molecules were examined in the literature for the recovery of Pd from HLW solutions [1]. In the present study, phosphonate based ligands such as Dibutylbutyl Phosphonate (DBBP) and Diamylamyl Phoshonate (DAAP) with higher extraction ability than TBP have been examined for the recovery of Pd from the nitric acid medium. In this context, these ligands were synthesized as reported in our earlier papers and characterized by FTIR and NMR[2]. The distribution ratios were measured from nitric acid by both the solvents. The extraction behavior of Pd by neat DBBP and DAAP has been studied as a function of nitric acid concentration. The *D* values by Pd by DBBP and DAAP are high at 0.5 M HNO$_3$, and it decreases sharply and gets flattened with an increase in nitric acid concentration (Fig.1). Both phosphonates and TBP are neutral type ligands which extract Pd through solvation *via* P=O group. Hence a similar extraction behavior is expected in the case of phosphonates. Density functional theory calculations were performed to understand the electronic structure of all ligands and complexation energies were computed for the interaction of Pd(II) with the ligands (Fig. 2). The calculated complexation energies of Pd(II) nitrate complexes with ligands, TBP, DBBP and DAAP are found to be in the order DBBP> DAAP >TBP. This is in agreement with the trend established by the experimental *D* values. The *D* values for Pd by phosphonates based solvent is significantly higher than that of the TBP system, indicating that phosphonate based solvents can be employed to extract Pd.

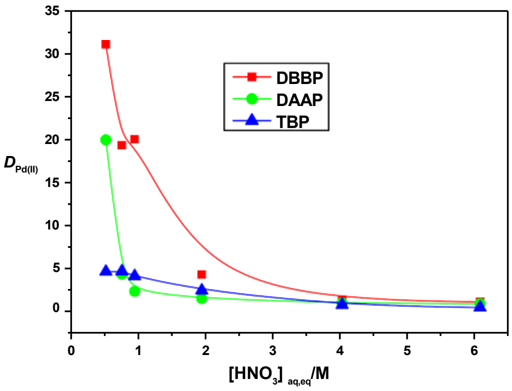

Fig. 1. Variation of *D* values for Pd as a function of nitric acid concentration by neat DBBP, DAAP and TBP

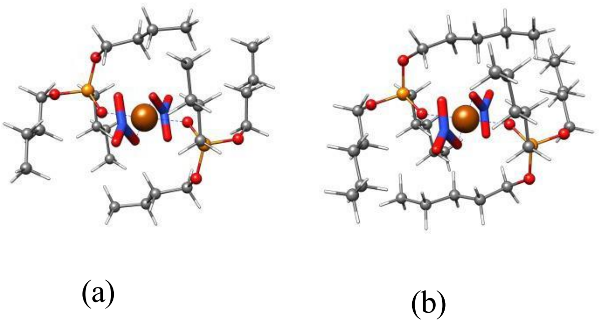

(a) (b)

Fig. 2. Energetically lowest–lying geometries of (a) $Pd(NO_3)_2.2DBBP$, (b) $Pd(NO_3)_2.2DAAP$

References:
1. R. Ruhela et. al., RSC Adv. **4**(2014)24344
2. C.V.S. Brahmmananda Rao et. al., *Solvent Extr. Ion Exch*., **25**(2007)771

Recovery of Uranium from different Matrices by Alicyclic Hydrogen Phosphonate in Supercritical Carbon Dioxide Medium

P. Rajani[1], B. Sreenivasulu[2], K. C. Pitchaiah[2§], C.V.S. Brahmananda Rao[1,2], N. Sivaraman[1,2]

[1]*HBNI-Training School Complex, Anushaktinagar, Mumbai -400094, India*
[2] *Indira Gandhi Centre for Atomic Research, Kalpakkam-603102, India*
[§] Email: nani@igcar.gov.in

Recovery of actinides from different matrices which are generated from the various nuclear fuel cycle operations is a challenging task. In recent past supercritical carbon dioxide ($SCCO_2$) based extraction methods acquired prominence for the progress of green separation techniques owing to their added advantages such as waste minimization and faster separations [1]. In this context, an alicyclic phosphonate namely, di-cyclohexyl hydrogen phosphonate (DCyHeHP) was synthesized and employed for supercritical fluid extraction (SFE) studies. Solubility of DCyHeHP in $SCCO_2$ was evaluated at temperatures (313, 323, and 333 K) with pressures varying from 10-20 MPa, shown in Fig. 1. Solubility of DCyHeHP was increased with pressure and reverse trend observed with temperature. DCyHeHP has significant solubility in $SCCO_2$ medium and employed for selective extraction of uranium from simulated dissolver solution (SDS). SDS containing U about 100 g/L and Zr about 5 g/L along with various other fission products in nitric acid medium. SFE of metal ions depends on solubility of ligand and metal-ligand complex as well as transportability of metal-ligand complex in $SCCO_2$ medium. Hence, the influence of temperature (313-333 K) and pressure (10-20 MPa) on the extraction behaviour was studied. The cumulative extraction of U (0.1M HNO_3) was found to be >95% and it has not improved significantly beyond 323 K and 16 MPa; therefore, extraction studies were performed at 16 MPa and 323 K. The extraction of uranium from SDS was carried out as a function of nitric acid concentration (0.1M, 1M, 4M) and extraction behaviour was shown in Fig. 2. The extraction efficiency of uranium was found to be >99% at all acid strengths. Under similar experimental conditions, the extraction efficiency of lanthanides and other fission products was found to be < 3%. Faster kinetics at 0.1M HNO_3 indicates that the ion-exchange mechanism (P-O-H) was predominant over solvation mechanism to extract uranium from SDS. These results have established potential application of SFE based process for recovery of uranium from different matrices.

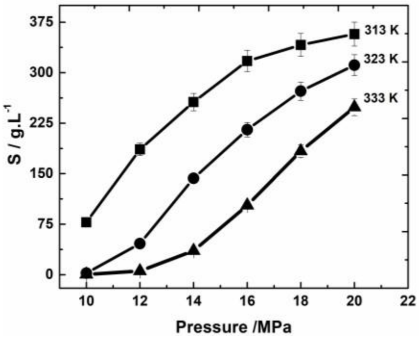

Fig. 1. Solubility of DCyHeHP in $SCCO_2$

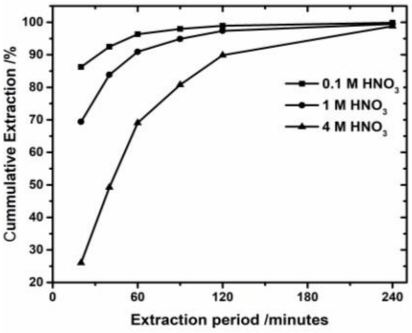

Fig. 2. Uranium extraction kinetics

References:
[1] A. Kongasseri, et. al., RSC advances, 13 (2023) 3317-3328.

Solvent extraction studies for recovery of Uranium from thiocyanate analytical waste using DAAP

B.Sivaramakrishna[1#], B.Sreenivasulu[2], G.Saipriya[1], P.Rajani[2#], G.S. Rao[1],
N.R. Jawahar[1], C.V.S.Brahmananda Rao[2, # §]
[#]HBNI – IGCAR, [1]INRPK, NRB Kalpakkam, [2]MC&MFCG, IGCAR, Kalpakkam.
[§] Email: brahma@igcar.gov.in

Analytical lab waste containing U in ammonium thiocyanate is generated in reprocessing laboratory. Recovery of U from such analytical waste is very important. Dialkaylalky phosphonate based extractants has high extraction efficiency over trialkyl phosphates. In the present study, the recovery of U from thiocyanate analytical waste has been examined by solvent extraction using diamylamyl phosphonate (DAAP) as extractant[1]. D_U in DAAP varies with pH and concentration of thiocyanate ligand [2]. Uranium forms a disolvate complex with DAAP in nitric acid medium. In the present study, solvation number of U complex extracted by DAAP from thiocyanate medium was studied by mole ratio method,absorption behavior of U extracted species in DAAP and back extraction studies of U with Na_2CO_3 as strippant were carried out. The following solutions were prepared for the experimental study i) DAAP (0.1, 0.275, 0.55, 0.82 and 1.1M) in n-Dodecane (DD), ii) U(10.79 mg/ml) solution in 0.26M thiocyanate and iii) sodium carbonate of 0.2, 0.6, 1.2, 1.8 and 2.25M.

Equilibration experiments carried out for 30 minutes by equal volume of U (10.79 mg/ml) thiocyanate solution with each [DAAP] extractant (0.1M, 0.27, 0.55, 0.82, 1.1M). U is estimated in aqueous and organic phase after phase separation. D_U is computed in each experiment. A plot between ln D_U Vs ln [DAAP] is shown in Fig.1. Solvation number of the U in DAAP extracted from 0.26M [SCN] is found to be 2.17 estimated by measuring the slope of the line obtained from the plot. Further to understand the nature of the U extracted species in DAAP, absorption spectra of U in organic phase is measured after a known amount of U (1.46 mg/ml) is extracted from 0.26 M [SCN]. The absorbance peak of the complex has a maximum wavelength of 297 nm due to U[SCN] complex in DAAP. However more studies are required to ascertain the exact nature of extracted species. Back extraction studies are carried out with Na_2CO_3 as strippant. Different molarities of Na_2CO_3 (0.2, 0.6, 1.2, 1.8 & 2.25M) are employed in 1:4 (Organic: Aqueous) ratio for stripping. Stripping of U is near complete with 2.25 M Na_2CO_3. Stripped U is brought into nitrate form for reuse. These studies conclude that the U is extracted as U-SCN complex from thiocyanate waste and it forms a disolvate complex in DAAP. Extracted U is recovered by stripping with 2.25M Na_2CO_3.

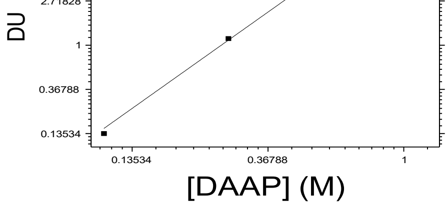

Fig.1: ln D_U Vs ln [DAAP]

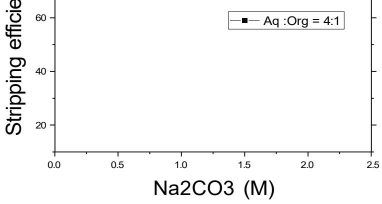

Fig.2: U stripping efficiency Vs Na_2CO_3

References:

1. C.V.S. Brahmmananda Rao et al. Solvent Extraction and Ion Exchange, 25 (2007) 771-789.
2. B.Sivaramakrishna et al. SESTEC 2022, ICT Mumbai, Nov 22-26, 2022, pp 90.

Thermodynamic Complexation and Decorporation Efficiency of N-(-2-acetamido)iminodiacetic acid for Th(IV)

S. Sharma[1,§], M. Ali[2], A. Kumar[2], N. Rawat[1,§]

[1] *Radiochemistry Division, Bhabha Atomic Research Centre, Trombay, Mumbai – 400 085*
[2] *Radiation Biology & Health Sciences Division, Bhabha Atomic Research Centre, Trombay, Mumbai, India – 400 085*
§ Email: sshikha@barc.gov.in

Owing to the presence of multiple strongly binding functional groups, amino carboxylates have been extensively used for sequestration, decontamination and decorporation of actinides [1]. In order to understand the effect of N-(2-acetamido) functionality of iminodiacetic acid on its complexation strength with actinides, a systematic study on thermodynamics of complexation of N-(2acetamido) iminodiacetic acid (AIDA) with Th(IV) has been carried out. In addition, the biocompatibility of AIDA [2] motivated us to ssess it‘s decorporation efficacy for Th(IV) in human red blood cells and blood.

Potentiometric titrations were carried out to know the speciation and stability constant values for the species formed during the course of reaction of Th(IV) and AIDA. The AIDA forms ML$_1$, ML$_2$, and ML$_3$ type of complexes with log K values 9.84, 8.23 and 5.70 respectively. The calorimetry studies were carried out to know the heat changes during complexation. Exothermicity of ML$_2$ formation is significantly higher compared to ML$_1$. The ESIMS (electrospray ionization mass spectrometry) studies further confirmed formation of ML$_1$, ML$_2$, and ML$_3$ (Fig 1a). The density functional theoretical studies were carried out to understand the coordination modes between Th(IV) and AIDA. The optimized structures of ML$_1$ and ML$_2$ showed the participation of two carboxylates in bond formation with Th(IV) in ML$_1$ while the participation of two carboxylate and amide oxygen in ML$_2$. The tridentate binding of ligand in ML$_2$ explains the experimentally obtained trend of enthalpy. Biological experiments using human erythrocytes and whole blood showed cytocompatibility and good decorporation ability of AIDA for Thorium. The decorporation efficiency of AIDA was found to be comparable with the clinical decorporating agent, DTPA (fig 1b).

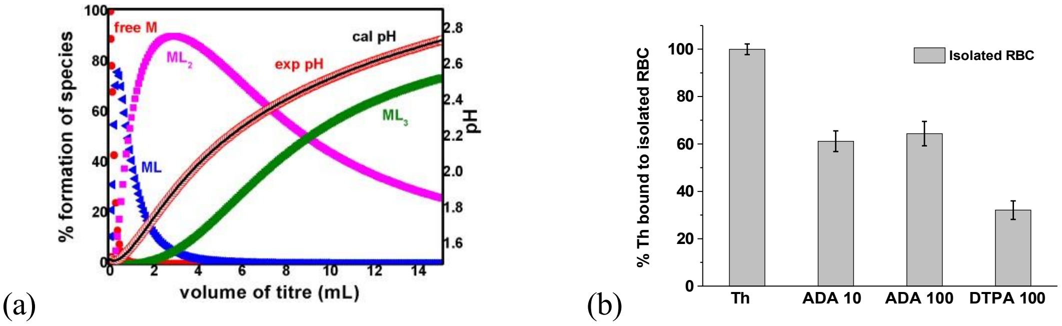

Fig. 1: (a) Experimental and fitted potentiometric data for titration of Th(IV) and AIDA (b) Decorporation efficacy of ADA to remove Th bound to the surface ligands of human RBC

References:

[1] E. P. C. Lai and C. Li, *Radiat Res*, **198** (2022) 430.

[2] M. Markowicz-Pi seck , P. Dębski, E. Mikiciuk-Olasik, and J. Sikora, *Molecules*, **22** (2017) 2265.

Complexation Studies of U/La-α-alanine by IR, Cyclic Voltammetry and PhotoluminescenceTechniques

Ritu Singh[1§], Ashutosh Srivastava[1], AnnuB[1, 2] and M. Mohapatra[1,2]

[1]*Radiochemistry Division, Bhabha Atomic Research Centre, Trombay, Mumbai-400085 India*
[2]*Homi Bhabha National Institute, Anushaktinagar, Mumbai-400094 India*
[§] Email: ritusing@barc.gov.in

Although there are many studies on complexes of amino-carboxylic acids with lanthanides and actinides, the complexation information on α-amino acid such as alanine and its derivatives are scarce [1]. The lanthanide/actinide-alanine complexes are used as luminescent markers in various fluor-immunoassay techniques especially using uranium[2]. In all these applications special emphasis has been given in order to understand the speciation of the metal ion. In this context, CV (cyclic voltammetry), IR (infra red) and photoluminescence (PL) spectroscopic studies were carried out on ‗U‘ incorporated La-αAlanine complexes prepared through a simple solution route. Comparison of the IR data of La-alanine and uranium incorporated La-alanine samples confirmed the formation of U-alanine bonding in the respective complexes [3]. A relatively small shift in peak position of Uranium-La-alanine complex vis-a-vislanthanum-alanine species was observed in the CV data suggesting weak complexation between uranium and alanine (figure 1). The PL excitation and emission data of only uranium solution (A) and uranium with alanine (B) are shown in figure 2. Although the emission and excitation spectra did not show any appreciable change, the decay time spectra of the uranium alanine complex showed a slight increase in the life time values.

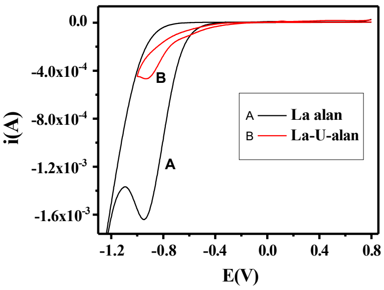

Fig 1: CV plots of La-Alanine and La-U-Alanine

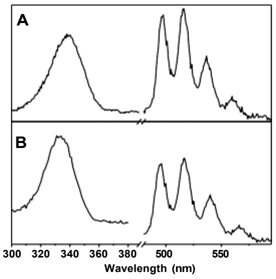

Fig 2:PL excitation and emission plot U (A)and U-alanine (B)

From the excitation and emission profile, it could be ascertained that uranium exists as uranyl ion (UO_2^{2+}) in the matrix. The life time spectra for both un-complexed and complexed system showed bi-exponential decay whose major fraction increased from 7.409 μs to 8.451 μs. The other long lived minor fraction could not be attributed to any species in the present set of investigation. An increase in the values of the decay time confirmed the formation of uranyl complex species.

Acknowledgements-: The authors thank Dr. P.K.Mohapatra, Head, RCD for his support during the course of the work.

References:
[1] M. Cefola, R. C. Taylor, P. **S.** Gentile, and A. V. Celiano, J, Phys. Chem.**,** **66** **(**1962) 790.
[2] E. Boros, P. Caravan, J. Med. Chem., **56** (2013) 1782
[3] John Knoeck,Anal. Chem., **41** **(**1969) 2069

Extraction behaviour of Pu(IV) into synthesized DES (TBACl:DA):30% TBP

Prashant Patil[1], Sharathbabu[1], Sachin Pathak[3], Ashutosh Srivastava[4,§]

[1, 2, 3] *Product Development Division,* [2]*Radiochemistry Division, BARC*
[§] Email: sriashu@barc.gov.in

Deep eutectic solvents (DESs) have emerged as new generation of solvents in 21st century and have found their potential applications in several fields including extraction and separation [1-2]. Their non-volatile and non-inflammable nature can make them a better alternative to the conventional volatile organic solvents [2]. They can be simply prepared by mixing two components in suitable mole ratio, one is hydrogen bond donor and other is hydrogen bond acceptor, which are capable of forming eutectic mixture with large depression in freezing point than the individual components due to hydrogen bonding interaction. DESs has similar physicochemical properties to ionic liquids (ILs), but unlike ILs, the DESs have several advantages such as speedy synthesis, easy handling, eliminating the laborious purification steps, biodegradability, non-toxicity. Therefore, DESs are a suitable option to replace the ILs in liquid-liquid extraction (LLE) process of actinides. In the present work, DES prepared by mixing tetra butyl ammonium chloride (TBACl) and decanoic acid (DA) in 1:1 mole ratio, which results in the formation of eutectic mixture. The as-synthesized TBACl-DA DES was used as hydrophobic solvent by adding 30% TBP for the extraction of Pu (IV) from nitric acid medium. Stock solution containing ^{239}Pu tracer in nitric acid was employed. The extraction studies were carried out by equilibrating equal volumes of acidic phase of required molarity containing Pu(IV) with (TBACl:DA):30%TBP organic phase . The solution was centrifuged to allow proper phase separation. The ^{239}Pu assayed in aqueous and organic phase by using alpha liquid scintillation counting for the computation of distribution ratio (D value). The kinetics of extraction studies illustrates (Fig.1a) more than 70% extraction completed in 20 minutes. However, around 40 mins is required to attain a constant D value. Variation of D value as a function of nitric acid concentration also demonstrated (Fig.1b). It reveals that D value increases from 1M and reaches maximum at 3M and later exhibits decreasing trend. It was also observed > 95% stripping of extracted Pu(IV) in DES:TBP phase could be achieved by using 1M oxalic acid+0.2M ascorbic acid medium.

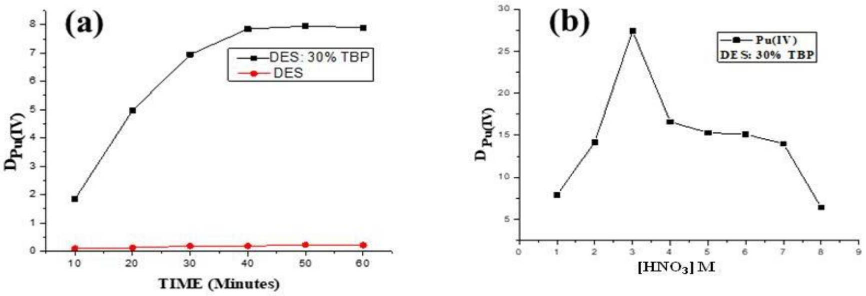

Figure 1. (a) D value with time of equilibration (b) D values with varying acidity of nitric acid

Acknowledgements- Authors would like to acknowledge Dr S C Parida, Head, PDD and Dr. P.K. Mohapatra, Head, RCD, BARC for their support during the course of this work.

References: [1] Zante, Guillaume, and Maria Boltoeva. *Sustainable Chemistry* 1, no. 3 (2020): 238-255.
[2] Kshirsagar, Asmita, P. K. Verma, and M. S. Murali. *Journal of Radioanalytical and Nuclear Chemistry* 330 (2021): 1053-1064.

Diluent free solvent extraction of Pu(IV) from TOPO-DEHPA eutectic

Sharathbabu[1], Sachin Pathak[1], Prashant Patil[1], Ashutosh Srivastava[4, §]

[1,] Product Development Division, [2] Radiochemistry Division, BARC
[§] Email: sriashu@barc.gov.in

Solvent extraction of Plutonium from acidic aqueous phase is essential step during reprocessing operations in nuclear industry. Deep eutectic solvents (DESs) are evolving as novel solvent media now a days and are finding their applications in different fields as environmentally benign sustainable alternative to the conventional organic solvents due to their promising solvent characteristics and tunable properties. Principally, DES is a mixture of hydrogen bond donor (HBD) and hydrogen bond acceptor (HBA) in proper mole ratio, which results in a liquid at room temperature with melting point lower than either of the components. Though, the physical properties of DES analogous to the conventional ionic liquids (ILs), however, DESs are better option in extraction in terms of their easy synthesis, non-toxicity and biodegradability. Usually, TOPO or DEHPA in organic diluents or in ionic liquid diluents [1-3] were used for the extraction of plutonium. To avoid the use of volatile organic solvents and ILs as diluent, the DES was prepared by combing 1:1 mole ratio of TOPO and DEHPA. This solvent was directly employed for liquid-liquid extraction of Pu(IV) from nitric acid medium. The stock solution of ^{239}Pu tracer was purified by TTA extraction. The Pu extraction studies were carried out by equilibrating equal volumes of aqueous phase containing ^{239}Pu tracer in required nitric acid molarity and TOPO-DEHPA solvent. The D value of extraction was evaluated by assaying ^{239}Pu in both the phases by using alpha liquid scintillation counting. In kinetic experiments, time of 25-30 minutes was found to be sufficient for equilibration. Fig.1 depicts that the extraction increases with increase in nitric acid concentration upto 3M, thereafter, it was found to be decrease at higher concentrations. About ~ 94 % stripping of extracted Pu(IV) could be accomplished with 1M oxalic acid in single contact (Table-1).

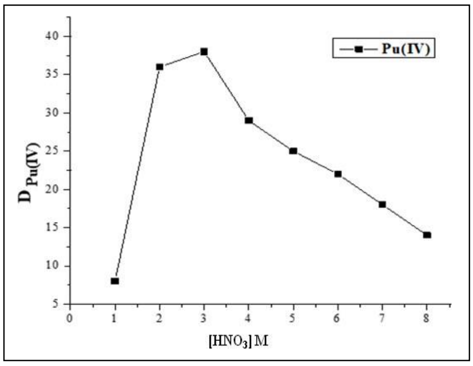

Figure-1: D values with nitric acid molarity

Table -1: Percentage of Pu stripping with various

Stripping agent	*% stripping*
1M oxalic acid	94
1M oxalic acid+0.2M ascorbic acid	88
6 M HNO_3	24
1M HNO_3+0.2M Sulphamic acid + 0.2M Fe^{+2}	65

Acknowledgements- Authors would like to acknowledge Dr S C Parida, Head, PDD and Dr. P.K. Mohapatra, Head, RCD, BARC for their support during the course of this work.

References: [1] M Gilmore et al. ACS Sustainable Chem. Eng.6,17323(2018).
[2] S.K.Patil et al.15(7), SEPARATION SCIENCE AND TECHNOLOGY, 15(7) (1980), 1459
[3] K. V. Lohithakshan, Prashant Patil ,J Radioanal Nucl Chem ,301(2014) ,153

Investigating the feasibility of using *N,N,N,N'*-tetraoctyl diglycolamide – *N,N*,-dioctyl hydroxyacetamide/*n*-dodecane for the minor actinide partitioning

N. Parvathy [1, 2], Satyabrata Mishra[1], T. Prathibha[1], N. Desigan[1], K. A. Venkatesan[§1, 2]

[1]*Indira Gandhi Centre for Atomic Research, Kalpakkam 603 102, India.*
[2]*Homi Bhabha National Institute, Anushakthi Nagar, Mumbai 400094, India.*
[§]E-mail: kavenkat@igcar.gov.in

N,N,N',N'-tetraoctyl diglycolamide (TODGA) is regarded as a potential ligand for the partitioning of minor actinides from high-level liquid waste [HLLW].[1] However, it possess third phase formation limitation when contacted with nitric acid concentration of 4 M or above. Addition of phase modifier is one of the effective methods for the prevention of third phase formation. One such phase modifier is *N,N*-dioctylhydroxyl acetamide (DOHyA),which is a major radiolytic degradation product of TODGA (Fig 1). Besides being an excellent phase modifier, it synergistically enhances the extraction performance of TODGA. The extraction and aggregation behaviour of this pair of extractants towards nitric acid and Nd(III) ion is well-established in literature.[2] However, in order to validate the applicability for real reprocessing scenario, it is necessary to study its extraction behaviour in the presence of various fission products present in the HLLW. In this context, we investigated the feasibility of TODGA-DOHyA/*n*-DD also termed as combined system (CS) for partitioning of minor actinides from HLLW. The extraction behaviour of fission products like lanthanides, PGMs, etc. were studied with this CS. Fig 2 shows the variation in the distribution ratio of the Ln(III) ions as a function of acidity. Extraction was carried out from the nitric acid containing 0.05 M of Ln‘s at the organic to aqueous phase ratio of unity. It can be seen that the D_{Ln} increases with increase of aqueous phase acidity and also D_{Ln} shows gradual increase across the period which can be attributed to the increase in effective nuclear charge of the Ln‘s across the period. It is to be noted that tetravalent Zr(IV) showed more D value compared to lanthanides, the distribution ratio of Zr(IV) is less in CS as compared to TODGA. Additionally, the extraction of various metal ions present in the simulated HLLW was also studied and it was found that this system indeed performs better that TODGA in terms of selective extraction of trivalent lanthanides. In view of this, the CS can be regarded as a potential candidate for minor actinides partitioning from high level liquid waste.

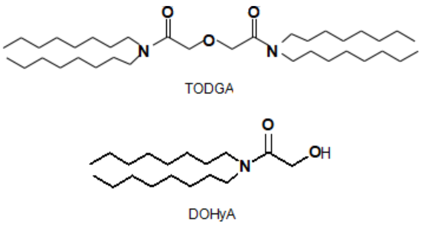

Fig 1. Chemical structure of extractants

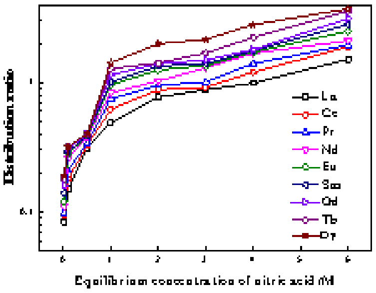

Fig 2. D_{Ln} as a function of initial HNO_3 concentration.

References

1. S.A. Ansari, et al., *Chem.Rev.***112,** 1751-1772 (2012)
2. N. Parvathy, et al., *J. Mol. Liq.* **317**, p.113940(2020).

Theoretical Studies on Tuning the Selectivity of Diglycolamide based Ligands Towards Lanthanide-Actinide Separation

Somnath Sengupta[1], G. Gopakumar[1], C.V.S. Brahmananda Rao[2§]
[1]*Fuel Chemistry Division, Material Chemistry and Metal Fuel Cycle Group, IGCAR, Kalpakkam-603102*
[2]*Homi Bhabha National Institute, IGCAR, Kalpakkam-603102*
(§ Email: brahma@igcar.gov.in)

Diglycolamides(DGA) are a novel class of extractant employed for the extraction of trivalent metal ions from high level liquid waste[1]. However, selective extraction between trivalent actinides and lanthanides is not possible with DGA based extractants. Hence, we attempted to understand computationally whether the DGA based extractants can be made more selective towards actinides by replacing the oxygen donor atoms in the ligand stracture with nitrogen atom. In this context, we obtained five ligands namely, L_{O-N-O}, L_{N-O-O}, L_{N-N-O}, L_{N-O-N} and L_{N-N-N}, by successive replacement of oxygen in the *N,N,N',N'*-tetramethyl diglycolamide structure by nitrogen. These structures were optimised at BP86/*def2*-TZVP level and lowest energy structures for each were obtained. As a next step, complexes of Am(III) and Eu(III) with the ligands were optimised at the same DFT level and the lowest energy structures were obtained. Harmonic frequency analysis was performed on all the lowest energy structures to confirm that they are minima in the potential energy surface. In order to understand the binding nature of the ligands with Am(III) and Eu(III), complexation energy was computed according to the following scheme:

$M(NO_3)(H_2O)_7^{2+} + 2NO_3^- + L \longrightarrow M(NO_3)_3L + 7H_2O$, where M=Am(III)/Eu(III) & L=ligand

Upon calculation of the complexation energies it was revealed that the ligands showed greater selectivity for Am(III) compared to Eu(III). Further, natural bond orbital (NBO) and atoms in molecules (AIM) analysis was done which confirmed stronger binding in Am(III)-ligand complexes. These calculations were performed with the ORCA version 4.2.1 quantum chemistry program package[2].

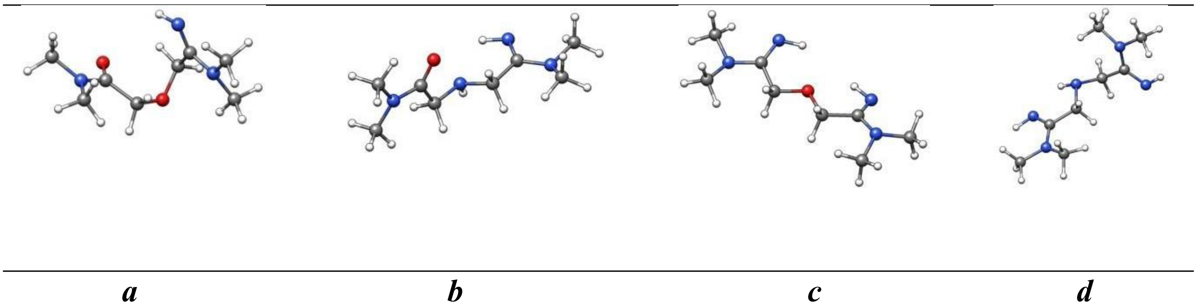

Figure 1. Optimized geometries of (*a*) L_{N-O-O} (*b*) L_{N-N-O} (*c*) L_{O-N-O} *(d)* L_{N-N-N} at RI-BP86-D3BJ/*def2*-TZVP level.

References:
[1] S.A. Ansari, et al *Chemical reviews*, **112(3)** (2012) 1751.
[2] F. Neese, The ORCA Program System. *WileyInterdiscip. Rev.: Comput. Mol. Sci.*, **2(1)** (2012) 73.

Speciation of Uranyl with varying pH in Ethylene glycol eutectic media

Jisha S. Pillai[1], Ashutosh Srivastava[2], Seraj Ansari[2], S. Chaudhury[1, §]
[1]*Fuel Chemistry Division,* [2]*Radiochemistry Division, Bhabha atomic research centre, Mumbai, india*
§ Email: saty@barc.gov.in

Deep eutectic solvents (DESs) are an emerging class of green solvents that can be considered as suitable alternate to nullify the major drawbacks of conventional aqueous based recovery of actinides from nuclear waste. A DES is the homogeneous liquid mixture of two or more solid compounds, generally a hydrogen bond acceptor (HBA) and a hydrogen bond donor (HBD), in a specific molar ratio with a melting point significantly lower compared to those of the neat individual constituents [1]. Major advantages of DESs are cheaper production, lower toxicity, higher biodegradability, low volatility and highly tunability. In addition, due to their inherent ionic conductivity and excellent solubilizing properties, the DESs are being used as novel electrolytic media. Uranium (U) being a nuclear fuel needs to be recovered and purified from nuclear waste for further use in the nuclear reactor. For development of methodology related to U recycling and recovery process using DES, it is necessary to understand the speciation of uranium with varying physiochemical conditions such Eh and pH in a particular DES media. Ethylene glycol (EG) is cheap and environmentally benign and DESs based on EG have low viscosity and wider electrochemical potential window compared to others. Therefore, in the present work, EG based DES was prepared by taking choline chloride (ChCl) as HBA and EG as HBD in 1:2 molar ratio and heating at 60°C in an oven for 1 hours. The uranyl nitrate (UN) was dissolved in ChCl-EG media. The IR and UV-visible absorption spectra studies indicate formation of UO_2^{2+} species through dissolution process. Electrochemical studies were carried out on dissolved sample of UN in ChCl-EG media with varying pH from 0.93 to 6.8 and the corresponding cyclic voltammograms are shown in Fig 1. The results show that below pH 2, three reduction peaks of uranyl were obtained at -0.584 V, -1.368 V, and -1.730 V while > pH 2 only one reduction peak is found at -0.646 V. The three reduction peaks at pH 0.93 and single peak at pH >2 of uranyl are found to be diffusion controlled. The calculated value of diffusion coefficients, n, and rate constant (k^0) in electron transfer step of uranyl are given in Table 1. Through UV-Visible absorption, the logK value of the interaction of uranyl with ChCl:EG was calculated.

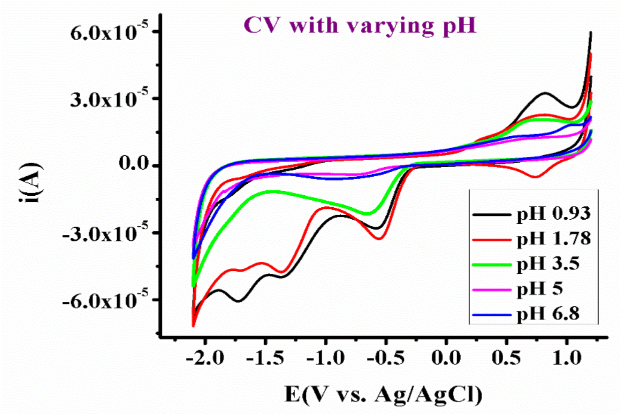

Figure 1. CV plots of UN in ChCl:EG with varying pH

Table 1: Redox and interaction parameters of Uranyl

Parameters	Values	
	pH 0.93	**pH 4**
D_0	9×10^{-9} cm^2/sec	1.42×10^{-8} cm^2/sec
αn	0.446	0.49
k^0	9.92×10^{-5} cm/sec	1.26×10^{-4} cm/sec

References:

[1] Smith, Emma L. et al. 114, no. 21 (2014): 11060-11082.

ADU precipitation in presence of oxalate ion

Arvind Prasad, Rekha V, K.S Vijayan, Bhanu Prasad CH.U, N Desigan§, K A Venkatesan and K Ananthasivan

Process, Radiochemistry and Reprocessing Research and Development Division,
Indira Gandhi Centre for Atomic Research, Kalpakkam – 603102
§E-mail: desi@igcar.gov.in

Fast reactor fuel reprocessing at CORAL adopts modified PUREX process. The process involves the co-extraction and co-stripping of uranium and plutonium in single cycle [1]. The plutonium from the co-strip product was selectively precipitated as oxalate using oxalic acid. The filtrate serving as a feed for uranium reconversion laboratory has 3-5 g/L of U in 2.5-3.5 M nitric acid and 0.07–0.15 M oxalate ion. In present work the effect of oxalate ion on ADU precipitation was studied. In course of experiment 50 ml solution from stock solution containing 3.80 g/L uranyl nitrate in 3.0 M nitric acid was taken in a conical flask and ammonium hydroxide solution was added drop wise to the solution kept under constant stirring. The flask was sealed immediately after precipitation with paraffin to avoid ammonia evaporation and interference due to atmospheric CO_2. A sample from the supernatant was taken at different time intervals and analysed for uranium and oxalate ion. In all experiments the pH was maintained at 9.0 ± 0.2.

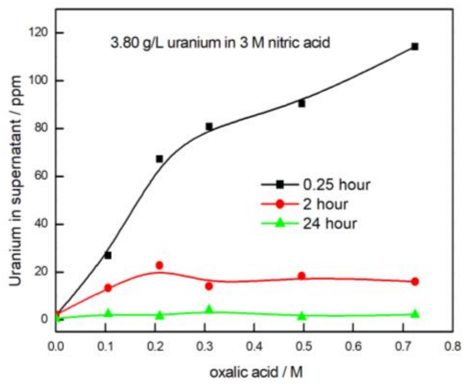

Fig.1.Variation in the concentration of uranium in the supernatant at different time intervals with oxalic acid

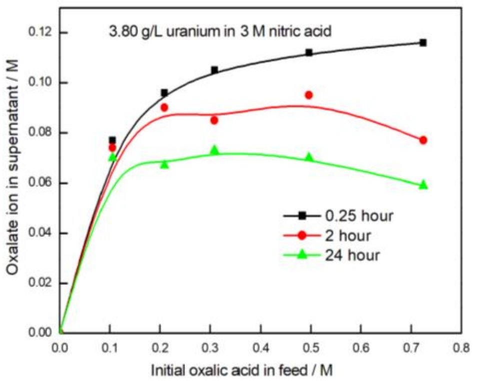

Fig.2. Variation in the concentration of oxalate ion in supernatant at different time intervals with oxalic acid.

The fig.1 shows that the uranium loss in supernatant increases with increase in the concentration of oxalic acid at 0.25 h , but decreases rapidly within 2 h with negligible uranium loss. Fig.2 shows the reduction in the oxalate ion concentration in supernatant with time which indicates a part of oxalate is consumed for precipitation. This may attributed due to the precipitation of other species like ammonium uranyl oxalate and ammonium oxalate along with ADU at higher pH. Since the sintering characteristics of ceramic powders, such as UO_2 are determined largely by their preparative history. Uranium oxide prepared by ADU precipitation in presence of oxalate ion might affect product quality, Hence uranium reconversion process will be require an additional step for oxalate optimization or killing of oxalate before ADU precipitation.

References :

1. R.Natarajan, IANCAS Bulletin ., 14(2) (1998) 27.

Simultaneous Determination of Uranium and Free Acidity in Uranyl Nitrate Solution by Chemometric Method

Mukesh Kumar, [1, 2] Saurabh Suman[1], S. Pugazhendi[1], K. Dhamodharan[1, §], K.A.Venkatesan [1,2] and K. Ananthasivan[1,2]
[1]*Reprocessing Group, IGCAR, Kalpakkam-603 102*
[2]*Homi Bhabha National Institute, IGCAR, Kalpakkam-603102*
[§] Email: kdn@igcar.gov.in

The modified PUREX process is being employed for the extraction of uranium and plutonium leaving bulk of fission products into high level waste (HLW) during reprocessing of spent fuel discharged from Fast Breeder Test Reactor. To accomplish a good decontamination factor, the process parameters such as free acidity, [U], [Pu] and fission product activities are monitored by analysing samples drawn at different stages of reprocessing. Therefore, the concentration of U, Pu and free acidity must be known in the feed solution before solvent extraction. There are several methods like titrimetry, spectrophotometry, photometry, or time resolved laser induced fluorescence (TRLIF) employed for the determination of concentration of uranium. Acid base titration is most commonly employed for free acidity determination after complexing heavy metal ion present in samples with suitable complexing agents [1]. Most of these methods for U and free acidity determination have several disadvantages like generation large volume of waste and difficult to recover nuclear material from the resultant analytical wastes. Conventional methods said above and existing procedure for recovery of valuable nuclear material from analytical wastes are time consuming causing more radiation exposure to analyst. Therefore, a chemometric method based on UV-Visible spectrophotometry can be regarded as a promising method amenable for online monitoring. The changes observed in UV-Visible absorbance spectra as a function of free acidity and uranium concentration was utilised as basis for this technique. Principle Component Regression (PCR) method was employed for the determination of free acidity and U concentration in Uranyl nitrate solution from UV-Visible spectra obtained for series of samples under simulated condition. Results obtained by this method for the samples consisting of uranium in the concentration range 2-21 g/L and feed acidity in 2-11 M has precision and accuracy of ± 6%.

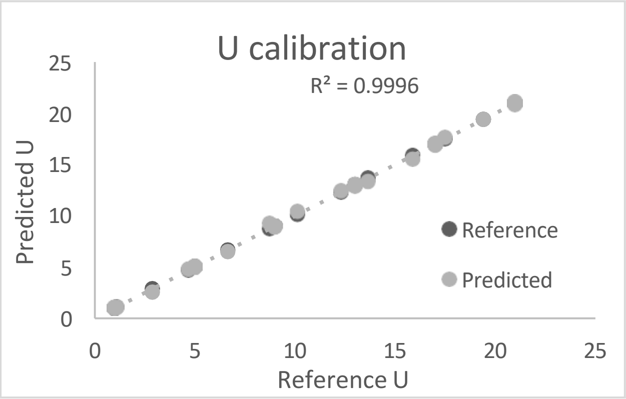

Figure 1: Calibration graph for the estimation of uranium using PCR modelling

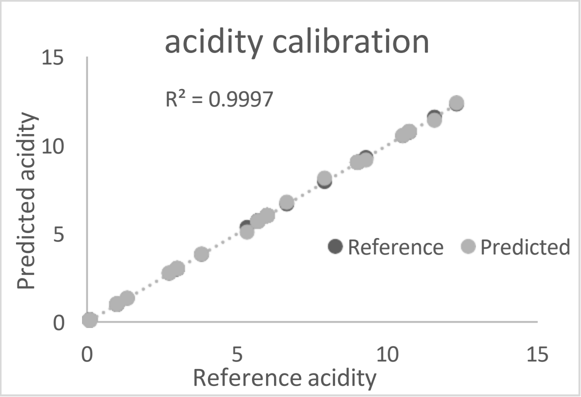

Figure 2: Calibration graph for the estimation of acidity using PCR modelling

References

1. T.G.Srinivasan, P.R.Vasudeva Rao, Free acidity measurement – A review, Talanta, 118 (2014) 162–171

Recovery of Pu from Analytical waste Solutions UsingDibutylbutyl Phosphonate and Diamylamyl Phosphonate based Solvents

K.N. Bikash[1], J.S. Brahmaji Rao[1], G.V.S. Ashok kumar[1], G. Gopakumar[1],
B. Sreenivasulu[1, §], C.V.S. Brahmmananda Rao[1]
[1]*Materials Chemistry and Metal Fuel Cycle Group, IGCAR, Kalpakkam – 603102.*
[§]E-mail: bsrinu@igcar.gov.in

Acidic radioactive waste solutions get generated during the various R&D activities in nuclear industry [1]. The waste solutions thus generated in each step need to be treated before final disposal considering its radio-toxicity to the environment. Waste solution is usually generated in large volumes with relatively lower levels of radioactivity (µCi/L to mCi/L).It is important to recover actinides from aqueous waste solutions due to its strategic significance, chemical and radio toxicity. In the present study solvent extraction based method were examined for the recovery of metal ions from waste solutions. Phosphonates exhibits superior metal ion extraction tendency than the phosphates due to the higher basicity of the oxygen atoms of the P=O groups of phosphonates [2]. In the present study, Dibutylbutyl pphosphonates (DBBP) and Diamylamyl pphosphonates (DAAP) were chosen and studied for the recovery of metal ions from acidic waste solutions in nitric acid medium. The acidity of the waste solution was found to be about 4M. Solutions of DBBP and DAAP (1.1M) in n-DD were prepared and solvent extraction experiments were carried out with equal volumes (5 mL) organic solvent and acidic waste solution. Activity of radio nuclides in the organic phase was estimated by HpGe detector. The maximum extraction of Pu into the organic phase was observed by 1.1M DAAP/n-DD followed by 1.1M DBBP/n-DD and 1.1M TBP/n-DD(Table 1). The extraction of other nuclides (Cs and Eu) by 1.1M solutions of DBBP and DAAP was found to be negligible. Density functional theory (DFT) calculations were performed to understand the electronic structure of all ligands and to compute complexation energies of Pu(IV) with all the ligands. Energetically lowest–lying geometries of ligands, DBBP and DAAP were established using DFT (Fig. 1). The computation of complexation energies of Pu(IV) nitrate complexes with ligands, TBP, DBBP and DAAP are in progress. The higher extraction of Pu by phosphonates based solvent than that of TBP system indicates that phosphonate based solvents can be employed for extraction of Pu.

Table 1. Activity of Radionuclide extracted in the organic phase(nCi)

Radionuclide	Initial Activity of the feed solution(nCi)	Activity of Radionuclide extracted in the organic phase(nCi)		
		1.1M DBBP/n-DD	1.1M DAAP/n-DD	1.1M TBP/n-DD
Cs^{137}	7600	0.2	0.66	0.22
Eu^{154}	53	0.6	0.2	0.4
Pu^{239}	40000	30000	35000	25000
Eu^{152}	3.95	1.3	0.4	0.8

Fig.1. Energetically lowest–lying geometries of ligands (a) DBBP (b) DAAP

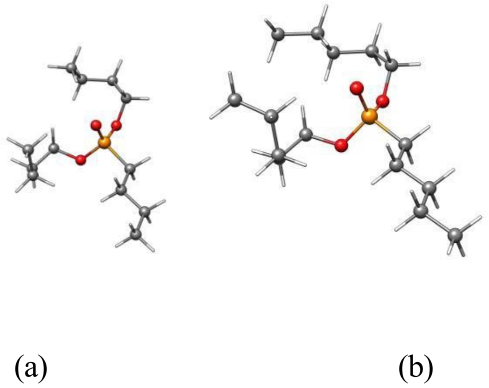

References:

1. B. Sreenivasulu, et. al., *J.Radioanal.Nucl. Chem.***331**(2022)362.
2. C.V.S. B. Raoet. al., *Solvent Extr. Ion Exch,***25**(2007)771.

Development of Magnetically Separable Fe_3O_4-SiO_2@Pt Catalyst for Uranium Reduction

Kuntal Kumar Pal, Ramakrishna Reddy, K. Ananthasivan§, P. Velavendan

Process Radiochemistry Reprocessing Research & Development Division
Reprocessing Group, IGCAR, Kalpakkam- 603102
§ Email: asivan@igcar.gov.in

In the PUREX process for spent nuclear fuel reprocessing 30% TBP-dodecane is used for the co-extraction of U(VI) and Pu(IV) from aqueous nitric acid solution. Once the U(VI) and Pu(IV) is extracted in the organic phase, the plutonium is selectively stripped back into the aqueous phase by contacting the loaded organic phase with an aqueous solution of U(IV), which reduces Pu(IV) to Pu(III) to strip it back to the aqueous phase while U(IV) gets oxidized to U(VI) and moves to the organic phase.

Hence, for the successful partitioning of Pu from U, U(IV) is essential and it can be obtained by reducing U(VI) to U(IV). Platinum particles dispersed over SiO_2 are known to catalyze the reduction of U(VI) to U(IV) under hydrogen atmosphere [1]. Fine catalyst particles are essential to improve the efficiency of the catalyst. However, their separation is more difficult owing to their smaller size.

This paper showcases the work pertaining to the development of a magnetically separable Fe_3O_4-SiO_2@Pt catalyst for the reduction of the U(VI) in an acidic aqueous solution followed by its separation by applying an external magnetic field.

Initially, Fe_3O_4-SiO_2 nanoparticles were synthesized as per the procedure reported in ref. [2] with a slight modification. In order to load the Pt on the host matrix, 1 g of dry Fe_3O_4-SiO_2 powder was initially dispersed in ethanol. Then, 1.4 ml 77 mM chloroplatinic acid was added to this dispersion and stirred for 30 min before the solvent was evaporated to obtain the dry powder. The powder was then heated in a tubular furnace at 150, 200, 250 and 300°C under 8%H_2-Ar atmosphere to obtain the Fe_3O_4-SiO_2@Pt catalyst.

The XRD patterns of Fe_3O_4, Fe_3O_4-SiO_2 and Fe_3O_4-SiO_2@Pt are shown in Fig. 1. Peaks corresponding to the planes of Fe_3O_4 appear in all the samples. In case of Fe_3O_4-SiO_2 a broad peak pertaining to amorphous SiO_2 appears at 2θ of 23 degree. Additional peaks corresponding to 111, 200 and 220 planes of Pt also appear at a 2θ of 39.75, 46.29 and 67.53 in the Fe_3O_4-SiO_2@Pt sample. Temperature dependent reduction behavior of chloroplatinic acid under 8% H_2-Ar atmosphere shows that 150°C is insufficient to reduce Pt^{4+} to Pt^0 and the phase identified from the XRD pattern is $PtCl_4$ appears in the XRD pattern. However, at 200°C and above a complete reduction of Pt^4 to Pt^0 was observed and XRD pattern of these samples reduced at 200, 250 and 300°C revealed the presence of Pt^0.

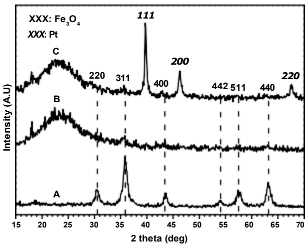

Fig. 1: XRD Pattern of (A) Fe_3O_4, (B) Fe_3O_4-SiO_2 (C) Fe_3O_4-SiO_2@Pt

Acknowledgements: Authors are thankful to Dr. Nithya Ravindran, SND, IGCAR for her support in XRD analysis.

References:
[1] N. K. Pandey et.al, *Ind. Eng. Chem. Res.*, **57** (2018) 3482.
[2] Li Zhou et.al, *Langmuir*, **26** (2010) 11217.

Monitoring the preparation of pyrochemicalsalt (LiCl-KCl-UCl_3) for bulk scale deposition of uranium using AAS &ICP-OES

S. Annapoorani[1], S. Sriram[1], R. Umamaheswari[1], Suganthi[2], K. Suryakumari2, K. Revathy[3], Sourabh Agarwal[3] and [§]S. Vijayalakshmi[1]

[1]*Analytical Chemistry & Spectroscopy Division,* [2]*Metal Fuel and Pyroprocessing Division,*
[3]*Pyroprocess Engineering Division, MC&MFCG, IGCAR,Kalpakkam*
[§]Email: sviji@igcar.gov.in

LiCl-KCl-UCl_3 is prepared by treating LiCl-KCl-$CdCl_2$ salt with metallic Uranium [1]. The complete oxidation of U to $UCl_3$with the reduction of $CdCl_2$ to Cd was ensured bymeasuring the concentration of $CdCl_2$ in the salt.Atomic Absorption Spectrometry (AAS) and Inductively Coupled Plasma Optical Emission Spectrometry(ICP-OES) were standardised for the determination of Cd in the pyrochemical salt. The standardised method has been applied to the monitoring of preparation of pyrochemical salt required for the bulk scale deposition of uranium by pyrochemical reprocessing method.

Standardisation of AAS and ICP-OES for the determination of Cd in pyrosalt:

Under the normal operating conditions of AAS,matrix interference for Cd at high salt level was investigated by measuring absorbance without and with D_2 correction and the studyclearly indicated the requirement of D_2 background correction at high salt concentrations. In ICP, spectral interference due to U matrix for Cd was studied for the recommended three wavelengths (214.438, 226.502 and 228.802 nm). All the three recommended wavelengths of Cd do not have spectral interference problem due to uranium till 5 mg/mL level and thus were recommended for analysis.Accuracy was established by the analysis of typical samples using both AAS and ICP-OES.

Standardisation of sampling and dissolution procedure and application to salt samples from various stages of process:

The preparation of LiCl-KCl-UCl_3at the operating temperatureof 773K involves the formation of Cd metal which is expected to get settled at the bottom due to density difference between Cd and salt.Therefore, to ensure the absence of contribution from the Cd metal to the measurement, sampling method was standardised and top of the salt phase was recommended for sampling. $CdCl_2$ is soluble in water whereas Cd metal is not soluble in water. Both $CdCl_2$ and Cd are soluble in HNO_3. The results of concentration of Cd measured using AAS in various samples taken in duplicate dissolved by both water and HNO_3 were compared and the results (Table 1) showed the contribution from metallic Cd vapour as salt dissolved in acid was found to give higher value than the salt dissolved in water.

Table 1 Results of salt samples by AAS

Sample Ref	Cd Conc. (%)	
	Acid soluble	Water soluble
Sample 1	0.06	0.03
Sample 2	0.05	0.03

Flame AAS is recommended for the regular analysis as the requirement is only for a single and sensitive element Cd. ICPOES was also standardised and the accuracy of AAS was established by the analysis of typical samples using both techniques. From the analytical results it was confirmed that complete conversion of LiCl-KCl-$CdCl_2$ to LiCl-KCl-UCl_3 was achieved.

Acknowledgements:Authors express sincere thanks toHead, MFPD and Sri.Muralidharan for providing the samples. Authors also thank AD, FMCG and Director, MCMFCG.

References:[1] B. Prabhakara Reddy, S. Vandarkuzhali, T. Subramanian, P. Venkatesh, ElectrochimicaActa, 49 (2004) 2471–2478

Aqueous speciation of pentavalent uranium with heterobifunctional phosphonocarboxylates

Ashutosh Srivastava[1, §], Rama Mohan Rao Dumpala[1], Neetika Rawat[1], P.K. Mohapatra[1]
[1]*Radiochemistry Division, BARC, Mumbai, India-400085*
[§] Email: sriashu@barc.gov.in

Pentavalent uranium (UO_2^+) is generally treated as an unstable species in aqueous solutions [1]. It undergoes rapid disproportionation [1] to form uranyl(VI) and U(IV) species. Hence, its aquatic speciation is highly challenging, resulting in a knowledge gap corresponding to the comprehensive understanding of its stability and structure in the aqueous medium. Further, compared to the hexavalent uranium (UO_2^{2+}), knowledge on the aqueous speciation of pentavalent uranium is scarce since most of the literature reports centered around its isolation and except for the carbonate ion, the data on log β values of pentavalent uranium are non-existent, to the best of our knowledge. The presence of uranyl(V) is of great importance to explain the geochemical behaviour of uranium and one-electron reduction of uranyl(VI) to the metastable uranyl(V) in abiotic and biotic environmental conditions [1].

In the present work, aqueous speciation studies on pentavalent uranium with three heterobifunctional phosphonocarboxylates (PCs: PFA, PAA and 3-PPA) chelators were carried out by electrochemistry and DFT methods to understand its stability and structure in aqueous solutions. The cyclic voltammograms (CV) [Fig. 1a] of uranyl in presence of the PCs were monitored with varying pH from 2 to 8, which indicated an interesting observation related to the redox stability of pentavalent uranium with PCs in a wider pH from 2 to 8 as only one reduction peak related to U(VI)-U(V) conversion was observed with varying pH. Through CV, the log β value of UO_2^+-PC complexes were calculated to be 10.17±0.06, 10.55±0.11 and 11.28±0.09. In-situ spectroelectrochemical measurements [Fig. 1b] validate the existence of pentavalent uranium species with PCs in aqueous solution. The appearance of new absorption peaks at 571 nm, 633 nm, 677 nm, 850 nm and 900 nm were found with applied cathodic potentials, which correspond to the UO_2^+ species in aqueous solution [2]. DFT calculations provide the optimized structure, binding modes, bond distances and partial charges of UO_2^+-PCs complexes.

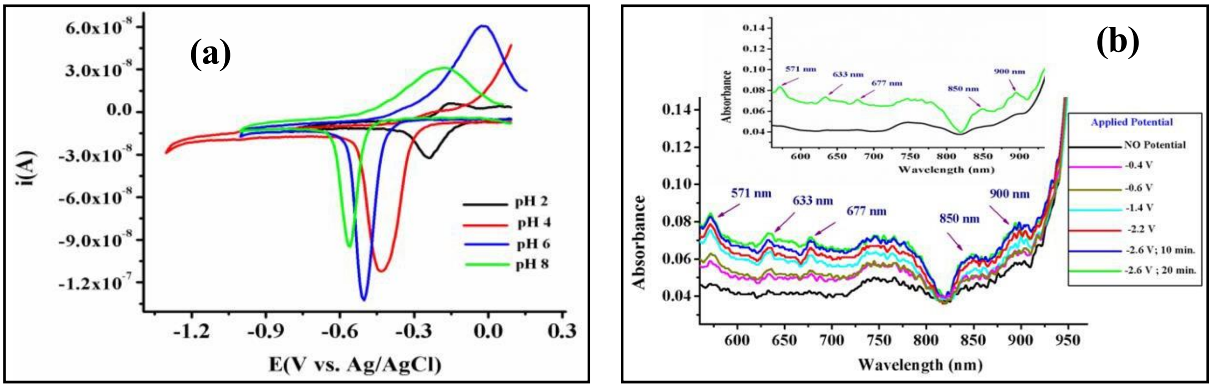

Figure 1: (a) CV plots with varying pH of UO_2^+ (10^{-5}M)-PFA (5×10^{-4}M) (WE: SMDE) (b) Spectroelectrochemical spectra with varying cathodic potential of UO_2^+ (4 mM)-PAA (40 mM), pH 4.

References: [1] Selbin, J. Ortego, J. D. (1969). Chemistry of uranium (V). Chemical Reviews, 69(5), 657-671.
[2] Ashutosh Srivastava, et al. New Journal of Chemistry 41, no. 24 (2017): 15094-15104.

Spectro-electrochemical studies of Neptunium complex of N,N,N’,N’,N”,N”-hexa-n-octylnitrilotriacetamide (HONTA) in $C_4mimNTf_2$

A. Srivastava[1], R. B. Gujar[1], B. Mahanty[1] P. K. Mohapatra[1] W. Verboom[2]
[1]*Radiochemistry Division, Bhabha Atomic Research Centre, Mumbai, India – 400 085*
[2]*Department of Molecules & Materials, University of Twente, the Netherlands*
§ Email: sriashu@barc.gov.in

N,N,N‘,N‘,N‖,N‖-hexa-n-octylnitrilotriacetamide (HONTA) (Fig. 1a, inset) is a promising extractant for the selective extraction of tetravalent actinides (Th^{4+}, Pu^{4+}) from acidic feed solutions [1, 2]. Room temperature ionic liquids (RTILs) are a class of diluents with very interesting extraction and electrochemical behaviour. This helps in developing better extraction systems leading to intersting extracted species. In the present investigation, we have carried out the extraction followed by spectro-electrochemical studies of the extracted neptunium complex of HONTA in $C_4mim.NTf_2$ as the ionic liquid medium. The extraction studies indicate a distribution ratio of Np(IV) as ca.5.0 with 0.9 mM HONTA in $C_4mim.NTf_2$. The cyclic voltammograms (CV) (Fig. 1a) were performed in the applied potential range from 1.1 V to -2.3 V at glassy carbon electrode, which indicated two reduction and two oxidation peaks at a scan rate of 10 mV/sec. These two reduction peaks at -0.993 V and -1.715 V correspond to the Np(VI)/Np(V) and Np(V)/Np(IV) couples, respectively whereas the two oxidation peaks at -0.479 V and -0.311 V correspond the Np(IV)/Np(V) and Np(V)/Np(VI) couples, respectively. The diffusion coefficients of Np-HONTA complex (monitoring Np(V)/Np(IV)) was determined by the scan rate variation. The reduction peak of Np-HONTA observed to be diffusion-controlled and its D_0 value is found to be 6.15×10^{-7} cm^2/sec. The recorded spectroelectrochemical spectra with varying cathodic potential from -2.2 V to -2.8 V indicate that the absorbance at 985 nm (Np(V)) decreases while that at 717 nm and 736 nm (Np(IV)) increases (Fig. 1, b) with above applied cathodic potential. This suggest that the reduction peak at -1.715 V is corresponding to the Np(V)/Np(IV) couple.

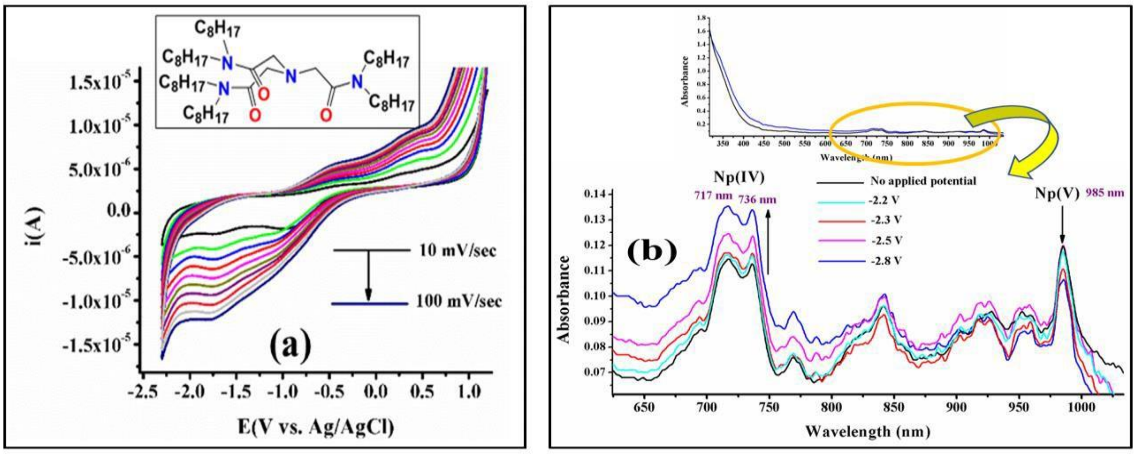

Figure 1: (a) CV plots with varying scan rates, [Np= 0.1 mM] (b) Spectroelectrochemistry plot of Np-HONTA [Np= 0.1 mM] recorded at ITO.

References:
[1] A. Karak et al Sep. Purif. Technol. 279 (2021) 119584.
[2] H. Huang, et al Sep. Purif. Technol. 138 (2014) 65–70.

Development of ATF –studies on variation in grain size of doped urania microsphere prepared by sol-gel process

Buddhadev Kanrar[1], Ashok Kumar[1,§], A.C. Deb[1], Rajesh V. Pai[1,2]

[1] *Fuel Chemistry Division, Bhabha Atomic Research Centre, Mumbai, India*
[2] *Homi Bhabha National Institute, Mumbai, India*
[§] Email: ashkumar@barc.gov.in

In new generation reactors, safety aspects are given prime importance. In this context, large grain size fuel materials which exhibit low radiation swelling, less Pellet Clad Interaction (PCI) and less Fission Gas Release (FGI) are considered a good candidate for Accident Tolerant Fuel(ATF). Grain size of UO_2 depends on various factors, such as, sintering condition, mixing process, presence of additives/dopant etc. Sol-gel process derived materials are known to have distinct sintering characteristics including densification and grain growth at a comparatively lower temperature.

In view of above, present study were undertaken to prepare urania microspheres doped separately with Cr_2O_3, TiO_2 and SiO_2. To assess effect of these additives one batch of undoped urania microspheres was also prepared. Content of dopant in each case was 0.1wt%. Microspheres were prepared by internal gelation process [1] using feed composition in each case as, [M] = 1.25M and [HMTA+ urea] = 1.74. [M] refers to total metal concentration including 0.1 wt% of the dopant, whereas as [HMTA+ urea] is concentration of equimolar mixture of Hexamethylenetetrammine (HMTA) and urea, each being 1.74 molar. After washing, drying , calcination and reduction processes all batches of microspheres, doped as well as undoped were sintered at 1400ºC in vacuum for 4 hours.

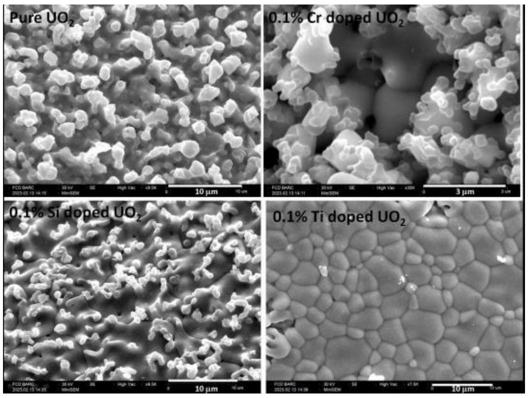

Fig-1 SEM images of pure and doped sintered UO_2 microspheres

Fig-1 gives SEM images of four types of sintered microspheres, undoped urania microspheres and those doped with 0.1wt% of TiO_2, SiO_2, Cr_2O_3. It can be observed that undoped urania microspheres as well as those doped with Cr_2O_3 and TiO_2 shoes almost same grain size about 5µm. On the other hand urania microspheres doped with SiO_2 shows larger grain size, about 20µm. It appears that in case of doping with TiO_2 and Cr_2O_3, mechanism of grain growth is matrix modification type which enhances diffusion process in UO_2 lattice [2,3]. Since such process may require higher temperature no significant increase in grain size was observed at 1400ºC. In case of doping with SiO_2, the mechanism of microstructure modification is through grain boundary [4] as silica forms glassy phase at the grain boundary which facilitates grain growth at lower temperature of about 1400ºC.

Acknowledgements

The authors thank Dr. S. Chaudhury, Head Fuel Chemistry Division for his keen interest and constant encouragement during the course of this work.

References

[1]. P.A. Haas, J.M.Bagovich, A.D.Ryon and J.S.Vavruska, *Ind. Eng. Chem. Prod. Dev.,* **19**(1980) 459.
[2]. I. Amato, et al, *J Nucl. Mater.*, **18**(1966) 252.
[3]. K.C. Radford, J.M. Pope, *J Nucl. Mater.*, **116**(1983)305.
[4]. K. Kawanishi, et al, *Proc. 1994, J14 Atomic Energy Society of Japan, Tokyo* (1966).

Optimization of process variables in solvent extraction separation of iron,cobalt and nickel from simulated PWR fuel crud solution

Pratyasha Panda, Sujata Mishra§

Department of Chemistry, Institute of Technical Education and Research (FET),
Siksha 'O' Anusandhan Deemed to be University, Khandagiri Square, Bhubaneswar-751030,
Odisha, India

§Email :drsujatamishra97@gmail.com/sujatamishra@soa.ac.in

All commercial solvent extraction plants suffer from crud, which mainly caused by solids. The crud results in serious work difficultyfor PWRs which can influence phase continuity, emulsion stability, aqueous solution and air distribution.The porous nature of crud leads directly to severalchallenges caused by its presence. The corrosion product deposit (crud) seen on a fuel rod surface of pressurized water reactors (PWRs) mainly consists of nickel ferrite and due to the activation of core deposits on the surface of pipes giving rise to discharge of these metals .The major elements present in the crud of PWR are Fe,Co and Ni in addition to Cr[1]. Low carbon pathway and use of green solvents have become a must in nowadays solvent extraction method. Due to the ease in operation ,handling and recyclability option, this method has been widely used in nuclear energy industries.In the present investigation the recovery of iron ,cobalt and nickel has been studied from simulated solution in nitrate medium using a novel green hydrophobic decanoic acid-menthol based deep eutectic solvent.Process variables like shaking time, aqueous pH,DES molarity were considered as input numeric factors and concentration of Fe,Co and Ni as response factors for design of experiments.Response surface methodology with Box Benken design , polynomial quadratic model showing maximum R^2 value was chosen for designing of solvent extraction experiments.Total 17 runs were performed and the response varibales were included to optimize the process.DES exhibited higher selectivity for Fe followed by Ni.Co extraction was very low.Fig.1 represents an overview of the abovementioned invesitgation.

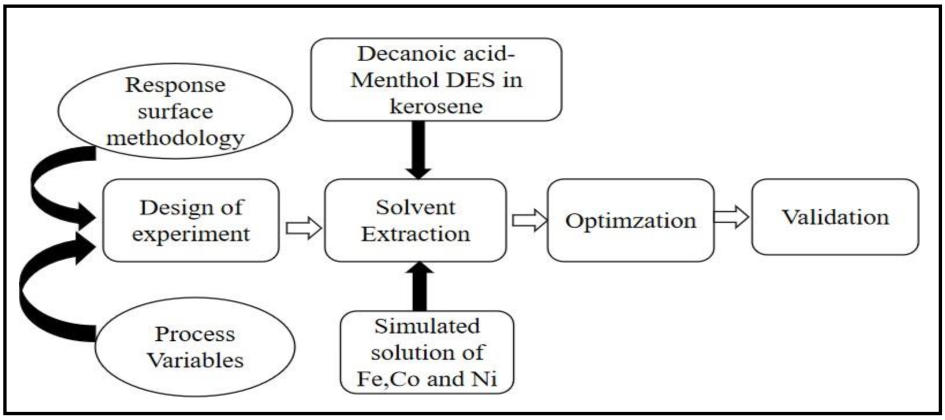

Fig.1.Representation of the summary of the research study

Acknowledgement

The authors are highly indebted and greatful for the generosity shown by Siksha „O" Anusandhan (Deemed to be) university to undertake this research investigation.

References:

1. C.A. Bergamann, J.Roesmer and D.W.Perone,Primary -side deposits on PWR steam-generator tubes. Westinghouse Electric Corp. Pittsburg, PA (USA),1983.

Conversion of lanthanide (Sm, Pr and Nd) oxides to their chlorides in molten LiCl-KCl using $AlCl_3$ for pyrochemical reprocessing

Nibedita Samanta[1,2], S. Maji[2], Satendra Kumar[1,2], Ashish Jain[1,2§]

[1]*Indira Gandhi Centre for Atomic Research, A CI of Homi Bhabha National Institute, Kalpakkam, Tamilnadu, 603102, India*
[2]*Materials Chemistry and Metal Fuel Cycle Group,IGCAR, Kalpakkam, Tamilnadu, 603102, India*
[§] Email: ashish@igcar.gov.in

In pyrochemical reprocessing of U-Pu-Zr metallic fuel, electrorefining (ER) is carried out under inert Ar atmosphere due to the hygroscopic and air sensitive nature of the metal (actinides, lanthanides) chlorides, spent metallic fuel, electrolyte salt (LiCl-KCl) and actinide electrodeposits [1]. Trace amount of O_2 impurity converts actinide and lanthanide (Ln) chlorides to their corresponding oxides or oxychlorides which is undesirable for ER process. Hence conversion of actinide oxides to corresponding chlorides is important step for pyrochemical reprocessing. During conversion of actinide oxides to its chlorides, Ln oxides may react with the chlorinating agent and form chlorides in molten salt. Therefore, a detailed study of the conversion process of Ln is necessary to increase the efficiency of the conversion process of actinides.

A mixture of lanthanide (Sm, Pr and Nd) oxides were chlorinated with double the stoichiometric amounts of $AlCl_3$ in LiCl-KCl media at 773 K for 45 minutes under constant stirring. The reaction products were dissolved in H_2O after sampling and filtered to remove oxides. The filtrate was analysed with UV-Vis absorption spectrophotometry. Fig. 1A shows absorption spectrum of a filtrate. Various absorption bands are observed corresponding to the intra 4f transitions of Sm^{3+}, Pr^{3+} and Nd^{3+} ions. These bands are well matched with the reported transitions [2]. For quantification 402, 444 and 797 nm peaks are used for Sm, Pr and Nd respectively and their values were obtained from the calibration plots (Fig. 1B) made with standards in presence of 50 mg mL^{-1} salt and 2 mg mL^{-1} $AlCl_3$ as the product always contains salt as matrix and some amount of unreacted $AlCl_3$.

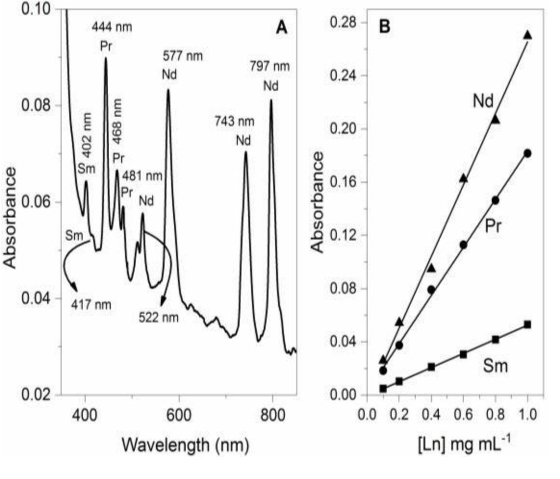

Fig. 1: (A) UV-Vis absorption spectra of the equilibrated product of Sm_2O_3 + Pr_6O_{11} + Nd_2O_3 + $AlCl_3$ in LiCl-KCl in 1 M HNO_3 (B) Calibration plots for Lns

It is observed that the individual lanthanide oxide reaches ~95% conversion efficiency within 45 minutes. The conversion efficiencies of Sm, Pr and Nd were found to be nearly 91%, 95% and 93% respectively in the chlorination of mixture of oxides. It indicates that the conversion efficiency of each lanthanide is not influenced in the presence of other Ln oxides.

References:
[1] J.J. Laidler et al., *Prog. Nucl. Energy*, **31** (1997) 131.
[2] L.M. Sharaf El-Deen et al., *J Alloys Compd.*, **465** (2008) 333.

Simulation of Gaseous phase, Liquid Phase, and Mass Transfer Reactions of Iodine Species in the Containment under severe accident conditions

Archana V.[1, §] and Mohammad Saif Osmani,[2]

[1]*Reactor Safety Division, Bhabha Atomic Research Centre, Mumbai, India*
[2]*Atomic Energy Regulatory Board, Mumbai, India*
[§] Email: archanav@barc.gov.in

Iodine is considered to be released during Beyond Design Basis Accident as well as postulated Design basis accident (DBA) like Loss of Coolant Accident. The extent of release depends on the fuel heat up under these scenarios. The released iodine subsequently will get released into the environment through containment leakage paths. Iodine radionuclide species are considered to cause thyroid damage and their concentration in the environment determines short term emergency planning for NPPs undergoing a severe accident [1]. Iodine is highly reactive and undergo many reactions in the containment. A module named RASAYAN is developed for studying the chemical behavior of iodine within the containment [2].

The RASAYAN module models various mass transfer processes between sump and gas, mass transfer of iodine species on dry and wet surfaces of the containment, chemical reactions in the gas phase, and chemical reactions in the liquid phase. The models are tested for a sample case having a total volume of 0.3 m^3 and a sump volume of 0.00332 m^3. The interfacial surface area between gas-sump is s 0.0051 m^2. The initial masses of various iodine species present in the sump and gas volume are specified. The various chemical reactions as mentioned earlier are simulated. The various iodine species namely elemental/molecular iodine, iodide ion, organic iodine, organic compound, and iodate in the containment are as shown in Figure 1. The mass of iodine adsorbed various dry and wet surfaces in the containment is shown Figure 2. The paper presents model descriptions of gas-sump mass transfer processes, and liquid, and gas phase reactions.

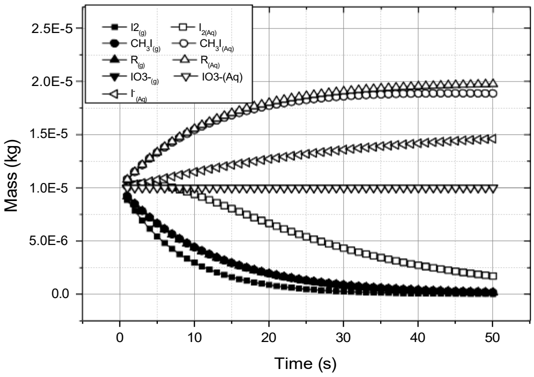

Figure 1: Evolution of various Iodine and organic species in gas phase and sump

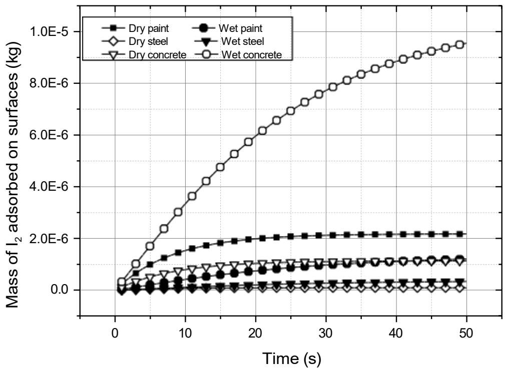

Figure 2: Mass of Iodine adsorbed on various surfaces

References:

1. AERB safety manual on methodology for radiational impact assessment of nuclear power plants under postulated accident conditions. Technical report, Atomic Energy Regulatory Board, Mumbai, 2019
2. Archana V., Mohammad Saif Osmani, RASAYAN Theory manual, RSD Report, Rep. No.RSD/CSSS/035/05/2022

Tracer technique to estimate the efficiency of radionuclide trap material in liquid sodium

A. Manivannan, P. Ravisankar, G. Saravanan, R. Sudha,§ and Kitheri Joseph
1. Materials Chemistry and Metal Fuel Cycle Group, Indira Gandhi Centre for Atomic Research, Kalpakkam 603102, Tamil Nadu, India. §email: rsudha@igcar.gov.in

In fast reactors, activated corrosion productsare formed due to activation of core structural materials. These activated corrosion products get transported by the coolant and get deposited on the surface of the primary heat transport components causing constraint on access for the maintenance of the components. ^{54}Mn, ^{58}Co&^{60}Coare the radionuclides of major concern due to their relatively long half-life and high gamma energy. The concentration of the radionuclides and in turn the activity burden can be reduced by incorporating a radionuclide trap using a suitable trap material [1]. Pure nickel is the best suited trap material for manganese and experiments were carried out at lab scale using inactive manganese. Subsequently trapping efficiency of the trap material is estimated using radiotracer technique in static sodium.Nickel foam and foil samples were exposed to liquid sodium containing 3µCi of $MnCl_2$. The samples were suspended by a sample holder and immersed in sodium as shown in Fig.1.The samples after sodium exposurewere taken out at intervals of 250, 500, 1000 and 2000 hat 773 K. The uptake of ^{54}Mn by the samples at various time duration was counted using well type NaI(Tl) detector with efficiency of 21 %. The measured activity (cps) was plotted as a function of time for both Ni foam and foil shown in Fig.2. The Ni foam and foil shows similar trend in their uptakeand Ni foam shows higher uptake than foil due to its large surface area. The efficiency of trap material is defined as

where, is the efficiency in percentage at a given temperature and time.
It is observed from the Fig.2thatthe uptake of ^{54}Mn by 1 g of Ni foamat 773 K for 2000 h is 2.7 µCi and itstrapping efficiency is 90 %.

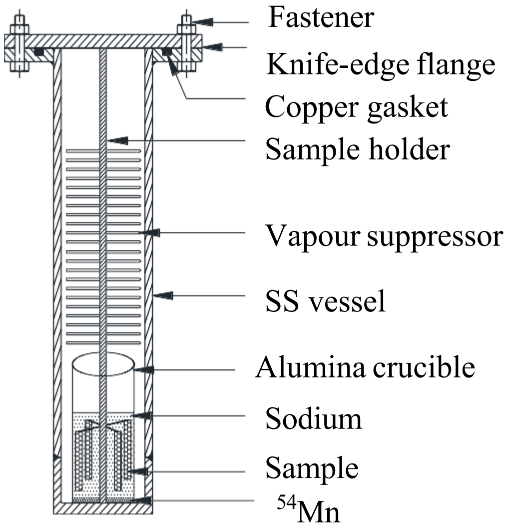

Fig.1.Schematic of an

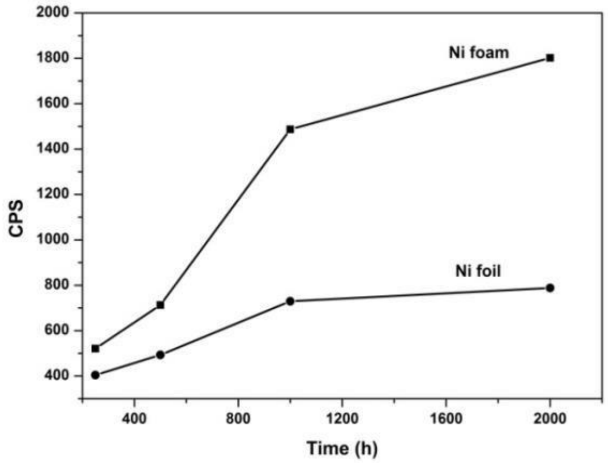

Fig.2. Uptake profile of ^{54}Mnat 773 K

Acknowledgement: The author grateful to Shri. Bramhaji Rao for his support during counting of samples and Mrs. J. Vithya for transfering of radioactive source.

Reference:[1] Fission and corrosion product behavior in liquid metal fast breeder reactors (LMFBRs), International Atomic Energy Agency, Tech document TECDOC- 687, (1993).

Extraction studies on Acidic Intermediate Level Radioactive Liquid waste (ILW) using composite solvent

G. Saipriya§, P. Revathi, V.K. Madhavan Kutty, G. Srinivasa Rao, N.R. Jawahar

INRP-K, NRB, BARC Facilities, Kalpakkam, India
§ saipriya2009@igcar.gov.in

Spent fuel reprocessing plants generate broadly three categories of liquid waste viz. high, intermediate and low-level liquid waste. The intermediate level liquid waste (ILW) arises from the condensates of co-decontamination and purification cycle raffinates. These are made alkaline and stored in carbon steel tanks for further management. Alkali addition increases the TDS and volume of ILW considerably and accumulation of precipitates at the bottom of the tank which poses difficulties in further management of the waste. Majority of the radioactivity of the waste is due to ^{137}Cs and traces of ^{90}Sr, ^{99}Tc & ^{106}Ru. Treatment of ILW in acidic medium itself would be highly beneficial in addressing problems related to handling of large quantity of alkaline liquid waste and it opens up ways to recover valuable isotopes from ILW. In this context, an attempt is made to evaluate a single step process for the management of ILW in acidic conditions by the composite solvents containing 1,3-di-octyloxycalix[4]arene-crown-6 (CC6) and bis-(2-ethylhexyl)diglycolamide (TEHDGA). Macrocyclic compounds (CC6) are promising extractants capable of selectively binding the cesium (Cs) from large concentration of interfering elements [1]. In earlier studies, we have used CC6 impregnated resin for the extraction of Cs in acidic waste [2] and TEHDGA to remove actinides and fission products. In the present study, batch experiments were conducted with a combination of CC6+TEHDGA and TEHDGA alone to separate radioactivity from ILW.

Extraction experiments were carried out in duplicate by equilibrating equal volumes of organic containing 0.03M CC6+0.4M TEHDGA and 0.4M TEHDGA in 50% Isodecyl alcohol (IDA) + 50% n-dodecane (n-DD) and aqueous phases having ILW in the acidic range of 3 M for about an hour. The concentrations of metal ions present in the aqueous phase before and after equilibration were determined by ICP-OES & radiometric measurements were carried out for the same to find out the gross α, β and γ activities (table.1). It is clear from the table that the gross beta & gamma activities are reduced by ~90% with composite solvent CC6+TEHDGA, indicating effective extraction of Cs by CC6 and extraction of gross alpha, U, Tc & Sr is due to the presence of TEHDGA. Along with these fission products, significant amounts of P (81.5 ppm) & Mn (360 ppm) were also estimated in feed sample. Studies are in progress to achieve higher extraction with respect to gamma activity and optimized conditions for Ru extraction. CC6+TEHDGA is found to be suitable composite solvent to reduce the radioactivity of ILW.

Table 1. Extraction behaviour of various elements / radionuclides present in ILW

Element		Feed	After extraction	
			0.03M CC6 + 0.4M TEHDGA	0.4M TEHDGA
Concentration (mg/L)	U	1360	<0.1	<0.1
	Tc	37.1	1.25	1.00
	Sr	1.85	0.045	0.046
	Ru	55.5	55.2	55.5
Gross Activity (mCi/L)	α	0.4	BDL	BDL
	β	53.3	4.25	36.0
	γ	42.0	4.10	38.0

References:
[1] J.N. Sharma et.al., *Sep. Sci. Technol.*, **135** (2014) 176.
[2] G. Saipriya et.al., 15th Biennial DAE-BRNS NUCAR symposium, India (2021) 167.

Synthesis, Characterization and Thermophysical Properties of Multi Lanthanide doped Calcium Fluorapatite

Pratik Das[1,3§], Bal Govind Vats[2,3§], Muhammed Shafeeq[1], S.C.Parida[1,3]

[1]*Product Development Division, Bhabha Atomic Research Centre, Mumbai 400085, India*
[2]*Fuel chemistry Division, Bhabha Atomic Research Centre, Mumbai 400085, India*
[3]*Homi Bhabha National Institute, Bhabha Atomic Research Centre, Mumbai 400085, India*
Telephone-+91-22-25594080, +91-22-25599079
[§]Email: pratikdas@barc.gov.in, bgvats@barc.gov.in

Fluoride containing nuclear waste generated from MSR (Molten Salt Reactor) reactor type is not suitable for vitrification in borosillicate glass due to poor solubility [1]. Natural apatites have been shown to be resistant to weathering for thousands of years and can accommodate various metal ions in different oxidation states. This observation led to the researchers to consider fluorapatite as a potential ceramic waste form for radioactive fluoride waste. Lanthanides are generated in nuclear fission in sizeable amount. In view of this, multi lanthanide doped, $NaPr_{0.125}Nd_{0.125}Sm_{0.125}Eu_{0.125}Gd_{0.125}Tb_{0.125}Dy_{0.125}Ho_{0.125}Ca_8(PO_4)_6F_2$ compound was synthesized by solid state reaction route by optimizing the synthesis temperature to obtain the pure apatite phase. The phase of the compound was identified by powder X-ray diffraction (XRD). To determine the thermal expansion of the compound, high temperature XRD data (HTXRD) was recorded starting from ambient temperature up to 1123K in argon atmosphere. The compound showed positive thermal expansion up to 1073 K. The HTXRD profile is shown in Fig.1(a). The obtained average thermal coefficients of the compound is given in Table-1. Molar heat capacity of this compound was also measured experimentally for the first time and shown to vary with temperature as $[C_{p,m}^{o}(T)] \pm 2 = 751.705+0.4174\times(T/K)-1.003\times10^{7}/(T/K)^{2}$ and shown in Fig.1(b) .

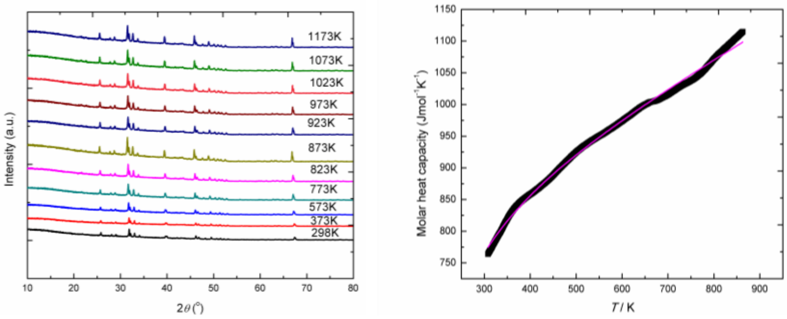

Fig.1. (a) HTXRD study (b) Molar heat capacity study of $NaLnCa_8(PO_4)_6F_2$ compound

Table 1: Average thermal expansion coefficient of $NaLnCa_8(PO_4)_6F_2$ compound

Compounds	**Temperature range(K)**	**Average thermal expansion coefficient [$\times10^{-6}$] K^{-1}**		
		$\alpha_a = \alpha_b$	**α_c**	**α_{vol}**
$NaLnCa_8(PO_4)_6F_2$	298-1123	14.024	12.904	41.220

References:
[1] P. Das, B. G. Vats, P. Samui, S. Kesari, M. Shafeeq, S. C. Parida, S. Dash, *Chem. Select*, **6** (2021),13817.

Computational study of interaction of aqueous strontium nitrate with Kaolinite clay

Shelly Goel[a,e,§], Amrit Pal Singh[b,e], Manish Chopra[c] and Niharendu Choudhury[d,e]

[a]Health Physics Division, Bhabha Atomic Research Centre, Mumbai 400085, India,
[b]Health Physics Unit, Nuclear Fuel Complex, Hyderabad 500062, India,
[c]Radiation Safety Systems Division, Bhabha Atomic Research Centre, Mumbai 400085, India,
[d]Chemistry Division, Bhabha Atomic Research Centre, Mumbai 400085, India,
[e]Homi Bhabha National Institute, Anushaktinagar, Mumbai 400094, India.
[§] Email: shellygarg@barc.gov.in

Long-lived radioactive fission products like Cs-137 and Sr-90 are the most important contaminants associated with nuclear fuel cycle. These radioisotopes pose key concern in the geological storage of radioactive waste. Understanding their behavior in aqueous solutions in the presence of soil minerals will help in evolution of advanced waste management strategies and studying their fate in case of leaching of these radionuclides into groundwater. In the present study, molecular dynamics (MD) simulations are carried out using the LAMMPS package to investigate adsorption behavior of Sr^{2+} ions on the surfaces of Kaolinite (clay) in its aqueous nitrate solution. The potential parameters for strontium and nitrate ions are taken from the literature [1-2] and the well-known SPC/E model [3] of water is used. The kaolinite is modelled based on CLAFF Force Field [4]. The simulations were performed at a target temperature of 300K and 1 atm pressure using periodic boundary conditions in all three directions. The cut-off distance of 12.5 Å was used for all short-range non-bonding interactions and Ewald summation was employed for Coulomb interactions. For a period of simulation of 20 ns, Radial (Pair) Distribution Function g(r) with respect to oxygen of water (O_W) showed a maximum at around 2.51 Å (Fig. 1a). The coordination number n(r) value of 9 for strontium ions w.r.t. O_W and zero w.r.t. nitrate oxygen (O_N), although not shown here indicates nil participation of nitrate ions in the first coordination shell (FCS) of Sr^{2+} ion. The peak near siloxane surface of Kaolinite in the single-particle atomic density profiles of Sr^{2+} indicates the adsorption of Sr^{2+} ions on kaolinite by forming the outer sphere complex through water molecules (Fig. 1b). We have identified different types of complexes formed by Sr^{2+} ions with water and nitrate ions and tried to explain their adsorption behavior based on these.

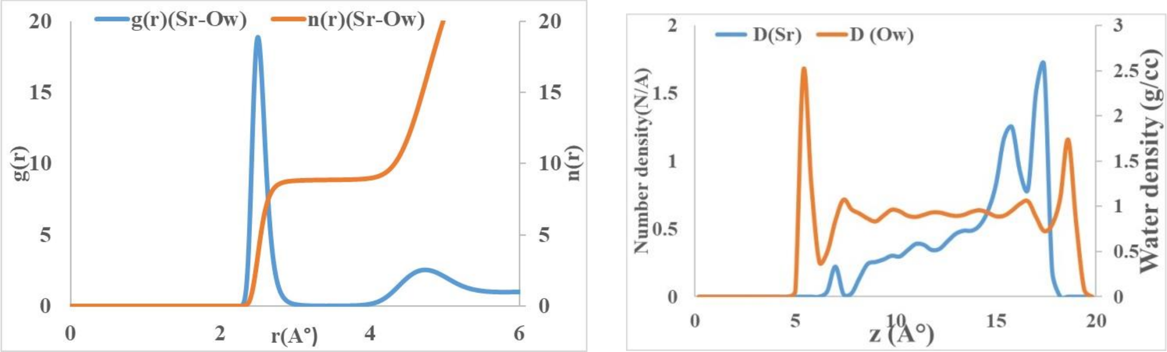

Fig. 1: (a) Radial distribution function (g(r)) and coordination number n(r) of Sr^{2+} w.r.t water (b) Density profiles of Sr^{2+} ion and water

References:
[1] A. Nikitin and G. D. Frate, J. Comput. Chem., 40 (2019) 2464.
[2] H. Krienke and D. Opalka, J. Phys. Chem. C, 111, (2007) 15935.
[3] H. J. C. Berendsen, J. R. Grigera, T. P. Straatsma, J. Phys. Chem., 91 (1987) 6269.
[4] R. Cygan, J. Liang and A. Kalinichev, J. Phys. Chem. B, 104 (2004) 1255

Enthalpy of formation of $RE_2(MoO_4)_3$[RE= La^{3+} and Sm^{3+}]

Manjulata Sahu[1, §],Rimpi Dawar[2], Kanaklata Pandey[1], M. K.Saxena[1]

[1]*Radio Analytical Chemistry Division,* [2] *Chemistry Division,*
Bhabha Atomic Research Centre, Mumbai-400085, India
[§]Email: manju@barc.gov.in

The nuclear waste is commonly immobilized in borosilicate glass. With time the borosilicate glasses degrades by changing to yellow colour due to presence of different molybedates of alkali and alkaline earth metal. Later, the rare earth elements have been found to substitute the alkali and alkaline earth metal in various molybedates and are hygroscopic [1]. Knowledge of thermodynamic properties of the yellow phases is vital in understanding their phase stability. Moreover, the rare earth elements and molybdenum were found to have very high fission yield during fission of uranium oxide based nuclear fuel [2]. High probability of interaction between the oxide of rare earth and molybdenum may occur at reactor operating conditions.The present work involves the measurement of standard enthalpy of formation of $RE_2(MoO_4)_3$[RE= La^{3+} and Sm^{3+}] employing a Calvet calorimeter (HT-1000, M/s Setaram, France). The solvent used was $3Na_2O.4MoO_3$ kept at 978 K. $La_2(MoO_4)_3$and $Sm_2(MoO_4)_3$were synthesized via pechini routeandcharacterized by powder XRD technique.

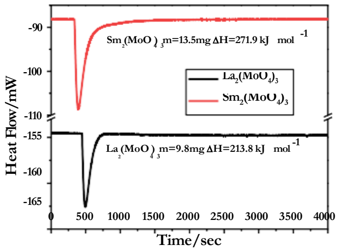

Fig. 1 Variation of heat flow with time for the dissolution of $La_2(MoO_4)_3$ (s) and $Sm_2(MoO_4)_3$ (s)

Table 1. The molar enthalpies of dissolution of $La_2(MoO_4)_3$(s) and $Sm_2(MoO_4)_3$(s) in $3Na_2O.4MoO_3$ solvent at T = 978 K

Sample Name	**Amount of sample / g ^{a}**	**ΔH (J/g)**	**(kJ mol^{-1})**
$La_2(MoO_4)_3$ (s) Molar mass = 757.62 g mol^{-1}	0.0098 0.0084 0.0048 0.0069	282.17 279.29 286.64 281.06	213.78 211.60 217.16 212.94 **Ave =213.87 ± 2.37**
$Sm_2(MoO_4)_3$ (s) Molar mass = 780.53 g mol^{-1}	0.0066 0.0135 0.0079 0.0058	353.35 348.42 356.25 350.14	275.80 271.95 278.06 273.29 **Ave = 274.78 ± 2.71**

The standard molar enthalpies of formation at 298 K of $La_2(MoO_4)_3$(s) and$Sm_2(MoO_4)_3$(s)were calculated by employing suitable thermochemical cycles (Table 1) and taking the required values from literature [3].The standard molar enthalpies of formation of $La_2(MoO_4)_3$ (s) and $Sm_2(MoO_4)_3$(s) at 298 K obtained in the present study are -4237.54 ± 1.66 and -4261.37 ±4.53 kJ mol^{-1}, respectively.

Reference(s):

[1]Y.Kinoshita at al, *Mater. Trans.*, **60**,111-120(2019).
[2]H. Kleykamp, *J. Nucl. Mater.* **131**, 221–246(1985).
[3]I. Barin, Thermochemical data of pure substances, third ed., VCH Weinheim (Federal Republic of Germany), 1995

Study of proton induced activations in natural Fe and steel composites

Sabyasachi Paul[1,§], A.A. Shanbhag[1], S. C. Sharma[2] and M. S. Kulkarni[1]

[1] *Health Physics Division, Bhabha Atomic Research Centre, Mumbai, India*
[2] *Nuclear Physics Division, Bhabha Atomic Research Centre, Mumbai, India*
[§] Email: spaul@barc.gov.in

The charge particle interactions with the structural materials are encountered at almost all radiation facilities and the study of induced activity becomes immensely important from the radiation protection perspective. Among the structural materials, the ^{nat}Fe or steel based composites are abundantly used in the radiation installations as machine components or as the primary barrier for the radiation sources. In the present study, induced activities were estimated in two different types of carbon steel (A-106 and A-333) and compared with earlier estimated [1-2] yields from ^{nat}Fe and stainless steel (SS-304). The irradiation of targets with 20 MeV proton beam was performed at the 6m port of BARC-TIFR Pelletron linac facility, Mumbai, India. The proton induced reactions on the carbon steel composite yielded intermediate and long lived radio-isotopes like ^{57}Co (271.8 d), ^{54}Mn (312.3 d), ^{56}Co (77.3 d), ^{58}Co (70.9 d), etc. through various nuclear reaction pathways like (p,γ), (p,n), (p,2n). The γ dose-rate for these samples was measured for estimation of the contributions from short lived isotopes and the quantification/decay profile for intermediate or long half-life radionuclides were followed up to 500 days using γ-spectroscopy. The γ-dose rate at a distance of 6 cm from the samples after 4 h delay was found to be ~1.5 mSv h^{-1} mC^{-1} g^{-1} and the dose rate reduces by 3 orders of magnitude upon a delay of 10^4 h. Among the two carbon steel samples irradiated, the A-106 showed marginally higher γ-dose rate compared to A-333. The spectrometric analysis identifies the presence of long-lived ^{56}Co, ^{57}Co, ^{58}Co and ^{54}Mn isotopes. The initial cumulative γ-dose rate from the irradiated SS-304 was found higher compared to ^{nat}Fe and carbon steel due to contributions from the short lived isotopes viz. ^{61}Cu (3.33h), ^{57}Ni (1.48 d),^{52}Mn (5.59 d), ^{51}Cr (27.7 d), produced from stable Cr and Ni isotopes used as additives in SS-304. The Fig. 1 represents the comparison of induced yield for short-lived ^{57}Ni and relatively long lived ^{58}Co isotopes. The study concludes that, utilization of SS-304 and carbon steel do not differ widely from the decommissioning aspects but SS-304 generates higher quantity of short lived induced activity per unit mass, a judicious selection of materials during facility commissioning would reduce radiation exposures during the maintenance activities.

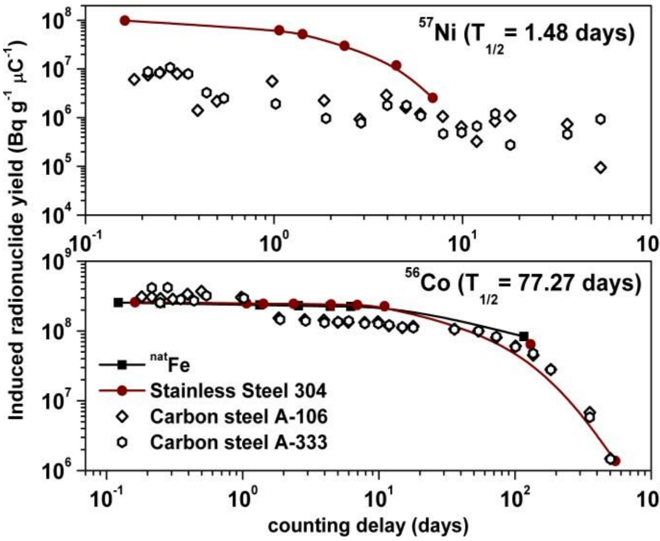

Fig. 1: Induced ^{57}Ni and ^{56}Co isotope yield comparison from 20 MeV proton bombardments on metal sample

References:
[1] S. Paul et. al., Journal of Radioanalytical and Nuclear Chemistry, **323** (2020) 1299.
[2] S. Paul et. al., Journal of Radioanalytical and Nuclear Chemistry, **325** (2020) 781.

Apparent enhancement in the mass transfer kinetics of Cs and Sr during microfluidic extraction/stripping conditions in nitric acid-CCD/PEG aqueous-organic pair

Shekhar Kumar[1,§], R.V. Subba Rao[1]
[1] FRPPCG, Reprocessing Group, IGCAR, Kalpakkam 603102, India
[§] Email: shekhar@igcar.gov.in

Removal of heat emitters like Cs-137 and Sr-90 from the HLLW is an important process step with two tangible benefits- societal usage of fission products as well as in lowering the temperature of vitrified waste for safe and sustained storage. In the literature [1], several processes like macrocyclic crown ethers or chlorinated cobalt dicarbollide (CCD) based methods are reviewed in detail. Kumar et al. [2-3] reported results of batch runs for Cs and Sr extraction and stripping in aqueous nitric acid-CCD/PEG-400 biphasic system as shown in Fig.1. Kumar and Rao [4] reported Cs/Sr co-extraction and co-stripping in 3D-coiled microfluidic microbore channel as shown in Fig.2. In the batch experiments, minimum time observed for reaching 90% the steady state for extraction/ stripping was about 10s/50s and 50s/5s for Cs(I) and Sr(II) respectively. However as 100 μm diameter based micro bore tubing has only a volume of 3.14 μL, it can provide a residence time of only about 0.38s for a combined throughput of 0.5 mL/min for both extraction and stripping experiments.

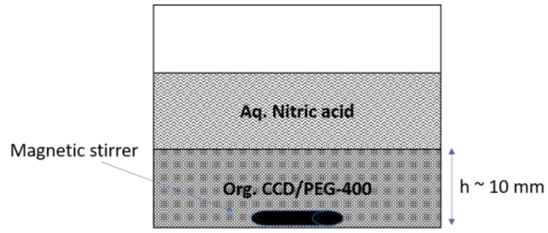

Fig. 1: Typical batch mixing setup.

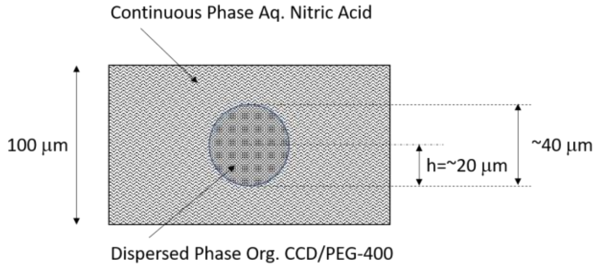

Fig. 2: Mixing in 100 mm dia microfluidic tubing.

The mixing time, required to cover the diffusion length, is given by the Eq.1,

$$t = \frac{h^2}{D_T} \tag{1}$$

Where, Taylor-Aris diffusivity D_T is given by the Eq.2,

$$D_T = D_{AB} + \frac{1}{210}\frac{u^2h^2}{D_{AB}} \tag{2}$$

The diffusivity of Cs-CCD complex D_{AB} was estimated at $2.0\text{x}10^{-11}$ m²/s. The Taylor-Aris effect causes significant enhancement in the effective diffusivity in both the cases, i.e., batch mixing as well as mixing in microfluidic flows. Hence the apparent enhancement in the extraction/stripping kinetics of Cs/Sr under microfluidic flow conditions may be explained on the basis shortening of the diffusion length due to Taylor-Aris effects.

References:
[1] T.A.Todd *et al.* Technical report INEEL/EXT-04-01895, INEEL, US, 2004.
[2] Shekhar Kumar *et al. Proc. SESTEC-2016*, 138, Guwahati 17-20 May 2016.
[3] Shekhar Kumar *et al. Proc. NUCAR-2017*, 314-315, Bhubaneswar 6-10 Feb 2017.
[4] Shekhar Kumar and R.V. Subba Rao, *J. Radioanal. Nucl. Chem.*, **329**, 351, 2021.

Leaching behavior of Technetium (^{99}Tc) trapped in Goethite and immobilized in CWP Matrix

R. K. Sah[§], V. K. Mittal, T. P. Valsala, D. B. Sathe, R. .B. Bhatt
Analytical Lab, TWMP, FF, NRB BARC Tarapur (India)
[§] Email: rksah@barc.gov.in

Technetium-99 is one of the fission products with very high yield (~6%) in thermal neutron induced fission of ^{235}U. The high solubility in water and high mobility of pertechnate ions, coupled with very high half-life of ^{99}Tc ($t_{1/2} = 2 \times 10^5\ y$, βmax = 290 keV) makes it a potential candidate for long term hazard to the environment [1]. The major radionuclide present in the Low level effluent waste (LLW) from the IX column is ^{99}Tc. In one novel process, technetium has been made captured in goethite by making use of in-situ formed corrosion products of mild steel [2]. In this paper, preparation of cement blocks with captured Technetium (^{99}Tc) in Goethite and subsequently leaching behavior of ^{99}Tc from active Cemented Waste Product (CWP) has been detailed.

Since nature of Tc sludge waste was acidic, it couldn"t be directly cemented. Hence, the waste was first neutralized with 4 molar NaOH solution and mixed with Ordinary Portland. The CWP were prepared with Tc sludge waste and cement in the ratio 0.9:1, 1:1, 1.1:1. The curing time of CWP blocks was 28 days. Compressive strength was tested on different inactive cement blocks which were prepared using Fe sludge in same proportion as active CWP blocks. Leaching study of ^{99}Tc from active cement blocks for in water is in progress.

The Tc sludge waste was characterized and the details is in Table 1. Primary investigation showed that, compressive strength (Table-2) of CWP blocks are less than that of cement blocks having no sludge waste. Leach rate of the CWP blocks are shown in Fig. 1 and after 30 days leach rate is given in Table 2. The leaching study will be continued for more time to established stabilized leach rate. The results are satisfactory.

Table1: Characterisation of Tc sludge waste:

Property	Nature		Sludge (%)	TS (%)	α (mCi/L)	β (mCi/L)	^{99}Tc (mCi/L)	Cs^{137} (mCi/L)	Sb125 (mCi/L)	Fe (g/L)
Values	Acidic		70	13	7.59 e-3	0.98	0.76	0.06	0.11	28

Table-2: Compressive strength & LR of CWP

Sl no.	Waste to cement ratio	Compressive strength (N/mm^2)	Leach rate after 30 days, g.cm^{-2}.d^{-1}
1	0	5.6	--
2	0.9:1	3.3	4.42×10^{-5}
3	1:1	2.2	4.48×10^{-5}
4	1.1:1	1.5	5.31×10^{-5}

Figure 1: Leach Rate of Tc for all CWP

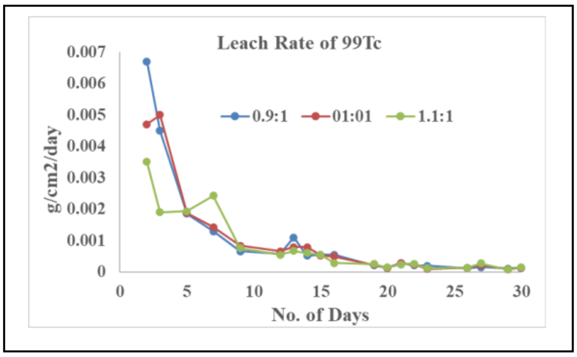

References:
1. R.E. Wildung, K.M. McFadden and T.R. Garland, J. Environ. Qual., 8 (1979) 156.
2. J.G. Shah, et. al., U.S. patent number 10,553,324 and EP3417461B1, 2020.

Elucidating the Corrosion Effect of Strontium on Plant Structural Material

Kankan Patra[§a], V. K. Mittal[a], Ashok Kumar Sahu[b], T. P. Valsala[a], D.B.Sathe[a], R.B.Bhatt[a]
[a]*Nuclear Recycle Board, Bhabha Atomic Research Centre, Tarapur 401504, India*
[b]*Glass & Advanced Materials Division, BARC,Mumbai-400085,India*
[§]E-mail: kankan.patra2010@gmail.com

Structural material like stainless steels (SS) was observed to be heavily contaminated during the processing of radioactive liquid waste. Their safe disposal is really challenging to nuclear industry[1]. If the chemical behavior steel metal corrosion could be determined, effective decontamination as well as successful decommissioning process could be planned. In view of this, studies were carried out to understand the chemical behavior of contamination on SS304L alloy under the exposure of strontium (Sr) under 70°C as the dissolution side the plant temperature reach up to 70°C, since Sr is one high yield fission product, most heat emitting and long half life. For understanding of Sr adsorption behavior on structural materials scanning electron microscope/energy dispersive X-ray spectroscopy (SEM/ EDX) was carried out before and after the exposure under HNO_3 medium at 70°C for 3 months. Figure 1a and 1b represent the SEM image of metal surface before and after exposure respectively. It was clearly observed that surface was corroded and found rough in nature. Figure 1c showed the EDX layered image of the exposed metal from the elemental mapping it was cleared that Sr metal was deposited on metal surface. Table 1 revealed the elemental composition of before and after exposure of metal surface. Around 1% Mn was also observed in both cases.

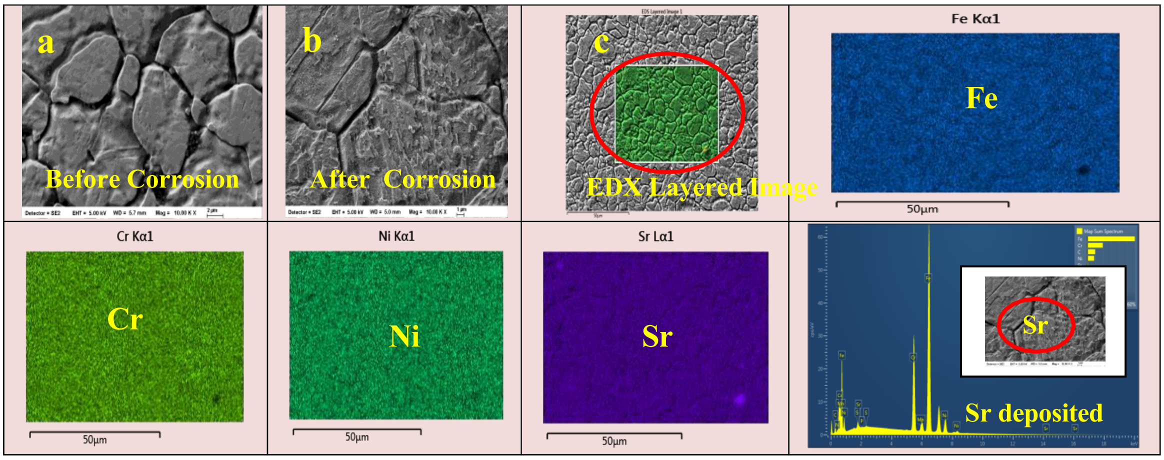

Figure 1: SEM image of (a) before exposure (b) after exposure (c) EDX image of exposed metal

The deposition of Sr was noticed, while SS coupons were exposed to Sr solution. It was found SS surface is mildly passivated under 3M HNO_3 and room temperature the by Cr enrichment by formation of Cr oxide layer on metal surface. This experimental result will facilitate to design a suitable corrosion inhibitor material and effective decontamination agent.

Table 1: Elemental composition of corroded SS metal

Element	**Before exposure composition (Wt %)**	**After exposure composition (Wt%)**
Cr	21.97	21.67
Fe	68.22	67.91
Ni	9.79	9.52
Sr	0.00	0.88
Total:	100.0	100.0

References: 1. C. Rivasseau, E. Farhi, A. Atteia, A. Couté, M. Gromova. Energy Environ. Sci.**6**,2013,1230−1239.

Treatment Feasibility of High Active Carbonate Waste

Soumya Sen[§], Gopal Sharma, V. K. Mittal, T. P. Valsala, D. B. Sathe and R. B. Bhatt

Fuel Fabrication, Nuclear Recycle Board, BARC, Tarapur, Maharashtra, India
[§] Email: ssen@barc.gov.in

In reprocessing plant, decontamination (DC) of various tools was carried out in the course of HL cell DC. The generated waste was mixed with carbonate washing of spent solvent used in PUREX cycle. The waste was difficult to treat by conventional IL (intermediate level) process due to presence of some organics generated in the HL cell DC, high concentration of salt and high activity of waste. Vitrification could not be done due to high concentration of sodium in waste [1].

Lab scale study was done to see the feasibility the high alkaline waste along with current low active IL waste. In IL process, the alpha DC steps and Cs removal through Resorcinol Formaldehyde (RF) resin steps must not disturb with this mixing. Hence, 2% of this high active alkaline waste was decided to mix with the IL waste and the above two steps of the IL process was checked prior to use in the running plant.

The detailed characteristics of the mixed waste was presented in Table 1. In alpha DC steps, the mixed waste was treated for carbonate killing by addition of Nitric acid up to pH 2. Alkali was added to increase the pH up to 12.5 for alkaline precipitation and details of the decanted solution is given in Table 2. The volume of precipitate was observed less than 1%, due to less quantity of uranium in the waste (~20ppm). In Cs removal step, decant was passed through 25 ml of NaOH soaked RF resin with controlled flow rate of 1 bed volume per hour. Total two bed volumes of waste were passed. The column was placed inside of heavily shielded hollow container to minimize the radiation field in working area. DF of around 1500 was observed with respect to beta activity and 90000 w.r.t Cs after passing through RF column (Table 2). Alpha DF was not significant after alkaline precipitation and considerably high (~1 x10^{-3} mCi/lt) in RF effluent may be due to less quantity of uranium. The Cs removal steps work efficiently. The high alkaline and high active waste can be treated with mixing with current IL waste.

Table 1:Characterization of waste

Sample	High active waste	IL waste	Mixed waste
α (mCi/lt)	6.76	0.04	0.12
β (mCi/lt)	1942	5.44	46.65
CO_3^{2-} (M)	0.57	0.63	0.46
HCO_3^- (M)	0.4	ND	ND
Free alkali (M)	ND	0.29	0.57
Cs^{137} (mCi/lt)	1770	4.6	42.61
$Sr^{90}Y^{90}$,Sb^{125}, Ru^{106}, Tc^{99} (mCi/lt) (calculated)	~170	~0.7	~4.04

Table 2 Result of streams generated during study

Sample	α (mCi/lt)	β (mCi/lt)	pH/ molarity	Cs^{137} (mCi/lt)
Mixed waste	0.12	46.65	CO_3^{2-} 0.46M alkali 0.57M	42.61
Acid addition	0.13	39.47	1.9	NA
Decant after alkaline pptn	0.11	34.87	12.5	32.16
Effluent	7.7x10^{-4}	2.34x10^{-2}	12.5	3.7x10^{-4}

ND= Not Detectable, NA= Not Analyzed

References:

[1] N. L. Sonar et al., *Journal of Radio analytical and Nuclear Chemistry* **331** (2022).

Performance evaluation of silvercoated alumina catalyst for the removal of iodine species from aqueous streams

Krishan Kumar[1,§], H. Seshadri[1], Shrikant S. Padhy[1]and D. K. Mohapatra[1]

[1]*Safety Research Institute, Atomic Energy Regulatory Board, Kalpakkam, Tamil Nadu, India,*
[§] Email: kgoyat55@igcar.gov.in

Iodine is the main fission product of the fuel used in Nuclear Power Plants (NPPs) and is generated in large quantities during power operation. The chemistry of iodine in the containment atmosphere and sump is complex since iodine can exist in several oxidation states (-1 to +7), including iodine (I_2), iodide (I^-), iodate (IO_3^-), periodate and organic iodide.[1].The major fraction of iodine-bearing aerosols will eventually reach the containment sump, where quite complex aqueous chemistry processes will take place. Since release behaviour and mitigation strategies depend on propertiessuch as pH, temperature, redox status and organic carbon content, studies related to Iodine speciation and its associated uncertainties are extremely important for accident management view point [2]. Therefore, it is essential to devisemethodologies to retain iodine species in the sump without making it airborne,thereby limiting its potential transport out of the containment.

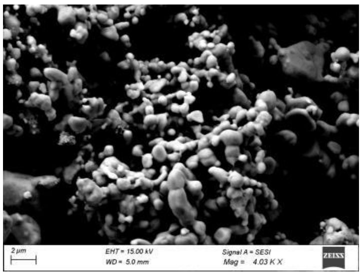

Fig. 1: SEM Image of silver coated alumina

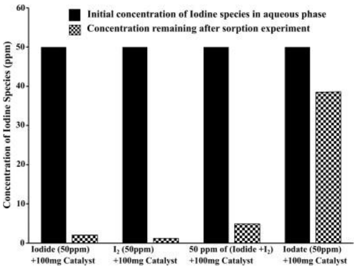

Fig. 2:Sorption of iodine species using silver coated alumina

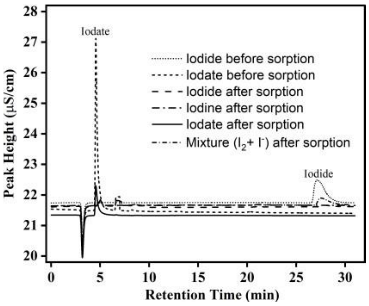

Fig. 3:Chromatogram of different iodine species before and after the sorption experiment

This study aims in the synthesis, characterization and evaluation of suitable sorbent for the retention of different iodine species in the sump phase. Silver coated alumina was synthesized in-house by chemical impregnation method. The synthesized catalyst was characterized using SEM-EDX to find out the morphology, extent of silver loading etc (Fig.1). For the experiments, simulated sump solutions containing 50mg/L of iodine species (I^-, I_2, IO_3^-, mixture of I_2 and I^-etc) were equilibrated with 100mg of catalyst for 2 hours and the extent of iodine retention was estimated using ion chromatographic method. The SEM EDX reveal that silver is distributed uniformly over the alumina matrix. More than 95% of iodine species (I^-, I_2 and mixture of I^- and I_2) and 23% of iodate could be retained by the catalyst(Fig. 2&3). The study demonstrates that the synthesised silver coated alumina catalyst is highly effective for the retention of iodine species, which could retain them in the aqueous phase itself.

References:
[1] Jungsook Clara Wren, Joanne M. Ball, Glenn A. Glowa “The Chemistry of Iodine in Containment”, Nuclear Technology, Vol.129, (2000), 297-325.
[2] Joffrey Huve, Andrey Ryzhikov, Habiba Nouali, Virginie Lalia, Gregoire Auge and T.Jean Daou, RSC Advances, 8 (2018), pp 29248-29273.

Loss of metal ions and HDBP during acidification of hydrazine carbonate based waste streamresulted during lean organic treatment

Satyabrata Mishra, Pankaj, Chayan Patra,Debojyoti Ghosh, N. Desigan*,P. Velavendan,
K.A Venkatesan, K.A Ananthasivan

Process, Radiochemistry and Reprocessing R& D Division,
Indira Gandhi Centre for Atomic Research, Kalpakkam, Tamil Nadu-603102
*Email: desi@igcar.gov.in

The lean organic generated during the reprocessing of Pu rich FBR spent fuel contains considerably high amount of di-butyl phosphate (HDBP). The use of Na_2CO_3 as wash reagent has few constraints during process operations. Hence, hydrazine carbonate (HC) was employed as an alternate reagent for the primary clean-up of radiolytically degraded 1.1 M TBP/n-dodecane.The aqueous waste generated during the clean-up,primarily contain HDBP and the retained metal ions such as Uand Pu. Further processing of this aqueous waste demands near quantitative removal of DBP along with the recovery of retained metal ions. Hence, investigations were carried out with simulated aqueous solution containing DBP and U. The aqueous alkaline waste was acidified to enable the separation of HDBP by diluent wash followed by evaporation forthe subsequent recovery of metal ions by solvent extraction.

Three sets of experiments were carried out using 1.5 M HC containing 1, 2 & 3 gL^{-1} of DBP. The U (VI) concentration was varied from 100-1000 mgL^{-1}, 250-2000 mgL^{-1} and 500-3000 mgL^{-1} in those sets respectively. During the process of acidification of HC solution for the separation of HDBP, formation of yellow precipitate and emulsion in some cases were observed which could be mainly due to the HDBP-U (VI) complex which has poor solubility in nitric acid medium. This led to some loss of HDBP as well as U (VI) during the acidification process. Present work is an effort to quantify these losses. All acidification experiment was carried out in two portions., A solution of 1.5 M HC with DBP & uranium was taken in two different vials. Equal volume of 7M nitric acid was added to both portions to get a final acidity of 2M. One portion was subjected to filtration followed by extraction with n-DD for HDBP separation where as another set was subjected to n-DD extraction without filtration.The HDBP and the U content after acidification followed by n-DD extraction with and without filtration were estimated to account for the loss in precipitate as given in figure 1 & table 1 respectively.

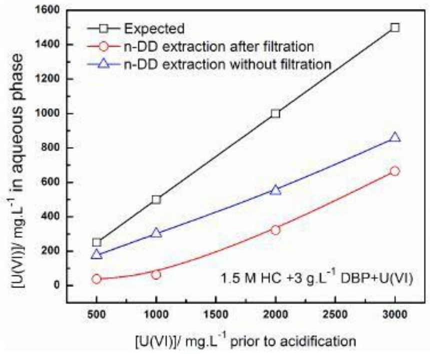

Fig1 Loss of U(VI) during acidification

Table 1 Loss of HDBP during acidification of 1.5 HC having 3 $g.L^{-1}$ DBP with various concentrations of U(VI)

[U(VI)] \ $mg.L^{-1}$ (before acidification)	Expected [HDBP]/ $mg.L^{-1}$ (after acidification)	Without filtration extraction with n-DD		Loss [HDBP]/ $mg.L^{-1}$	With filtration extraction with n-DD		Loss [HDBP]/ $mg.L^{-1}$
		$[HDBP]_{Aq}$ / $mg.L^{-1}$	$[HDBP]_{Org}$ / $mg.L^{-1}$		$[HDBP]_{Aq}$ / $mg.L^{-1}$	$[HDBP]_{Org}$ / $mg.L^{-1}$	
500	1500	244	1140	116	213	918	369
1000	1500	229	1033	238	202	570	728
2000	1500	102	647	751	83	267	1150
3000	1500	83	451	966	37	240	1223

The loss of U(VI) could be clearly attributed to the solid formation during acidification. In the case of extraction without filtration, some of the U(VI) trapped in the solids are getting extracted and hence the apparent lost is less. Further work is in progress to overcome this loss by adopting a different procedure for processing this aqueous alkaline waste.

Effect of Assorted Functional Groups in Highly Stable Zirconium based Metal organic frame works on Hydrogen Adsorption under various Pressures

V. Venkata Sravani,[1,2] M. Bootharajan,[2] B. Sreenivasulu,[2§] A.Suresh,[1,2] and C.V.S. Brahmmananda Rao,[1,2]
[1]HBNI, Training School Complex, Anushaktinagar, Mumbai-400094, India
[2]MC&MFCG, IGCAR, Kalpakkam-603102, Tamil Nadu, India
[§]*E-mail: bsrinu@igcar.gov.in*

Hydrogen has a wide range of applications in various fields, including petroleum refining, aerospace applications, pharmaceuticals due to its peculiar properties. In addition, Hydrogen gas is a promising candidate for future use as an energy carrier in vehicles and air-crafts [1]. Metal–organic frameworks (MOFs) have emerged as an advanced generation of nanoporous materials [2]. Numerous research studies have been carried out to develop MOFs for solid-state hydrogen storage applications [3]. Herein, three distinct functionalized zirconium based MOFs such as UiO-66-MOFs; UiO-66-SO_3H@Si (2-monosodium sulphoterephthalic acid), UiO-66-PDCA (2, 5 pyridine dicarboxylic acid), and UiO-66-AO@Si (amidoxime), with Zr^{4+} metal, are synthesized and examined for hydrogen adsorption at distinct pressures from 0.67 to 2.1 bar and at a fixed temperature (77 K). The functionalized UiO-66-MOFs showed variations in surface area, porosity, thermal, chemical stability, and hydrogen adsorption efficiency. Besides this, UiO-66-SO_3H@Si and UiO-66-AO@Si showed outstanding chemical stability in nitric acid medium up to 8 M and 6 M, respectively. The increasing order of hydrogen adsorption by three UiO-66-MOFs are as follows: 0.12 wt.% (UiO-66-SO_3H@Si) < 0.25 wt.% (UiO-66-PDCA) < 0.35 wt. % (UiO-66-AO@Si) at 2.1 bar and 77 K (**Table 1**). In comparison to the other two MOFs, UiO-66-AO@Si exhibited the highest hydrogen adsorption making amidoxime-based MOFs as an attractive contender for potential H_2 storage materials at 77 K. Hydrogen storage in these functionalized UiO-66-MOFs is accomplished through solely physical adsorption. The high surface area and porosity of UiO-66-AO@Si are important factors in achieving the high hydrogen adsorption than other two MOFs. The successful desorption of hydrogen gas from MOFs was achieved at room temperature (**Figure 1**).

Table 1: **Hydrogen adsorption values for UiO-66-MOFs**

Pressure (bar)	UiO-66-SO_3H@Si	UiO-66-PDCA	UiO-66-AO@Si
	H_2 capacity (wt.%)	H_2 capacity (wt.%)	H_2 capacity (wt.%)
0.67	0.040	0.10	0.2
1.13	0.062	0.14	0.23
1.35	0.076	0.16	0.25
1.67	0.081	0.17	0.28
2.1	0.101	0.25	0.35

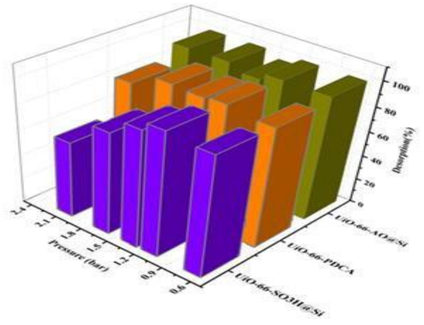

Figure 1. Hydrogen desorption capacities (wt.%) of UiO-66-MOFs with respect to pressure.

Acknowledgement: I am thankful to Dr. N. Sivaraman for his keen interest in this

References:

1. E. Tsivion, et al. *Journal of the American Chemical Society,* **136** (2014) 17827-17835.
2. L. Chen, et al. *ACS Applied Materials & Interfaces*, **9** (2017) 32446-32451.
3. M. P.Suh, *Chemical Reviews*, **112** (2012) 782-835.

Recovery of Calix-Crown-6 from Actual Spent Calix Solution for efficient Spent Solvent Management

Deepika Nair[1§], Prema Gireesan[2], D. Banerjee[1], R. K. Mishra[2], A. D. Dharashiokar[2],
Sanjay Kumar[1], Smitha Manohar[2]

[1] *Process Development Division,* [2] *Waste Management Division*
Nuclear Recycle Group, Bhabha Atomic Research Centre, Trombay, Mumbai – 400 085
[§] E-mail: deepikan@barc.gov.in

1,3-dioctyloxycalix[4]arene-18-crown-6 (Calix-Crown-6 or CC-6) is a solvent successfully deployed for the selective separation of ^{137}Cs from High Level Liquid Waste (HLLW) in Waste Immobilization Plant (WIP), Trombay [1]. It is a highly selective extractant which specifically complexes Cs(I) and separates it from the other radio-nuclides present in HLLW. The separated ^{137}Cs is used for the fabrication of cesium pencils which are regularly supplied as blood irradiators to different hospitals. The removal of ^{137}Cs also has the additional advantage of reducing the radio-toxicity as well as the heat load of the waste. The separation of Cs(I) from HLLW is achieved by solvent extraction using an organic phase composition of 0.03 M CC-6 in 50% Isodecyl alcohol (IDA)/n-dodecane (DD). After multiple cycles of Cs(I) extraction, it was observed that while the extraction of Cs(I) remained same, the alpha decontamination factor reduced. This was due to the formation of interfering degradation products, and thus this solvent was removed from the plant for disposal via incineration.

Since CC-6 is an expensive chemical, it was attempted to recover the un-degraded CC-6 from this spent CC-6 solution with the aim of recycling it. For this, in the first step, from 500 mL spent CC-6 solution, isodecyl alcohol/n-dodecane (~ 370 mL) were distilled off under vacuum (0.05 mm Hg, T = 60 ^{0}C) leaving behind a dark red oily residue. The activity of the distilled IDA/n-DD mixture was observed to be background level. An attempt to precipitate the CC-6 crystals directly from the oily residue by adding excess methanol in which CC-6 is insoluble was found to be unsuccessful. Hence, purification of CC-6 from this oily residue was attempted using column chromatography. For this, the oily residue was passed through a silica-gel column and subjected to gradient elution using dichloromethane-petroleum ether as mobile phase. The impurities were removed at this stage, which was confirmed by TLC. The CC-6 was retained in the column which was eluted using ethyl acetate. Finally, ethyl acetate was distilled off to give a dark orange residue which was pure CC-6 as established by TLC, although its physical properties were different. Total recovery of CC-6 from spent CC-6 solution after column purification was approximately 13%. The recovered CC-6 was constituted using IDA/n-DD and analysed for Cs(I) and alpha extraction. The results are presented in Table 1, which clearly indicate that the alpha extraction by CC-6 post purification is significantly reduced, making this solvent suitable for recycling.

0.03 M CC-6 in 50% IDA/n-DD	D_{Cs}	D_{Am}
Spent CC-6	4.0	0.255
Recovered CC-6	3.9	0.007

Table 1. Extraction Studies for Recovered CC-6

References:
[1] C. P. Kaushik et. al., *BARC Newsletter*, (2017) Mar-Apr, 3-4.

Nitric acid effect on oxalate destruction with and without catalyst

Arvind Prasad, K.S Vijayan, N Desigan§, K A Venkatesan and K Ananthasivan

Process, Radiochemistry and Reprocessing Research and Development Division,
Indira Gandhi Centre for Atomic Research, Kalpakkam – 603102
§E-mail: desi@igcar.gov.in

The oxalate supernatant generated in CORAL contains 40-60 mg/L of Pu, 3-5 g/L of U, 0.1–0.15 M oxalate ion in 2.5-3.5 M nitric acid. The presence of oxalate ion in the supernatant can hinder the recovery of plutonium in the subsequent processing step. Therefore this is a need to remove or destroy the oxalate ion present in the supernatant before processing. The destruction of oxalate ion using Mn^{2+} catalyzed nitric acid process at higher temperature was studied in our laboratory [1]. For understanding the process the effect of nitric acid on oxalate destruction was studied in the presence and absence of Mn^{2+} catalyst. The concentration of oxalic acid was fixed to 0.098 M and concentration of nitric acid was varied from 3 M to 12 M (Fig.1) in these experiments. To understand the effect of catalyst on oxalate destruction the experiments were repeated in the presence of 0.01 M Mn^{2+} catalyst (Fig.2). The oxalic acid concentration during course of experiment was determined by titration using $KMnO_4$.

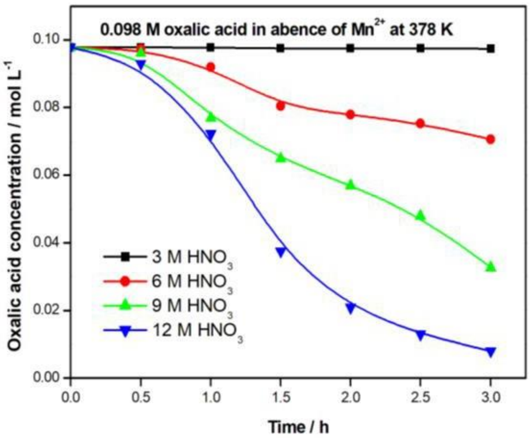

Fig.1. Variation in the concentration of oxalic acid remaining in the solution as a function of time in the absence of catalyst

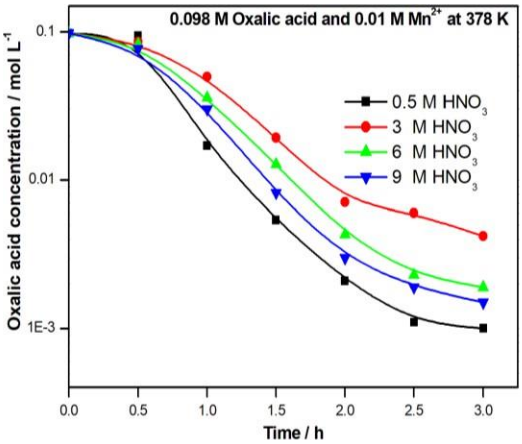

Fig.2. Variation in the concentration of oxalic acid remaining in the solution as a function of time in the presence of catalyst

The mechanism involves the oxidation of oxalate ion to CO_2 by nitric acid. Therefore, the rate of destruction of oxalate ion increases with increase in the case of nitric acid as shown in (Fig.1). The Fig.2 show combined effect of catalyst and nitric acid on the rate of destruction of oxalate ion. This trend indicates some kind of catalytic retardation at higher acidity. The catalytic retardation probably could be attributed to the formation of low spin stable Mn(II)-NO complex [2] at higher HNO_3 concentration, which decrease the availability of Mn^{2+} ion for the reaction with the oxalate ion, inhibiting the destruction.

References:

[1] Arvind Prasad et al in proceedings of the fourteenth biennial DAE-BRNS symposium on nuclear and radiochemistry, BARC, Mumbai(2019), B15, p26 .

[2] Wayland, B.B.; Olson, L.W.; Siddiqui, Z.U. (1976) Nitric oxide complexes of manganese and chromium tetraphenylporphyrin. *Journal of the American Chemical Society*, 98(1): 94-98.

Investigations on the Extraction and Aggregation behavior of Zr loaded Dibutylbutyl Phosphonate and Diamylamyl Phosphonate Solvents

K.N. Bikash[1], G. Sushanthini[1], A. S. Suneesh[1], B. Sreenivasulu[1, §],
C.V.S. Brahmmananda Rao[1],
[1]*Materials Chemistry and Metal Fuel Cycle Group, IGCAR, Kalpakkam – 603102.*
[§] E-mail: bsrinu@igcar.gov.in

Third phase formation is major concern during the extraction of tetravalent metal ion such as Pu(IV), Th(IV) and Zr(IV) with tri- n-butyl phosphate (TBP) based solvent extraction process. Our earlier studies on development of alternative extractant to TBP revealed that phosphonate based solvent such as dibutyl butylphosphonate(DBBP) and diamyl amylphosphonate(DAAP) exhibit lower third phase forming tendency than TBP[1]. Dynamic Light Scattering technique is considered to be an important technique to study the aggregation behaviour in solvent extraction systems.. In this context the aggregation behaviour of TBP, DBBP and DAAP loaded with Zr(IV) was studied using DLS. The number of stages required for quantitative extraction of Zr(IV) has been examined in cross-current mode by 1.1M solutions of DBBP and DAAP in n-DD and compared with 1.1M TBP/n-DD. The concentration of Zr in the organic phase decreases with stage number and the cumulative extraction of Zr were found to be about 97.7, 98.3 and 32.6%, respectively in the case of 1.1M solutions of DBBP, DAAP and TBP in n-DD. The aggregation tendency of the Zr-ligand complex was further examined by DLS experiments. Results of the study indicated that the aggregate size of the Zr-TBP formed was more widely distributed, suggesting the formation of a less stable complex. However, DBBP exhibited a sharp peak of around 20 nm during the first extraction stage, and DAAP peaked at approximately 25 nm. It can also be seen that the aggregate sizes of Zr-DAAP and Zr-DBBP are more intense than the Zr-TBP complex, suggesting that Zr-DBBP and Zr-DAAP complexes are relatively more stable. The decrease in size of the Zr-ligand aggregate with the increase of stage numbers is due to the reduced amount of Zr loaded to the organic phase. Based on the DLS observation and the solvent extraction experiments on zirconium extraction, it can be concluded that DBBP exhibited superior Zr extraction behaviour compared to DAAP and TBP.

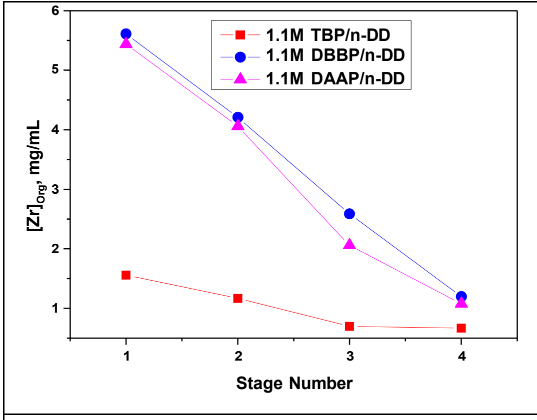

Fig. 1. Organic stage profiles for Zr during the extraction from 4M HNO_3 by 1.1M TBP, DBBP and DAAP at 303K.

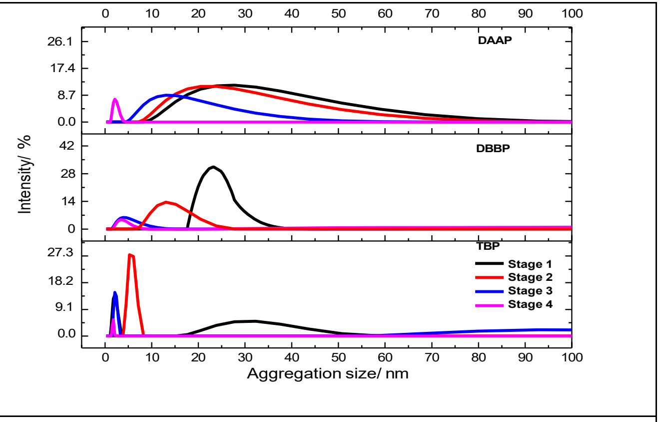

Fig. 2. Variation of Aggregate size with stage number during the extraction from 4M HNO_3 by 1.1M solutions of TBP, DBBP and DAAP in n-DD at 303K

References:

1. C.V.S. B. Rao et. al., *Solvent Extr. Ion Exch*, **25**(2007)771
2. R. Chiarizia et. al., *Langmuir*, **20**(2004)10798

Extraction Studies of Pd(II) by Metal Organic Framework from Aqueous Medium

Somnath Sengupta[1], S. B. Shrikala[2], B. Sreenivasulu[1§], C.V.S. Brahmananda Rao[1]

[1]*Fuel Chemistry Division, Material Chemistry and Metal Fuel Cycle Group, IGCAR, Kalpakkam-603102*
[2] *Amrita Vishwa Vidyapeetham, Coimbatore*
[§] Email: bsrinu@igcar.gov.in

Palladium is a precious and scarce metal that is widely employed in many industries, including electronics, pharmaceutics, catalysis, and other fields. However, extraction of palladium from sources other natural resources is necessary because of its high demand. Owing to the substantial palladium content along with other noble metals, spent nuclear fuel is a good source for palladium. Pd(II) can be extracted using a number of methods, including liquid phase extraction and ion exchange. Solid-phase extraction techniques have various benefits over liquid-phase extraction methods, including higher selectivity, lower cost, etc. Due to their large surface area and porosity, metal-organic frameworks are attractive solid-phase extraction materials. Iso-reticular metal-organic framework-3 (IRMOF-3) and UiO-66-NH_2 have been employed extensively in recent years for a variety of purposes, including membranes, heterogeneous catalysis, gas storage and separation and sensing of different metal ions. In this context, we synthesized two MOFs, viz. Zn and Zr based MOFs for sorption of Pd(II) from aqueous solutions. UiO-66-NH_2 was synthesized according to the procedure reported by Costa *et al* [1] and IRMOF-3 was synthesised as per the procedure reported by Gascon *et al* [2]. The synthesized MOFs were characterised using different techniques like PXRD(Fig.1), FTIR, TGA etc. The IRMOF-3 showed greater sorption towards Pd(II) compared to the UiO-66-NH_2 MOF, which can be attributed to the greater porosity of the former MOF(Fig. 2). Further the effect of temperature and amount of palladium on the sorption behaviour was studied, which also showed that IRMOF-3 has higher affinity towards Pd(II) sorption compared to UiO-66-NH_2.

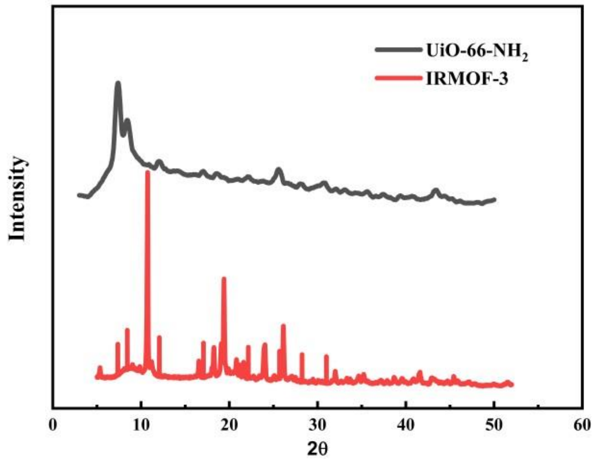

Fig. 1. Powder XRD for UiO-66-NH_2 and IRMOF-3

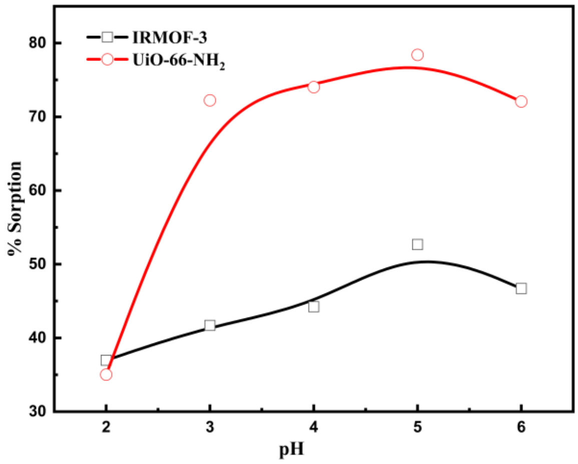

Fig. 2. Variation of sorption(%) with pH of the Pd(II) solution

References:

[1] J. S. Costa *et al*. Eur. J. Inorg. Chem, **10** (2018) 1551-1554.

[2] J. Gascon *et al*. J. Catal., **261** (2009) 75–87.

A new composite of Potassium Cobalt hexacyanoferrate for sequestration of radio-cesium from contaminated water

Prithwish Sinharoy[§], Pallavi Yevale, Dayamoy Banerjee, Sanjay Kumar, Smitha Manohar
Process Development Division, Nuclear Recycle Group, Bhabha Atomic Research Centre,
Mumbai, India
[§]Email: psroy@barc.gov.in

Potassium Cobalt hexacyanoferrate can quantitatively and selectively remove radio cesium over other alkali metal cation from waste water[1]. The selectivity arises from their cubic structures with thin channels having channel diameter compatible for the diffusion of smaller hydrated ions like Cs^+. However, the material is powdery in nature and cannot be directly used in column mode[2] and hence necessitates development of composite granular beads. Zirconium based cement fulfills all the prerequisites of a binder and hence in this study granular beads were prepared by blending zirconia based cements with Potassium Cobalt hexacyanoferrate. Their efficacy towards cesium uptake was evaluated from near neutral water solution. The cesium uptake capacity was calculated as follows:

_ (—) .... (1)

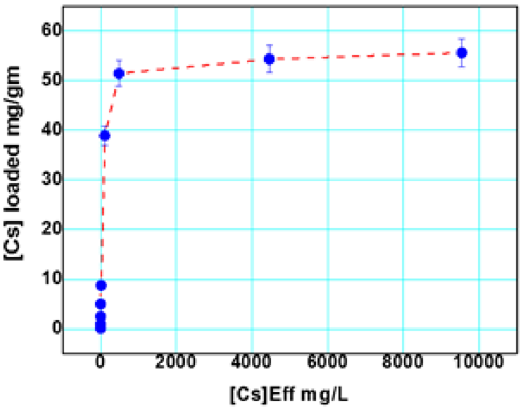

Figure 1. Cs uptake isotherm by composite

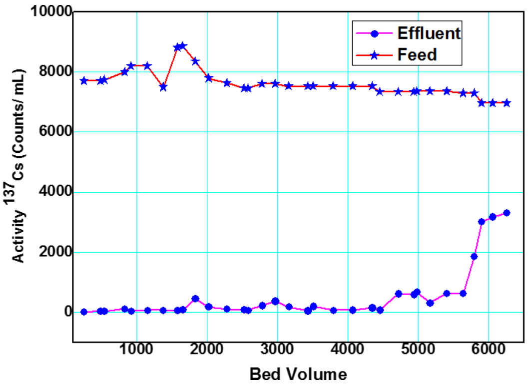

Fig 2. Cs uptake performance in column

The material was found to have a high K_d of $1x10^5$ at a feed solution of 5000 ppm $NaNO_3$ and pH 7.4 spiked with ^{137}Cs. The material retains it uptake performance for a wide range of pH 4 to 10. Maximum metal sorption capacity was found to be 55 mg/gm of the composite when tested at batch mode (**Figure 1**). The metal sorption follows Freundlich isotherm model and K_f was found to be 1.2 & „n‟ value 1.4 indicating a monolayer adsorption. The kinetics was very rapid and equilibrium was reached within 30 minutes. The uptake capacity was also tested at varying concentration of sodium nitrate and it was found that material retains its performance even up to 50 g/L. The material is also tested in column mode and 4500 bed volumes of simulated waste spiked with ^{137}Cs was treated with less than <1 % break through (**Figure 2**). High uptake capacity and fast kinetics makes this composite material a potential candidate for sequestration of radio cesium from waste water solution.

References:

1. Thierry Vincent et.al. , *Molecules,* **20**, 20582 (2015).
2. Julien Kiener et. al. , *Materials,* **12**,1253 (2019).

Characterization of Ruthenium Deposited Silver Disc: The core component of Ru-brachytherapy sources

Prithwish Sinharoy[§], Annie Joseph, Dayamoy Banerjee, Sanjay Kumar Smitha Manohar
Process Development Division, Nuclear Recycle Group, Bhabha Atomic Research Centre, Mumbai, India
[§]Email: psroy@barc.gov.in

^{106}Ru based sealed sourceshave been indigenously developed in BARC, Mumbai and deployed for eye cancer treatment. The source utilizes ^{106}Ru isotope, which is electrodeposited on a silver disk to obtain a uniform dose distribution throughout the surfaces. Physical properties like uniformity, roughness and thickness of Ru coating in surface of silver have significant impact on further process steps of plaque fabrication as well as in treatment. Detailed characterizations of the surfaces obtained under different experimental conditions have been carried out and the highlights of salient characteristics features are presented in this paper.

The physical properties of the coating are function of two major parameters in electrodeposition step viz. current density and electrolytic medium. The cell used for deposition of Ruthenium on silver was as follows:

$$Pt \,|\, HCl\ (aq)\ |HCl,\ Ru(III)\ (aq)|Ag$$

The SEM micrograph of Ruthenium deposit (**P1**) obtained under optimum condition (5 mA/cm^2 current density and 0.1 M HCl solution as catholyte) is shown in **Figure 1**. It can be seen that the deposits is uniform and has no cracks and crevices. The EDS mapping of the plate (shown inset of figure 1) ascertains uniform distribution of Ru (green) on top of silver (red).Higher acidity beyond 0.5 M HCl in catholyte resulted in poor quality deposition with less current efficiency which could be due to formation of anionic species like $[Ru(Cl)_6]^{-3}$.Higher current density resulted in rough black colour deposition probably due to formation of RuO_2 on surface. The AFM surface topography and three-dimensional scan of deposition P1 is shown in **Figure 2**. The RMS roughness values of the coatings deposited is 5.041 nm. Thermal stability of the deposit was analyzed from the TG-DTA profile and it is observed that there is insignificant mass loss up to 800 ^{O}C. Information gathered from present study helped to develop an optimized process flow sheet for fabrication of actual Ru plaques.

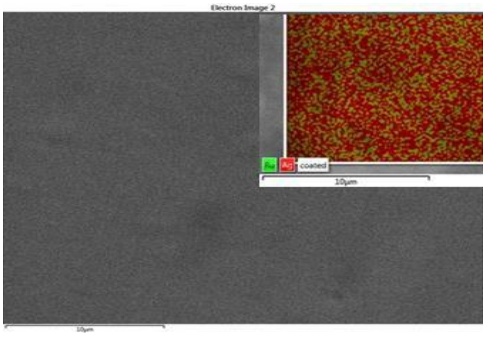

Fig 1: SEM micrograph

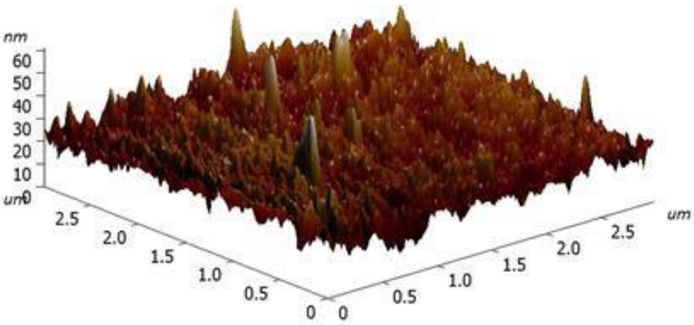

Fig 2: AFM Micrograph of Ru deposited disc

References:

1. M. Jayakumar et.al. Materials Chemistry and Physics 128 (2011) 141–150.

Metal retention behaviour of diluent degradation products

Satyabrata Mishra[1], Debojyoti Ghosh[1],Puspalata Rajesh[2], N. Desigan[1§], K A Venkatesan[1]
andK. Ananthasivan[1]

[1]Process, Radiochemistry and Reprocessing R& D Division,
[2]Water & Steam Chemistry Division, BARC (F), Kalpakkam
Indira Gandhi Centre for Atomic Research, Kalpakkam, Tamil Nadu-603102
[§]Email:desi@igcar.gov.in

The PUREX solvent, tri-butyl phosphate (TBP) in n-dodecane (n-DD),during the reprocessing of spent fuel, undergoes hydrolysis and radiolysis due to the intense ionizing radiation environment and decay heat from the short-lived radio isotopes in addition to the chemical environment due to presence of nitric acid. The primary degradation products resulted during solvent degradation are aqueous washable unlikethe secondary degradation products like high molecular weight phosphates and the diluent degradation products which are responsible for the retention of metal ions. There is a scarcity of information on the metal retention behavior of the diluent degradation products. In this context, investigations were carried out on the gamma radiolysis of n-DD in monophasic as well as biphasic system in presence of 4M HNO_3. Gamma radiolysis was carried out up to 500 kGy.The zirconium metal retention behavior of the irradiated diluent was determined before and after alkali wash upon diluting the degraded n-DD up to 1.1 M using fresh TBP and was compared with un-irradiated solvent.

For Zr metal retention test, the irradiated organic phases (made up to 1.1 M using fresh TBP) were equilibrated with 1.2 gL^{-1} of Zr (IV) in 4M HNO_3. The metal loaded organic phase was stripped using 1M HNO_3. The Zr(IV) distribution behavior by the n-DD solutions irradiated in presence of nitric acid (made up to 1.1 M using fresh TBP) before and after alkali wash is compared in figure 1.The Zr (IV) metal retention by the irradiated diluents before and after alkali wash are given in Table 1.

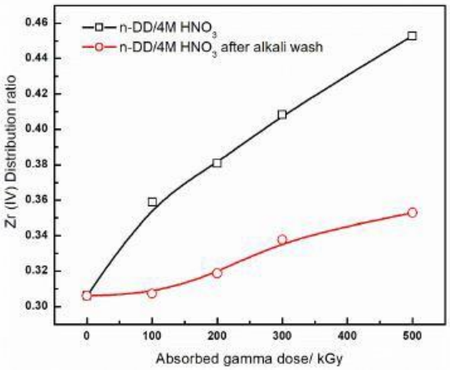

Fig1 Zr(IV) distribution in the Purex solvent with irradiated diluent

Table 1 Zr(IV) retention by Purex solvent with diluent degradation products

System	Before wash				After wash			
	loading	1st strip	2nd strip	Retained Zr	loading	1st strip	2nd strip	Retained Zr
Unirradiated 1.1 M TBP/n-DD	281	145	21	115	281	145	21	115
1.1 M TBP/ [(n-DD+4M)-100 kGy)	317	128	9	180	282	118	12	152
1.1 M TBP/ [(n-DD+4M)-200 kGy)	331	119	8	204	290	110	8	172
1.1 M TBP/ [(n-DD+4M)-300 kGy)	348	114	8	226	303	91	7	205
1.1 M TBP/ [(n-DD+4M)-500 kGy)	374	103	7	264	313	89	1	223

The D value obtained for the unirradiated 1.1 M TBP/n-DD was about 0.31 which gradually increased up to 0.45 as the absorbed gamma dose by the diluent increased.As can be seen from table 1, beyond 2nd strip, the measured Zr(IV) concentration in the aqueous phase during stripping was below detection limit. Alkali wash could remove some of the metal retaining degradation products which account for about 20-40 mgL^{-1} of Zr(IV) retention.

VapourPressure Measurements on Nd-TeSystem

S. Shyam Kumar[1,2,§],V Dhibojini[3]and Rajesh Ganesan[1,2]

[1]*Materials Chemistry and Metal Fuel Cycle Group,* [2]*Homi Bhabha National Institute,*
Indira Gandhi Centre for Atomic Research, Kalpakkam, India
[3]*Guru Nanak College (Madras University),Chennai, India*
[§] Email:*shyam.igcar@gmail.com*

Nuclear reaction produces myriad of fission products. Rare earth elementscontributes to about ~25 % of the total fission products[1]. Neodymium has the highest fission yield of 16.4 % in Pu 239 fission among the rare earth fission products. Tellurium is one of the fission products known to be responsible for fuel clad chemical interactions (FCCI) [2]. FCCI could be minimized by formation of intermetallic compounds between tellurium and rare earth metal[3].

Isopiestic method of investigation was used to probe the Nd-Tesystem. The experimental technique used for studying the system is well known in the literature [4]. As the Nd is air and moisture sensitive, handling of metal was carried out in an inert atmosphere conditions.

Experimental results of isopiestic experiments of Nd-Tesystem for reservoir temperatures of 731 K which is superimposed on the reported Nd-Tephase diagram[5] in Fig 1. The overall composition of the samples obtained from these experiments lies from 64 to 74 at% which lies between 821 and 1100 K.

It can be seen that the majority of the data are clustered at intermetallic compound $NdTe_2$, clearly establishes higher thermodynamic stability of this compound. They also clearly reveal the existence of non-stoichiometry in this compound. Two of the samples are found to be in the two phase regions $NdTe_2$ + Nd_2Te_5 and Nd_2Te_5 + $NdTe_3$. The existence of these phases were confirmed by XRD analysis, chemical activity of Te were determined for the samples. Details of investigation on the system will be presented in the conference.

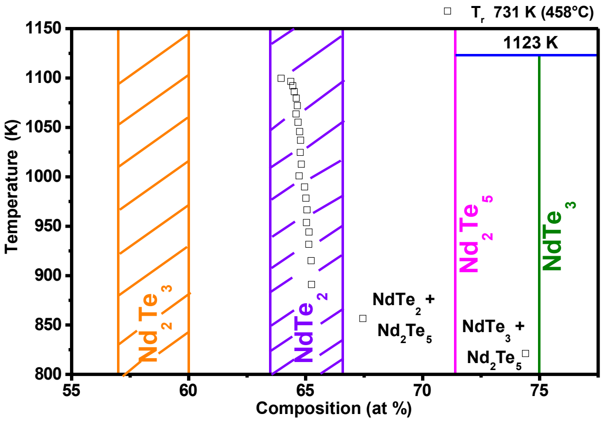

Figure 1: Isopiestic results superimposed on Nd-Te phase diagram

Reference(s):

[1] E.A.C. Crouch, Atomic Data and Nuclear Data Tables, Academic Press Inc., 1977.

[2] C.K. Mathews, Thermochemistry of Transition Metal Tellurides of interest in Nuclear Technology, J. Nucl. Mater. 201 (1993) 99–107.

[3] N.D. Jerred, R. Khanal, M.T. Benson, E. Perez, J.A. King, M. Dubey, J. Burns, I. Charit, S. Choudhury, R.D. Mariani, Evaluation of Tellurium as a Fuel Additive in Neodymium-Containing U-Zr Metallic Fuel, Sci. Rep. 9 (2019) 10643.

[4] R. Ganesan, A. Ciccioli, G. Gigli, H. Ipser, Thermochemical investigations in the tin - phosphorus system, Int. J. Mat. Res. 102 (2011) 93–103.

[5] T.B. Massalski, H. Okamoto, P.R. Subramanian, L. Kacprezak, Binary Alloy Phase Diagrams, 2nd ed., ASM International, The Materials Information Society, Ohio, 1990.

Investigationon Gd-Te Systemby Isopiestic Method

Chita Ranjan Patra[1,§], S Shyam Kumar[1,2], Sowndharya R P Samy[3]and Rajesh Ganesan[1,2]

[1]Materials Chemistry and Metal Fuel Cycle Group,[2]Homi Bhabha National Institute,
Indira Gandhi Centre for Atomic Research, Kalpakkam, India
[3]PSGR Krishnammal College for Women, Coimbatore, India
[§] Email: *crpatra143@gmail.com*

Nuclear fission results in the formation of several fission products. Rare earth elements has a share of ~25% of the fission products. This investigations attempts to probe into interactions of one of the rare earth fission product viz., gadolinium with tellurium. Formation of intermetallic compounds among them, reduces fuel clad chemical interaction (FCCI)[1].Some of the isotopes of Gd viz., 155 and 157 have very high fission cross section for thermal neutrons, hence reducing the neutron economy in the reactor [2].In this context, investigation on Gd-Te system is carried out.

The experimental set up used for investigation is described elsewhere[3]. Experimental results of isopiestic experiments of Gd -Te system for reservoir temperatures of 731 Kis superimposed on the reported Gd-Tephase diagram[4] in Fig 1. The overall composition of the samples obtained from these experiments lie from 60 to 74 at % which lies from temperature 810 K and 1095 K.

It can be seen that the majority of the data were clustered between Gd_2Te_3 and $GdTe_{1.75}$ intermetallic compounds. Existence of non-stoichiometry in these compounds is evident from the distribution of the samples in the phase diagram. Two of samples lie in the two phase regions viz., $GdTe_2 + Gd_2Te_5$ and $Gd_2Te_5 + GdTe_3$. Thermochemical activity of Te was determined and the results will be discussed.

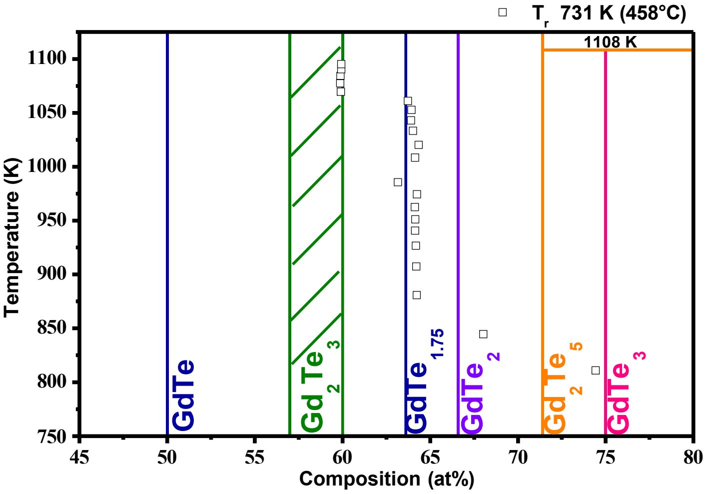

Fig.1: Isopiestic results superimposed on Gd-Te phase diagram.

Reference(s):

[1] N.D. Jerred, R. Khanal, M.T. Benson, E. Perez, J.A. King, M. Dubey, J. Burns, I. Charit, S. Choudhury, R.D. Mariani, Evaluation of Tellurium as a Fuel Additive in Neodymium-Containing U-Zr Metallic Fuel, Sci. Rep. 9 (2019) 10643.

[2] S. Glasstone, A. Sesonske, Nuclear Reactor Engineering, 4th ed., CBS Publishers and Distributors Pvt. Ltd., India, 2012.

[3] S. Shyam Kumar, G. Rajendra Prasad, J.P. Rao, V. Suresh Kumar, R. Ganesan, V. Jayaraman, Design, Development, and Instrumentation of Isopiestic Experimental Setup, Rev. Sci. Instrum. 93 (2022) 44105.

[4] T.B. Massalski, H. Okamoto, P.R. Subramanian, L. Kacprezak, Binary Alloy Phase Diagrams, 2nd ed., ASM International, The Materials Information Society, Ohio, 1990.

Thermodynamic Studies on La-Te System

S. Shyam Kumar[1,2,§], K. Uvarani[3]and Rajesh Ganesan[1,2]

[1]*Materials Chemistry and Metal Fuel Cycle Group,* [2]*Homi Bhabha National Institute,*
Indira Gandhi Centre for Atomic Research, Kalpakkam, India
[3]*Department of Chemistry, Pondicherry University, Puducherry, India*
[§] Email: *shyam.igcar@gmail.com*

Various fission products are formed as a result of nuclear fission in the reactor core. Among the fission products, rare earth elements constitute ~25 % of the total fission products[1]. Yield of lanthanum is about 5.8 at% in Pu-239 fission[1]. Tellurium is one of the fission products known to cause corrosion of cladding materials[2]. Tellurium also interacts with rare earth elements. Investigation of thermodynamic behavior of La-Te binary system is discussed in this work.

Tellurium vapor pressures were determined over La-Te samples by an isopiestic method. The principle and experimental details of the isopiestic method were described elsewhere[3]. After equilibration, the isopiestic apparatus was quenched in cold water. The samples were weighed again and their compositions were derived from the mass difference which was attributed to the uptake of Te. Representative samples were analyzed by XRD. Activity of tellurium in the La-Te samples is arrived by the following relationship:

$$a_{Te}(T_s) = \sqrt{\left(\frac{p_{Te_2}(T_S)}{p^o_{Te_2}(T_S)}\right)} = \sqrt{\left(\frac{p^o_{Te_2}(T_R)}{p^o_{Te_2}(T_S)}\right)} \qquad (1)$$

where, T_S and T_R are sample and reservoir temperatures, respectively. $a_{Te}(T_s)$ is the activity of the tellurium, $p^o_{Te_2}$ and p_{Te_2} are the saturated and vapor pressure of the tellurium dimer, respectively.

Experimental results of isopiestic experiments of La - Te system for reservoir temperatures of 731 K which is superimposed on reported La - Te phase diagram [4] in Fig 1 . The overall composition of the samples obtained from these experiments range from 65 to 73 at% Te which is lies between 807 K and 1094 K.

It can be seen that the majority of the data were near $LaTe_2$ region showing non-stoichiometry in the compound. One of the samples was found to be in the two phase region which shown to be a mixture of La_2Te_5 and $LaTe_3$. It can be observed that the latest reported phase diagram does not shown the existence of La_2Te_5. These phases are confirmed by XRD analysis and their thermodynamic data were determined.

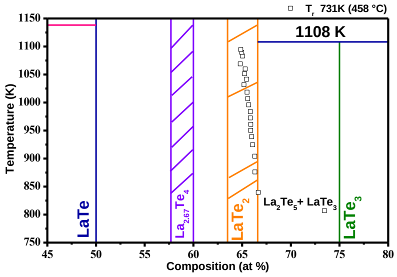

Figure 1: Equilibrated samples superimposed on La-Te phase diagram

Reference(s):

[1] E.A.C. Crouch, Atomic Data and Nuclear Data Tables, Academic Press Inc., 1977.

[2] R.D. Mariani, D.L. Porter, T.P. O'Holleran, S.L. Hayes, J.R. Kennedy, J. Nucl. Mater. 419 (2011) 263–271.

[3] S. Shyam Kumar, G. Rajendra Prasad, J.P. Rao, V. Suresh Kumar, R. Ganesan, V. Jayaraman, Rev. Sci. Instrum. 93 (2022) 44105.

[4] T.B. Massalski, H. Okamoto, P.R. Subramanian, L. Kacprezak, Binary Alloy Phase Diagrams, 2nd ed., ASM International, The Materials Information Society, Ohio, 1990.

Studies on the extraction behaviour of Zr (IV) in HNO_3-TBP-HDBP/ n-dodecane system

Pranay Kumar Sinha, Alok Kumar Mishra, M. Sampath, P Velavendan§, K. A. Venkatesan and K. Ananthasivan

Reprocessing Group, Indira Gandhi Centre for Atomic Research, Kalpakkam-603102
§Email: velp@igcar.gov.in

The dibutyl phosphoric acid (HDBP) is formed as radiolytic degradation product of TBP during reprocessing of spent fuel. The presence of HDBP in organic phase leads to the retention of metal ions[1] in the organic phase during stripping cycle. The objective of the present study was to evaluate the influence of HDBP during the extraction of Zr (IV) from acidic solution. Zr (IV) solution was prepared by dissolving zirconyl nitrate in concentrated HNO_3 for six hours under reflux conditions and suitably diluted to achieve the desired concentration. For experimental studies, two sets of organic phases were prepared. In the first set, TBP in n-dodecane (n-DD) solution containing HDBP concentration (2.5mM, 5mM, 10mM, and 15mM) was prepared. In the second set, the TBP concentration in n-DD was varied (0.5M, 0.7M, 0.9M, and 1.1M) at the fixed concentration of HDBP (5 mM). The organic solution was pre-equilibrated with various concentrations of a nitric acidic solution followed by contacting the organic phase with an equal volume of an aqueous solution containing 5.5 mM Zr(IV) in various nitric acid concentrations (0.1M, 0.5M, 1M, 2M, 3M, 4M, 5M) for 15 minutes. The organic and aqueous phases were separated, and the Zr (IV) in the aqueous solution was analysed spectrophotometrically at 665 nm using Arsenazo (III) as a chromogenic reagent. The concentration of Zr (IV) in the organic phase was determined by a difference in aqueous phase concentrations. The extraction results are shown as the variation in the distribution ratio (D_{Zr}) of Zr (IV) in fig. 1 and 2.

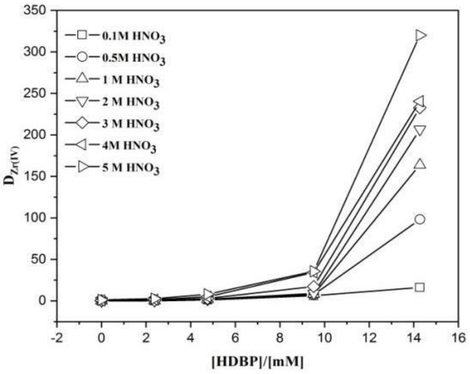

Fig. 2: Variation in distribution ratio of Zr(IV) with HDBP concentration

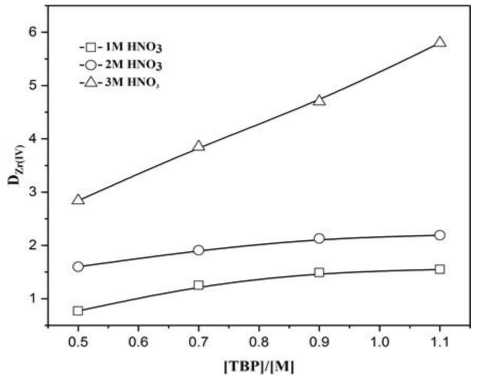

Fig. 3: Variation in distribution ratio of Zr(IV) with TBP concentration ([HDBP]=5mM)

Fig.1 shows that D_{Zr} increases with the increase in the HNO_3 concentration. At HDBP concentrations of more than 5 mM, the D_{Zr} increases rapidly at all HNO_3 concentrations. Fig. 2 shows that the D_{Zr} increase with the increase in the TBP concentration and at 3M HNO3 D_{Zr} is high even at lower TBP concentration. It can be concluded that the presence of HDBP, a primary degradation product of TBP increases the D_{Zr} multi-fold and needs to be removed before solvent reuse.

References:
1. Siczek, A. A. and Meisenhelder, J. H., Zirconium Retention in 30% Tributyl Phosphate/n-Dodecane. Radiochimica Acta, 27, 4, 1980, 217.

Studies on chemisorption and physisorptioncapacity of I_2 capture by Ag zeolite-13X and Ag-Pb impregnated zeolite-13X for iodine trap application

S.Sriram, S. Annapoorani, V. Mahalakshmi, S. Vijayalakshmi§ and V.Jayaraman

*Analytical Chemistry & Spectroscopy Division,MC&MFCG, IGCAR,Kalpakkam,*Rajeswari Vedachalam Government Arts College, Chengalpattu*
(§Email: sviji@igcar.gov.in

Iodine, an important fission product is of great concern in nuclear reactor accidents due to its volatile nature and its environmental impact.Activated charcoal traps are incorporated in nuclear reactors to trap iodine. Due to the limitation of the flammability of charcoal, variousporous sorbents for I_2 capture have been reported [1]. In this study, measurement ofphysisorption and chemisorption capacity of I_2 in commercial Ag zeolite-13X, in house prepared Ag impregnated and Ag-Pb impregnatedzeolite-13X were carried out usingAr flow, solubility ofphysisorbed I_2 in toluene and chemisorbed iodides with thiosulphate.

Physisorption and chemisorption of I_2 in zeolites:Ar containing I_2vapourwas passed through zeolitesloaded in „V‟tubeat 423K. The unabsorbed I_2 was collected in the scrubber. The capture capacity was calculated from the total amount of I_2 captured for 1g of zeolite.The difference between dry weight and weight after trap experiment is the sum of chemisorbed and physisorbed I_2.The physisorbed I_2 is slowly released at room temperature. Therefore, to find outphysisorption, after the trap experiment i.e. after noting down the weight of „V‟ tube, I_2 containing tube was removed and V tube with „ I_2sorbed zeolite‟ was connected to the setup. Only Ar was passed through the V tube containing „I_2 sorbed zeolite‟. Thereleased physisorbedI_2 was collected in the fresh scrubber solution (50 mL of 0.5M NaOH). Periodically scrubber solutionwas analysed(every 2h) for iodide by ICP-OES.The experiment was stopped when iodide saturates in the scrubber for 2h. The amount of iodide in the scrubber corresponds to thephysisorbed I_2 and subtracting this valuefrom the total weight gain reveals the chemisorbed I_2(Table 1)

Physisorption and chemisorption based on solubilityintoluene and thiosulphate: Physisorbed I_2 issoluble in toluene whereas the chemisorbed iodidessuch as AgI and PbI_2 are not soluble in toluene,but dissolve in thiosulphate. Hence, „I_2 sorbed zeolites‟ were added to cold toluene.On adding thiosulphate to toluene in separate beaker, It wasfound that I_2 was completely extracted into thiosulphate. Thus, analysis of thiosulphate by ICP-OES or by iodometry was found to give physisorbed I_2.Subsequent to toluene treatment, zeolite samples wererepeatedly heated with fresh 1M thiosulphate to ensure the complete removal of AgI and PbI_2.Analysis of thiosulphatesolutionsfor $I^-$was found to give chemisorbed I_2.

Table 1.Physisorption and chemisorptions capacity of various zeolite-13X

zeolite	Capacity (I_2) mg/g	Physisorption (Ar flow)mg/g	Physisorption -toluene (mg/g)	Chemisorption (thiosulphate) mg/g
Commercial Ag zeolite-13X	272	37	36	191
Ag impregnated 13X (Inhouse)	270	83	-	-
Ag,Pb impregnated 13X (Inhouse)	260	--	60	--

Physisorbed and Chemisorbed iodine were separately determined in various zeolites.

Ref: 1. Joffrey Huve, et. al. RSC Advances (2018) Porous sorbents for the capture of radioactive iodine compounds : A review

Decay power measurements from P91, SS316L, SS304L and D9 steels using Whole Energy Absorption Spectrometer

G. Pandikumar[1,§], D.V. Subramanian[1], A. John Arul[1,2], Adish Haridas[1] and S. Raghupathy[1]

[1]Indira Gandhi Centre for Atomic Research, Kalpakkam, Tamilnadu 603102, India
[2]Homi Bhabha National Institute, Training School Complex, Mumbai-400094, India.
[§]Email: pkg@igcar.gov.in

Decay power from P91, SS316L, SS304L and D9 steels are measured using Whole Energy Absorption Spectrometer (WEAS) and compared with ORIGEN2 predictions. The principle of WEAS is to measure the beta and gamma energies that are deposited in the detector simultaneously with detection efficiency close to 100%. The essential part of WEAS set-up is a pair of large bismuth-germanate (BGO) scintillators. An irradiated sample is sandwiched tightly by the BGO scintillators to make 4π geometry.

Samples of P91, SS316L, SS304L and D9 steels are irradiated in KAMINI PFTS location for 60 minutes at 20kW reactor power. To determine neutron flux, gold foils are also irradiated along with each sample. The decay powers from the samples are calculated using ORIGEN2 code. Neutron flux, obtained from Au activity, is used in decay power prediction. The reactor spectrum averaged one group cross sections, which are prepared using the KAMINI neutron flux spectrum, is used in the calculation. The measured decay power is smaller than predicted due to (a) gamma attenuation in the sample (b) energy absorption efficiency of BGO detectors for beta and gamma particle and (c) self-absorption and scattering of beta particles in the sample. Table 1 gives a comparison of measured and predicted decay power (D) from the samples for cooling periods T_c. So, the estimated decay power is corrected accordingly. From this study, it is possible to predict decay powers from P91, SS316L, SS304L and D9 steel samples within ± 6%, ± 7%, ± 4% and ± 8% respectively with respect to measurements. The study also validates the spectrum averaged one group cross section and the neutron flux.

Table 1: P91, SS316L, SS304L and D9 measured decay power comparison with prediction

P91			SS316L			SS304L			D9		
T_c (h)	D (pW)	C/E	T_c h)	D (pW)	C/E	T_c (h)	D (pW)	C/E	T_c (h)	D (pW)	C/E
21.91	3803.72	1.01	22.31	14818.92	1.07	22.89	10218.45	1.01	27.48	5105.09	1.01
71.56	299.23	1.06	46.89	1411.72	1.07	46.63	1401.5	1.02	46.37	697.65	0.95
166.66	176.76	1.01	72.52	811.33	1.05	166.10	312.63	1.04	71.87	481.06	0.99
238.51	155.62	1.01	239.24	312.60	0.99	239.52	282.92	1.02	166.92	306.33	1.06
362.06	133.20	1.02	382.61	262.50	1.01	383.02	256.84	1.02	238.92	261.69	1.08
697.91	102.19	0.98	698.46	213.80	0.99	698.23	218.57	1.02	698.69	165.61	1.07
865.89	89.21	0.97	866.56	198.15	0.97	866.84	211.16	0.99	866.22	145.80	1.07
1009.92	80.78	0.96	1010.64	184.28	0.96	1010.95	197.72	1.00	1010.31	131.65	1.06

References:

[1] Fujio Maekawa, et al, Development of whole energy absorption spectrometer for decay heat measurement, Nucl. Inst. and Meth. Phys. Res. A 450 (2000) 467 – 478.

[2] A. G. Croff, ORIGEN2: A versatile computer code for calculating the nuclide composition and characteristics of nuclear materials, Nucl. Tech. **62,** 1983.

Synergistic aqueous biphasic separation of ^{90}Nb from natural yttrium

Sayantani Mitra[1], Nabanita Naskar[2], Susanta Lahiri[2,3§], Punarbasu Chaudhuri[1]

[1]*University of Calcutta, 35, Ballygunge Circular Road, Kolkata, India*
[2]*Diamond Harbour Women's University, Sarisha, South 24 Parganas, India*
[3]*Sidho Kanho Birsha University, Purulia, India*
[§] Email: susanta.lahiri.sinp@gmail.com

^{90}Nb {mean β^+ energy 662.2 keV, positron branching 51%, $E_{\beta max}$ = 1.5 MeV, $T_{1/2}$ = 14.6 h) is a positron emitter which has application in diagnostic nuclear medicine. Now-a-days, radioanalytical separation experiments are guided by the mandates of green chemistry and more attention is given to the resources obtained from nature [1]. In this work, we have combined the concept aqueous biphasic separation and nature resourced chemistry to develop a separation route for ^{90}Nb from natural yttrium target.

A natural yttrium foil of thickness 3 mg cm^{-2} was irradiated with 34 MeV α- particles for ~10 h at VECC, Kolkata. The irradiated yttrium foil was dissolved in 1M HCl. To monitor bulk Y, another yttrium foil of same thickness was irradiated with 46 MeV α- particles which produced ^{87}Y, ^{90}Nb and ^{89}Zr in the matrix. ^{87}Y was separated by already established method [2] and was spiked in the radioactive stock solution. To perform radiochemical separation, ABS comprised of 2M $NaHSO_3$ and 2M $(NH_4)_2SO_4$ and PEGs (M.W 4000, 6000) were made. 3 mL 50% PEG solution was mixed with equal volume of salt solution and 0.1 mL radioactive stock solution. 30 mg catechins was added in the ABS before the addition of radioactive stock solution. After shaking, settling and complete phase separation, 1.8 mL of each phase was subjected to gamma spectrometric analysis and counted for 300s in a HPGe detector.

Fig 1 represents the extraction profile ^{90}Nb and bulk yttrium in the PEG 6000 phase after the addition of catechins. In case of $NaHSO_3$, extraction of ^{90}Nb increased from 28.9% to 96.9% in PEG rich phase after the addition of catechins where as in case of $(NH_4)_2SO_4$, extraction of ^{90}Nb increased from 31.8% to 90.8% in PEG rich phase after the addition of catechins. The contamination from bulk yttrium was less than 2% in both the cases. To minimize the contamination from bulk, the ^{90}Nb rich catechin-PEG phases were 2nd time extracted with the respective salt phases.

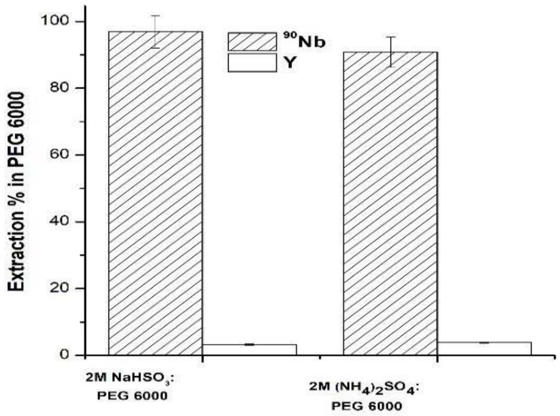

Fig. 1: Extraction profile of ^{90}Nb and bulk Y in catechin-PEG 6000 phase

The nature-resourced chemicals are powerful green reagents in chemical processes. In this paper, catechins showed rewarding synergistic effect to separate ^{90}Nb in the PEG rich phase.

Authors gratefully acknowledge the cooperation of VECC cyclotron staffs.

References:

[1]. S. Lahiri et al., *J. Radioanal. Nucl. Chem.,* **318(3)** (2018) 1543.
[2]. S. Lahiri et al., *J. Radioanal. Nucl. Chem*. **218(2)** (1997) 229.

HR GRS-HPGe as NDT method for quantification of uranium and U^{235} content in process stream samples from UO_2 fuel production facilities

Y. Balaji Rao[1§], Vinod.K. Ray[1], P.V. Nagendra Kumar [2], Dinesh Srivastava[1]

[1 & §] Nuclear Fuel Complex, Dept. of Atomic Energy, ECIL post, Hyderabad- 500062, India
[2]Asst Professor, Dept of Chemistry, GITAM University, Hyderabad-502329, India
[§]Email: ybr4793@gmail.com / ybr@nfc.gov.in

As an industrial arm of Department of Atomic Energy (DAE), Nuclear Fuel Complex (NFC) is engaged in manufacturing and supply of UO_2 fuel sub-assemblies for all the operating nuclear power reactors in India. Different raw materials such as Heat Treated Uranium Peroxide (HTUP), Sodium Di-Uranate (SDU), Uranium Ore Concentrate (UOC) are used for producing the sintered UO_2 fuel pellets. The production process involves several steps like acid dissolution of raw materials, solvent extraction, calcination, reduction followed by fabrication processes. During wet processing, several process stream solutions are generated like Crude Uranyl Nitrate Solution (CUNS), Uranyl Nitrate Feed Solution (UNFS), Uranyl Nitrate Pure Solution (UNPS), Uranyl Nitrate Extract (UNE), Uranyl Nitrate Lean Solvent (UNLS) and Uranyl Nitrate raffinate (UNR). Measurement of concentration of uranium in these process stream solutions is essential for different purposes like for material input in UNFS/CUNS, for extraction efficiency in UNE, for effective stripping in UNPS and for over all material balance in UNLS and UNR. In addition, it is required to measure U^{235} content in raw material for qualifying them for production. Further, the isotopic measurement helps in segregation of uranium based materials with different enrichments. Several methods are cited in literature for this purpose. For uranium determination gravimetric [1], volumetric [2], X-Ray Fluorescence Spectrometry [3] etc., methods are available in literature. For U-235 content, thermal ionization mass spectrometer [4] etc., are cited in the literature. However, the limitations of each of these techniques make them as un-preferred choices for an industrial lab attached to production facility. Quick analytical feed-back with reliability to the production plant and generation of minimum of liquid analytical waste are the important requirements for any industrial lab. In view of the above, a High Resolution Gamma Ray Spectrometric (HR GRS) technique with High Purity Germanium (HPGe) detector as a non-destructive testing (NDT) method has been developed for the estimation of uranium and U^{235} content in solutions from uranium process stream. In the present work, γ-rays of 143.8 keV & 185.7 keV emitted from U^{235} and 63.3 keV & 92.8 keV from daughter products of U^{238} are included for determination of uranium. Apart from this, self-induced uranium X-rays are also emitted ($U_{k\alpha1}$ 98.4 keV and $U_{k\alpha2}$ 94.7 keV) are included in the study. The calibration was done with uranium standards in the concentration range of 10-140 g/L in nitric medium for both aqueous and organic stream measurements. Uranium spectra centred around 80-120 keV has been used for U^{235} content measurements. The developed method was successfully employed for UOC, UO_2 powders, UO_2 pellet and U bearing process stream solutions.

References:

1. P.L. Lopez-de-Alba, S. Gonzalez, J.GomezLara, *J. Radioanal. Nucl. Chem.*, **136** (1989)
2. W. Davis, W. Grey, *Talanta***,** **11** (1964) 1203.
3. Y . Balaji Rao, B. V. V. Ramana, P. Gayathri Raghavan, R. B. Yadav, *J J. Radioanal. Nucl. Chem.*, **294** (2011), 371.
4. O. Pereira de Oliveira, W. De Bolle, S. Richter, A. Alonso, H. K¨uhn , J.E.S. Sarkis, R. Wellum, *International Journal of Mass Spectrometry* , **246** (2005) 35.

Potentiometric end point detection for destruction of oxalic acid using $KMnO_4$ in oxalate supernatant-treatment

Suman Panja[§], N S Rathore, S K Gupta, T P Valsala

R&WM, INRPO, Nuclear Recycle Board
Bhabha Atomic Research Centre, Tarapur-401501
[§]Email: sumanp@barc.gov.in

In reconversion, plutonium nitrate solution is precipitated and converted into plutonium dioxide powder using the conventional oxalate precipitation method. During the precipitation excess oxalic acid above the stoichiometric is added to ensure quantitative precipitation of plutonium. The plutonium oxalate precipitate is then filtered and collected in hold up tank of 1000 liters capacity. This oxalate supernatant contain plutonium up to 100 mg/L is transferred to process cell for further recovery. Before recycling, oxalate ions need to be completely destroyed because at elevated temperature, oxalate ions are highly corrosive to process equipment‟s made-up of SS 304L.This supernatant is treated with 0.3M KMnO4 solution to kill the oxalate ions followed by addition of hydrogen peroxide solution to remove the excess KMnO4. Presently the addition of calculated volume of KMnO4 in treatment tank is carried out in multiple batches with slow rate (~20 lph) by applying suction in tank. After addition of each batch, air sparging is done for assuring proper mixing, and then 2 liter of solution is taken out in trap bottle and its pink colour change is observed, which ensures complete destruction of oxalic acid. If it is colourless then again KMnO4 is added, followed by air sparging and colour test. The step is repeated until the pink color persists, which ensures absence of any traces of oxalic acid. This process required manual operation and more time. Hence an alternative method for in-situ end point detection during the treatment was studied using potentionmetric method which gives a clear sharp indication of the completion of the treatment without withdrawing samples during the treatment. Present paper describes details of this study.

Experimental & observations: The initial potential of the oxalic acid in acidic medium is around 0.59 volt, on addition of incremental volume of $KMnO_4$; the potential is increased, at the end point there is sharp jump in potential (Fig. 1). After addition of excess $KMnO_4$ the potential remains around 1.25 volt which is near the standard potential of the $KMnO_4$.

Thus, by immersing the electrode of the potentiometer in the supernatant tank and adding $KMnO_4$ solution for oxalate ion destruction the end point can be obtained in-situ without withdrawing samples in-between. This method will reduce the treatment time and hence the radiation exposure.

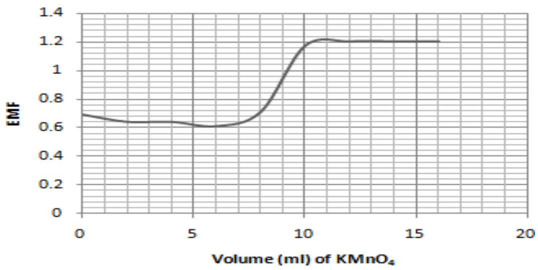

Fig.1: Change of EMF (volt) of oxalic acid with volume (ml) of $KMnO_4$ addition

Acknowledgements: During the course of work, the help rendered by Shri D. Thakur, FF, NRB(T) greatly acknowledged.

References: [1] Electrolytic and ozone aided destruction of oxalate ions in plutonium oxalate supernatant of the PUREX process: A comparative study by S. Ganesh, N. Desigan, A. Chinnusamyl and N. K. Pandey, *Journal of Radioanalytical and Nuclear Chemistry*, **328**, (2021), 875-885.

Systematic investigation of inter-element effects during EDXRF measurements on mixed oxides of yttrium, aluminium and silicon

P.S. Remya Devi[§], T.A. Chavan, M. Sarma, and K.K. Swain

Analytical Chemistry Division, BARC, Mumbai, India
[§] Email: psremya@barc.gov.in

Mixed oxides of yttrium (Y), aluminium (Al) and silicon (Si) are used in the medical field for radiotherapy. Quantification of the major constituents, Y, Al, Si, is inevitable for optimizing the amounts and efficacy of the material [1]. Compositional characterization of mixed oxide powders by wet chemical routes is always a challenge to the analysts, owing to the refractory nature of constituents. Classical methods, though very accurate and precise, require proficient analysts, large material inventory, rigorous chemical treatment, and time. Atomic absorption /emission techniques are not suitable for these, due to both the difficulty in dissolution and multi-step dilutions, which in turn will hamper the measurement precision. An instrumental technique, with minimal sample preparation, is ideal to tackle such situations. Energy dispersive X-ray fluorescence (EDXRF) spectrometry is a convenient tool. However, a thorough understanding of inter-element effects is inevitable to ensure accuracy & precision.

Systematic investigations were carried out to understand the inter-element effects during EDXRF measurements on mixed oxides of Y, Al and Si. Unary (individual oxide), binary (one oxide fixed; the other varied) and ternary (two oxides fixed, one varied) mixtures of Y, Al, Si were made with cellulose, pelletized, and analyzed by EDXRF. The K_α X-rays were monitored for Al and Si. In the case of Y, both the K_α and L_α X-ray intensities were noted. Calibration curves were obtained by plotting the net counts vs amount of analyte varied, in each case. Sensitivity (counts / mg) and intercept of the calibration curves for Al, Si, Y were determined and the effects of presence of other elements were studied. Results are summarized in Table 1. The sensitivity was found to increase, as per the atomic number, reported mass absorption coefficients and fluorescence yields [2]. Addition of other oxides affected the instrumental sensitivities, which was the accumulated effect of factors such as the characteristic X-ray energies, absorption of source X-rays by the matrix, enhanced interactions near the absorption edge and attenuation of analyte X-rays in the matrix. Addition of SiO_2 increases the sensitivity of Al, as the Si X-rays act as secondary excitation source for Al, owing to the proximity of Si X-ray energy (1.74 keV) to the Al absorption edge (1.56 keV). Presence of interfering impurities, overlap of peaks, scattering and absorption by the matrix are the causative factors for the variation in intercepts of the calibration. The insights from present studies were applied during compositional analysis of process samples. Results on two representative samples are shown in Table 2. Accuracies (relative errors < 2 %) were ascertained by standard addition-recovery as well as gravimetry for Si.

Table 1 Inter-element effects in EDXRF

Fixed	Varied	Sensitivity	Intercept
--	Al_2O_3	516	7736
--	SiO_2	3250	4448
--	Y_2O_3	7585	33339
SiO_2	Al_2O_3	899	10755
Y_2O_3	Al_2O_3	753	8954
Al_2O_3	SiO_2	2545	-3463
Y_2O_3	SiO_2	2196	17430
Al_2O_3	Y_2O_3	6130	19365
SiO_2	Y_2O_3	5281	-2828
Y_2O_3, SiO_2	Al_2O_3	503	8814
Y_2O_3, Al_2O_3	SiO_2	2291	11916
Al_2O_3, SiO_2	Y_2O_3	3975	22671

Table 2 Percentage composition in samples

Sample	Al_2O_3	SiO_2	Y_2O_3
1	18.03 ± 1.57	39.27 ± 0.25	43.18 ± 3.03
2	19.38 ± 1.26	40.36 ± 0.24	40.08 ± 2.61

References:

[1] M.R. Ghahramani, A.A. Garibov and T.N. Agayev, *Int. J. Radat. Res.,* **12 / 2** (2014) 179.

[2] E.P. Bertin, Principles and practice of X-ray spectrometric analysis, 2nd Edition, (1984) Plenum Press, New york-London pp 89-11

Quantifying the Loss in Reactivity Value of PFBR Fuel due to Am-241 Buildup over Time Employing Differential Perturbation

Bilal Hassan Khan[1,§]

[1]*Reactor Design group, Indira Gandhi Centre for Atomic Research, Kalpakkam, India*
[§] Email: bhk780@igcar.gov.in

Fuel refabrication and its intended usage are sometimes not in synch due to reactor non operatibility, commissioning delays or other non-technical factors, leading to enhanced shelf life for some fuel batches. Maximizing fuel economy of active reprocessed fuel poses optimization challenge in terms of utility considering reactivity worthiness, shutdown margins, refuelling batch size and cycle length etc. Decay becomes the primary factor affecting the fuel isotopic characterisation once fuel is extracted from thermal reactor. The reactivity worth of fuel gradually decreases over time as shorter-lived isotopes, such as fissile Pu-241 with a half-life of around 14.4 years, are transformed into neutron-absorbing Am-241.

To quantify the effect of Am-241 buildup accounting different shelf lives, A differential perturbation feature, consequently validated with exact 2-K_{eff} difference of Monte Carlo transport was employed in simulations. Due to extended shelf life of PFBR fuel, the reference Pu vector {Pu-239(68.8%), Pu-240(24.6%), Pu-241(5.1%), Pu-242(1.2%), Am-241(0.3%)} gets changed marginally owing to radioactive decay. Since each Pu-241 atom is equivalent to 1.5 times Pu-239 atom reactivity, which is established by relative comparison of isotopic fission rates and Am-241 being neutron absorbing, so roughly there is a loss of reactivity worth of two atoms of Pu-239 per atom decay of Pu-241. The 3000 pcm decrease in fuel reactivity value over a span of 11 years which is equivalent to worth of 10 fresh fuel SA‟s, can impact many reactor parameters from operational perspective. The results tabulated in table (1) and displayed in figure (1 & 2) have been established by tallying reaction rates and K_{eff} for PFBR BOL core configuration performing multiple fuel vector perturbations.

Table 1 Am-241 build-up and reactivity loss with shelf life

Shelf life (Years)	Am-241 (g/SA)		Differential pertubation	2K Difference
	Core-I	Core-II	$\Delta\rho$ (pcm)	$\Delta\rho$ (pcm)
1	49.46	66.2	267.17	219.31
2	89.73	93.83	656.31	644.47
3	126.2	120.1	1015.26	1057.72
4	159.1	145.2	1346.31	1397.23
5	188.9	168.9	1650.96	1726.96
6	202.7	191.6	1841.63	1875.28
7	215.8	233.5	2107.98	2094.83
8	228.2	271.4	2352.97	2364.73
9	240.1	305.6	2579.17	2569.34
10	251.3	336.5	2788.26	2822.71
11	262	364.3	2980.13	2968.64

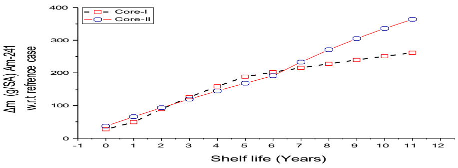

Figure 1 Am-241 build-up for core-I & II

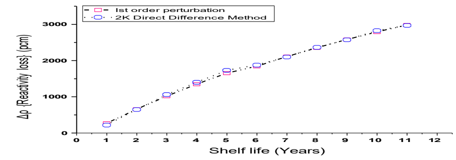

Figure 2 Reactivity loss with shelf life

The results of the study indicate that the rate of reactivity loss is solely contingent upon the isotopic composition of plutonium at the time of its removal from thermal reactor. High burnup LWR fuel with a higher initial concentration of Pu-241 will experience a more rapid loss in reactivity value compared to less irradiated fuel with a lower Pu-241 content.

References: [1] H. RIEF, “Generalized Monte Carlo Perturbation Algorithms for Correlated Sampling and a Second-Order Taylor Series Approach,” *Ann. Nucl. Energy*. 11, 9, (1984) 455-476.

Determination of Nitrogen and Oxygen Content in Uranium Metal using Glove Box Adapted Twin Determinator System and Related Studies

Seema Raul, Revati Gaikwad, Rakesh Pandey, Namrata Kumar, D.R. Raut, Ashish Pandey, Anoop Kelkar[§], T.P. Valsala, D.B. Sathe, R.B. Bhatt

Fuel Fabrication, INRP(O), Nuclear Recycle Board, , B.A.R.C., Tarapur - 401502, India
[§]Email : anoop@barc.gov.in

The fabrication of plutonium based nuclear fuel for the fast reactors envisaged in the second stage of nuclear power programme is a challenging and tough task. Fuel Fabrication (FF), INRP(O), B.A.R.C, Tarapur, India is involved in the fabrication of plutonium based nuclear fuels for various types of reactors and fabricated fuel is tested at various stages from quality assurance and control point of view. One of this crucial parameters includes determination of non-metallic impurities content like nitrogen. Recently, we have successfully demonstrated the glove box adaption of Twin determinator as it detects simultaneously Oxygen-Hydrogen (O-H) and Oxygen-Nitrogen (O-N) contents in samples. This instrument uses thermal conductivity detector and extra pure nitrogen and extra pure helium gases are used as carrier gases for (O-H) & (O-N) mode respectively. At present, it is being used for the analysis of fuel samples on routinely basis. Details are mentioned elsewhere [1].

Present works is associated with the determination of nitrogen and oxygen content in the uranium metal samples and optimization of instrument conditions for the same. The in-house stock of uranium metal was used for the determination of hydrogen and nitrogen content. It was found that, optimized conditions required for complete removal of oxygen and nitrogen content from the uranium metal are same as required for analysis of mixed oxide fuel sample analysis for O-N, O-H determination. Here, for the O-H mode, out gassing temperature was optimized as 1850ºC while analysis temperature was kept as 1650ºC while for O-N mode it was 2500ºC and 2350ºC respectively. For analysis, uranium metal was carefully cut into required small size pieces and were subjected for the analysis where sample was put in to the furnace part with required quantity of flux. For this, sample (0.1g) was put in to the nickel basket with one tin capsule as flux. The sample to flux ratio is maintained as the 1:10 (w/w). Then outgas of empty crucible was carried out and sample falls in to hot crucible automatically avoiding external exposure of the hot crucible to atmosphere. Later the gases evolved were measured for the nitrogen detection. The nitrogen & oxygen content was found to be 46.0 ± 9.3 & 460.1 ± 54.0 and were as per expectations. Twin determinator was found much superior in terms of stabilisation period, ON-OH mode shifting, total analysis time and safety features etc. as compared to old Twin determinator unit. For Twin determinator, sample analysis time was maximum up to 300 seconds after 20-25 minutes stabilization time which was 45 minutes and minimum two hours respectively for old instrument. Also, the route is dry with inert gas fusion technique which is much better than old micro-kjehdahl method of wet route for nitrogen. Twin determinator instrument performance was compared for hydrogen determination in MOX samples employing „Paired t test‟ for each pair of results for same MOX batch samples obtained by Twin and other instruments revealed Practical t < theoretical t indicating no significant difference between two methods / instruments.

Reference:
[1] Analysis of DDUO$_2$ Pellets for Hydrogen & Nitrogen Content Using Glove Box Adapted Twin Determinator System, D.R. Raut *et al*, *In the Proceedings of NUFUC-2022, pp 113*.

Pulsed Fast Thermal Neutron Activation for Characterization of Coal

Tushar Roy[§], Shefali Shukla, Yogesh Kashyap, Mayank Shukla, Prashant Singh, M. R. More
and L. M. Pant

Technical Physics Division
Bhabha Atomic Research Centre, Mumbai, India
[§] Email: tushar@barc.gov.in

Coal materials are classified for better combustion and minimum detrimental effects to environment. Nuclear analytical techniques can be used to determine coal quality parameters non-destructively.

In this paper, we describe the development of Pulsed Fast Thermal Neutron Activation (PFTNA) based coal analysis system using in-house developed 14.1 MeV D-T neutron source. The system is capable of measuring the content of major and minor elements in coal. It utilizes reactions produced from both fast and thermal neutrons for elemental characterization of coal. In PFTNA technique, a pulsed 14.1 MeV neutron source is used. During the neutron pulse ON time, the coal material interacts with neutrons via neutron inelastic scattering (*n, n'γ*) and during the neutron pulse OFF time, the interaction is via thermal neutron capture (*n, γ*). During both the interactions, characteristic gamma rays produced are detected using a BGO detector and these gamma rays are fingerprints of elements present. PFTNA method gives information for some critical elements such as C and O in the fast spectrum and H, Si, Al, S etc. in the thermal spectrum, thereby helping in identification of the various chemical elements crucial in determining properties of coal samples such as calorific value, sulphur content and ash content. Since fast neutrons have higher penetration power, this technique can be used for bulk characterization of coal samples of the order of few kilograms. Fig.1 and Fig.2 show gamma spectrum from different coal samples for neutron inelastic scattering and thermal neutron capture processes respectively.

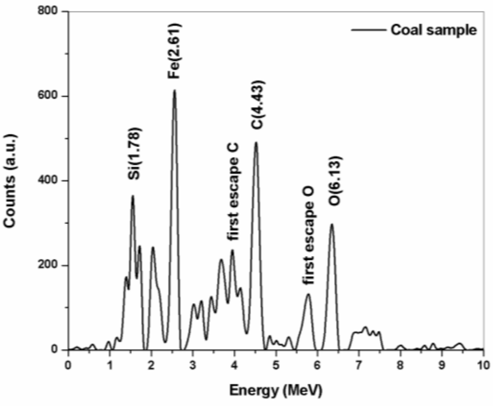

Fig. 1: Gamma spectrum of coal samples for (*n, n'γ*) process

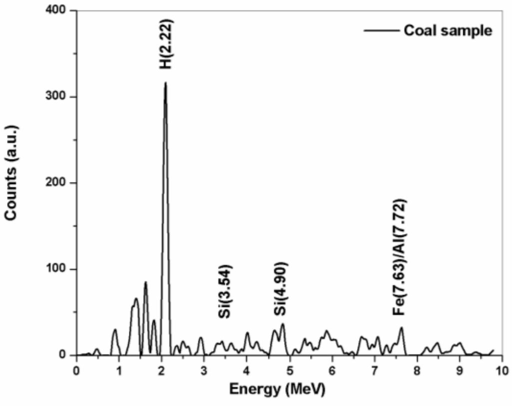

Fig. 2: Gamma spectrum of coal samples for (*n, γ*) process

References:

[1] L. Dep et. al., *Journal of Radioanalytical and Nuclear Chemistry,* **234** (1998) 107

Quantification of Zr in Simulated Dissolver Solution of U-Zr Fuel by LIBS

U. K. Maity[1, §], J. Namitha[1], P. Manoravi[2],

[1]*MC&MFCG, IGCAR; Kalpakkam – 603102, India.*
[§] Email: ujjwalm4@gmail.com

Laser induced break down spectroscopy (LIBS) is a versatile multi-element analytical technique, which has several inherent advantages over other similar techniques, such as irrespective of the state of the material, μg-ng sample requirement, remote analysis, field portable, real time response and drift free results. LIBS is suitable for analysis of highly radioactive samples kept at remote locations, namely, inside glove box (GB) or lead shielded hot-cell [1]. In the present study, quantitative estimation of Zr in the simulated dissolver solution of U-Zr fuel is demonstrated using LIBS.

Five different compositions of Zr and U, where Zr/U ratio varies 0.02-0.26 in ppm level solutions, were prepared from their stock solutions of 81.4 mg/mL and 83.4 mg/mL, respectively. In-house designed liquid sample cell kept inside a single module GB was used to analyse the samples. The liquid samples were taken as a thin film over rotating Al wheel, dried with hot air jet and LIBS measurements were carried out over the dried thin film. The details of the liquid sample cell and its superiority are described elsewhere [2]. Four U-Zr oxide pellets (Zr/U ratio ~ 0.05-0.2; each element is in percentage level) were also prepared through sol-gel route from the same stock solutions, calcined in reducing atmosphere (Ar + 4% H_2) at 800 °C for 8 hrs, and subjected to LIBS analysis.

Non-overlapping emission lines at 414.8 and 556.42 nm were identified for Zr and U, respectively. The measured intensity ratio (IR) of Zr/U is plotted against their corresponding weight ratio (WR) [Fig. 1]. It fits linearly with good correlation coefficient (R^2) of 0.995 and 0.998 for liquid and solid, respectively. Relative standard deviation (RSD) calculated for 10 measurements varies from 3-6% for solid pellet samples and it is 4-7% for liquid samples. The R^2 is also comparable, although it is marginally better for solid pellets. However, the slope, i.e., measured IR of Zr/U is ~ 6 times higher for liquid samples. This observation can be attributed to the surface enhanced laser plasma from a dried thin film over pure Al metal wheel, resulting a higher plasma temperature, therefore, higher yield of excited/ionic species. Since Zr has larger 1st ionization energy (6.63 eV) than U (6.19 eV), the relative increase of excited/ionized species for Zr are expected to be more than that of U for higher plasma temperature. Hence, IR of Zr/U is higher for liquid sample for a given composition. Even though Zr/U ratio is similar, LIBS could detect individual concentration of ppm range in aqueous solution, whereas it is in percentage level in solid pellet.

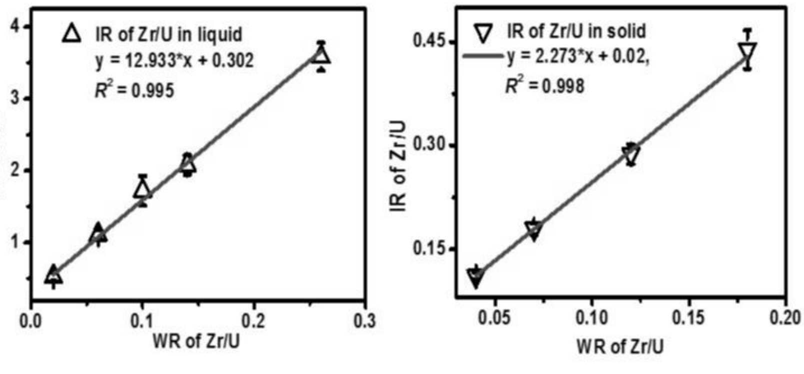

Fig. 1: Plot of intensity ratio verses weight ratio of Zr/U.

References:

[1] Amrita Sen *et. at.*, Abstract book, *NUCAR-2019*, (2019), p.318

[2] U. K. Maity *et. al.*, *Spectrochim. Acta Part B*, 190 (2022), 106393.

Survival Probability of Selenium-induced fusion reactions

H.S.Anushree[1,§], N. Sowmya[1,§] and H.C.Manjunatha[1,§]

[1] *Department of Physics, Government College for Women, Kolar*
[§] Email: manjunathhc@rediffmail.com, sowmyaprakash8@gmail.com

The study of the fission of highly excited nuclei is still a hot issue [1-2]. For almost two decades,it has been recognized that the "conventional" statistical theory of fission underestimates the amount of recorded pre-scission neutrons released in heavy-ion processes [3-4]. It is generally accepted that the main cause of this discrepancy is associated with the viscosity of hot nuclear matter [5]. Giant dipole resonance γ-ray emission has also been used to infer inadequacies in our models of nuclear fission decay widths [6]. These inadequacies have been compensated for by adjusting the viscosity of hot nuclear matter to reproduce experimental data. Earlier researchers [7] investigated neutron and fission decay width for the fusion reaction of ^{25,26}Mg+^{248}Cm. Hence, the neutron and fission decay width becomes an important factor in the estimation of survival probability. In the present work, we motivated to investigate Selenium-induced fusion reactions for the synthesis of superheavy element. The decay width of emitted light particle is evaluated as follows;

$$a(A,E^*) = \tilde{a}\left[1+\delta E\,\frac{1-\exp(-\gamma E^*)}{E^*}\right] \qquad (1)$$

here, $\tilde{a} = 0.073A + 0.095B_s\beta_2A^{2/3}$, δE is the shell correction and γ =0.0061 is the shell damping parameter. The level density is defined as;

$$\rho(J,E^*) = \frac{1}{24}\left(\frac{\hbar^2}{2I}\right)^{3/2}(2J+1)a^{1/2}U_J^{-2}\times\exp[2(aU_J)^{1/2}] \qquad (2)$$

and

$$U_J = E_* - E_r(J) \qquad (3)$$

Here $E_r(J)$ is the yrast energy. The figure 1 shows a plot of level density parameter, level density and survival probability as a function of excitation energy for the fusion reaction of **^{76}Se**+ **^{211}**At. As the excitation energy increases the level density parameter and level density increases with excitation energy. In case of survival probability the maximum value is observed to be 17.43MeV. Further, the accurate level density parameter, shell correction energy, and fission barriers can be used to evaluate neutron decay width and fission decay width. This is used in the evaluation of survival probability. Hence, accurate survival probability is further helpful in the prediction of evaporation residue cross-sections for the super heavy element Z=119.

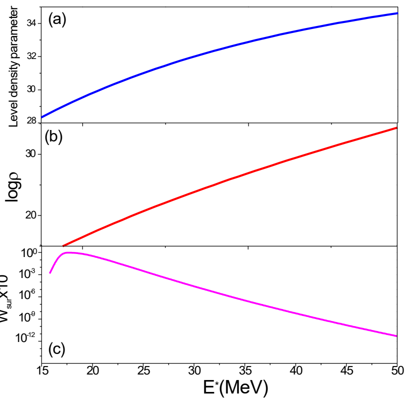

Fig. 1: A plot of (a) level density parameter, (b) level density and (c) survival probability as a function of

References:
[1] V. V. Sargsyan et al., *Phys. Rev.* **C 76**, 064604 (2007).
[2] P. N. Nadtochy, A. Kelić, K.-H. Schmidt, *Phys. Rev.* ***C*** **75**, 064614 (2007).
[3] E. Holub et al., *Phys. Rev. C* **28**, 252 (1983).
[4] W. P. Zank et al., *Phys. Rev.* ***C*** **33**, 519 (1986).
[5] D. Hilscher and H. Rossner, *Ann. Phys. (Paris)* **17**, 471 (1992).
[6] P. Paul and M. Thoennessen, *Annu. Rev. Nucl. Part. Sci.* **44**, 65 (1994).
[7] N. Sowmya, et al., *Phys Rev* ***C*** **105**, 044605 (2022).

Tritium release from new ceramics of heavy elements

N. Sowmya[1,§], H.C.Manjunatha[1, §] and K.N. Sridhar[2]

[1] *Department of Physics, Government College for Women, Kolar*
[2] *Department of Physics, Government First Grade College, Kolar*
[§] Email: sowmyaprakash8@gmail.com, manjunathhc@rediffmail.com

These fast-moving neutrons with large energy leave the fusion reactor in all directions. These neutrons leave the reactor and come to rest in a blanket component. Further, the nuclear processes induced by neutrons can yield tritium. The average energy required to make a triton is orders of magnitude more than the energy that can eventually be eliminated by burning the tritium produced in a fusion reactor. Tritium may be produced with a high particle efficiency in neutron-induced processes [1]. The main challenge is to identify the processes that create the required neutrons at an acceptable energy, low cost with sufficient quantity. Earlier study [2] found that neutron irradiation of LiOH and Li_2O caused tritium to be released. The tritium produced in the ceramic breeder by neutron reactions with ^6Li and/or ^7Li is thought to be transferred out via a different method [3]. Several models have been developed (e.g. by Federici et al., [3], and by Billone et al., [4]). The rate of diffusion control reaction is expressed as follows;

$$\alpha = 1 - \frac{6}{\pi^2} \sum_{n=1}^{\infty} \left(\frac{1}{n^2} \right) \exp\left(\frac{-Dn^2\pi^2 t}{a^2} \right) \qquad (1)$$

Here, D is the diffusion coefficient. Figure 1(a) shows a plot of fraction of tritium released with the grain size in case of Li_2SrPb ceramic breeder. It is noticed from the figure that the fraction of tritium released decreases with increase in grain size. Figure 1 (b) shows a comparison of the diffusion coefficient for different studied compounds at temperature 445K. The larger diffusion coefficient is observed for NaLi2Sn when compared to other studied compounds. Hence, the detail investigation on studied different compounds gives an information regarding larger tritium release among the studied compounds.

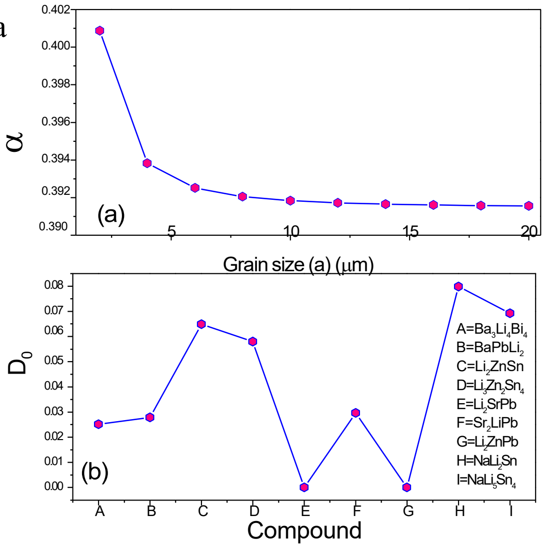

Fig. 1: (a) Variation of a fraction of tritium released with the grain size in the Li_2SrPb ceramic breeder and (b) Comparison of the diffusion coefficient for different studied compounds.

References:

[1] D P Jackson, et al., Canadian Fusion Fuels Technology Project., (1985).

[2] H Kudo and K Okuno. J. Nucl. Mater., **101** (1981) 43.

[3] Federici, et al., J. Nucl. Mater., **173** (1990) 2013.

[4] S Hofmann, et al., Argonne National Lab (1992).

Uncertainty analysis in estimation of radioactivity in the soil samples using gamma-ray spectrometry

B. Arun[1, §], I. Vijayalakshimi[1], S. Viswanathan[1], M.Menaka[1], V. Subramanian[1, 2], and B. Venkatraman[1, 2].
[1] *Safety, Quality, and Resource Management Group, [2]Homi Bhabha National Institute, Indira Gandhi Centre for Atomic Research, Kalpakkam-603102, Tamilnadu, India.*
[§] Email: arunhcu09@igcar.gov.in

The Naturally Occurring Radionuclide Material (NORM) concentrations in the soil samples are quantified using High Purity Germanium (HPGe) detector. Only the random error due to counting statistics (Sample and background counts) is usually taken into consideration for estimation of standard deviation in NORM estimations. However, in order to optimize the measurements and to achieve the ISO 17025 principles, it is necessary to include all the other sources of error to study their relative effect on the total error. So the aim of this study is focused on the calculation of combined uncertainty value and relative contribution of all sources of uncertainties to combined uncertainty value in estimation of NORM (^{238}U, ^{232}Th & ^{40}K) in soil samples using gamma ray spectrometry.

The uncertainty in quantification of specific activity comes from the uncertainty in net count rate, efficiency of the system, mass of sample and gamma emission probability. The combined uncertainty in specific activity is calculated using the eq-1.

$$\sigma_A = \left(\frac{C}{E * g * t * m}\right) * \sqrt{\left(\frac{\sigma_c}{C}\right)^2 + \left(\frac{\sigma_m}{m}\right)^2 + \left(\frac{\sigma_g}{g}\right)^2 + \left(\frac{\sigma_E}{E}\right)^2} \quad [1]$$

Where, σA is is uncertainty in specific activity of sample, σE is uncertainty in efficiency (cps/photons), σm is uncertainty in sample mass, σg is uncertainty in photon emission yield, σc is uncertainty in net counts, C is sample net counts, E is efficiency of the system, t is counting time, m is sample mass and g is gamma emission yield (photons/Bq).

The figure-1 shows the percentage contribution to combined uncertainty value due to different variables for ^{40}K, ^{238}U and ^{232}Th. It was observed that even though counting statistics (sample and background counts) was major contributor to the combined standard uncertainty for all the three radionuclides but other sources of uncertainties also contributes significantly to combined uncertainty values. In case of ^{40}K, relative contribution of uncertainty in photon yield and uncertainty in efficiency values to combined uncertainty values was 6.0% and 12.7% respectively. In case of ^{232}Th, relative contribution of uncertainty in efficiency values to combined uncertainty value was 45.42%.

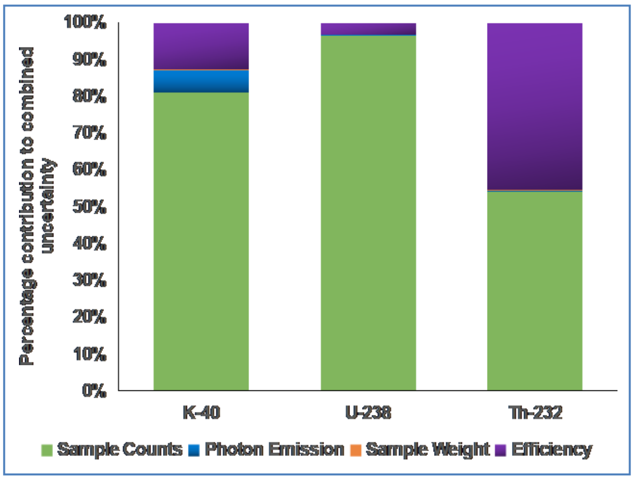

Figure-1: Percentage contribution to combined uncertainties for different radionuclides

References

1. Denis GC et.al, Measurement uncertainty arising from sampling of environmental samples. Applied Radiation and Isotopes 156, 2020, 108978.
2. IAEA, Quantifying uncertainty in nuclear analytical measurements. IAEA, 2004, IAEA-TECDOC-1401.

Measurement of ^{144}Sm(p, γ) Cross Section using Activation Techniques for Astrophysical p-process Study

Tanmoy Bar[1,2,§], Dipali Basak[1,2], Sukhendu Saha[1,2], Lalit Kumar Sahoo[1,2], Jagannath Datta[3], Sandipan Dasgupta[3] and Chinmay Basu[1]

[1]*Saha Institute of Nuclear Physics, 1/AF Bidhannagar, Kolkata 700 064, INDIA*
[2]*Homi Bhabha National Institute, Anushaktinagar, Mumbai, Maharashtra 400094, INDIA*
[3]*Analytical Chemistry Division, BARC, 1/AF Bidhannagar, Kolkata 700 064, INDIA*
[§]Email: tanmoy.bar@saha.ac.in

Beyond Fe, there is a class of 35 proton-rich nuclides, between ^{74}Se and ^{196}Hg, called p-nuclei. They are bypassed by the s and r neutron capture processes and are typically 10–1000 times less abundant than the s and r isotopes in the solar system. There is a typical abundance of ~1% for lighter nuclei with $34 \leq Z \leq 50$ and 0.01-0.3% for medium and heavier nuclei with an atomic number >50. Generally, the abundance of p-nuclei decreases with an increase in atomic number, but for neutron magic p-nuclei ^{92}Mo and ^{144}Sm, it is 14.52% and 3.08%, respectively. So the study of these nuclei is important to understand why they are more abundant! For this reason, more detailed and precise information about the reaction cross-section in the astrophysical energy region is extremely important. The primary aim of experimental nuclear astrophysics is to determine the rates of nuclear reactions taking place in stars under various astrophysical conditions. The reaction rates are determined from the cross sections, which need to be measured at energies as close as possible to the astrophysically relevant ones (near the Gamow window) [1]. With information on its production and destruction, the final abundance of any nuclei in nucleosynthesis can be estimated. The ^{144}Sm(p,γ) reaction, a destructive pathway of ^{144}Sm nuclei, has been chosen for investigation [2]. Molecular deposition techniques have been used to prepare enriched (67%) ^{144}Sm targets from a $^{144}Sm_2O_3$ powder sample. Prepared targets have been used in a cross-section measurement experiment with activation techniques at the K130 cyclotron, VECC, Kolkata. Two stacks of targets have been used for different irradiation energies between 4.2 and 7 MeV. Irradiation current was approximately 250 nA, and irradiation time for the first stack (for energies 7–5 MeV) was 17 hours, whereas the second stack for lower energy was done for 39 hours. The typical gamma spectrum of the ^{144}Sm (p,γ) ^{145}Eu reaction ($T_{1/2}$ 5.93 d) is depicted in Fig. 1, with the most intense gamma-rays from ^{145}Eu has been highlighted in box, rest are background and impurities in backing Al-foil. The details of the data analysis of the reaction cross sections will be presented during the conference.

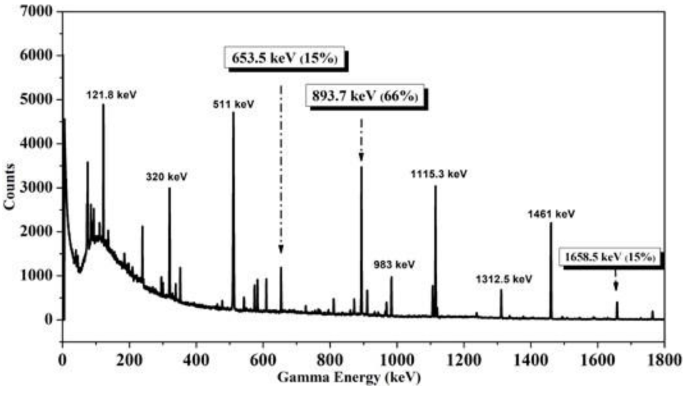

Fig. 1: Gamma Spectrum from $^{144}Sm_2O_3$ target at proton energy ~ 6 MeV

We acknowledge the help of K130 accelerator people for their co-operation.

References:
[1] Gy. Gyürky, et al., Eur. Phys. J .A, 55 (2019) 41.
[2] N. Kinoshita, et al., PHYSICAL REVIEW C, 93 (2016) 025801.

Estimation of Fission Product and other Radioisotope Activities and Shielding Requirement of Storage Bay of Advanced Water Cooled Reactor

Suryanarayana P.[§], and Maheshwari N.K.

Bhabha Atomic Research Centre, Mumbai, India
[§] Email: surya@barc.gov.in

The nuclear fuel undergoes fissions in Reactor Core. These fissions generate fission products, which are different Isotopes of various elements. These Isotopes of different elements emit gamma radiation of different energies. Shielding is needed around the Storage Bay where these spent fuel assemblies are stored. The fuel is basically Pu-239 and U-233 based thorium MOX fuel in the ratio 1.45, 1.91 and 96.64% with a burn-up of 57,500 MW-D/ton. The spent fuel assemblies will be shifted to Temporary Storage Bay inside Reactor Building using Fuelling Machine. These reach the bay after 3 hours (cooling time) of transit time from the reactor core. The storage capacity of the bay is 15 number of spent fuel assemblies. Later, these will be shifted to permanent storage bay located outside Reactor Building.

In the present work, Fission Products and other Radioisotope Activities, gamma source strength are estimated due to all isotopes of all elements. Based on curies, the dominant activity is Pa-233. The gamma energy groups are collapsed to three groups of 0.5, 1.5 and 2.5 MeV. Using the estimated gamma source strength, dose limits based on occupancy requirement, shielding requirements around the Storage Bay are estimated. Point-kernel technique-based code is used to check adequacy of existing shielding, which is 150 cm Heavy Concrete and 400 cm water in radial direction. The paper deals with the estimation of source strength, method of analysis and the shielding estimated around the Storage Bay.

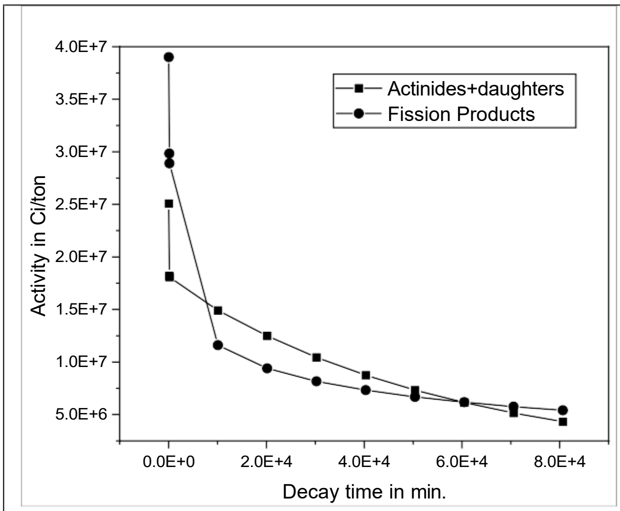

Fig. 1: Variation of Fission Product and Actinides Activity with decay time

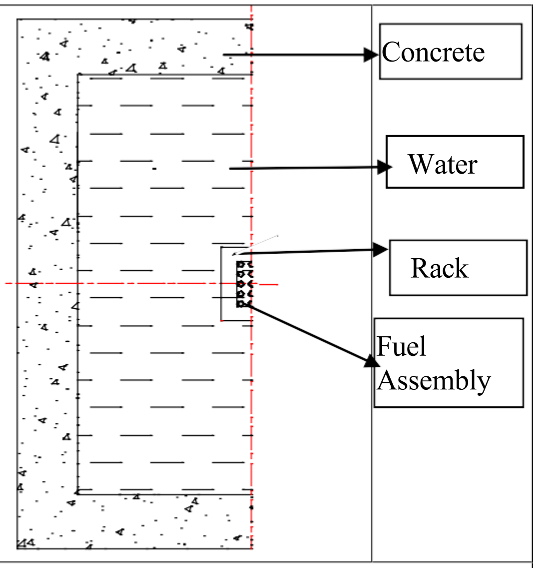

Fig. 2: Geometry of Storage pool with Spent Fuel Assemblies - Plan View

References:
[1] Theodore Rockwell III, *Reactor shielding design manual,* **First Edition** (1956).
[2] Argonne National Laboratory, *Reactor Physics Constants,* **ANL-5800 Second Edition** (1963).

Coulomb fission and Coulomb time scales of superheavy nuclei Z=120

Vasudha.G.S[1&2], N. Sowmya[1], H.C.Manjunatha[1, §], and D. Prakash Babu[2]

[1] *Department of Physics, Government College for Women, Kolar*
[2] *Department of Physics, REVA University, Bangalore.*
[§] Email: manjunathhc@rediffmail.com, sowmyaprakash8@gmail.com

The long-range Coulomb interaction can cause the excitation of a range of collective nuclear modes when a heavy ion approaches a heavy nucleus. The target nucleus may experience distortion up to a saddle-point before sliding down to scission as a result of this interaction. If the experiment is carried below the interaction barrier, only Coulomb forces are involved in initiating the process, and no nuclear matter is transferred between the projectile and the nucleus. The induced fission in this scenario is known as Coulomb fission. Earlier researchers investigated Coulomb fission time-scales [1]. Characteristics of fusion reactions are studied for Xe+U fusion reactions [2]. Earlier studies show Coulomb fission cross-sections for light projectiles [3-5]. Coulomb fission is also of the hindrance in the formation of superheavy nuclei Z=120. Hence, this motivated us to investigate Coulomb fission cross-sections and Coulomb fission life-times.

The Coulomb fission cross-sections are evaluated as follows;

$$\sigma_A^{C_f} = \int_{b_{\min}}^{\infty} 2\pi b db \int_{E_{\min}}^{E_{\max}} N_B(E,b)\sigma_A^{\gamma f}(E)dE \qquad (1)$$

Here

$$N(E) = \frac{2\alpha Z_1^2}{\pi\beta^2 E}\left(xK_0(x)K_1(x) - \frac{x^2\beta^2}{2}[K_1(x)^2 - K_0(x)^2]\right) \qquad (2)$$

here α , β , E , $K_1(x)$ and $K_0(x)$ are with usual notations as explained in the literature [6]. Coulomb fission lifetimes are evaluated as follows;

$$\frac{1}{\tau[s]} = 1.225\times10^{13}.E_\gamma[MeV]^5.B(E_2;I_i \rightarrow I_f)(e^2b^2) \qquad (3)$$

$E_\gamma[MeV]$ and $B(E_2;I_i \rightarrow I_f)$ are taken as explained in reference [7]. Figure-1 shows a plot of Coulomb fission life-times and Coulomb fission cross-sections as function of atomic number of projectiles and mass number of compound nuclei respectively for the synthesis of superheavy nuclei Z=120. The detail investigation on Coulomb fission cross-sections and lifetimes gives an hint for the formation of superheavy nuclei Z=120.

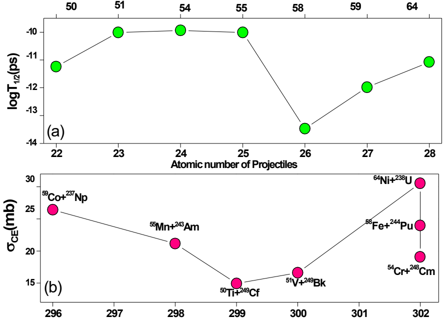

Fig. 1: (a) A plot of Coulomb fission life-times as a function of mass number of projectiles. **(b)** A plot of Coulomb fission cross-sections as function of mass

References:

[1] T Nandi et al., *Pramana – J. Phys*. **96:230** (2022).
[2] Oberacker, et al., *Phys Rev C*, **20(4)**, (1979) 1453.
[3] Oberacker, et al., *Reports on Progress in Physics*, **48(3)**,(1967) 327.
[4] Ngô, C., et al., *Nuclear Physics A,* **221(1),**(1974)37.
[5] Backe, *Physical Review Letters*, **43(15)**(1979) 1077.
[6] M. Vidovi´c, et al., *Phys Rev C* **48**, 2011 (1993).
[7] Single-particle transition,https://web-docs.gsi.de/~wolle/BUCH/HTML/MODEL/weisskopf.pdf.

Bayesian neural networks for the evaluation of reaction cross-section of interest in nucleosynthesis studies

Aparna Chakraborty*, Aman Sharma, and Ajay Kumar§

Banaras Hindu University, Varanasi 221005, India
Email: *aparnarra1123@gmail.com ; § ajaytyagi@bhu.ac.in

Nuclear reaction cross-sections are of primary interest in the nucleosynthesis studies. The nuclear reactions involved in such studies are difficult to be measured experimentally at all the projectile energies of interest. Therefore, the theoretical model predictions are generally optimized using the experimental data available. However, difficulty arises in the estimation of the uncertainties appropriately with such predictions.

There have been general advancements in the field of machine learning in recent years. It has seen a great success in diverse fields of application including nuclear physics. Neural networks are one of the machine learning tools which can help in automating the process of nuclear data evaluation. It requires a large volume of good quality data to train a neural network. However, the experimental data is sparse in the field of low energy nuclear physics and thus, the neural networks cannot provide uncertainty estimates associated with their predictions.

In this study we have used a Bayesian neural network to produce cross-section predictions along with their uncertainty estimates. In order to leverage on the data from the available theoretical models, we have used a low-fidelity Bayesian neural network. As a test case we have trained a multi-fidelity learning model by the data from the Talys prediction and available experimental data. We have used experimental data for $^{14}N(n,p)^{14}C$ reaction from EXFOR data library and theoretical predictions from TENDL data library for our low-fidelity estimate which will be discussed at length in the conference.

References:
[1]Aman Sharma, A.Gandhi and Ajay Kumar, Phys.Rev.C 105, L031306 (2022)
[2]X.Meng and G.Em Karniadakis, Journal of Computational Physics 401, 109020 (2020)
[3]Karniadakis,G.E. et.al., Nat.Rev.Phys. 3, 422-440 (2021)

Exploring the Neutron Self-Shielding Factor of Scattering-Dominated Activation Foils

Kavya S.[1], Subhrojit Bagchi[2, §] , D. Sunil Kumar[2] and A. John Arul[2]
[1] *Dept. of Physics, Ramaiah University of Applied Sciences*
[2] *Indira Gandhi Centre for Atomic Research, Kalpakkam*
[§] Email: bagchi@igcar.gov.in

The use of foils in neutron activation analysis can cause self-shielding induced perturbations in the neutron flux due to resonances in the epithermal region of the reactor neutron spectrum. To obtain accurate sample activation results, it is necessary to apply resonance self-shielding factors. Conventional models may not be sufficient due to their neglect of multiple scattering. In cases where energy loss is comparable to or less than the resonance width and scattering cross-section exceeds capture cross-section, alternative methods such as using the Monte Carlo code to consider multiple scattering must be used to calculate the self-shielding factor. The goal is to develop a calculation method for resonance self-shielding factors in foils such as Mn and Co for 1000 isolethargic groups using Monte Carlo for versatility.

The resonance self-shielding factor, G_{res}, in a foil of thickness 't' (0.02 cm) is defined as the ratio between the reaction rates per atom in the actual sample and an infinitely diluted sample.

$$G = \frac{\int_{E1}^{E2} \Phi(E)\sigma_{n,\gamma}(E)dE}{\int_{E1}^{E2} \Phi_0(E)\sigma_{n,\gamma}(E)dE} = \frac{RR(E,\rho_0)}{RR(E,10^{-6}\rho_0)} \ldots(1)$$

$\Phi_0(E)$ represents the non-perturbed epithermal neutron flux in the infinitely diluted sample, while $\Phi(E)$ is the perturbed flux in the actual sample. $RR(E,\rho_0)$ and $RR(E,10^{-6}\rho_0)$ represent the reaction rates for energy E, corresponding to the densities ρ_0 and $10^{-6}\ \rho_0$ respectively. The perturbed neutron flux, $\Phi(E)$, takes into account neutron scattering in the sample and is calculated using the total neutron cross-section. The details of the foil are as follows.

Nuclide	ρ_0 (g/cc)	A(g)	E_{res}(eV)	σ_γ (b)	σ_n (b)	σ_{tot} (b)	Γ_γ (eV)	Γ_n (eV)	Γ_t (eV)
Co59	8.9	58.9	132	$8.49\text{x}10^2$	$9.52\text{x}10^3$	$1.04\text{x}10^4$	0.47	5.15	5.62
Mn55	7.3	54.9	336	46	$3.24\text{x}10^3$	$3.29\text{x}10^3$	0.435	22	22.4

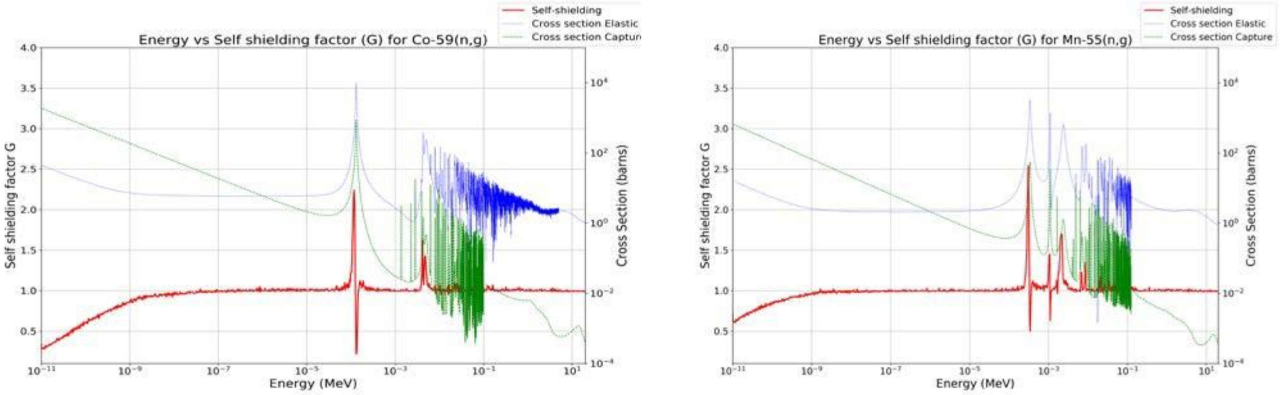

Fig1: Self shielding factor G(E) for Co and Mn

It's clear from Fig1, for cobalt and manganese, which are excellent neutron scatterers ($\sigma_s > \sigma_\gamma$), the self-shielding factor $G_{res}>1$ when the neutron energy E is less than E_{res}. The effect is due to multiple scattering processes, where a neutron with energy $E=E_{res}$ may undergo one or more scattering interactions before being captured, ultimately resulting in absorption when $E < E_{res}$. The values for G_{res} and G_{epi} will be used in different theoretical validations.

References

[1] Eastwood, T.A et al. "Resonance and thermal neutron self-shielding in cobalt foils and wires." *Nucl. Sci. Eng.* **13**, 385–390.

Laser Decontamination of SS304 and T91 Clad Material

D. Bola Sankar[1], M. Rahman[1], U. K. Maity[1], ~~P.~~ Manoravi[1, §]

[1]MC&MFCG, IGCAR; Kalpakkam – 603102, India.
[§] Email: pmravi@igcar.gov.in

Surface decontamination of nuclear facilities and various components (reactor pressure vessels, steam generators, pipes, pumps, valves) with respect to radioactive contaminants is essential to be carried out periodically or irregularly during routine maintenance, overhaul and decommissioning. Decontamination is essential for the reduction of occupational exposure, limiting the release and absorption of potential radioactive contaminants and thereby reduction of collective radiation dose of operating personnel to ensure safe operation of nuclear power plants and nuclear application units. The surface contaminants in nuclear facilities mainly exist both as loose contaminated layer and fixed oxide layer. The types of radionuclides and contamination layer thickness are closely related to the operation status of nuclear facilities. Among the various method, laser can be used for efficient and precise decontamination of these components [1]. In the present, 193 nm ArF excimer laser is employed to decontaminate SS304 and T91 clad.

The substrate of SS304 and T91 clad (10 mm x 10 mm) was coated with uranyl nitrate solution by spreading a few µm over it and dried under infra-red lamp. Then, the substrate was subjected to laser decontamination with 193 nm ArF excimer laser of 2 mJ energy, 10 Hz frequency and spot size 150 x 150 µm. The α and β activities of UO_2 coated substrates were measured before and after decontamination. The calculated decontamination factors (DF) is plotted against number of exposure (laser irradiation) in Fig. 1. Though, DF increases initially with number of exposures it saturates after 3rd exposure. DF for T91 was found to be higher compared to SS304 in the initial exposures. It may be attributed to the higher thermal conductivity of T91 (26 W/m.K) than that of SS304 (14 W/m.K). High DF (>99%) were obtained after 3rd exposure for both the structural materials with such small laser energy (2 mJ) and frequency (10 Hz). Although high power laser is reported for laser decontamination, present study shows power laser of shorter wavelength can also be effect to decontaminate with DF value (>99%).

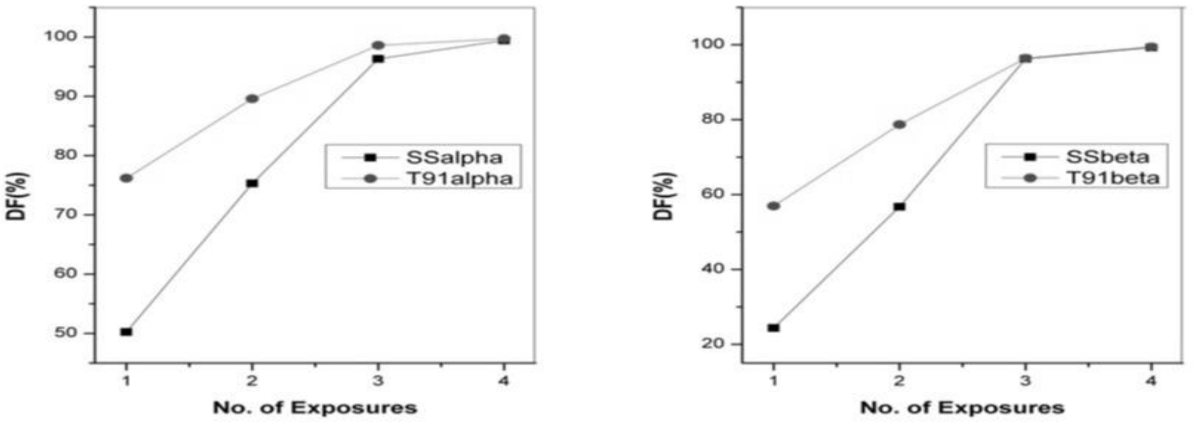

Fig. 1: Plot of decontamination factor (DF) verses number of exposure.

References:
[1] Qian Wang *et. al.*, *Nucl. Eng. Technol.*, **55** (2023), 12.

Hydrogen diffusivity studies in Niobium using Neutron Imaging

Shefali Shukla[1,2§], Tushar Roy[2] , Y.S.Kashyap[1,2] , Prashant Singh[1,2], Mayank Shukla[1,2]
R.N.Singh[2,3] and L.M.Pant[1,2]

[1] *Technical Physics Division, BARC, Mumbai, India*
[2] *Homi Bhabha National Institute, Mumbai, India*
[3] *Mechanical Metallurgy Division, BARC, Mumbai, India*
[§] Email: shefali@barc.gov.in

Niobium is a rare earth metal having high melting point, good superconductivity and corrosion resistance and is currently being widely used in various applications like superconducting cavities, spacecraft industry, atomic energy industry, medical and chemical industry. The structural and mechanical properties of niobium can however be degraded in the presence of hydrogen which can result in problems like hydrogen embrittlement, softening and stress corrosion cracking. Hydrogen transport studies thus become essential to understand this degradation phenomenon. Several techniques have been used for determining diffusion coefficients of hydrogen in Niobium like resistivity measurements, permeation techniques [1] and techniques based on Gorsky effect.

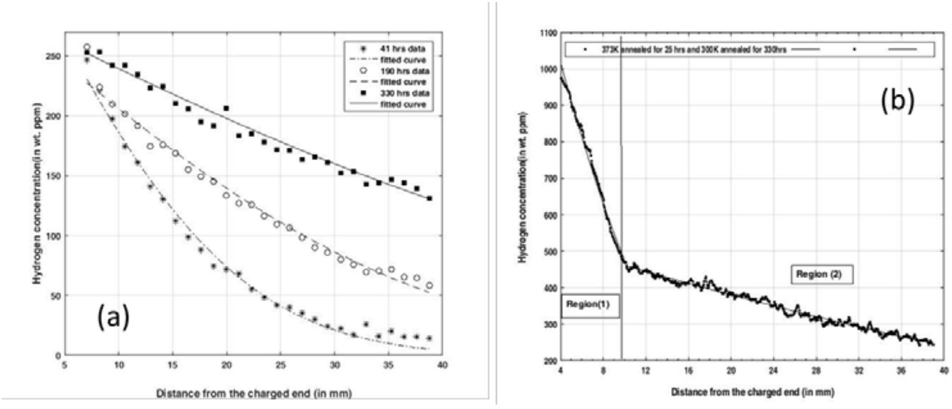

Fig. 1: Hydrogen concentration v/s distance from the charged end at different times for sample kept at RT. (a) ; and at 473K (b)

Neutron imaging is a non-destructive technique which can be used for detecting the presence of light elements like hydrogen in metals [2]. Upon calibration this technique can estimate the absolute amounts of hydrogen and also the diffusion parameters. Present work aims at measuring the diffusion coefficient of hydrogen in niobium in the temperature range (300K-500K) using Neutron Imaging. Diffusion samples were prepared by creating a hydride layer at one end and then annealing the sample at said temperature. The hydrogen concentration v/s depth profile was mapped using neutron radiography. Fig 1 shows the diffusion profiles for the same sample kept at RT (373K) at different times (a) and sample annealed at 473K (b).

References:

1. H.Yukawa, et al Analysis of hydrogen diffusion coefficient during hydrogen permeation through pure niobium. J.of alloys and compounds, 476 (2009) 102-106.
2. Shefali Shukla, et al Investigation of hydrogen diffusivity in Zr-2.5%Nb alloy pressure tube material using Metallography and Neutron Radiography. JNM 544 (2021), 152679.

Decay power uncertainty estimation from nuclear reaction covariance data

G. Pandikumar[1,§], A. John Arul[1,2] and S. Raghupathy[1]

[1]*Indira Gandhi Centre for Atomic Research, Kalpakkam, Tamilnadu 603102, India*
[2]*Homi Bhabha National Institute, Training School Complex, Mumbai-400094, India.*
[§] Email: pkg@igcar.gov.in

The decay power is being estimated using the versatile point depletion code ORIGEN2.1 [1]. The code is associated with nuclear database suitable for various reactors. Accuracy of ORIGEN2.1 prediction depends on the accuracy of the nuclear data used for calculation. Consequent to uncertainty in nuclear data, usually an uncertainty of 20% is added over the predicted decay power. With an intention to reduce uncertainty and also to validate calculation methods, decay power measurements are being done at IGCAR. Recently, decay power measurements are performed for several elements and in various SS materials. Using ORIGEN2.1, the decay powers, from the said samples, are estimated considering their respective irradiation power, irradiation period, mass and cooling periods. The C/E values, for most of the samples, were found in the range from 0.9 to 1.10. In order to find the consequence of such deviations, uncertainty in the predicted decay power, due to uncertainty in decay constant (λ), decay energy (E) and neutron cross section (σ) are estimated for Cr, Na, Ni, Fe and for P91, SS316L, SS304L and D9 steel samples. The total uncertainty in the predicted decay power (Table 1) is estimated using the sensitivity analysis method [3] as follows:

$$\left(\frac{\Delta f(t)}{f(t)}\right)_T = \left[\left(\frac{\Delta f}{f}\right)_E^2 + \left(\frac{\Delta f}{f}\right)_\lambda^2 + \left(\frac{\Delta f}{f}\right)_\sigma^2\right]^{1/2}$$

The uncertainty data for λ and E are considered from JEFF-3.1 [4]. The covariance data given in ENDF/B-VIII [5] is processed using NJOY [6] for obtaining uncertainty in cross sections.

Table 1: Uncertainty in predicted decay power

Sample		Cr	Na	Ni	Fe	P91	SS316L	SS304L	D9
Decay time (h)		20.67	20.31	2.50	2.50	22.14	72.52	46.63	27.48
Decay power (pW)		66.41	1517.0	3584	1974.0	3653.18	851.15	1425.95	5165.03
C/E		1.02	1.04	1.01	1.02	1.01	1.05	1.02	1.01
Uncertainty (%)	$(\Delta f/f)_\lambda$	0.02	0.01	0.16	0.19	0.15	0.10	0.17	0.16
	$(\Delta f/f)_E$	0.52	0.01	0.21	0.90	0.72	0.26	1.81	0.08
	$(\Delta f/f)_\sigma$	2.24	4.50	0.98	1.11	1.27	1.09	0.26	1.39
	$(\Delta f/f)_T$	2.30	4.50	1.02	1.55	1.47	1.13	1.84	1.40

References

[1] A. G. Croff, ORIGEN2: A versatile computer code for calculating the nuclide composition and characteristics of nuclear materials, Nucl. Tech. **62,** 1983.

[2] Jun-ichi Katakura, Uncertainty analyses of decay heat summation calculations using JENDL, JEFF, and ENDF files, J. Nuc. Sci. Tech. Vol. 50, No. 8, 799–807, 2013.

[3] Santamarina A, et al, The JEFF-3.1.1 nuclear data library, Paris: OECD/NEA Data Bank; 2009.

[4] Brown, D.A., Chadwick, et al., 2018. ENDF/B-VIII.0: The 8th major release of the nuclear reaction data library with CIELO-project cross sections, new standards and thermal scattering data. Nucl. Data Sheets 148, 1–142. https://doi.org/10.1016/j.nds.2018.02.001

[5] R. E. MacFarlane, D. W. Muir, R. M. Boicourt, A. C. Kahler and J. L. Conlin, The NJOY Nuclear Data Processing System, Version 2016, Los Alamos: Los Alamos National Laboratory, 2016.

Effect of aging in the performance of resin in reprocessing facility

P K Sharma[§,1], P Banerjee[1], R Saini[1] , A Kelkar[1]T P Valsala[1], D B Sathe[1], and R B Bhatt[1]

[1]*NRB, FF, INRPO, BARC Tarapur, India*
[§]Email : pksharma_ta@barc.gov.in

In reprocessing facility fuel pool area is considered as interim storage for fuel rods before being sent for reprocessing. Adjustment of pH in the pool water is a mandate to avoid accumulation of activity in the muck and build up of activity in the fuel pool. pH of the pool water is adjusted by anion exchange resin(styrene DVB copolymer with quaternary ammonium group). Due to prolong exposure strongly basic anion exchangers in the hydroxyl form are subject to considerable degradation of functional groups at temperatures above 40°C, leading to a loss of strongly basic functionality [1] and also become active source that needs to be disposed. Before disposal, removal or reduction of activity is required for safe disposal. An attempt was made to reduce activity from that resin and presented here.

Measured quantity of resin was taken and directly counted in high resolution gamma spectrometry to assess the presence of radionuclides. Physical change in resin was also seen in XRD results. For leaching of activity equal measured quantities of resin were taken in sets and subjected to contacts separately with different leachants in batches of 5 ml for the stage when activity stripped in the leachant is observed below detectable level i.e.2.0Bq alpha and3.8Bq gamma for Pu and Am estimation respectively. 0.5M sodium sulphate, 1 M sodium chloride, 1 M sodium hydroxide and 4 M nitric acid were used for the study. Activity leached from resin is tabulated here.

Table 1: Leaching study of resin with different leachant

Sample	**^{241}Am (Bq/gm)**	**Pu (Bq/gm)**	**^{137}Cs (Bq/gm)**	**Alpha (Bq/gm)**	**Beta (Bq/gm)**	**Gamma (Bq/gm)**
Solid resin (initial)	167	-	233	-	-	310
0.5M Na_2SO_4	24	BDL	55	26	80	60
1M NaCl	20	BDL	74	21	92	77
1M NaOH	141	BDL	134	144	173	165
4M HNO_3	163	12	174	180	255	237
Solid resin (after leaching with 4M HNO_3)	BDL	-	50	-	-	64

As shown in table 1, 4M nitric acid has highest leaching efficiency for Am (around 94%) and Cs (around 75%. In all cases gross gamma content is less than total gamma contribution from Cs and Am as NaI (Tl) counter (for gross gamma) is Cs specific but individual contribution was determined by gamma spectroscopy.^{90}Sr contribute to Beta activity in fuel pool. Exposure to heat and radiation causes irreversible chemical change in resin. Hence Am and Cs ions can be seated into the interstitial position of linkage and leached out accordingly. Poor efficiency of leaching by sodium sulphate and sodium chloride can be explained in this way that they only able to extract exchangeable part of resin, not effectively any interstitially seated ion. At highly acidic and alkaline medium, Am and Cs leached out easily. Acid leaching can be adopted for this type of exchanger in plant compatible condition to reduce alpha activity, which can lead to safe disposal of waste.

References: [1] Anion Exchangers: Ion Exchange, W.H. Höll Encyclopedia of Separation Science, 2000, 4477

Radioactivity of Francium

P.S.Prabhavathi[1§], N.Sowmya[1§], H.C. Manjunatha[1§], and L. Seenappa[2]

[1.] *Department of Physics, Government College for Women, Kolar, Karnataka, India*
[2.] *Department of Physics, Government First Grade College, Mulbagal, Karnataka, India*
[§] Email: manjunathhc@rediffmail.com, sowmyaprakash8@gmail.com

The decay modes of the compound nucleus formed by fusion include β^- -decay, β^+ -decay, alpha decay and spontaneous fission. The investigation of these many decay modes plays a critical role in determining the presence of heavy nuclei. Flerov and Glasoe [1,2] investigated the spontaneous fission of uranium atoms experimentally. β-decay is also one of the decay mode for neutron/proton rich nuclei [3,4]. α-decay is also investigated both for heavy and superheavy nuclei using Coulomb and Proximity potential model, effective liquid drop model and many empirical relations [5,6]. Huyse et al., [7] studied α-decay chains of odd Fr-At-Bi. Ritchie et al., [8] studied alpha-decay properties of Fr isotopes.

Hence, in the present study we investigated different decay modes of Fr-isotopes in the mass number range 206-247 using β^- -decay, β^+ -decay, alpha decay and spontaneous fission. α-decay half-lives are evaluated using the following formula is as follows;

$$T_{1/2} = \frac{\ln 2}{\lambda} = \frac{\ln 2}{\nu P} \qquad (1)$$

Here ν is the assault frequency and P is the penetration probability and it is evaluated using WKB approximation as follows;

$$P = \exp\left\{ -\frac{2}{\hbar} \int_{R_a}^{R_b} \sqrt{2\mu\left(V(r) - Q\right)}\, dr \right\} \qquad (2)$$

The total potential is evaluated using Coulomb and proximity potential. The spontaneous fission half-lives are evaluated using empirical-formula by Xu et al., [8]. Figure 1 shows comparison between studied different decay modes. $^{206, 208, 210, 212}$Fr is dominant in for β^+ -decay, α-decay half-lives are dominant for $^{207, 209, 211, 213\text{-}221}$Fr. β^- -decay is dominant in isotopes of $^{222\text{-}247}$Fr nuclei. Hence, this study finds an important in the identification of isotopes of francium nuclei.

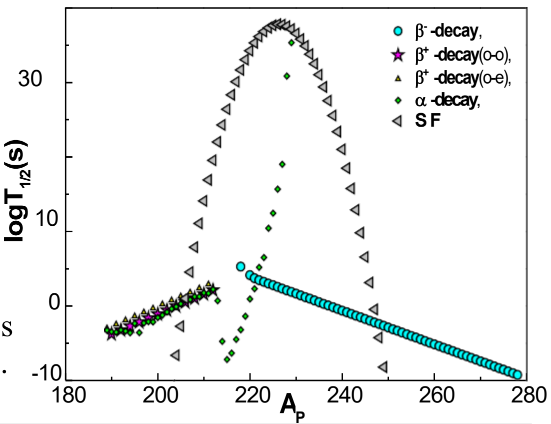

Fig. 1: Comparison of logarithmic half-lives of β^- - decay β+ - decay, α-decay and spontaneous fission half-lives as function of mass number of parent nuclei.

References:
[1] G.N. Glasoe, J. Steigman, *Phys. Rev.* **58** (1940) 1.
[2] Petrjak Flerov, *Phys. Rev*. **58** (1940) 89.
[3] S.Z. Qiang, S.L. Ping, et al., *Chin. Phys. C* **38(12)** (2014) 124101.
[4]X.P. Zhang, Z.Z. Ren, Q.J. Zhi, et al., *J. Phys. G, Nucl. Part. Phys*. **34** (2007) 2611.
[5] H.C. Manjunatha, et al., *Nucl Sci Tech* **32**, 130 (2021).
[6]H. C. Manjunatha, et al., *Phy Rev C* **98**, 024308 (2018).
[7] M. Huyse, et al., *Phys. Rev. C* **46**, 1209 (1992).
[8] Z Ren and C Xu, *Nucl. Phys. A* **759**, 64 (2005).
[9] B. G. Ritchie, et al., *Phys. Rev. C* **23**, 2342 (1981).

A Re-assessment of 620 group SAND-II cross-section set based on IRDF-90

Deep Bhandari § , Kapil Deo, Sudipta Samata, Amod Kishore Mallick, Rajeev Kumar and Umasankari Kannan

Reactor Physics Design Division
Bhabha Atomic Research Centre, Mumbai, India-400085
§ Email: dbhan@barc.gov.in

An accurate knowledge of neutron spectrum is essential for various fields like Reactor Physics, NAA, Isotope Production etc. Owing to its various advantages, Activation Foil method is often used for neutron spectrum measurement. Estimating of accurate spectrum is not possible without having a proper neutron unfolding code. At RPDD, the neutron unfolding code SAND-II [1] has been routinely used along with activation detector measurements, for estimating neutron spectrum due to different sources. Apart from the foil activities, SAND-II requires cross-section of all the reactions of interest in 620 energy group, as input. Such a cross-section has earlier been extracted from IRDF-90 library [2]. A new version of IRDF library (IRDFF-II) [3] was recently released which addresses neutron dosimetry needs for fission and fusion applications for incident neutron energies from 0 to 60 MeV. In light of this development, the cross-section set for SAND-II (retrieved from IRDF-90) was re-assessed.

Using IRDFF-II library, 620 energy group cross section of various reaction of some well-known activation foils have been extracted and a comparative study was carried out between the old cross section data and updated cross section data extracted from IRDF-90 and IRDFF-II respectively. Also, there were some missing cross section data of some specific isotopes in the earlier cross-section set. The 620-group cross section of those isotopes were also extracted from IRDFF-II library. Using this updated SAND-II cross-section set, neutron spectrum unfolding for a photo-neutron source was carried out. The spectrum thus obtained was compared with that corresponding to cross-section set based on IRDF-90.

As an example, the relative difference between the $Au^{197}(n, \gamma)$ Au^{198} reaction cross-section obtained from IRDF-90 and IRDFF-II library using nuclear data processing code PREPRO [4] is shown in Fig 1. The maximum and minimum difference in cross-section was 46% (at energy 230eV) and -3.9% (at energy 840eV) respectively.

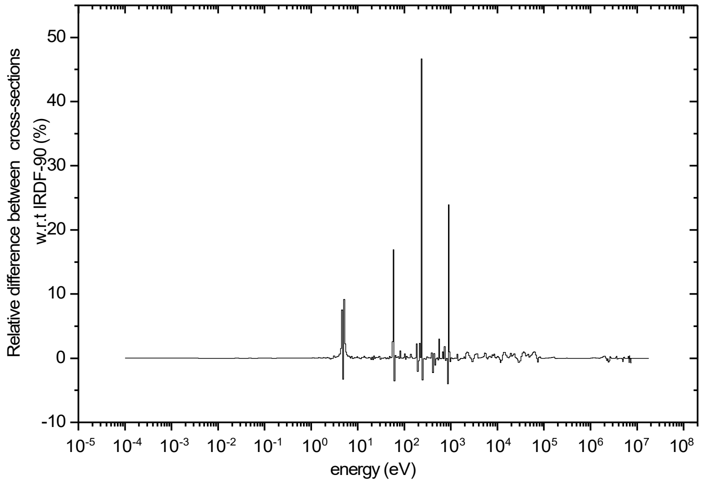

Fig1. Relative difference between the Au197(n,y) Au198 reaction cross-section obtained from IRDF-90 and IRDF-II library

References: [1] Patrick J. Griffin, J. (Jake) G. Kelly; "User's Manual for SNL-SAND-II Code"; April 1994
[2] N.P. Kocherov, and P.K. McLaughlin; "The International Reactor Dosimetry File (IRDF-90 Version 2)"; Oct 1993.
[3]A. Trkov, P.J.Griffin, S.P Simakov; "IRDFF-II: A New Neutron Metrology Library"2020.
[4] Dermott E. Cullen, "PREPRO 2021ENDF/B Pre-processing Codes" July 2021.

Study of entrance channel effect on shell-closure in fission dynamics for Rn^{212*}

Punit Dubey [§], Utkarsha Mishra, and Ajay Kumar*

Department of Physics, Banaras Hindu University, Varanasi, India
[§] Email: punitdubey@bhu.ac.in *Email: ajaytyagi@bhu.ac.in

It is evident from the published research work that the nuclear fission dynamics are critically based on the entrance channel mass asymmetry (α), shell effect, and N/Z. In fission dynamics, pre-scission neutron multiplicity (ν_{pre}) is the best way to understand the dependence of these parameters. Experimental studies show neutron multiplicity decreases for the shell-closed nucleus compared to the non-shell-closed nucleus [1].

In our present calculation, the systematics used by us to find the pre-scission neutron multiplicity ($\tilde{\nu}_{pre}$) is based on Ref. [2]. We have added the shell correction energy δW to excitation energy by using the NRV JINR web application.

$$\tilde{E}^*=E^*+\delta W \quad (1)$$

Where $\tilde{E}^*$ is the liquid-drop excitation energy, E^* is the excitation energy, and δW is the shell correction which is a function of Z and A. The $\tilde{\nu}_{pre}$ $(A,\tilde{E}^*)$ dependence is described by the expression below:

$$\tilde{}_{pre}(A,\tilde{E}^*)=-10.64+0.0979A-0.0154\tilde{E}^*-0.000234A^2+0.000305A\tilde{E}^* \quad (2)$$

By using equation (2), we can find $\tilde{\nu}_{pre}$, and here we add an error of $\Delta\tilde{\nu}_{pre}=6\%$, which we have taken from Ref. [2].

In the present work, we have calculated the $\tilde{\nu}_{pre}$ for compound system Rn^{212} by using the systematic given in Ref. [2], which is a shell-closed system (N=126). Here, the systematically calculated data have been compared with the available experimental data for Rn^{212} [3-4]. From Fig.1, we can clearly observe that systematics data coincide with experimental data at low excitation energy, indicating that shell effects are more predominant at low excitation energy (~50 MeV or below). Here, we can also observe deviation in both the experimental data due to the entrance channel effect, as shown in Fig.1. Also, the appearance and disappearance of shell closure effects critically depend on the excitation energy of the system [1,3]. From here, we can predict that we can get more fascinating results if we form the same compound nucleus using different entrance channels by varying excitation energy.

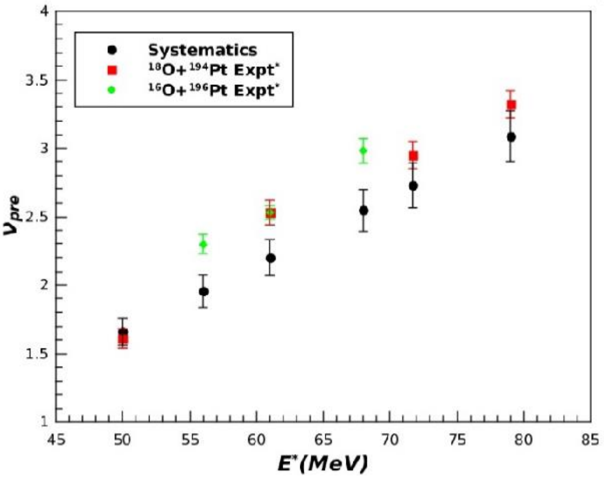

Fig. 1: A plot between pre-scission neutron multiplicity w.r.t Excitation energy for Rn^{212}.

The author (Punit Dubey) gratefully thanks the Prime Minister Research Fellowship (PMRF) for the financial support for this work.

References:

[1] Varinderjit Singh *et al.,* Phys. Rev., C **86** (2012) 014609.
[2] E.M Kozulin *et al.,* Yad. Fiz., **56** (1993) 37-54.
[3] Rohit Sandal *et al.,* Phys. Rev., C **87**, (2013) 069901.
[4] K. Kapoor *et al.,* Phys. Rev. C **100**, (2019) 014620

Decay power measurements from Na, Al, Sb and Cr using Whole Energy Absorption Spectrometer

G. Pandikumar[1,§], D.V. Subramanian[1], A. John Arul[1,2], Adish Haridas[1] and S. Raghupathy[1]

[1]Indira Gandhi Centre for Atomic Research, Kalpakkam, Tamilnadu 603102, India
[2]Homi Bhabha National Institute, Training School Complex, Mumbai-400094, India.
[§]Email: pkg@igcar.gov.in

Decay power from reactor grade sodium, aluminium, antimony and chromium are measured using Whole Energy Absorption Spectrometer (WEAS) and compared with ORIGEN2 [1] predictions. The principle of WEAS is to measure the beta and gamma energies that are deposited in the detector simultaneously with detection efficiency close to 100%. The essential part of WEAS set-up is a pair of large bismuth-germanate (BGO) scintillators [2]. An irradiated sample is sandwiched tightly by the BGO scintillators to make 4π geometry.

Samples of Na, Al, Sb and Cr are irradiated in KAMINI PFTS location. To determine neutron flux, gold foils are also irradiated along with each sample. The decay powers from Na, Al, Sb and Cr samples are calculated using ORIGEN2 code. Neutron flux, obtained from Au activity, is used in decay power prediction. The reactor spectrum averaged one group cross sections, which are prepared using the KAMINI neutron flux spectrum, is considered in the calculation. The measured decay power is smaller than predicted due to (a) gamma attenuation in the sample (b) energy absorption efficiency of BGO detectors for beta and gamma particle and (c) self-absorption and scattering of beta particles in the sample. So, the estimated decay power is corrected accordingly. Table 1 gives a comparison of measured and predicted decay power (D) from Na, Al, Sb and Cr samples for cooling periods T_c. From this study, it is possible to predict decay powers from Na, Al, Sb and Cr samples within 4%, 7%, 9% and 8% respectively with respect to measurements. The study also validates the spectrum averaged one group cross section and the neutron flux.

Table 1: Comparison of calculated and measured decay powers from Na, Al, Sb and Cr

Sodium			Aluminium			Antimony			Chromium		
T_c (h)	D (pW)	C/E	T_c (h)	D (pW)	C/E	T_c (h)	D (pW)	C/E	T_c (h)	D (pW)	C/E
0.65	3752.42	1.02	1.04	4541	1.07	71.39	14077.81	0.97	20.67	65.07	1.02
20.31	1460.86	1.04	3.53	2233	0.99	95.61	10480.99	1.03	164.55	53.55	1.06
24.91	1174.22	1.04	45.77	322	0.97	287.24	2161.37	1.09	308.27	45.27	1.08
43.93	487.36	1.02	51.72	242	0.97	478.94	1132.56	1.02	403.42	41.67	1.07
47.82	405.39	1.02	70.12	100	1.01	600.58	972.48	1.01	572.50	35.24	1.06
67.85	156.98	1.02	75.63	78	1.00	1107.06	773.53	0.95	859.07	26.04	1.06
71.28	133.56	1.02	-	-	-	1463.44	641.55	0.96	907.88	25.15	1.04

References

[1] Fujio Maekawa, et al, Develpoment of whole energy absorption spectrometer for decay heat measurement, *Nucl. Inst. and Meth. Phys. Res*., A 450 (2000) 467 – 478.

[2] A. G. Croff, ORIGEN2: A versatile computer code for calculating the nuclide composition and characteristics of nuclear materials, Nucl. Tech. **62,** 1983.

Understanding Temporal Evolution of Diatomic Rovibrational Molecular Spectra of BO Molecule

Anandhu Mohan[1,2], Anannya Banerjee[2] and Arnab Sarkar[1,2,§]

[1] *Homi Bhabha National Institute, Mumbai -400094, India*
[2] *Fuel Chemistry Division, Bhabha Atomic Research Centre, Mumbai-400085, India*
[§]E-mail: arnab@barc.gov.in

Boron, a well-known element in analytical and technical industry especially in nuclear industry. Due to its high neutron absorption cross-section, several purposes arises for the use of natural and enriched boron materials. Laser Ablation Molecular Isotopic Spectroscopy (LAMIS) is one of the distinct method for real time analysis of isotopic ratio. The higher isotopic shift in the boron oxide emission band (0.73 nm) draws attention to this method since the isotope splitting of boron atomic lines (0.0025 nm) is comparatively small [1].

In the present study, the temporal evolution of rotational-vibrational (rovibrational) bands of $B^2\Sigma^+ \rightarrow X^2\Sigma^+$ (B-X) transition was analysed for the diatomic boron oxide molecule using boric acid pellets. The B-X transition is primarily observed in UV region (~220-330 nm) and the band origins were calculated using the diatomic constants reported by Mélen et.al. [2]. The temporal analysis of these BO bands were carried out by varying the acquisition delay time (t_d) from 0.2 μs to 15 μs and gate width (t_w) were kept same as that of t_d. The data was normalized by t_w. Along with BO molecular emission, temporal evolution of boron atomic and ionic lines, B(I)261.35 nm, B(II)345.13 nm and B(III)247.9 nm were also studied.

On careful analysis of the data, it can be observed that the atomic, ionic and molecular species follows an exponential decay pattern. The ionic emission lines were found to be decay at a faster rate than atomic emission lines in the order B(III) > B(II) > B(I). Likewise, the initial temporal studies of B-X band showed different decay rates for different vibrational bands. A closer look reveals, one B(III) line and two B(I) lines spectrally interfere the (0-1) rovibrational band. Whereas, B(I)261.35 nm is spotted at the observable tail-end of (2-0) band. The (0-3) band were also found to be spectrally interfered at early plasma evaluation time. The removal of atomic and ionic species influenced information from the earlier plasma evolution time period, revels that all the vibrational bands of B-X transition shows same decay profile with an average exponential rate constant, k = ~ 0.28 μs^{-1}.

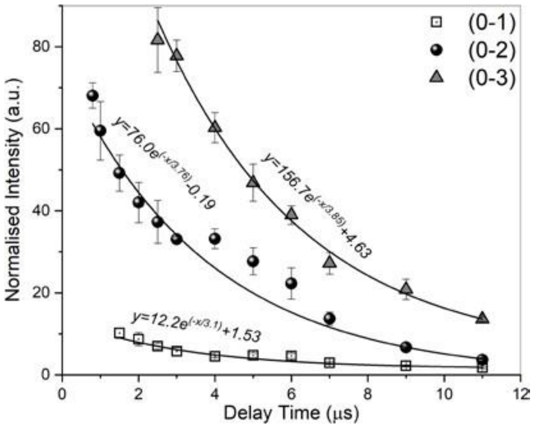

Fig. 1: The temporal decay profile of (0-1), (0-2) and (0-3) $B^2\Sigma^+ \rightarrow X^2\Sigma^+$ vibrational transitions of BO.

The study gives an idea about the time dependent influence of atomic and ionic species in molecular information of B-X transition of boron oxide. The (0-2) vibrational band showed better intensity and less spectral interference. The study shows, that the (0-2) band is the best choice for boron isotopic ratio calculation using LAMIS technique.

References:
[1] R.E. Russo et.al., *Spectrochimica Acta Part B.*, 66 (2011) 99-104.
[2] F. Mélen et.al., *J. Phys. B: Atom. Mol. Phys.*, 18 (1985) 2423

Polyatomic Molecular Band and its Temporal Evaluation in a Laser Induced Plasma: BO_2 Molecules

Anandhu Mohan[1,2], Anannya Banerjee[1] and C.D.E. Arnab Sarkar[1,2,§]

[1] *Homi Bhabha National Institute, Mumbai -400094, India*
[2] *Fuel Chemistry Division, Bhabha Atomic Research Centre, Mumbai-400085, India*
[§]E-mail: arnab@barc.gov.in

Various species such as ionic, atomic, diatomic, and polyatomic species were formed in laser induced-plasma. Analysis of diatomic and polyatomic molecular spectra using LIBS in the analytical and nuclear industry became popular in recent times [1]. This study investigates the possibility of formation and temporal evaluation of polyatomic (BO_2) molecular bands in ambient air conditions using boric acid pellets.

The band origins were calculated using database [2]. The $A^2\Pi_i \rightarrow X^2\Sigma^+$ transition of BO and $A^2\Pi_u \rightarrow X^2\Pi_g$ transition of BO_2 are in similar wavelength region. The temporal analysis of these bands was carried out by varying the acquisition delay time (t_d) from 0.2 to 30 μs.

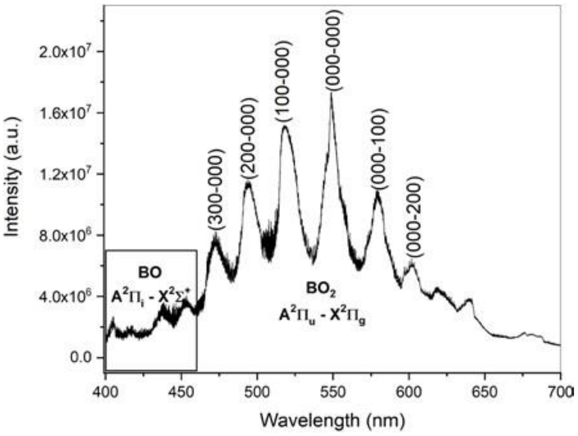

Fig. 1: Molecular emission spectrum of BO $A^2\Pi_i \rightarrow X^2\Sigma^+$ and BO_2 $A^2\Pi_u \rightarrow X^2\Pi_g$ transition

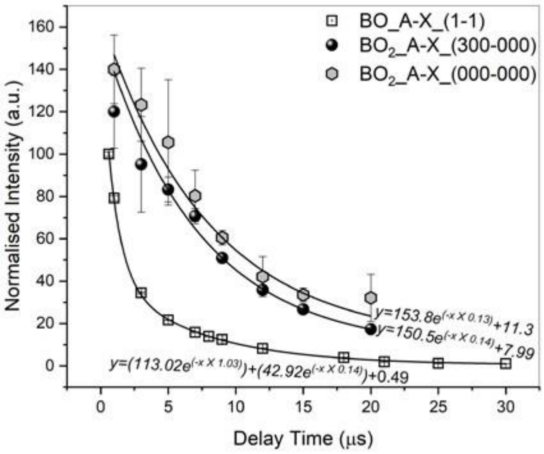

Fig. 2: The temporal decay profile of diatomic (BO) and polyatomic (BO_2) molecular bands.

The BO_2 $A^2\Pi_u \rightarrow X^2\Pi_g$ bands were observed in the 450 – 650 nm region in ambient air conditions. The diatomic BO molecule's $A^2\Pi_i \rightarrow X^2\Sigma^+$ transition which emits in the 400-500 nm region, interferes with the (300-000) band originating at ~450 nm. In comparison with BO $A^2\Pi_i \rightarrow X^2\Sigma^+$ bands, BO_2 $A^2\Pi_u \rightarrow X^2\Pi_g$ bands started to appear at higher delay times. This shows that the formation of triatomic species requires lower plasma temperature. BO_2 molecular bands show significantly high intensity when compared to BO molecular bands. The (1-3), (1-2), and (1-1) rovibrational bands of BO A-X transition were identified in the range of 400 – 450 nm. On analyzing, the temporal evolution of A-X's (1-1) band, a second-order exponential decay with two different rate constants (k = 1.03 and 0.14 μs^{-1}) was obtained. The second rate constant in the decay curve clearly indicates the interference of BO_2 $A^2\Pi_u \rightarrow X^2\Pi_g$ on BO $A^2\Pi_i \rightarrow X^2\Sigma^+$ molecular bands. This study provides an understanding of how the BO_2 molecular spectra are evolved and the influence on the BO molecular spectra.

References:
[1] A. Sarkar et.al., *Spectrochimica Acta Part B*, 92 (2014) 42-50.
[2] J.W.C Johns., *Canadian Journal of Physics*, 39 (1961) 1738-1768.

Wavelet analysis of Autoradiography Images

Rajashree Dixit[§], K.V. Vrinda Devi, S. Mukhopadhyay and Amrit Prakash
Bhabha Atomic Research Center
[§] Email: rajashree@barc.gov.in

Nuclear fuel characterization utilizes different forms of radiation imaging by means of external radiation sources as well as the emissions from the object to be imaged (fuel element). Plutonium bearing fuels have strong emissions of γ-rays, α radiations, neutrons etc. which can be used for generating self radiation images known as autoradiograph. It is important to identify the presence of plutonium heterogeneity in MOX fuel pins to ensure conformity with the stringent specifications. Image analytical studies have been reported to obtain quantitative estimations of plutonium heterogeneity in fast reactor fuels [1]. Wavelet analysis has been reported to be effective in denoising radiation images and hence was envisaged to improve delectability in GAR images of nuclear fuel pins too. Wavelet analysis GAR images of (U, Pu)O_2 mixed oxide (MOX) fuel pins for the upcoming Prototype Fast Breeder Reactor (PFBR) have been carried out and results are reported in this paper.

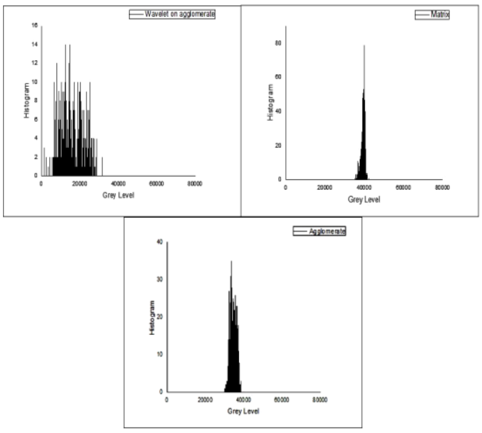

Fig 1: Histograms of (clockwise from left) wavelet transformed image and original images .

Wavelet transforms are efficient mathematical tool for analyzing data where characteristics vary over different layers [2, 3]. The image is first converted into a pixel based data matrix of 17 x 30. Wavelet transform is applied on this data matrix to segregate different grey levels and classify patterns based on the type and levels of wavelet applied. The transformation denoises and enhances the image through dilation and compression property of the wavelet. There are two types of Wavelet Transforms (WT): Continuous (CWT) and Discrete (DWT) out of which DWT was used in this work as it is usually used for analysis of stationary signals and images. DWT breaks a signal into set of time series representing a particular frequency band.

Few rejected MOX fuel pins detected with plutonium agglomerates were chosen for the experiment and their GAR images were used for the analysis. The images were converted into corresponding pixel data matrix containing grey level values. Relative standard deviations were calculated for the matrix portion of the image to estimate the inherent statistical fluctuations in a homogeneous fuel matrix due to various factors. Any deviation from these statistical values would indicate heterogeneity (agglomerate) in plutonium distribution. These deviations were computed on original GAR images as well as wavelet transformed images for a direct comparison. A fivefold improvement was found in the deviation values owing to wavelet transformation of the images indicating a significant improvement in detectability of presence of plutonium agglomerates in MOX fuel pins.

Acknowledgement: The authors acknowledge Shri. Vivek Bhasin (Director, NFG), Shri. R. B. Bhatt, (ED (FF&QA), NRB) and Shri D. B. Sathe, (AGM (TS), NRB) for their support during this work.

References:
[1] K.V.Vrinda Devi et al (2019). Plutonium Heterogeneity in MOX Fuel: A Quantitative Analysis *J. Nucl. Mat.*518 : 129-139, DOI: 10.1016/j.jnucmat.2019.02.048.
[2]Chui, C.K. (1992). An Introduction to Wavelets. Academic Press, New York.

Reverse-Phase Liquid Chromatographic method for the measurement of Uranium in Process Stream Solutions from Uranium Extraction Facility

Y. Balaji Rao[1§], Shehanaz Bano [1], P.V. Nagendra Kumar [2], Dinesh Srivastava[1]

[1 & §] *Nuclear Fuel Complex, Dept. of Atomic Energy, ECIL post, Hyderabad- 500062, India*
[2]*Asst Professor, Dept of Chemistry, GITAM University, Hyderabad-502329, India*
[§] Email: ybr4793@gmail.com / ybr@nfc.gov.in

Natural UO_2 pellets are being used as fuel in Pressurized Heavy Water Reactors (PHWRs) and are produced by following chemical conversion and fabrication processes at Nuclear Fuel Complex (NFC). Different raw materials such as sodium di-uranate (SDU), heat treated uranium peroxide (HTUP) and uranium ore concentrate (UOC) are used for the production of nuclear grade natural UO_2 pellets. Solvent extraction is the important step of chemical conversion process and as part of QA/QC program, process efficiency is monitored by measuring the concentration of uranium in uranyl nitrate pure solution (UNPS) and uranyl nitrate raffinate (UNR). UNPS is an aqueous solution obtained after stripping the uranium from the organic phase into aqueous phase and UNR is an aqueous solution left after extracting the uranium from the aqueous feed into the organic phase. Apart from finding the process efficiency, another important requirement of the process is the disposal of active ammonium nitrate (AN) solution which is obtained after precipitating the uranium in UNPS with ammonia as ammonium di-uranate. Prior measurement of uranium in AN solution is required for its disposal. The concentration range of uranium in UNPS, UNR, AN solutions is about 120-150 gm/l, 1-10 gm/l and 1-200 mg/l respectively. In view of wide range of uranium concentration to be measured in these process stream solutions, different techniques are employed as one technique will not meet the requirements. Gamma Ray Spectrometer (GRS) is suitable for higher uranium concentration of >5 gm/l, X-Ray Fluorescence Spectrometer (XRFS) [1] is suitable for measurement in the range of 1-10 gm/l and Inductively Coupled Plasma Optical Emission Spectrometry (ICP-OES) is suitable for lower concentration[2]. Therefore, a successful effort has been made to develop a single and simple method of Reversed-Phase Liquid Chromatography (RPLC) using C18 column(medium capacity,150x4.0mm) and spectrophotometer as detector for measuring uranium content in the above mentioned process stream solutions. For this purpose, sample solutions are diluted suitably to bring into the linear dynamic range of 0.5 mg/l – 20mg/l of the developed method. Different eluents and several parameters like pH, concentration of eluent are studied during the development of method. A typical chromatogram of UNR sample using eluent with optimized conditions is shown in Fig-1. The developed RPLC method is devoid of interferences from other elements during elution. Comparison of sample results obtained by the developed method and regularly used techniques is also given in the paper. A RSD of less than 10% is achieved in the developed method and the effort has resulted in increasing of through-put by removing use of multiple techniques and also reduced the analytical waste generated.

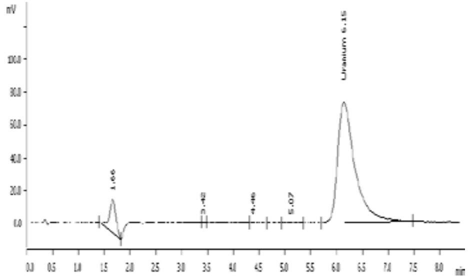

Fig. 1: A typical chromatogram of UNR sample (eluent 0.2M α-HIBA+10% methanol, pH 4, 1.2ml/min, λ_{652nm})

References:

1. Y. Balaji Rao etal, J. Radioanal. Nucl. Chem.294 (2011), 371.
2. Gupta etal, J. Radioanal. Nucl. Chem. 314(3) (2017), 2129-2135.

Quantitative estimation of microgram level of Pu in plutonium nitrate solution using controlled potential coulometry

S.R.Guchhait[1,2,§], P.J. Wagh[1], M.P.Phadke[1], A.Sankhe[1], V.De[1], A. Kelkar[1], T.P. Valsala[1],
D.B. Sathe[1], R.B. Bhatt[1]
[1] *TRP, NRB, BARC, Tarapur, India*
[2] *Homi Bhabha National Institute, Mumbai, India*
[§]Email: srguchhait@barc.gov.in

The controlled potential coulometry, being an absolute method and highly selective, is one of the best methods for quantitative estimation of Pu in dissolved solution of PuO_2 powder. Plutonium being a radiotoxic and strategic material its precise and accurate estimation is highly important for nuclear material accounting purpose. Although controlled potential coulometry is perfectly meeting these requirements but mg level of the sample required for this analysis leads to loss of greater amount of Pu in the analytical waste. Presence of small amount of iron in the Pu sample seriously affect the precision and accuracy of this method for Pu estimation as the ratio of their equivalent weight (Fe:Pu) is 1:5. In the present study iron has been used purposefully to reduce the quantity of plutonium required in the sample for its precise and accurate estimation.

The in-house Pu stock solution was diluted on weight basis and microgram level of Pu aliquots were taken for coulometry containing known quantity of iron. The analysis was carried out in a 3 limbed coulometric cell in 0.5M HNO_3 medium keeping the potential fixed at 0.35V and 0.78V during reduction and oxidation respectively in an inert atmosphere. Complete analysis was carried out within 1 hr. Total charge consumed/liberated–in the analysis was attribution of plutonium and iron. The charge consumption for plutonium was calculated by subtracting the contribution from known quantity of iron added. The results are shown in table1. It is evident from the table that when microgram quantity of plutonium is analysed along with iron, in most cases the precision and accuracy obtained is better than 0.2% which can be considered better or same as the existing method of analysing plutonium in milligram level. Whereas it was found that the same microgram level of plutonium when analysed alone showed very poor precision and accuracy (>10%).

Table1. Results of Pu analysis in presence and absence of Fe

Sample no	Fe added(g)	Pu added(µg)	Calculated Q (mC)	Expt. Q (mC)	%E
1	0.0372	209.8	1238.8	1236.9	0.15
2	0.0371	206.2	1234.2	1231.9	0.19
3	0.0378	242.6	1270.7	1267.9	0.22
4	0.0374	210.7	1245.4	1244.2	0.09
5	0.0376	217.1	1253.9	1252.3	0.15
6	0	206.1	83.1	73.5	11.54
7	0	199.3	80.3	69.1	13.99
8	0	207.6	83.68	74.9	10.49

Hence, it may be concluded that the adoption of this new method will drastically reduce the quantitative handling of plutonium as well as man-rem exposure with subsequent loss into analytical waste and will ease the waste management.

References:
[1] V. N. Momotov and E. A. Erin et.al, *RADIOCHEMISTRY*, Vol. 59 (2017), pp. 3
[2] Sharma et. al., *Nuclear Technology*, Vol.89, (1990), pp. 391

Determination of trace level uranium content in Mild Steel wastes from uranium oxide plant at various stages of decontamination using LED based Fluorescence spectrometer.

U.B. Misra[§], B.Rajendra, M.Dutta, Y.Balaji Rao, R.K.Chaube and K.Kpoor

Nuclear Fuel Complex, Hyderabad, India
[§]Email: ubhayabharati@yahoo.in

Nuclear Fuel Complex, is a pioneer unit for manufacturing of nuclear fuel from ore to core for Indian PHWRs and BWRs. In the years of operation some of the MS scrap generated in uranium oxide plant needed to be disposed after decontamination. The homogenous melted samples were sent to CLAB, NFC for uranium estimation from various stages of decontamination.

There are various methods for quantification uranium in trace & ultra-trace level like ICP,ICP-MS,α-spectrometry, scintillation counting, fluorescence spectrometry, UV spectrometry TXRF,NAA etc. Every method suffers from their own limitations of high DL, tedious matrix separation and availability of the facility in the laboratory etc.

In the present work the high fluorescence quantum efficiency of uranium[1] was exploited to determine the uranium content. In literature quenching effect of many elements on the fluorescence of uranium are discussed [2,3,4,5].As quenching effect of Fe is studied by various authors, it was challenging to analyze uranium content with Fe matrix. In the present work it is observed that the quenching effect is not pronounced up to the 80 mg/L of Fe concentration in the solution. Hence the sample received were dissolved in aqua regia, followed by addition of $HClO_4$ and fumed on hot plate till dense white fume. Suitable dilution was done to bring down the Fe concentration. Optimized quantity of tri-sodium-pyrophosphate as fluorophore and NaF as enhancer was added .Calibration is done by standard addition method without and with matrix matching standard and $R^2=0.999$ is obtained for both.CRM of Uranium with concentration 1004 ±4 µg/ml, Plasm CAL from SCP-Science is used for calibration. The LOQ is found to be 10ppm in MS steel matrix. The real time samples with uranium concentration ranging from 10ppm to150ppm were analyzed using the method. LED based fluorescence spectrometer model no UA2 from Quanta Lase Enterprises Pvt. Ltd was used for the determination. The method was validated with standard recovery using CRM and also with ICP-AES for samples with higher uranium content. Interference free emission line of uranium 385.985nm was used for analysis in ICP-AES . The LOQ by ICP-AES in MS matrix is 100ppm due to the limitation of maximum 10% solid in solution for aspiration and high background. Hence fluorescence spectrometry was used for lower concentration. The quenching effect of Cr ,Ni & Mo are studied for feasibility of determination of uranium in SS and molybdenum matrix to meet the requirements of ceramic fuel fabrication plant of NFC .

Acknowledgement: Authors express their sincere thanks to Smt. N.Bhavani for carrying out experimental works.

References:1 G. Geipel, Coordination Chemistry Reviews 250 (2006) 844.
2.T. Matsui et-al J. Nucl. Sci. Tech, 25 (1988) 868.
3.P.S. Rathore, M. Kumar, Talanta, 62 (2004) 343
4.P. K. Tarafder1 et-al, J Radioanal Nucl Chem, (2017) 313:353
5. Sanjukta A. Kumar et-al, Talanta 77 (2008) 422.

Alpha induced gamma emission spectroscopy for determination of carbon in steel

G. L. N. Reddy[§], Y. Sunitha, A. A. Sukumar, D. V. Lakshmipathy and J. V. Ramana

National Centre for Compositional Characterisation of Materials (NCCCM), BARC, Hyderabad, India, 500062
[§] Email: glnreddy@barc.gov.in

Carbon is one of the most important element in steels. The carbon content and its distribution determines its strength, hardness, toughness, weldability and corrosion resistance, among other properties. Accurate determination of carbon content in steels and in other materials is crucial for the material to meet the desired quality and performance standards. Among the many analytical techniques, Ion Beam analysis (IBA) offers sensitive, non-destructive and rapid compositional characterisation of materials. IBA techniques such as PIGE, RBS, EBS, NRA have been extensively utilised for the determination of overall content as well as depth profiling of carbon. [1]. However, the detection limit of PIGE, using protons as the incident particles is often limited to sub-percentage levels due to elevated backgrounds and interference from other competing reactions.

In the present study we have standardised a methodology to determine carbon using $^{12}C(\alpha, \gamma)^{16}O$ (Q=7.16 MeV)and $^{13}C(\alpha, n\gamma)^{16}O$ (Q=2.22 MeV) nuclear reactions which emits 6.1 MeV characteristic γ-rays. NIST steels were used as standards. Samples and standards were irradiated with 4.0 - 6.4 MeV α-particles, produced from 3 MV Tandem accelerator. The characteristic γ-rays emitted from the above reactions were detected using HPGe detector placed at 0° w.r.t. the beam direction (Fig 1(a)). The calibration curve was constructed using standards at 6.0 MeV beam energy and it exhibited good linearity with a regression coefficient (goodness of fit) of 0.99981 (Fig 1(b)). This methodology can be utilized to determine carbon down to 500 ppm in stainless steels. The higher beam energies have resulted in higher yields which gives better sensitivity. However, the beam energy is limited to 6.0 MeV to avoid the interferences from oxygen. The advantages of this method are simple, non-destructive and provides quantification with a precision of 5%.

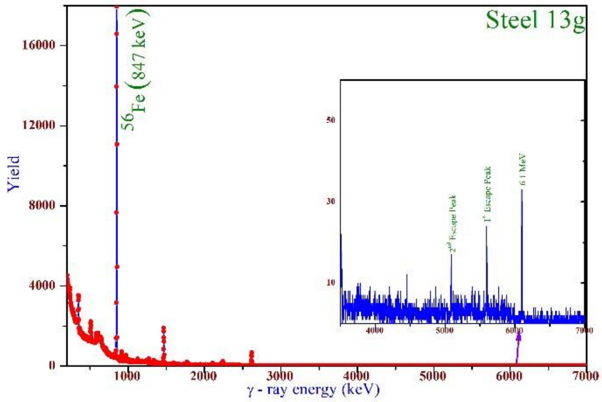

Figure 1(a). 6.0 MeV α induced γ-ray spectrum of steel samples

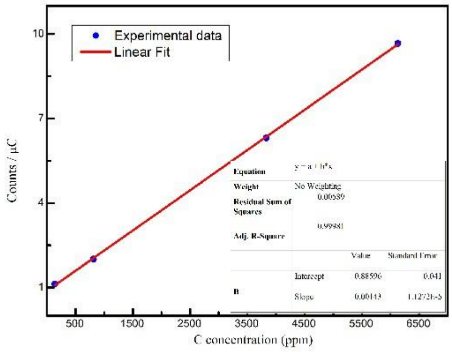

Figure 1(b). Calibration curve at 6.0 MeV α energy

Reference(s):

[1] R.D . Vis., *Nucl. Inst. and Meth B 66 (1992) 139–145*

Improving the Sensitivity Thermal Ionization Mass Spectrometric Analysis of Thorium

Preeti Goswami, K. Sasi Bhushan§, Sumana Paul and P.G. Jaison

[1] *Fuel Chemistry Division, Bhabha Atomic Research Centre, Mumbai*
§ Email: sasiakp@gmail.com

Thermal Ionization Mass Spectrometry (TIMS) is the method of choice for the disequilibrium investigations of the naturally occurring radioactive decay series such as uranium-series to yield valuable insights in the field of geochemistry, geochronology, paleoclimatology etc [1]. Though TIMS can measure $^{234}U/^{238}U$ ratio with high precision and accuracy, ratio measurement of Th isotopes is impaired by the poorer sensitivity of thorium ions (Th^+) or thorium oxide ions (ThO^+) in the thermal ion source.

Recently our laboratory has developed a novel TIMS methodology for the minor abundant isotope ratio of $^{234}U/^{238}U$ in ground water samples. This was possible by the pyrolysis of uranium pre-loaded DEHPA-Dod@PP [bis(2-ethylhexyl)phosphoric acid-Dodecane@PolyPropylene] membrane on the vaporization filament leading to significant enhancement of ion intensity of UO^+ ions (~ 10 fold) [2]. Present work explores the possibility of utilizing similar approach for the enhancement of ThO^+ ions by employing Th pre-loaded DEHPA-Dod@PP membrane on the filament. The preparation of Supported Liquid Membrane of DEHPA-Dod@PP membrane is given elsewhere [2].

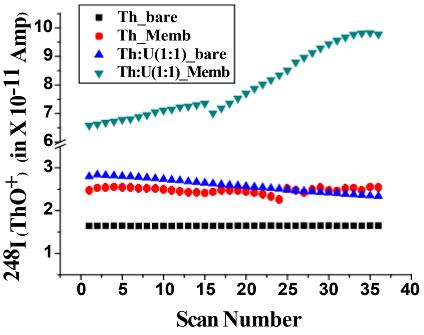

Fig. 1. Stability of ion intensity of ThO^+ under different conditions

TIMS analysis for various loadings on VF, such as pure Th and U-Th mixture (1:1) on bare VF and pure Th and U-Th mixture (1:1) pre-loaded on DEHPA-Dod@PP membrane, were carried out to check the stability of Th^+ and ThO^+ ion currents at m/z 232 and 248 respectively using double filament assembly. Similar to bare filament analysis, DEHPA-Dod@PP membrane analysis also required heating of the VF to high temperatures in order to get maximum ion currents. As can be seen in Fig. 1, Th pre-loaded DEHPA-Dod@PP membrane along with U (1:1) yielded relatively higher ion currents of ThO^+ ions when compared to the respective bare filament combinations. For the first time in the thermal ion source, 10×10^{-11}A ion current for ThO^+ is obtained. It is also seen from the Figure that certain amounts of uranium is required in the filament to obtain such an enhanced ion current of ThO^+, however, no isobaric interference is expected in the case of natural samples. Such type of measurements could be very helpful for achieving better precision analysis for $^{230}Th/^{232}Th$ isotope ratio, provided ion counter like SEM or DALY is available for recording the ion current of ^{230}Th due to its very low abundance.

References:

[1] M. Ivanovich, R. S. Harmon, *Claredon Press, Oxford*, (1982) 571.

[2] Preeti Goswami, K. Sasi Bhushan, Sumana Paul, Applied Polymer Materials (2022) https://doi.org/10.1021/acsapm.2c00919

Studies on ion Source Chemistry of Molybdenum

Preeti Goswami, K. Sasi Bhushan§, P. G. Jaison

[1] *Fuel Chemistry Divison, Bhabha Atomic Research Centre, Mumbai*
§ Email: sasiakp@gmail.com

High precision isotope ratio measurements of molybdenum is required to support its isotopic enrichment studies. It is also required in geochemistry –for monitoring the minute natural variations. The isotopic analysis of Mo is also important for obtaining valuable information regarding the structure of the nucleus, as ^{96}Mo is a radiogenic product of ^{96}Zr formed through double beta decay. The established positive mode analysis by thermal ionization mass spectrometry involves, the use of ascorbic acid (AA) on Re filament to reduce Mo (+VI) to Mo (+III), which is a less volatile species and the method also uses silica gel (SG) to coat over the sample to improve the sensitivity (by minimizing the evaporative loss of the sample) [1]. In this context, efforts were made to understand the ion source chemistry of molybdenum by changing different loading conditions.

About 25µg of molybdenum in 6MHCl solution was loaded on the bare vaporization filament of a double filament assembly. Same amount of Mo was loaded on Re filament with (i) Mo in ascorbic acid & coating with silica gel and (ii) Re filament coated with graphite. Graphite alone was used as the modifier as it acts as a reducing agent and is known to trap volatile species because of its layered structure. From Fig. 1, it can be noticed that the ion current of ^{96}Mo is much higher for AA+SG method when compared to the case where Mo was loaded on bare filament. In the case of graphite coated filament, ion current for ^{96}Mo is almost constant about 80x10^{-14}A for the whole range of filament currents. This is in contrast to AA+SG method which yielded increased ion intensities only at significantly higher filament temperatures. It can also be seen from Fig.1 that the stability in the isotope ratio of ^{100}Mo/^{95}Mo with the change in filament current is much better for the graphite loading method and is the worst for bare filament. In the case of bare filament loading, Mo isotopes might have subjected to severe fractionation due to high volatility resulting in a higher isotope ratio of ^{100}Mo/^{95}Mo compared to the true ratio. Though the stability of ^{100}Mo/^{95}Mo ratio from AA + SG method is comparable to that of graphite loading method at low filament currents, the trapping capability of SG might be insignificant at higher filament temperatures resulting in much fractionated ratio of ^{100}Mo/^{95}Mo.

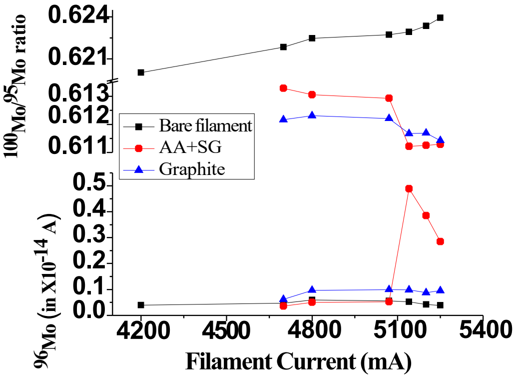

Fig. 1: Shows the stability of the ion current of ^{96}Mo and the variation in the isotope ratio of ^{100}Mo/^{95}Mo with different loading conditions

From the present studies, it can be concluded that the reductive behavior and layered structure of graphite minimized the volatility of molybdenum resulting in a stable ion current along with the better precision in the isotope ratio measurement of Mo isotopes.

References:
[1] Michael E. Wieser et. Al., *Inter. J. Mass Spectr.*, **197** (2000) 253
[2] Radhika M. Rao et.al., *Inter. J. Mass Spectr.* **364** (2014) 21

Rapid screening technique for gross α and gross β estimation in aqueous samples during radiation emergency

Sonali P.D. Bhade[§], Rajesh Sankhla and Pramilla D. Sawant
Internal Dosimetry Section, Radiation Safety Systems Division
[§]Email: sonali@barc.gov.in

Alpha/beta discrimination based on Pulse Length Index (PLI) using Liquid Scintillation Counting (LSC) is a well-established screening technique for gross α and gross β measurements with conventional 2 or 3 PMTs detector systems. However, these LSCs have limited applicability in fieldwork. Objective of the present study was to standardize a methodology for simultaneous estimation of gross α and gross β activities in aqueous samples using field deployable, portable, single PMT LSC system (Triathler LSC: 425-034).

In contrast to conventional LSCs, β spectra in Triathler LSC showed prominent luminescence peak in the lower energy region (1-200channels). Therefore, to avoid these spurious counts, the lower limit of β ROI was set at 200 channels. The luminescence peak doesn't interfere in α measurement as α peaks are confined to higher energy region (>300channels). Initially, sensitivity of the portable LSC for gross measurements in aqueous samples was investigated for different counting times, various sample loads (scintillator: sample ratios-10:1, 10:10, 12:8 and 15:5) and four different scintillators (Optiphase Hisafe-3, Ultima Gold AB, Optiphase HiSafe-2 and Aqualight AB) using glass vials. Later, Triathler LSC was calibrated with a set of quenched ^{90}Sr/^{90}Y (~100 Bq) standards (BRIT; Reference No.5279). A calibration plot of counting efficiencies (CE) against subsequent quench parameter (QP) was generated. CE for gross β was then obtained from the quench correction plot and used for estimation of gross β activity in mixed α/β sample. CE for α measurements was found to be ~ 100% irrespective of degree of quenching. Further, various aqueous samples labelled with α (^{241}Am, ^{233}U) and β (^{90}Sr/^{90}Y, ^{36}Cl) standards in different activity ratios(α:β)(1:200 and 200:1) (fig.1a) were analysed to check the efficacy of the standardized method. These spiked samples were initially counted in the β mode to obtain the QP and later counted at optimized PLI settings using 2D spectrum analysis tool (fig.1b). Gross activities derived using portable LSC system were validated using HIDEX 300SL LSC.

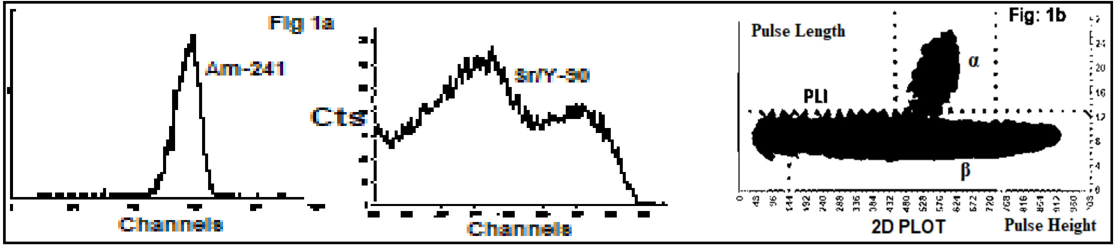

Figure 1. Discriminated α/β spectra of spiked test sample (fig.1a) with the 2D plot (fig. 1b)

Minimum Detectable Activities (MDA) obtained for gross α (3.4 BqL^{-1}) and gross β (14.7 BqL^{-1}) activities in aqueous samples using portable LSC (counting time: 30min) are sufficiently lower than the interventional levels (OILs) suggested by AERB during emergency scenarios (gross α: 5 Bqkg^{-1} and gross β:100 Bqkg^{-1}) [1]. Gross activities estimated using portable LSC in aqueous test samples were found to be comparable with HIDEX 300SL LSC (within ± 8%). Thus, portable LSC offered rapid and reliable results with adequate sensitivity and provides a useful tool for radiological characterization and in situ measurement of aqueous samples during emergency scenario.

References:

[1] AERB Guidelines No. AERB/NRF/SG/EP-5 (Rev.1) 2014.

Electrochemical determination of Thorium in aqueous medium

Rahul Agarwal[1, §], Jayashree S Gamare[1], Rama Mohana Rao Dumpala[2] and Manoj K. Sharma[1]

[1] *Fuel Chemistry Division,*
[2] *Radiochemistry Division*
Bhabha Atomic Research Centre (BARC), Trombay, Mumbai 400 085
[§] Email: rahulmarru@barc.gov.in

Thorium is radiologically and biologically toxic element and the exposure poses threats to human health.[1] Inhalation of Th dust may cause lung, pancreas and bone cancer.[3] Thus, it is of great importance to develop a sensitive method for trace level determination of Th to limit its exposure to aquatic and biological environments as well as to check the suitability of nuclear effluents to fall below the disposal limits.

The most stable oxidation state of Th is Th^{4+} and electrochemical reduction of Th^{4+} in aqueous medium is extremely difficult. Therefore, it is very difficult to quantify Th in aqueous medium by voltammetry.[1] The decrease in the peak-current density of UO_2^{2+} to UO_2 reduction on PEDOT-PSS/GC (poly(3,4-ethylenedioxythiophene)-poly(styrenesulfonate)-coated glassy carbon electrode) electrodes is selective for the presence of Th^{4+} and the decreasing trend of peak-current density may be correlated with Th concentration. The decrease in the peak-current of U(VI) to U(IV) reduction provides an indirect route for Th determination in aqueous medium which is otherwise very difficult by electrochemistry. The present study will widen the roots of voltammetry for determination of low level of Th in natural water. But the present approach needed the presence of U(VI) in solution for determination of Th(IV).

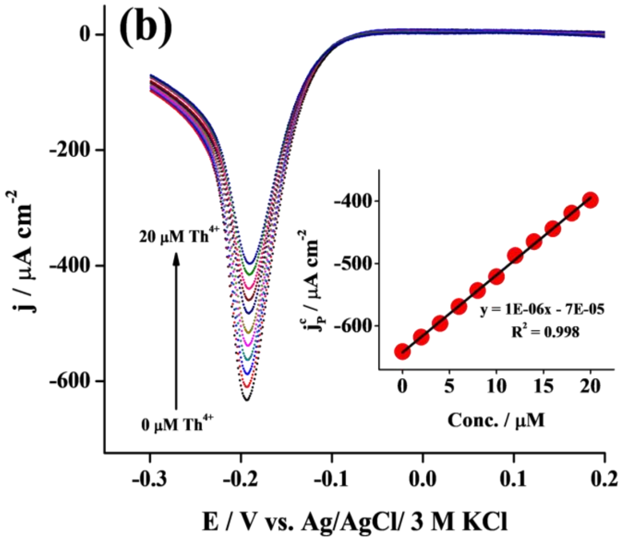

Figure 1. LSVs of PEDOT-PSS/GC electrode for Th determination at a scan rate of 100 mV s^{-1}.

References:
[1] Y. Peled, E. Krent, N. Tal, H. Tobias, D. Mandler, *Analytical Chemistry* 87(2015) 768-776.

EPR dosimetric investigations of a tissue equivalent $Li_2B_4O_7$ host for high dose applications

Hemachandar V[1], Saparya Chattaraj[1, 3 §], D. K. Patre [1], Reshmi T. P.[3], M. Mohapatra[2, 3],
Ashok Kumar P.[1], R. V. Kolekar [1]
[1] *Health Physics Division, Bhabha Atomic Research Centre, Mumbai, India*
[2] *Radiochemistry Division, Bhabha Atomic Research Centre, Mumbai, India*
[3] *Homi Bhabha National Institute, Mumbai, India*
§ Email: saparya@barc.gov.in

Radiation dosimetry is a prerequisite for the radiation protection programme. Electron Paramagnetic Resonance (EPR) spectroscopy is a well-established method for dosimetric assessment, as this process does not damage the irradiated sample. Further, the dose information is not lost after several rounds of reading, unlike in thermo-luminescent (TL) dosimetry. Moreover, the International Atomic Energy Agency (IAEA) recommends EPR dosimetry as the standard technique for high dose measurements [1]. The suitable dosimetric materials that can be used for personnel monitoring and other instances involving biological systems should have an effective 'Z' (Z_{eff}) value close to that of the tissue for accurate dose-response measurements. Lithium tetra-borate (LTB, $Li_2B_4O_7$). LTB is one such tissue equivalent material with Z_{eff} = 7.2 [2]. In this present work, we report the synthesis, characterization and EPR dose response studies of LTB samples. LTB samples were prepared from its individual precursors namely, Lithium Carbonate and Boric Acid via high temperature reaction route. XRD studies confirmed the formation of a single phase compounds without any impurity. The identification of the chemical nature of the radical along with its saturation behavior were also investigated.

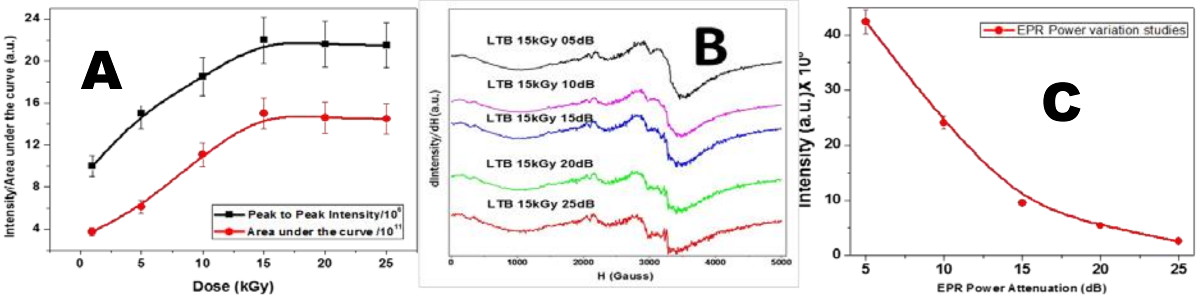

Fig1. **A**: Variation of peak area and intensity as function of radiation dose; **B**: Actual EPR spectra for the samples studied at different power; **C**: EPR signal intensity for 15 kGy irradiated sample as function of microwave power.

From the EPR analysis, it was observed that, the radical intensity and the area under the absorption curve saturated at 15 kGy dose. Even at a very low power of 0.6 mW (25dB), significant EPR intensity was observed. From the observed 'g' value at 3200 Gauss (2.09) and the observed features, the radical formed due to gamma irradiation was identified as a borate based hole-trapped centre.

Acknowledgements: Authors extend their gratitude to Dr. M. S. Kulkarni, Head HPD and Dr. P. K. Mohapatra, Head RCD for their support and encouragement.

References:
[1] Kishor Mehta, *Appl. Radiat. Isot*. **47** (1996) 1155
[2] O.M. Pop et. al., *Opt. Mater.*, **132** (2022) 112791

Study of Degree of Disequilibrium inJahazUranium Deposit, Jhunjhunu District, Rajasthan, India

M. K. Sandilya, L. K. Sharma§, B. Kishan, A. R. Nayak, B. R. M. Reddy and S. K. Sharma

Atomic Minerals Directorate for Exploration and Research (AMD)
Jaipur -302033, Rajasthan, India
§Email: lksharma.amd@gov.in

Disequilibrium studies of uranium deposit play a vital role in optimizing the value of deposit. Study of U_3O_8 and Ra(eU_3O_8) data of core samples of Jahaz uranium deposit was carried out to quantify the degree of disequilibrium. eU_3O_8 is the amount of U_3O_8 present (irrespective of presence of thorium oxide and potassium) in the sample to support the observed count. Jahaz uranium deposit is situated in Jhunjhunu district, Rajasthan, wherein a small size-medium grade U-deposit is established by AMD. Geologically Jahaz U-deposit occur in North Delhi Fold Belt of Khetri sub basin and hosted mainly by quartz-biotite-schist and to some extend by quartz-amphibolite-schist. Uranium occurs in sheared host rocks with albitic alterations.

The present study is based on the data obtained from radiometric analysis of 1,966 active core samples ($eU_3O_8 \geq 100$ ppm) from 52 boreholes drilled in the area. Data considered are found to be normally distributed (Fig.-1). The study has significance in connection with the ore reserve estimation. The study reveals that the Disequilibrium Factor (DF) is 1.031 indicating equilibrium condition of the Jahaz Uranium deposit(Fig.-2). It is also revealed that the samples having high grade show lesser deviation from the state of equilibrium.

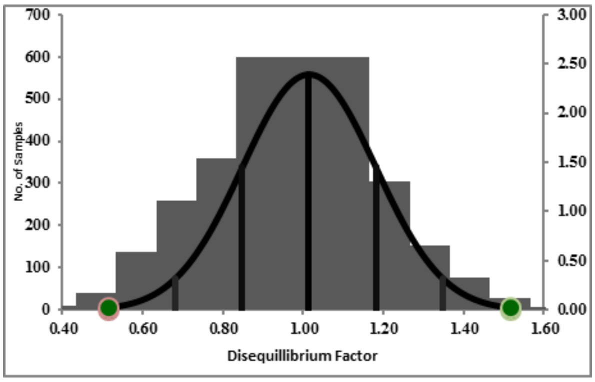

Fig.-1: Histogram with Normal Distribution Curve Fitting

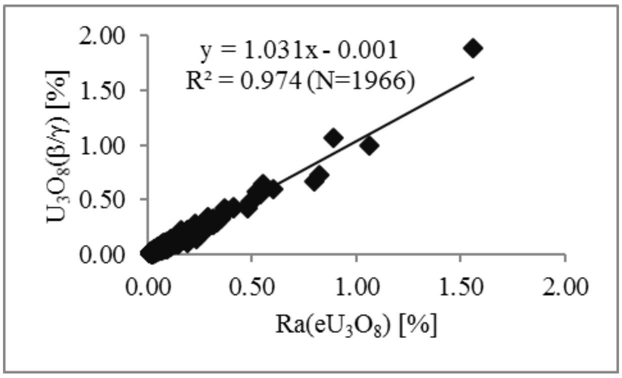

Fig.-2: Linear regression between U_3O_8 and Ra(eU_3O_8)

References:

[1] Das Gupta, S. P. (1968) The structural history of the Khetri Copper Belt, Jhunjhunu and Sikar districts, Rajasthan. Memoir, Geological Survey of India No. 98, 170pp.

[2] Levinson, A.A., Coetzee, G.L., 1978. Implications of disequilibrium in exploration for Uranium ores in the surficial environment using radiometric techniques – a review, Mineral Sci. Engg., Vol. 10, No. 1, 19-27.

Study of equilibrium status among uranium series radionuclides in ore samples

Amar D. Pant[1, §] , Aashna Gupta[2], Chetan Dusane[1], Suchismita Mishra[1], Anilkumar S. Pillai[1] and Vinod Kumar A.[1]

[1] *Environmental Monitoring and Assessment Division,* [2] *Radiation Safety Systems Division,*
Bhabha Atomic Research Centre, Trombay, Mumbai 400085, India
§ Email: amarp@barc.gov.in

Uranium is one of the main nuclear fuel, which needs to be developed to sustain the growth of nuclear energy. In India, an extensive exploration programme is being carried out in different geological domains to establish new uranium resources and reserves. In uranium exploration procedure based on gamma spectrometry method, it is assumed that uranium exists in secular equilibrium with its progenies. In many cases, the disequilibrium in ore sample will lead to improper assessment of the uranium deposit. The equilibrium status depends on the geological and physico-chemical process prevailing on the location [1]. In short, the activity ratios of nuclides in the decay chain can act as signature of the location. The activity concentrations and activity ratios estimation of U-series radionuclides can be done by radio analytical techniques such as gamma and alpha spectrometry. In the present study, uranium ore samples from the different mining locations were processed and analysed using high resolution gamma spectrometry.

The activity ratios of ^{235}U to ^{231}Pa and ^{235}U to ^{227}Ac (in ^{235}U decay series) and ^{234m}Pa to ^{226}Ra (in ^{238}U decay series) is shown in figure 1. It is evident from the figure 1 that in case of ^{238}U decay series, the activity ratio of ^{238}U to ^{226}Ra was found in the range of 0.92-1.12 and in ^{235}U decay series, the activity ratio of ^{235}U to ^{231}Pa and ^{235}U to ^{227}Ac was spread in range of 0.98-1.26 and 0.99-1.05 respectively. The activity ratio of ^{235}U to ^{231}Pa was found more than 1.13 in 7 out of 10 ore samples, which revealed the radioactive disequilibrium between ^{235}U to ^{231}Pa. Further, extensive studies with large number of samples at different depth and location give better information of equilibrium status between ^{235}U to ^{231}Pa. The mean values of activity ratios were found close to unity in ^{238}U to ^{226}Ra and ^{235}U to ^{227}Ac which conveys the fact that, there is prevalent radioactive equilibrium among them.

Figure 1: Measured activity ratio of different radionuclides in ore samples

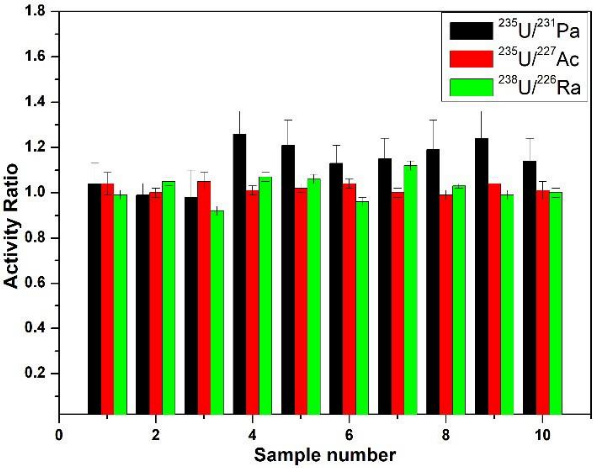

Acknowledgements: The authors express their sincere thanks to Dr. D K Aswal, Director, HS&E Group for his constant encouragement and support in this work.

References:

[1] Ivanovich, M., Uranium series disequilibrium: concepts and applications, *Radiochimica Acta*, **64** (1994), 81-94.

Studies on alpha radiolysis of tri-butyl phosphate/n-dodecane system

Chandan Mukhopadhyay[1, 3], Satyabrata Mishra[1], R. Karthick[1], D. Saha[2], D. Sivakumar[1],
K. Dhamodharan[1], N. Desigan[1], K.A. Venkatesan[§], [1, 3] and K Ananthasivan[1, 3]

[1]Process, Radiochemistry and Reprocessing R& D Division,
[2]Analytical Chemistry Division, MC&MFCG
[3]Homi Bhabha National Institute,
Indira Gandhi Centre for Atomic Research, Kalpakkam, Tamil Nadu-603102
[§]Email: kavenkat@igcar.gov.in

Aqueous reprocessing of plutonium (Pu) rich fuel from fast reactor leads to severe degradation of the PUREX solvent 1.1 M tri butyl phosphate (TBP) in n-dodecane (n-DD). This results in the formation of a number of degraded products which can alter the solvent performance during subsequent cycles. Vast literature is available on the degradation of the solvent-diluent by gamma irradiation and in most of the studies the solvent is subjected to very high absorbed gamma dose to correlate with alpha degradation. However, such correlation are not appropriate for assessing the degradation due to difference in the energy and mode of interaction of γ and α radiation. Limited literature is available on alpha radiolysis of PUREX solvent. In this context, a systematic study was taken up to evaluate the alpha radiolytic degradation of 1.1 M TBP/n-DD system resembling the actual reprocessing plant condition.

A freshly prepared 1.1 M TBP/n-DD solution after pre-equilibration with 5.5 M HNO_3 was contacted with 18 g.L^{-1} of Pu (IV) in 5.5 M HNO_3. The metal loaded organic phase (16 g.L^{-1}) was kept as such till the organic phase receives the absorbed dose up to 100 kGy. The samples were withdrawn at regular intervals of time to find out the effect of α-dose on the formation of degradation products of TBP. Also, the change in TBP concentration upon alpha radiolysis was estimated. The Pu metal retention behavior of the radiolyzed samples were compared against the unirradiated solvent to quantify the degree of degradation. To determine the effect of dose rate during alpha radiolysis, similar experiments were performed with a lower loading of Pu (IV) [8 g.L^{-1} of Pu (IV) in 5.5 M HNO_3] to the same absorbed dose of 100 kGy. Another set of experiment was carried out with a Pu loading of 8 g.L^{-1} in 0.1 M HNO_3 to nullify the effect of nitric acid during alpha radiolysis. During radiolysis the average energies of the α-particles emitted by Pu isotopes are calculated to be 5.2 MeV. The acidic degradation products of TBP such as HDBP and H_2MBP were analyzed by ion-chromatography and the change in TBP concentration was estimated by gas chromatography. The Pu content and β, γ activity in organic phase was analyzed by radiometry. Some results are given below and complete details will be discussed in the presentation.

Table 1. Pu retention behavior of the radiolyzed solvent

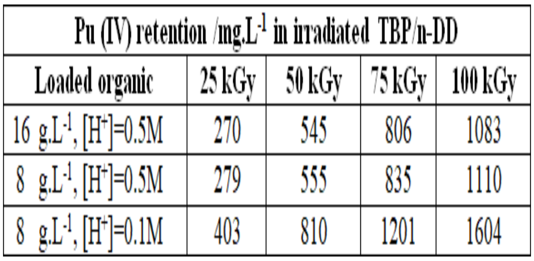

Pu (IV) retention /mg.L^{-1} in irradiated TBP/n-DD				
Loaded organic	25 kGy	50 kGy	75 kGy	100 kGy
16 g.L^{-1}, [H$^+$]=0.5M	270	545	806	1083
8 g.L^{-1}, [H$^+$]=0.5M	279	555	835	1110
8 g.L^{-1}, [H$^+$]=0.1M	403	810	1201	1604

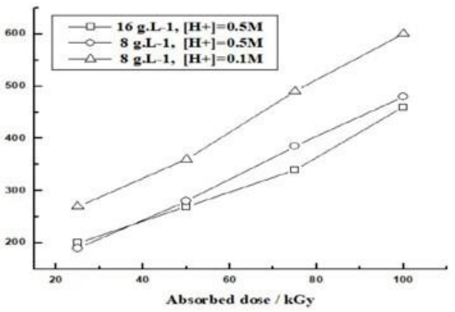

Fig 1. DBP concentration upon alpha irradiation

Spectrophotometric Determination of Boron in Boron doped Zr-Nb alloy Employing Methylene Blue-BF_4^- complex

K.L. Pandey[1,], P.S. Ramanjaneyulu[1,§], M.K. Saxena[1]
[1]*Radioanalytical Chemistry Division, B.A.R.C., Mumbai-85.*
[§] Email : psr@barc.gov.in

Boron doped zirconium – niobium alloy is being used for neutron reactivity control in advanced compact light nuclear reactors. **An** accurate knowledge of the boron content in these materials is essential for reactivity calculations. In view of the refractory nature of the alloy, determination of boron in these type of matrices is a challenging task for analytical chemists. Few methodologies have been reported for determination of boron in Zr matrices including spectrophometric determination employing curcumin as a complexing agent and BF_4^- ion selective electrode method in author's laboratory [1]. However, these all methods either require matrix matched reference materials for method calibration or highly laborious methods. With this in view, a simple and sensitive method based on spectrophotometric determination of boron as tetrafluoroborate-methylene blue complex has been developed. In this methodology about 100 mg of the sample was taken in 25 mL PVC volumetric flask, added 5.0 mL of de-ionized water and then added 0.3 mL of concentrated HF (40% by volume) for dissolving the sample. After dissolution of the sample, volumetric flask was kept in water bath maintained at 60 °C for two hours for quantitative conversion of B to BF_4^- ion [2]. After cooling the flask to room temperature, 0.5 mL of conc. H_2SO_4 was added and then made total volume of the solution as 25.0 mL. From this solution an aliquot of 3.0 mL was taken in a 25 mL quartz beaker and added 2.0 mL of de-ionized water. To this solution 5.0 mL of 0.005 M methylene blue in H_2O and then 5.0 mL of dichloroethane was added and stirred well for 5 minutes with magnetic stirrer. Allowed for 3 minutes for phase separations and then organic phase was separated employing weight burette suction. Along with BF_4^- -MB complex partially pure MB will also get extracted into organic phase. This extracted MB was stripped by treating separated organic phase with deionised water and then again organic phase was separated and then diluted to 10 mL with dichloroethane. Absorbance of BF_4^- -MB was measured at 658 nm. Calibration plot was constructed employing standard $NaBF_4$ solution and followed above procedure after conversion of B into BF_4^-. Calibration plot is shown in Figure 1. Method has been standardised employing standard boric acid solution in the place of sample and repeated entire procedure mentioned above. Method has been validated by an independent method namely spectrophotometric determination with curcumin as a complex agent and results are agreed well at 95% confidence level. Precision and accuracy of methodology is ± 5%.

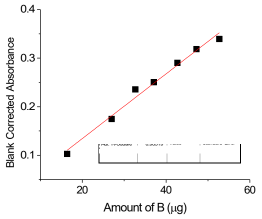

Fig.1. Calibration plot

Table 1. Method validation

Sr. No.	Sample ID	Present Method (wt%)	Reported method
1	BR-01	0.41± 0.04	0.38 ± 0.04
2	BR-03	0.33 ±0.03	0.33 ±0.03

References:

1. P.S. Ramanjaneyulu et. al., , B.A.R.C. Report No., BARC/2009/R/003.
2. P.S. Ramanjaneyulu et. al., Accre. and Quality Assur. journal **15** (2010) 665-671.

Characterization of insoluble residue found in Centrifuge Extractor bowl

D.Sivakumar, Satya Narayan Das, C. S.Suganyadevi, G.Santhosh Kumar, K.Dhamodharan §,
K.A.Venkatesan and K.Ananthasivan
Reprocessing Group, Indira Gandhi Centre for Atomic Research, Kalpakkam-603 102
§ Email: kdn@igcar.gov.in

Compact Reprocessing of Advanced fuel in Lead cell (CORAL), is a pilot plant being operated successfully for the past two decades. The objective of CORAL was to validate process flow sheet and equipment for continuous reprocessing of irradiated spent fuel to be discharged from prototype fast breeder reactor. In CORAL, the centrifugal extractor is employed for solvent extraction and stripping. Operating experience indicates that the centrifugal extractor got choked on few occasions which resulted flooding and it is due to accumulation of solid materials. Therefore, it is essential to characterise these materials and to find suitable solvent to dissolve it. A known weight of insoluble residue was collected from a CE bowl, and experiments were conducted to dissolve it using various reagents as described in Table 1. A portion of residue from CE bowl was washed with alcohol to remove organic moiety followed by acidified water and dried using Whatman-541 filter paper. The resulting residue was then accurately weighed, dissolved in sodium carbonate solution and made to known volume. The phosphate content in this solution was determined by spectrophoto metric method with and without fuming with $HClO_4$. The sample solution was also analysed for plutonium. A similar experiment was conducted with other reagents as well. Results from Table I indicates that sodium carbonate (10%) was found to be promising solvent for the dissolution of insoluble residue to the extent of 90-95 %. Results of this study indicate that insoluble residue is plutonium phosphate complex and spectrophotometric studies confirm there is no inorganic phosphate in insoluble residue. Therefore, flooding in CE is due to accumulation of organic Pu-Phosphate complex. The results shown in Table 2 further confirms that the insoluble residue is mainly consisting of plutonium nitrate DBP complex (Pu $(NO_3)_4$.2DBP), which is found to be soluble >90 % in 10 % sodium carbonate solution. Hence, it was recommended to use 10 % sodium carbonate for de-choking.

Table1 Dissolution of residue with different reagents

Sl. No	Nature of reagents	solubility	$HClO_4$ treatment		Nature of PO_4^{3-}
			With	without	
1	HNO_3, 8 M	Insoluble	-------	--------	--------
2	HNO_3 + H_2O_2	Insoluble	------	--------	------
3	Na_2CO_3 (5%)	Partially soluble	PO_4^{-3} found	No PO_4^{-3}	Organic
4	Na_2CO_3 (10 %)	Soluble ≈90-95%	PO_4^{-3} found	No PO_4^{-3}	Organic

Table 2 Determination of PO_4^{3-} , Pu content & mole ratio

S.No	Volume of aliquot	Wt. of PO_4^{3-} (mg)	Wt. of Pu (mg)	$[PO_4^{3-}]/[Pu]$ Mole ratio
1	0.05	1.89	2.37	1.98
2	0.10	1.94	2.45	1.96
3	0.15	1.93	2.48	1.92
4	0.20	1.94	2.41	2.00

Extraction of U(VI) by phenoxy acetic acid modified zirconium phosphate

B.Robert [§] , Selvan, A.S.Suneesh, M.Amutha Suba, N.Ramanathan

Fuel Chemistry Division, MC&MFCG
Indira Gandhi Centre for Atomic Research, Kalpakkam, India
[§]Email: robert@igcar.gov.in

Uranium separation from unconventional sources such as seawater or contaminated mine water solutions is gaining widespread popularity due to its limited supply from uranium mines to fulfill the enhanced utilization in commercial nuclear reactors for producing energy. Based on uranium-selective ligands attached to different solid phase matrices, solid phase separation techniques are highly appropriate for recovery from seawater or similar solutions wherein uranium abundance is extremely lower. Apart from the above, these solid-phase adsorbents are also helpful for the analytical pre-concentration of uranium. This paper reports the feasibility of uranium separation from aqueous solutions using zirconium phosphate-modified phenoxy acetic acid (ZrP-PhAc).

The adsorbent, ZrP-PhAc, was prepared by chemical modification of zirconium phosphate. Zirconium phosphate is a rigid and stable material prepared by reacting phosphoric acid (250 mL, 1 M) with zirconyl chloride (100 mL, 0.1 M). Phenolic acetic acid (5 g) was added to the above (zirconium phosphate). The reaction mixture was refluxed at 333 K for 6 hours. The precipitate was separated by filtration and was washed thoroughly with distilled water. The white-colored residue was further heated to 343 K for 24 hours before the use.

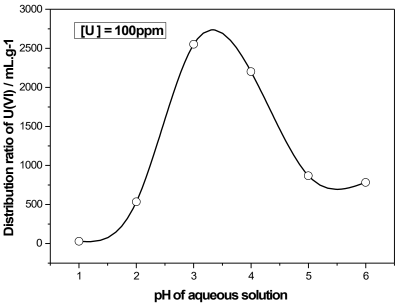

Figure 1. Uranium adsorption behavior of ZrP-PhAc

The feasibility of ZrP-PhAc to remove uranium from the aqueous phase was evaluated by batch adsorption experiments involving measurement of uranium concentration before and after the contact of uranium-bearing aqueous solutions with ZrP-PhAc. Uranium concentration in these aqueous solutions was assayed by UV-Visible spectrophotometry using Arsenazo-III as a coloring agent. ZrP-PhAc exhibited a higher removal tendency of uranium from aqueous solutions at pH 3, as seen in figure 1. The separation tendency of uranium by ZrP-PhAc appears to be increased with the increase of pH up to 3, and subsequently there is a decrease. The increased uranium adsorption by the phenoxy acetate anchored adsorbent suggests that the adsorption could be governed by weakly acidic moieties, and due to the matrix effects governed by zirconium phosphate. The intricate mechanism involved for the decrease of adsorption observed above pH is not known at present. However, more studies are underway to establish the above observation. The study's results summarized that ZrP-PhAc can be employed as a material suitable for the recovery of uranium from uranium-bearing lean solutions.

References:

[1] A.Behera et al, Materials Chemistry and Physics , 290 (2022) 126540
[2] H.Alhendaw et al, 2014. Journal of Chemical Sciences, 126 (2014) 1721.

Simultaneous removal of NOx and RuO_4 from dissolver off gas stream of Reprocessing Plant

Chandan Mukhopadhyay, R. Karthick, D. Sivakumar, K. Dhamodharan, K.A. Venkatesan and K Ananthasivan
Process Radiochemistry and Reprocessing R&D Division, Indira Gandhi Centre for Atomic Research, Kalpakkam – 603 102
[§]E-mail: kdn@igcar.gov.in

Uranium dioxide, mixed uranium plutonium carbide and mixed uranium plutonium dioxide are important nuclear reactor fuels. During reprocessing of these irradiated fuels, they are dissolved in strong oxidising nitric acid to produce a dissolver solution, which is subjected to a solvent extraction process. In a typical PUREX process, the $NO_{x\ gas}$ generated during the dissolution of spent nuclear fuel is one of the poisonous gases, as it poses health hazards at levels above 25 ppm. Additionally, the discharge of NO_x through the stack off gas creates air pollution, formation of smog and acid rain, as well as affecting tropospheric ozone. Apart from NO_x the ruthenium is one of the fission product present in spent nuclear fuel is also oxidized to highly volatile and radiotoxic RuO_4 during dissolution. The gaseous RuO_4 is deposited as black ruthenium dioxide (RuO_2) particles when RuO_4 contact with cooler parts of the SS duct and equipment, causing a serious concern to the reprocessing plant. Therefore, the dissolver off gas is scrubbed via dissolver off gas treatment, before releasing into the environment. In order to have effective removal of NO_X and RuO_4, the caustic solution re-circulated in to the scrubber unit by a pump. During this operation, the pumps malfunction frequently due to soapy nature of caustic solution resulting in frequent intervention, which increases the man-rem expenditure. Therefore, an alternative scrubbing reagent is required to overcome this problem. Acidified urea is one of the promising reagents to absorb NOx and RuO_4 with equal efficiency to NaOH. Urea ($(NH_2)_2CO$) is a mild reducing agent and reduces NO_x and RuO_4 to N_2 & non volatile Ru-Nitrate respectively.[1-2] In this content, experiments have been carried out to determine the scrubbing efficiency of urea for removal of NO_X and RuO_4. NO_x gas was generated by mixing sodium nitrite and nitric acid in a closed container. The NO_X gas was passed through acidified urea column followed by caustic solution column. The NO_X escaped from urea column was trapped by a caustic scrubber was estimated by ion chromatography (IC). In another set of experiment, Ruthenium nitrosyl nitrate solution in 1 M HNO_3 was taken in the glass electrolytic cell. Electrolysis was performed with the anodic current density of 10 mA cm^{-2} in the presence of cerous/ceric redox couple, at 318 K temperature. The RuO_4 gas generated due to the oxidation of ruthenium at anode was absorbed in the gas wash bottle containing acidified Urea solution and the ruthenium concentration in urea was analysed by spectrophotometry. The scrubbing efficiency of acidified urea solution with respect to NO_x and RuO_4 were calculated and the results are presented in Table 1.

Table 1. Scrubbing efficiency of NO_x and RuO_4 in 0.5 M urea Column

Experiment No.	**% Scrubbing efficiency of Urea**	
	NO_x	**RuO_4**
1	95 ± 2.5	92 ± 2.1
2	93 ± 2.5	91 ± 2.1
3	92 ± 2.5	93 ± 2.1

References:

1. P. Fang et al., Chemical Engineering Journal, 168 (2011) 52
2. P. Swain et al., J Radioanal Nucl Chem, 303 (2015) 1865

Analytical estimation of ^{241}Am in the irradiated U-Zr fuel

T. Prathibha, A.S.Suneesh[§], B.Robert Selvan, Alok Rout, M.Amutha Suba, N. Ramanathan, D. Bola Sankar, S. Rajeswari, J.S.Brahmaji Rao, G.V.S.Ashok Kumar

Fuel Chemistry Division, MC&MFCG
Indira Gandhi Centre for Atomic Research, Kalpakkam, India
[§]Email: suneesh@igcar.gov.in

U-Zr or U-Pu-Zr-based metal fuel is considered a plausible nuclear fuel option for futuristic fast reactors owing to advantages such as high thermal conductivity, fissile atom content, superior breeding capacity, etc. To understand the irradiation behavior, a typical metal fuel, U-Zr, was irradiated up to burn-up of ~1580 MWd/t. This paper reports the analytical estimation of americium produced in the above-irradiated fuel. Analytical assessment of americium is challenging as the fuel has experienced significantly lower burn up, and the americium produced also should be relatively in lower proportions. Since the radiometric assay of americium is seemingly challenged by the presence of uranium and plutonium, it was intended to remove uranium and plutonium by TBP extraction, and thereupon, americium was planned to be separated from the TBP raffinate by TODGA extractant and assayed by alpha spectrometry.

The U-Zr fuel (1.1 g) was dissolved in ~12 M nitric acid (50.8 mL) with traces of HF. 5 mL of this dissolver solution was evaporated under an IR lamp for nearly three hours for removal of excess nitric acid. After cooling, the solution was again diluted to 5 mL with 4 M nitric acid. The acidity of the resulting solution was found to be 4.5 M. 2.5 mL of the above solution was transferred to a 10 mL vial. This aqueous phase was subjected to four extraction stages, as shown in the scheme described in figure 1. Two extraction stages were performed with 1.1 M TBP/n-dodecane as the organic phase after contacting the aqueous phase with 0.05 mL of saturated sodium nitrite solution for bringing all the plutonium ions into the +4 oxidation state in the solution. This was followed by two more extraction stages using 0.2 M TODGA/n-dodecane + 5 vol% 1-octanol as the extracting phase. The gross alpha and beta counts recorded for 0.05 mL of aqueous and organic phases at each extraction stage were monitored to evaluate the quantitative removal of uranium and plutonium by TBP and americium removal by TODGA. The alpha spectra were recorded for the original solution and for the aqueous and organic phases of stage 1. The analysis reports agrees with the revelation that TBP extraction quantitatively removed Pu and U in two contacts, and the aqueous raffinate left out after the extraction is devoid of Pu and U. The analysis of alpha spectrum on the organic phase after the extraction from the aqueous phase obtained after TBP extraction showed the presence of Am. The americium was quantitatively removed by TODGA in two contacts, as revealed by the alpha spectrum of the aqueous phase obtained after two extractions by TODGA. The amount of americium extracted from the TODGA organic phase was quantified by alpha spectrometry by comparing it with in-house prepared americium standard. According to the results, the alpha activity of americium in 0.05 mL of the extracted organic phase was ~ 1840 pCi, and the total americium content of the irradiated pellet is estimated to be ~ 0.5 µg/ g.

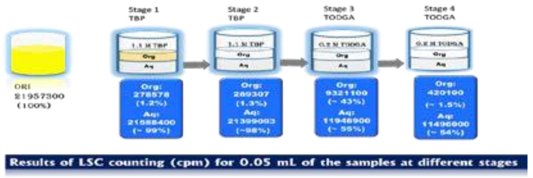

Figure 1: Gross alpha and beta counts of the fuel solution at different stages of extraction

Dependence of Resonance Self-Shielding Factor on Foil Thickness

Subhrojit Bagchi[§], D. Sunil Kumar and A. John Arul
Indira Gandhi Centre for Atomic Research, Kalpakkam
[§] Email: bagchi@igcar.gov.in

Materials used in neutron dosimetry and radionuclide production for medical purposes exhibit resonances in epithermal region, leading to perturbation of the neutron flux due to self-shielding. To obtain accurate sample activation results, it is necessary to apply resonance self-shielding factors (SSF). The Monte Carlo method is ideal for determining self-shielding factors due to its capability to consider the intricate relationships between the sample material and neutrons, incorporating multiple scattering and energy loss into the calculations. Additionally, Monte Carlo methods can be easily updated with the latest cross-section data, allowing for accurate predictions of self-shielding factors even as the underlying physics and nuclear data evolve. In this study, we demonstrate the dependence of self-shielding factor on the thickness of the foil, with gold foil being used as a case example.

The resonance self shielding factor, G_{res}, in a foil of thickness 't' is defined as the ratio between the reaction rates per atom in the actual sample and an infinitely diluted sample.

$$G = \frac{\int_{E1}^{E2} \Phi(E)\sigma_{n,\gamma}(E)dE}{\int_{E1}^{E2} \Phi_0(E)\sigma_{n,\gamma}(E)dE} = \frac{RR(E,\rho_0)}{RR(E,10^{-6}\rho_0)} \ldots(1)$$

$\Phi_0(E)$ represents the non-perturbed epithermal neutron flux in the infinitely diluted sample, while $\Phi(E)$ is the perturbed flux in the actual sample. $RR(E,\rho_0)$ and $RR(E,10^{-6}\rho_0)$ represent the reaction rates for energy E, corresponding to the densities ρ_0 and $10^{-6}\rho_0$ respectively. The $\Phi_0(E)$ and $\Phi(E)$ inside a real sample can be calculated by Monte-Carlo simulation based on the ENDF/B-VII nuclear data library. The details of the foil are as follows.

Nuclide	A (gm)	ρ_0 (g/cc)	E_{res}(eV)	σ_γ (b)	Γ_γ (eV)
Au-197	196.96	19.3	4.9	2.7×10^4	0.124

In this work, the gold foil samples with 6 mm in diameter and thickness varying from 10^{-5} mm to 2 mm were used for MCNP simulations. These simulations were conducted for flat neutron energy spectrum.

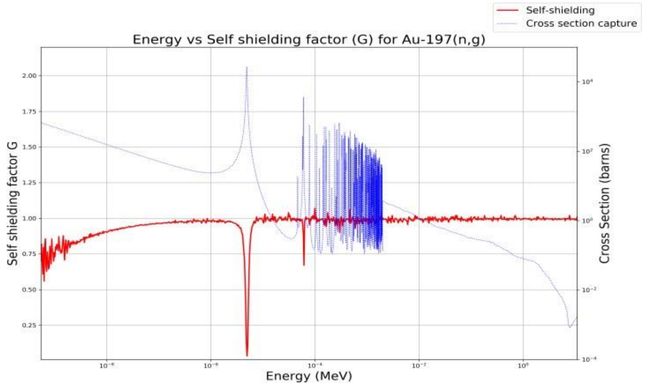

Fig1: SSF vs Energy for Au-197

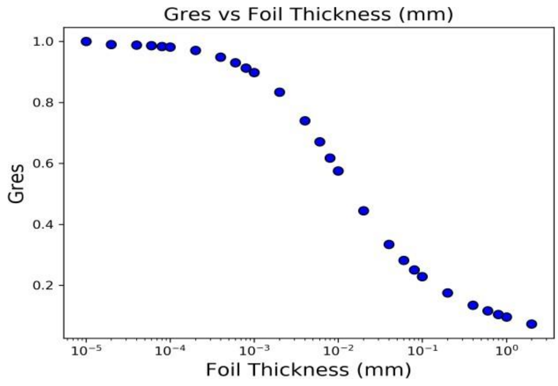

Fig2: G_{res} vs Foil Thickness

The Monte Carlo simulation was utilized to accurately simulate the resonance SSF G_{res} for Au-197. Fig:1 depicts the variation of self-shielding factors (SSF) with energy across 1000 isolethargic groups. Fig:2 illustrates the variation of G_{res} as a function of foil thickness.

References

[1] Eastwood, T.A., Werner, R.D., 1962. "Resonance and thermal neutron self-shielding in cobalt foils and wires." Nucl. Sci. Eng. 13, 385–390.

Optimizing the fusion reactions to synthesis Lr

L.Reddi Rani[1], N. Sowmya[1§], and H.C.Manjunatha[1§]

[1] *Department of Physics, Government College for Women, Kolar*
§ Email: manjunathhc@rediffmail.com, sowmyaprakash8@gmail.com

Experimentally and theoretically, there has been significant advancement in the synthesis of superheavy nuclei (SHN). ^{208}Pb and ^{209}Bi targets with excitation energies of 10–20 MeV are used for cold fusion reactions. ^{48}Ca-projectiles on actinide targets with excitation energies of 30 to 50 MeV are used in hot fusion processes [1, 2]. Numerous theoretical investigations into the SHN production process have been conducted [3–7] using advance statistical model and dinuclear system model. Effect of entrance channel parameter on projectile-target combinations and deformation effect of the same were investigated. Hence, in the present work we motivated to investigate possible fusion reactions, optimal center of energy and evaporation residue cross-sections to synthesize superheavy element Z=103. Evaporation residue cross-sections are evaluated using dinuclear system model is as follows;

$$\sigma_{ER}^{xn} = \frac{\pi}{k^2}\sum_{l=0}^{\infty}(2l+1)T(E,l)P_{CN}(E,l)P_{sur}^{xb}(E^*,l) \qquad (1)$$

Where, $P_{CN}(E,l)$ is the compound nuclei formation probability, $P_{sur}^{xb}(E^*,l)$ is the survival probability and $T(E,l)$ is the transmission probability. $P_{sur}^{xb}(E^*,l)$ is evaluated as follows;

$$P_{sur}^{xb}(E^*,l) = P_{xn}(E^*)\prod_{i=1}^{i_{\max}=b}\left(\frac{\Gamma_n}{\Gamma_{tot}}\right)_{i,E^*} \qquad (2)$$

Γ_n and Γ_{tot} is the neutron and total decay width respectively [8]. For instance, evaporation residue cross-sections are evaluated for ^{48}Ca+^{209}Bi fusion reaction. Figure-1 shows a plot of fusion cross-sections, survival probability and evaporation residue cross-sections as function of center of mass energy. The fusion cross-sections increases with increase in energy, whereas survival probability decreases with increase in energy. Figure 1(c) shows a plot of evaporation residue cross-section for 2n channel with center of mass energy. The evaporation residue cross-section is found to be maximum at 65.46nb at 175 MeV. However, experimental cross-section of 2n channel at 174.09 MeV is found to be 12nb. Hence, using dinuclear system model we can predict evaporation residue cross-sections of the unexplored new isotopes of Lr.

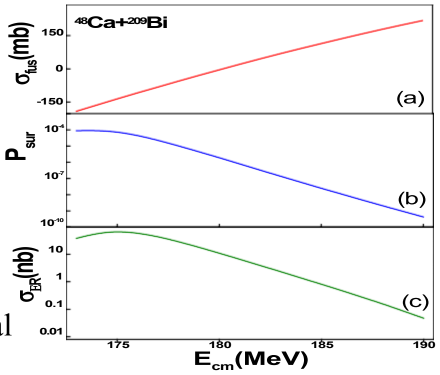

Fig. 1: A plot of (a) fusion cross-sections, (b) survival probability and (c) evaporation residue cross-sections as a function of center of mass energy.

References:

[1] S. Hofmann and G. Munzenberg, *Rev. Mod. Phys*. **72,** 733 (2000).
[2] S. Hofmann, et al., Eur. Phys. J. A **14,** 147 (2002).
[3] H.C. Manjunatha, et al., *Phys. Rev. C* **102**, 064605 (2020).
[4] H.C. Manjunatha, et al., *Phys. Rev. C* **98,** 024308 (2018).
[5] H.C. Manjunatha, et al., *Nucl. Phys. A* **987,** 382 (2019).
[6] H.C. Manjunatha, et al., *Can. J. Phys*. **99,** 16 (2021).
[7] H.C. Manjunatha, et al., *Phys. Rev. C* **104,** 024622 (2021).
[8] N. Sowmya, et al., *Phys. Rev. C* **105,** 044605 (2022).

Resolving Isobaric interference and accurate quantification of Cs and Sr in dissolver solution by using Isotopic Dilution Thermal Ionisation Mass Spectrometry (ID-TIMS)

J. Namitha[1§], Suranjan Bera[1,2], M. Joseph[1,3], N. Sivaraman[1,2]

[1]*HBNI, IGCAR, Kalpakkam – 603102, India.*
[2]*MC&MFCG, IGCAR, Kalpakkam – 603102, India.*
[3]*Raja Ramanna Fellow, IGCAR, Kalpakkam – 603102, India.*
[§]Email: namitha.jpm@gmail.com / namithaj@igcar.gov.in

The effective management of highly radiotoxic active waste produced by nuclear reprocessing plants is one of the main objectives of a nuclear energy programme. Determining ^{90}Sr and ^{137}Cs in HLLW is a serious concern due to environmental risk, long half-life, high energy radiation, and higher fission yield [1]. For radiometric measurement of ^{90}Sr and ^{137}Cs in HLLW, conventional techniques demands for their separation into pure fractions, or in the case of mass spectrometric methods, their removal from isobaric interfering elements [2]. The present study demonstrates potential applications of thermal ionisation mass spectrometry (TIMS) technique for direct quantitative estimation of ^{90}Sr and ^{137}Cs in dissolver solution.

Initial experiments were conducted with a non-radioactive sample mixture containing Sr, Rb, Cs, Zr, and Ba, prepared from spectroscopic grade reference solutions, in order to optimise the experimental conditions for the radioactive samples. Solution of H_3PO_4 and Ta_2O_5 is used as an activator. Preferential evaporation method was adopted for analysis of elemental species that are present in the mixture solution, as there are considerable differences exist in some of their thermophysical properties. During analysis, Cs ions start appearing at 1.1 A of filament current and measurements were carried out at 1.3 A to have stable and sufficient ion intensity for precise isotopic ratio measurement. A typical mass spectrum obtained (for a mass range of 130 to 140 amu, covering all the possible isotopes of Cs and Ba) at a filament current of 1.3 A is shown in Fig. 1. As can be seen, no isotopes of Ba are observed in the mass spectrum. Thus, it is possible to measure the Cs isotopes without any isobaric interference from isotopes of Ba.

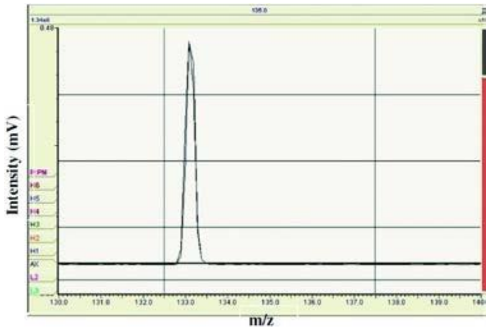

Fig. 1 *Mass spectrum of Cs obtained at a filament current of 1.3 A; no interference from Ba is observed*

After Cs analysis, the filament was maintained at high temperature of 2.1 A for up to 3 hrs to remove the isobaric interference of Rb in the isotopic ratio (IR) measurement of Sr. Sr isotopic ratio measurement was carried out at 2.6 A where a sufficient ion intensity for Sr isotope was observed. For mass spectrum covering a mass range of 83–90 amu, only isotopes of Sr were observed and no isotope of Rb was detected. The other possible isotope that could interfere with ^{90}Sr measurement is ^{90}Zr. At this filament current of 2.6 A, Zr did not appeared in the mass spectrum. The dissolver solutions obtained from spent fuel of uranium plutonium mixed oxide (MOX) discharged from FBTR is taken up for analysis. The concentration of Cs and Sr in dissolver solutions were measured by ID-TIMS method. The present study established the assay of ^{90}Sr, ^{135}Cs and ^{137}Cs present in dissolver solutions without prior chemical separation.

References:

1. C. R. Minitha et al., *Ind. Eng. Chem. Res.*, **57 (**2018) 1225.
2. J. Namitha et al., *J. Anal. At. Spectrom.,* **37 (**2022) 563.

Deep eutectic solvent modified supported liquid membrane for Actinide extraction

Sumana Paul and Ruma Gupta§

Fuel Chemistry Division, Bhabha Atomic Research Centre, Mumbai 400 094
§Email: rumac@barc.gov.in

Several extractants have been synthesized and employed for the selective separation of actinides from complex aqueous matrices like fuel materials, dissolver solution of irradiated fuel or high level liquid waste (HLLW) solution [1]. In recent times, deep eutectic solvents (DESs) have gained immense attention due to their unique properties as green solvents, efficient dispersants and as large-scale media for chemical and electrochemical synthesis of advanced functional materials [2]. The present work involves the development of a hydrophobic DES pore filled membrane (C_7DES@PP) and its application for actinide extraction from acidic medium. The DES used in the present work comprises of two components viz. heptyltriphenylphosphonium bromide as the hydrogen bond acceptor and decanoic acid as the hydrogen bond donor. Heptyltriphenylphosphonium bromide salt (C_7PPh_3Br) was mixed with decanoic acid (DA) in 1:2 molar ratio and stirred at 60°C until the formation of a colourless DES, which was then vacuum dried and stored in a desiccator. To prepare the pore filled membrane, commercially available polypropylene (PP) membrane was immersed in the DES for overnight – during the process, the DES was physically immobilized within the pores PP membrane by capillary force. The extraction of Pu(IV), U(VI) and Am(III) by C_7DES@PP was investigated as a function of nitric acid concentration in aqueous medium. 2 mL of aqueous solutions, having varying concentrations of nitric acid and containing known activity of ^{233}U/^{239}Pu/^{241}Am tracer, were equilibrated with 1cm x 1cm pieces of C_7DES@PP for 2–3 hours with continuous stirring. 20 μL of aliquot was taken out from each solution, before and after equilibration with the membrane samples. The amount of U/Pu/Am extracted by C_7DES@PP was calculated from the difference in alpha activities in each solution, before and after equilibration using equation (1).

$$\text{Sorption efficiency} = \frac{(A_i - A_f)}{A_i} \text{ X } 100 \quad (1)$$

where, A_i and A_f are the alpha activity of U/Pu/Am in solution, before and after equilibration with the membrane, respectively. Fig. 1 represents the extraction efficiency of C_7DES@PP for Pu(IV), U(VI) and Am(III) as a function of HNO_3 concentrations in the aqueous phase. It can be seen from Fig. 1, the sorption efficiency for Pu(IV) increases with increasing HNO_3 concentration in the aqueous phase and reached a maximum value of ~90±3% at 4–5M HNO_3. On the other hand, the sorption efficiencies for U(VI) and Am(III) were found to be around 20±1% and 5±1%, respectively, in 1−5 M HNO_3 concentration. This indicates that C_7DES@PP can be employed for the selective separation of Pu(IV) from U(VI) and Am(III) in 4M HNO_3 medium.

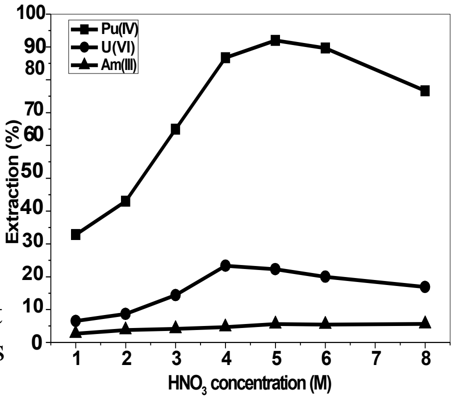

Fig. 1: Actinide sorption efficiency of C_7DES@PP as a function of HNO_3 concentration.

References:
[1] N.Vajda, C.K. Kim, Anal. Chem. 83 (2011) 4688−4719.
[2] V. Andruch, P.M. Chełstowska, J.P. Wasylka, Microchemical Journal 179 (2022) 107498.

Preliminary Investigation on eye lens dose measurement during ^{106}Ru plaque making operation

Susheela Sivakumar[1, §], Sanjay Singh[1], D. Banerjee[2], M Bhattacharya[1],A. K. Bakshi[1],
M. K. Suresh Kumar[1] and M. S. Kulkarni[1]
Health Safety & Environment Group[1], Process Development Division[2]
Bhabha Atomic Research Centre, Mumbai-400085
[§]Email : susheela@barc.gov.in

Introduction: ^{106}Ru is used as an important ophthalmic brachytheraphy source. High Level Liquid Waste (HLW) from nuclear fuel reprocessing is a rich source of this isotope. BARC has developed an indigenous technology for the fabrication of eye plaque using ^{106}Ru recovered from HLW [1]. The fabrication process has three important steps, separation of pure ^{106}Ru from HLW, electroplating, sealing the source and polishing of plaque. In the present pilot scale facility these steps involves very close handling of the source, resulting in a likelihood of getting significant dose to the eye lens in addition to whole body dose. International Commission of Radiological Protection (ICRP) has revised the life time eye dose threshold for induction of cataract from 2000 mGy to 500 mGy and occupational annual dose limit of eye lenses from 150 to 20 mSv [2]. Hence, it is important to generate data on eye lens dose during the plaque fabrication. The generated data will be useful for optimizing the dose consumption, suggesting engineering automation and also to assure regulatory compliance.

Material and methods: For dose measurement TLD badge calibrated with respect to operational quantity $H_P(3)$ is used [3]. Head TLD badge is worn on forehead of individual along with the regular Chest TLD during the plaque fabrication process.The data presented here is the dose consumption during one batch processing starting with approximately 20 mCi/L of ^{106}Ru in HLW. All activities except the final polishing of the product is carried out in adequately shielded fume-hoods. Though, the sample size is limited to two individuals due to current limited scale processing, the observed results have considerable safety significance.

	Whole body gamma dose (mSv)	**Whole Body Beta dose (mSv)**	**Dose to the eye lenses (mSv)**	
			Gamma	Beta
Worker-1	0.75	5.30	0	1.05
Worker-2	2.20	4.35	1.35	9.30

Results and Discussion: The results of the measured dose is presented in Table. It is seen that in operations, eye lens dose can be higher than whole body dose. This is more pronounced for worker-2 who is involved in brazing and polishing of the plaque, in which case the total eye lens dose is almost five times that of whole body gamma dose.T hough the measured Hp(3) value is much lower than the present dose limit of 150 mSv, considering ALARA well defined procedure and radiation protection measures is justified so that if the annual dose limit to eye lens is reduced to 20 mSv, exposure remains well below the limit.

References:

[1] Prithwish Sinharoy et.al., “Developed of ^{106}Ru bearing sealed source for eye cancer treatment application”,BARC Newsletter, July – Aug 2018, (Pages 1-4).

[2]International Commission on Radiological Protection (ICRP). Statement on Tissue Reactions (2011). www. icrp.org//page.asp, retrieved 10-2011.

[3]Madhumita B et. al., Radiation Protection Dosimetry (2018), Vol. 178 (4), 364–373.

Determination of U(IV) concentration by ferric sulphate titration

T. Aneesh [1], Neeraja Chandran[1], S.Sagunthala Devi [1], Bhavya.S.Nair[1], D.Shravan Kumar [1], D.Jebaraj Mahildoss[1,§], K.Dhamodharan[1], KA. Venkatesan[1], K. Ananthasivan[1]

1 Reprocessing Group, IGCAR, Kalpakkam, Tamilnadu-603102
§ Email: djm@igcar.gov.in

The uranous nitrate solution is employed as a reducing agent for Pu(IV) in PUREX process for the mutual separation of uranium and plutonium from the loaded organic phase. This reagent is also used for recovery of plutonium from degraded solvent, removal of plutonium from surface of the process equipments and tanks etc. The uranous nitrate of concentration of 5-100g/L is usually employed for the recovery of plutonium in reprocessing plant. As uranium in +4 oxidation state undergoes aerial oxidation and also by the nitrite ion present in nitric acid, it is important to determine the concentration of U(IV) before treatment. In general, concentration of uranous ion in feed sample is determined by redox titration method using potassium dichromate as the titrant and ferroin as indicator. In this method, hydrazine nitrate interferes in the analysis, which is being employed as a scavenger for nitrous acid. Direct spectrophotometric method has several advantages such as resultant analytical waste of this method is free from corrosive chemicals, foreign metal ion and waste is amenable to mix with process stream. However, lower molar extinction coefficient of U(IV) system decreases sensitivity of the analysis of U(IV). In view of above, a new titrimetric method for the analysis of uranous nitrate has been developed which was based on reducing property of U(IV)/(U(VI) system as described by chemical equation (1) .

$$U^{4+} + 2\,Fe^{3+} + 2H_2O \rightarrow UO_2^{2+} + 2\,Fe^{2+} + 4\,H^+ \qquad (1)$$

In this method, known volume of aliquot was transferred into the titration flask containing sulphuric acid (0.05 M, 20ml). The solution in the flask was titrated against standard solution ferric sulphate using potassium thiocyanate as an indicator. The colorless solution changes to pale red in colour at the end point due to the formation of ferric thiocyanate complex. The ammonium ferric sulphate employed in this titration was standardized by complexometric titration. The concentration of uranous in the test samples were also analyzed by redox titration and spectrophotometric methods. The concentration value obtained by the present procedure is in good agreement with the value determined by the conventional method.

Table1. Uranous concentration determined for a set of samples by three different methods

Sl No	$[U^{4+}]$, g/L		
	Titration using ferroin indicator	Spectrophotometric method	By present method.
1	9.89	9.77	9.72
2	38.99	39.53	38.65
3	67.17	68.25	67.75

Composition of test sample: $[U^{4+}]$ = 10-70 g/L; $[HNO_3]$ =0.5-1.0 M; $[N_2H_4]$ =0.5 M

The precision and accuracy of the present method and the conventional ferroin based titration method are found to be less than ±1.75 % and ± 1% respectively for 3-25 mg of U^{4+}.

References

[1] Ernest Miller Wylie, Katherine Garduno, Kattathu Mathew, Comparison of the Davies and Gray titrimetric method with potassium dichromate and ceric titrants, Journal of Radioanalytical and Nuclear Chemistry, August 2018.

Calculation of Isotopic Composition of Boron Using Calibration-Free LAMIS

Anannya Banerjee[1], Anandhu Mohan[1,2] and Arnab Sarkar[1,2,§]

[1]Fuel Chemistry Division, Bhabha Atomic Research Centre, Mumbai-400085, India
[2]Homi Bhabha National Institute, Mumbai -400094, India
[§]E-mail: arnab@barc.gov.in

Laser Molecular Isotopic spectrometry (LAMIS) is an emerging technique, capable of giving the information about the molecular transient species, formed in a laser induced plasma [1]. Due to the larger isotopic shift in ro-vibrational bands (RVB) compared to electronic transition for the isotopologue molecules, LAMIS can be used for isotopic composition analysis. The method has an added advantage of being a direct solid analysis. Boron (B) is one of the most important elements used in nuclear reactor and is used as neutron absorber. Boron contains two natural isotopes, ^{10}B and ^{11}B with thermal neutron absorption cross section (σ_{th}) of 3840 b and 0.005 b, respectively. Due to the large difference in σ_{th}, it is important to accurately ascertain the isotopic ratios of ^{10}B and ^{11}B in a given sample.

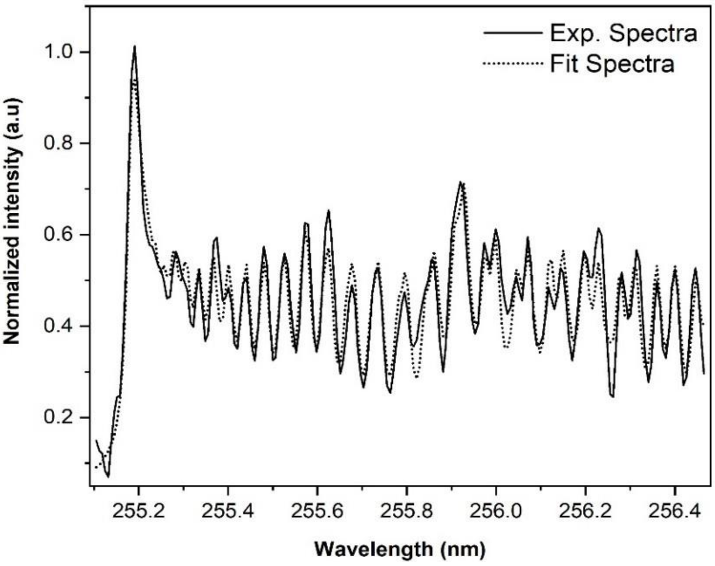

Fig. 1: Correlation of the experimental and theoretical

Natural boric acid pellets were prepared and used in the present study. The (0-2) vibrational band of $B^2\Sigma^+ \rightarrow X^2\Sigma^+$ (B-X) transition with band head at 255.23 nm was selected for this study, due to its relatively simpler RVB structure. An analytical figure of merit, signal to envelope ratio (SER) was used to optimize the experimental conditions. To theoretically simulate this RVB, all the possible ro-vibrational transitions of B-X (0-2) band was calculated using diatomic constants of B available in literature [2]. An in-house written Levenberg-Marquardt method of least square error based non-linear curve fitting based algorithm was developed on LabView platform. The algorithm generates a theoretical spectra of BO B-X molecular band with different $^{10}B/^{11}B$ ratio and compared the same with experimental spectra recorded using high resolution Czerny-Turner spectrograph. Least weighted mean square error was used for terminating the fitting procedure. The isotopic concentration of ^{11}B and ^{10}B in the sample were obtained from the best fitted parameters. The calculated isotopic composition was found to be accurate to the natural isotopic abundance of ^{11}B and ^{10}B with a prediction error of ~ 1 %. Due to the simplicity of the process and being a calibration free method, the CF-LAMIS may prove to be beneficial for applications in nuclear industry especially for remote application.

References:
[1] Bol'shakov et.al., *J.Anal.At. Spectrom.*, **31**(2016), 119.

Non-destructive assay of SNMs in samples having high gamma spectral interference

Sanhita Chaudhury[§], Ashwani Kumar, Sabyasachi Patra, Rahul Tripathi[§]

Radiochemistry Division, Bhabha Atomic Research Centre, Mumbai-85
[§] Email: sanhita@barc.gov.in/ rahult@barc.gov.in

Absolute non-destructive assay of special nuclear materials (SNMs) involves use of gamma spectrometry (GS) in combination with neutron multiplicity counting (NMC)/ calorimetric measurement (CM). The isotopic composition (IC) of Pu, as obtained from GS, is a requirement for its absolute estimation by either of these non-destructive techniques. Considering the low intensity of the Pu gamma rays, the ^{241}Am contribution can sometime be too dominating to subtract and carry out IC analysis. Use of gamma spectrum for IC analysis is limited even in the heavily shielded samples too. Herein, we propose an empirical analysis method for absolute estimation of Pu, involving NMC and CM and most importantly without using GS. The method is described as follows-

Step 1- The unknown sample is counted in a NMC [1] and the corresponding α (alpha to fission ratio) is obtained from the multiplicity data analysis. The ^{241}Am fraction (f_{Am}) in the sample is then obtained from the theoretically generated (using standard decay and reaction parameters [2], Fig. 1) f_{Am} vs α plot. *Step 2*- Using a set of standard Pu samples, the calibration plot for doubles rate (D) vs $^{240}Pu_{eff}$ is obtained. Then, using the standard specific power of different Pu isotopes [2], the calorimetric heat output (W_{Pu}) for a Pu sample corresponding to a particular D (hence particular $^{240}Pu_{eff}$) was calculated for PR grade Pu. A linear plot of W_{Pu} vs D is thus obtained for a particular IC. A slight variation in the IC will lead to varying slope in this plot. Four such calibration lines having ^{239}Pu in the 70-74% range are shown in Fig. 2. *Step 3*- The unknown sample is counted in a calorimeter and the heat output is corrected for the ^{241}Am fraction (as obtained from step 1). Using this corrected W_{Pu} and the D (from NMC) in Fig. 2, one can determine the IC of the sample and hence the absolute amount of Pu from the calibration plot in Fig. 2. The uncertainty on the measured Pu amount may arise mainly from the variation in IC. The proposed method is experimentally verified from the obtained IC and absolute Pu amount of an unknown sample, as shown in Fig. 1 and 2. The obtained ^{240}Pu composition (and hence also the Pu amount) was within ±4% of the previously estimated standard GS based IC. It is to be noted that presence of any low Z matrix in the samples can enhance only the singles rate and hence will not affect the D vs W_{Pu} plot.

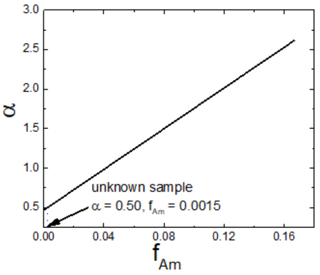

Fig. 1: Variation of α as a function of f_{Am}

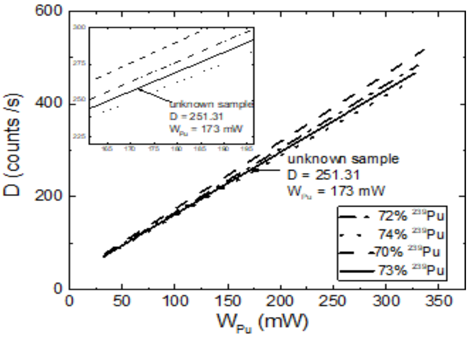

Fig 2: Doubles rate vs W_{Pu} plot

References:

[1] S. Chaudhury, M. Y. Ali, S. Patra, C. Agarwal, R. T. Jadhav, P. K. Pujari. BARC report, BARC/2018/I/008

[2] D. Reilly, N. Ensslin, H. Smith, S. Kreiner, 1991. Passive Nondestructive Assay of Nuclear Materials. Los Alamos National Laboratory, United States.

Determination of Plutonium concentration in dissolver samples

S.Pugazhendi, Saurabh Suman, Mukesh Kumar, V.Rekha, D. Sivakumar, K.Dhamodharan§,
K.A.Venkatesan and K.Ananthasivan
Reprocessing Group, IGCAR, Kalpakkam-603 102
§ Email: kdn@igcar.gov.in

The spent nuclear fuel discharged from Fast Breeder Test Reactor is being reprocessed in a Compact Reprocessing of Advanced fuel in Lead cell, IGCAR, Kalpakkam. The concentration of plutonium present in the dissolver tank needs to be determined with good precision and accuracy. Currently, the isotopic dilution mass spectrometry (IDMS) is employed for the determination of plutonium in these samples. However, it requires the separation of plutonium from uranium and fission products by ion exchange chromatography. This entire process is time consuming and significantly contributes the radiation exposure to operating personnel, as the high level of fission products activities are associated with the dissolver sample. Therefore, there is a need to look for other methods to minimise the man-rem exposure. In this context, the extractive redox titrimetric method is regarded as a method for the determination of plutonium in sample associated with high level of FPs activities. In this method, tri-octyl phosphine oxide (TOPO) diluted with o-xylene was employed as an extractant for the quantitative extraction of plutonium from dissolver solution, followed by stripping of plutonium using 0.2 M oxalic acid from the loaded organic phase. The strip product was transferred into titration flask and the plutonium present in the strip solution was oxidised to Pu (VI) with fuming perchloric acid. Fuming perchloric acid also destroys oxalate ion completely. The hexavalent plutonium thus formed was treated with known volume of excess ferrous ammonium sulphate in H_2SO_4 and H_3PO_4 medium and un-reacted excess Fe^{2+} was titrated with standard potassium dichromate (0.0251 N) using barium di-phenyl amine sulphonate (BDAS) as an indicator. From the value of dichromate equivalent to Fe^{2+} in the sample and in the blank, the concentration of plutonium was determined. To validate this method, standard plutonium solution was analysed and the results are compared in Table 1. The results indicate that the error in this method was ±3.0 % for the aliquot having plutonium in the range of 0.5 -1.0 mg/aliquot. The developed procedure was employed for the determination of plutonium in the dissolver sample and concentration of plutonium is in good agreement with plutonium concentration obtained by IDMS as shown in table 2. Since 0.1 M TOPO/xylene can quantitatively extract plutonium in a single contact, it is possible to use this extractant for carrying out solvent extraction inside hot-cell and transfer the loaded organic layer to the lab for analysis. As a result, radiation exposure to analysts can be significantly reduced.

Table 1 Determination of Pu concentration in standard samples

Sl.No	Pu in feed solution/mg	Pu in organic phase/mg	Pu in strip product/mg	% error (±)
1	3.39	3.31	3.29	2.9
2	3.39	3.33	3.32	2.9
3	6.78	6.75	6.65	2.2
4	6.78	6.76	6.75	1.4
5	6.78	6.73	6.73	1.0

Table 2 Determination of Pu concentration in plant sample

Sample Id	Volume aliquot	[Pu]/ g.L^{-1}	
		Present method	By IDMS
Dissolver-1	0.2	20.39	20.55
Dissolver-1	0.2	20.43	20.47

Method development for determination of Li isotopic abundance using LIMS

T. Bapuji[2], D. Bola Sankar[1,2], J. Namitha[1], U. K. Maity[1,2], P. Manoravi[2,§]

[1]*HBNI, IGCAR, Kalpakkam – 603102, India.*
[2]*MC&MFCG, IGCAR, Kalpakkam – 603102, India.*
[§]Email: pmravi@igcar.gov.in

Lithium being precious metal (natural isotopic composition of ^{6}Li and ^{7}Li is 7.59 & 92.41%, respectively) has wide area of applications with different isotopic enrichment. As for examples, enriched ^{6}Li is used in Li-ion battery, whereas in thermal nuclear power plant (NPP) lithium hydroxide of 99.995% pure ^{7}Li is used as a pH adjustment agent in coolant systems [1]. Highly enriched ^{7}Li is used in NPP because ^{6}Li undergoes (n,α) reaction to produce highly radioactive tritium (^{3}T). Hence, it is essential to determine the isotopic abundance of Li before its use. Conventionally, inductively coupled plasma mass spectrometry (ICP-MS), laser ablation (LA) ICPMS and thermal ionization mass spectrometry (TIMS) are used for the above purpose. These instrument are sophisticated, costly and they are applicable either for solid (LA-ICPMS) or liquid (ICPMS & TIMS). The present study demonstrates potential use of in-house designed laser ionization mass spectrometry (LIMS) technique for measuring the isotopic abundance of Li. The advantages of LIMS are simple technique to handle, cheap, applicable to solid as well as liquid samples, and the mass analyzer (TOF-MS) can be home made [2].

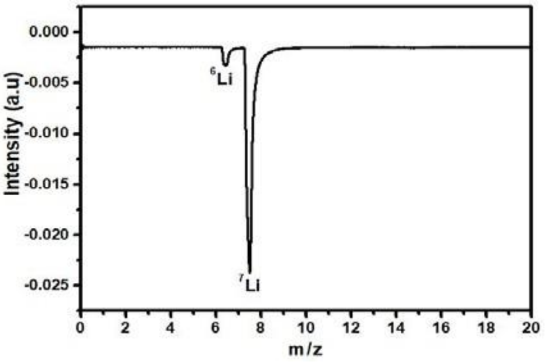

Fig. 1: Mass spectrum obtained for the sample by LIMS

The liquid sample containing natural isotopic composition of Li, is made a slurry using graphite powder, which has high laser absorption capacity and serves as a matrix. The slurry is then dried on a stainless steel sample plate to form a thin layer, which is loaded into a sample chamber and analyzed using LIMS.

The typical mass spectrum obtained for the sample by LIMS is shown in Fig. 1. The isotopic abundance obtained from LIMS is given in Table 1. It is obvious from the table that the present method can determine the isotopes of lithium with an accuracy and precision better than 2.6% and 4.5%, respectively. Hence, the present method using LIMS, can be an alternative technique to measure the isotopic abundance, which can overcome the shortcomings of conventional techniques, where direct solid as well as liquid sample can be analysed.

Isotopes	Abundance obtained from LIMS	Nat. abundance	RSD	Error
^{6}Li	7.39%	7.59%	4.5%	2.6%
^{7}Li	92.29%	92.41%	0.2%	0.13%

Table.1 Comparison of isotopic abundance of lithium from LIMS with that of natural abundance values

Reference

[1] P. Aaltonen et.al,"Water chemistry and behavior of materials in PWRs and BWRs" (1997)
[2] J. Namitha et.al, *J. Anal. At. Spectrom.*, **36**, 1503 (2021)

Artificial Neural Network based Direct Non-Destructive Compositional Analysis of (Th, U)O_2 Fuel Pellets by X-Ray Fluorescence Technique

B. Kanrar[1, §], K. Sanyal[1] and R.V. Pai[1,2]

[1] *Fuel Chemistry Division, Bhabha Atomic Research Centre, Mumbai, India*
[2] *Homi Bhabha National Institute, Mumbai, India*
[§] Email: buddha@barc.gov.in

Mixed Oxide (MOX) fuels like (Th,U)O_2 and (Th,Pu)O_2 are the proposed fuels in Advance Heavy Water Reactor (AHWR) which is a forerunner to demonstrate the thorium fuel technology in the third state of Indian nuclear power programme. X-Ray Fluorescence (XRF) is a well known non destructive analytical technique with aided advantage of multi-elemental analytical capability. Chemometric method like Artificial Neural Network (ANN) is capable to perform spectroanalysis. Major advantages of ANN based methodology are the robustness of the technique in analyzing spectra for quantification, efficiency of exploring quantitative information for noisy as well as high variance data, flexibility of not knowing the underlying mathematical model for analysis. Here we have exploited the applicability of ANN based micro-XRF technique for direct, non destructive compositional analysis of MOX fuel pellets samples.

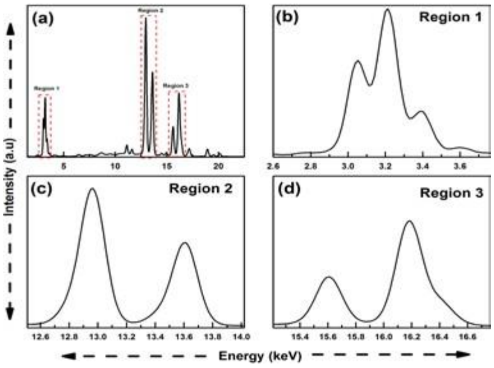

Fig 1: XRF spectra with three different energy ranges in consideration.

The regression relationship between counts from various channels with elemental concentration is established in the presently developed ANN based methodology. After exploiting various ANN configurations with different no of hidden layers, different activation function optimized ANN architecture was obtained. In this study seven (Th, U)O_2 MOX fuel pellet with varying U concentration were used. Each pellet was measured 10 times to form input data set. Among them data from six pellets were used to training and the rest one was used for validating the model. The entire XRF spectra were splitted into three regions: Region 1 is selected by considering the elemental U/Th fluorescence M lines, region 2 is for elemental fluorescence Lα1 lines of U/Th and region 3 is for the Lα2 lines of U/Th. Data from all the regions were used for training and validating. We obtained from the present study accuracy for the U determination in the validation sample of 3.40%, 3.19% and 5.56% for region 1, 2 and 3 respectively. Similarly the precisions for the U determination in the validation sample are 4.40%, 1.90% and 6.52% for region 1, 2 and 3 respectively. Superiority of region 2 in terms of precession and accuracy of the results can be explained due to higher counting statics of U/Th Lα1 line.

The authors would like to thank Dr. S. Kannan; Director, Radiochemistry and Isotope Group and Dr. S. Chaudhury Head, Fuel Chemistry Division, for their support in this work.

References:
[1] B. Kanrar, K. Sanyal and R.V. Pai, *Journal of Analytical Atomic Spectrometry*, **37** (2022) 741.
[2] M. Kaniu, K. Angeyo, A. Mwala and M. Mangala, *Analytica chimica acta*, **729 (**2012) 21

Quality control of external Particle Induced Gamma-ray Emission (PIGE) method for quantification of low Z elements in cement samples

Sonika Gupta[1], S. K. Samanta[1,2, §], R. Acharya[1,2,§]

[1] *Radiochemistry Division, Bhabha Atomic Research Centre, Mumbai – 400085, India*
[2] *Homi Bhabha National Instituite, Mumbai – 400094, India*
[§]Email: sksamanta@barc.gov.in / racharya@barc.gov.in

Particle Induced Gamma-ray Emission (PIGE) is an accelerator based online nuclear analytical technique which utilizes several nuclear reactions (p,nγ), (p,γ) and inelastic scattering (p,p'γ) for excitation of the atomic nucleus [1]. The excited nucleus decays via emission of prompt γ-rays which is generally assayed using HPGe detector. Low energy proton beam (< 5 MeV) can be suitable for determination of low Z elements (Li – S). External (in air) PIGE has already been standardized for rapid estimation of elements using Ta window as current normalizer. Quality control parameters (accuracy, precision, sensitivity, detection limit) are studied for external PIGE using several geological certified reference materials (CRMs) such as PCC-1, MAG-1, SDC-1, GSP-1, BCR-32 and AGV-1. Direct samples (~300 mg) were packed in thin mylar foils and irradiated in 3.5 MeV proton beam. Elements such as Na, Mg, Al and Si are quantified in these CRMs with error (%) within ± 6%, Z-score and Zeta-score within ± 2 at 95.5 % confidence level. The uncertainties in concentration are within ± 5%. **Table 1** shows the determined concentrations in **AGV-1**. The methodology was applied for quantification of Si in three cement samples ($CT_1 – CT_3$) and the analytical results were compared with EDXRF as alternative technique. Statistical evaluation of the analytical results was done using **t-test** and **F-ratios** (**Table 2**). T-test and F-ratios was found to be less than their critical values.

Table 1. Determined concentration of elements in AGV-1

Element	Certified Conc (%)	Obtained Conc (%)	Error (%)	Z-Score	Zeta - Score
Na	3.16±0.09	3.08±0.02	-2.5	-0.9	-0.9
Al	9.07±0.18	9.4±0.07	3.6	1.8	1.7
Si	29.42±0.29	30.05±0.42	2.1	2.2	1.2
Mg	0.92±0.06	0.98±0.01	6.5	1.0	1.0

Table 2. Si determined in cement samples ($CT_1 – CT_3$) and its intercomparison with EDXRF

Sl. No.	Cement samples	Si concentration (%) [n=3]			
		PIGE	EDXRF	t-test	F-test
1.	**CT_1**	10.47 ± 0.32	10.88 ± 0.44	0.91	0.53
2.	**CT_2**	9.98 ± 0.31	10.59 ± 0.41	1.42	0.57
3.	**CT_3**	4.57 ± 0.11	4.98 ± 0.23	2.23	0.19

References:

[1] S. Chhillar et.al., *Analytical Chemistry*, **86 (22) (2014) 11167**.

Chemical characterization of coal samples using Ion Beam Analysis (IBA) and Instrumental Neutron Activation Analysis (INAA) for Coal Quality: An Intercomparison Study

S. K. Samanta[§], R. Acharya[§]
Radiochemistry Division, Bhabha Atomic Research Centre, Mumbai – 400085
Homi Bhabha National Institute, DAE, Mumbai – 400094
[§]Email: sksamanta@barc.gov.in / racharya@barc.gov.in

Quality of coal used for energy production is very important to get high calorific value and lower ash content, though the coal agencies provide different grade coal with their ash content value it is necessary to further check the same before its intended use. Presently, in India, wet chemical analysis is used for quantifying ash content from the oxide concentrations of mainly Si, Al, Fe, Na, Mg, Ca. There is a scope to analyze coal samples by faster nondestructive methods to assess the coal quality with high accuracy and precision. In this respect, nuclear analytical techniques neutron and proton play a pivotal role for analyzing small to large size coal samples. In the present work, Ion Beam Analysis (IBA) techniques like PIGE and PIXE using proton beam have been used to determine low Z (Si, Al, Na, Mg) and medium Z (Fe, Ca, Ti) respectively. PIGE experiment was carried out in FOTIA, BARC using 3.5 MeV external proton beam. PIXE is an online, accelerator-based technique where the proton beam is used for electronic excitation. PIXE experiment was carried out at Ion Beam Laboratory at IOP, Bhubaneswar. For PIGE, direct samples packed in Mylar foils were irradiated in proton beam along with the NIST standards followed by its radioactive assay using HPGe detector. For PIXE experiment, 100 mg each of coal samples were mixed with 50 mg of 5% Y_2O_3 stock and 300 mg graphite followed by its pelletization using 2-ton hydraulic press. The pellets were irradiated in proton beam of 3 MeV (1-2 nA current) and the emitted X-rays from electronic excitation were recorded using Si(Li) detector. In addition, trace elements (Sc, Cr, Co, Zn, Se, Cs, Ce, Sm, Hf, U and Th) were determined using INAA (**Figure 2**), and it was observed that the coal with higher ash content contains high concentration of trace elements. In future, PGNAA will be used for rapid and non-destructive determination of all inorganic constituents relevant for coal ash contents.

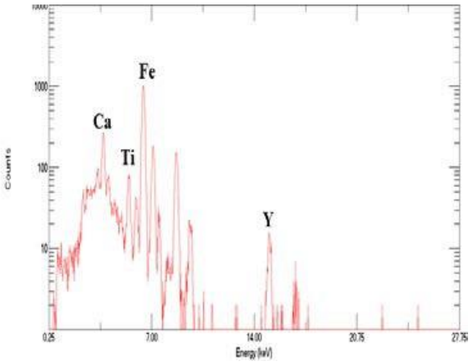

Figure 1: PIXE Spectrum of Coal

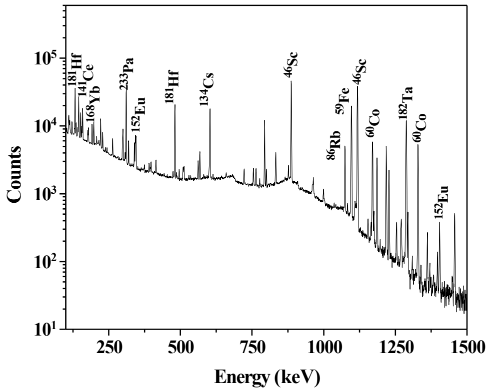

Figure 2. NAA spectrum of a coal sample

Acknowledgements: Authors thank operation crew members of FOTIA and Dhruva reactor, BARC and IBL, IOP for their support during the experiment.

Quantification of low Z elements and improvement of their detection limits in uranium matrix using external PIGE facility at FOTIA, BARC

Sk Wasim Raja[1,3,§], R. Acharya[2,3]

[1] *RCD (BARC), Variable Energy Cyclotron Centre, Kolkata-700064, India*
[2] *Radiochemistry Division, Bhabha Atomic Research Centre, Mumbai-400085, India*
[3] *Homi Bhabha National Institute, Anushaktinagar, Mumbai-400094, India*
[§] Email: sw.raja@vecc.gov.in

Particle Induced Gamma-ray Emission (PIGE) method using low energy proton beam (3 to 5 MeV) has successfully been applied for chemical characterization of reactor materials by quantifying low Z elements like Li, Be, B, F, Na, Mg, Al, Si, Ti etc. [1]. We have set up external PIGE facility at Folded Tandem Ion accelerator (FOTIA), BARC for non-destructive analysis of as received samples without any sample pretreatment in a greener way. In this work, we present our developmental work on non-destructive quantification of low Z elements like Si, Al etc. in synthetic samples of uranium matrix without any sample preparation and instrument contamination and improvement of their detection limits for practical applications in nuclear materials.

In the external PIGE facility, proton beam was extracted in air through a 25 µm thick Ta window [2]. Samples were doubly wrapped using a thin Mylar film (1mil thickness). For 5 MeV proton beam, beam energy on target was ~3.5 MeV and beam current was ~10-20 nA depending on the samples. Synthetic samples of Al_2O_3 and SiO_2 in U_3O_8 matrix were prepared by homogeneously mixing the stoichiometric compounds. For detection limits, various samples in U_3O_8 with different ppm of low Z elements (50 to 500 ppm) were prepared by mixing the U_3O_8 samples with required Merc IV solution and dried under IR lamp. All sample preparation works were done inside the fume hood and the outside Mylar was cleaned using alcohol to avoid any surface contamination.

Samples wrapped in Mylar were irradiated using 3.5 MeV proton beam using the external PIGE facility at FOTIA, BARC. The obtained mass fraction of Si, Al etc. were in good agreement with the theoretically calculated values. We were able to detect up to 50 ppm for Li and Na and 100 ppm for Si, Al and Ti in the U_3O_8 samples using the present experimental set up. The advantage of this external (in air) PIGE set up is that fast non-destructive quantification of direct samples can be done in a greener way without any instrumental contamination. It is especially useful for chemical quality control purposes when a large no of samples need to be analyzed in a shorter time. Improvements of detection limits will be done by optimizing experimental parameters like proton beam current, spatial resolution of the beam and target-detector arrangements.

Acknowledgements: Dr. S. Kannan, Director, RC&IG, BARC and Dr. P. K. Mohapatra, Head, RCD, BARC are acknowledged for their constant support for this work. We thank Dr A. Sengupta, RCD, BARC for providing the uranium oxide samples. FOTIA operation crew are acknowledged for their help during the experiment.

References:
[1] Sk Wasim Raja, R. Acharya and P. K. Pujari., *J Radio. Nucl. Chem.*, **323(2)** (2020) 1359.
[2] Sk Wasim Raja et al., *Anal. Chim. Acta*, **1202 (310)** (2022) 339686.

Electro-refining of FBTR irradiated U-6Zr(Wt%) in hot cells

D. Bolasankar[1], T. Kalaiyarasu[1], R. Karunakaran[1], S. Rajeswari[1],
Gurudas Pakhui[2], S.Suganthi[2], K. Suriyakumari[2],
Kakkum Perumal[3], A.S.Ganapathi[3], S. Mariyappan[3], S.Rajarajeswari[3],
R. Padmanaban[4], Arul Kumar[4], N. Ravi[4],
P. Manoravi[1], R. Kumaresan[2], P. Venkatesh[3], V. Suresh kumar[4], J. Prabhakar Rao[4] ,
and V.Jayaraman[1§]

[1] *Mini & Hot Cell Section, ACSD, FMCG*
[2] *Pyro-chemical Process Studies Section, MFPD, MFRG*
[3] *Pyro-chemical & Engineering Studies Section, PPED, MFRG*
[4] *Chemical Facilities Engineering Division, MFRG*
Materials Chemistry & Metal Fuel Cycle Group, IGCAR, Kalpakkam
[§] Email: vjram@igcar.gov.in

Electro refining (ER) of irradiated U-6Zr(%) alloy fuel was carried out in the laboratory scale pyro-process augmented hot cell experimental facility of MC&MFCG. About 22.9g irradiated fuel (with clad) was loaded with 21g of fresh U-6Zr(w%) alloy in anode basket. Total weight of U-6Zr(wt%) alloy loaded inside anode basket was 43.9g. ER was carried out employing 2.819 Kg of LiCl-KCl-UCl_3 (Salt) as electrolyte (3.55 wt% UCl_3), 10 mm dia SS rod as cathode and FBTR irradiated U-6Zr(%) as anode. Ag wire along with LiCl/KCl/AgCl salt loaded inside a quartz tube was used as reference electrode.

Before starting the ER runs, potential of cathode (*vs.* $Ag^+|Ag$ ref.) and anode (*vs.* $Ag^+|Ag$ ref.) was measured to be -0.310 and -1.236 V, respectively at 500 °C. ER was carried out at 500 °C in potentiostatic mode by varying the potential at -1.4 V to -1.5 V for 15 hrs. The total cathode deposit recovered is 15.9g. The salt and deposit samples were taken out of hot cell for characterization under hot condition using indigenously fabricated samplers. [Figure 1-4]

Figure 1: Salt and Cd balls loaded to vessel

Figure 2: Fuel loaded to anode basket

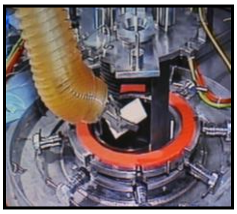

Figure 3: Eutectic salt loaded to reaction vessel

Figure 4:Deposit at SS cathode

Three salt samples taken in different time durations were analysed for uranium content using spectrophotometric method. The concentration of uranium after electrolysis was found to be about 3.1 wt.%. The diluted salt sample was analysed by gamma spectrometry. The radioisotopes ^{134}Cs, ^{137}Cs, ^{144}Ce, ^{154}Eu and ^{155}Eu were found to be present. The cathode deposit was analyzed for uranium and zirconium contents and their concentrations were estimated to be 70 mg and 210 µg respectively.

Acknowledgements:
The authors hereby acknowledge with thanks Dr. N.Sivaraman, Director, MC&MFCG, Dr.Kitheri Joseph, AD, MFRG, Dr. Suddhasatwa Ghosh, Head, MFPD and Shri.T.V.Prabhu, Head, CFED for their participation and support rendered throughout the course of this work.

Effect of temperature on the selectivity coefficient of a polymeric membrane sensor for Gd^{3+} detection

D. B. Sharma[1,§], B. Mahanty[1], P. K. Mohapatra[1], W. Verboom,[2]

[1]*Radiochemistry Division, Bhabha Atomic Research Centre, Mumbai – 400085, India*
[2]*Laboratory of Molecular Nanofabrication, MESA+ Institute for Nanotechnology, University of Twente, P.O. Box 217, 7500 AE Enschede, The Netherlands*
[§] Email: dbsharma@barc.gov.in

In nuclear industry, gadolinium as gadolinium nitrate is used as neutron poison in the moderator system owing to its very high thermal neutron absorption cross section [1]. Due to the same reason presence of gadolinium in the nuclear fuel is also not desirable. Therefore determination of gadolinium at trace level is very important. Potentiometric sensor has many advantages over other analytical techniques [2]. However, determination of Gd^{3+} potentiometrically suffers from the possible interference from other lanthanide elements. Selectivity coefficient is a parameter by which the effect of interference is measured. Temperature can play a vital role to tune the selectivity coefficient of the sensor. In the present investigation the effect of temperature on the selectivity coefficient of Gd^{3+} over La^{3+} (model lanthanide) was determined using a Gd^{3+} based sensor prepared in house with a 9-membered aza crown ether scaffhold tethered with three diglycolamide (L_I) (Fig.1, inset) as ionophore in a polyvinyl chloride matrix [3].

The selectivity coefficient (K_{ij}^{Pot}) of a neutral ionophore based cation selective membrane for same charge of primary and interfering ions with constant concentration of ionophore and ionic additive is given by the following equation.

$$\ln\frac{K^{Pot}_{ij,T2}}{K^{Pot}_{ij,T1}} = \frac{\Delta H^{0}_{ex}+\Delta H^{0}_{jL}-\Delta H^{0}_{iL}}{R}\left[\frac{1}{T_1}-\frac{1}{T_2}\right] \qquad (\Delta H= \Delta H^{\circ}_{ex}+ \Delta H^{\circ}_{jL}- \Delta H^{\circ}_{iL})$$

ΔH°_{ex}, ΔH°_{jL}, ΔH°_{iL} are the standard enthalpy of ion exchange, complex formation of the interfering and the primary ion with the ionophore respectively [4]. T is the temperature in kelvin and R is universal gas constant.

The selectivity coefficient was determined at different temperature by matched potential method (Fig. 1). As can be seen there is a linear correlation between logarithms of selectivity coefficient versus inverse of temperature. The overall ΔH found for the present case is −39.3 kJ mole^{-1}. Therefore, by determining the values of ΔH°_{jL} & ΔH°_{iL} using calorimetry, one can determine ΔH°_{ex} which is a very important thermodynamic parameter. The selectivity coefficient data suggest that the La^{3+} is less interfering in the Gd^{3+} determination at lower temperature.

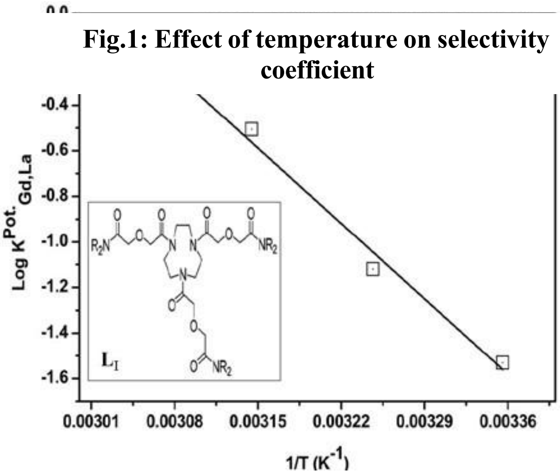

Fig.1: Effect of temperature on selectivity coefficient

References:
[1] Rufus et al., J.hazard. mater., 342 (2018) 77-84.
[2] Bakker et al., Trends Anal. Chem. 24 (2005) 199–207.
[3] Sharma et al., G-08, SESTEC 2022, p.226.
[4] Zahran et. al., Analytical chemistry, 82 (2010) 3622.

Chemical Characterization of salt and deposit from the electro-refining of FBTR irradiated U-6Zr(Wt%) in hot cells

D. Bolasankar[1], T. Kalaiyarasu[1], R. Karunakaran[1], S. Rajeswari[1], Gurudas Pakhui[2],
P. Manoravi[1], R. Kumaresan[2] and V. Jayaraman[1§]

[1]*Mini & Hot Cell Section, ACSD, FMCG*
[2] *Pyro-chemical Process Studies Section, MFPD, MFRG*
Materials Chemistry & Metal Fuel Cycle Group, IGCAR, Kalpakkam
[§] Email: vjram@igcar.gov.in

Electro refining (ER) of irradiated U-6Zr(wt%) alloy fuel was carried out in the laboratory scale pyro-process augmented hot cell experimental facility of MC&MFCG. About 22.9g irradiated fuel (with clad) was loaded with 21g of fresh U-6Zr(%) alloy in anode basket. ER was carried out by employing 2.819 Kg of LiCl-KCl-UCl_3 (Salt) as electrolyte (3.55 wt% UCl_3), 10 mm dia SS rod as cathode and irradiated U-6Zr(wt%) as anode. Ag wire along with LiCl/KCl/AgCl salt loaded inside a quartz tube was used as reference electrode. ER was carried out at 500 °C in potentiostatic mode by varying the potential at -1.4 V to -1.5 V for 15 hrs. The total cathode deposit recovered is 15.9g. The metal deposit was scrapped from the cathode under hot condition. Three samples of salt solution and two samples of metal deposit were taken using manipulators during the run under hot condition using indigenously fabricated samplers. The samples were taken out of hot cell for characterization.

Uranium content of the salt samples was analyzed using spectrophotometric method using bromo-PADAP as a colouring agent. The concentration of uranium after electrolysis was found to be about 3.1 wt.%. However, the presence of chloride ions suppressed the signal and interfered in uranium analysis. The diluted salt sample after electrolysis was analyzed by gamma spectrometry. The radioisotopes and its radioactivity are given in the table.

S.No.	Radioisotopes	Radioactivity (Bq)
1	^{134}Cs	85.6 ± 1
2	^{137}Cs	4440 ± 30
3	^{144}Ce	146 ± 13
4	^{154}Eu	25.1 ± 1
5	^{155}Eu	167 ± 5

The cathode deposit after the electrolysis run was analyzed for uranium and zirconium contents. After sufficient washing, the sample was dissolved in conc. HNO_3 and the residue was dissolved separately by HNO_3-HF mixture. The dissolved samples were analyzed for uranium and zirconium content by Davies and Gray and spectrophotometric methods respectively. The concentration of uranium and zirconium was estimated to be about 70 mg and 210 µg respectively.

Acknowledgements:
The authors hereby acknowledge with thanks Dr. N.Sivaraman, Director, MC&MFCG, Dr. Kitheri Joseph, AD, MFRG and Dr. Suddhasatwa Ghosh, Head, MFPD for their participation and support rendered throughout the course of this work.

Development of a process flow-sheet for the chemical separation and reconversion of plutonium and uranium in fast reactor fuel reprocesssing

K S Vijayan, Arvind Prasad, Akhilesh K Nair, Dhanesh P R, Bhanu Prasad CH.U, Chokkalingam R N, Rekha V,N Desigan§ ,K A Venkatesan and K Ananthasivan

Process, Radiochemistry and Reprocessing Research and Development Division,
Indira Gandhi Centre for Atomic Research, Kalpakkam – 603102
§E-mail: desi@igcar.gov.in

Reprocessing of high burn-up spent fuel (70%PuC/30%UC) discharged from FBTR is being carried out at CORAL facility, IGCAR.A modified PUREX process is employed for the co-decontamination of plutonium and uranium from fission products in this facility [1]. Plutonium and uranium recovered together with respective concentration in the range of 6-12 g/L and 3-6 g/L is received in the reconversion laboratory. Studies have been carried out for the separation of plutonium and uranium from the nitric acid co-strip product solution by chemical precipitation method [2] and an advanced flow-sheet has been developed.

In the first step, bulk quantity of plutonium was selectively precipitated as plutonium oxalate using oxalic acid, leaving the bulk of uranium (2-4 g/L) and soluble plutonium (30-40 mg/L) in the filtrate. Further separation of plutonium from the bulk of uranium was achieved by uranous oxalate carrier precipitation and by ammonium uranyl carbonates (AUC) precipitation. Uranous nitrate solution having 2g/L concentration was added to the filtrate to remove 95% of soluble plutonium as oxalate along with uranous oxalate precipitate. The filtrate was subjected to hydroxide precipitation using ammonia and the hydroxide cake containing uranium was converted to AUC using ammonium carbonate. The plutonium oxalate and AUC cakes were calcined to their respective oxides. The flow sheet is given in Fig.1

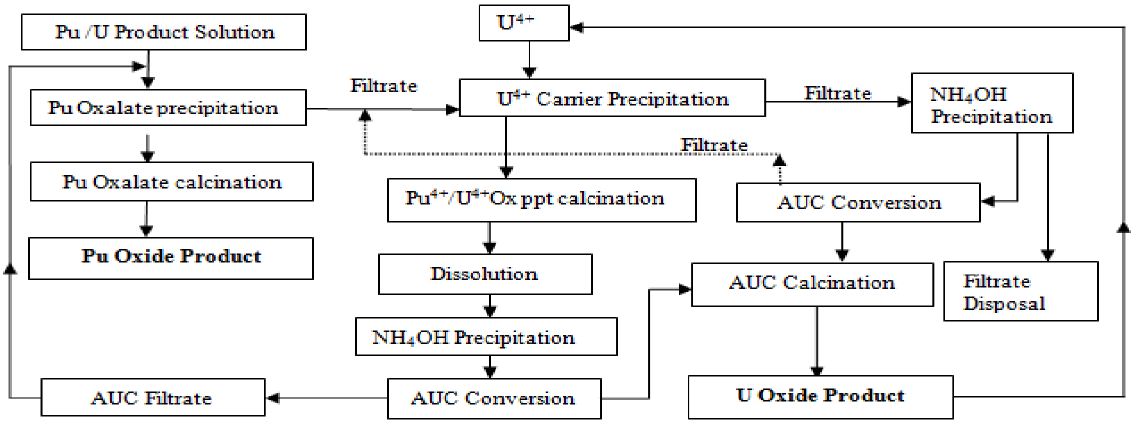

Fig.1.Process flow sheet

The flow- sheet was tested under realistic concentrations of plutonium and uranium and successfully deployed in CORAL reconversion laboratory. The recovery of uranium with less than 200 ppm of Pu and plutonium with less than 5000 ppm of U was nearly quantitative (>99.9%).

References:
[1] R.Natarajan, IANCAS *Bulletin*, 14(2), (1998)27
[2] K.S.Vijayan and P Govindan, in *proceedings of the twelfth DAE-BRNS symposium on nuclear and radiochemistry*, BARC, Mumbai (2015)110.

Development of a chemically functionalized polystyrene for the bulk removal of yttrium from strontium

M.Amutha Suba, B.Robert Selvan, A.S.Suneesh [§], N.Ramanathan

Fuel Chemistry Division, MC&MFCG
Indira Gandhi Centre for Atomic Research, Kalpakkam, India
[§]Email: suneesh@igcar.gov.in

^{89}Sr is being produced using yttrium target via the nuclear reaction ^{89}Y(n,p)^{89}Sr in Fast Breeder Test Reactor (FBTR), IGCAR. The separation of high purity ^{89}Sr for the requirement of pain palliation in cancer patients requires sophisticated separation technique. For the requirement of radiopharmaceutical grade pure ^{89}Sr, the bulk separation of ^{89}Y need to be carried out. In this context, diglycolamide anchored polystyrene resin (PS-DGA) was developed and was studied for the selective separation of Y(III) so that the aqueous solution will be devoid of Sr(II).

The adsorbent, PS-DGA was prepared by chemical modification of commercially available polystyrene chloromethylated resin (ALDRICH, 20-60 Mesh, 4-5 % functionalization and 4 % cross linking with DVB). This involves an initial conversion of the above to an amine functionalized resin (PS-NH2) by reacting with diethylene triamine in the presence of pyridine, at 85 °C. The PS-NH2 resin was further reacted with diglycolic anhydride in the presence of dichloromethane, at 40 °C to form a diglycolamic acid resin (PS-DGAH). The PS-DGAH resin was further reacted with thionylchloride in the presence of triethylamine, using acetonitrile as solvent form PS-COCl resin. The PS-COCl resin was further modified to PS-DGA by reacting the former with diethyelene triamine in the presence of triethylamine, using chloroform as solvent at 50 °C. Figure 1 shows the sketch of the preparative route of PS-DGA. PS-DGA exhibits higher adsorption of Y(III) and negligible adsorption of Sr(II), as seen in table 1. As seen for the diglycolamides systems like TODGA or TEHDGA, the PS-DGA also exhibits higher adsorption of Y(III) at nitric acid concentrations above 2 M. Table 1 indicates the summary of adsorption tendency of PS-DGA for different concentration ratios of Sr(II) and Y(III). Results of the study indicated that PS-DGA can be utilized for the bulk removal of Y(III) for the production of radiopharmaceutically pure grade ^{89}Sr.

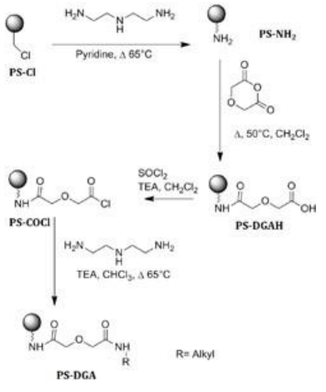

Figure 1. Synthetic scheme for the preparation of PS-DGA

Table 1. Adsorption tendency of Y(III) and Sr(II) by PS-DGA.

Concentration of Y/ ppm	Adsorption efficiency of Y	Concentration of Sr
10	99 %	10 ppm
1000	98 %	10 ppm
10000	97 %	10 ppm
20000	95 %	10 ppb

References:
[1] S.A. Ansari et.al., *Chemical reviews. 112 (2012) 1751-72.*

Assessment of potassium element concentration in vegetables using gamma spectrometry

Joshy P. James[1,§],T.K.Reji[1], R.M.Joshi[1], M.S.Vishnu[1], I. V. Saradhi[2]

[1]*Environmental Survey Laboratory, EMAD, BARC, Kaiga 581400,*
[2]*Environmental Monitoring and Assessment Division, BARC, Mumbai 400085*
[§] Email: joshyvandanam@gmail.com

Using gamma spectroscopy to measure the ^{40}K activity concentration in food is an efficient method to estimate the total potassium in food samples [1]. Methodology for the estimation of potassium element concentration from ^{40}K activity concentration is well described and calibration factor is derived [2] and using the factor the potassium elemental concentration in vegetables from the environment of Kaiga, Karnataka is estimated.

^{40}K activity in vegetables was determined by gamma spectrometric analysis of ash samples. The background spectra were measured under the same conditions of sample measurements and were used to correct the calculated sample activities. ^{40}K activity and the potassium elemental concentration in vegetable samples are presented in **Table 1.** The maximum value of potassium is observed in green spinach samples and minimum value is observed in papaya samples.^{40}K activity levels in vegetables reported in different parts of the world is in the range of 40-240 Bq kg^{-1}. The determination of potassium content using gamma spectrometry is found to be simple, reliable and less time consuming.

Table 1-^{40}K activity and potassium content in vegetables from Kaiga environment

S No.	Type of vegetables	No. of samples	^{40}K activity (Bq kg^{-1} fresh weight)		Potassium concentration (g kg^{-1} fresh weight)	
			Range	Mean	Range	Mean
1	Raw Banana	5	113.2-141.8	126.9	3.64-4.56	4.08
2	Bitter gourd	2	80.3-86.7	83.5	2.58-2.79	2.69
3	Brinjal	8	67.5-128.2	92.4	2.17-4.12	2.97
4	Ladies finger	2	61.0-115.0	88.0	1.96-3.70	2.83
5	Papaya	3	36.2-54.0	49.2	1.16-1.84	1.58
6	Tomato	6	62.6-95.0	74.36	2.01-3.05	2.39
7	Green spinach	1	177.6	177.6	5.71	5.71
8	Red spinach	1	131.0	131.0	4.21	4.21
9	Raw mango	1	93.6	93.6	3.01	3.01
10	Beans	1	108.2	108.2	3.48	3.48
11	Ginger	2	40.6-67.0	53.8	1.30-2.15	1.73
12	Green chilli	1	97.0	97.0	3.12	3.12
13	Torai	1	71.0	71.0	2.28	2.28
14	Lemon	1	83.9	83.9	2.70	2.70

References:

[1] Dedawan S. Saleh1, Saddon T. Ahmad and Sarmad R. Kareem,The Scientific Journal of Koya University Vol. X, No. 2 (2022),http://dx.doi.org/10.14500/aro.11053

[2] Abt, I., Garbini, L. and Schulz, O. *Detection*,(2016) **4**, 73-85. http://dx.doi.org/10.4236/detection.2016.43010

Elemental composition of soil samples collected from Uttarakhand state using X-ray fluorescence technique

M Tiwari[1], T. D. Rathod[1,2], R. C. Bhangare[1], S. K. Sahu [§,1,2], V. Pulhani[1,2]
[1]*Environmental Monitoring and Assessment Division, Bhabha Atomic Research Centre, Trombay, Mumbai – 400085, India*
[2]*Homi Bhabha National Institute, Anushaktinagar, Mumbai – 400094, India*
[§]Email: sksahu@barc.gov.in; Phone: +91-2225592375

The monitoring of trace and toxic elements in soil samples is crucial for environmental and human health, agricultural production, and compliance with regulations [1]. 35 soil samples were collected from different districts od Uttarakhand to assess levels of trace and toxic elements. EDXRF is an effective technique for monitoring these elements in soil due to its non-destructive nature, accuracy, versatility, fast analysis time, and cost-effectiveness [2]. 0.8 gram each of freeze dried and fine sieved (<63 µm) soil sample was homogeneously mixed with0.2 g cellulose powder (Sigma Aldrich). The homogenized mixture was then compressed under a hydraulic pressure of 25 tones for 3 minutes to make pellets. One filter-based (W) and four different secondary targets (Ge, Zr, Ti, Si) EDXRF (Xenemetrix's Genius IF) methods were optimized to excite the elements in the soil sample. The secondary targets were chosen to reduce relevant background intensities at specific line energies. The concentrations of 22 elements are reported using this technique. Calibration was done using a filter membrane for individual elements and a matrix-matched certified reference material (IAEA-433).

Table 1: Mean, and range (min, max) of elemental concentration (mg kg^{-1}) in soil samples collected from state of Uttarakhand.

	Min	**Max**	**Mean**		**Min**	**Max**	**Mean**
Mg	7242	77547	19663	**Cs**	0.8	28.1	8.3
Al	56221	95201	70991	**Rb**	73	30491	1044
V	58.2	337.9	178.5	**Zr**	77.8	428.6	224.7
Cr	64.6	251.9	126.6	**U**	2.48	8.66	5.26
Mn	218.9	3017.3	951.1	**Ce**	9.94	133.76	55.89
Fe	17778	92307	41941	**K**	8842	45142	23234
Co	5.6	28.3	13.2	**Sc**	0.97	15.77	4.94
Ni	11.2	63.4	40.3	**As**	8.87	40.74	16.26
Cu	28.5	51.7	35.5	**Br**	4.36	17.50	7.92
Zn	55.5	476.7	185.5	**Sr**	14.60	173.42	79.93
Ba	235	1587	575	**Pb**	14.54	52.79	27.27

Elemental concentrations (mg kg^{-1}) in soil samples from the state of Uttarakhand are shown in **Table 1**. To evaluate the level of soil pollution with toxic elements and the anthropogenic input various indices such as contamination factor, index of geoaccumulation and pollution load index (PLI) were calculated [3]. Average PLI values for soil samples collected from Uttarakhand is 1.35, which higher than 1 indicates with respect to the earth crust anthropogenic trace element contribution to the soil.

References:

[1] Piekut A, Baranowska R. et al., *Environ Monit Assess.* **16** (2018) 190(1): 25.
[2] Marguí E. et al., *Chemosphere* **303** (2022) 135006.
[3] Tomlinson,D.C.,et al., *Mar.Res.***33** (1980) 566–575.

BODIPY based Fluorescent Dosimeter for Gamma Radiation

<u>Manoj K. Choudhary</u>[1], Soumyaditya Mula[1,2] §*

[1]*Bio-Organic Division, Bhabha Atomic Research Centre, Mumbai 400085, India.*
[2]*Homi Bhabha National Institute, Anushaktinagar, Mumbai 400094, India.*
§ Email: smula@barc.gov.in

Accurate measurement of gamma (γ) doses is highly important to avoid any damage to human being and the materials used for γ-exposure. Although various γ-detectors such as ionization chambers, scintillators, thermoluminescent and semiconductor detectors etc are available but many of these techniques are highly costly with several limitations. Thus, it is extremely desirable to develop highly sensitive, low cost and easy to use γ–dosimeter for practical uses. Fluorescence sensors are highly popular due to their high sensitivity, selectivity, low cost, easy operation etc. But fluorescence sensor for γ-radiation is rarely explored.[1] Here, we report a highly sensitive fluorescent γ–dosimeter based on anilino-BODIPY dye (**1**).

The dye **1** in chloroform showed broad absorption profile with λ_{abs} at 496 nm and a shoulder peak at 540 nm. The dye showed weak reddish fluorescence with λ_{fl} at 609 nm. The broad absorption peak at 540 nm and highly red shifted fluorescence peak of dye **1** is due to the photoinduced charge transfer (PCT) from amino group to the BODIPY core. With increasing γ-exposure doses, the shoulder peak at 540 nm started decreasing and λ_{abs} was red shifted by 11 nm. The purple colour of the solution changed to orange colour after the γ-exposure which is visible by naked eyes. Remarkable change was observed in the fluorescence of the chloroform solution of **1** after γ-irradiation. With increase in γ-exposure doses, the fluorescence peak at 609 nm started decreasing and fluorescence peak at 530 nm sharply increases. Thus, the low reddish fluorescence of dye **1** changed to intense greenish-yellow showing ratiometric "off-on" fluorescence sensing of γ–radiation (Figure 1). The fluorescence intensity at 530 nm increased 100 folds after 200 Gy of γ-exposure. Interestingly, the fluorescence intensity ratio, I_{530}/I_{609} increases linearly with increase gamma doses upto 150 Gy, after that it started saturating (Figure 1). The limit of detection (LOD) was calculated to be very low (0.5 Gy). Therefore, the new dosimeter can be used for detection of gamma radiation in the range of 0.5-150 Gy very efficiently. The developed fluorescence dosimeter will be very useful for the accurate measurement of the absorbed doses in food irradiation processes.

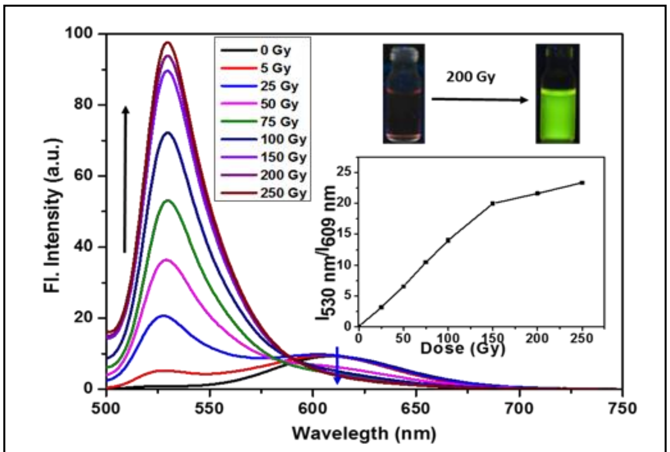

Fig1: Fl. spectra of dye **1** in $CHCl_3$ after γ-irradiation with different doses. Inset: change in fl. of dye **1** after 200 Gy of γ-irradiation and fluorescence intensity ratio ($I_{530\ nm}/I_{609\ nm}$) changes with γ -irradiation doses.

References:
[1] J.-M. Han, M. Xu, B. Wang, N. Wu, X. Yang, H. Yang, B. J. Salter and L. Zang, *J. Am. Chem. Soc.* **136** (2014) 5090.

Determination of $^{10}B/^{11}B$ in Boric Acid and B_4C using LA-ICPMS

U. K. Maity[1,§], P. Bavya[2], K. Ushalakshmi[1], P. Manoravi[1] and S. Viajyalakshmi[1]

[1]*MC&MFCG, IGCAR, Kalpakkam – 603102, India.*
[2]*Stella Maris College, Chennai-600086, India.*
§ Email: ujjwalm4@gmail.com

B isotopic ratio measurement is very important in nuclear industry because it is used as (i) ^{1}n poison (boric acid) in thermal reactor, (ii) a control rod material (B_4C pellet) in fast reactors. Since ^{10}B has higher neutron absorption cross-section, enriched ^{10}B is used in nuclear power plants and the extent of enrichment varies from 50-90%. Therefore, it is essential to determine $^{10}B/^{11}B$ ratio in boric acid and B_4C. B_4C can be dissolved either by fusion using sodium carbonate or by microwave digestion using the mixture of HF, HNO_3 and H_2O_2. Though the interference from ^{12}C is not expected at ^{11}B peak in high resolution inductively coupled plasma mass spectrometry (ICPMS), still to ensure the above fact, investigation for precise determination of $^{10}B/^{11}B$ ratio was carried out using laser ablation (LA) ICPMS. The prime purpose of the present study is to utilize LA-ICPMS for measuring $^{10}B/^{11}B$ ratio both in solution (boric acid & dissolved B_4C) and solid (B_4C pellet) without any pre-treatment so that the difficulty in dissolution or powdering process of B_4C (2nd hardest material) can be avoided and B_4C pellet can be reused. The results obtained from LA-ICPMS were compared with solution ICPMS data. The solution of boric acid (natural abundance) and dissolved B_4C (natural & ~67% enriched isotopic composition) was analysed by ICPMS and LA-ICPMS. B_4C pellet (enriched ~67%) was analysed by LA-ICP-MS. LA-ICPMS has 193 nm ArF laser (matrix independent due to shorter wavelength) and in-house designed multi-sampler which mimics the auto-sampler in liquid sample. The details of LA system and advantages of in-house designed multi-sampler are described elsewhere [1]. For solution, laser was directly focused on the liquid sample and ablated droplets were carried to ICP plasma by Ar carrier gas. Less than 100 µL solution was sufficient for LA-ICPMS analysis.

The results obtained for ^{10}B atom percentage from LA-ICPMS in boric acid and B_4C are comparable with solution ICPMS data [Table 1]. Both precision (relative standard deviation, RSD) and accuracy are better than 1%. A single method (LA-ICPMS) provides ^{10}B atom percentage data with good accuracy and precision in both solid and solution samples without any pre-treatment. Moreover, the method has many advantages over other conventional techniques such as fast, no sample preparation, minimal sample requirement (µg-ng level), almost non-destructive, suitable for highly radioactive samples, negligible radioactive waste generation and insignificant radiation exposure.

Table 1: Atom percentage of ^{10}B measured by ICPMS and LA-ICPMS.

Nat. Abn.	Boric acid		Natural B_4C		Enriched B_4C		
^{10}B (%)	Solution		Solution		Pellet	Solution	
19.89	ICPMS	LA-ICPMS	ICPMS	LA-ICPMS	LA-ICPMS	ICPMS	LA-ICPMS
^{10}B (%)	19.96	19.75	19.98	19.82	67.16	67.25	67.56
SD	0.10	0.13	0.12	0.15	0.25	0.27	0.35
RSD (%)	0.5	0.7	0.6	0.8	0.4	0.4	0.5
Error (%)	0.4	0.7	0.5	0.4	-	-	-

References:

Determination of thorium at trace level in plutonium matrix by total reflection X-ray fluorescence spectrometry

Sangita Dhara[a,b, §,] S. K. Singh[c]
[a]*Fuel Chemistry Division, Bhabha Atomic Research Centre, Mumbai 400085, India*
[b]*Homi Bhabha National Institute, Anushaktinagar, Mumbai 400094, India*
[c]*Fuel Reprocessing Division, Bhabha Atomic Research Centre, Mumbai 400085, India*
[§] Email: sdhara@barc.gov.in

The Plutonium scraps generated during the fuel fabrication process contain a significant amount of Pu which can be recovered, purified and reused as nuclear fuel. The method of Pu purification involves dissolution of the scrap in nitric acid, followed by separation of Pu using TBP. The impurities remain in the aqueous phase and Pu is extracted in organic phase which is further purified and converted to oxide. Thorium is a contaminant which is likely to get incorporated into Pu during this process. The specifications dictate that the PuO_2 for nuclear fuel purpose must contain metallic impurities less than 5000 ppm i.e. 0.5% in PuO_2. Determination of at trace level Th in presence of bulk amount of Pu is a very challenging and tedious task. Inductively Coupled Plasma (ICP) based methods require separation of the major matrix, Pu, for trace determination of Th in it. X-Ray Fluoresence (XRF) methods can be used for such analysis, however, it suffers from severe matrix effect. Further, handling of large amount of sample for XRF analysis (100 mg) requires glovebox [1]. Total reflection XRF (TXRF) is a geometrical variant of XRF having superior features like negligible matrix effect, requires less sample amount (500 ng) and generates very less radio-analytical waste. For development of a TXRF anlytical method, for trace determination of Th in presence of bulk Pu, the preliminary studies were carried out using Th and U samples. The detection limits and recovery rates of Th in presence of bulk U were studied and collodion was used to fix the activity on the quartz sample support. The detection limt of Th in presence of uranium was 40 ng/mL, upto the U concentration of 500µg/ml, and then increased as the U concentration increased. Similar trend was observed in case of the deviation from expected values which increased with increasing U concentration. These observations clearly show the introduction of matrix effect above 500 µg/ml of U in the sample. The analytical results showed a deviation and precision within 10%. After validation of the developed methodology real Pu scrap samples from FRD were analysed for trace Th.

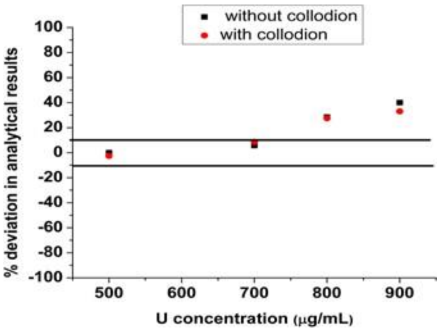

Fig 1: Variation in the recovery rates with U concentration

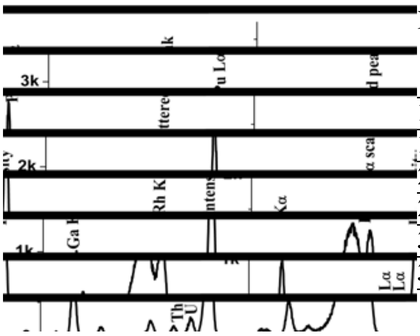

Fig 2: TXRF spectrum of a real Pu sample

Sample No.	Concentration in (µg/ml)	
	Th	Pu
1A	4.1±0.3	130 ± 1
1B	4.4±0.3	133 ±1
2A	3.2±0.3	337±1
2B	4.0±0.3	343±1
3A	7.8± .1	165 ±1
3B	17.2±0.3	349±3

Table1: TXRF analysis results of Th and Pu in samples

Acknowledgements**:** The authors are thankful to Dr. S. Chaudhury, Head Fuel Chemistry Division and Dr. R. V. Pai for their constant support during this work.

References: [1] H. A. Woltermann, R.R. Eckstein, P.L. Redding and S.A. Tomes, *Journal of Nuclear materials*, **54** (1974) 117-120.

Studies on the elemental Concentration determination in protein powder by Instrumental Neutron Activation Analysis (INAA)

Surekha U. Sane[1, §], S. K. Samanta[2,3,§], Tapas Das[1,3]

[1]*Radiopharmaceutical Division, Bhabha Atomic Research Centre, Mumbai – 400085, India*
[2] *Radiochemistry Division, Bhabha Atomic Research Centre, Mumbai – 400085, India*
[3] *Homi Bhabha National Instituite, Mumbai – 400094, India*
[§]Email: sksamanta@barc.gov.in / susane@barc.gov.in

Neutron Activation Analysis (NAA) is widely used in determination of micronutrients and vital elements in dietary items at trace and ultratrace level [1]. Concentration of elements in protein powder has been estimated by NAA. Essential elements important for haemoglobin, normal cellular functioning, synthesis of some hormones and tissue buildup of infants were analyzed by this technique. Breast milk is most important food for growth of infants but, it will give all the elements needed for the first 6 months. At around 6 months, baby will need complementary food which contains iron iodine, zinc and cobalt and other essential elements. Essential elements important for growth, development, normal cellular functioning, and synthesis of some hormones and tissue build up of infants. The main purpose of the present study was to determine some of the elements using Instrumental Neutron Activation Analysis (INAA) technique. In the present investigation, samples, reference standards and control samples were sealed in quartz tubes and irradiated in tray position of Dhruva reactor at an average neutron flux of 0.5 ×1013 cm-2.s-1. The induced activity was measured in a pre calibrated High Purity Germanium (HPGe) detector coupled to MCA and the peak areas were calculated using in-built peak-fit software. It was observed that elements like, Ca, P, Co, Fe, K, Mn, I, Zn, Mg, were present in the samples. Among these elements, Co was found to be in the range of 275 mg kg-1whereas other elements were found to be in the range of 1-280 mg kg-1. It has been observed that Fe concentration is about 185 mg kg-1, indicating these samples are good sources of Fe, may be in the bioavailable form. The study showed that the toxic elements found in the samples were below the levels prescribed by health regulations. The precision and the accuracy of the results were evaluated by analyzing the certified reference materials of leafy origin (Apple Leaves, NIST SRM 1515). The variation in elemental concentration is mainly attributed to the differences in botanical structure as well as in the mineral composition of the soil in which the plants are cultivated. Though the concentrations were in ppm/ppb concentration ranges, they could be determined by this method due to high sensitive nature of INAA at a higher neutron flux. The results will be used for obtaining information on their bioaccessibility in terms essential/toxicity values by calculating regulatory dietary intake (RDI) of each element.

Acknowledgements

Authors are thankful to Dr. S.Kannan, Director, RC&IG, BARC, Mumbai for his kind support and encouragement. Thanks are due to Dr. Archana Mukherjee, Head, RPES, RPhD, and BARC for her support. We also thank operation crews of ROD, BARC and Dr. S.V. Thakare, RPhD for their help in planning the neutron irradiations.

References

1. S.D. Kulkarni et al., NUCAR ,2003, pp-421

Filament surface modifiers in Thermal Ionization Mass Spectrometry for Nd isotope ratio measurement

Preeti Goswami, K. Sasi Bhushan§, Pranaw Kumar and P.G. Jaison

[1] *Fuel Chemistry Division, Bhabha Atomic Research Centre, Mumbai*
§ Email: sasiakp@gmail.com

Precise atom ratio of Nd isotopes is required for obtaining the concentration of fission monitor (^{148}Nd) for the experimental determination of burn-up of spent fuel. The isotope ratio measurement of Nd by TIMS suffers from isobaric interference from Sm at various isotopes e.g. 148, 150. Conventionally, Interfering Element Correction Methodology and two stage ion exchange separations are being employed for minimizing the interference from Sm. Direct analysis of Nd, without chemical separation in nitrate medium has also been carried out based on the difference in the evaporation rates of oxides of Nd and Sm [1]. But, this approach demands exceptionally longer degassing periods for the complete elimination of isobaric interference of Sm. However, as compared to the nitrates, the differences in the volatilities of compounds of Nd and Sm are higher for their chloride as well as carbide species and this may lead to preferential evaporation of Sm over Nd [2].

In this context, single filament assemblies were pre-coated with various surface modifiers such as Graphite (Gr), Graphene Oxide (GO), Nano-Horns (NH) and Porous Carbon (PC), in order to compare their efficiencies in bringing down the isobaric interferences. About 80 µg of each of these modifiers were loaded on filament in acetonitrile medium and degassed at 1A Filament Current (FC) for about half an hour in the ion source under high vacuum conditions. Thereafter, 200 ng of Nd in chloride medium from the synthetic mixture of Nd/Sm ~ 10 was loaded on the above filaments coated with modifiers. Analysis was carried out at various filament currents and the % deviation of measured atom ratios of Nd from the true value was plotted for all the isotope ratios at low and high FCs. It can be seen from Fig. 1 that % deviation from true for all the isotope ratios at lower FCs are larger compared to those measured at higher FCs. Significant bias observed in the atom ratios of Nd at lower FC can be attributed to the partial removal of Sm. At higher FCs, the removal of Sm becomes almost complete and this helps in bettering the atom ratios. From Fig. 1, we can also observe that among all the above surface modifiers PC yielded almost isobaric free ion currents of Nd isotopes even at relatively low FCs and found to be the most suitable for the initial experiments. However, about 0.5% deviation from the true ratio is still observed and this could be corrected by internal normalization using ^{145}Nd/^{146}Nd ratio for samples of natural origin. Studies are in progress to minimize the bias for the non-natural samples such as irradiated nuclear fuels.

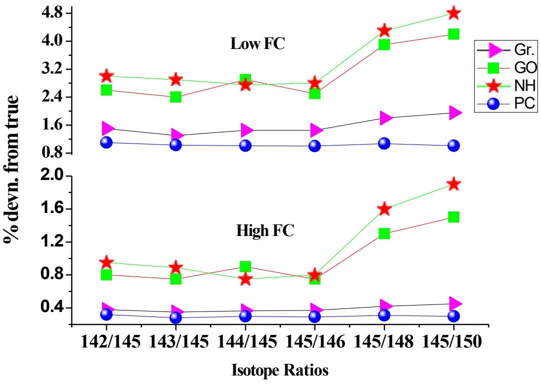

Fig. 1 Effect of surface modifiers on the bias in the isotope ratios of Nd

References:
[1] R. Sajimol et. al., J. Radioanal. Nucl. Chem., DOI 10.1007/s10967-015-4631-2
[2] T. Uda et.al., Science 289(2000) 2326.

Elemental analysis of ceramic insulation materials by INAA

J. S. Brahmaji Rao§,[1], T. Raghunath[2], M. Neelamegam[3], G. V. S. Ashok Kumar[1],
V. Ramakrishna[2], K. Sundararajan[1]

[1]*Materials Chemistry & Metal Fuel Cycle Group, IGCAR, Kalpakkam, India – 603 102*
[2]*Health Physics Division, Bhabha Atomic Research Centre, Mumbai, India*
[3]*Reactor Facilities Group, IGCAR, Kalpakkam, India – 603 102*
§Email: brahmaji@igcar.gov.in

The in-core detectors used in nuclear reactors for neutron flux measurements are usually exposed to the high temperatures around 300°C. The detectors are shielded for thermal and electrical using insulation ceramic spacers and tapes respectively to enhance their durability [1]. The identification of the isotopes produced in the irradiated ceramic insulation materials during reactor operation is important for health physics activities in any radiological surveillance checks and in turn to provide better radiation safety to the operational personnel. In this context, the elemental analysis of ceramic insulation materials using Instrumental Neutron Activation Analysis (INAA) technique was carried out. INAA technique is widely used in anlysing the samples of various matrices using KAMINI research reactor [2] in IGCAR. Around 50 and 100 mg of ceramic spacer powder and tape respectively were taken along with standard reference material (SRM) NIST 1633b coal fly ash. The prepared samples and standard were irradiated in pneumatic fast transfer system (PFTS) position of KAMINI reactor for 4 h at 20 kW. The irradiated samples were cooled for an overnight inside the reactor after its shutdown.

The samples and standards were collected and assayed by high-resolution gamma spectrometry using 30% Baltic HPGe p-type detector connected to 8 k MCA quadADC module and InterWinner 7.0 MCA acquisition software. The acquired spectra were analysed using PHAST gamma spectra analysis software. The counting time was varied from around 4000 to 55000 s, to get better counting statistics. The obtained counting data of various activation products present in the acquired spectra were used in the calculation of INAA and obtained elemental concentration of the irradiated samples. The results of the same for ceramic tape and spacer powder samples were given in the Table 1. In conclusion, INAA technique was found to be the suitable non-destructive technique for simultaneous determination of multi elements in the ceramic insulation materials which otherwise demands stringent quantitative dissolution protocols for conventional wet chemical analytical methods.

Table1. Results of Ceramic materials

Conc. (μg/g) of ceramic materials		
Element	Tape	Spacer
As	884 ± 7	-
Ce	69.26 ± 2.98	-
Cr	13.44 ± 2.05	6.54 ± 1.13
Eu	0.63 ± 0.08	-
Hf	3.77 ± 0.25	-
La	33.71 ± 0.41	-
Na	446 ± 6	337 ± 4
Sb	11.68 ± 0.55	-
Sc	3.79 ± 0.05	-
Ta	1.60 ± 0.12	1.60 ± 0.12
Th	6.72 ± 0.37	-
W	-	0.66 ± 0.17
Zn	-	17.93 ± 2.86

References:
[1] T. Raghunath and V. Ramakrishna et.al, 6th Asian and Oceanic Congress for Radiation Protection (AOCRP6), held in Mumbai, India during 07 - 11, Feb. 2023.
[2] J.S. Brahmaji Rao and E. Senthilvadivu et.al, J Radioanal Nucl Chem 294(2012)137.

Assessment of cement quality via rapid determination of Ca and Si in cement samples using NAA and PIGE methods

Sonika Gupta[1], S. K. Samanta[1,2,§], R. Acharya[1,2,§]
[1] *Radiochemistry Division, Bhabha Atomic Research Centre, Mumbai – 400085, India*
[2] *Homi Bhabha National Instituite, Mumbai – 400094, India*
[§]Email: racharya@barc.gov.in

The compressive strength of cement samples depends on Ca/Si ratio. The compressive strengths of C-S-H pastes increases with decreasing Ca/Si ratio [1]. Thus, it is important to determine Ca and Si content in the samples for its quality assessment. Moreover, Ca/Si ratio influences the micromechanical properties of cementitious materials. Ca/Si ratio varies in the range (0.6 – 1.8). Ca and Si can be quantified using conventional analytical techniques, but nuclear analytical technique (NAT) is known for being non-destructive, highly sensitive and accurate with very low detection limit. Neutron based technique such as Neutron Activation Analysis (NAA) is well-known where samples are irradiated in high neutron flux ~5x10^{13} n/cm^2/s (Dhruva reactor) followed by the radioactive assay of delayed γ-rays (**Figure 1(a)**) using High Purity Germanium (HPGe) detector. Ca has been estimated in cement samples using NAA with short time irradiation (~1 min). Accelerator based technique like Particle Induced Gamma-ray Emission (PIGE) is an online NAT which utilized various nuclear reactions including in-elastic scattering of proton beam for excitation of nucleus followed by the assay of prompt γ-rays (**Figure 1(b)**). Si has been quantified using external PIGE where the beam has been extracted out in air. Mass of about (~200 mg) cement samples were directly packed in mylar foils and irradiated in 3.5 MeV proton beam. Thus both NAA and PIGE techniques are optimized with less turnaround time of analysis. Method validation was carried out using several geological reference materials. In the present work, five cement samples (CT_1 – CT_5) were analyzed for Ca and Si and the results are shown in **Table 1**.

Table 1. Ca and Si concentrations (%)

Sl. No.	**Sample**	**Determined Concentrations (%)**		**Ca/Si Ratio**
		Ca (NAA)	**Si (PIGE)**	
1.	**CT_1**	30.78±1.39	10.88±0.44	2.83
2.	**CT_2**	29.78±1.37	10.59±0.41	2.81
3.	**CT_3**	31.19±1.50	10.02±0.43	3.11
4.	**CT_4**	26.62±1.09	17.38±0.71	1.53
5.	**CT_5**	1.3±0.06	4.98±0.23	0.26

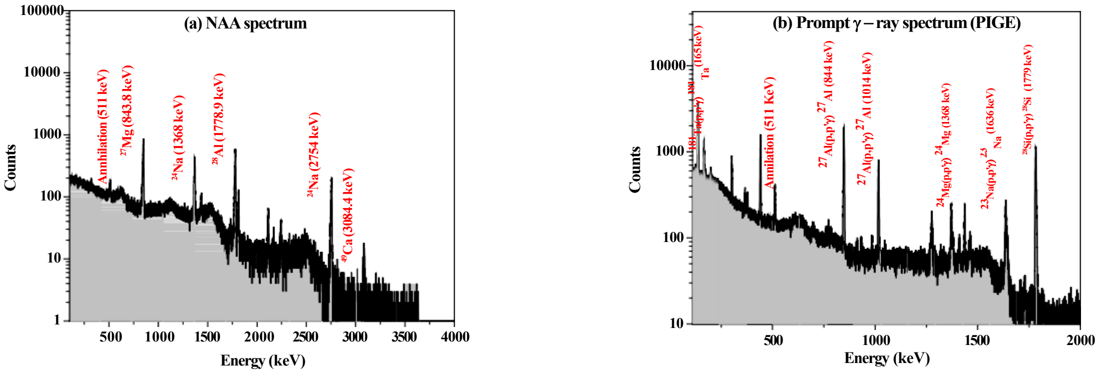

Figure 1 (a) NAA spectrum **(b)** PIGE spectrum for a cement sample

References:

[1] W. Kunther et.al., *Journal of Material Chemistry A,* **5 (2017) 17401**.

Utilization of Pneumatic Carrier Facility of Dhruva reactor for Quality Assurance of INAA by determining elements in CRMs through their short-lived activation products

Sonika Gupta[1], S. K. Samanta[1,2, §], Priya V Mestry[1], R. Acharya[1,2,§]

[1] *Radiochemistry Division, Bhabha Atomic Research Centre, Mumbai – 400085, India*
[2] *Homi Bhabha National Instituite, Mumbai – 400094, India*
§Email: sksamanta@barc.gov.in / racharya@barc.gov.in

Neutron based technique such as Neutron Activation Analysis (NAA) is well-known where samples are irradiated in high neutron flux ~5x10^{13} n/cm^2/s (Dhruva reactor) followed by the radioactive assay of delayed γ-rays (**Figure 1(a)**) using High Purity Germanium (HPGe) detector [1]. Conventional NAA method involves longer decay time after irradiation followed by longer counting period. PCF at Dhruva is air cooled facility used for short time irradiation of samples. The irradiation time is limited to 1 minute. The time limits on irradiation are based on the assessment of temperatures (heating in the sample < 500 mW) and post irradiation dose rate (< 10 R/hr). The facility helps for simultaneous rapid quantification of short-lived isotopes upto ppb level. Mass of about (~ 5 mg) of geological certified reference materials (CRMs) such as RGM, PCC-1, GSP-1, AGV-1, BCR-32 were packed in polythene pouch and irradiated in polypropylene capsules. Quality control parameters (accuracy, precision, sensitivity, detection limit) are studied. Elements such as Na, Mg, Al and Ca are quantified in these CRMs with error (%) within ± 5%, Z-score and Zeta-score within ± 1.5 at 95 % confidence level. The uncertainties in concentration are within ± 5%. **Table 1** shows the determined concentrations in **AGV-1**. **Figure 1** shows the delayed gamma spectrum of AGV-1 irradiated in PCF.

Table 1. Determined concentration of elements in AGV-1

Element	Certified Conc (%)	Obtained Conc (%)	Error (%)	Z-Score	Zeta - Score
Na	3.16±0.09	3.28±0.09	3.8	1.3	0.9
Al	9.07±0.18	9.23±0.59	1.8	0.9	0.3
Mg	0.92±0.06	0.88±0.1	-4.3	-0.7	-0.3
Ca	3.53±0.1	3.63±0.13	2.8	1.0	0.6

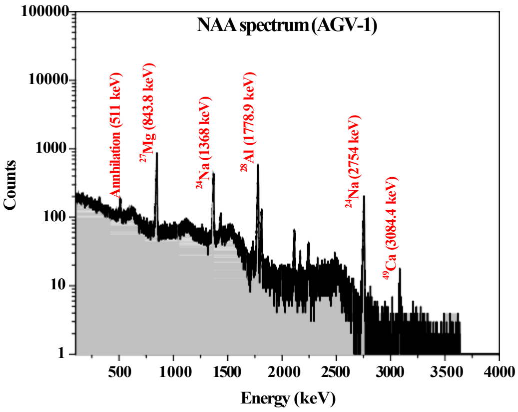

Figure 1. NAA spectrum of AGV-1

Determination of Carbon in Niobium by Charged Particle Activation Analysis (CPAA)

Y. Sunitha[§], G.L.N. Reddy, A.A. Sukumar, D.V. Lakshmipathy, Sk. Jayabun, J.V. Ramana

[a]*National Centre for Compositional Characterization of Materials, Bhabha Atomic Research Centre, ECIL Post, Hyderabad-500062, India*
[§] Email: sunitha@barc.gov.in

Niobium (Nb) and its alloys are candidate structural materials for advanced nuclear (fission) and fusion reactors due to their excellent physical, chemical, mechanical and metallurgical properties. Nb, NbTi and Nb_3Sn exhibit superconducting properties, hence are used in the manufacturing of superconducting magnets. Carbon is an alloying element in some materials, while in others, it may be present as an impurity. Therefore, the determination of carbon in niobium or its alloys is required in the preparation of materials for desired applications. This paper describes the determination of carbon in niobium coupons by charged particle activation analysis (CPAA) using $^{13}C(p,n)^{13}N$ nuclear reaction (Q= −3.0 MeV). Nitrogen-13 is a pure positron (β^+) emitter with a 10 min half-life. Therefore, the 511 keV annihilation photons were detected, through off-line mode for the quantitative analysis.

The coupons of Nb (NFC, Hyderabad) were irradiated at the 3 MV Tandetron (HVEE) facility of NCCCM, BARC, Hyderabad with 4.0 MeV protons (current = ~ 500 nA) for 30-45 minutes in a scattering chamber maintained at a vacuum pressure of 5×10^{-6} torr. Since ^{13}N isotope is short-lived, special arrangements were made for the transportation of the coupons from scattering chamber to an off-line HPGe (efficiency: 36%, energy resolution: 1.78 keV at 1332 keV of ^{60}Co) based detection system within 3-4 minutes after irradiation. High purity graphite was used as the standard. Quantification of carbon was done by comparator method. Charge normalized counts of annihilation photons, duly corrected for delayed counting and the stopping powers of the standard and the sample(s) (calculated by SRIM-2003) were used for quantification.

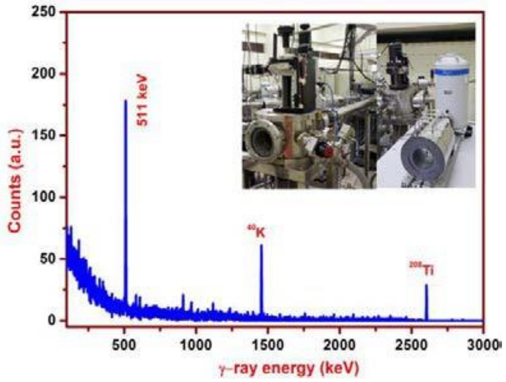

Fig.1 Typical γ-ray spectrum of Nb sample measured off-line after irradiating with 4 MeV protons. Experimental setup for irradiation the coupons and counting are shown in inset

Fig.1 shows a typical γ-ray spectrum of the irradiated coupon acquired by the off-line counting system. The limit of quantification (LOQ) of the method, under the present experimental conditions is 40 μg/g. The content of carbon in a typical Nb coupon on three replicate measurements was determined to be 58.0 ±4 μg/g.

In summary, low energy particle accelerator has been used, to the best of our knowledge for the first time, for the determination of carbon at ≥ 40 μg/g levels in niobium by CPAA. It is facilitated by installing special provisions at the beamline that enables the off-line counting of ^{13}N (short-lived) nuclei, without any significant loss of activity.

Reference(s)

1. C. Vandecasteele, K. Strijckmans, Ch. Engelmann, H.M. Ortner, Talanta **28** (1981) 19-23.

Determination of iodine in water by polarized energy dispersive X-ray fluorescence spectrophotometry: A comparison of Mo, Al_2O_3 and HOPG secondary targets

Y. Sunitha[§], J.V. Ramana

[a]*National Centre for Compositional Characterization of Materials, Bhabha Atomic Research Centre, ECIL Post, Hyderabad-500062, India*
[§]Email: sunitha@barc.gov.in

X-ray fluorescence spectrometry (XRF) is one of most widely used analytical techniques. Compared to conventional XRF, polarized X-ray fluorescence spectrometry (p-XRF) provides higher sensitivity due to reduced background and, therefore, has recently attracted numerous applications. The present paper explores the capability of plane polarized energy dispersive X-ray fluorescence spectrometry (p-EDXRF) in determining iodine, an important micronutrient for human health, in water. Measurements are performed using Mo, Al_2O_3 (Barkla scatterer), and highly oriented pyrolytic graphite (HOPG) (Bragg crystal) as the secondary sources of excitation and their analytical potentials, in terms of limits of detection, linearity and reproducibility, compared to assess their suitability for the detection of iodine in aqueous systems.

The XRF measurements were performed using Spectro Xepos spectrometer (X-Lab^{Pro} 5) equipped with an X-ray tube made up of Pd anode, and Mo, Al_2O_3, and HOPG secondary targets. The standard solutions of iodine were prepared by dissolving potassium iodide (KI) in deionised (DI) water. The typical experimental conditions/ parameters were as follows: sample/standard volume: 7 mL; data acquisition time: 300 s, detector resolution: 125 eV.

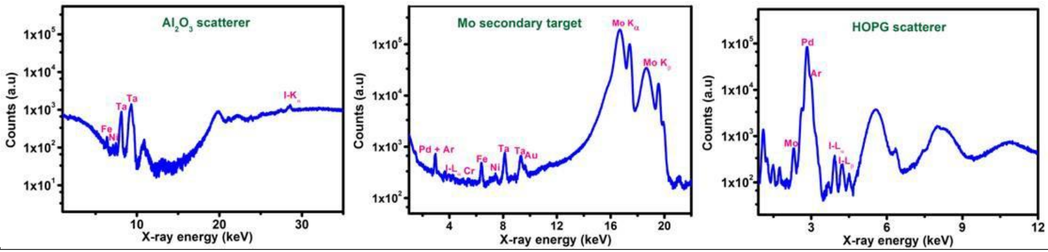

Fig.1 X-ray spectra of the aqueous solution containing 100 µg/mL iodine

Fig. 1 shows the XRF spectra of the aqueous solution containing 100 µg/mL iodine recorded using Mo K-X rays and, Al_2O_3 and HOPG scatterers. The iodine L_α-X-ray (3.93 keV) peak is most prominent in the spectrum acquired with HOPG. It suggests the suitability of only HOPG scatterer for the determination of iodine. Incidentally, the potassium K_α X-rays are not observed in any spectrum due to high background around the relevant energy region. The experiments with the standard solutions in DI showed that HOPG scatterer provides (a) good linearity in 10-1000 µg/mL range (regression coefficient= 0.997), (b) limit of detection (LOD) of 1 µg/mL and (c) ~2% precision at >100 µg/mL and ~ 8% precision at ~ 10 µg/mL levels of iodine. In the case of groundwater (Ca content: 90 µg/mL), the LOD was measured to be ~3 µg/mL. The higher LOD is attributed to the interference from Ca K_β X-rays (4.0 keV). The content of iodine in groundwater samples collected from the surrounding areas was below the detection limit. The method can be adopted for the determination of iodine in food materials and pharmaceuticals in solid form as well.

Reference(s)

1. P. J. Potts, A. T. Ellis et. al, J. Anal. At. Spectrom. 2004, 19, 1397-1419.

Estimation of Essential Trace Elements of Baby Food Samples using PIXE and Comparison of Results with EDXRF: Possible Application of Food Forensics.

Reetta Sara George[1], Arpita Datta[1,§], V. Sharma[2], R. Acharya[2,3]

[1]*Amity Institute of Nuclear Science & Technology, Amity University, Uttar Pradesh-201313*
[2] *Radiochemistry Division, Bhabha Atomic Research Centre, Mumbai - 400 085, India*
[3]*Homi Bhabha National Institute, Department of Atomic Energy, Mumbai – 400094, India*
[§]Email: adatta@amity.edu

Adulteration of infant food supplement has received world-wide attention as this is not only compromises the nutritional quality of the baby food products, but also may bring significant health effect [1-2]. Food forensic of baby food samples is the process of an investigation of food safety and quality control of products to ensure if the nutrients are present as per specification or not. In presented work, PIXE method is utilized to quantify minor and trace elements of mostly used 10 baby food samples due its versatility and high sensitivity. Baby food samples along with two certified reference materials were irradiated by a proton beam of 3 MV and emitted X ray analysis was carried out with Si (Li) detector (ORTEC) using Maestro V7 software. Total of five major elements (Ca, Cl, K, P, S) and seven trace elements (Fe, Mn, Ni, Co, Cr, Sc, Ti) and one toxic elements (Al) were detected [**Fig. 1**]. Method validation was done by analyzing the INCT certified reference materials Tea leaves and mixed polish herb. In the baby food samples, Ca, Cr, Cl, Fe, K, Mn, P, S, Ti are found to be in the range of 0.45-2.14 wt%, 0.50-58.9 mg/kg, 1.19-2.70 wt%, 245-5163 mg/kg, 0.33-2.5 wt%, 0.6-1263 mg/kg, 0.2-0.5 wt%, 0.3-0.7 wt% and 3.5-79 mg/kg respectively. The amount of most of the minor and trace elements contained in the baby food samples are found to be higher than the value specified by the brands as well as permissible limit as per FSSAI [3]. Results obtained using PIXE was also compared with EDXRF and concentration of minor elements like K and trace elements like Fe, Mn and Zn are well matched with the results obtained using PIXE.

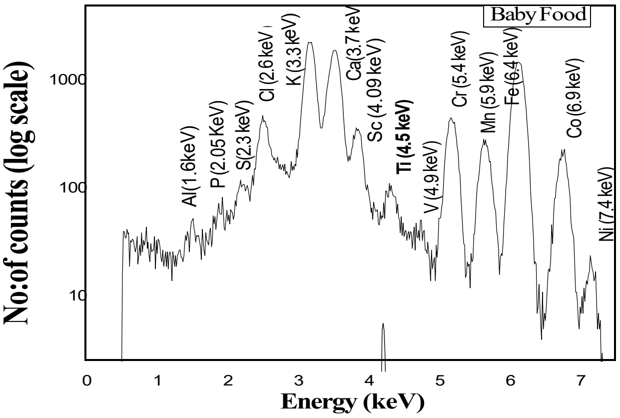

Fig. 1: Typical energy spectrum of baby food sample obtained using PIXE

Acknowledgements: This work is a part of project UGC-DAE-CSR (Mumbai Centre) of AINST, Amity University. Authors thanks Dr P.K. Mohapatra, Head, RCD, BARC for his kind support and encouragement in this work and UGC DAE CSR Mumbai Centre for financial support. Authors sincerely thanks to Operation Crews of IBA facility at IOP, Bhubaneshwar and EDXRF facility at UGC-DAE-CSR Kolkata. Ms. Reetta thanks UGC-DAE-CSR for the financial assistance as a project fellow at Amity University. Mr. V. Sharma is thankful to Dr. H.K. Bagla, Vice Chancellor, HSNC University for encouraging him. He also wants express his gratitude to CSIR, New Delhi for providing senior research fellowship (SRF).

Reference(s):

1. Liu-Yisen et al., Foods, 10 (2021) 785.
2. M. Savin et al, Int. J. Environ. Res. Public Health, 19 (2022) 13452
3. Food Safety and Standards (Foods for Infant Nutrition) Regulations, 2019

Neutron Activation Analysis using PCF Dhruva Reactor for the Determination of Trace Rare Earth Elements (REEs) in bulk REE

Sonika Gupta[1], V. Sharma[1],Pranaw Kumar[2, §], S. Chaudhury[2], R. Acharya[1, §]
[1]*Radiochemistry Division,*[2]*Fuel Chemistry Division, Bhabha Atomic Research Centre,*
Mumbai – 4000845
[§]Email: pranaw@barc.gov.in / racharya@barc.gov.in

High purity rare earth elements (REE)have applications in various fields such as nuclear industries particularly in existing PHWRs and in areas having phosphors and luminescent applications.Dysprosium pelletized with zirconium oxide is proposed to be used for reactivity control in nuclear reactors. For these applications, a stringent are laid down for the purity of the REEs. For example, presence of ^{157}Gd (σthermal=257000 barn & ϴnatural=15.7%)can affect the neutron absorption properties of other REEs. In view of their similar chemical and physical properties, determination of rare-earth elements in bulk of a rare-earth element is a difficult task. Classical methods for the determination of rare earths including gravimetry, complexometry and colourimetry are typically non-selective and hence are useful for the total rare-earths determinations. Multi-elemental analysis techniques such as mass spectrometry, X-ray fluorescence, etc. are capable of determining individual rare-earths with good sensitivity but are susceptible to spectral interferences when these elements are present in mixtures. Chromatographic techniques and solvent extraction are used to minimize the interferences and thus improve the selectivity of analysis [1]. However, these techniques are time consuming, destructive, cumbersome in nature and need blank correction.In order to obviate the stringent sample preparation and spectral interference a simple, non destructive method for the quantification of trace amount of REE in Dy matrix using short lived activation product by neutron activation analysis using Pneumatic carrier facility (PCF) of Dhruva research reactor was optimized. Samples were prepared by drying the different proportion of Dy to REE and irradiated with the high flux reactor neutrons (~10^{13} neutrons cm^{-2} s^{-1}) for 1 min [2]. Typical gamma-ray spectrum of REEs irradiated with neutron flux for a 1 min using PCF of Dhruva is shown in the **Figure 1**.Radioactive assay was carried out using HPGe detector of 50% relative efficiency. Quantification of REEs (e.g. Eu and Gd) was carried out by comparing the count rate of sample and standards after correcting the self absorption within a sample. Further, this approach will be utilized for the quantification of REEs in real samples.

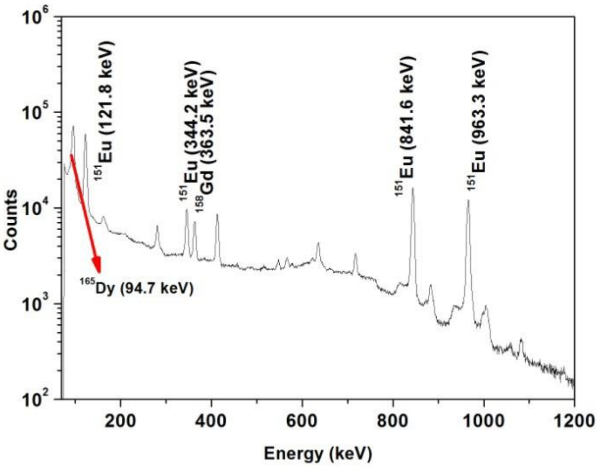

Figure 1: Typical gamma-ray spectrum neutron irradiated REEs samples for a 1 min using PCF of Dhruva

Acknowledgements: Authors thank Director, Reactor Group, Head, ROD, BARC, RS, Dhruva and operation crews of Dhruva reactor for their support and co-operation during experiment.

References: [1] P. Kumar et. al., J. Liq.Chromatogr. Rel. Technol. 36 (2013)1513.
[2] Acharya et al., J. Radioanal Nuc. Chem. 302 (2014) 1525-1530.

Determination of Hydrogen Content and its Possible Buildup in the DDUO$_2$ Pellets using Glove Box Adapted Twin Determinator System

Seema Raul, Revati Gaikwad, Rakesh Pandey, Namrata Kumar, D.R. Raut, Ashish Pandey, Anoop Kelkar[§], T.P. Valsala, D.B. Sathe, R.B. Bhatt

Fuel Fabrication, INRP(O), Nuclear Recycle Board, , B.A.R.C., Tarapur - 401502, India
[§]Email : anoop@barc.gov.in

Fabrication of deeply depleted uranium oxide (DDUO$_2$) fuel pellets is being regularly carried out at Fuel Fabrication (FF), INRP(O), B.A.R.C, Tarapur, India. Hydrogen is one of the critical impurity in said fuel pellet with allowed limit of 3 ppm for PFBR as it may combined with coolant sodium to form the sodium hydride resulting in deterioration of reactor performance. Therefore, extreme care is taken to keep hydrogen content within the specification limit. During fabrication process, pellets gets exposed to glove box atmosphere for certain time period where sorption of hydrogen can takes place on fuel pellets. The present work has been taken up to study this hydrogen build up in DDUO$_2$ pellets.

Determination of hydrogen content, has been carried on glove box adapted ONH Determinator (Twin determinator). Instrument uses inert gas fusion technique and an impulse furnace with temperature > 3000ºC to analyze hydrogen content with extra pure (> 99.995%) nitrogen gas as carrier. Thermal conductivity cell and infrared measuring cells detects the released gases. For the O-H mode out gassing temperature was set as 1850ºC & analysis temperature was 1650ºC respectively [1]. Hydrogen detection range at 300 mg sample is 0.1 – 3ppm for lower side and 1-3000ppm for higher content. System calibration was done by extra-pure He gas and SS standards. In general relative standard deviation (RSD) was 0.16% for n=7 and accuracy was7% for SS standards of H conc. 2.40±0.80 ppm level.

For study, required number of DDUO$_2$ pellets of single batch were taken and divided into three sets. One set containing required number of fuel pellets have been kept under air tight SS container inside glove box while for other set of DDUO$_2$ pellets, lid was kept open resulting the open exposure to glove box atmosphere to the pellets. In third case, 8 Sintered pellets were dipped in 50mL distilled water for 10 minutes and kept in glove box environment for drying. Out of this, 6 dry pellets were degassed at 150°C at 10^{-2} torr for 4 hours while 2 dry pellets were heated at 150°C for 4 hours where the hydrogen content found were 0.45 ± 0.10 and 0.45 ± 0.11 respectively revealing negligible hydrogen uptake as initial value were 0.35 ± 0.03 for sintered and 0.45 ± 0.10 for degassed pellet. Table 1 presented the data for first two sets where also, negligible hydrogen uptake was observed. It's very important from the storage point of view as it reveals the very good quality control during each & every stage of fuel fabrication and assures the qualitative storage of pins for required time period without rise in hydrogen content.

Table 1: Hydrogen content in DDUO$_2$ pellet as a function of storage

Day	Hydrogen, (ppm)	Remark (Closed system)	Day	Hydrogen, (ppm)	Remark (Open system)
0	0.35 ± 0.03	*Avg. of two sintered pellets*	0	0.45 ± 0.10	*Avg. of two degassed pellets**
7	0.27	*Single sintered pellet*	5	0.44 ± 0.14	*Avg. of two degassed pellets**
15	0.46	*Single sintered pellet*	**:- Degassed at 150°C at 10^{-2} torr for 4 hours.*		
30	0.59 ± 0.07	*Single sintered pellet crushed into two parts and analysed*			

Reference:
[1] D.R. Raut *et al*, *In the Proceedings of NUFUC-2022 (2022) 113.*

Extraction of U (VI) by iminodiaceic acid functionalized mesoporous silica

B.Robert Selvan[§] , A.S.Suneesh, M.Amutha Suba, N.Ramanathan

Fuel Chemistry Division, MC&MFCG
Indira Gandhi Centre for Atomic Research, Kalpakkam, India
[§]Email: robert@igcar.gov.in

Uranium, the integral element of the nuclear energy program as a nuclear fuel, yields energy by atomic fission. There has been an enhanced interest in separating uranium from seawater as its land-based conventional mines have limited availability and the enhanced requirement of nuclear reactor-based power plants. Uranium separation from seawater is challenged by its lesser abundance and competitive chemical behavior with other interfering elements. A separation system exhibiting high separation efficiency from seawater needs a sophisticated uranium-selective ligand. In this context, we developed iminodiacetic acid-functionalized mesoporous silica (MS-IDA) to selectively remove uranium from aqueous solutions similar to seawater, wherein uranium concentrations will be of the order of a few ppb or lower [1,2]. The definitive surface area offered by mesoporous silica and the increased tendency of iminodiacetic acid to complex with uranium is responsible for the enhanced separation.

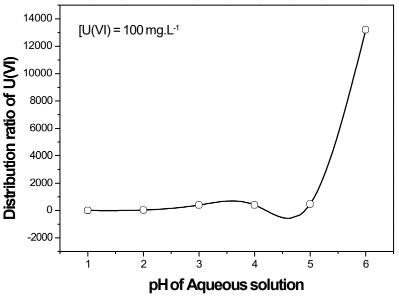

Fig. 1: Distribution ratio of U (VI) at various pH

Functionalization of iminodiacetic acid on mesoporous silica was carried out by chemical modification reactions. Mesoporous silica was initially prepared by hydrolysis of tetra ethoxy silane using water in the presence of CTAB. The above-prepared mesoporous silica was further transformed into amine-functionalized silica by reacting with (3-Aminopropyl) triethoxysilane. The amino-functionalized silica was reacted with iminodiacetic acid to form the adsorbent, iminodiacetic acid functionalized silica (MS-IDA).

The adsorption tendency of MS-IDA on uranium separation was carried out from an aqueous phase varying from pH 1 to 6. For this purpose, 100 ppm of uranyl solution in acetic acid-sodium acetate buffer was employed as an aqueous phase for the adsorption studies. The removal efficiency of uranium from the aqueous phase was measured based on the uranium present before and after the contact with MS-IDA. Uranium concentrations in the aqueous phase were measured by UV-Visible spectrophotometry, using Arsenazo-III as a coloring indicator. Figure 1 shows the adsorption behavior of uranium from the aqueous phase. Since the adsorption of uranium by MS-IDA could be guided based on the ion exchange of uranium, as seen in figure 1, the adsorption tendency was expected to increase pH in the aqueous phase. The adsorption trend in Figure 1 indicates that maximum uranium adsorption was observed at pH 6. Based on the above studies, the preliminary observations indicated that MS-IDA can remove uranium from sub-micron uranium-bearing feeds similar to seawater. However, more studies must be conducted to establish the suitability of using MS-IDA for uranium recovery.

References:

[1] J.Huynh et.al., *ACS Applied Materials & Interfaces,* 9 , 18 (2017) 15672
[2] F.Zhang et. al., *Journal of Hazardous Materials* , 435 (2022) 129022.

Method for estimation of ^{99}Tc activity content in low level liquid waste generated during Geltech (^{99}Mo/^{99m}Tc) generators production at RPL, BRIT.

A.S. Chindarkar[1§], D.K. Sawant[1], S.V. Chavan[1], Ranjit Sharma[1],
Abhishek K. Sharma[2],Balender Singh[2],Ajay Thamke[2], N. Jaychandran[2]

Bhabha Atomic Research Centre[1], Mumbai 400085, India
Board of Radiation and Isotope Technology[2], Vashi, NaviMumbai 400703, India
[§] Email: amitsc@barc.gov.in

Geltech generator facility of Radiopharmaceutical laboratory (RPL), BRIT, Vashi produces ^{99}Mo/^{99m}Tc Gel generators for^{99m}Tc based Radiopharmaceuticals. This generator is produced using neutron activated Sodium Molybdate(^{99}Mo) solution along with fission- based Sodium Molybdate (^{99}Mo) solution for desired specific activity. Every production batch of Geltech generator creates about 5 to 8 litres of low level aqueous liquid waste having beta gamma emitters like ^{60}Co, ^{134}Cs,^{65}Zn and ^{99}Tc (Refer1). Liquid waste of each production batch is collected separately. ^{99}Tc is pure beta emitter having maximum beta energy of 294 KeV and physical half-life of 2.13x10^{5} years. To comply with regulatory limits of effluent discharge, it is necessary to quantify ^{99}Tc content of liquid waste. Method for separation and quantification of ^{99}Tc content in this low level liquid waste is discussed here.

Method for separation and quantification of ^{99}Tc:

10 ml representative sample of liquid waste was taken and ^{99}Tc is extracted at $_{p}$H = 10 in equivalent volume of Methyl Ethyl Ketone (MEK) by solvent extraction. Gamma spectrometric analysis of both organic (MEK-^{99}Tc) layer and aqueous waste layer was done with HPGe detector. Vial with MEK-^{99}Tc solution was dried under IR lamp. 1 ml of distilled water and Dioxane based cocktail was added to this vial and ^{99}Tc was quantified in pre-calibrated liquid scintillation counter (LSC). Efficiency calibration of LSC was done using in-house ^{99}Tc standard.

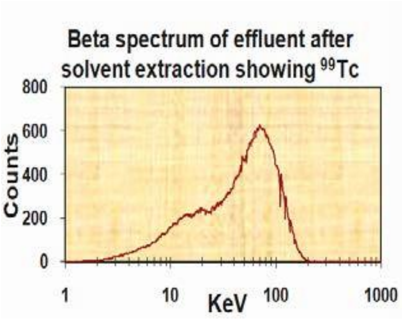

Figure: 1

Result and discussion:

HPGe based gamma spectrometric analysis of 10 liquid waste batches prior to solvent extraction process showed average concentration of ^{134}Cs, ^{60}Co and ^{65}Zn as 3.95, 16.56 and 0.34 Bq/ml respectively. Solvent extracted MEK-^{99}Tc solution of individual waste batch showed 96 % to 97.8 % reduction in these gamma impurity levels. Solvent extraction recovery yield of ^{99}Tc in spiked aqueous sample was observed to be 94%. In Fig.1, beta spectrum of solvent extracted liquid waste samples showed a spectral shifting of typical ^{99}Tc peak from 98KeV to 70KeV, due to hydrolysed pertechnate ions of ^{99}Tc. The area under beta spectrum showed efficiency of 92%. ^{99}Tc content in 10 effluent batches varied from 2.51 ± 0.89 Bq/ml to 18.93 ± 1.61 Bq/ml. The average ^{99}Tc content in ten liquid waste batches was 10.31 ± 1.29 Bq/ml.This method effectively separates ^{99}Tc from other beta gamma emitters of Geltech liquid waste and can be used for quantification of ^{99}Tc in liquid waste.

References:

[1] D.K. Sawant et.al " Regulatory aspects in liquid effluent generated during the production of the novel ^{99m}Tc Gel Generator System developed at BRIT" IARP conference 2010.

Standardization of various parameters for the estimation of Iodine by Gas Chromatography-Electron Capture Detector (GC-ECD)

A. Arul Kumari, J. Vithya, Debasish Saha[§], K. Sundararajan
RCSSS, Analytical Chemistry and Spectroscopy Division, FMCG, MC&MFCG, Indira Gandhi Centre of Atomic Research, Kalpakkam, Tamil Nadu-603 102, India
[§]Email : dsaha@igcar.gov.in

^{131}I (8.02d) and ^{129}I (16.1x10^{6} a) radioisotopes poses environmental hazards in case of nuclear fallout as it concentrates in thyroid and deliver radiation dose. It is essential to install iodine traps in the exhaust stack before it gets discharged to the environment. Various experiments are in progress to find out suitable iodine traps either by physisorption or by chemisorption mode. All this experimental efforts require efficient chemical method for the estimation of iodine in various samples. Redox titration, ICP OES, ICP MS, GC-ECD etc. are few techniques that are in use for the estimation of iodine[1]. In this study we have used GC-µECD system (M/s YoungIn, Korea). GC-ECD technique offers advantages over other techniques as it can be used for the estimation of total iodine as well as can offer information about various species of iodine present in the sample.

In this work, we have estimated iodine (b.p. 184°C) by derivatization with acetone (b.p. 56°C), which forms iodoacetone (b.p. 163°C) [2-3]. The operating condition of the GC-ECD was as following: column stationary phase: CA5, 5% phenyl methyl silicone, capillary injector temperature 300ºC, oven temperature 70ºC, mobile phase (UHP N_2) flow rate 1 mL/min, column length: 30m, film thickness: 0.25µm, ID: 0.25mm, µECD temperature: 300ºC. Elevated temperature of capillary injector vaporises acetone as well as iodoacetone and due to the flow of mobile phase and oven temperature they were eluted out from the column and finally reaches µECD, where they are detected. Chromatogram and calibration graph can be seen from Fig1 and 2. The present method can be used for the estimation of iodine in various matrices as well as towards the standardization of suitable radioiodine traps in the field of nuclear safety. Since this facility is available in a shielded facility for radioactive sample analysis, this system is suitable for the analysis of toxic iodine compounds e.g. methyl iodide as well as radioactive iodine.

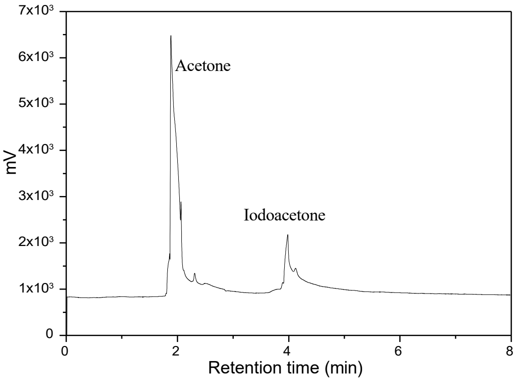

Fig.1: GC-µECD Chromatogram for the assay of Iodine.

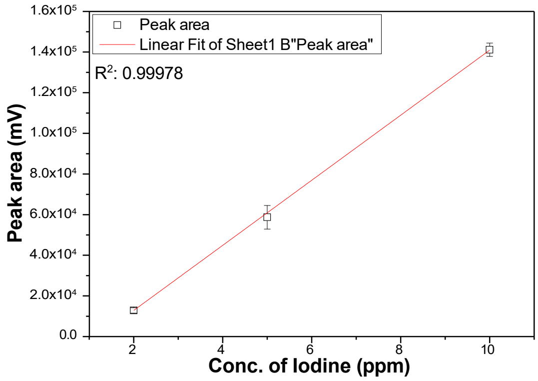

Fig.2: Calibration graph for the determination of Iodine using GC-ECD.

Reference

[1] Shelor, C. Phillip, and Purnendu K. Dasgupta. Analytica Chimica Acta 702.1 (2011): 16-36.
[2]Haynes, William M. CRC handbook of chem. and physics. 97th Ed., CRC press, 2016, p3-320.
[3] Christopher M. Timperley et al, Table S1. RSC Adv., 2018, 8, 41731

Quantification of Micronutrients in the Baby Food Samples by INAA utilizing high flux reactor neutrons from Dhruva reactor

Arpita Datta[1, §], Reetta Sara George[1], V. Sharma[2], R. Acharya[2,3]
[1]*Amity Institute of Nuclear Science & Technology, Amity University, Uttar Pradesh-201313*
[2] *Radiochemistry Division, Bhabha Atomic Research Centre, Mumbai - 400 085, India*
[3]*Homi Bhabha National Institute, Department of Atomic Energy, Mumbai – 400094, India*
[§] Email: adatta@amity.edu

Quality control of baby foods in terms of authenticity is mandatory under the quality assurance of infant food supplements to prevent food fraud as insufficient quantity of the nutrients can affect the growth and development of the infant. On the other hand, if these nutrients are present in higher amount from specified, can induce toxicity. Adulterated baby foods in terms of presence of toxic elements like As, Pb, Hg is an alarming situation due to sever health effect [1-2]. So, the evaluation of elemental profile of essential micro-nutrients like Ca, Cu, Fe, Mn, Se, Mn and Zn in the baby foods is important to confirm whether these are as per specifications or not [3]. In view of this, some of baby food products are analyzed by INAA for food forensic study. Ten branded baby foods were collected and irradiated using reactor neutrons (~10^{13} n/cm^2/sec) along with two INCT CRMs using self-serve facility of Dhruva reactor for quantification of essential trace elements. Typical gamma-ray spectrum of baby food irradiated for 5 h in self-serve facility of Dhruva is shown in **Fig. 1**. Total of 12 elements namely Na, K, Ca, Sc, Cr, Fe, Co, Zn, Rb, Cs, Br and Eu are identified in the samples. Method was validated by analyzing the biological certified reference material i.e. INCT Tea leaves (as reference standard) and INCT mixed polish herb as control sample. All the determined elements are found in the range as Na (311-889ppm); K (0.51-1.6%); Ca (0.49-1.13%); Sc (0.46-3.1ppb); Cr (0.09-0.13ppm); Fe (2.5-98ppm); Co (22-162ppb); Zn (28-44ppm); Rb (2.5-22ppm); Cs (6-34ppm); Br (4-65ppm) and Eu (1.8-5.7ppb) in all the analyzed baby food samples. Br and Rb are considered as toxic contaminant in baby food samples.

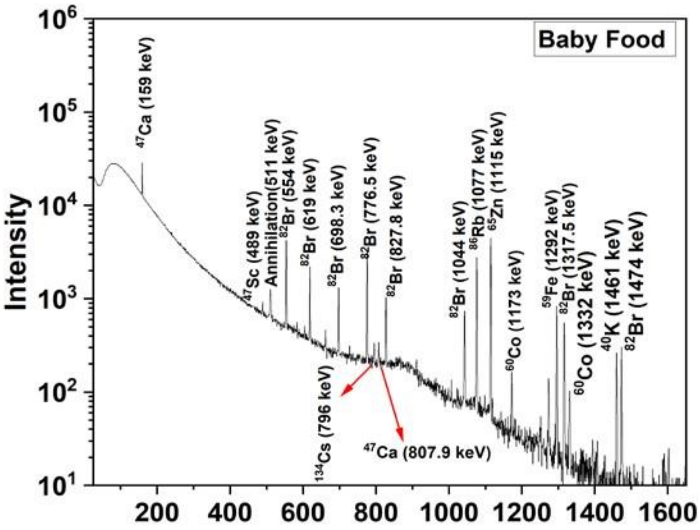

Fig 1: Typical gamma-ray spectrum of baby food sample irradiated for 5h using self-serve facility of Dhruva reactor

Acknowledgements: This work is a part of project UGC DAE CSR (Mumbai Centre) of AINST, Amity University. Authors are sincerely thanks to Operation Crews of Reactor Group; Dr. S. Kannan, Director, RC&IG and Dr. P.K. Mohapatra, Head, RCD, BARC. Ms. Reetta thanks UGC-DAE-CSR for the financial assistance as a project fellow at Amity University. Mr. V. Sharma is thankful to Dr. H.K. Bagla, Vice Chancellor, HSNC University for encouraging him. He also wants express his gratitude to CSIR, New Delhi for providing senior research fellowship (SRF).

Reference(s): 1. Liu-Yisen et al., Foods, 10 (2021) 785-800. 2. Anita Mielech et al., Nurtients, 13 (2021) 2358-2379. 3. A. Datta et al, J Radioanal Nucl Chem 325 (2020) 967-975.

Fission product ^{95}Zr corrections for Zr analysis in U-Zr alloy samples by Instrumental Neutron Activation Analysis

J. S. Brahmaji Rao[1], G. V. S. Ashok Kumar[§,1], D. Venkata Subramanian[2], M. Elumalai[3], K. Sundararajan[1]

[1]*Materials Chemistry & Metal Fuel Cycle Group,* [2]*Reactor Design and Technology Group,* [3]*Reactor Facilities Group, IGCAR, Kalpakkam, India – 603 102*
[§]Email: gvs@igcar.gov.in

U-Zr and U-Pu-Zr metallic alloys are considered as nuclear fuel for future fast breeder reactors (FBRs) in India. These alloys consist of 6-10% of zirconium to increase their melting temperature. Fabrication of metallic slugs involves the preparation of alloy from pure metals, melting of prepared alloys and injection casting at high pressure. It has been decided to use U-6wt%Zr alloy for developing the technologies like fuel slug fabrication [1]. However, the chemical analysis of prepared U-Zr slugs for their homogeneity is a challenging task and potential concern. The various analytical techniques can be employed to analyze their individual elemental composition. Neutron activation analysis (NAA), is a nondestructive analytical technique for the analysis of prepared U-Zr alloys.

NAA is regularly being practiced in IGCAR for variety of samples using KAMINI research reactor [2]. North thimble location of the reactor was chosen for carrying out NAA which is having high neutron flux in the order of 10^{10} $cm^{-2}s^{-1}$ among the allowed locations for analyzing uranium rich samples. However, the analysis of zirconium in U-Zr samples required corrections from fission of ^{235}U. To determine the correction factors, various in-house prepared standards having 1 to 15 mg of uranium were irradiated. The overnight cooled samples which showed a maximum radiation dose of 15 μSv/h were taken for counting using 150% BSI p-type HPGe detector and the spectra were analyzed using BARC developed PHAST peak fitting software. The fission product ^{95}Zr was taken due to its relative long half-life and calculated the corrected CPS by normalizing activity to the end of irradiation. Corrected CPS as a function of uranium standard concentration was plotted and presented in Fig.1 which showed R^2 as 0.99. The fission product ^{95}Zr correction factors are known from the plot for analyzing Zr content in the samples of U-Zr metallic slugs using KAMINI reactor. The study confirmed that the response function (corrected CPS) is linear and hence can be applied for analyzing U-Zr samples having similar weight as that of uranium standard used for fission product correction. Similarly, activities of various other fission products which can interfere in their elemental analysis (Mo, Ce, Sm etc.) in presence of uranium were also studied.

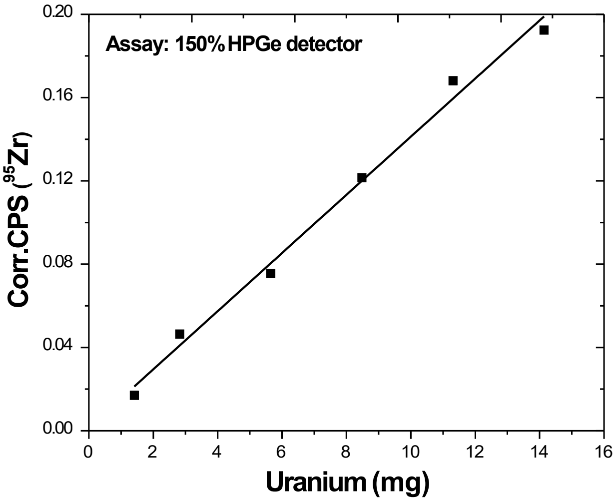

Fig. 1 Corrected CPS as a function of uranium concentration

References:

[1] https://wwwpub.iaea.org/MTCD/Publications/PDF/SupplementaryMaterials/P1665CD/Track5_Fuels.pdf, visited on dated 14.02.2023

[2] J.S. Brahmaji Rao and E. Senthilvadivu et.al, J Radioanal Nucl Chem 294 (2012) 137.

Fusion-Fission and Quasifission lifetimes of fusion reactions attempted to synthesize the superheavy element Z=120

N.Manjunatha[1&2], N. Sowmya[1,§], H C Manjunatha[1,§], T. Ganesh[2]

[1]*Department of Physics, Government College for women, Kolar-563101, Karnataka, India*
[2] *Rajah Serfoji Government College (Autonomous), Thanjavur-613005, Tamilnadu, India*
Affiliated to Bharathidasan university, Tiruchirapalli-Tamilnadu
[§] Email: manjunathhc@rediffmail.com, sowmyaprakash8@gmail.com

Numerous nuclear phenomena, including deep inelastic, complete fusion, fast fission, fusion-fission, quasifission and particle evaporation, result from the collision of two heavy nuclei. The formation of the excited and rotating dinuclear system is a crucial stage for all channels. Typically, two heavy ions that collide go through three phases of evolution. The first step is the capture mechanism. Secondly, formation of an asymmetric dinuclear system (DNS) and The DNS's binary decay, also known as the "quasi-fission process, is the final stage in crossing the "quasi-fission barrier on the radial distance. Earlier studies show detailed investigation of quasifission and fusion-fission lifetimes [1–5]. Since the quasifission and fusion-fission processes are also hindrances in the formation of superheavy nuclei, We investigated fusion reactions such as ^{59}Co+^{237}Np, ^{55}Mn+^{243}Am, ^{50}Ti+^{249}Cf, ^{51}V+^{249}Bk, ^{58}Fe+^{244}Pu, ^{64}Ni+^{238}U, and ^{54}Cr+^{248}Cm that were attempted to synthesize the SHE Z=120. This motivated us to investigate quasifission and fusion-fission systematics for the SHE Z=120. The quasifission lifetimes are evaluated as follows:

$$\tau_{qf} = \frac{1}{\lambda_{qf}} \tag{1}$$

and

$$\lambda_{qf} = \frac{\omega_m}{2\pi\omega_{qf}}\left(\sqrt{\left(\frac{\Gamma}{2\hbar}\right)^2 + \omega_{qf}^2} - \frac{\Gamma}{2\hbar}\right)\exp\left(-\frac{B_{qf}(Z, A,\ )}{\Theta_{DNS}(Z, A)}\right) \tag{2}$$

The fusion-fission lifetime is given by $\tau_{ff} = \frac{1}{\lambda_{ff}}$

$$\lambda_{ff} = \frac{1}{2\pi}\left(\sqrt{\left(\frac{\Gamma_o}{2\hbar}\right)^2 + \omega_{qf}^2} - \frac{\Gamma_o}{2\hbar}\right)\times\exp\left(-\frac{B_f(Z, A,\ )}{\Theta_{DNS}(Z, A)}\right) \tag{3}$$

And the above formulae were evaluated as explained in the literature [1-3].Figure 1 shows a plot of quasifission and fusion-fission lifetimes as function of different projectiles for the synthesis of SHE Z=120. It has been observed that the τ_{qf} are in the order of zeptoseconds (zs) and τ_{ff} are in attoseconds (as). The larger τ_{qf} and τ_{ff} lifetimes were observed for the fusion reaction ^{59}Co+^{237}Np. Hence, quasifission and fusion-fission process are less pronounced for the fusion reaction of ^{59}Co+^{237}Np. Hence, further microscopic investigations were required to predict evaporation residue cross-sections for the fusion reaction of ^{59}Co+^{237}Np. Hence, it finds its importance in the study of quasifission and fusion-fission lifetimes in the SHE Z=120.

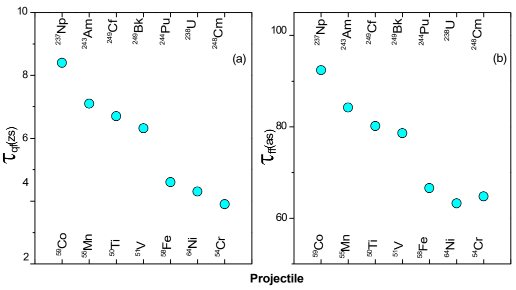

Fig. 1: (a) A plot of quasifission lifetimes (b) fusion-fission lifetimes as a function of different projectiles.

References:
[1] S. Soheyli and M. V. Khanlari, *Phys Rev C*, **94**, 034615 (2016).
[2] Khanlari, M. et al., *Phys Rev* ***C*** **95**, 024617 (2017).
[3] H. C. Manjunatha, et al., *Phys. Rev.* ***C*** **103**, 024311(2021).
[4] P. S. Damodara Gupta, et al., *Pramana-J of Phy*, (2022).
[5] P.S.Damodara Gupta, et al., *Phys. Rev.* ***C*** **106**, 064603 (2022).

Non-destructive determination of uranium and plutonium in annular (U, Pu)O_2 mixed oxide sintered pellets using Matrix Matched Standard by WDXRF Spectrometer

A. Pandey[1,] , M. Singh[1],D. L. Meena, Lopamudra Pradhan, Aakash ranjan, Anoop Kelkar[1§],
T. P. Valsala, D. B. Sathe[1] and R. B. Bhatt[1]
[1]*Fuel Fabrication, Bhabha Atomic Research Centre, Tarapur 401502, India*
Email: anoop@barc.gov.in

FF Plant at Tarapur is fabricating annular (U, Pu)O_2 Mixed Oxide (MOX) sintered pellets in a definite compositions using conventional powder metallurgical route to be used in FBRs. After fabrication, chemical quality of sintered MOX pellets is checked in terms of fissile content, impurities (metallic and non-metallic), stoichiometry etc. to assess whether the fuel can deliver the expected output without failure. The analysis of U and Pu in sintered (U, Pu)O_2 MOX pellets is a very important step to check the fissile content and must be done accurately. U and Pu in sintered MOX pellets are determined by using Davies & Gray and Drummond & grant method respectively. Earlier, in our laboratory, we have developed WDXRF based methodology for quick and non-destructive determination of U and Pu in annular MOX sintered pellets using homogeneously blended calibration standard powders pressed with hydraulic press [1].

In the present work, the suitability of WDXRF for direct non-destructive determination of uranium and plutonium in annular (U, Pu)O_2 MOX sintered fuel pellets has been studied using matrix matched calibration standards in the form of annular (U, Pu)O_2MOX sintered pellets. U(wt%) and Pu (wt%) in the sintered standards were in the range 65.71-69.29 % and 20.46-22.28% respectively. The U and Pu values were obtained by conventional potentiometric titration. U or Pu (wt%) were plotted against the corresponding analytical line intensity ratio (U L_α or Pu L_α). The calibration equation obtained for U & Pu was $y=0.2301*x-12.28$ (R-square =0.9597)& $y=0.018*x-0.058$ (R-square =0.9928) respectively. Sintered MOX pellets were analyzed directly using WDXRF by means of calibration plots. The WDXRF results were compared with the conventional potentiometric methods used for quantification of U and Pu in sintered (U, Pu)O_2 MOX samples after their dissolution and were found in good agreement some of the results are shown in table1.

Table 1.

Sample No.	U (wt%) by WDXRF (x̄ ± 2σ)	U (wt%) by Titration (x̄ ± 2σ)	Pu (wt%) by WDXRF (x̄ ± 2σ)	Pu(wt%) by Titration (x̄ ± 2σ)
1	66.97±0.09	67.36±0.11	20.78±0.09	20.62±0.06
2	67.82±0.15	67.28±0.12	20.01±0.13	20.37±0.10
3	67.80±0.12	67.82±0.15	20.02±0.10	20.06±0.08
4	67.85±0.11	67.72±0.10	19.98±0.09	19.87±0.06
5	67.18±0.13	67.34±0.13	20.58±0.13	20.39±0.10

References:

[1] Pandey A, Khan FA, Kelkar A, Purohit P, Kumar Pradeep, Kumar Vijay, Sathe DB, Bhatt RB, Behere PG ; J Radioanal Nucl Chem 326 ((2020):423.

Chemical characterization of sodalime glass by PIGE and INAA methods for the preparation of *in house* glass reference material

Vishal Sharma[1], R. Acharya[1,2,§]
[1] *Radiochemistry Division, Bhabha Atomic Research Centre, Mumbai – 400085, India*
[2] *Homi Bhabha National Instituite, Mumbai – 400094, India*
[§]Email: racharya@barc.gov.in

Chemical characterization of glass samples is important in various fields including material science, archaeological and Forensic studies [1-6]. Among various classes of glass samples, soda-lime is ubiquitously applied or utilized in day to day life and mainly composed of Si-Na-Ca along with minor and trace elements including transition elements and rare earth elements. Chemical characterization of glass samples using suitable analytical technique or optimization of new methodologies required the analysis of a matrix matched certified/standard reference materials (CRMs/SRMs). These RMs procured from various agencies including NIST are not readily available or otherwise costly. So, every institute are encouraged to prepared in house reference materials using already standardized methodologies. In view of this, a big piece of soda-lime glass (automobile windshield glass) is procured from market and cut into the various small pieces for its chemical characterization using nuclear analytical techniques. Out of these, ten different pieces were analyzed by External (in-air) Particle Induced Gamma-ray Emission (PIGE) method utilizing 3.75 MeV proton beam from particle accelerator FOTIA, BARC for quantification of major elements like Si, Mg, Al and Na and Instrumental NAA (INAA) for quantification of major (Na, Ca, Fe) and 15 minor and trace elements obtained from irradiating the sample for 5h in high flux reactor neutrons [1-6]. Figs. 1 and 2 shows the typical gamma-ray spectra of soda-lime glass analyzed by PIGE and INAA. Concentrations of 18 elements: Na, Ca, Sc, Cr, Fe, Co, Zn, Ba Rb, Cs, La, Ce, Eu, Yb, Hf, Sm, Ta and Th were determined, in which Na, Ca and Fe are in percentages and other elements are in trace level (ppm). Average results were obtained from a replicate (n=10) sample analysis and the associated uncertainties (at ±1s) are expressed in terms of standard deviation and are found to be in the range of 1-7%. NIST SRM 610, 620 and geological CRMs were analyzed for validation of methods. Further, replicate samples will be analyzed by other radioanalytical techniques namely ED-XRF, DC Arc AES and ICP-OES for assuring the quality of the results.

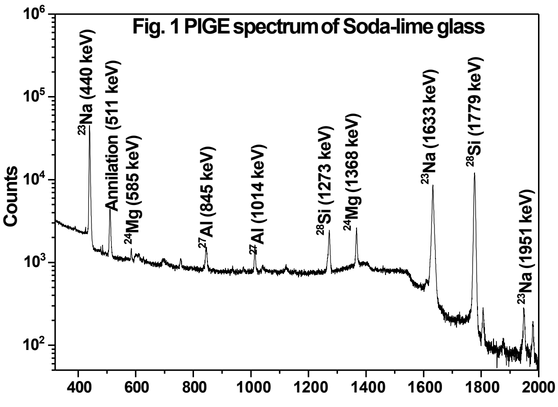

Fig. 1 PIGE spectrum of Soda-lime glass

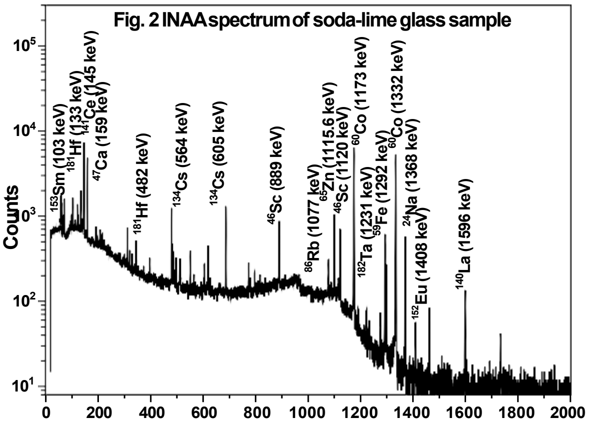

Fig. 2 INAA spectrum of soda-lime glass sample

Acknowledgements: Mr. Vishal Sharma, CSIR-SRF & PhD student of Univ. Of Mumbai at K.C. College, is thankful to CSIR for the Fellowship and Principal, KC College, Mumbai for her encouragement.

References: 1. Acharya & Pujari, Forensic Chemistry, 12 (2019) 107 (2) Sharma et al., *J. Radioanal. Nuc. Chem.*, 2019, 323, 1451–1457 (3) Sharma et al., *J. Anal. At. Spectrom.*, 2021, 36(3), 630-643 (4) Sharma et al.*, Forensic Science International*, 2022, 334(3), 111262 (5) Sharma et al., *J. Radioanal. Nuc. Chem.*, 2022, 331, 1769–1778 (6) Sharma et al., *RSC Advances*, 2023, 13, 5118-5133.

Study on analytical parameters of TXRF Spectrometer-A tool for trace elemental analysis.

Manjunatha[1], A. S. Bennal[1,§], N. M. Badiger[2]
[1] *Department of Studies in Physics, Karnatak University, Dharwad 580003, India*
[2] *School of Advanced Sciences, KLE Technological University, Hubli 580031, India*
[§]Email: arvindbennal@gmail.com

Abstract: Total reflection X-ray Fluorescence spectrometry (TXRF) is a well-established analytical technique for qualitative and quantitative analysis of trace elements in various kind of samples. This technique is modified version of the EDXRF with detection limits in the ppb-level. The S2-PICOFOX TXRF spectrometer was the first commercial and benchtop spectrometer installed in India. In this study, the analytical parameters are involved in TXRF measurements was tested. A mono and multi-elemental standards, quartz and acrylic sample carriers was used for the analysis. The analytical results of parameters such gain correction, spectroscopic resolution (FWHM), absolute sensitivity, lowest limits of detections (LLD), accuracy and precision of some elements in mono and multi-elemental standards by using quartz and acrylic sample carriers were obtained. A TXRF spectrum of MES and LLD values of some elements as given below.

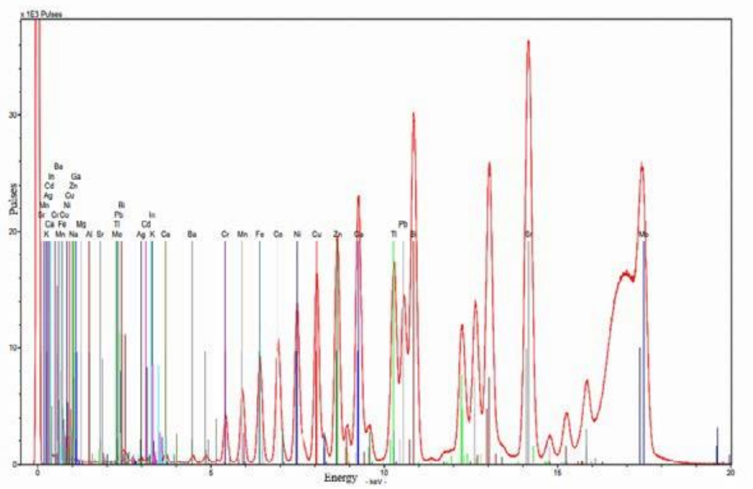

Figure: Typical spectrum of MES-IV solution

Table: LLD values of some elements

Lowest limit of detections (LLD) in mg/l		
elements	Quartz carrier	Acrylic carrier
K	21.8 ± 2.3	25.6 ± 2.0
Ca	22.6 ± 2.3	26.2 ± 2.03
Cr	1.82 ± 0.18	2.06 ± 0.16
Mn	2.06 ± 0.21	2.38 ± 0.18
Fe	0.9 ± 0.09	1.02 ± 0.08
Co	0.82 ± 0.08	0.98 ± 0.07
Ni	0.74 ± 0.07	0.86 ± 0.06
Cu	0.68 ± 0.07	0.82 ± 0.06

at both sample carriers

An experimental result on the recovery ranging from 90 to 110% and relative standard deviation values (1 to 5%) of several elements in multi-element standard were obtained. The accuracy and precision of several elements shows that, the S2-PICOFOX TXRF approach exhibits a good analytical potential for multi trace elemental analysis.

Acknowledgements: A.S. Bennal would like to thank UGC-DAE CSR for funding the research project and Manjunatha is thankful to UGC-DAE CSR for the financial assistance in the form of Project Fellow (CSR-IC-ISUM-16/CRS-299/2019-20/1351 dated 05.03.2020).

Development of methodology for Improvement of Minimum Detectable Activity(MDA) for ^{131}I&^{60}Co measurement in coolant water at KGS-3&4 using HPGe based Gamma spectrometer

G. S Salunke§****,Veerendra. D* ,G.K Sunil* , M.Seshaiah*,B.Vinod Kumar****
***N. Karunakara*[1] *G.K. Nagaraja*[2]**
*****NPCIL** *KAIGA GENERATING STATION3&4 Karnataka, 581 400*
[1]Center for Advanced Research in Environmental Radioactivity (CARER), Mangalore University, [2]Department of Chemistry Mangalore University Mangalagangothri-574199 Karnataka INDIA§ Email: gssalunke@npcil.co.in

Even though the activity levels are low it is essential to measure the activity as indicators. Coolant ^{131}I activity monitoring is being done as an indicator of presence of failed fuel in the Nuclear reactor core. Coolant ^{131}Iactivity in KGS-3 is ≥ 1.0 µCi/lit and in KGS-4 is a ≤0.1 µCi/lit. For improvement in MDA of ^{60}Co measurement need was felt since Co-NU were bundles were loaded in coolant system of KGS#3 for production of ^{60}Co activity. ^{60}Co generated is used for DAE 's ambitious project of Radioisotopes production for Medical purpose. Also ^{60}Co activity measurement in low level in coolant water is required to meet the regulatory requirement. For improving MDA of the High Purity Germanium(HPGe)based gamma ray spectrometer optimization of distance between sample and detector, counting time for sample and background etc were carried out. The gamma spectrometer was calibrated with certified reference source (National Metrological Institute, ROSSSTANDART) epoxide resin granules size not more than 1mm&density 1.0g/cm^3,it consists of mixture of radionuclide's of ^{241}Am,^{133}Ba and ^{152}Eu in 10 ml, 60 ml, 500 ml and 1000 ml geometries to cover the entire energy range of interest, Efficiency calibration was carried out from the contact of detector (0 mm) to various distances from the detector(50 mm ,100mm 150mm).Since the density of the reference standards and the sample medium was same, there was no need for gamma attenuation correction. Details of radionuclide and the MDA are given in the following table.

Sr. No	**ISOTOPE**	**Sample size - 60ml & counting time for sample/background - 2000 sec**							
		60ml, 0 mm		**60ml, 50 mm**		**60ml, 100 mm**		**60ml, 150 mm**	
		MDA (Bq/ml)	**MDA (µCi/l)**	**MDA (Bq/ml)**	**MDA (µCi/l)**	**MDA (Bq/ml)**	**MDA (µCi/l)**	**MDA (Bq/ml)**	**MDA (µCi/l)**
1	I 131	0.018	0.0005	0.046	0.0012	0.079	0.0021	0.110	0.003
2	Co-60	0.030	0.0008	0.074	0.0020	0.129	0.0035	0.186	0.005
3	Co-60	0.034	0.0009	0.082	0.0022	0.141	0.0038	0.220	0.006

From the above data it is observed that the MDA increases as the distance from the detector increases. By following this methodology for a sample volume of 60 ml, counting time of 2000 s and at 150mm distance from the detector, the MDA for ^{131}I was determined to be 0.003 µCi/l (0.11Bq/ml)and^{60}Co is 0.006 µCi/l (0.22Bq/ml) respectively, which is an improvement of about two orders of magnitude when compared to conventional method. Validation of the results was carried out by an inter comparison study with Center for Advanced Research in Environmental Radioactivity (CARER), Mangalore University Karnataka, India.

References;[1].“Introduction to Health physics” by Herman Cember&; Thomas E Johnson (IVth edition).[2].High Resolution Gamma-Ray Spectrometry Analyses for Normal Operations and Radiological Incident Response EPA United States Environmental Protection Agency dated: Oct 2019.

Theoretical Modelling of Proton Induced Ionisation Cross-section of elements for their application in PIXE analysis of some Indian Medicinal Plants

Manpreet Kaur[§] and Amandeep Singh

Department of Physics, University Institute of Sciences, Chandigarh University, Gharaun, Mohali, Punjab-140413, India.
[§]Email: manpreetjangra7@gmail.com

Particle induced x-ray emission (PIXE) is one of the most widely used ion beam techniques for the elemental analysis of solid materials. Simultaneous multi-element detection, non-destructive nature and sensitivity to mid and high Z elements down to trace levels are some of its attractive features. PIXE is usually performed with 2-3 MeV proton ion beam. It involves high resolution spectrometry of X-rays, emitted as a result of ion-atom interaction, for the qualitative and quantitative analysis of materials. PIXE can be performed on thin and also on thick targets. The preparation of thin targets of a material is often cumbersome but the data analysis/quantification is easy while the preparation of thick targets is simple but the quantitative analysis is complex due to matrix effects. The quantitation of an element is based on its X-ray yield which depends on a number of factors including shell-ionisation cross-section. A precise knowledge of the shell-ionisation cross-section is desirable for an accurate analysis, particularly, of thick targets and, in general, for the selection and optimization of experimental parameters.

This paper presents the theoretical modelling of proton induced ionisation cross sections of the different levels of such toxic elements as As, Hg and Pb. The cross-sections are calculated in 0.5 - 2.5 MeV proton energy region by ISICS software [1-2] and are shown in Fig.1. It is observed that the ionisation cross-sections increase with the increase in beam energy implying that the X-ray production is comparatively higher in the surface region of the materials. The above calculated cross section will be utilized and will be employed in the analysis of medicinal plants at FOTIA (BARC) with the help of NPD, BARC using PIXE technique. Importantly the samples would also be examined by NAA at DHRUVA Research Reactor at BARC for the purpose of cross validation.

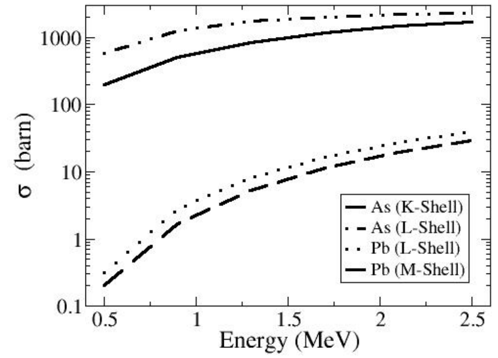

Fig.1: Calculated ionisation cross-sections of different levels of As and Pb.

Acknowledgement: We thank Dr. A. K. Gupta, Head NPD, BARC and Dr. R. Acharya, RCD, BARC for their encouragement to pursue this work in future at BARC under UGC DAE CSR Mumbai Centre. We also thank Dr. Sanjiv Kumar, Ex-Head, NCCCM, Hyderabad for his guidance and support.

References:
[1] M. Batic et al., Computer Physics Communications 183 (2012) 398–404.
[2] S.J. Cipolla., Computer Physics Communications 182 (2011) 2439–2440.

Nondestructive Determination of Fuel-Blanket Gap in 1-m Metal Fuel Pin

J. S. Brahmaji Rao, R. Senthilvadivu, G. V. S. Ashok Kumar [§], P. Ravisankar, R Padmanabhan, D. Saisubalakshmi, K. Sundararajan

Materials Chemistry & Metal Fuel Cycle Group, Indira Gandhi Centre for Atomic Research, Kalpakkam, India – 603102
[§]Email: gvs@igcar.gov.in

India's future fast breeder reactors contain metallic fuel fabricated using slugs of binary or ternary alloys made with zirconium and fissile element viz. uranium and plutonium (U-Zr, U-Pu-Zr). The metallic slugs containing U-6wt.%Zr were prepared using injection casting method at IGCAR [1]. As a quality control protocol, the fabricated sodium bonded metallic fuel pins using casted metallic slugs were subjected to an active gamma scanning for the fuel homogeneity using an attenuation source. The fuel pin scanning system used earlier for sol-gel fuel pins was upgraded to inspect the 1 m metallic fuel pins made with U-Zr. The system was modified to accommodate 1 m length of fuel pins by increasing the length of SS plate which firmly holds the pin and coupled with $LaBr_3$(Ce) detector, its associated electronics and MCA acquisition software. The VB software was developed in-house and coupled with APTEC MCA to automate the gamma spectra acquisition at desired locations of fuel pin by moving the pin.

1 m fuel pins with 100 and 320 mm of U-Zr slugs used as blanket and fuel respectively were assayed by active gamma scanning method using ^{137}Cs source through 3 mm Pb collimation. The fuel pin was moved vertically and attenuated gamma spectrum was registered from bottom at every 3 mm step up to a total length of 537 mm. All the acquired spectra were analysed, the net counts of attenuated photo peak of 661.6 keV as a function of scanned length of fuel pin was plotted. The system was used to scan several metal fuel pins successfully (Fig 1a) to obtain the profile of fuel slug and determined the length of fuel and blanket about 420 mm. A discontinuity i.e., a gap of more than 1 mm between the blanket and fuel in one of the pin was identified (Fig.1b) which can be attributed to the presence of sodium between the two slugs. Thus, the present study could non-destructively profile the length of the fuel slug in 1-m metal fuel pin and discontinuity between slugs as well.

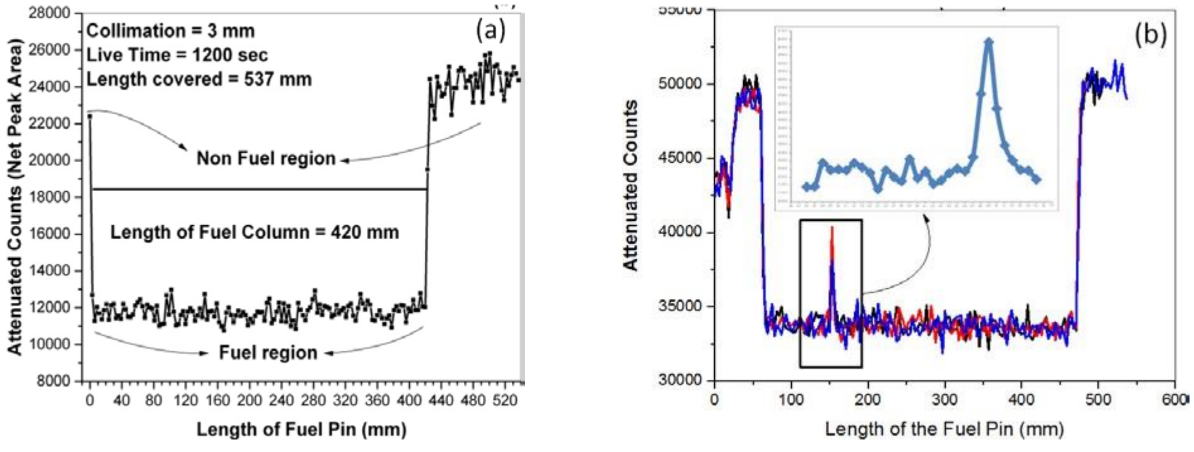

Fig. 1 Profile of fuel homogeneity in metal pins (a & b)

References:
[1] P. Muralidaran and T.V. Prabhu et. al, Internatl. Conf. characterization and quality control of nuclear Fuels (CQCNF-2012), Hyderabad, 27-29 Feb 2012, p. 114-115.

Determination of Iron and Chromium in bulk uranium matrix using Energy Dispersive X-ray Fluorescence (EDXRF) technique

R. Senthilvadivu, G.V.S. Ashok Kumar§, K. Sundararajan

Materials Chemistry & Metal Fuel Cycle Group, Indira Gandhi Centre for Atomic Research,
Kalpakkam, India – 603 102
§Email: gvs@igcar.gov.in

Metallic uranium in the form of (U,Pu)O_2 or U-Zr or U-PuZr alloy is the proposed nuclear fuel in the future fast breeder reactors in India. The quality of metallic uranium as well as the nuclear fuel depends on the presence of various elemental impurities at different concentration level. Iron (Fe) and Chromium (Cr) are the most important and common impurities which strongly influence the mechanical properties of metallic uranium fuel beyond a limit of 350 and 150 $\mu g.g^{-1}$ respectively [1]. In this context, energy dispersive X-ray Fluorescence (EDXRF) method was explored to determine these impurities in bulk uranium matrix towards its final product qualification. A series of uranium standard solutions containing 50 to 350 mg mL^{-1} were prepared to which Fe and Cr standards were added with a varying concentration from 10 to 50 $\mu g.mL^{-1}$. The solutions were assayed by EDXRF (Make: Xenemetrix, Model: Genius IF) instrument having the primary target Rh and excited with the help of a secondary target, Ge Kα radiation produced at 25 kV and 1.0 mA current. 2 mL sample and blank solutions were taken on an X-ray film in a sample holder and data acquisition carried out for 600 s for each measurement. The blank corrected peak areas of Kα lines of Fe (6.403 keV) and Cr (5.414) were plotted for various uranium concentrations as a function of Fe and Cr concentration (Fig.1). From the graphs, as the concentration of U is increasing, the counts of Fe and Cr are decreasing due to matrix absorption effects. However, it is observed that for each concentration of uranium, counts of Fe and Cr are increasing linearly with their increasing concentration. With increase in uranium concentration up to 100 mg mL^{-1} there is no specific positive or negative bias observed in the linearity of Fe and Cr which indicates the method is matrix independent till this U concentration. Thus, the present method can be used to determine Fe and Cr in uranium concentration solution of 100 mg mL^{-1}. Further studies are in progress to estimate the concentration of Fe and Cr in U_3O_8 solution and powder samples.

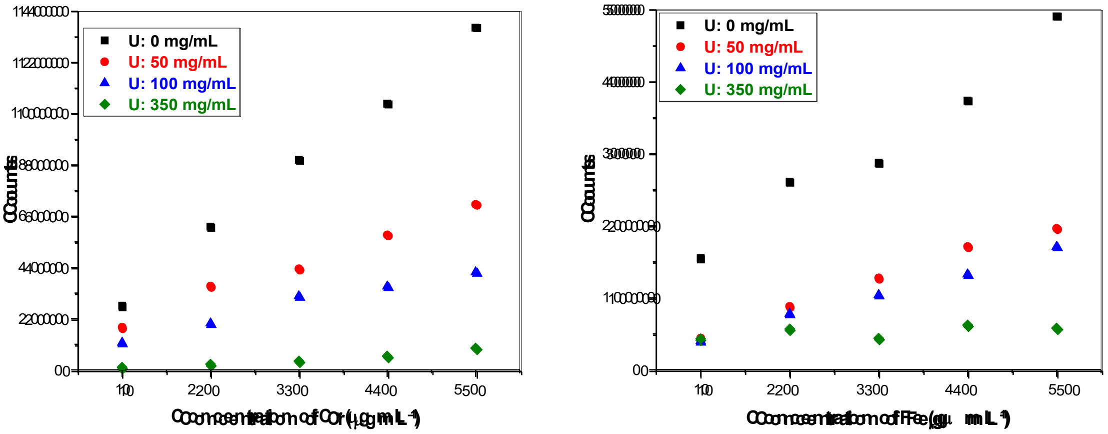

Fig.1 Calibration graphs for Fe and Cr with different Uranium concentrations

References:
[1] S.C. Ravi Chandar etal., Specification from manufacturer of sodium bonded metallic fuel pin for test irradiation, FBTR/31411/SP/38/R-1.

Establishing a Nondestructive Identification method for Pu Samples with high ^{241}Am content for Nuclear Reactor applications

G. V. S. Ashok Kumar[§], J. S. Brahmaji Rao, K. Sundararajan

Indira Gandhi Centre for Atomic Research, Kalpakkam, India
[§]Email: gvs@igcar.gov.in

Uniform radial flux is a mandatory prerequisite for any nuclear reactor which can be achieved using different fissile content materials (%PuO_2 in case of MOX) inside the core. Towards this, fuel subassemblies with higher and lower fissile content are positioned in outer and inner side of the core respectively [1]. This would increase fission rate at the periphery of active core which in turn increases the neutron flux to flatten it radially. Though the FSAs are tagged during the manufacturing for identification, there is a need to confirm the same before their loading into the core. In order to identify and ascertain the Pu level of a subassembly, a non-destructive gamma spectrometric method was established at our laboratory using standard solutions of Pu and Am. $LaBr_3$(Ce) and CZT detectors were explored whereas HPGe detector was not considered due to its difficulties in maintaining at cryogenic temperatures in plant ambience. The method proposes to use the 413.7 keV photo peak area of ^{239}Pu to distinguish the subassemblies. The major challenge in resolving this photo peak is the presence of ^{241}Am that keeps building from ^{241}Pu with the age of the subassembly which has several gammas at the vicinity of 413.7 keV of ^{239}Pu.To simulate the same, standard solution of plutonium and americium were assayed individually and combinedly by gamma spectrometry using $LaBr_3$(Ce) and CZT detectors [2] with APTEC MCA software. The studies using $LaBr_3$(Ce) detector could not resolve the 413.7 keV photo peak of ^{239}Pu in presence of ^{241}Am due to its inadequate energy resolution and higher ^{241}Am background even after positioning low energy cut-off foil (Cd) in front of the detector (Fig.1). The detector was changed to CZT and recorded the gamma spectra for same configuration and registered the counts of the ^{239}Pu 413.7 keV photo peak. The CZT detector could identify the 413.7 photo peak in presence of ^{241}Am (Fig.1) due to its superior resolution compared to $LaBr_3$(Ce) detector. In addition, due to its smaller crystal size, the overall background also reduced to a great extent which reduced the dead time of the detector. Thus, the use of this detector can help to increase both the efficiency and effectiveness of NDA methods applied in the nuclear safeguard fields and can be adopted to distinguish subassemblies with different PuO_2 content.

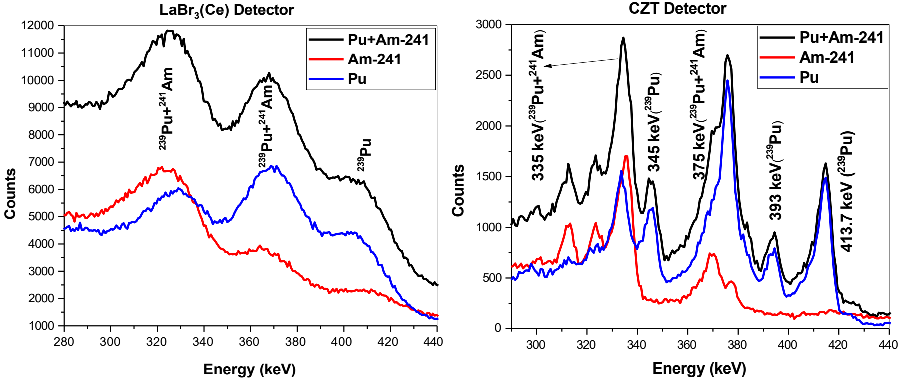

Figure 1: Gamma Spectra of Pu and Am solutions by $LaBr_3$(Ce) and CZT detectors

References:

[1] Swaminathan et al., Design Calculations of Fissile Zone Identification System (2002) FChD/CG/17/2002.

[2] Ashok et al., FIZIDS experiments with CZT detector (2021) PFBR/35141/DN/1010 RevA.

Utilization of external PIGE and INAA methods for the radio-purity analysis of rock samples relevant for nuclear astrophysics

Sonika Gupta[1], Priya V. Mestry[1], Naresh Gamre[2], S.V. Thakare[2],
P.C. Rout[3], A.K. Gupta[3], M.K.Pradhan[4], R. Acharya[1,2,§]
[1] *Radiochemistry Division,* [2]*Radiopharmaceuticals Division,*
[3]*Nuclear Physics Division* [4]*Civil Engineering Division*
Bhabha Atomic Research Centre, Trombay, Mumbai – 400085, India
[§] Email: racharya@barc.gov.in

Three different rock samples were analysed for low Z elements (F, Na, Al, Si, Mg) using 3.75MeV Proton beam from tandem accelerator by External Proton Induced Gamma ray Emission (PIGE) method [1]. For the determination of elements at major to trace level, samples were irradiated with high neutron flux (~10^{13} n/cm^2/s)for 1 min using PCF (for short lived activation products) and 5hrs using self serve facility (for medium to long lived activation products) of Dhruva reactor [2,3]. Radioactive assay was carried out using High Purity Germanium (HPGe) detector having 40% relative efficiency [1-3]. **Figures 1 (a) and 1 (b)** are showing the typical gamma ray spectra of rock sample by PIGE and NAA using short lived activation product, respectively. The elements namely Na, Al, Mg, As, Ba, Br, Ce, Co, Cr, Cs, Eu, Hf, K, La, Lu, Mn, Rb, Sb, Sc, Sm, Th, U, V, Yb, and Zr were determined in all the analyzed samples. The methods were validated by analyzing geological certified reference materials namely AGV-1, RGM-1 and PCC-1. The obtained results were found to be in good agreement with the certified values and the % deviation was found to be within ±5%. The uncertainties on the results were expressed as propagated uncertainties (at ±1s) and found to vary from ±0.8% to ±7%.

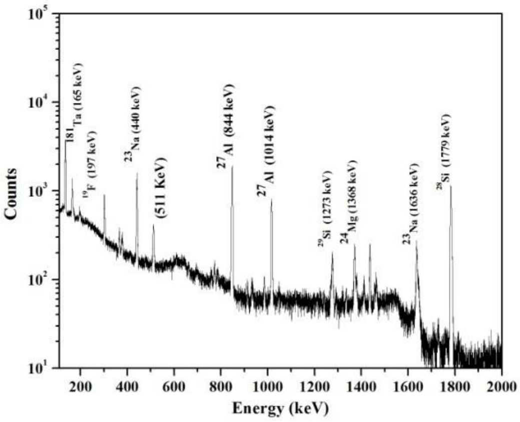

Figure: 1(a) Prompt Gamma ray spectrum of rock sample by PIGE using 3.75 MeV proton beam

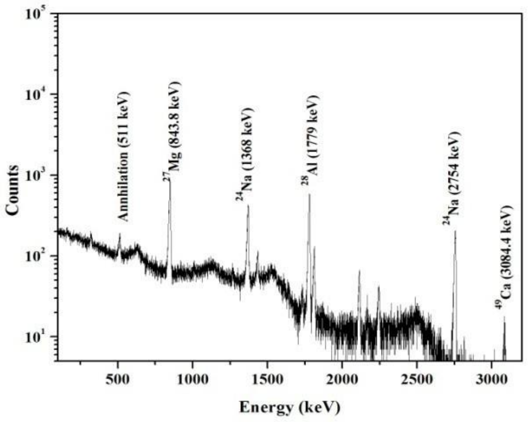

Figure: 1(b) Gamma ray spectrum of rock sample by NAA using PCF of Dhruva reactor

Acknowledgements: Authors would like to thank reactor personnel of Dhruva, reactor, BARC for their help during the irradiation at PCF and Self Serve facility. Authors would like to thank Dr. P. K. Mohapatra, Head, RCD, Dr. S. Krishnagopal, Head, IADD, Mr. A. Agarwal, OIC, FOTIA, IADD and FOTIA operation crews for their support and co-operation during experiment.

References:

1) Sharma et al., *J. Anal. At. Spectrom.*,2021, 36(3), 630-643
2) Sharma et.al., *J Radioanal Nuc Chem*, 323 (1) (2019) 1451.
3) Sharma et al., *RSC Advances*, 2023, 13, 5118-5133.

Application of PIGE and INAA using pneumatic carrier facility of Dhruva research reactor for chemical characterization of agricultural soils from Punjab

Vaishali Dadwal[1], Sonika Gupta[2], Vishal Sharma[2], Deep Shikha[1, §], R. Acharya[2,3]
[1]*Sri Guru Teg Bhadur Khalsa College, Punjab-140118, India*
[2] *Radiochemistry Division, Bhabha Atomic Research Centre, Mumbai - 400 085, India*
[3]*Homi Bhabha National Institute, Department of Atomic Energy, Mumbai – 400094, India*
[§]Email: deep_shikha79@yahoo.co.in

In India the hike in agriculture output came after Green revolution with the adoption of hybrid seeds, pesticides, herbicides, fertilizers and many other cultures[1]. Continuous use of artificial fertilizers may change the physic-chemical properties of the soil, thus degrade the quality of soil. A repetitive cultivation on agricultural land also contributes toward the exploitation of soils.[2] By the year 2050 population of India touches to 166.8 crore thus to safeguard their food intensive farming was done[3]. This practice may be beneficial to us but in long run we are heading toward degrading soil quality. Soil mainly composed of Si, Al, Fe, Ca, Mg, Mn, Na, K, N, Ca, P and Ti along with trace elements. Essential micronutrients present in soil has tendency to occur into crop and crop yield. This imbalance of mineral was thus entering in food cycle leads to various health issues. In order to understand the status of nutrients in agricultural soils of Nawanshshar-Hoshiarpur region of Punjab, different soil samples and artificial fertililizers were collected. Samples were irradiated using reactor neutrons (~10^{13} n/cm^2/sec) along with two geological CRMs (AGV-1 and RGM-1) for 1 min using PCF of Dhruva reactor, BARC. Radioactive assay was carried out using HPGe detector. Typical gamma-ray spectrum of soil samples irradiated for 1 min in PCF of Dhruva is shown in **Fig. 1**. Total of 10 elements, out of which 5 were determined by PIGE (Si, Mg, Al, Na and F) and other elements namely U, Co, and Mn, were determined from INAA. The obtained results were found to be in good agreement with the certified values with % deviation vary from ±1% to ±7% of almost all elements and corresponding Z-score values are within ±1. All the determined elements were found in the range as Si (20-25%); Al (5.4-6.3%); Na (0.9-1.5%); F(769-939ppm); Mg (0.11-0.26%); Mn (52-177ppb%); Co (1-2ppm) and U (1-2ppm) in all the analyzed soil samples.

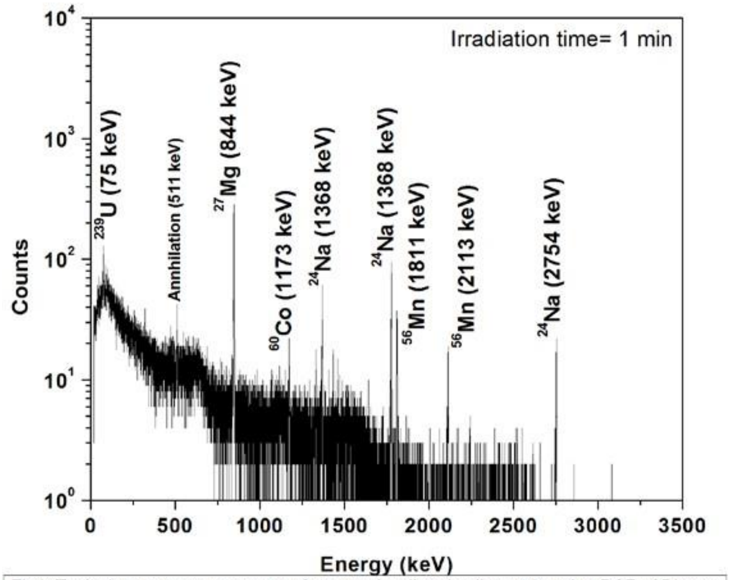

Fig1: Typical gamma ray spectrum of neutron irradiated soil sample using PCF of Dhruva

Acknowledgements: Authors are sincerely thanks to Operation Crews of Reactor Group; Dr. S. Kannan, Director, RC&IG and Dr. P.K. Mohapatra, Head, RCD, BARC. Ms. Vaishali Dadwal thanks UGC-DAE-CSR for the financial assistance as a project fellow at SGTB Khalsa college, Punjab.

Reference(s): 1.David Pimentel et al. Environment, 188(1996) 86-98. 2. Shukhla et al. Fertilizers18(2022) 218-237. 3 Andhra, L et al., *Academia.Edu*, (2009) 45–52.

Rapid estimation of Uranium concentration in aqueous process solutions

Shekhar Kumar[1,§]

[1] FRPPCG, Reprocessing Group, IGCAR, Kalpakkam 603102, India
[§] Email: shekhar@igcar.gov.in

Based on the Masson relation, Kumar and Koganti[1] proposed a re-parameterized equation of density of aqueous solutions of mixed electrolytes of interest to the reprocessing of spent nuclear fuel as

$$\frac{\rho_m}{\rho_o} = 1 + \sum_{i=1} a_i C_i + \sum_{i=1} b_i C_i^{3/2} \tag{1}$$

The same equation can be re-arranged in the following form for two solutes- U(VI) (i=1) and nitric acid (i=2) as

$$b_1 C_1^{3/2} + a_1 C_1 + \left(b_2 C_2^{3/2} + a_2 C_2 + 1 - \frac{\rho_m}{\rho_o} \right) = 0 \tag{2}$$

Eq.2 is a polynomial in $C_1^{1/2}$. The adjustable parameters a_1, a_2, b_1, b_2 were regressed by multiple linear regression from the huge data base of PUREX density data containing more than 1000 points. Now the uranium concentration C_1 can be simply estimated by finding roots of the cubic Eq.2 numerically, provided density ρ_m and acidity of the solution C_2 are available. Experimental data, generated at RpG [2] and reported data of NFC [3], was used to estimate uranium concentrations by ***roots*** function of GNU Octave 7.3.0 [4]. Out of three roots, only one root will be real and will have to be taken.

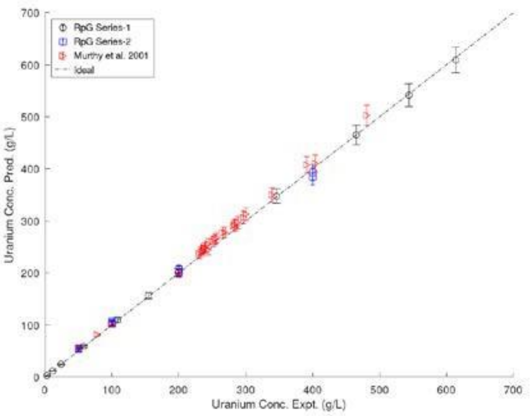

Fig. 1: A parity plot between the experimental and predicted aqueous Uranium concentrations.

Table 1. Range of expt. concentrations

Ref.	U Range (g/L)	HNO_3 Range (mol/L)	Std.Dev. (%)
[2]*	50.0-400.0	0-6.0	3.84
[2]*	2.57-613.8	0	1.35
[3]	52.1-481.0	0.25-3.75	1.53

*Temperature was 298.15 K

The parity plot is shown in Fig.1. An excellent comparison between experimental and predicted uranium concentrations was observed as shown in Fig.1. Table 1 lists the range of experimental concentrations and the standard deviation for Eq.2 for different data sets.

Proposed method can be utilized for rapid estimation of Uranium concentration in aqueous solution just by measuring its density and acidity by instrumental means.

References:

[1] Shekhar Kumar, S.B. Koganti, *J. Nucl. Sci. Technol.* **34**(1997) 410
[2] Shekhar Kumar, Unpublished data RpG, IGCAR.
[3] Murti B.N. *et al*. Proc. NUCAR 2001. 7-10 Feb. 2001, Pune.
[4] Internet info link https://docs.octave.org/interpreter/index.html accessed on 27/02/2023.

Study of Non-linear Behaviour of Photo-peak area in NaCl aqueous solutions using Prompt Gamma Measurement

D. Meena[1,§], S.K.Gupta[2] and P.Meena[2]

[1] *Department of Physics, University of Rajasthan, Jaipur, India*
[2] *Department of Zoology, University of Rajasthan, Jaipur, India*
[§] Email: dalpat11phdmeena@gmail.com

The Prompt Gamma Neutron Activation Analysis (PGNAA) is an efficient method for qualitative and quantitative analysis. PGNAA is widely used for the determination of elements. It is on-line, in situ and non - destructive elemental analysis technique. This method is mostly used in the analysis of bulk materials such as those performed in heavy metal detection in aqueous solution, explosive detection, mines, salinity measurement, cement industries, copper and ore with the capability of isotopic analysis [1]. In the present work, we estimated minimum detectable limit (MDC) of PGNAA setup for chlorine (Cl) in aqueous solution for low counting time (1800 sec) using 5 Ci Am-Be neutron source (emitting ~ 1.25×10^7 n/sec and HPGe detector. In this work, thermal neutron self-shielding effect is observed in aqueous bulk samples containing neutron absorbing materials using prompt gamma neutron activation analysis[2].

In order to describe the detection limit of chlorine (Cl) element measured by this setup for low irradiation time (1800 s), the minimum detectable concentration (MDC) of the setup was calculated for chlorine element. The following formulas were used to calculate the MDC and error [2].

$$MDC = 4.653 \times \frac{C}{N_p} \times \sqrt{N_B} \quad , \quad \sigma_{MDC} = \frac{C}{N_P} \times \sqrt{2N_B} \qquad (1)$$

where C is the concentration of the interested element , N_P and N_B are the net count and background count of the characteristic peak respectively.

Table.01 MDC and error of the Chlorine(Cl)

Element	**Energy (keV)**	**Cross-section $\sigma_\gamma(E_\gamma)$ b**	**MDC(ppm)**		
			Irradiation Time		
			14400 s [2]	**7200 s** [2]	**1800 s**
^{35}**Cl**	6110.842 (18)	6.59(6)	175±53	280±85	781±273

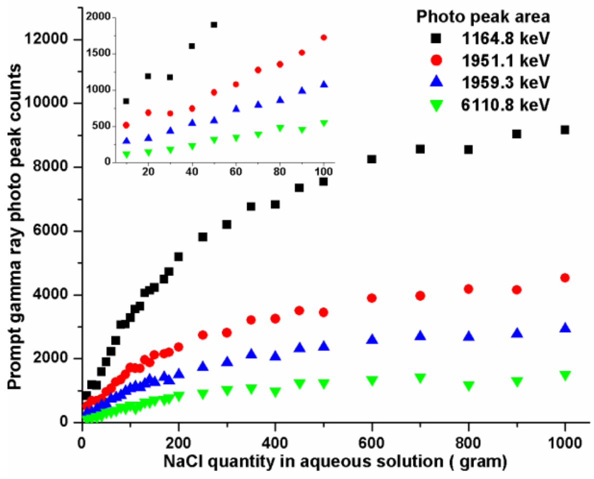

Fig.1.The peaks areas of Cl at 1164.8, 1951.1, 1959.3 and 6110.8 keV prompt gamma rays

References:

[1] R.R. Greenberg, P. Bode, and E.A. De Nadai Fernandes, Spectrochimica Acta Part B: Atomic Spectroscopy volume **66** (2011) 193.

[2] D. Meena, S.K. Gupta and H.S.Palsania, et.al. Heavy metal detection in aqueous solution using PGNAA technique, Adv. Sci. Eng. Med., vol. **11** (2019)11.

Xe-induced fusion reactions to synthesize SHE Z=119

S.Madhu[1], N. Sowmya[§], H.C.Manjunatha[§] and L. Seenappa[2]
[1] *Department of Physics,Govt. First Grade college,Srinivasapur-563135,karnataka,India*
[§] *Department of Physics,Govt. College for women,Kolar-563101,karnataka,India*
[2] *Department of Physics,Govt. First Grade college,Mulbagal-563131,karnataka,India*
[§] Email: manjunathhc@rediffmail.com, sowmyaprakash8@gmail.com

The neutron-rich heavy nuclei with N = 126 are not only significant in terms of nuclear structure, but they also help us understand the mechanism of heavy element synthesis in the process. As a result, substantial effort has been expanded in recent years to produce neutron-rich heavy nuclei [1-4] using fusion reactions such as ^{136}Xe + ^{208}Pb and ^{136}Xe + ^{198}Pt. Earlier researchers predicted optimal energies, compound nucleus formation probability, survival probability and evaporation residue cross-sections in the formation of superheavy element [5-8]. Many fusion reactions using ^{59}Co, ^{55}Mn, ^{50}Ti, ^{51}V, ^{58}Fe, ^{64}Ni, and ^{54}Cr projectiles were used to synthesize superheavy element Z=119 and 120 [5]. But all these experiments failure to synthesize the superheavy element Z=119 and 120. Hence, this motivated us to investigate Xe-induced fusion reactions to synthesize superheavy element Z=119. Fusion cross-section is evaluated as follows;

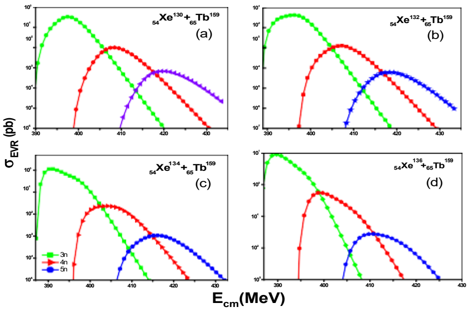

Fig. 1: A plot of evaporation cross-sections as function of center of mass energy for (a) ^{130}Xe+^{159}Tb, (b) ^{132}Xe+^{159}Tb, (c) ^{134}Xe+^{159}Tb and (d) ^{138}Xe+^{159}Tb for 3n, 4n and 5n evaporation residue channels.

$$\sigma_{fus} = \frac{\pi\hbar^2}{2\mu \times E_{cm}} \sum_{l=0}^{l_{max}} (2l+1) \times T_l(E_{cm}) \times P_{CN}(E_{cm}, l) \tag{1}$$

The following boundary conditions are used to evaluate barrier height V_B and barrier position R_B

$$\left.\frac{dV(r)}{dr}\right|_{r=R_B} = 0 \quad \text{and} \quad \left.\frac{d^2V(r)}{dr^2}\right|_{r=R_B} \leq 0 \tag{2}$$

Here $V(r)$ is the total interacting potential barrier for two spherical nuclei is given by

$$V = V_N(R) + V_C(R) + \frac{\hbar^2 l(l+1)}{2\mu \times r^2} \tag{3}$$

The evaluation of cross-sections are in detail explained in literature [6]. Figure 1 shows a plot of plot of evaporation cross-sections as function of center of mass energy for (a) ^{130}Xe+^{159}Tb, (b)^{132}Xe+^{159}Tb, (c)^{134}Xe+^{159}Tb and (d) ^{138}Xe+^{159}Tb for 3n, 4n and 5n evaporation residue channels. The larger evaporation cross-sections are observed for 3n channel in all the studied Xe-induced fusion reactions. The observed cross-sections are in the range of 0.01pb to 0.1pb. Since, these predicted cross-sections are in the measurable range, the Xe projectiles can be used to extend periodic table.

References:
[1]] L. Corradi, et al., *J. Phys. G, Nucl. Part. Phys*. **36** (2009) 113101.
[2] V. Zagrebaev, W. Greiner, *Phys. Rev. Lett*. **101** (2008) 122701.
[3] J.S. Barrett, et al., *Phys. Rev. C* **91** (2015) 064615.
[4] E.M. Kozulin, et al., *Phys. Rev. C* **86** (2012) 044611.
[5] H.C. Manjunatha, et al., *eur. phys. J. plus* **137**, (2022) 693.
[6] H. C. Manjunatha, et al**.,** *Phys Rev C* **98**, (2018) 024308.
[7] H.C. Manjunatha, et al**.,** *Phys. Rev. C* **102**, (2020) 064605.
[8] H.C. Manjunatha, et al., Phys. Rev. C **98**, (2018) 024308.

Development of a cesium-specific solid phase adsorbent

B. Robert Selvan, M. Amutha Suba, A. S. Suneesh, N. Ramanathan

Fuel Chemistry Division, MC&MFCG
Indira Gandhi Centre for Atomic Research, Kalpakkam, India
Email: suneesh@igcar.gov.in

Safe practice of civilian nuclear programs relies on the management of radioactive wastes to avoid the burden of radiotoxic waste being transferred to the future generation. To achieve the goal of radioactive waste management, the recovery of harmful radioactive elements deserves paramount importance [1]. Aside from the immobilization of radioactive elements, recovery of useful isotopes that find scope in industrial and medical applications is also important in nuclear waste management. Among the different radioactive fission products, radioactive cesium separation is gaining wide attention due to the huge industrial demand for radioactive cesium for being used as a sealed radiation source. Different isotopes of cesium, viz. ^{137}Cs, ^{135}Cs etc. being produced by fission of both ^{235}U and ^{239}Pu, are produced in substantial levels, ^{137}Cs. Solid phase separation methods are beneficial for recovering radioactive cesium owing to the large separation efficiency and selectivity. This paper reports the development of nickel ferrocyanide anchored magnetite (MAN-NFCN) for the selective removal of cesium from aqueous solutions. The adsorbent, MAN-NFCN, exhibits ferromagnetic properties due to the presence of magnetite (Fe_3O_4) that enables the faster physical separation of the adsorbent from the aqueous phase. Unlike the conventional solid phase adsorbents based on column-based extraction chromatographic separations, the separations can be carried out in batch operations. The larger surface area of the magnetic matrix facilitated the incorporation of the ligand (nickel ferrocyanide) responsible for cesium separation.

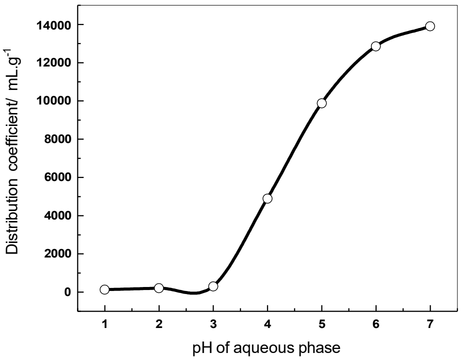

Figure 1. Cesium adsorption behavior of MAN-NFCN

The adsorbent, MAN-NFCN, was prepared by chemical modification of magnetite (Fe_3O_4). Fe_3O_4 was initially prepared by co-precipitation of Fe^{2+} and Fe^{3+} salts using ammonia. The magnetite was further modified to a silica-coated matrix by reacting the former with tetra ethoxy silane. The silica-coated Fe_3O_4 was further reacted with 3-aminopropyltriethoxysilane to form an amine-functionalized Fe_3O_4, which upon reaction with nickel nitrate and potassium ferrocyanide, resulted in MAN-NFCN. The adsorbent exhibited superior adsorption features for cesium separation at pH values above 3, as seen in figure 1. All the cesium present in the aqueous phase was quantitatively recovered to MAN-NFCN within 60 minutes of contact. The adsorption studies indicated that MAN-NFCN could be considered a suitable solid phase adsorbent for the cesium recovery from radioactive wastes.

References:

[1] P.A. Haas PA, *Separation Science and Technology*, 28 (1993) 2479-506

Correlation of Pendrin with ^{131}Iodine uptake in post-NAI treated thyroid cancer animal model

C.S. Gholve, Y.H. Shete, S. Rakshit, S. Basu, S.P. Kulkarni[§], A.K Tyagi

Radiation Medicine Centre, BARC, C/o TMH Annexe, Parel, Mumbai-400 012
[§]Email: savitapk@barc.gov.in

Radioactive iodine (RAI) refractoriness develops in the background of a loss of thyroid differentiation features representing major therapeutic challenges in thyroid cancer management. Studies have reported decreased or loss of pendrin (SLC26A4 gene) expression in thyroid tumours, signifying the role of pendrin in the impaired ability of thyroid cancer cells for uptake and concentration of iodine. As acute iodide treatment has been shown to increase SLC26A4 mRNA [1], the study of pendrin expression in malignant tissues is of interest. Hence, we focused to evaluate the pendrin expression and ^{131}I uptake in an N-bis-(2-hydroxypropyl) nitrosamine (DHPN) induced thyroid cancer model in Wistar rats followed by a single dose of sodium iodide (NAI) treatment to see if any change occurs in RAI uptake.

DHPN (83 mg/animal) was administered in Wistar rats ((n=18)) by i/p route. After 17 weeks, metabolic alteration in the thyroid gland was checked by giving ^{131}I (8 μCi) orally and thyroid uptake imaging was performed at 24h followed by excess NAI (2mg/animal) treatment with 2h, 24h, 48h and 72h uptake. Animals were sacrificed after 20 weeks and thyroid tissues were processed for histopathology (HP) and immunohistochemistry (IHC).

^{131}I uptake by scintigraphy showed thyroid uptake values of 10.16±1.6 and 13.13±0.115 in DHPN-treated and control groups respectively at 24h. However, post-NAI treatment decreasing patterns at 24h, 48h and 72h were observed in a few animals similar to the control (Fig.1). This could be attributed to a phenomenon known as the „Wolff-Chaikoff effect‟ which results due to acute iodide excess that transiently impairs thyroid hormone synthesis. However, the rising pattern of ^{131}I uptake was also observed in a few DHPN-induced thyroid cancer animals compared to the control (Fig. 2), which could perhaps be related to the effect of iodide excess treatment influencing the expression and functionality of pendrin [2].

In conclusion, further research is warranted to verify the role of NAI in the expression of Pendrin in conjunction with animal species and age; along with the dose and exposure time of NAI. In addition, the expression and quantification of pendrin at the molecular level entail being assessed to enhance its utility in the management of RAI refractory human thyroid cancer patients.

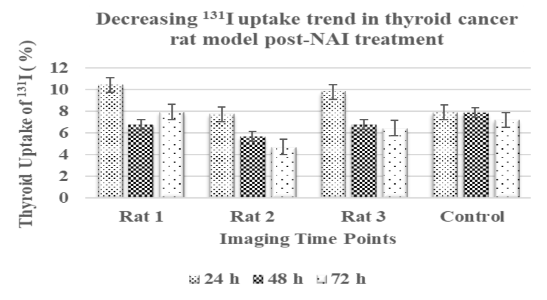

Fig. 1: Decreasing ^{131}I uptake in NAI-treated rats

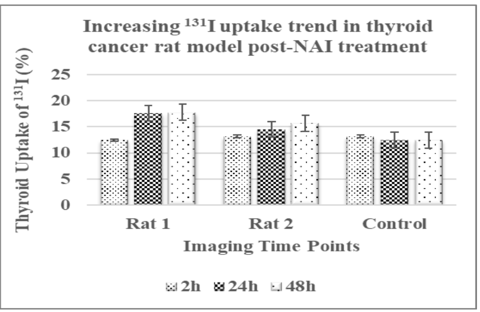

Fig. 2: Increasing ^{131}I uptake in NAI-treated rats

References:
[1] Calil-Silveira J, et al., Mol Cell Endocrinol. 350(1) (2012) 118-24.
[2] Calil-Silveira J, et al., AJP-Cell Physiology. 310(7) (2016) C576-82.

Effect of different doses of gamma radiation on the shelf life of chicken sausages in refrigerated storage

Shobita R. Muppalla[§] and S. Gautam

Food Technology Division, Bhabha Atomic Research Centre, Mumbai, India
[§]Email: shobitar@barc.gov.in

Demand for convenient ready-to-cook (RTC) / ready-to-eat (RTE) meat products such as sausages, salami, frankfurters etc. is on rise in urban areas in India [1]. Many such products are marketed in frozen conditions to ensure their quality during storage period. However, lack of adequate freezing facilities, its inability to eradicate pathogens and adverse effect on texture are limitations encountered during marketing of these products. Gamma irradiation is a promising technology to improve microbiological safety and extension of shelf life of such products in refrigerated storage. The objective of this study was to evaluate the effect of gamma irradiation (1, 2 and 3 kGy) on shelf life of chicken sausages in refrigerated storage. At day 1 of irradiation, the pH, colour, texture, moisture, water activity was not significantly influenced. Dose dependent decrease in total viable counts (TVC), *Staphylococcal* counts and coliforms counts were observed with total elimination of coliforms at doses more than 1kGy. Lipid oxidation increased with increasing dose of radiation as measured by thiobarbituric acid reactive substances (TBARS) assay. No significant differences ($p \leq 0.05$) in taste, aroma and overall acceptability due to radiation treatment were observed during sensorial evaluation. The non-irradiated samples spoiled microbiologically in refrigerated storage within 4 days followed by samples (1 kGy and 2 kGy) in 7 and 10 days respectively. Chicken sausages (3kGy) had a shelf life of 15 days at refrigerated storage and were organoleptically acceptable till end of storage period. This study provides an insight in use of gamma radiation in extending the shelf life of convenient meat products by controlling microbial growth without significant effect on its sensory quality in refrigerated storage.

References:

[1] S.Temgire et.al.,*Pharma Innovation*,**10(5)** (2021) 211.

Cross section measurements of ^{nat}Mo(α,n)^{103}Ru for production of Auger emitter for immunotherapy

Mahima Upadhyay[1], [§] A. Gandhi[1], Aman Sharma[1], Mahesh Choudhary[1], Namrata Singh[1], S. Dasgupta[2], J. Datta[2] and A. Kumar[1§]
[1]Department of Physics, Banaras Hindu University, Varanasi - 221005, INDIA [2]Analytical Chemistry Division, Bhabha Atomic Research Centre,
Variable Energy Cyclotron Centre, Kolkata – 700064, INDIA
[§]*Email: mahimaupadhyay@bhu.ac.in; § ajaytyagi@bhu.ac.in*

Auger electron emitter ^{103m}Rh is used for internal radiation therapy which has a short half-life of 56.11 min. It is produced via β- decay of ^{103}Ru which has a half-life of 39.26 days [1]. This measurement is to study the cross section for the production of ^{103}Ru with the help of alpha induced reaction on molybdenum.

The experiment was accomplished using the K-130 cyclotron at Variable Energy Cyclotron Center (VECC), Kolkata, India. We have used stacked foil activation method and offline γ- ray spectroscopy. We arranged the stack as ^{nat}Al accompanied by ^{nat}Mo followed by ^{nat}Cu. ^{nat}Cu acted as both catcher and monitor foil. All are the dimensions of 1cm x 1cm. The thickness of ^{nat}Al, ^{nat}Mo, ^{nat}Cu foils were 6.75 mg/cm^2, 12.75 mg/cm^2, 9 mg/cm^2 respectively. 28 MeV of alpha beam was smitten on the stack. We employed Stopping and Range of Ions in Matter, SRIM-2012.03 code to calculate energy degraded of our stack.

High-Purity Germanium (HPGe) detector was used to measure the gamma-ray activity of the irradiated sample. The efficiency calibration was done using the ^{152}Eu point source ($T_{1/2}$=13.517 years of known activity A_0 = 39080 Bq as on 17 May 1982) [2,3]. The cross section was calculated using the following equation: -

$$\sigma_s = \sigma_m \eta \frac{A_s \lambda_s a_m N_m I_m f_m}{A_m \lambda_m a_s N_s I_s f_s} \times \frac{C_{attn.(s)}}{C_{attn.(m)}} \qquad (1)[4,5]$$

We also employed the statistical nuclear model code TALYS-1.96 for the theoretical calculations of the reaction. We compared the result with different level density models in TALYS-1.96. The present experimental data has also been rationalized with the existing cross sections data available in the EXFOR.

Experimental obtained cross section followed the same trend as theoretical results but no theoretical model is in good agreement with the present work.

We would like to thank Prof. Chandana Bhattacharya and K-130 Cyclotron staff, VECC for their cooperation and smooth working of the experiment.

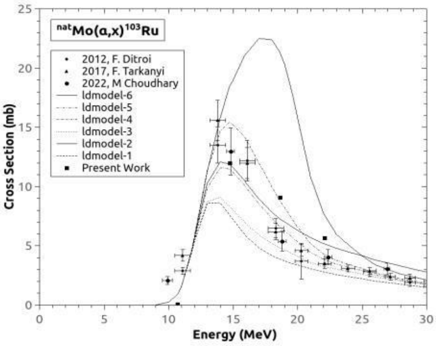

Fig. 1: The measured cross sections of ^{nat}Mo(a,n)^{103}Ru.

References:
[1] B. Bartoś et.al., *Journal of radioanalytical and nuclear chemistry*, **279** (2009) 655.
[2] M. Choudhary et.al., *The European Physical Journal A* **58** (2022) 95.
[3] M. Choudhary et.al., *Journal of Physics G: Nuclear and Particle Physics* **50.1** (2022) 015103
[4] A.Gandhi et.al., *European Physical Journal A* **57** (2021) 1.
[5] A.Gandhi et.al., *European Physical Journal Plus* **136.8** (2021) 819

Semi-empirical systematics for the cross-sections of the (n,p), (n,α) and (n,2n) reactions at 14.5 MeV neutron energy

Namrata Singh§, A. Gandhi, Aman Sharma, Mahesh Choudhary, Punit Dubey, Mahima Upadhyay and A. Kumar

Department of Physics, Banaras Hindu University, Varanasi-221005, INDIA
§ Email: namratasingh.jwala@gmail.com

Neutron induced reaction cross-section data are essential for many technical applications in nuclear physics and medical fields around 14.5 MeV neutron energy. These data are needed to estimate induced radioactivity, gas production, nuclear transmutation and radiation damage [1]. Nuclear data are important for the application of nuclear reactors and for the protection measurements of accelerator facilities [2].

In the present work, semi-empirical formulae have been obtained for the (n,p), (n,α) and (n,2n) reaction cross-sections at 14.5 MeV incident neutron energy in the target mass regions $23 \leq A \leq 206$, $23 \leq A \leq 142$ and $45 \leq A \leq 204$ respectively. The reaction cross-section can be expressed on the basis of the statistical model as follows:

$$\zeta_{n,x} = \zeta_R(\Gamma_x/\Gamma_n) \qquad (x = p, \alpha, 2n)$$

where ζ_R is reaction cross-section for the incident neutrons, Γn and Γx are the decay width for a neutron and for a proton, an α-particle and 2n emission respectively.

The systematic formulas proposed by us for (n,p), (n, α) and (n,2n) reactions are given below:

Even-A	**Odd-A**
$\zeta_{n,p} = 20.97(1 + A^{1/3})^2\exp(-18.89(N - Z)/A)$	$\zeta_{n,p} = 7.02(1 + A^{1/3})^2\exp(-16.67(N - Z)/A)$
$\zeta_{n,\alpha} = 21.79(1 + A^{1/3})^2\exp(26.49(N - Z)/A)$	$\zeta_{n,\alpha} = 18.17(1 + A^{1/3})^2\exp(-23.82(N - Z)/A)$
$\zeta_{n,2n} = 5.58(1 + A^{1/3})^2\exp(22.85(N - Z)/A - 63.51(N - Z)^2/A^2)$	$\zeta_{n,2n} = 8.93(1 + A^{1/3})^2\exp(8.76(N - Z)/A)$

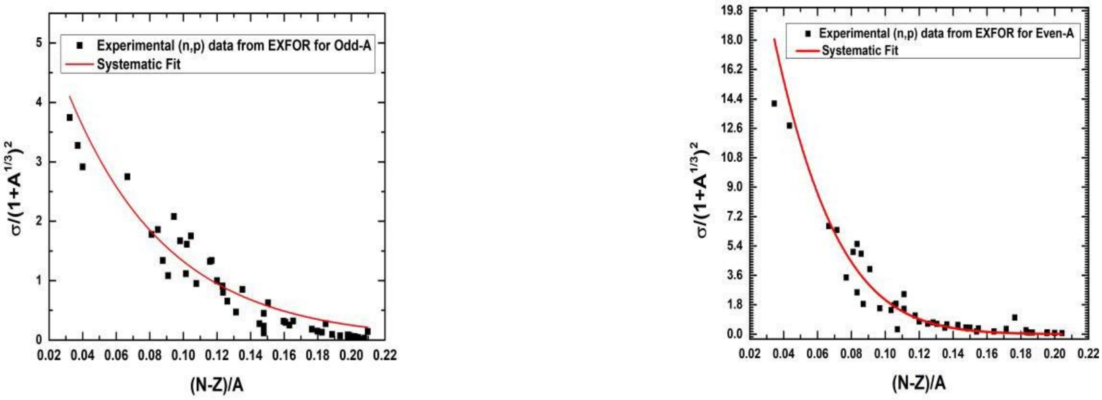

Fig.1: Systematic fitting of the odd-A (n,p) and odd-A (n,2n) reaction cross-sections

References:
[1] A. Gandhi et al., *European Physical Journal Plus*, **136** (2021) 8.
[2] Namrata Singh et al., *Indian Journal of Pure and Applied Physics,* **54** (2020) 314.

Excitation function analysis of α+^{95}Mo reaction to produce medically relevant ^{97}Ru up to 60 MeV

Malvika Sagwal and Moumita Maiti[§]

Department of Physics, Indian Institute of Technology Roorkee, Roorkee-247667,
Uttarakhand, INDIA
[§]Email: moumita.maiti@ph.iitr.ac.in

^{97}Ru ($T_{1/2}$ = 2.83 d) is an application-based radioisotope that finds enormous demand in the present-day healthcare industry. It decays through e^- capture (100%) followed by intense γ-ray emission of 215.7 keV (85.6%), which offers efficient tumor diagnosis through imaging. The current study attempts to understand the reaction mechanism of ^{97}Ru production through the excitation function (EF) analysis of ^{95}Mo(α,2n)^{97}Ru reaction. The experimental data have been taken from the IAEA-EXFOR database [1], and the reactions have offered a reasonable production of ^{97}Ru. The production cross section has been compared with evaluated nuclear data from the data library TENDL-2019, 2021 [2] based upon the reaction code TALYS. Additionally, we have incorporated the nuclear reaction code PACE4 [3] and EMPIRE-3.2.2 [4]. PACE4 works on the Hauser-Feshbach (HF) formalism for the equilibrium (EQ) mechanism during the compound nuclear formation, while EMPIRE embodies a combination of distorted-wave Born approximation (DWBA) for the direct reactions, HF formalism, and Exciton model for the EQ and pre-equilibrium (PEQ) reaction processes, respectively. The EGSM (Enhanced Generalized Superfluid Model) level density has been invoked. The reproducibility of EF using EMPIRE code has been found excellent for the experimental data in the entire energy region. The lower energy part can be explained by the inclusion of coupled channel code CCFUS for heavy-ions reactions, while the stark contrast in the high-energy part compared to PACE4 can be accounted to the PEQ emission of light particles and clusters, holistically covered by EMPIRE model code. The systematics can be further implemented for the efficient forecasting of unmeasured application-based isotopic data.

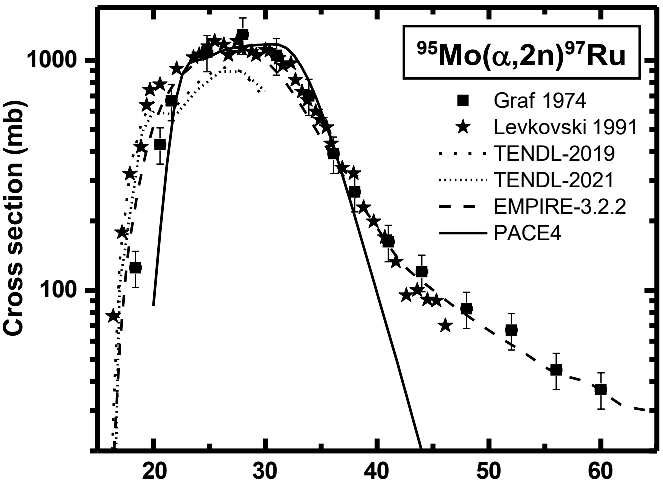

Fig. 1: Cross section data of ^{95}Mo(α,2n)^{97}Ru reaction and its theoretical prediction using various model codes.

Acknowledgements
MS sincerely thanks the MHRD, Govt. of India, for its financial assistantship during research.

References

[1] N. Otuka, E. Dupont et al., *Nucl. Data Sheets*, **120** (2014) 272.
[2] A. J. Koning, D. Rochman et al., *Nucl. Data Sheets,* **155** (2019) 1.
[3] A. Gavron, *Phys. Rev. C,* **21** (1980) 230.
[4] M. Herman, R. Capote et al., *Nucl. Data Sheets,* **108** (2007) 2655.

Dual Mode Automated Module for Radiolabelling of ^{68}Ga Produced from both Generator and Medical Cyclotron

Yuva Raj Nitin [1], Shrinibas Nayak[2], Amit Kumar[3], B K Sharma[4] and Savita Kulkarni[5, §]
[1,2,5] *Radiation Medicine Centre, BARC, Parel, Mumbai-400 012, India.*
[3,4] *Board of Radiation and Isotope Technology, Navi Mumbai-400 703, India*
[§] Email: *savitapk@barc.gov.in*

Introduction: ^{68}Ga is produced either using a ^{68}Ge-^{68}Ga generator or in a Medical Cyclotron using ^{68}Zn (p, n) ^{68}Ga route. Here we present an in-house developed automated synthesis module which can separate and label peptides using ^{68}Ga obtained from either of the sources.

Materials and Methods:

Hardware and Software: The control system is based on a custom STM32 microcontroller board, which is controlled by HMI software that sends commands to the hardware controller board through the USB port.

Synthesis: The radio synthesis module was used to synthesize ^{68}Ga-PSMA-11, using ^{68}Ga produced from both Medical Cyclotron using ^{68}Zn(NO$_3$)$_2$ aqueous solution as a target and ^{68}Ge/^{68}Ga generator. ^{68}Ga was purified and pre-concentrated using solid phase extraction method. Post purification, ^{68}Ga was added to reaction vial containing sodium acetate buffer and peptide. Post incubation at 95ºC for 12 minutes, the reaction mixture was cooled by adding water and then it was transferred to preconditioned tC18 column for purification of product, followed by washing the column with 2 mL saline. ^{68}Ga -PSMA-11 was eluted using 50% Ethanol (0.8-1.0 ml) followed by rinsing the column with 5 mL saline.

Results: The automated synthesis module had been successfully used to produce ^{68}Ga-PSMA-11 using ^{68}Ga produced from both Medical Cyclotron and generator. The radiolabelling yield (decay uncorrected) of ^{68}Ga-PSMA-11 was found 70-80 % which was comparable with yield obtained using a commercial module procured from Eckert & Ziegler.

Conclusion: The automated synthesis module is easy to operate and serves the purpose of reducing the running costs in the production of ^{68}Ga-PSMA-11 peptide while easily allowing labelling of ^{68}Ga from either generator or Medical Cyclotron. Moreover, the separated ^{68}GaCl$_3$ can also be used to radio label other peptides commonly used in nuclear medicine.

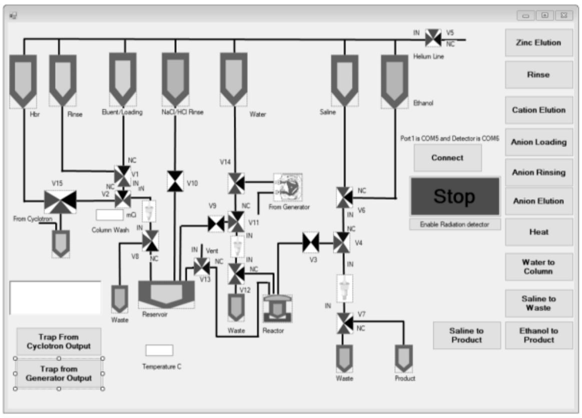

Fig: Schematic of process in the Automated Module

Total chemical synthesis PSMA-617: An API for prostate cancer endotherapeutic applications

K. S. Ajish Kumar [1,2,§], and Anupam Mathur[3]

[1]Bio-Organic Division, Bhabha Atomic Research Centre, Mumbai, India
[2]Homi Bhabha National Institute, Anushaktinagar, Mumbai 400094, India
[3]Radiopharmaceuticals Program, Board of Radiation and Isotope Technology,
Navi Mumbai 400703, India
§Email: ajish@barc.gov.in

Prostate-specific membrane antigen (PSMA), a cell surface bond protein that is ubiquitously present in the prostate cancer cells[1] has received considerable attention in recent past as an excellent target for both imaging and therapy. Significant preclinical studies targeting this membrane bound protein resulted in the identification of many small molecule ligands that could specifically bind to it. The first clinical breakthrough using small molecule PSMA inhibitors was achieved with ^{68}Ga-PSMA-11 for PET imaging and ^{131}I-MIP-1095 for endoradiotherapy of metastatic prostate cancer. Subsequently, rigorous research in this area culminated in the development of ^{177}Lu-labeled PSMA-617, which is currently a subject of multicenter studies.

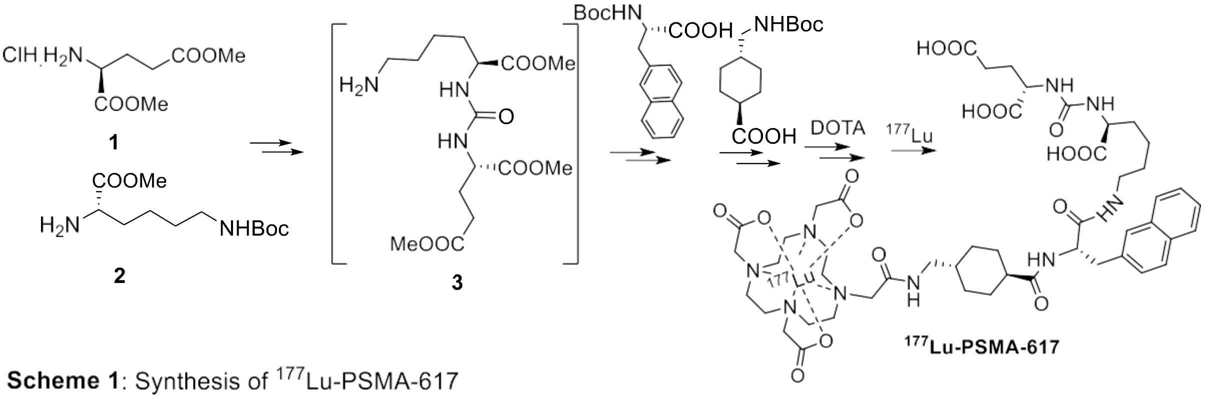

Scheme 1: Synthesis of ^{177}Lu-PSMA-617

Development of economically benign methodology for the synthesis of PSMA-617 is particularly important to have a better access to this highly important active pharmaceutical ingredient (API). In this respect, we have recently reported a synthesis of PSMA-617 using a protocol that involves the use of flow reactor based catalytic hydrogenation as the key step.[2] Alternatively, herein we demonstrate the synthesis of PSMA-617 using Boc-approach (Scheme 1). Using this method ligand with purity >99.5% was achieved. Radiolabelling with ^{177}Lu generated endotherapeutic agent ^{177}Lu-PSMA-617 with purity >99% which is sufficient enough to use it for direct human applications.

Acknowledgements: KSAK is thankful to Prof. B. S Patro, Head, Bio-Organic Division, Prof. T. K. Ghanty, Group Director, Bio Science Group, BARC and former Group Directors for their constant support and encouragement throughout the course of this activity.

References:
[1] J. Horoszewicz, E. Kawinski, G. Murphy *Anticancer Res*. **7**, (1987), 927.
[2] K. S. Ajish Kumar, A. Mathur *Eur. J Med. Chem. Rep.* **3**, (2022), 100084.

Measurement of ^{109}Ag(n, γ)^{110m}Ag reaction cross section in the incident neutron energy 0.5- 1.6 MeV

Mahima Upadhyay[1], [§] A. Gandhi[1], Aman Sharma[1], Mahesh Choudhary[1], Namrata Singh[1], Sumit Bamal[1], Akash Hingu[2], S. Mukherjee[2], G. Mishra[3], Sukanya De[3], A. Mitra[3], L. S. Danu[3], Saurav Sood[4], Sajin Prasad[4], Ajay Kumar[3], R. G. Thomas[3] and A. Kumar[1§]

[1]Department of Physics, Banaras Hindu University, Varanasi - 221005, INDIA
[2]Department of Physics, The Maharaja Sayajirao University of Baroda, Vadodara – 390002, INDIA
[3]Nuclear Physics Division, Bhabha Atomic Research Centre, Mumbai- 400085, INDIA and
[4]Health Physics Division, Bhabha Atomic Research Centre, Mumbai- 400085, INDIA
[§]Email: mahimaupadhyay@bhu.ac.in; § ajaytyagi@bhu.ac.in

^{110m}Ag is composed by ^{109}Ag. ^{110m}Ag undergoes β - decay into ^{110}Cd which is used for the production of ^{110}In, ^{113m}In radioisotopes which have vital role in health care, medical applications and pharmaceutical industries. There is inadequacy of the experimental data for ^{109}Ag(n,γ)^{110m}Ag reaction at low energy of neutrons. In this study, we have measured the cross section and covariance of our interested reaction.

The experiment was carried out using the 6-MV Folded Tandem Ion Accelerator (FOTIA) facility, BARC, Mumbai, India. The proton beam of energies 2.5, 3, 3.6 MeV were impinged on a 56.18 μm thick Lithium target producing neutrons of average energies 0.53 ± 0.02, 1.05 ± 0.02, 1.66 ± 0.02 MeV. The reaction p + ^{7}Li → n + ^{7}Be is the neutron source reaction [1]. These neutrons bombarded on silver targets of thickness 0.125, 0.125, 0.1 mm respectively. We have used EPEN code [2] to obtain the spectrum averaged neutron energies at the three proton energies. The time for irradiation for each target was 24 hours.

We have used High-Purity Germanium (HPGe) detector to measure the gamma-ray activity of the irradiated sample [3]. The efficiency calibration was completed using the ^{152}Eu point source ($T_{1/2}$=13.517 years of known activity A_0 = 6614.71 Bq as on 1 Oct. 1999). The cross section was computed using the following equation given in Ref [4]: -

$$<\sigma_s> = <\sigma_m> \eta \frac{A_s \lambda_s a_m N_m I_m f_m}{A_m \lambda_m a_s N_s I_s f_s} \times \frac{N_{Corr(s)} C_{attn.(s)}}{N_{Corr(m)} C_{attn.(m)}} \qquad (1)$$

We also employed the statistical nuclear model code TALYS-1.96 for the theoretical calculations of the reaction. The present experimental data has been rationalized with the existing cross sections data available in the TENDL-2019, IRDFF-II, JENDL/AD and IRDF-2002G.The initial results of cross section are presented in Fig.1. The computational results estimated by TALYS by using ldmodel-6 fit well with the present data.

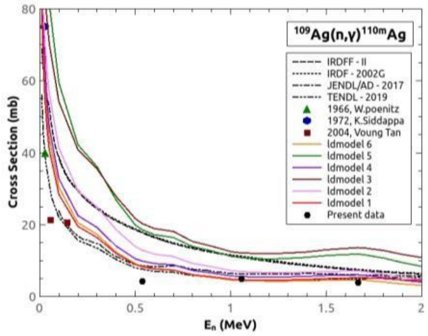

Fig. 1: The measured cross sections of ^{109}Ag(n, γ)^{110m}Ag.

References:
[1] A. Gandhi et.al., *European Physical Journal A,* **57** (2021) 1.
[2] Rebecca Pachuau *et al*., Nuclear Physics A **992** (2019) 121613.
[3] A.Gandhi *et al.*, Chinese Physics C **46.1** (2022) 014002.
[4] A.Gandhi et.al., *European Physical Journal Plus* **136.8** (2021) 819

Standardization of an efficient method for the removal of toxic Crown Ether from process solution containing ^{89}Sr Radioisotope

J. Vithya, Debasish Saha§, A. Arul Kumari, K. Sundararajan
RCSSS, Analytical Chemistry and Spectroscopy Division, FMCG, MC&MFCG, Indira Gandhi Centre of Atomic Research, Kalpakkam, Tamil Nadu-603102, India
§Email: dsaha@igcar.gov.in

Sr specific crown ether, DtBuCH18C6 in Octanol medium has been reported for the extraction of ^{89}Sr from FBTR irradiated yttriatarget [1,2]. Due to the toxicity associated with the crown ethers, it is mandatory to reduce its content in the final $^{89}SrCl_2$ radiopharmaceutical solution, which has application in metastatic bone cancer. The LD_{50} limit for 4′,4″(5″)-Di-tert-butyldicyclohexano-18-crown-6 is 100mg/kg for oral administration, whereas the limit for inhalation is only 3mg/L [3]. The LD_{50} values through intravenous injection is usually much lower than oral administration.

Extraction using organic solvent, elution through macro porous polymeric adsorbent resin, calcination etc. are probable options available to remove the dissolved organic content from aqueous phase. In this study calcination route has been implemented to avoid multiple stages of operation, cross contamination and radiation dose. Thermogravimetry analysis (TGA) of DtBuCH18C6 shows its complete removal at 400ºC. A fraction (1 ml) of 0.1M DtBuCH18C6 in octanol standard solution was added to a Pt crucible, and was subjected to calcination at 450ºC and 800ºC for 5h under identical conditions. The calcination step is also effective in removing the diluent 1-octanol as well (b.p.195ºC). Calcination at 800ºC, removes both dissolved organic phase as well as excess nitrate content, present in the sample since the chemical processing was done in HNO_3 medium, which thereby eases the conversion of$^{89}Sr(NO_3)_2$ to $^{89}SrCl_2$. Calcined sample was removed from Pt crucible using chloroform. A fraction of the chloroform wash was injected into the Radioactive Gas Chromatography-Flame Ionization Detector (GC-FID) system for the determination of crown ether and octanol. For both the calcination temperatures, the residual conc. of DtBuCH18C6 and Octanol in the calcined sample was found less than detection limit of the GC FID, which establishes the complete removal of toxic crown ether and octanol by calcination (Fig.1). Post calcination retention of Sr in Pt crucible was quantitative i.e. 99.9(±0.1)%.

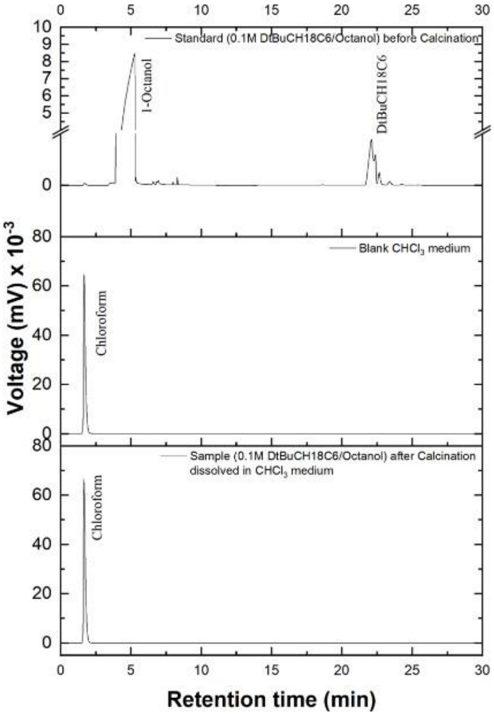

Fig.1: Assay of aqueous phase containing dissolved organic, post calcination (800ºC)using Radioactive Gas Chromatography (GC-FID)

Reference

[1] Saha, Debasish, et al. Journal of Radioanalytical and Nuclear Chemistry (2023): 1-14.

[2] Saha, Debasish, et al. RadiochimicaActa 104.3 (2016): 1-10.

[3] Aldrich, 2021. Safety data sheet 4′,4″(5″)-Di-tert-butyldicyclohexano-18-crown-6 (No. Version 6.4)

Production and Radiochemical Separation of ^{64}Cu from Enriched ^{68}Zn Target in 30 MeV Cyclotron

S. Chattopadhyay[1,§], S. Ash[1], S. Singha[1], L. Barua[1], D.G. Mahesh[1], S. Saha Das[1], Madhusmita[1], Md. N. Alam[1], U. Kumar[1], S. Roy[2] and P. Dhang[2]

[1] *Medical Cyclotron Facility, Regional Centre, Board of Radiation and Isotope Technology, Kolkata, India*
[2] *VECC, MCF, Chakgaria, Kolkata – 700094*
[§] Email: sankha@vecc.gov.in

Copper-64 ($t_{1/2}$: 12.7 h, decays: 17.5% β^+, 38.5% β^-, 44.0% EC) is a multipurpose radionuclide with many potential applications in monitoring of cancer growth and its development (PET imaging) as well as for theranostic purposes. This isotope can be produced in reactor as well as in cyclotron. No-Carrier-Added ^{64}Cu is generally produced in a small cyclotron through ^{64}Ni(p, n)^{64}Cu nuclear reaction (specific activity: 740-7400 MBq/µg); however it can also be prepared via ^{68}Zn(p, αn)^{64}Cu nuclear route in a medium or high energy cyclotron. The utilization of exorbitantly priced enriched ^{64}Ni as a target compared to enriched ^{68}Zn makes the ^{68}Zn target a more economic route in target utilization.

The indigenously prepared electroplated enriched ^{68}Zn target (area: 11.69 cm^2) was irradiated for 5.3 hours (total integral beam current: 500 µAh) using 28 MeV proton beam in 30 MeV cyclotron. The irradiated target was transferred from the vault to the solid target processing hotcell via the pneumatic target transfer system. It was dissolved in acid and chemically processed in an indigenous separation module using Dowex 50W-X8 (H^+ form), Dowex 1-X8 (Cl^- form) and solvent extraction (DIPE/ 7N HCl solvent system) to yield pure nca ^{64}Cu, (radionuclidic purity of >99.5% EOS, yield: 40.5 MBq/ µAh EOB, specific activity: 500 MBq/µg) in the form of $^{64}CuCl_2$ which may be further utilized for the preparation of other Cu-based radiopharmaceuticals. Therefore, it may be concluded that appreciable quantity of pure ^{64}Cu can be produced using ^{68}Zn(p, αn)^{64}Cu nuclear route.

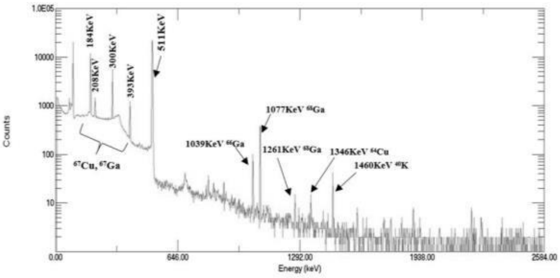

Fig. 1: Gamma Spectra of impure irradiated ^{68}Zn target

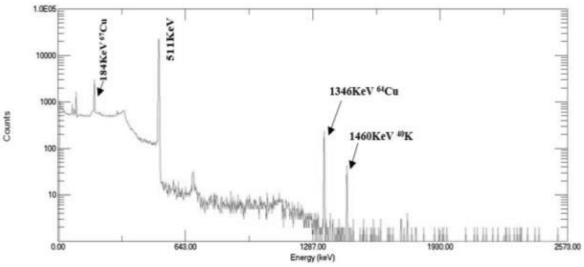

Fig. 2: Gamma Spectra of pure ^{64}Cu after radiochemical separation

The authors acknowledge cyclotron personnel for their contribution in cyclotron operation.

References:
[1] L.V. So et.al., *Journal of Radioanalytical and Nuclear Chemistry*, **277** (2) (2008) 451.
[2] S.V. Smith et.al., *Radiochimica Acta*, **75** (1996) 65.
[3] Rubel Chakravarty et.al., *Applied Radiation and Isotopes*, **165** (2020) 109341.

Production and Radiochemical Separation of ^{68}Ge from irradiated Ga-Ni Alloy Target in 30 MeV Cyclotron

S. Chattopadhyay[1,§], S. Singha[1], S. Ash[1], L. Barua[1], D.G. Mahesh[1], S. Saha Das[1],
Madhusmita[1], Md. N. Alam[1], U. Kumar[1], S. Roy[2] and P. Dhang[2]

[1] *Medical Cyclotron Facility, Regional Centre, Board of Radiation and Isotope Technology, Kolkata, India*
[2] *VECC, MCF, Chakgaria, Kolkata – 700094*
§ Email: sankha@vecc.gov.in

Gallium-68 [$t_{1/2}$: 67.7 min, β^+ (89%)] has application in PET imaging mainly for prostate cancer and neuroendocrine tumors. This isotope can be produced directly from enriched ^{68}Zn solid/liquid targets via ^{68}Zn(p, n)^{68}Ga reaction in a medical cyclotron and supplied to local hospitals. However, due to short half-life of ^{68}Ga, the supply of cyclotron produced ^{68}Ga-radiopharmaceutical is restricted to local regions only. Therefore, it is important to prepare ^{68}Ge ($t_{1/2}$ = 271 days) radiochemical for the manufacture of ^{68}Ge/^{68}Ga generator to cater to various nuclear medicine centers. ^{68}Ge has been produced in 30 MeV Medical Cyclotron from an indigenous electroplated Ga-Ni alloy target.

The Ga-Ni alloy target was prepared from sulphate bath (pH – 1.5) using constant current electrolysis technique on a gold-plated Cu-base material [1]. The target was irradiated with 28 MeV proton beam for 80 hours (total integral beam current: 4000 μAh) and chemically processed using Sephadex G-25 column after sufficient cooling in an indigenous automated module. The irradiated target (n=3) was dissolved in HNO_3 by repeated circulation of the hot acid solution in a closed loop. The dissolved solution was mixed with 1M Na-citrate (pH =12-13) and NaOH solution followed by loading on a preconditioned Sephadex G-25 column [2]. The column was washed with 1M Na-citrate (pH adjusted to 12-13), dilute Na-citrate (pH adjusted to 12-13), dilute NaOH solution and deionized water successively. ^{68}Ge-chloride was eluted using 0.1M HCl solution. The chemical separation yield and radionuclidic purity of ^{68}Ge was about 70% (n=3) and >98% (n=3), respectively. Thus pure ^{68}Ge-chloride may be used for the preparation of ^{68}Ge/^{68}Ga generator.

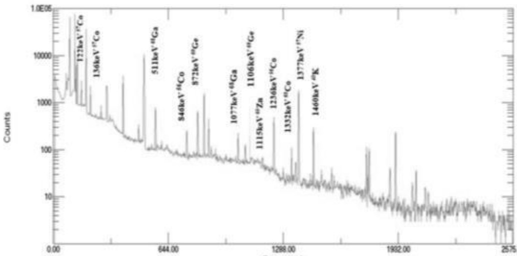

Fig. 1: Gamma Spectra of impure irradiated Ga-Ni alloy target

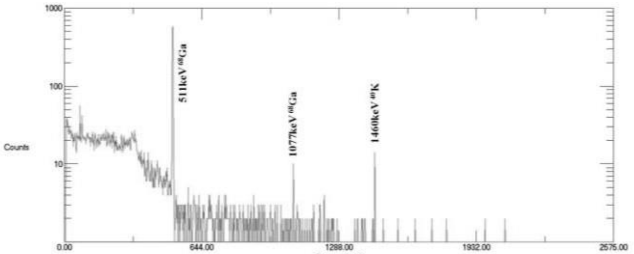

Fig. 2: Gamma Spectra of pure ^{68}Ge after radiochemical separation

The authors acknowledge cyclotron personnel for their contribution in cyclotron operation.

References:

[1] R. Adam-Rebeles et.al., *Radiochim. Acta*, **101** (2013) 481.
[2] J. M. Fitzsimmons et.al., *Radiochim. Acta*, **103**(2) (2015) 117.

Preparation and supply of ^{90}Sr/^{90}Y large area check sources for the hand and foot contamination monitors

Manoj Kumar[§], Shyamala Gandhi, Yugandhara Y. Yadav, S. K. Saxena

Radiopharmaceuticals Division, BARC, Mumbai, INDIA
[§]Email: mkjangir@barc.gov.in

The hand and foot monitoring devices can be installed at the exit of radiation control areas in nuclear power plants and other nuclear facilities such as radiological laboratories where radioactive material is handled. Hand-foot contamination monitors are used to check radioactive contamination adhered on working personnel‟s hands, feet and clothes while leaving radioactive laboratory. It occurs alarm and display the affected locations on the LCD screen when the count exceeds user programmable alarm level. For routine calibration of such instruments for beta radiation an external radioactive source of large area containing ^{90}Sr/^{90}Y is required. At the request of PLA Electroappliances, Mumbai, development of a rectangular large area ^{90}Sr/^{90}Y sources were undertaken. ^{90}Sr is a pure beta emitter and it decays to ^{90}Y with beta energy of maximum 0.546 MeV and half-life of ~28 years. ^{90}Y, too is a pure beta emitter with a shorter half-life of 64 hours and considerably higher beta energy of max. 2.27 MeV. In response to the above demands development of a rectangular large area sources having 150mm (L) x 100 mm (W) x 3 mm (H) was done which was further housed in another rectangular aluminum frame having the dimension of 152 mm (L) x 102mm (W) x 1 mm (thick). For this a required quantity of ^{90}Sr/^{90}Y radioactivity (~4000 dpm) each was prepared by chemical absorption using special chromatography paper manually [1]. After the absorption the absorbing paper was dried under normal environmental conditions and the dried paper was adhesively mounted on the aluminum base followed by an Al foil of 11micron thickness was placed to prevent the possible contamination during the end use. Finally, sources were cover with Aluminum frame for safe handling [Fig.1].

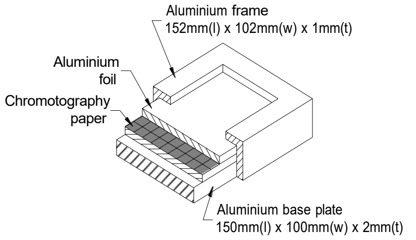

Fig.1: ^{90}Sr/^{90}Y Source assembly

The activity strength of each ^{90}Sr/^{90}Y sources were measured in liquid scintillation counter using suitable aliquots before and after absorption.

Also, the gross count rate was checked by hand-foot contamination monitor itself as per our previous experience. Before the supply of these sources all the necessary quality control test such as swipe test and spectrum check etc. were carried as per AERB, India norms towards the safe use of ^{90}Sr/^{90}Y radioactive sources. In conclusion, the reported method can be used for preparing large area sources of wide variety of long-lived radionuclides.

References:

[1] Manoj Kumar, Shyamala S. Gandhi, Rubel Chakravarty, J. Nuwad, J. Udhayakumar, Ashutosh Dash, *Applied Radiation and Isotopes*, Vol. 79 (2013), Pages 5-11.

Selection of DNA aptamers against epidermal growth factor receptor-1 for tumor scintigraphy

Chandan Kumar[§]
Radiopharmaceuticals Division, Bhabha Atomic Research Centre, Mumbai,400085, India
[§]*Email ID: ckumar@barc.gov.in*

Introduction:
Aptamers are single-stranded DNA (deoxyribonucleic Acid) or RNA (ribonucleic acid), similar to antibodies, for target recognition. It has become a promising biomolecule in recent decades due to the ease of chemical synthesis, modification, and manipulation, and its cost effectiveness enable its affordability for economically compromised people. The great chemical stability, low molecular weight (10–14 kDa), and minimal immunogenicity of aptamers provide an additional benefit in comparison to antibodies. These characteristics make aptamer an interesting and effective probe for target recognition. HER1 (Human Epidermal growth factor receptor-1) is overexpressed in various cancers, and thus it is an important target for tumors and can be used for diagnosis and therapy.

Material and Methods: The SELEX (systematic evolution of ligands by exponential enrichment) process was employed to select aptamers against the HER1 tumor receptor. In brief, the DNA library was designed, and the probable DNA sequence that was supposed to bind HER1 was screened. The probable DNA sequence was enriched after repeated screening for seven rounds of selection. The final DNA pool was sequenced using next generation sequencing (NGS). Out of 2 million aptamer sequences, only 20 sequences were chosen after analysis of the NGS data. Selected sequences were synthesized. A431 cells, which are HER1-overexpressing cells, were used to test the aptamer's specific binding. Cell binding was carried out in the A431 cell line with ^{125}I-nimotuzumab (an anti-HER1 antibody), along with an excess amount of the respective aptamers. Again, these selected aptamers were radio iodinated, and cell-binding studies were carried out in the A431 cell line and MCF-7 (Michigan Cancer Foundation-7) a low level of HER1 expressing cell line.

Results: It was discovered that these 20 sequences demonstrated different percentage binding, of which a few sequences show 10% binding.

Conclusions: The distinctive DNA sequences that specifically bind to HER1 receptor may be exploited to develop radiopharmaceuticals for diagnosis, radioimmuno assays, and other appropriate assays for monitoring HER1-expressing cancer.

Acknowledgements: Author would like to thank Head, Radiopharmaceuticals division and Head RPES, RPhD for their support in carrying out this study.

Study of alpha induced reactions for the production of ^{57}Ni

Namrata Singh[1§], A. Gandhi[1], Mahesh Choudhary[1], Aman Sharma[1], Mahima Upadhyay[1], Punit Dubey[1], Nitin Dubey[1], Utkarsh Mishra[1], J. Datta[2], S. Dasgupta[2] and A. Kumar[1]

[1]*Department of Physics, Banaras Hindu University, Varanasi-221005, INDIA*
[2]*Analytical Chemistry Division, BARC, Variable Energy Cyclotron Center, Kolkata-700064, INDIA*
[§] Email: namratasingh.jwala@gmail.com

Measurement of the reaction cross-sections for the induced reactions with target materials are of great interest in many fields such as production of medical radioisotopes, astrophysics and improvement of physical properties [1]. The radioisotope 57Ni (t1/2 = 35.6 hours), having Eγ=1377.63 keV (Iγ = 81.7%) is used in biomedical and agricultural research. Excitation functions were measured for natNi(α,x) reactions from 20-40 MeV and compared with the experimental data from EXFOR and also with the theoretical data using TALYS-1.9. Improving the activation cross-section data for natNi(α,x) reactions associated with covariance analysis [2-3] was the aim of this measurement.

The experiment was performed using the K-130 cyclotron at the Variable Energy Cyclotron Center (VECC), Kolkata, India. We have used the stacked foil activation technique followed by the offline gamma ray spectroscopy using HPGe detector. natNi, natAl and natCu foils were used in the stacks as a target material, energy degrader and as a monitor, respectively. The stacked targets were made with 6 and 5 sets of Cu-Ni-Al foils (10 X 10 mm2). Both stacked targets were irradiated for 3 hours by a 40 MeV and 28 MeV alpha beam with the average intensity of 150 nA.

The measurement of the reaction cross-section was done after the cooling of 7 days. The result of the present measurement and other experimental values reported in the literature of the reaction natNi(α,x)57Ni along with the theoretical calculations are shown in the Fig. 1.

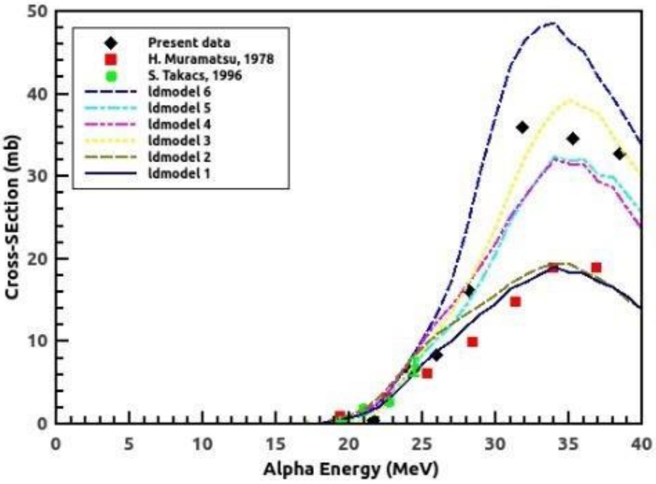

Fig. 1: Excitation function of ^{nat}Ni(α,x)^{57}Ni reaction

References:
[1] Namrata Singh et al., *Indian Journal of Pure and Applied Physics,* **54** (2020) 314.
[2] Mahesh Choudhary et al., *The European Physical Journal A*, **58** (2022) 1.
[3] A. Gandhi et al., *Chinese Physics C*, **46** (2022) 014002.

The detailed covariance analysis of ^{nat}Sn(α,x) nuclear reactions

Mahesh Choudhary[1§], Namrata Singh[1], Aman Sharma[1], A. Gandhi[1], Mahima Upadhyay[1]
S. Dasgupta[2], J. Datta[2] and A. Kumar[1]
[1]*Department of Physics, Banaras Hindu University, Varanasi-221005, India*
[2]*Analytical Chemistry Division, BARC, VECC, Kolkata-700064, India*
[§]Email: maheshchoudhary921@gmail.com

The data on alpha-induced reactions with various target materials are used in various fields such as nuclear medicine, the study of astrophysical phenomena and nuclear reaction studies [1]. The radioisotopes such as ^{118}Te, ^{119}Te, ^{121}Te, ^{119}Sb, ^{120m}Sb, ^{122}Sb, ^{124}Sb, ^{126}Sb, ^{117m}Sn, ^{111}In can be produce from alpha induced reaction on ^{nat}Sn. In the present work, we present measured nuclear reaction cross sections of ^{nat}Sn(α,x) reactions in the incident energy range 17-40 MeV. The uncertainty in the measured reaction cross sections was calculated from covariance analysis [2-4]. In the covariance study, we can describe uncertainty propagation with cross correlation between different measured quantities [5-7]. In this study, we have used TALYS nuclear code for theoretical prediction of the ^{nat}Sn(α,x) nuclear reaction.

For the present study, the experiment was performed at K-130 cyclotron, VECC, Kolkata. In this experiment, we have irradiated two stacks of target to measure the excitation function of ^{nat}Sn(α,x) reactions in the energy range 17-40 MeV. The foils ^{nat}Cu, ^{nat}Sn and ^{nat}Al were used to make a stacked target. The ^{nat}Cu foil was used as a monitor, the ^{nat}Sn foil was our main target and the ^{nat}Al foil was used as an energy degrader as well as used as catcher foil. The energy loss in the foils was calculate by using SRIM code. The measured excitation function of ^{nat}Sn(α,x)^{119}Te nuclear reaction along with the theoretical calculations is shown in figure 1. More details about the data analysis of cross sections and uncertainty quantification will be presented during the conference.

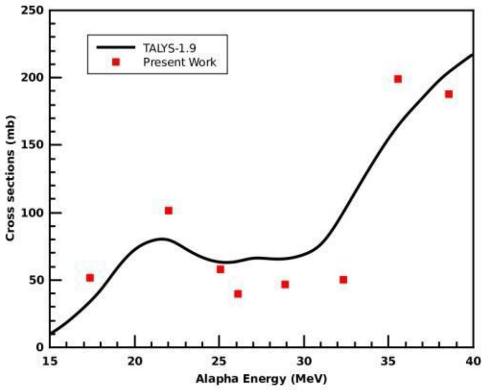

Fig. 1: The measured excitation function of ^{nat}Sn(α,x)^{119}Te nuclear reaction along with the theoretical calculations

References:

[1] B. Mukhopadhyay and K Mukhopadhyay, J. Nucl. Med. Radiat. Ther, 2 (2011) 1000115.
[2] A. Gandhi et al., European Physical Journal Plus, 136 (2021) 8.
[3] Mahesh Choudhary et al., The European Physical Journal A, 58 (2022) 1.
[4] A. Gandhi et al., The European Physical Journal A, 57 (2021) 1.
[5] Mahesh Choudhary et al., Journal of Physics G: Nuclear and Particle Physics, 50 (2022) 015103.
[6] A. Gandhi et al., Chinese Physics C, 46 (2022) 014002.
[7] R. Pachuau et al., Nuclear Physics A, 992 (2019) 121613.

Application of Nuclear Imaging Techniques in Veterinary Disease Diagnosis for Laboratory Animals

Y. Shete[1,§], P. Bhatkar[2] S. Rakshit[1], A. Damle[1] , A.K. Tyagi[1]
[1] *Radiation Medicine Centre, BARC, C/o TMH Annexe, Parel, Mumbai-400 012*
[2] *Department of Biotechnology Mumbai University*
Email: §yogeshwarivet@gmail.com

Laboratory animals are an integral part of preclinical studies and many key factors govern the outcome of experimental results. Healthy animals are important for preclinical testing hence, early detection and diagnosis of subclinical disease conditions is important before beginning of the testing.

Nuclear imaging method is explored for laboratory animals to identify the disease status and its correlation with tissue histopathology which is the gold standard [1]. Under this study, laboratory animals mice (n=54) and rabbits (n=8) were involved in the routine health monitoring programmes. Based on clinical examination suspected animals were subjected to a whole-body PET-CT scan with ^{18}F-FDG.The activity was injected intravenously at doses of 100 µCi and 1mCi in mice and rabbit respectively.

The observed and confirmed PET-CT scan lesions were categories as inflammation, infection and benign tumor lesion of animals. In BALB/C mice (n=1) suspected for lung infection with increased uptake of radiotracer (Max 10.8 SUV) as compared to control (Max 3.2 SUV) animal (Fig. 1). Lung histology showed infiltration of polymorphonuclear cells and congestion indicating the pneumonic changes. A case of mice skin infection ruled out by obscure contrast of CT scan of the skin surface compared to the control mice (n=2). Skin scraping and histopathology confirm the mange infection (Fig. 2). New Zealand rabbit (n=1) had penial skin growth with bleeding and PET-CT showed local inflammation (Max 0.5 SUV) which was supported by cell cytology, presented more population of heterophils (Fig. 3). Rabbit (n=1) having subcutaneous skin nodules displayed uptake of ^{18}F-FDG radiopharmaceutical at site. The cell cytology and histopathology showed fibrous connective tissue with whorl formation indicative of benign tumor of fibroma in rabbit.

In conclusion the combined PET-CT imaging offers deeper insights in the invasive and non-invasive behaviour of the lesion with accurate anatomical location which helps to differentiate and identify the pathological conditions. Further confirmatory diagnosis is supported by histopathology and cell cytology of the samples. Hence, nuclear imaging is one of the highly sensitive, less time consuming, non-invasive technique endorsed with histopathology as a quick and effective diagnostic aid in laboratory animals.

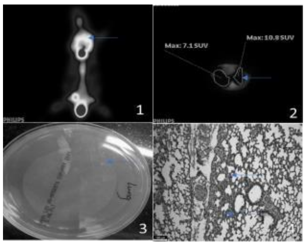

Fig.1: Mice Lung Infection with PET-CT scan

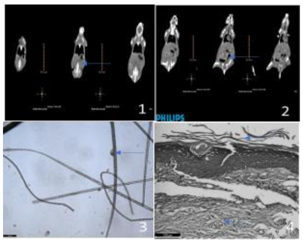

Fig.2: Mice Skin Mange Infection with CT scan

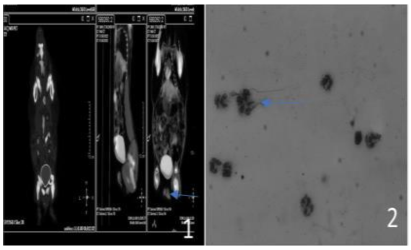

Fig.3: Rabbit Penial Papillary Growth with PET-CT scan

References:
[1] Song, S.L., et al., JNM., *49*(2) (2018) 303 - 309.

Evaluation of differential cross section data of alpha induced reactions using Bayesian neural network

Avika Chatterjee[§], Aman Sharma and Ajay Kumar[§]

Department of Physics, Banaras Hindu University, Varanasi-221005, India
[§]Email: avikachatterjee7@gmail.com ; ajaytyagi@bhu.ac.in

Alpha-induced nuclear reactions are crucial to understand nucleosynthesis effectively. Differential cross-sections provide us insight into the reaction mechanisms happening during the reaction. Such cross-sections are also helpful in effectively determining the respective reaction rates during nucleosynthesis.

Direct measurement of cross-section of certain reactions of interest is difficult. Therefore theoretical models provide us with a tool to estimate the cross sections. But data provided by most of the theoretical models are of low fidelity. Generally evaluated data which contains the information in available experimental data and the theoretical predictions are used for the applications. But the process of nuclear data evaluation is cumbersome and thus poses a challenge. In the past decade the field of machine learning has such significant progress.

In this study, we are using neural networks to obtain the evaluated data for alpha-induced reactions. Since neural networks do not provide the uncertainties in their predictions, we have used Bayesian neural networks to estimate the aleatoric uncertainties. We have used $^{12}C(\alpha,el)^{12}C$ reaction as the test reaction. We have developed a multi-fidelity Bayesian neural network to benefit from the theoretical model prediction and available experimental data. We used theoretical estimation of the differential cross-section from TALYS and experimental data from the EXFOR data library. The result obtained from the multi-fidelity Bayesian neural network trained for 18000 data points is shown in Fig. 1. The differential cross sectional data has been scaled by multiplying with 100.

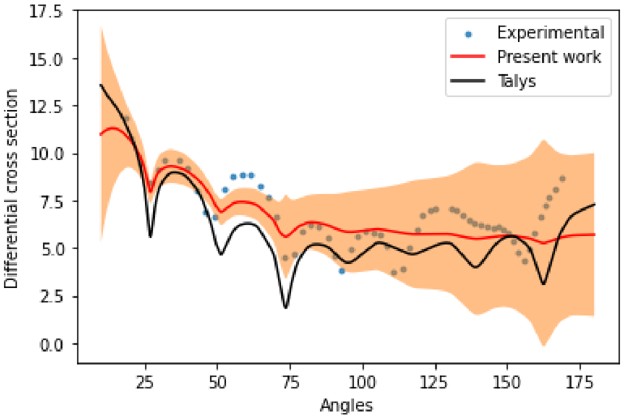

Fig. 1

References:
[1] Aman Sharma, A. Gandhi and Ajay Kumar, Phys.Rev.C 105, L031306 (2022)
[2] X.Meng and G.Em Karniadakis, Journal of Computational Physics 401,109020 (2020)

Comparison of ZnS (Ag) scintillation detector-based contamination monitor and GM detector-based contamination monitor while handling ^{225}Ac for radiopharmaceutical preparation.

Shriram Tervankar[1], Kamaldeep[2§], Gaurav Wanage[1], Pravind Maletha[1], Rahul Bhoite[1], Sandip Basu[1], Sureshkumar M K[2]
[1]*Radiation Medicine Centre, Bhabha Atomic Research Centre, Mumbai, India.*
[2]*Health Physics Division, Bhabha Atomic Research Centre, Mumbai, India.*
[§]Email: kdeep@barc.gov.in

Targeted alpha therapy (TAT) is a promising treatment option for wide spectrum of metastatic malignancies.^{225}Ac is a promising radionuclide for TAT due to its long half-life (9.9 days), emission of four alpha particles in its decay chain and emission of beta and gamma radiations (gamma emission of 217.6 keV (12.5%) and 440.4 keV (28%) by its daughters ^{221}Fr and ^{213}Bi respectively; beta emissions of 1.4 MeV (98%), 1.8 MeV (100%) and 0.6 MeV (100%) by its daughters ^{213}Bi, ^{201}Tl and ^{209}Pb respectively)[1]. Recently, Radiation Medicine Centre (RMC) has started TAT based on ^{225}Ac labelled radiopharmaceuticals. Being the first alpha emitter introduced in the therapeutic armamentarium in the domain of clinical nuclear medicine, ^{225}Ac based therapies are fraught with radiation safety related challenges. ^{225}Ac and its daughters emit both alpha particles and gamma radiations. In such situations choice of right radiation monitoring device especially for contamination monitoring is of paramount importance. The present study aimed to compare the sensitivity of ZnS (Ag) scintillation detector-based α contamination monitor and GM detector-based β/γ contamination monitor for contamination monitoring during handling of ^{225}Ac for radiopharmaceuticals.For this study, two contamination monitors viz. ZnS (Ag) scintillation detector-based alpha contamination monitor (Model ALS939, Pla, surface area 90 cm^2) and GM detector-based gamma contamination monitor (Model PCRM 162D, Pla , surface area 17.3 cm^2) were used. Both were used simultaneously to detect the contamination on hand gloves during the handling of ^{225}Ac-labelled radiopharmaceuticals and the observed response is presented in table 1.

Table1: Level of contamination detected over the hand gloves by both the contamination monitors.

S. No.	Contamination Level over the hand gloves (Counts/Sec)		Ratio of two monitors
	ZnS (Ag) based contamination monitor	GM based contamination monitor	
1	0.6	2.1	3.5
2	0.6	2.0	3.3
3	1	3.4	3.4
4	4.6	8	1.74
5	2761	5414	1.96

From this study it is found that, GM based pan cake contamination monitor is more sensitive in detecting the contamination due to ^{225}Ac and its daughter products in comparison to ZnS (Ag) based contamination monitor. The higher overall efficiency of pan cake detector for ^{225}Ac is due to its good response to both α and β particles and can be a suitable instrument for checking contamination in nuclear medicine facilities handling ^{225}Ac labelled compounds.

References:

[1] Andrew Kyle Henderson Robertson, Caterina Fortunata Ramogida, Paul Schaffer et.al., *Current Radiopharmaceuticals*, **11** (2018) 156.

Preparation and evaluation of a novel [^{177}Lu]Lu-labeled antibody-drug conjugate for targeted radionuclidic therapy of non-Hodgkin lymphoma

Naveen Kumar[1,2], Shishukant Suman[1], Mohini Guleria[1,2], Jeyachitra Amirdhanayagam[1],
Archana Mukherjee[1,2], Tapas Das[§1,2]
[1]*Radiopharmaceuticals Division, Bhabha Atomic Research Centre, Trombay, Mumbai-400085, INDIA*
[2]*Homi Bhabha National Institute, Anushaktinagar, Mumbai-400094, INDIA*
[§]Email: tdas@barc.gov.in

The ability of the antibody (mAb)-based agents towards targeting the receptors of choice with high specificity and selectivity put them in the category of sought-after ligands for the development of agents for various onco-targeting applications [1]. However, treatment using mAbs alone is often sub-optimum, leading to less satisfactory therapeutic results [1]. Hence, the use of antibody-drug conjugate (ADC), was envisaged to bring the mAb and cytotoxic drug together for the improvement of the therapeutic efficacy of immunotherapy. ADC is typically composed of a monoclonal antibody (mAb) covalently attached to a cytotoxic drug via a chemical linker. It combines both the advantages of highly specific targeting ability of antibody and highly potent killing effect of cytotoxic drug to achieve accurate and efficient elimination of cancer cells. Rituximab is a US-FDA approved drug for immunotherapy of non-Hodgkins‟ lymphoma whereas Chlorambucil has also been approved by US-FDA for chemotherapy of lymphomas. In the present work, a novel ADC comprising Rituximab and Chlorambucil was synthesized by employing the amine-carboxylic acid conjugation reaction between two resulting into formation of amide linkages. The average number of drug molecules conjugated per Rituximab was determined using MALDI-TOF mass spectrometry and found to be four. In order to further enhance the therapeutic efficacy of in-house synthesized ADC, it was radiolabeled with a therapeutic radionuclide viz. ^{177}Lu [$T_{1/2}$ =6.73 d, $E_{\beta(max)}$ = 497 KeV, E_{γ} = 208(11%), 113(6.4%)] via DOTA, a bi-functional chelating agent with a final radiochemical purity of >95%. The efficacy of the immunoconjugate in comparison to bare antibody and drug was ascertained via *in-vitro* studies in Raji cells. *In-vitro* studies revealed higher cytotoxicity associated with the immunoconjugate at different concentrations (Figure 1). During cell binding assay, [^{177}Lu]Lu-labeled immunoconjugate exhibited higher cell binding in cancer cells compared to unconjugated radiolabeled antibody. The results showed the improved therapeutic potential of the radiolabeled ADC ([^{177}Lu]Lu-Rituximab-Chlorambucil) compared to the unconjugated radiolabeled antibody ([^{177}Lu]Lu-Rituximab).

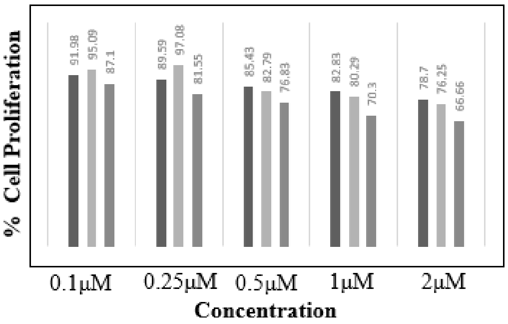

Figure 1: Cell cytotoxicity of Rituximab, Chlorambucil and Rituximab-Chlorambucil conjugate in cancer cell lines performed at different ligand concentrations viz. 0.1, 0.25, 0.5, 1 and 2 micromolar

Acknowledgements: The authors gratefully acknowledge Dr. S. Kannan, Director, Radiochemistry and Isotope Group, Bhabha Atomic Research Centre (BARC) for his constant support and encouragement. The authors are also thankful to their colleagues from Radiochemicals Section, Radiopharmaceuticals Division, BARC for providing ^{177}Lu used during the present study.

Reference:

[1] F. Zhiwen et. al., *Signal Transduct. Target Ther.,* **93** (2022)

Study of the effect of electron beam irradiation on polyethylene / ethylene-octene copolymer blends

Manjeet Singh[1,2], Rohini Agarwal[2], *Subhendu Ray chowdhury*[2§], Harish Jagat Pant[2]

[1]*Fuel Chemistry Division, Bhabha Atomic Research Centre & Homi Bhabha National Institute, Anushaktinagar, Mumbai, India*
[2]*Isotope & Radiation Application Division, Bhabha Atomic Research Centre & Homi Bhabha National Institute, Anushaktinagar, Mumbai, India*
[§] *Email: rcsubhen@barc.gov.in; rcsubhendu@gmail.com*

The blending of polymers is a way for the development of new materials in a less hazardous and more economical way compared to the synthetic route. Linear Low-density polyethylene (LLDPE) is used in various industries such as packaging, agriculture, construction, and automotive. It is mixed with other polyolefins to reduce costs or to improve its processability [1]. Polyolefin elastomers (POEs) possess long shelf life, good tear resistance, excellent chemical resistance and environmental stability, processing ease, and moderate cost. They are extensively used in the automotive sector, have biomedical applications including catheters and blood bags, and are used for the manufacturing of high-performance elastic fibers wires, cables, adhesives, footwear, soft foams, etc. Electron beam irradiation (EBI) is commonly used method for crosslinking of polymers [2]. EBI has many advantages such as fast reaction time, low operating temperatures, and low emission of volatile materials. Herein, effects of electron beam irradiation on LLDPE/ ENGAGE blends is carried out

Blends of LLDPE/ENGAGE are prepared in a twin-screw extruder. Stress-strain curve data obtained from UTM are used for the calculation of mechanical properties. With the increase in LLDPE content, the young"s modulus and tensile strength increased, whereas the percentage elongation decreased. The rheological data are presented by reporting the elastic modulus (G"), viscous modulus (G”), the dynamic viscosity (η) and the loss tangent (tan δ). EBI dose from 50 to 250 kGy are used for irradiation of prepared blends. The tensile strength and Young"s modulus values of blends increases with the increase EBI dose upto 200 kGy. Interfacial strength increases with increase in EBI dose due to formation of chemical bonds between polymer during the exposure of the blends to the radiation. Increasing irradiation dose led to increased cross-linked density and hence hindered the extension of chains which resulted in lower value of elongation at break.

Dynamic Mechanical Analysis (DMA) and hardness studies are performed for the irradiated samples. The hardness of the samples are measured using SHR-D Durometer and found to increase with the irradiation dosage. The EB treated samples are dissolved in hot Xylene for 24 hours for gel content determination. Gel content increases with increase in EBI dose

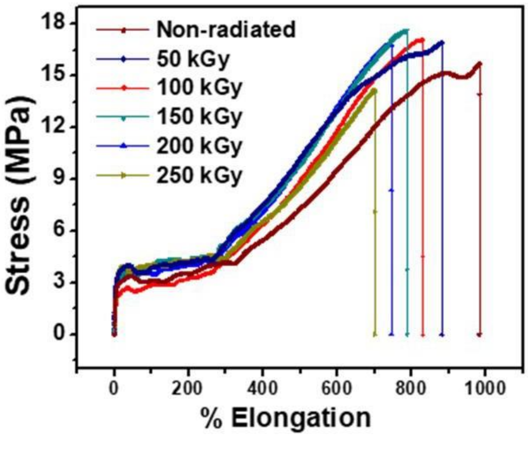

[1] M.C.G Rocha et.al., *Polimeros* 24 **(2014)** 23.
[2] A. J. Berejka et.al., *Radiat. Phys. Chem.*, 63 **(2002)** 551.

Investigation on the effect of Gamma Radiation on Structural and Optical properties of Mg doped SnO_2 nanoparticles

Ruchi Bisht[1], G.C. Joshi[1,2, §] and Jagat Pal Singh[1]

[1] *Department of Physics, G.B. Pant University of Agriculture & Technology,*
Pantnagar-263145 (Uttarakhand), India
[2]*Radiation and Isotopic Tracers Laboratory, Pantnagar, India*
§ Email: gc.joshi@gbpuat-cbsh.ac.in

Gamma radiation is the most energetic, highly penetrating EM radiation. When metal oxides are exposed to high energy γ-radiation, causing ionization in material, lattice defects in the form of vacancies, defect clusters, atomic excitation and dislocation loops near the interface which in turn can have a significant impact on the optical, electrical, and physical properties of materials.

In this light, the purpose of this study is to investigate the effect of γ-irradiation on Magnesium doped SnO_2 nanoparticles synthesized by simple co-precipitation method. The two gamma ray doses of 30 kGy and 60 kGy were chosen for irradiating the samples from ^{60}Co source (GC-5000) at RITL, GBPUA&T, Pantnagar and one of the samples was used as control (non-irradiated).

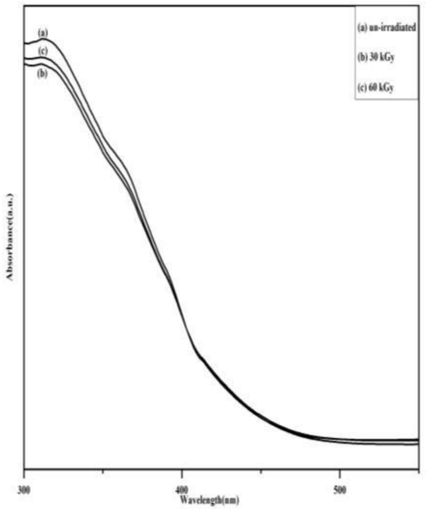

Fig. 1 UV-Absorption Spectrum

The induced modification caused by γ-irradiation on the structural, optical and functional properties have been systematically studied using X-Ray diffraction, UV-Vis spectroscopy, Photoluminescence (PL) and Fourier Transform Infrared (FTIR) Spectroscopy. XRD pattern reveals the formation of sample in tetragonal rutile structure, slight peak shifts and variation in crystallite size which was found to be in the range of 3-8nm when treated with both the gamma ray doses[1]. The optical properties were obtained using UV-Vis spectrophotometry before and after gamma ray irradiation and the energy band gap values were found to be gamma dose dependent and decreased with increasing dose of 30kGy and 60kGy. The decrease in the optical band gap could be attributed to the creation of localized states as a result of structural defects[2]. Photoluminescence measurements at room temperature using 300 nm wavelength excitation were investigated to unfold γ-irradiation effect on the defects and luminescence properties of the sample through PL spectra. In addition to demonstrating near band edge emission, the PL investigation also supports blue and green emissions caused by defects such as singly and doubly ionized oxygen vacancies. FTIR spectra revealed an O-H symmetric vibration band at 3100-3800cm^{-1} and corroborated chemical bonding and the position of the O-Sn-O band at around 673cm^{-1} [3]. The resultant changes in Mg doped SnO_2 nanoparticles were significantly impacted by the gamma-ray dose and are related to energy transfer and defect creation all through the irradiation process.

References:

[1]. Oryema et.al., *Radiation Physics and Chemistry*, *176* (2020), 109077M.
[2]. El-Nahass et.al., *Optical and Quantum Electronics*, *50* (2018), p1.
[3]. Gu, F et.al., *Chemical Physics Letters*, *372* (2003),(3-4), p451.

Efficiency of Gamma rays in developing mutants of Bhagwa pomegranate and their stratification through ISSR Marker

Mandeep Rawat [1,§], V. P[2] .Singh, G.C Joshi[3], S.K Verma[4], Ratna Rai[5] and Kanchan Karki[5]

[1,§,2,5] Department of Horticulture, [3]Radiations and Isotopic Tracer Laboratory , [4]Department Genetics and Plant Breeding and [5]Uttarakhand Council of Biotechnology,
G. B Pant University of Agriculture & Technology, Pantnagar. India. Uttarakhand, India.
[§] Email:- mandeeprawat107@gmail.com

Nuclear technology is currently used as one of the tools in mutation breeding to improve crops by increasing genetic variations. Induced mutation through gamma rays is a promising method to create variability. Gamma rays are categorized as ionizing radiation and considered as one of the potential mutagens due to its high penetrating ability. Presence of long juvenile period in fruit crops serves as hindrance for fruit breeders. Mutation breeding through gamma radiation can help breeders in overcoming this problem. Pomegranate is an important crop in terms of nutritional security, has high amount of anthocynin, phenolics, tannins, organic acids etc. But the crop is prone to fruit cracking, so the present study was carried out on a less cracking prone cultivar Bhagwa with five different treatments along with control (15Gy, 25Gy, 35Gy, 45Gy and 55Gy) to check the ability of gamma rays in developing cracking resistant mutants. The irradiation treatment of gamma rays was given in Radiations and Isotopic Tracer Laboratory (RITL, CBSH) and further carried out in Medicinal Plant Research and Development Center, GBPUAT, Pantnagar. A total of 3 replications per treatment with 10 cuttings in each replication were taken. Lethal dose or $\mathrm{LD}_{50/60}$ was obtained at 22.015 Gy for hardwood cuttings of pomegranate. Obtained mutants were analyzed using morphological, biochemical and molecular basis. On morphological basis tall and dwarf plants were obtained with 35Gy and 15Gy respectively [1]. A positive influence was observed in peroxidase, total sugars and catalayse activity of plant. Increase in the enzymatic activity of plants indicates activation of defense system ROS mediated cellular signaling [2]. Also, molecular characterization of mutants showed that the highest numbers of amplicons as well as maximum polymorphism were produced by primer 812 and 827, showing the variations produced due to gamma radiation treatments. So, it is concluded that gamma radiation has potential in developing mutants for pomegranate as well in fruit crops.

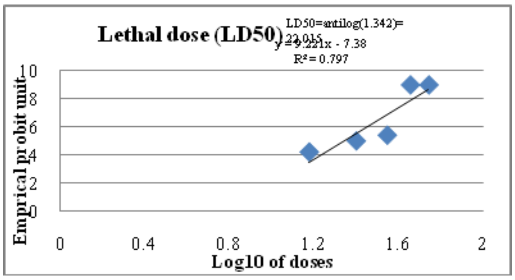

Fig1: Probit analysis based on corrected mortality rates of pomegranate

Fig 2: Types of leaves obtained with different treatments

References:
[1] Helaly, M.N.M., and Hosieny, A.M.R.H. *American Journal of Plant Physiology,* 4 (2011): 190-208.
[2] Ghosh, S. and Ganga, M. *Chemical Science Review and Letters*, 8(2019): 06-10.

Radiolytically Synthesized Photoluminescent Silicon Oxide Nanomaterials: Effect of Doping and Applications in Cr (6+) Sensing

Abina Hari[1], Apurav Guleria[2,4,§], Madhab C Rath[2,4] and Soumyakanti Adhikari[3,4]

[1]*School of Chemical Sciences, Kannur University, Kerala*
[2]*Radiation & Photochemistry Division,* [3]*Scientific Information Resource Division,*
Bhabha Atomic Research Centre, Mumbai 400085, India
[4]*Homi Bhabha National Institute, Trombay, Mumbai 400094, India*
§ Email: aguleria@barc.gov.in

Silicon (Si) has received a great deal of attention in the field of nanoscience and nanotechnology over the past three decades due to its excellent biocompatibility, natural abundance and cost-effectiveness [1]. Considering the imminent importance of Si nanomaterials (NMs) in various areas, a highly rapid, eco-friendly, and one-pot scalable approach based on radiation-induced technique is being reported for their preparation.

In a typical one-pot synthesis, the sample solutions were prepared by dissolving an optimized amount of Si precursor in double-distilled water. The resultant solution was bubbled with N_2O gas and irradiated with 7 MeV electron beam. The optimum absorbed dose imparted was ~ 40 kGy. The as obtained photoluminescent Silicon oxide nanocomposites (SiONCs) were functionalized *in situ* with different biocompatible ligands [2,3].

In order to tune the photoluminescence (PL) properties, different metal ions were doped into SiONCs. For instance, on doping with Mn^{2+} ions, the PL of SiONCs exhibited tunability from blue to green region. This is an indication of the tetrahedrally coordinated Mn^{2+} ions in the matrix of SiONCs. In addition to this, lanthanides such as Eu^{3+} and Tb^{3+} were doped into SiONCs, which resulted in significant changes in their PL properties. The as obtained doped SiONCs were explored for the sensing of toxic metal ions. Figure 1 shows the plot of F/F_0 versus metal ions (F_0 and F are SiONCs PL intensity in the absence and presence of metal ions, respectively. As can be seen, SiONCs exhibited remarkable effectiveness in the trace level detection of Cr^{6+} ions. Detailed analysis and the possible sensing mechanism will be discussed.

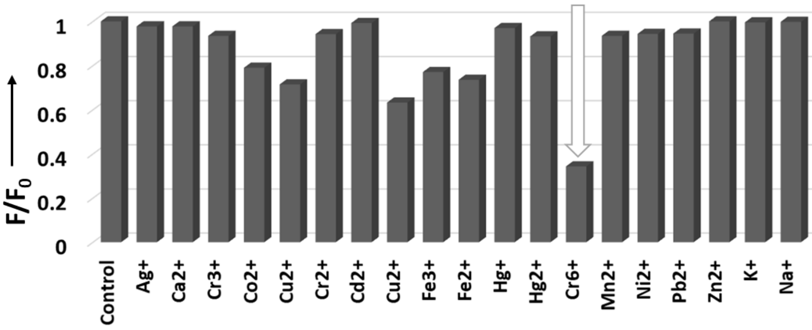

Fig. 1: Effect of various metal ions on the PL of SiONCs.

References:
[1] B. F. P. McVey and R. D. Tilley, *Acc. Chem. Res.*, **47** (2014) 3045.
[2] A. Guleria, A. P. Chavan, S. Neogy, V. V. Gandhi, A. Kunwar, A. K. Debnath and S. Adhikari, *ACS Appl. Nano Mater.*, **3** (2020) 5123.
[3] A. Guleria, V.V. Gandhi, A. Kunwar, S. Neogy, A. K. Debnath and S. Adhikari, *Colloids Surf. A Physicochem. Eng.*, **640** (2022), 128483.

Radiation Assisted Modification of Cellulose Paper for Application in Paper based Analytical Devices (PADs)

S. Rawat[1,2,§], N. Misra[1], S. A. Shelkar[1] and V. Kumar[1,2]

[1] *Radiation Technology Development Division, Bhabha Atomic Research Centre, Mumbai, India*
[2] *Homi Bhabha National Institute, Mumbai, India*
[§] Email: swarnima@barc.gov.in

Paper based Analytical Devices (PADs) have garnered a lot of research interest in the past few decades for on-site detection of several pollutants such as, toxic metal ions, pesticides etc. PADs are cost-effective, portable, easy to use and do not require sophisticated instrumentation or trained professional, which makes them a suitable alternative to the cumbersome conventional analytical techniques. Furthermore, paper as the analytical template offers ease of modification owing to the presence of hydroxyl groups of cellulose.

In the present work, cellulose paper has been modified via a green process of gamma radiation induced mutual irradiation grafting, wherein poly(acrylic acid) (PAA) has been grafted on paper substrate. This introduces acidic moieties on the paper in the form of -COOH groups of PAA, which can generate localized acidic conditions in-situ. Therefore, this PAA grafted paper (PAA-*g*-paper) can be used to fabricate PADs for estimation of pollutants (e.g., Cr(VI), boron etc.) that have established estimation protocol requiring acidic conditions. This eliminates need of external acid handling altogether and makes the on-site usage of PADs much safer. The grafting process was optimized by studying effect of various parameter such as, monomer concentration, absorbed dose, homopolymer inhibitor concentration and acid concentration. The grafting yield was found to increase with increase in the absorbed dose up to 25 kGy and got saturated beyond that (Fig. 1). Characterization of the samples was carried out via SEM, FTIR, DSC, TGA, and XRD.

Colorimetric estimation of Cr(VI) in water can be carried out water as per the American Public Health Association (APHA) protocol 3500-Cr using a spectrophotometer [1]. This colorimetric reaction between Cr(VI) and sensing species requires acidic conditions, necessitating addition of external acid during estimation. PADs fabricated from PAA-*g*-paper post loading sensing agent onto it were ably demonstrated for estimation of Cr(VI) in water. Cr(VI) could be visually detected with naked eyes and quantified via RGB analysis. The measurement range of these PADs for estimation of Cr(VI) is 1 mg.L^{-1} – 40 mg.L^{-1}.

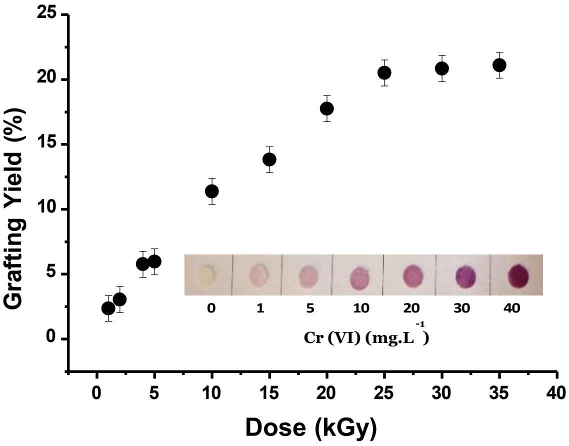

Fig. 1: Effect of Adsorbed Dose on Grafting Yield (Inset: Digital images of the colour developed on PADs for different Cr(VI) concentrations)

References:
[1] E. W. Rice et al. Standard methods for the examination of water and wastewater. 22nd ed: American Public Health Association; 2012.

Application of the magnetizable cellulose particle in development of CRP radioimmunoassay

T. S. Ghodke[1], V. Kadwad[2], S N Paradkar[1], N Karunakara[1] and K. B. Shenoy[1§]
[1] *Department of Applied Zoology/CARRT, Mangalore University, Mangalore 574199, India*
[2] *Radiopharmaceutical Programme, Board of Radiation, and Isotope Technology, Vashi complex Vashi, Navi Mumbai 400057, India.*
[§] Email: kshenoyb@gmail.com

Solid phase-based radioimmunoassay (RIA) procedure for quantification of C-reactive protein (CRP) is an important tool for the clinical analysis. CRP, an inflammatory protein belongs to pentameric protein family was described by Tillet and Francis in 1930 [1] while working with *Streptococcus pneumoniae*. Quantification of the CRP by a sensitive immunoassay is the need, and to fulfill this we have developed a rapid and user-friendly RIA by employing separation system based on antibody coupled with magnetizable cellulose nanoparticle.

In the present study development of separation system is achieved by coupling of anti-CRP antibody with magnetizable particle coated with cellulose residues. The coupling reaction was carried out by 1, 1' carbonyl-di-imidazole (CDI) activation method [2]. The magnetizable nanoparticle-based separation system was found responsive, it had better S/N ratio which reduces non-specific binding (NSB) and results in increased assay sensitivity. These magnetizable cellulose particles were prepared by wet grinding method, where a mixture of iron oxide containing manganese ferrite core and cellulose are stirred in a ball mill [3]. Size of prepared particles was below 3.11 µm. The wet grinding process is established in-house (Indian patent no.193445) by BRIT, Mumbai.

RIA is a competitive immunoassay [4]. RIA procedures using these particles have been tested by standard methods for sensitivity, linearity, reproducibility *etc.* and found to be user-friendly, inexpensive, reduced assay time and highly sensitive when compared with antibody-coated tubes or PEG-based liquid phase separation system. The coupling efficiency of antibodies to these particles was about 80-90% and titre for the coupled CRP antibody to magnetizable particle is shown in figure 1. Antibody functionalized micro-magnetizable cellulose particles can be used as a universal separating reagent in any immunoassays employing primary antibodies. The developed assay has the added advantage of flexibility in using solid-phase magnetizable immunosorbent as per the specific requirement of any assay or research.

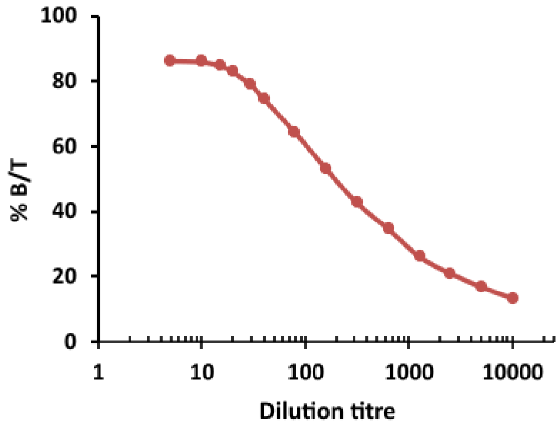

Figure 1. Magnetic particle coupled antibody titre

Acknowledgements: Authors like to thank BRNS and DAE, Govt. of India for funding the research.

References:

1. Tillet and Francis *J Exp Med*. **52(4)** 561 (1930)
2. Al-Abdulla *et al*. *J. Immunol. Methods* **122.2,** 253 (1989).
3. Yalow B.R.S, and Berson S.A. *J. Clin. Investig*. **39,** 1157 (1960).
4. Kadwad, V., *et al*. *J. Radioanal. Nucl. Ch.* **210.1,** 27 (1996)

Synthesis of Intrinsically Radiolabelled Gum Arabic Coated [^{169}Yb]Yb_2O_3 Hybrid Nanoparticles for Potential Use in Nanoscale Brachytherapy

Sanchita Ghosh[1,5], Sourav Patra[1], Santosh Gupta[2], Apurav Guleria[3], Avik Chakraborty[4], Sudipta Chakraborty[1] and Rubel Chakravarty[1,5,§]

[1]Radiopharmaceuticals Division, [2]Radiochemistry Division, [3]Radiation and Photochemistry Division, [4]Radiation Medicine Centre, Bhabha Atomic Research Centre, Trombay, Mumbai, 400058, India. [5]Homi Bhabha National Institute, Anushaktinagar, Mumbai 400094, India.

[§] Email*:* rubelc@barc.gov.in

Intrinsically radiolabelled nanoparticles have tremendous prospective in offering an easier, faster, stable, and more specific radiolabelling technique in cancer treatment. In this study, intrinsically radiolabelled ^{169}Yb ($t_{1/2}$ = 32d; $\gamma_{avg.}$ = 93 keV) nanoparticles have been developed for potential use in nanoscale brachytherapy. Nanoscale brachytherapy is an emerging field in cancer care because functionalized nanoparticles can be synthesized to match the sizes of tumor vasculature so that optimal therapeutic payloads with minimum leakage away from target sites can be achieved [1]. Ytterbium-169 was produced by irradiation of enriched (~ 10 % in ^{168}Yb) Yb_2O_3 target at a flux of 1×10^{14} $n.cm^{-2}.s^{-1}$ for 14 d in the Dhruva reactor. The irradiated target was radiochemically processed and intrinsically radiolabelled gum arabic coated [^{169}Yb]Yb_2O_3 nanoparticles were synthesized by controlled hydrolysis in aqueous medium for potential application in nanoscale brachytherapy. Non-radioactive gum arabic coated Yb_2O_3 nanoparticles were also synthesized and extensively characterized by various techniques.

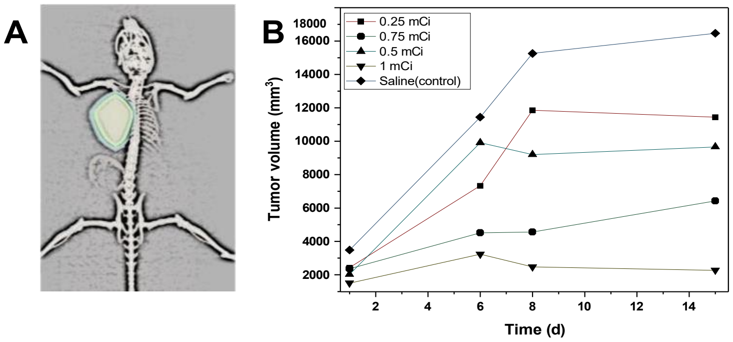

Fig.1 A) SPECT/CT image of tumor bearing mice. **B)** Tumor regression studies.

A clear and crystalline solution of gum arabic coated Yb_2O_3 nanoparticle, having high colloidal stability, was prepared with particle size 12±1 nm. The radiochemical purity of intrinsically radiolabelled nanoparticles was > 99%. Uniform distribution and enhanced retention of the agent was observed in SPECT/CT image after intratumoral injection in melanoma (B16F10) tumor bearing C57BL/6 mice (**Fig. 1A**). The therapeutic efficacy of the nanoparticle was evaluated by tumor regression studies in melanoma tumor bearing mice after intratumoral administration of 0.25, 0.5, 0.75, 1 mCi doses. We observed that after 15 days tumor growth was significantly arrested with all the doses compared to the control and the best treatment effect observed with 1 mCi dose (**Fig. 1B**). Overall, we have successfully developed intrinsically radiolabelled gum arabic coated [^{169}Yb]Yb_2O_3 nanoparticles which shows potential as a cancer theranostic agent in preclinical settings.

Reference:

[1]. R. Chakravarty, S. Chakraborty, A. Guleria, R. Shukla, C. Kumar, K.V. Nair, H. D. Sarma, A. K. Tyagi, and A. Dash. *Ind. Eng. Chem*. Res. 57 (**2018**) 14337−14346.

Gamma Irradiation Induced Effect on Structural, Optical and Elastic Properties of Nickel-Cobalt Ferrite

Deepak Kholiya[1], Komal[1, §], R C Srivastava[1], G. C. Joshi[2] and Chandra Shekhar Joshi[1]

[1]*Department of Physics, G. B. Pant University of Agri. & Tech., Pantnagar, India*
[2]*RITL, C.B.S.H., G. B. Pant University of Agri. & Tech., Pantnagar, India, 263145*
[§]Email: kanakbhatheja0509@gmail.com

In present study, the structural, optical and elastic properties of $NiFe_2O_4$, $CoFe_2O_4$ and $Ni_{0.5}Co_{0.5}Fe_2O_4$ nanoparticles were investigated before and after gamma irradiation with total dose of 1 kGy and 5 kGy. The sol-gel auto combustion method was used to synthesize ferrite nanoparticles. The XRD pattern of all the samples indicated the formation of single phase cubic spinel structure. Different structural parameters were calculated using XRD data and the effect of dose of gamma irradiation on these parameters were also studied. UV-Vis diffuse reflectance spectroscopy was used to find the optical band gap values and are represented in Fig. 1. The values of energy band gap showed that all samples were semiconductor in nature. The elastic parameters were evaluated using the method based on infrared spectroscopy and it was observed that these parameters are affected due to the change in crystallite size and cation distribution. The elastic moduli were observed to be in increasing trend with gamma irradiation which indicates that interatomic bonding amid various atoms in crystal is getting strengthened continuously due to redistribution of cations.

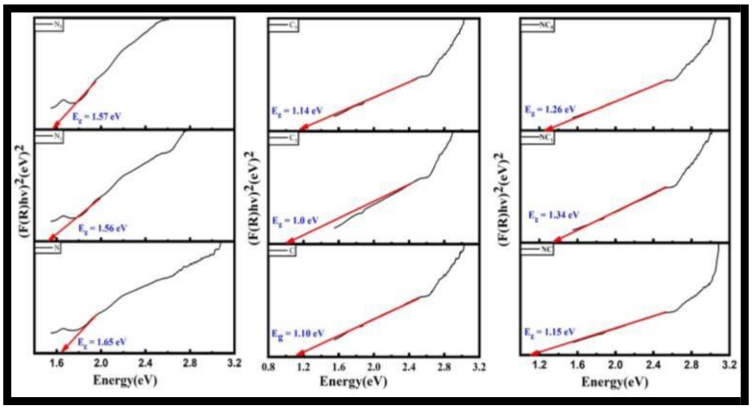

Fig. 1: Tauc plot for pristine and irradiated of (a) $NiFe_2O_4$ (b) $CoFe_2O_4$ (c) $Ni_{0.5}Co_{0.5}Fe_2O_4$

Keywords: Spinel ferrite; optical band gap; elastic properties; gamma irradiation; structural properties.

References:

[1] Sen, S. K., Babu et. al., *AIP Advances*, *11* (2021) 075308.
[2] Kalunge, S., Surase, et. al., In *Journal of Physics* 1644 (2020) 012020.

Radiosynthesis of ^{99m}Tc-labeled albumin binder- cNGR peptide conjugate

Kusum Vats[1], Haladhar D Sarma[2] and Drishty Satpati[1§]

[1]*Radiopharmaceuticals Division,*
[2]*Radiation Biology and Health Science Division*
Bhabha Atomic Research Centre, Trombay, Mumbai-400085, India
[§]Email: drishtys@barc.gov.in

The peptide sequence asparagine-glycine-arginine (NGR) binds specifically to aminopeptidase receptor (APN/CD13) over-expressed in various human solid tumors [1]. Hence radiometalated NGR peptide constructs have been explored as molecular imaging probes for detection and monitoring of APN/CD13 receptor-expressing malignant sites [2]. In previous studies we observed rapid blood clearance of radiolabeled NGR peptide constructs which resulted in lower accumulation of radioactivity in tumor [2]. Thus with an aim to enhance the bioavailability, albumin binder [4-p-(tolyl)butyric acid] was conjugated to cyclic NGR peptide which was then radiolabelled with technetium-99m [3].

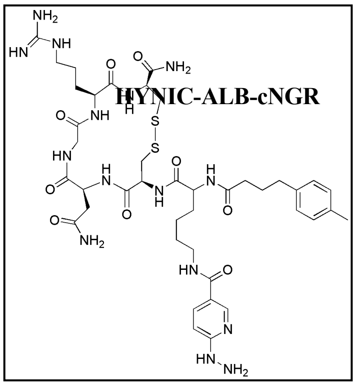

The fully protected peptide chain Fmoc-Lys(Alloc)-Cys(Acm)-Asn(Trt)-Gly-Arg(Pbf)-Cys(Acm)-NH_2 was assembled on rink amide MBHA resin manually by standard Fmoc solid phase peptide synthesis. The albumin binder, 4-p-(tolyl)butyric acid was attached to the α-amino group of lysine and HYNIC chelator was conjugated at the ε-amino carboxylic group of lysine. On-resin cyclization of cysteine sulphides was carried out with 1.2 eq of thallium(III)trifluoroacetate in DMF. Followed by cleavage from the solid phase crude peptide conjugate was purified using semi-preparative HPLC and characterized by mass spectrometry (m/z (obs) = 994.41) $[M+Na]^+$ (calcd for $C_{41}H_{61}N_{15}O_9S_2$: 971.42). The peptide conjugate HYNIC-ALB-cNGR was radiolabeled with ^{99m}Tc by incubation with EDDA, tricine and stannous chloride. ^{99m}Tc-HYNIC-ALB-cNGR was formed with >95% radiochemical purity (RCP). Bio-distribution studies were carried out in C57BL/6 mice bearing melanoma tumor. Blood uptake of ^{99m}Tc-HYNIC-ALB-cNGR was 1.71 ± 0.27% ID/g and 0.86 ± 0.22% ID/g at 1 h and 3 h p.i. respectively. Corresponding tumor uptake values were 2.12 ± 0.19% ID/g and 1.89 ± 0.17% ID/g which were higher than those observed for ^{99m}Tc-HYNIC-cNGR (0.63 ± 0.11 and 0.38 ± 0.08% ID/g). Present results indicate that introduction of 4-p-(tolyl)butyric acid as an albumin binder enhanced circulation in bloodstream which ultimately led to 2.7-fold increase in tumor activity of ^{99m}Tc-HYNIC-ALB-cNGR as compared to ^{99m}Tc-HYNIC-cNGR (without albumin binder).

References:

[1] A. Corti, F. Curnis, W. Arap and R. Pasqualini, *Blood*, **112 (**200) 2628.
[2] K. Vats, D. Satpati, R. Sharma, C. Kumar, H. D. Sarma and S. Banerjee, *J. Label. Comp. Radiopharm.*, **61 (**2018) 68.
[3] J. Lau, O. Jacobson, G. Niu, K. S. Lin, F. Bénard and X. Chen, Bioconjugate Chem., **30** (2019) 487.

Interaction of Rhenium-188 labelled microspheres with primary hepatic cell-lines

Aarti Aggarwal[1], Gurjeet Kaur[2],Ravjit Singh Jassal[3], Bikash Medhi[2], Bhagwant Rai Mittal[1]and Jaya Shukla[1,§]
[1]*Department of Nuclear Medicine, Post Graduate Institute of Medical Education and Research, Chandigarh, India*
[2]*Department of Pharmacology,PGIMER, Chandigarh, India*
[3]*Department of Biochemistry, PGIMER, Chandigarh, India*
[§] Email: shuklajaya@gmail.com

Hepatocellular carcinoma (HCC) is one of the common causes of mortality worldwide. Chemo and radiotherapy are not suitable because of hepatic intolerance. Trans-arterial delivery of chemo(TACE) and radiotherapeutic drugs (TARE) are main palliative treatments. However, TACE is contraindicated when portal vein is thrombosed. Indigenous microsphere cold kit has been developed at PGIMER. The aim of the present study is to evaluate the behaviorof microspheresand therapeutic potential of ^{188}Re-Microspheres on primary hepatic cancer cell lines (HepG2).

The microspheres were first labelled with FITC and the labelling efficiency was determined with the flow cytometer. The cellular uptake of FITC labelled microspheres in HepG2 cells was studied at different time points. The cytotoxic effect of ^{188}Re-Microspheres and the mode of cell death in HepG2 cells was studied using MTT and Annexin FITC-V/PI apoptosis assay respectively.

More than 99% labelling was achieved with FITC and $^{188}ReO_4^-$. The Z-stacking analysis obtained from confocal microscopy showed 6 h as maximum uptake time for microspheres in HepG2 cells. Results indicated that the exposure to ^{188}Re-Microspheres decreased the cellular viability of HepG2 cells. The observed mean viability was 77.81 ± 0.015% to 42.03 ± 0.148% at 192 h incubation (more than 10 half-lives) with 0.07 to 1.97Gy delivered by^{188}Re-Microspheres (Fig. 1). TheAnnexin FITC-V/PI apoptosis assay showed that 60.59 ± 0.030%cells entered into the early apoptotic phase after treatment with ^{188}Re-Microspheres and only 36.5 ± 0.020% remained in viable phase. The data revealed that ^{188}Re-Microspheres show significant growth inhibition even after 11 half-lives (192 h). However, cells treated with alone ^{188}Re showed early cell death (48 h). After 192 h, the cells regrown and 50.32 ± 0.004% were in viable phase and1.2 ± 0.025% cells in early apoptotic phase after 11 half-lives (Fig. 2).

The optimum uptake time for microsphere uptake in HepG2 cells was noted as 6 h. ^{188}Re-Microspheres showed better cytotoxicity as compared to ^{188}Re alone. The ^{188}Re-Microspheres entered inside the cells, behaved as permanent radiation source, and delivered continuous radiation exposure for a sufficient time, induced apoptosis and better cytotoxicity was obtained.

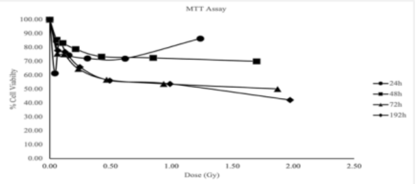

Fig 1. Cytotoxicity effect of ^{188}Re-Microspheres was studied for more than 10 half-lives of ^{188}Re in HepG2 cell lines by MTT assay

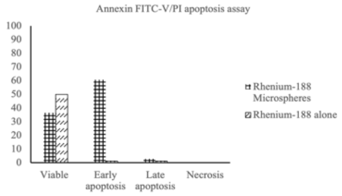

Fig 2. Comparison of mode of cell death by ^{188}Re-Microspheres and alone ^{188}Re in HepG2 cell lines studied with Annexin FITC-V/PI apoptosis kit and analyzed by flow cytometry. The data here represents cells in various phases of cell cycle after 11 half-lives of ^{188}Re.

Improvement of Anti-fouling Properties of Ethylene Propylene Diene Elastomer (EPDM) by Modifying Surface Properties

R. Agarwal, S. Ray Chowdhury§ and H. J. Pant

Isotope & Radiation Application Division, Bhabha Atomic Research Centre & Homi Bhabha National Institute, Anushaktinagar, Mumbai, India
§ *Email: rcsubhen@barc.gov.in; rcsubhendu@gmail.com*

EPDM is extensively used in water system O-rings, hoses, and gaskets. It is used for making portable water gaskets and seals for drinking water containers. Certain gram-negative bacteria, *P. aeruginosa, K. pneumoniae* and *L. pneumophila,* are found to colonise on its surface and persists as biofilms on it [1]. Biofilms are developed by the microbial cell adhesion followed by colonization on the surfaces through extra-cellular polymeric substances. The adhesion and proliferation of bacteria on abiotic surfaces and the subsequent biofilm formation pose challenges in both healthcare and industrial applications. Biofilm formation on EPDM gaskets led to the washing of bacteria in the purified drinking water and hence, has been reported as a source of infection to a healthy body [2].

Membrane surface properties play important roles in determining the rate and severity of membrane fouling. In the study, EPDM was surface modified by covalent attachment of Methacrylic acid (MAA), Dodecyl methacrylate (DMA), and Isodecyl methacrylate (IDM) using Co-60 gamma radiation. Various reaction parameters like monomer concentration and radiation dosage were optimized. The fouling property of the modified membranes was studied.

The modified surface was characterised by attenuated total reflection - Fourier transform infrared spectroscopy and scanning electron microscopy. The contact angle was measured to study the change of surface wetting property. The EPDM modified with different functional groups was tested for biofouling using colony forming units (cfu) count and resazurin fluorescence assay technique. The biofouling assay data showed the strong resistance to fouling of *K. pneumoniae* on MAA grafted EPDM. The proliferation of bacteria was observed to be higher for DMA and IDM grafted surface compared to pure EPDM. The study revealed that the hydrophilic nature of MAA attributed to the anti-fouling property of the modified EPDM.

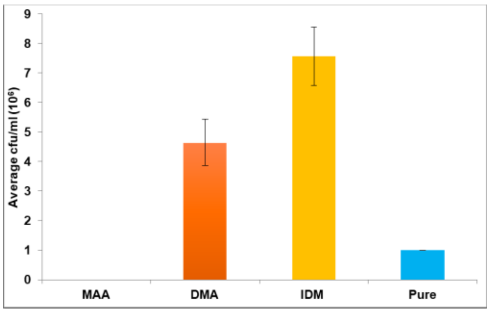

Figure 1. Spread plate count of samples immersed with *K. pneumoniae* for 30 days.

References:

[1] G. Moore et.al., *Journal of Bioadhesion and Biofilm Research,* **31** (2015) 677.
[2] C.F. Hutchins et.al., *Journal of Hospital Infection,* **106** (2020) 429.

Studies on the Selective Adsorption of Strontium by Surface Modified Fe_3O_4-TiO_2

Chayan Patra, Kuntal Kumar Pal, P.Velavendan§, K. A Venkatesan, K. Ananthasivan

Process, Radiochemistry and Reprocessing R& D Division,
Indira Gandhi Centre for Atomic Research, Kalpakkam, India
§ Email: velp@igcar.gov.in

Separation and recovery of useful isotopes from radioactive waste and their deployment for societal application makes it as a wealth. Radioisotope of strontium, ^{89}Sr, is one of the beta emitting radio nuclides, which has immense potential for use in therapeutic application [1]. Here, Fe_3O_4@TiO_2 was synthesized as a precursor for the selective recovery of strontium from the radioactive aqueous solution [2]. Initially, $FeCl_3$ and $FeCl_2$ (2:1) solutions were mixed together and poured into NH_4OH solution under stirring condition. The precipitate formed was separated using external magnets and treated with 2(M) perchloric acid and centrifuged. To make the Fe_3O_4 sol, the solid was re-dispersed in the water. 5 ml Fe_3O_4 sol in 95 ml water and 50 ml 0.1 M Ti acylate was mixed together, stirred at 60°C for 1 hr. $NaHCO_3$ was also added into the reaction mixture to complete the hydrolysis. The precipitate was separated by centrifugation and washed several times with water and ethanol. The product (Fe_3O_4-TiO_2-CO_3) was dried under vacuum, and the surface was modified by using NaOH solution for the adsorption studies.

The maximum adsorption efficiency of strontium by this adsorbent was found to be 98.9% in aqueous solution containing an initial strontium concentration of 185.6 mg/ L. This adsorbent was treated with strontium nitrate solution in the pH range from 5-12 in various batches in presence of sodium nitrate solution. In each experiment, samples were collected at regular intervals and Sr analyses were carried out by Ion chromatography by suitable dilution. The results were compared with the known Sr standard to get the sample results. Experimental result shows that the sorption of strontium begins at pH = 5 and it increases with increase of pH. So, sorption capacity is much higher at higher pH levels. Strontium analysis method was standardized by preparing known concentrations of Sr from Sr $(NO_3)_2$ (assay: 99.995%), Sigma Aldrich by ion chromatography technique after appropriate dilution with high purity water to get the calibration plot. Strontium is calibrated from 1 to 5 ppm (Fig. 1) with RSD 1.00%. Experimental results prove that surface modified Fe_3O_4-TiO_2 exhibit high adsorption capacity and selectivity particularly for the strontium in the presence of cesium and potassium metal ion.

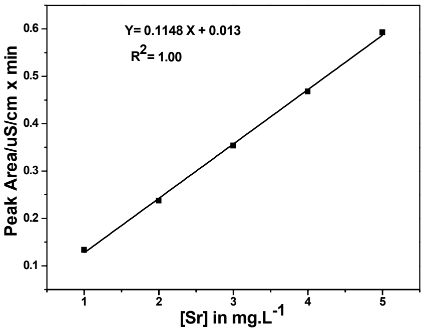

Fig. 1: Calibration graph for Sr standard (1-5 ppm) by Ion chromatography.

Acknowledgements: Authors are thankful to Mr. Suvra Sil, MC&MFCG, IGCAR for his support in Ion Chromatographic analysis.

References:
[1] Debasish Saha et.al, *Journal of Radioanalytical and Nuclear Chemistry*, **298** (2013) 1309
[2] N. Li et. al, *Advanced Funcional Material*, **22** (2012), 835

Hydrophobic Modification of Jute Fibre: Reaction Parameters Optimization and Structure-Property Analysis

A. Jha[1, 2], A. Thite,[3] S. Ray Chowdhury[§ 1,2] and H. J. Pant[1, 2]

[1]Homi Bhabha National Institute, Anushaktinagar, Mumbai-400094, India.
[2]Isotope and Radiation Application Division, Bhabha Atomic Research Centre, Trombay, Mumbai-400085, India.
[3]The Bombay Textile Research Association, Ghatkopar (W), Mumbai 400086, India.
[§] Email: rcsubhen@barc.gov.in; atanujha@barc.gov.in

In this work we report an easy, economic, environment friendly, single step, and high throughput method for hydrophobization of jute fibre. Surface wettability of jute fibre is modified by gamma radiation assisted covalent attachment of long chain hydrocarbon molecules (LCHM). Lauryl methacrylate (LMA) is found to be the most suitable agent among the acrylates used, for effective grafting and generation of the desired surface wettability (superhydrophobicity, with very high water contact angle). Extent of modification in terms of grafting yield is measured gravimetrically. Characterization of unmodified and modified jute fibre is performed by Fourier-transform infrared spectroscopy (FTIR), contact angle measurement, surface wettability study, tensile testing, scanning electron microscopy (SEM), and thermogravimetric analysis.

Effect of degree of modification with extent of hydrophobicity is studied and accordingly required grafting yield is determined as ~25-30 wt%. Important reaction parameters are optimized to achieve the required extent of modification (i.e., 25-30 wt%). These optimized parameters are fixed at 15 kGy total dose, 2 kGy/hr dose rate, 20 vol% LMA concentration and 12 vol% water content in the reaction mixture.

Modified jute fibre is turned to be superhydrophobic (water contact angle 151°) from superhydrophilic (water contact angle 12°) one (Fig. 1). Mechanical and thermal analysis reveals that there is no considerable alteration of mechanical performance and thermal stability after modification. Results of SEM analysis support the findings of contact angle measurement and surface wettability study.

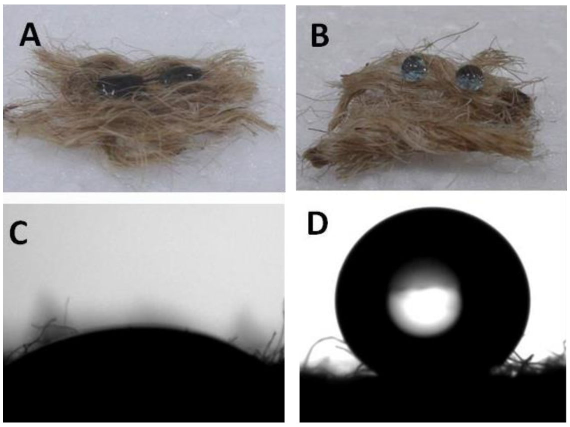

Fig. 1: Water drop beading and water contact angle (WCA) on unmodified (A, C) and modified jute fibre (~30 wt% modified) (B, D)

Keywords: Jute fibre, hydrophobization, radiation technology, polymer

Synthesis of scandium oxide microspheres by microfluidic route and their characterization

Jayashree Biswal[1,2,§], Nirvik Sen[3], Sunil Goswami[1], Annie Joseph[4], Arvind Ananthanarayanan[4], V. K. Sharma[1], K. K. Singh[3] and H. J. Pant[1]

[1]Isotope and Radiation Application Division, [3]Chemical Engineering Division,
[4]Process Development Division
Bhabha Atomic Research Centre, Mumbai 400085, India
[2]Homi Bhabha National Institute, Mumbai 400094, India
§ Email: jayashreebiswal@gmail.com

Radioactive scandium-46 oxide microspheres (RMSs) have applications in mapping flow in a chemical reactor through a technique known as radioactive particle tracking (RPT) [1]. The microspheres should be designed in a such a way that nuclear properties and other physical properties such as shape, size and density of the microsphere have to be optimised for their suitability in RPT applications. Therefore, designing an experimental method plays a vital role in preparation of tailor-made scandium oxide microsphere (Sc-MS) with desirable physical properties. Microfluidic technique deals with controlling chemical reactions by flow of liquid through micrometer-sized channels. This technique requires small amounts of liquid to perform chemical reactions with by fast mixing inside the droplets. In the present study a microfluidic technique was developed for synthesis of scandium oxide microspheres through sol-gel reaction of the reactants. The aqueous solution of the reactants, i.e, scandium nitrate, hexamethylene tetramine (HMTA) and urea were dispersed in dodecane in a microfluidic device. The device consists of two microfluidic T-junctions for mixing of different liquid stream and three syringe pumps were used to maintain a specific flow rates of the reactant solutions.

The scandium hydroxide microspheres were first obtained by allowing a residence time of 30-60 s to the reactants inside the device at a temperature of 90 ^{0}C. The reaction conditions were optimised to obtain microsphere with appreciable mechanical properties. 3 mol dm^{-3} scandium nitrate, 4 mol dm^{-3} HMTA and 4 mol dm^{-3} urea were used and the flow rates of aqueous and organic phases were maintained at 1.2 ml min^{-1} each for synthesis of the microspheres. The obtained microspheres were heated in a furnace at 300 ^{0}C to produce Sc-MS (Fig 1). The Sc-MS were characterized by XRF and optical microscopy. The size of the SMS was in the range 500-2000 μm. The Sc-MS were irradiated in a nuclear reactor to obtain RMS. The activity produced on each RMS was about 35 MBq.

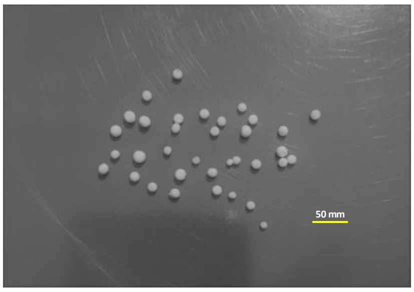

Fig 1. Photograph of scandium oxide microspheres

References:
[1] Roy, S., Larachi, F., Al-Dahhana, M.H., Dudukovi!ca, M.P., Appl. Radiat. Isot. 56 (2002) 48.

Evaluation of corrosion rate of heat-treated carbon steel by using TLA method

Jayashree Biswal[1,2,§], B. P. Mandal[3], V. K. Sharma[1] and H. J. Pant[1]

[1]Isotope and Radiation Application Division, [3]Chemistry Division
Bhabha Atomic Research Centre, Mumbai 400085, India
[2]Homi Bhabha National Institute, Mumbai 400094, India
§ Email: jayashreebiswal@gmail.com

Corrosion of metallic components or alloys is a common problem in industry and various technological areas. Measurement and quantification of corrosion is often desired for quality control and assessment of reliability and durability of various mechanical parts. Thin layer activation (TLA) method, a nuclear method is widely used for corrosion, wear and tear measurements of various metallic, industrial and automobile components [1]. TLA method has several advantages over conventional methods and is adaptable in various situations. Carbon steel (CS) is material of construction in many industrial systems due to its low cost and easy to perform machining. However, carbon steels are susceptible to corrosion under the industrial operation conditions. Often heat treatment is an approach employed to modify the material property and it may increase the corrosion resistance of a material. The objective of the present study is to evaluate the corrosion rate of heat-treated carbon steel by using TLA method. In this study the CS coupons were first subjected to different heat treatment procedures. The CS coupon which was not subjected to any heat treatment/ control was labelled as CS-1. All other CS coupons were first heated to 900 ^{0}C in a muffle furnace for two hours and cooled in different conditions, such as air cooled (CS-2), fast cooling by dipping in water bath (CS-3), controlled cooling inside the furnace after switching off the furnace (CS-4). Subsequently, the coupons were labelled with cobalt-56 radioisotope using 13 MeV proton beam (current: 200 nA) from BARC-TIFR Pelletron accelerator, Mumbai.

The irradiated coupons were subjected to corrosion media containing 0.1 M HCl solution. The measurement of remnant activity of the coupons as a result of corrosion was performed in a multichannel gamma spectroscopy analyzer. Figure 1 shows gamma spectrum of proton irradiated carbon steel coupon. The corrosion resistance was evaluated based on the lowest corrosion rate of the heat-treated CS coupons. It was observed that the rate of corrosion was lowest, i.e, 50.6 nm h^{-1} in case of CS-4, hence the corrosion resistant was highest in CS-4 coupon.

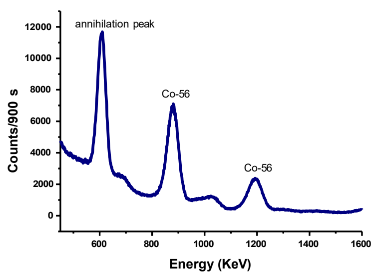

Fig 1. Gamma spectrum of irradiated carbon steel coupon

[§] Email: jayashreebiswal@gmail.com

References:
[1] D. P. Chowdhury, J. Datta, A. V. R. Reddy, Radiochim. Acta, 139 (2012) 100.

Liquid-liquid extraction studies of Np(IV) using *N,N,N',N',N",N"*-hexa-*n*-octylnitrilotriacetamide (HONTA) in C4mimNTf2

R.B. Gujar§,[1] B. Mahanty,[1] P.K. Mohapatra[1] W. Verboom[2]

[1]*Radiochemistry Division, Bhabha Atomic Research Centre, Mumbai, India – 400 085*
[2]*Department of Molecules & Materials, University of Twente, the Netherlands*
§*Email: rgujar@barc.gov.in*

It was reported that *N,N,N',N',N",N"*-hexa-*n*- octylnitrilotriacetamide (HONTA, Fig. 1, inset) has a promising extraction ability and selectivity towards tetravalent actinide ions over a wide range of nitric acid concentration when extracted in molecular solvent[1, 2]. There are reports where extraction of actinides by the extractant increases many fold in presence of room temperature ionic liquid (RTIL) [3]. Albeit the extraction of actinides ions by HONTA is well reported in molecular solvent, however there is no report on its extraction behaviour in presence of RTIL. The present investigation deals with the extraction of Np(IV) by HONTA in $C_4mimNTf_2$ in nitric acid medium.

Extraction kinetics of Np(IV) with HONTA in $C_4mimNTf_2$ at 3 M HNO_3 was found to be very slow (nearly 5 hrs required to attend equilibrium distribution ratio) which can be related to its higher viscosity in RTIL medium. The extraction of Np(IV) was carried out at different nitric acid concentration and the result is shown in Fig. 1. The increasing extraction pattern was observed with increase in acidity indicating a solvation type mechanism. Subsequently, C_4mim^+ and NTf_2^- variation study carried out at 0.5 M HNO_3 indicates no linear correlation on either C_4mim^+ or NTf_2^- concentration, thus ruling out the possibility of cation or anion exchange mechanism respectively at 0.5 M HNO_3. As a comparison purpose, Pu(IV) extraction was carried out under similar condition, which indicated similar extraction trend (Fig.1). Nitrate variation at wide concentration range (0.5−4 M) and ligand concentration variation indicated mixed species of $Np(NO_3)_4.2L$ and $Np(NO_3)_5^-.2L$ get extracted in the medium which suggest both solvation and anion exchange mechanism may be predominantly operating depending on the acidity of the aqueous medium. The anion exchange mechanism was confirmed at 3 M HNO_3 by the NTf_2^- variation at 3 M which indicated a slope of −1.25 ± 0.09. The plateau observed on and above 3 M HNO_3 (Fig. 1) may be due to a competition reaction of extraction by anion exchange mechanism and the availability of free ligand concentration, the latter decreases due to protonation of the ligand. Stripping study was carried out with extracted Np(IV) using various stripping agents, however only 1 M guanidine carbonate in 0.05 M EDTA was found to back extract Np(IV) quantitatively.

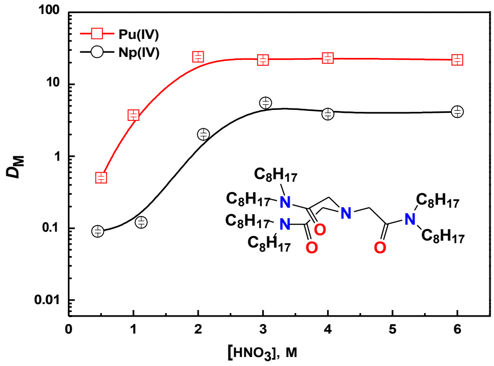

Fig. 1. $D_{Np(IV)}/_{Pu(IV)}$ with nitric acid, [L]: 0.9 mM HONTA in $C_4mimNTf_2$

References:

1. A. Karak et al Sep. Purif. Technol. 279 (2021) 119584.
2. H. Huang, et al Sep. Purif. Technol. 138 (2014) 65–70.
3. P.K.Mohapatra, Dalton Trans., 2017,46, 1730-1747

Freeze-dried ^{99m}Tc-HYNIC-PSMA kits for SPECT imaging of prostate cancer: Formulation and in vitro evaluation

Sweety Mittal[1] , Ajish Kumar[2], Avik Chakraborty[3], Archana Damle[3], Madhava B. Mallia[1, §]

[1] *Radiopharmaceuticals Division, Bhabha Atomic Research Center, Mumbai, India*
[2] Bioorganic Division, *Bhabha Atomic Research Center, Mumbai, India*
[3] *Radiation and Medicine Center, Parel*
[§] Email: sweetys@barc.gov.in

Prostate specific membrane antigen (PSMA) is considered a promising target for prostate cancer imaging and therapy. ^{68}Ga-HBED-CC-PSMA (PSMA-11) is an FDA approved clinically used PET imaging agent for prostate cancer. Herein, we report the formulation of a freeze-dried ^{99m}Tc-HYNIC-PSMA kit using in-house synthesized Hynic PSMA.

The wet chemistry protocol for the preparation of ^{99m}Tc-HYNIC-PSMA was optimized with respect to the amount of ligand, reagents and conditions. The optimized formulation was then transformed into a freeze-dried kit. A batch of 10 freeze-dried kit was made and extensively tested for physicochemical parameters such as radiolabeling efficiency, pH of the formulation, etc. The ^{99m}Tc-HYNIC-PSMA was prepared by adding 1 mL activity of freshly eluted [^{99m}Tc]TcO$_4$ (40 mCi) to the freeze-dried kit vial followed by heating on boiling water bath for 30 mins. The radiolabeling yield and radiochemical purity of the radiotracer ([^{99m}Tc]Tc-HYNIC-PSMA) was determined by HPLC as well as paper chromatography (PC). In vitro binding studies were carried in PSMA positive LNCaP cells at six different concentration of radiotracer (0.1 nM, 0.5 nM, 2.5 nM, 12.5 nM, 30 nM, 62.5 nM). The activity associated with cell pellet was determined in a gamma counter to calculate %cell binding of the radiotracer at each concentration. The K_d value was calculated by fitting the data using a nonlinear regression algorithm (GraphPad software). For inhibition studies excess of cold HYNIC-PSMA ligand (1000x) was used.

Results and Discussion: Each 10 mL kit vial contains a sterile, non-pyrogenic, lyophilized mixture of HYNIC-PSMA (20 ug), Stannous chloride dehydrate (40 µg), EDDA (10 mg), Tricine (20 mg) and phosphate buffer. The radiolabeling yield of the [^{99m}Tc]Tc-HYNIC-PSMA prepared from kit vial was more than >95% by HPLC as well as PC. The in vitro binding studies in LNCaP cells displayed very good affinity and specificity of [^{99m}Tc]Tc-HYNIC-PSMA (K_d =1.22 ± 2.3) towards the PSMA receptor. During inhibition studies significant decrease in the % binding of the radiotracer was observed in presence of excess of cold ligand (HYNIC-PSMA).

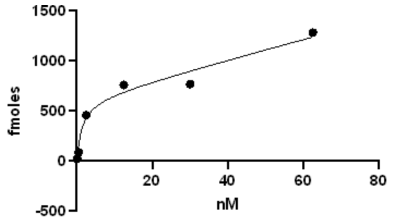

Figure 1: Determination of binding affinity of [^{99m}Tc]Tc-HYNIC-PSMA by saturation binding assay in LNCap cells.

Conclusion: The preliminary in vitro results showed excellent affinity and specificity of the radiolabeled ligand towards PSMA-receptor. In vivo evaluation of the radiotracer will be carried out in near future to further establish its feasibility as a SPECT imaging agent for the detection of PSMA positive prostate cancer.

References:

[1] M. Eder, M. Schafer, U. Bauder-Wust, W. Hull, C. Wangler, W. Mier, U. Haberkorn, M. Eisenhut, *Bioconjugate Chem*., **23**, 2012, 688.

Preparation of [^{64}Cu]Cu-NOTA complex as a renal PET imaging agent using ^{64}Cu produced in direct activation route

Sourav Patra[1], Shachin Jhadav[1], Avik Chakraborty[2], A. Rajeswari[1], Priyalata Shetty[1], K. V. Vimalnath[1], Rubel Chakravarty[1], Sudipta Chakraborty[1,§]

[1] Radiopharmaceuticals Division, BARC, Trombay, Mumbai, India
[2] Radiation Medicine Centre, BARC, Trombay, Mumbai, India
[§]Email: sudipta@barc.gov.in

Kidney function, such as glomerular filtration rate (GFR) can be evaluated more accurately by positron emission tomography (PET) compared to conventional gamma imaging. We have demonstrated the utility of carrier ^{64}Cu produced by direct neutron activation route as potential renal PET imaging agent using 1,4,7-triazacyclononane-1,4,7-triacetic acid (NOTA) as a hydrophilic chelator. The preparation of ~370 MBq doses of [^{64}Cu]Cu-NOTA complex was optimized using different amounts of NOTA (5-20 mg/mL). It was found that minimum concentration of NOTA required to achieve > 98 % radiolabeleing yield was 10 mg/mL. The excellent stability of the [^{64}Cu]Cu-NOTA complex was investigated over a period of 48 h. The in vitro stability of the complex was also found to be excellent in physiological saline upto 48 h. Further, the kinetic inertness of the complex was established by challenging with apoferritin protein which acts a scavenger for Cu^{+2} ion. Small animal PET/CT imaging study was carried out in healthy Wistar rats, which shows rapid clearance of the administered [^{64}Cu]Cu-NOTA radiotracer through renal route without any accumulation or uptake in any organ/tissue. Typical whole body PET and PET/CT images of a healthy Wistar rat acquired 30 min post-administration of ~ 20 MBq of [^{64}Cu]Cu-NOTA given in Fig. 1 clearly demonstrate this. Fast uptake of injected radiotracer in kidney with subsequent rapid excretion through urinary bladder proved the feasibility of using [^{64}Cu]Cu-NOTA formulation prepared as an affordable formulation for renal PET imaging and measurement of GFR.

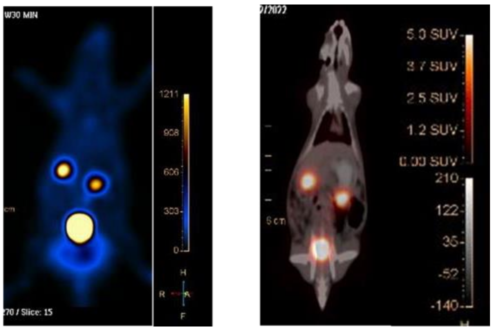

Fig. 1: PET (left) and PET/CT images of a healthy Wistar rat acquired 30 min post-administration of [^{64}Cu]Cu-NOTA

Recovery of radiochemically pure ^{106}Ru from CORAL dissolver off gas scrubber

Chandan Mukhopadhyay, R. Karthick, T. Selvi, G Santhosh Kumar, K. Dhamodharan§,
K.A. Venkatesan and K Ananthasivan
Process Radiochemistry and Reprocessing R&D Division, Indira Gandhi Centre for Atomic Research, Kalpakkam – 603102
§E-mail: kdn@igcar.gov.in

High burn-up (155GWd/t) spent nuclear fuels with a cooling period of 2 years discharged from Fast Breeder Test Reactor (FBTR) are being reprocessed in Compact Reprocessing of Advanced fuels in Lead Cell, IGCAR, Kalpakkam. Unlike, the spent fuel discharged from thermal reactor, the spent fuel from fast reactor contains high concentration of Ru isotopes. During dissolution, Ru is oxidized to highly volatile and radiotoxic RuO_4. The volatile RuO_4 is scrubbed in a dissolver off gas scrubber containing DM water. The solution in the scrubber system becomes acidic due to absorption of NOx. Based on the radioactivity present in the scrubber solution, it is categorized as intermediate level waste. The analysis of scrubber solution indicated the presence of fission products such as ^{106}Ru, ^{137}Cs, ^{125}Sb and $^{155\text{-}154}$Eu. Since, the scrubber solution contains Ru in order of mCi/L, it is considered as a valuable resource for recovery of Ru, which is used for eye cancer treatment. However, ^{106}Ru need to be separated from other isotopes for medical applications. The present study was carried out to develop a process for the recovery of radio chemically pure ^{106}Ru from the dissolver off gas scrubber solution. The Ru species present in scrub solution was oxidised to RuO_4 using KIO_4 as oxidising agent. The produced RuO_4 was extracted into CCl_4, which was equilibrated with Cl_2 gas. The extracted Ru was stripped back using 0.1M hydrazine sulphate in 1M HNO_3. The final stripped solution generated during study was analyzed using HPGe detector for gamma-emitting radionuclides. A typical γ-spectrum of the product solution is presented in Fig.1, it can be seen that there is no other γ-emitting radionuclides are present in CCl_4 phase. About 68-70 % of Ru separation was achieved in demonstrated process. The recovered ^{106}Ru solution generated from the process is radiochemically pure and suitable for further purification required for the brachytherapy.

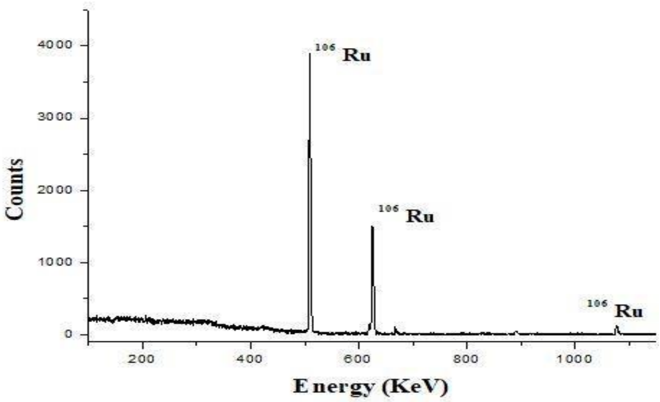

Figure 1. γ-spectrum of radio chemically pure ^{106}Ru recovered from dissolver off gas scrub solution

References: 1. Singharoy et.al, Separation Science and Technology, 56 (2021) 8

Preparation of [2,5-^{14}C]-tetrahydrofuran by catalytic cyclodehydration of 1,4-butanediol using tungsten-substituted-phosphoric acid

R. K. Sahu[1], S. P. Patil[1], D. B. Kalgutkar[1§], K. M. Mathew[1], N. Jayachandran[1]

[1]Labelled Compounds & Technical Services
Board of Radiation & Isotope Technology,
BRIT / Vashi Complex, Navi Mumbai – 400 703, India
[§]Email : dbkalgutkar@britatom.gov.in

Polymeric coatings[1] are an important part of a variety of industries including textiles, electronics automobiles and food etc. They are the protective layers that are used to extend the life of a material or surface by shielding it from moisture and preventing it from cracks. Water-based coatings rather than organic-based coatings are extensively used nowadays to develop biocompatible and eco-sustainable coatings[2]. Tetrahydrofuran labelled with carbon-14 was required to study diffusion of the solvent inside the coating and to study the effect of surfactant on the solvent removal rate in polymers and solvent coatings.

Tetrahydrofuran is prepared either from1,4-butanediol[3]by reacting acetylene with formaldehyde by Reppe process and followed by hydrogenation of 1,4-butynediol or from the chlorination of the butadiene.We prepared [2,5-^{14}C]-tetrahydrofuran from [1,4-^{14}C]-butanediol[4] by cyclodehydration using dodecatungstophosphoric acid[1,5,6] as a catalyst with a radiochemical yield more than 75 %. Product was isolated from the polymerized radiolabeled impurities by reactive distillation.The reaction scheme employed is as shown below.

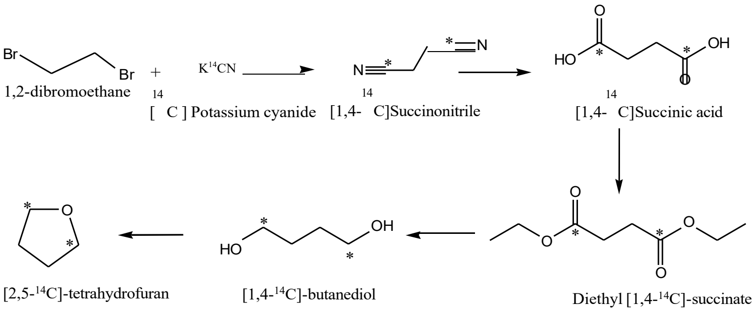

Acknowledgments

The authors sincerely thank Shri.Pradip Mukherjee, Chief Executive, BRIT for his support in the work.

References

1. Wu Huixiong, Zhou Mei, QU Yixin, Li Haixia and YinHengbo, Chinese Journal of Chemical Engineering, 17(2) (2009), 200
2. Raj Kumar Arya, Jyoti Sharma, Rahul Srivastava, DevyaniThapliyal, George D Verros, Coatings, 11(12) (2021) ,1529
3. Arpad Moliner and Mihaly Bartok, Helvetica ChimicaActa, Vol 64(1981), 389
4. Takeshi Hara, Yong Jixn, Hitomi Sasaki, Masaru Niitu and KeijiroSamejina, Journal of Labelled Compounds & Radiopharmaceuticals, 43 (2000), 1005
5. US Patent 709834 B2 (2006)
6. S H Vaidya, V M Bhandari, R V Chaudhari, Applied Catalysis A : General 242 (2003), 321

An efficient synthesis of phenyl barbituric-[2-^{14}C] acid

S. P. Patil[1], D. B. Kalgutkar[1§], Dr. K. M. Mathew[1], N. Jayachandran[1]

[1]Labelled Compounds & Technical Services
Board of Radiation & Isotope Technology
BARC/ BRIT Vashi Complex , Navi Mumbai – 400703, India
[§]Email:- dbkalgutkar@britatom.gov.in

Barbituric acids are sedative drugs consisting of variety of synthetic substances with closely related chemical structures and similar pharmacological activities.Barbituric acid itself does not possess hypnotic property but when alkyl, aryl or alicyclic groups are introduced into the 5-position, the resultant compounds show marked physiological activity. Barbiturates[1,2] are prepared by the condensation of urea with malonic acid or its alkylated esters in presence of a slight excess of sodium alkoxide in alcohol[3,4,5]. In reported procedures the condensation reaction of phenyl diethyl malonate and urea was carried out in ethyl alcohol and sodium ethoxide but the yield obtained was very low[5]. In general,arylated malonic esters are difficult to prepare than alkylated ones[6]. We carried out reactions in methyl alcohol and sodium methoxide in place of ethyl alcohol and sodium ethoxide.In cold runs, yield of phenyl barbituric acid obtained was consistently more than 70 % andhence employed for the preparation of phenyl barbituric-[2-^{14}C] acid. Radiolabelled barbituric acid obtained is further used for the preparation of its labelled analogues.The reaction scheme employed is as shown below.

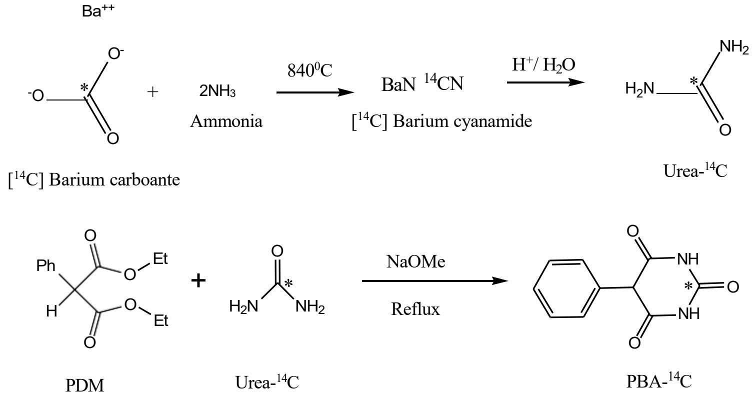

Acknowledgements

The authors wish to thank Shri. PradipMukharjee , Chief Executive , BRIT for his kind support and encouragement in this work.

References

1) Organic Syntheses, Coll. Vol. II (1943), 60
2) Haley EE&Lambooy J P, J. Am.Chem. Soc., 76 (1954), 2926
3) Brain S F, Antony P W G, and R T Austin, Vogel‟s textbook of practical organic chemistry 5th edition (1989) , 1177
4) S. Goldschmidt and R. Wher, Hoppe-Seyler‟s, Z. Physiol. Chem., 301(1955),107
*5) A.*Murray &D. L.Williams, Organic Syntheses with Isotopes (1958), 711
6) Dox A W & Thomas A, J. Am. Chem. Soc., 57 (1935), 1303

Synthesis and radiolabelling of triple negative breast cancer targeting GE11 peptide analogue

Akanksha Jain[1] and Drishty Satpati[1,2§]

[1]Radiopharmaceuticals Division,
[2]Homi Bhabha National Institute,
Bhabha Atomic Research Centre, Trombay, Mumbai-400085, India
[§]Email: drishtys@barc.gov.in

Triple-negative Breast Cancer (TNBC) is a highly aggressive breast cancer and comprises of 20% of human breast cancers. Since it lacks expression of estrogen receptors, progesterone receptors and human epidermal receptor 2 (HER2), conventional targeted therapies such as hormonal and anti-HER2 therapies are ineffective on TNBC.[1] However TNBC‟s exhibit elevated expression of epidermal growth factor receptors (EGFR) which can be targeted by receptor-based radiopharmaceuticals for molecular imaging and therapy.[1]

This work reports solid phase synthesis of EGFR-targeting GE11 peptide analogue (YHWYGYTPENVI). The peptide was synthesized manually using chlorotrityl resin followed by conjugation with Fmoc-NH-PEG$_4$-COOH. N-terminal of pegylated peptide was conjugated with chelator, DOTA and finally cleaved from the resin. The crude peptide was purified using semi-preparative HPLC and characterized by MALDI.

The peptide, DOTA-YHWYGYTPENVI (200 µg) was radiolabeled with ^{177}LuCl$_3$ (74 MBq) in presence of sodium acetate buffer (pH 5) and incubated at 90 ºC for 10 min. The radiolabeling yield obtained was 80% as assessed using radio-HPLC. It was further purified using Sep-pak column to get a purity of ≥95%.

The radiolabeled compound would be further assessed for its uptake in EGFR positive TNBC cell lines, MDA-MB-231.

References:

[1] H.N. Ariani and K. Kaur et al. *Scientific Reports*. **9** (2019) 2723.

Extension of shelflife through post harvest Gamma radiation along with surface edible coating of litchi cv. Rose Scented

Nikesh Chandra[1], Satish Chand[2], Ranjan Srivastava[3], G.C Joshi[4], Omveer Singh[5], Mandeep Rawat[6§]

[1,2,3,5,6§] Department of Horticulture, [4]Radiations and Isotopic Tracer Laboratory
(G.B. Pant University of Agriculture and Technology,Pantnagar, Uttarakhand 263145
[§]Email: mandeeprawat107@gmail.com

Nuclear technology in agriculture has great impact in controlling pest, diseases as well as in creating variability; it is also used as preventive quarantine tool due its germicidal properties. The joint expert committee of FAO, IAEA and WHO has approved the permissible dose of up to 10 kGy in food processing as it has no hazardous effect on nutrition and microbes [1]. Litchi is an important member of Sapindaceae (soapberry) family and preferred for its sweet taste as well as nutritional properties. Litchi is highly perishable crop and availability of fruits was from May to June in the market. So, the current study aimed to extend the shelf life of litchi fruit through utilization of gamma rays and aloe vera edible coatings. *Aloe vera* commonly referred to as a "medicinal plant", is known for its wide range of therapeutic properties, has two most common species are *Aloe barbadensis* and *Aloe arborescence* [2]. The gamma radiation processing was applied to samples weighing 2 kg each (0.8 kGy, 1.0 kGy and 1.2 kGy) in Radiations and Isotopic Tracer Laboratory (RITL, CBSH). Then, *Aloe vera* gel (10%, 25% and 50%) coating treatments were applied to the entire gamma irradiated samples except 1 to 4 treatments. After that irradiated samples along with control were stored at low temperature of 4°C in perforated plastic bags. The evaluation of irradiated samples was carried out at an interval of 4 days. To determine the acceptability of the stored litchi samples, a number of biochemical parameters and an organoleptic evaluation were examined. The best of all the samples, with an extended shelf life of 20 days at 4 °C, came from 1 kGy irradiated samples, followed by 1kGy + 50% *Aloe vera* gel (shelf life at ambient temperature without any treatment being 3–4 days). So with the above mentioned findings we can conclude that 1 kGy dose of gamma rays has potential to extend the shelf life of litchi along with low temperature.

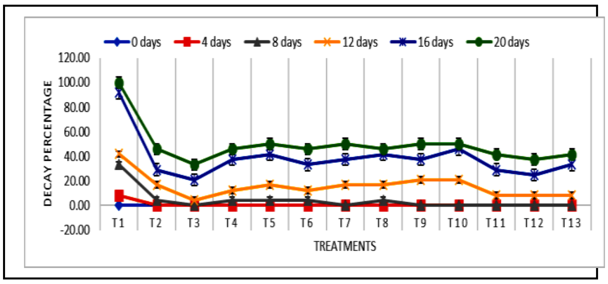

Fig1: Decay percentage gamma-irradiated and *Aloe vera* gel coating litchi samples

References

[1] Khalil *et al., International journal of food science & technology*, 44(2009): 927-931.
[2] Ahmed *et al., International journal of food science & technology*, 44(2009).

Understanding Efficient Sequestration of Radioiodine using Human Hairs

Jyotsna A. Sapkal§, Pankaj Sorate and R.V. Kolekar

Health Physics Division, Bhabha Atomic Research Centre, Mumbai, 400085, India
§Email: jyots@barc.gov.in

Radiopharmaceutical division (RPhD), RLG is engaged in radiochemical processing of reactor produced ^{131}I using well known dry distillation method. During radiochemical processing of ^{131}I there is generation of large quantity of airborne activity / contamination inside the shielded glove box. Therefore, during handling of ^{131}I there is always possibility of surface contamination of individual personal body parts specially on hair and subsequently decontamination of hair becomes very challenging job. In view of this, it is interesting to understand the nature of interaction between ^{131}I with human hair i.e., normal as well as coloured hair. Efforts were put to understand and investigate the nature of the sorption mechanism in terms of different isotherm modelling and chemical kinetics. This paper describes in brief about the experiments related to the interaction mechanism of ^{131}I with hairs. Normal hair was found to have more affinity towards radioiodine compared to coloured one as observed from the partition coefficients (K_d) values generated from experimental data. Experiments were carried out with ~ 1.2 ml of radio iodine in aqueous phase in specified acidic condition with 50 mg of hair samples with varing equlibriation time inside the fume hood. The K_d of iodine was monitored as a function of aq. feed acidity in the range of 0.01 – 6 M HNO_3. Maximum uptake of iodine for normal hair was found at 2 M HNO_3 while for coloured hair showed flat response. "F" (F is the ratio of concentration of iodine at time „t‟ to concentration of I_2 at equlibrium) is the fraction of sorption reaction completed w.r.t. time hence 60 min (Fig – 1) was found to require to attain equilibrium for normal and cloured hair for iodine uptake. To understand the adsorption mechanism, different isotherm models were used. It was found that the sorption of radio iodine on both hair samples were predominatly followed Langmuir adsorption isotherm [1] having mono layer coverage without any neighbouring group participation. The rate constant for sorption and linear regression of different kinetics model were studied. From the experimental data, Fig – 2 indicated that q_t is the amount of radio iodine adsorbed on the sorbent at the equlibration time „t‟ and it was found that the reaction have been predominatly followed Pseudo 2nd order rate kinetics.

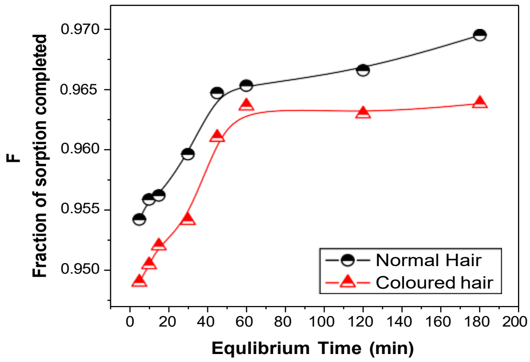

Fig- 1 Variation in fraction of sorption reaction completed with function of time

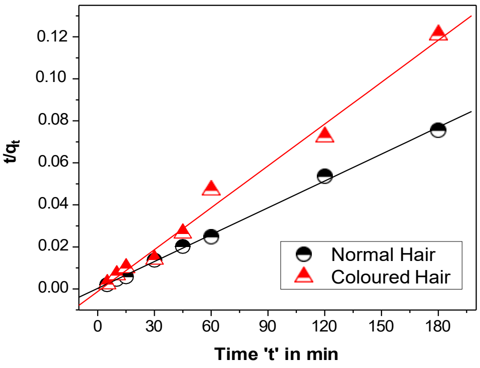

Fig – 2 Pseudo second order kinetics

References:

[1] S. Pahan, A Sengupta, Sk. M. Ali, A. K. Debnath, D. Banerjee, T. Vincent, G. Sugilal, C.P. Kaushik, Sep Purif Technol., 279 (2021) 119703.

Reverse osmosis membrane based separation of solute containing Sr radioisotopes from bulk acidic solution

Debasish Saha§, J. Vithya, A. Arul Kumari, K. Sundararajan

RCSSS, Analytical Chemistry and Spectroscopy Division, FMCG, MC&MFCG,
Indira Gandhi Centre of Atomic Research, Kalpakkam, Tamil Nadu-603102, India
§Email:dsaha@igcar.gov.in

Application of membrane based separation techniques are on increasing demand due to their inherent advantages of continuous operation capability, durability and ease of operation. Reverse osmosis based potable water purification system has become indispensable part of our daily life.^{89}Sr radioisotopes, is produced by^{89}Y(n,p)^{89}Sr reaction at fast flux reactor, FBTR for its application as a therapeutic radiopharmaceutical. During the chemical processing of irradiated yttria pellets, batch wise dissolution using 9M HNO$_3$, solvent extraction using 0.1M DtBuCH18C6/Octanol performed at hotcell due high radiation dose associated with the irradiated pellets. Remaining processes like back extraction and quality control processes gets completed in the laboratory [1-2]. Pertraction of ^{89}Sr from FBTR irradiated yttria has been demonstrated in our laboratory using supported liquid membrane technique [3]. In this study, we are investigating the separation of bulk acidic solvent from Sr containing solute using reverse osmosis technique which is originated post back extraction stage. A 10,000 mL simulated sample solution was prepared with $^{85+89}$Sr radiotracer solution in 0.1M HNO$_3$. Reverse osmosis membrane with pore size of 0.1-1nm is known to transport only solvents but reject all solutes. A RO booster pump i.e. diaphragm pump with capacity 100 Gallon per day (GPD)with max pressure of 150 psi, flow rate of 1.5L/min and a flow restrictor 350mL/min was used for this study. Solution after passage through RO membrane which was made of polysulfone coated with aromatic polyamides [4], gotdistributed between solvent (permeate) and solute (concentrate) chambers (Fig.1). The solvent collected in concentrate chamber was further recirculated through RO membrane to minimise the volume of solvent of concentrate chamber. After the transport study, RO membrane was washed with several rounds of solvent phase. The samples were collected from concentrate as well as permeate chambersand contentof ^{89}Sr, a pure β^- emitter in the samples were assayed by cerenkov counting using liquid scintillation counter (Tri Carb 5110 TR LSC). Overall recovery of Sr content was found 85.5(±11.7)% within ~1,000 mL solvent in concentrate chamber, whereas ~9,000 mL solvent was collected in permeate chamber with an average of 45 minutes. Sr content in the permeate chamber was less than the minimum detectable activity (6nCi/L). Large variation associated with the Sr recovery may be due to error associated with final volumes of permeate and concentrate chambers. A fast method is standardised for the separation of bulk solvent from trace solute Sr, which can be utilised for the continuous production of^{89}SrCl$_2$ radiopharmaceutical using bulk scale irradiation of yttria target.

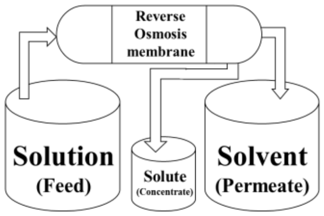

Fig.1: Experimental setup for the separation of solute containing Sr Radioisotopes from bulk acidic solution

Reference

[1] Saha, Debasish, et al. Journal of Radioanalytical and Nuclear Chemistry (2023): 1-14.
[2] Saha, Debasish, et al. RadiochimicaActa 104.3 (2016): 1-10.
[3] Saha, Debasish, et al. Ind.& Eng. Chem. Res. 61.11 (2022): 3817-3830.
[4] Maynard, E., and C. Whapham. Decontamination in Hospitals and Healthcare.2020.45-69.

On the optimization of the protocol for automated radiosynthesis of [^{68}Ga]Ga-Pentixafor, [^{68}Ga]Ga-FAPI-4 and [^{68}Ga]Ga-DOTATATE in an EZ Modular Lab

Sreeja Raj Menon[1,2], Arpit Mitra[3], Sudeep Sahu[4], Avik Chakraborty[2,4], Mukti Kanta Ray[4], Sharmila Banerjee[2,5,§]

[1]*Health Physics Division, Bhabha Atomic Research Centre, Mumbai, India.*
[2]*Homi Bhabha National Institute, Mumbai, India.*
[3]*Radiopharmaceutical Laboratory, Board of Radiation and Isotope Technology, Navi Mumbai, India.*
[4]*Radiation Medicine Centre, Bhabha Atomic Research Centre, Mumbai, India.*
[5]*Advanced Centre for Treatment, Research and Education in Cancer (ACTREC), Tata Memorial Centre, Navi Mumbai, India.*
[§] E-mail: banerjees@tmc.gov.in, banerjeesharmila2207@gmail.com

PET/CT scintigraphy using ^{68}Ga-labeled agents has gained prominence in diagnostic nuclear medicine. The present work describes the automated radiochemical syntheses of multiple and promising PET radiotracers like [^{68}Ga]Ga-Pentixafor, [^{68}Ga]Ga-FAPI-4 and [^{68}Ga]Ga-DOTATATE, which are in regular clinical use [1]. The strategy involves optimization of a single protocol to be used in the automated Eckert-Ziegler Modular Lab, without any modification in the time list of inbuilt human machine interface (HMI) software. [^{68}Ga]Ga^{3+} was sourced from an organic matrix based ^{68}Ge/^{68}Ga generator, housed inside a biosafety cabinet. Each of these ligands (30 - 50 µg, concentration: 1µg/µL) and 1N CH_3COONa buffer (2mL) were taken in the reaction vial of EZ Modular Lab, before radiochemical synthesis. The precursor [^{68}Ga]$GaCl_3$ (~4 mL, in 0.05N HCl medium) was eluted from the generator and pre-concentrated with strata SCX cartridge. [^{68}Ga]$GaCl_3$ from SCX cartridge was taken inside the reaction vial with 512µL acidified NaCl solution (0.2N HCl in 5N NaCl). The reaction mixture was incubated for 15 minutes at 95 ^{o}C, with the pH maintained ~4.0. The reaction mixture was cooled using 3 mL of ultrapure water and loaded to preconditioned light/plus C18 Sep Pak cartridge. 2mL of saline was passed through the column to remove unlabeled [^{68}Ga]Ga^{3+}. The product was eluted from the light/plus C18 cartridge through 0.22µm PES membrane syringe filter using 50% aqueous ethanol (1mL). The resultant product was diluted with sterile pyrogen free saline. Using ~30 mCi [^{68}Ga]$GaCl_3$, all the three products (~25 mCi) could be prepared (product pH: 5.0-6.0), with RAC of 1-3 mCi/mL and RCP >98%, as estimated by radio-TLC (SG-60 ^{o}A, 0.1M Citrate buffer, R_f: 0.0-0.1) and radio-HPLC (H_2O/CH_3CN, gradient mode). The endotoxin limit (EL) was <6 EU/mL, as quantified by gel-clot BET assay method. The sterility of the products were analyzed by direct inoculation method. The consistent and reliable RCY and RCP of multiple ^{68}Ga-labeled PET tracers by single optimized automated radiochemistry protocol exhibits the versatility of the EZ Modular Lab.

Reference:

[1] Alireza Aslani, Graeme M Snowdon et. al., *Asia Ocean J Nucl. Med. Biol.*, **2**(2014)75.

Trastuzumab Fragments labeled with Gallium-68 for PET imaging of HER-2 expression in cancers

Shishu Kant Suman[1,4, §], Archana Mukherjee[1, 4], Usha Pandey[5], Avik Chakraborty[3,4], Sutapa Rakshit[3], Megha Tawate[3,4], and Haladhar Dev Sarma[2]
[1]*Radiopharmaceuticals Division,* [2]*Radiation Biology & Health Science Division,*
[3]*Radiation Medicine Centre, Bhabha Atomic Research Centre (BARC), Mumbai, India*
[4]*Homi Bhabha National Institute, Anushaktinagar, Mumbai, India*
[5]*Board of Radiation & Isotope Technology, Navi Mumbai, India*
§ Email: shishu@barc.gov.in

Trastuzumab is the first humanized FDA approved monoclonal anti-human epidermal growth factor receptor 2 (HER2) antibody for the treatment of HER2-positive breast, gastroesophageal, and ovarian cancers [1]. The grading of HER2 status of breast tumors is the standard protocol for its typing, prognosis, and optimization of treatment protocol. Radiolabeled trastuzumab and its fragments have been employed for visualizing HER2 expression status in various cancers [2]. The present study envisages the development and application of trastuzumab fragments radiolabeled with Gallium-68 (^{68}Ga) as promising immunoPET agents in gradation and early diagnosis of HER2 positive tumors. Although half-life of ^{68}Ga is relatively short for immunodiagnostic applications, clinical studies have been reported and feasibility of imaging up to 3 h is demonstrated with target specific ^{68}Ga labeled radioformuations [3].

Trastuzumab fragments **[**F(ab′)$_2$ and F(ab′)] were prepared, purified and conjugated with chelator NOTA for labeling with ^{68}Ga. Intact trastuzumab was also radiolabeled for comparison. Radioformulations could be prepared with >98 % radiochemical purity (% RCP) and were found to be stable with RCP>98 % in saline and serum at 37 °C up to 4 h. *In-vitro* binding studies revealed high affinity (Kd) and specificity of the formulations towards HER2 receptors. The immunoreactive fraction (IRF) of the radio formulations were greater than 77 %. Biodistribution and PET imaging studies showed faster clearance of ^{68}Ga-NOTA-F(ab′)-trastuzumab than ^{68}Ga-NOTA-F(ab′)$_2$-trastuzumab predominantly through renal route. Radioformulations showed specific tumor uptake and could detect lesions in HER2 positive tumors in SCID mice at 3 h p.i.

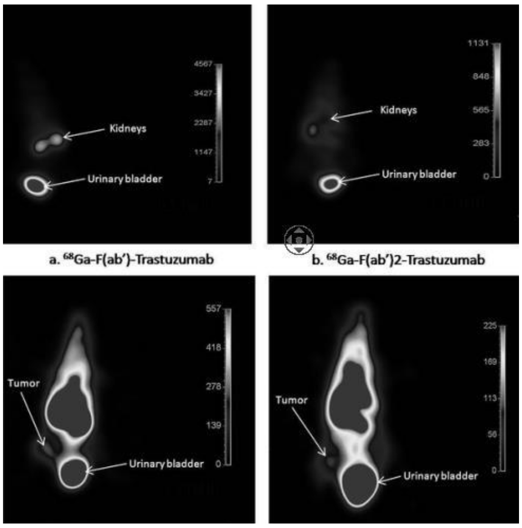

Fig. 1: PET images showing uptake of radioformulations in SK-BR-3 tumors
a. ^{68}Ga-NOTA- F(ab')-trastuzumab uptake in kidneys
b. ^{68}Ga-NOTA- F(ab')$_2$-trastuzumab uptake in kidneys
c. ^{68}Ga-NOTA- F(ab')-trastuzumab uptake in tumor
d. ^{68}Ga-NOTA- F(ab')$_2$-trastuzumab uptake in tumor

Formulation of ^{68}Ga-NOTA-F(ab′)-trastuzumab and ^{68}Ga-NOTA-F(ab′)$_2$-trastuzumab for targeting HER2 overexpressing tumors was successfully achieved. These radioformulations could be effective immunoPET agents for management of HER2 overexpressing breast and other solid tumors.

References:
[1] Wang J and Xu B., Signal Transduction and Targeted Therapy, **4** (2019) 34.
[2] Ge S et.al., Molecules, **26** (2021) 6482.
[3] Beylergil V et.al., Nuclear Medicine Communications, **34** (2013) 1157.

In-house developed freeze-dried kit of Trastuzumab-DOTA: Efforts towards convenient clinical translation of [^{177}Lu]Lu-Trastuzumab

Jeyachitra Amirdhanayagam[1], Mohini Guleria[1,2] and Tapas Das[1,2§]

[1]Radiopharmaceuticals Division, Bhabha Atomic Research Centre, Trombay, Mumbai-400085, INDIA
[2]Homi Bhabha National Institute, Anushaktinagar, Mumbai-400094, INDIA
[§]Email: tdas@barc.gov.in

Trastuzumab is a US-FDA approved humanized monoclonal antibody used for the treatment of human epidermal growth factor receptor 2 (HER2) positive breast cancer (ca breast). In clinical cases where immunotherapy using monoclonal antibodies fail to respond, the possible use of „radioimmunotherapy" involving radiolabeled antibodies has been envisaged to improve the therapeutic efficacy [1]. The aim of the present work is to optimize a freeze-dried formulation of Trastuzumab-DOTA conjugate for the preparation of [^{177}Lu]Lu-Trastuzumab patient dose for radioimmunotherapy of ca breast. The whole procedure for the preparation of [^{177}Lu]Lu-Trastuzumab takes long time, primarily due to involvement of synthesis and purification of Trastuzumab-DOTA conjugate (takes roughly one and half day) and thus, such a process is not suitable for routine preparation of this potent radiolabeled agent in hospital radiopharmacies. However, this could be circumvented by using a pre-synthesized Trastuzumab-DOTA conjugate in the form of a freeze-dried formulation. Working in this direction, we have formulated a freeze-dried kit of Trastuzumab-DOTA by optimizing Trastuzumab to DOTA ratio, buffer medium, radio-protectant and cryoprotectant. In the present work, a pre-optimized Trastuzumab to DOTA molar ratio (1:10) was utilized for the synthesis of Trastuzumab-DOTA conjugate. The purified Trastuzumab-DOTA conjugate was obtained in 0.2 M sodium acetate buffer (0.2 M, pH=5.6) to which varying amounts of radio-protectant (ascorbic acid) and cryoprotectant were added before subjecting the solution mixture to freeze-drying process. Evaluation of freeze-dried kits containing varying amounts of excipients was performed by radiolabeling with ^{177}Lu and subsequent determination of the percentage radiochemical purity. The radiochemical purity of [^{177}Lu]Lu-Trastuzumab prepared using freeze-dried formulations was determined employing paper chromatography (0.01M sodium citrate, pH 5.0) as well as high performance liquid chromatography (HPLC). [^{177}Lu]Lu-Trastuzumab formulated using the freeze-dried kit was evaluated for the following parameters: appearance post re-constitution (clear), pH (5-6), percentage radiochemical yield (>95) and product stability up to 24 h post-preparation. The results of the present study indicated a significant effect of nature and amount of excipients on the percentage radiochemical yield of [^{177}Lu]Lu-Trastuzumab prepared using freeze-dried formulation. The availability of the freeze-dried Trastuzumab-DOTA kit will promote convenient clinical translation of [^{177}Lu]Lu-Trastuzumab for routine application in nuclear medicine centres of our country.

Acknowledgements: The authors gratefully acknowledge Dr. S. Kannan, Director, RC&IG Group (BARC) for his constant support and encouragement. The authors are also thankful to their colleagues from RCS, RPhD, BARC for providing ^{177}Lu used during the present study.

References:
[1] G. L. Ray et al. *Pharmaceuticals,* **5**, (2012) 1.
[2] M. Guleria et al. *RSC Med Chem,* 12, (2021) 263.

Study of Microwave Irradiation Induced Expanded Graphite: Synthesis and Characterization

Neetu Bora[1§], Deepika P. Joshi[2]

1Department of Physics, Govind Ballabh Pant University of Agriculture and Technology, Pantnagar, 263145 Uttrakhand, India
§**Email**: neetubora95@gmail.com

In the present work, Different Expanded Graphite (EG) samples have been prepared by microwave irradiation method for various irradiation times (30, 60, and 90 sec) to find the highest exfoliation volume (EV). Characterization techniques such as XRD, FESEM, FTIR, and N_2 adsorption isotherm have been used to study prepared samples. The findings have supports that the produced expanded graphite is chemically and structurally stable with varying expanded times. The FESEM image of EG has shown the expanded layers of graphite forming a porous structure. The adsorption isotherm curve of EG exhibits a sharp increase in the amount of adsorbed capacity at very low relative pressure, which denotes the presence of microspores. In the BET analysis, the specific surface area of EG has found $12.5 m^2/g$.

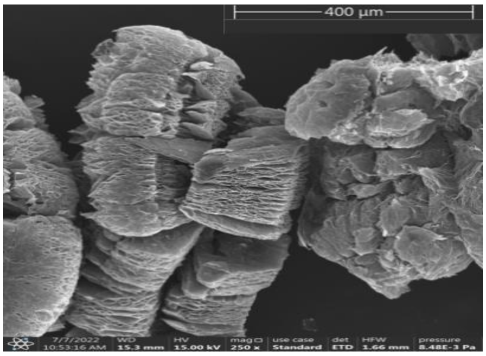

Figure 1. FESEM image of EG

References:

[1] Zhan B, Liu Y, Zhou WT, Li SY, Chen ZB, Stegmaier T, & Ren LQ (2021). Multifunctional 3D GO/g-C3N4/TiO_2 foam for oil-water separation and dye adsorption. *Applied Surface Science*, 541, 148638.

[2] Liu Y, Jiang Z, Fu J, Ao W, Siyal AA, Zhou C, & Zhang C (2022) Iron-biochar production from oily sludge pyrolysis and its application for organic dyes removal. *Chemosphere*, 301, 134803.

[3] Sabir R, Waheed A, Moazzam AM, & Mushtaq U (2021) “Graphene-based photocatalysts for organic pollutant removal from waste-water: recent progress and future challenges,” *Environmental Technology Reviews*, vol. 10, no. 1, pp. 323–341.

Application of Radioactive Ion Chromatography System for medical radioisotopes production using FBTR

J. Vithya, Debasish Saha§
RCSSS, Analytical Chemistry and Spectroscopy Division, FMCG, MC&MFCG, Indira Gandhi Centre of Atomic Research, Kalpakkam, Tamil Nadu-603 102, India
§Email: dsaha@igcar.gov.in

Fast neutron reactors are known to produce no carrier added (nca) radioisotopes by (n,p), (n,α) reactions, which mandatorily require chemical separation from its targets. Determination of the target, produced element and other co-produced elements are required for standardization of chemical separation methods using a multielement estimation technique. HPLC, Ion Chromatography, ICPOES, ICPMS are well known techniques for multi element estimation. At IGCAR, Kalpakkam, we are producing ^{89}Sr and recovering^{60}Co produced by fast neutron irradiations in FBTR using ^{89}Y(n,p)^{89}Sr and ^{60}Ni(n,p)^{60}Co reactions, where target, product and coproduced impurities are Y, Sr, Rb, Co, Na, Fe, Mn, Mo, NH_4^+ etc. elements are present in the target post irradiation [1-2]. We have standardized radioactive ion chromatography technique for this application using various eluents and chromatography columns. Determination of various anions e.g. NO_3^-, Cl^-, PO_4^{3-}, SO_4^{2-} and radiochemical purity of $^{89}SrCl_2$ has already been studied in our previous publication [3]. Metrohm 930 Ion chromatography system along with conductivity detector in non supressed condition was used for the study. Metrohm cation column, Metrosep C4-150/4.0 with silica gel with carboxyl groups stationary phase with particle size of 5 µmand Nucleosil 5SA - 125/4.0 cation column with spherical silica gel with sulphonic acid groups with particle size of 5 µmwere used for the work with Oxalic acid and dilute HCl as eluent respectively. List of elements studied, their retention time and peak area are tabulated in Table 1. Further experiments are in progress with IC-UV Vis detector.

Table 1: Assay of various cations using Radioactive Ion Chromatography System

Sl.	Element	Retention time (min)	Peak area (µS/cm) x min for 1mg/ L concentration	Separation conditions (Column, eluent, flow rate)
1.	Y(III)	5.4	0.50	Nucleosil cation column with 10mM alpha HIBA/2mM EDA eluent, 1.0mL/min
2.	Sr(II)	14.4	0.16	
3.	Na(I)	3.7	3.00	Cation column with 2.5mM HNO_3, 0.9mL/min
4.	NH_4(I)	3.8	3.50	
5.	Ni(II)	3.3	0.63	Cation column with 3mM oxalic acid, 0.9mL/min
6.	Co(II)	4.3	1.15	
7.	Fe(II)	5.6	0.51	
8.	Mn(II)	7.0	1.71	
9.	Mo(II)	9.2	0.06	

Reference

[1] Saha, Debasish, et al. Journal of Radioanalytical and Nuclear Chemistry (2023): 1-14.
[2] Vithya et al, Procedings for the fifth International Conference on Application of RadiotraCers and Energetic Beams in Sciences (ARCEBS 2023), 135-136.
[3] Saha, Debasish, et al. Applied Radiation and Isotopes 192 (2023) 110566.

Preparation and evaluation of ^{175}Yb produced by (n,γ) activation of indigenously produced isotopically enriched [^{174}Yb]Yb(NO_3)$_3$ target

Sharad P. Lohar[1], K. V. Vimalnath[1], Avik Chakraborty[2], Sudipta Chakraborty[1,§]

[1] Radiopharmaceuticals Division, [2] Radiation Medicine Centre, BARC, Mumbai, India
[§]Email: sudipta@barc.gov.in

Owing to suitable decay properties, ^{175}Yb [$T_{½}$ = 4.18 d, $E_{\beta(max)}$ = 466 keV (86.5%), Eγ = 282.5 keV (3.05%), 396.3 keV (6.5%)] is be envisaged as a promising radionuclide for use in therapeutic nuclear medicine. Production of ^{175}Yb with adequate radionuclidic purity requires use of isotopically enriched ^{174}Yb target to avoid co-production of ^{169}Yb and ^{177}Lu on thermal neutron irradiation. In the present article, we report formulation, quality control and pre-clinical evaluation of [^{175}Yb]Yb-DOTMP (DOTMP = 1,4,7,10-tetraazacyclododecane-1,4,7,10-tetracaetic acid) for use in palliative care of bone pain due to cancer metastases using isotopically enriched ^{174}Yb produced in house.

Ytterbium-175 was produced via ^{174}Yb(n,γ)^{175}Yb route by neutron irradiation of indigenously produced isotopically enriched Yb(NO_3)$_3$ target (I.E. 98.3 atom% in ^{174}Yb) at a thermal neutron flux of 1×10^{14} n/cm^2/sec for 14 d in Dhruva. Isotopic enrichment of natural Yb was achieved using Atomic Vapor Laser Isotope Separation (AVLIS) technique at ATLAF, BTDG, BARC. Yield of ^{175}Yb was 21.5 GBq/mg (580 mCi/mg) with >99.9 % radionuclidic purity, as demonstrated in the gamma ray spectrum (Fig. 1) recorded 6 h after end of irradiation. Around 2.6 GBq (70 mCi) dose of [^{175}Yb]Yb-DOTMP was prepared in high yields having radiochemical purity 98.8 ± 0.5% and the preparation showed excellent in vitro stability. Imaging studies in healthy Wistar rats showed preferential localization of the formulation in skeleton (52.6% of injected activity in skeleton from ROI analysis) with fast clearance of residual activity through renal route, as shown in the whole body image of the animal recorded 3 h post-administration of the formulation (Fig. 2). The accumulated activity in skeleton was found to be retained upto 14 d post-administration studied by serial whole body imaging of the animal.

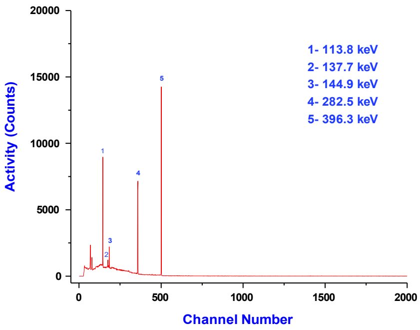

Fig. 1: Gamma ray spectrum using HPGe-MCA system

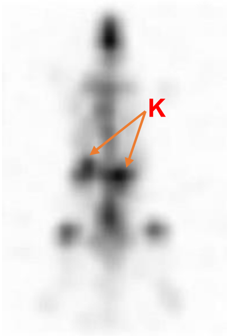

Fig. 2: Whole body gamma image of health Wistar rat recorded 3 h post-administration of the [^{175}Yb]Yb-DOTMP (K denotes kidneys)

Acknowledgements: Authors express their sincere gratitude to the scientists of ATLAF, BTDG, BARC, for providing isotopically enriched ^{174}Yb target used in the present study.

Elemental purification of indigenously produced isotopically enriched ytterbium precursor for radiopharmaceuticals

Anupama Prabhala[1,§], Dheeraj Kumar[2], Arpit Mitra[2] Anupam Mathur[2], Manisha V.[3],
Usha Pandey[2], and Sanjay Sethi[1]
[1]ATLA-F, Beam Technology Development Group, BARC, [2]Board of Radiation & Isotope Technologies[1], Mumbai, [3]Analytical Chemistry Division, BARC
[1, §] Email: anuvivek@barc.gov.in

The radioisotope ^{177}Lu is being widely used in therapeutic applications for cancer treatment. ^{177}Lu can be produced by both the direct and indirect routes. In the direct route, enriched ^{176}Lu target (> 74%) is neutron activated to produce the desired radio isotope ^{177}Lu with medium specific activity. In the indirect route, enriched ^{176}Yb target (> 95%) is neutron activated to form ^{177}Yb which by β-decay produces ^{177}Lu of high specific activity.

Atomic vapor-based laser isotope separation (AVLIS) process is being used to indigenously prepare these isotopically enriched lanthanide targets viz., ^{176}Lu (> 74%) and ^{176}Yb (> 95%) for the radiopharmaceutical applications. In the AVLIS process, a composite tunable dye laser beam of required wave-lengths shines on ytterbium atomic vapor and selectively excites & ionizes the targeted isotope. The ionized enriched product is extracted by applying a suitable electric field and is collected on a metallic substrate. The enriched product is then leached with nitric acid, the quantity and isotopic composition of the target determined before neutron activation [1]. ^{176}Yb with specifications of >99% nuclidic purity, ≥ 97% and having a low concentration of metallic impurities is required.

Using analytical reagents and Millipore water (18.2 MΩ), the product is recovered in the AVLIS process from the metallic substrate. In spite of this, ingress of impurities like sodium mainly due to handling issues has been observed in some batches in the stages from product recovery to post neutron activation. To meet the chemical purity requirements of the target, it is necessary to remove the sodium impurity.

In this work, column chromatography separation using extraction chromatography resins has been carried out for the sodium removal from two separate isotopically enriched ^{176}Yb and ^{174}Yb targets using commercially available DGA resin (M/s. Triskem make) [2]. Loading was done with 4M HNO_3 medium and the sodium was removed both in the loading steps as well as the subsequent washing step with 1.4 M HNO_3. The enriched Yb on the resin was finally eluted with dilute HCl. The eluted Yb and Na in various product fractions were quantitatively estimated by ICPOES method. With this process, the two batches of enriched ^{176}Yb and ^{174}Yb targets could be cleaned of sodium to bring it to acceptable limit with respect to radio-nuclidic impurities. Around 25.2 mg of enriched ^{176}Yb with 0.026 mg Na/mg Yb was obtained as the final product. The lower detection limit for Na was 0.1 ppm in the product solution. Further work is in progress to standardize the above purification protocol and to minimize the enriched product losses in the purification process.

Fig: Indigenously produced isotopically enriched ytterbium precursors prior to elemental purification.

Acknowledgements: The authors acknowledge Dr. Archana Sharma, Director, BTDG, Chief Executive, BRIT, Shri S. Kundu, Advanced Tunable Laser Application Facility, BTDG for the encouragement and the support. Dr. Sudipta Chakraborty, RPhD is acknowledged for arranging the irradiation and for evaluating the quality of enriched Yb-176 target.

[1] Anupama Prabhala et al., In *E-Proceedings of NLS-30*, 114, January 19-22, (2022)
[2] Horwitz, E.P., et al. Applied Radiation and Isotopes. 2005, Vol. 63, pp. 23 (2005)

Materials development for laser isotope separation process to produce stable radiopharmaceutical precursors of ytterbium and samarium

Nagaraj Alangi[§], Mukesh K Verma and Sanjay Sethi

Advanced Tunable Laser Applications Facility, BTDG, BARC, Mumbai, India
[§] nagaraj@barc.gov.in

Isotopically enriched isotopes of Ytterbium (Yb), Samarium (Sm) and Lutetium (Lu) by Laser Isotope Separation (LIS) are widely used in nuclear medicine and imaging applications after irradiating in a nuclear reactor. For example, Sm-153 is widely produced with high yield and purity by neutron irradiation of isotopically enriched $^{152}Sm_2O_3$ [1]. BTDG is actively pursuing a LIS program to produce ^{152}Sm enriched samarium and has demonstrated a sizeable quantity of product, which has been clinically administered. ^{176}Yb enriched ytterbium product prepared is awaiting regulatory approvals. However, Sm and Yb, both in vapour and liquid form, are highly reactive with common engineering metallic materials and oxides. Hence, all the components for handling Sm and Yb require a protective barrier. This work reports materials development for handling Sm and Yb in spectroscopic and vapour generator studies. Typically, vapour generator components are exposed to Sm/Yb metal or vapour in the range of 1173 K to 1373 K for a duration of 10 h in the vacuum of 1E-4 Pa. Selection and evaluation of materials was based on thermodynamic calculations in the temperature range of 300 K to 1300 K by FACTSAGE software [2]. TiC-coated titanium crucibles were shortlisted for testing against Sm/Yb in the vacuum of 1E-4 Pa due to their excellent machinability and availability, resistance to nitro-hydrochloric acid, and good thermal cycling endurance.

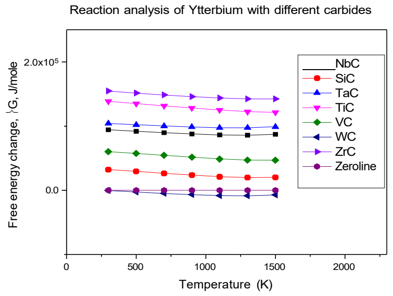

Fig 1. Free energy change for reaction with ytterbium metal for different carbides

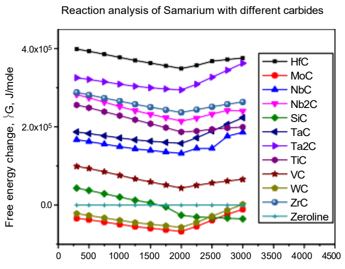

Fig 2. Free energy change for reaction with samarium metal for different carbides

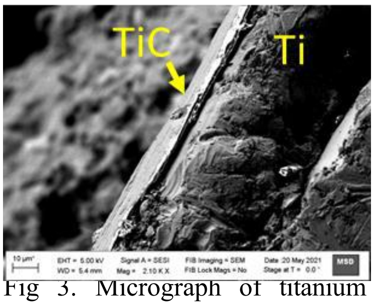

Fig 3. Micrograph of titanium crucible carburized at 1373K for 6 h

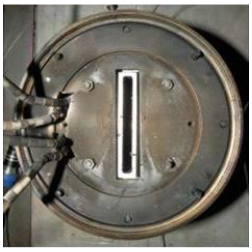

Fig 4. TiC coated Ti used as samarium vapour generator

We have produced durable coatings of TiC on titanium substrates for Sm and Yb handling based on the optimized carburizing parameters. TiC was found to be a stable, protective barrier against Sm and Yb at 1273K up to 10 h. The coating was durable without cracks or spalling, and the Sm/TiC and Yb/TiC interface was free of any reaction products during line scan analysis. A metal vapour generator for the samarium was fabricated and qualified for LIS applications.

Authors acknowledge the support and guidance provided by Dr Archana Sharma, Director, Beam Technology Development Group.

References:

[1] International Atomic Energy Agency, Manual for Reactor Produced Radioisotopes, IAEA-TECDOC-1340, IAEA, Vienna (2003).
[2] C. W. Bale and E. Bélisle, Fact-Web suite of interactive programs, www.factsage.com

$Ce(OH)_4$-Polymer (Poly-Ether-Sulfone/Chitosan) Composite: Ru selective Adsorbent in highly saline solution

J. Selvakumar[1,3,§], Kumari Anshul[1], Padala A Nishad[2] Anupkumar Bhaskarapillai[2,3],
S. Srinivasan[1], N.R. Jawahar[1], A L Rufus[2,3], J.K. Gayen[1], T V Krishna Mohan[2]

[1]*Nuclear Recycle Board, Bhabha Atomic Research Centre, Kalpakkam 603 102, India*
[2]*Water and Steam Chemistry Division, Chemistry Group, BARC, Kalpakkam 603 102, India*
[3]*Homi Bhabha National Institute, Anushakthi Nagar, Mumbai 400 085, India*
[§] Email: jselva@igcar.gov.in

Ruthenium is one of the troublesome fission products present in radioactive waste, and its chemistry is complex, especially in highly alkaline saline solutions. In an alkaline medium, ruthenium exists mainly in the form of RuO_4^{-} and RuO_4^{2-} in the pH range of 9-13 [1]. Most of the literature on ruthenium separation from Low-level Liquid Waste (LLW) is based on the ion-exchange, liquid-liquid extraction, and chromatographic separation. Unfortunately, none of the above processes qualifies for the industrial application since the recovery of Ru is poor in all studied cases, and the required acidity for re-extraction is >8M HNO_3, which is the bottleneck. In addition, the residual activity with the solvent system poses an issue during the spent solvent/ion exchanger management using incineration/destruction. Hence, inorganic ion exchangers, based on Ce, Zr, Ti, and Ni were selected and screened for Ru removal from highly saline LLW solution. The Ce-based adsorbent was found to be promising [2], and the Ru-loaded ion exchanger can be immobilized in a suitable matrix without any adverse effect.

In this paper, we describe the performance of in-house made Ce-based adsorbent (Fig. 1), $Ce(OH)_4$-PES and $Ce(OH)_4$-chitosan, in actual plant conditions. The phase purity of $Ce(OH)_4$ in the prepared adsorbents was assessed using X-ray diffraction (XRD). The XRD pattern revealed no phase change in $Ce(OH)_4$ (Fig. 1). The feed solution, ILW IX-effluent, was used as received from the process stream. The characteristics of the feed solution before and after equilibrium with the adsorbent are given in Table 1. The batch studies (2mL test solituon: 0.1g adsorbent, 60 min equilibration) are promising. Further, the role of pH, [Ru], $[Ce(OH)_4]$, polymer additive, and relevant kinetic studies are in progress.

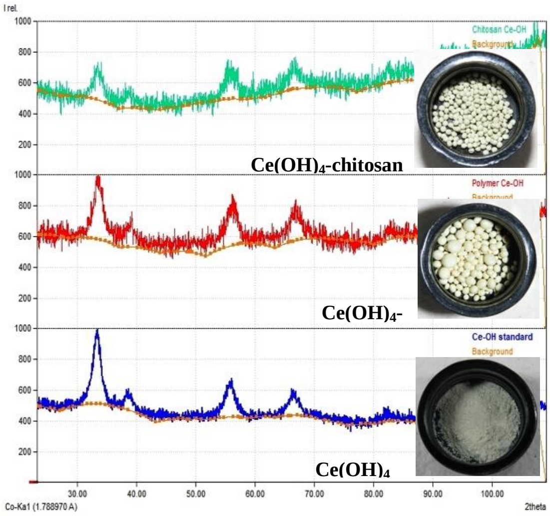

Figure 1. X-ray diffraction pattern of adsorbent

Table 1. Characteristics of feed and effluent

Parameters	**Adsorbent**						
	Initial	$Ce(OH)_4$-PES Comp.			$Ce(OH)_4$-Chitosan		
	Contacts→	I	II	III	I	II	III
pH	12.8	12.7	12.6	12.5	12.8	12.8	12.7
Gross β, ×10^{-3} mCi/L	259	235	234	225	228	226	224
^{106}Ru, ×10^{-3} mCi/L	38	7.5	4.2	ND	2.5	1.9	1.1
^{137}Cs, ×10^{-3} mCi/L	4.9	4.9	4.2	3.4	4.9	4.8	4.3

References:
[1] P.K. Verma et al., *Sep. Purif. Technol*. 275 (2021) 119148
[2] Kumari Anshul et al., Proc., NUCAR 2022, pg. 292

Selective separation of Lanthanides from High-level Liquid Waste using 2-ethylhexylphosphonic acid mono-2-ethyl-hexyl ester (HEH[EHP]) – 1,4-diisopropyl benzene (DIPB)

J. Selvakumar[1,2,§], N. Geetha[1], S. Srinivasan[1], N.R. Jawahar[1] and J.K. Gayen[1]

[1]*Nuclear Recycle Board, Bhabha Atomic Research Centre, Kalpakkam 603 102, India*
[2] *Homi Bhabha National Institute, Anushakthi Nagar, Mumbai 400 085, India*
[§] Email: jselva@igcar.gov.in

An efficient and socio-economical means to separate Transuranic (TRU) elements, such as Am and Cm, from fission product Lanthanides, especially Eu, Ce, and Nd, on an industrial scale would be a significant step in fully closing the nuclear fuel cycle. Partitioning the Lanthanides from TRU fuels is needed to improve neutron efficiency since the Lanthanides have high neutron cross-sections. A two-step approach, coextraction, and partitioning are commonly proposed for separating the Lanthanides from acidic high-level liquid waste (HLW) [1]. Mainly studied process for the two-step approach is TALSPEAK, but it has not yet been deployed in a complete industrial setting. TALSPEAK solvent system showed an inadequate separation factor between Lanthanides and TRU for industrial applications.

To improvise the present solvent system, we have replaced bis-(2-ethyl-hexyl)phosphoric acid (D2EHPA)-dodecane with the 2-ethylhexylphosphonic acid mono-2-ethyl-hexyl ester (HEH[EHP])-1,4-diisopropyl benzene (DIPB) systems. In this paper, we describe the performance of the proposed system with the known TALSPEAK approach: coextraction of the TRU and Lanthanides from HLW using Diglycolamide (DGA) and partitioning of Lanthanides into a proposed system. The buffered aqueous solution (pH 3.5) containing diethylenetriaminepentaacetic acid (DTPA) is used as TRU holding agent.

The role of HEH[EHP] concentration on distribution coefficient and separation factor was calculated based on the ratio of the measured activity of targeted metal ion in the organic phase to that in the aqueous phase. The determined distribution coefficient and separation factor are summarized in Table 1.

Table 1. Distribution coefficient and separation factor (feed: ^{241}Am: 572.9mCi/L; ^{154}Eu: 307.5mCi/L; Experiment: A/O = 1; equilibration time: 40 min.; Aqueous pH 3.5)

HEH[EHP], mol/L	D_{Am}	D_{Eu}	$SF_{Eu/Am}$
0.3	12.11	71.79	5.93
0.5	17.28	162.82	9.11
0.7	17.28	214.10	12.39
0.9	16.37	285.34	17.43
1.2	32.59	952.00	29.22
1.5	59.45	1034.69	17.40
1.8	76.88	1417.77	18.44

The above results are promising, especially when HEH[EHP] is 1.2 mol/L. Experiments are in progress to study the role of solvent, feed solution acidity/alkalinity, and temperature on separation factors.

References:
[1] S. Manohar et.al., *BARC Newsletter*, **332** (2013) 13.

Determination of indoor and outdoor gamma dose rate in soils of leather industrial area of Tirupattur district, Tamil Nadu, India

S. Karthikayini[1], A. Chandrasekaran[1§]

[1] *Department of Physics, Sri Sivasubramaniya Nadar College of Engineering (Autonomous)*
Kalavakkam-603110, Tamil Nadu, India
[§] Email: chandrasekarana@ssn.edu.in

Soil is one of the natural resources which contains the natural radionuclides ^{238}U, ^{232}Th, and ^{40}K and the levels of natural radioactivity vary based on the type of rocks and local geology. Humans have continuously exposed to gamma radiation when soils are used as a building material and it makes adverse effects such as cancer and non-cancer diseases [1]. Hence, soil samples are collected from 17 different locations in and around the leather industrial area of Tirupattur district, Tamil Nadu by random sampling method to determine the activity concentration of natural radionuclides using NaI(Tl) detector-based gamma-ray spectrometry and the associated indoor and outdoor annual effective dose rate are calculated. The energy and efficiency calibrations are carried out using the standard sources ^{137}Cs (662 keV) and ^{60}Co (1173-1332 keV), and reference grade materials given by International Atomic Energy Agency (IAEA), RGU-I, RGTh-I, and RGK-I, respectively. The activity concentrations (A_c) of radionuclides ^{238}U, ^{232}Th and ^{40}K for each sample were determined using the net area under the photo peaks using equation 1,

$$A_c\ (\mathrm{Bq\ kg^{-1}}) = \frac{NCPS}{w \times \eta} \qquad (1)$$

NCPS is the net count per second, w is the weight of the respective sample in kg, and η is the efficiency factor (cps/Bq). From obtained results, mean activity concentrations of ^{238}U, ^{232}Th, and ^{40}K are 68±6, 101±7, and 731±26 Bq kg^{-1}, for soil samples and it is slightly higher than the world average value of 33, 45, and 420 Bq kg^{-1} respectively [2]. Using activity concentrations, the calculated mean indoor and outdoor absorbed dose rates are 123±8 and 233±15 nGy h^{-1}, respectively. The indoor and outdoor annual effective dose equivalent rate ($AEDE_{in}$ and $AEDE_{out}$) due to natural radionuclides in soil samples was estimated using the below equations.

$$AEDE_{in}\ (\mathrm{mSv\ y^{-1}}) = DR_{in} \times 8760\ (\mathrm{h\ y^{-1}}) \times 0.8 \times 0.7 \times 10^{-6}\ (\mathrm{Sv\ Gy^{-1}}) \qquad (2a)$$

$$AEDE_{out}\ (\mathrm{mSv\ y^{-1}}) = DR_{out} \times 8760\ (\mathrm{h\ y^{-1}}) \times 0.2 \times 0.7 \times 10^{-6}\ (\mathrm{Sv\ Gy^{-1}}) \qquad (2b)$$

where, DR_{in} is the indoor absorbed dose rate, DR_{out} is the outdoor absorbed dose rate, 8760 is the exposure time in one year (in hours), 0.8 is the occupancy factor for indoors and 0.2 is for the outdoors, and 0.7Sv Gy^{-1} is the dose conversion coefficient. The mean indoor and outdoor annual effective dose equivalents were 0.60±0.04 and 0.29±0.02 mSv y^{-1}, which are greater than the world average value of 0.48 and 0.07 mSv y^{-1} recommended by UNSCEAR [2].

References:
[1] V.Sathish, A.Chandrasekaran, A.Tamilarasi, V.Thangam, V. Journal of Radioanalytical and Nuclear Chemistry, 331(11), 2022, pp.4513.
[2] UNSCEAR (2000) United Nations Scientific Committee on the Effect of Atomic Radiation. Sources and Effects of Ionizing Radiation, Report to General Assembly, with Scientific Annexes, United Nations, New York.

Measurement of ambient gamma dose rate in Urban Areas of Mumbai and its neighboring cities

P.G. Shetty[1], M. Swarnkar[1], R. A. Takale[1], S. K. Sahu*[1,2], V. Pulhani[1,2]
[1]Environmental Monitoring and Assessment Division, Bhabha Atomic Research Centre,
Trombay, Mumbai – 400085, India
[2]Homi Bhabha National Institute, Anushaktinagar, Mumbai – 400094, India
(Corresponding Author: Email: sksahu@barc.gov.in; Phone: +91-2225592375)

The exposure of human beings to ionizing radiation from natural sources is a continuing and inescapable feature of life on earth. The main contributors to external exposure from gamma radiation are the members of Uranium (radium) and Thorium series together with potassium. These nuclides are present in all soils and rocks with strong variation from one place to another. In this context, it is important to measure the dose rates at different geological areas. These radionuclides impart not only external dose to the population, they also enter the human body through food chain and inhalation thus resulting in the internal radiation dose to population.

To measure the ambient gamma dose rate in the environment of urban areas, twenty-seven locations from Mumbai, Navi Mumbai and Thane cities were identified. The study was carried out for one year on quarterly basis the ambient gamma radiation was measured using Thermoluminescent Dosimeter (TLD) based on $CaSO_4$: Dy Teflon discs. TLD is a passive device for the measurement of gamma dose and in this the dose is acquired and stored for a long period of time until the system is stimulated by heat. The advantage of this system is that since it acquires the dose continuously the variation of dose during different periods of time is averaged out. These TLDs were placed outside of residential building for a period of three months. After three months these exposed TLDs are replaced by new set of TLDs. Annual values for all the locations are evaluated based on the average quarterly values by normalizing to 365 days. These TLDs have been thoroughly characterized based on ANSI 545[1] criteria for the environmental radiation monitoring using TLDs. The average air dose rates in Mumbai and its neighbouring urban cities are summarized in Table .1 The values are in the range of 0.43 mGy/a to 0.47 mGy/a with an average of 0.45 mGy/a. Urban spaces are more complex environments, in which terrestrial background gamma radiation depends not only on the soil and bedrock level of radionuclides, but also on the content of radionuclides in building materials used for the construction of roads, pavements and buildings.

Monitored Place	**Avg. Air Dose Rate(mGy/a)**
South Mumbai	0.47 ± 0.04
South Central Mumbai	0.45 ± 0.03
North Mumbai	0.45 ± 0.01
Western Suburban	0.44 ± 0.04
Central Mumbai	0.46 ± 0.01
Harbor Mumbai	0.43 ± 0.01
New Mumbai	0.43 ± 0.04
Thane City	0.45 ± 0.03
Average	**0.45 ± 0.03**

Table 1: Outdoor Ambient Annual Gamma Air dose

References:
[1] ANSI N-545, American National Standard, Performance, Testing, and procedural specifications for Thermoluminescent Dosimetry, Environmental Applications (1975).

Scintillating Polystyrene Adsorptive Membrane for Alpha-Beta Particle Discrimination

Utkarsh Alset[1], Suparna Sodaye[§2], Atul Kulkarni[§1]

[1] *Symbiosis Centre for Nanoscience and Nanotechnology (SCNN), Symbiosis International (Deemed University), Pune – 412 115, Maharashtra, India.*
[2] *Radiochemistry Lab, Bhabha Atomic Research Centre, Trombay, Mumbai – 400 085, Maharashtra, India.*
[§] E-mail Address: atul.kulkarni@scnn.edu.in, suparna@barc.gov.in

Environmental radioactivity is a major concern due to the release of radioactive elements from human activities. The monitoring of radioactive contamination is vital for protecting the environment and human health. Discrimination between alpha and beta particles is crucial in understanding the nature of environmental radioactivity. In this study, we present a newly developed scintillating polystyrene adsorptive membrane for discrimination between alpha and beta particles. These particles have different penetration depths and can be differentiated based on their energy spectra. Various scintillating membranes, such as polycarbonate and polyvinyl-toluene, have been developed in previous studies, but the use of polystyrene as an adsorptive scintillating membrane has not been explored further. Thus, we synthesized a polystyrene adsorbing polymer with primary and secondary organic scintillators with appropriate chemical composition and tested it with varying degrees of water uptake and thickness using a solution polymerization method. The use of ^{241}Am and ^{152}Eu is evaluated as an active source and measured efficiency and discrimination between alpha and beta particles. Our results demonstrate that membrane was highly sensitive to alpha and beta particles with a detection efficiency of 96 %, while also maintaining a low background count rate (illustrated in Fig. 1). The newly developed scintillating polystyrene adsorptive membrane offers a cost-effective and efficient alternative to existing photomultiplier (PMT) devices. This research has significant applications in public health and safety, which can be extended to various sectors such as medical diagnostics and radiation detection.

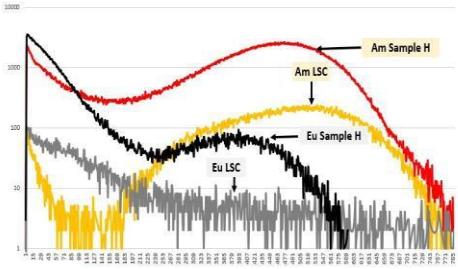

Fig. 1: Characteristic illustration of Alpha and beta particle spectrum using liquid scintillation count (LSC) and scintillating polystyrene

Acknowledgements:
This research project is funded by the Board of Research in Nuclear Sciences (BRNS) Project No. 58/14/16/2020-BRNS.

References:
[1] Luo, Jian-Bin, et al. "A Melt-Quenched Luminescent Glass of an Organic–Inorganic Manganese Halide as a Large-Area Scintillator for Radiation Detection." *Angewandte Chemie* **135.7** (2023): e202216504.
[2] Kwak, S., et al. "Comparison of existing and new optical fiber-based scintillation detectors for spent-fuel verification equipment." *Nuclear Instruments and Methods in Physics Research Section A: Accelerators, Spectrometers, Detectors and Associated Equipment* **1048** (2023): 167914.

Assessment of gross alpha and gross beta activities in beach sediments along the northeast coast of Tamil Nadu, India

V. Sathish[1] and A. Chandrasekaran[1,§]

[1] *Department of Physics, Sri Sivasubramaniya Nadar College of Engineering, Chennai, India*
[§] Email: chandrasekarana@ssn.edu.in

In this study, 63 shoreline sediment samples were collected from twenty-one locations at three different depths (0 – 20 cm, 20 – 40 cm, and 40 – 60 cm) along the northeast coast of Tamil Nadu and examined to estimate the Natural gross α and gross β activities using the low background Gas-less Automatic Alpha/Beta counting system (Canberra iMatic™) calibrated with alpha (^{241}Am) and beta (^{90}Sr) standards [1]. The mean counting efficiencies of α and β activity concentrations in the counting system were 33–40 % and 95–98 %, respectively. The background counting of the detectors was made using an empty, clean planchette for each detector [2]. From the top layer of sediment samples (0 – 20 cm), activity concentration ranges for gross α and gross β are 6 – 180.86 Bq kg^{-1} with an average value of 32.39 Bq kg^{-1} and 270.16 - 2371.27 Bq kg^{-1} with an average value of 621.26 Bq kg^{-1} respectively. In the same way, in the middle-layered samples (20 – 40 cm), the activities of gross α and gross β are 6 - 122.99 Bq kg^{-1} with an average value of 29.09 Bq kg^{-1} and 216.46 - 578.61 Bq kg^{-1} with an average value of 307.91 Bq kg^{-1} respectively. Finally, the ranges of the activities of gross α and gross β in bottom layered samples (40 – 60 cm) are varied from 6 - 340.81 Bq kg^{-1} with an average value of 32.66 Bq kg^{-1} and 100 - 2664.5 with an average value of 433.77 Bq kg^{-1} respectively. These results were compared with previous studies throughout the world [3-6], and the study could be reference data for future research related to radiological mapping or environmental monitoring in the northeast coast of Tamil Nadu, India.

Keywords: Alpha activity; Beta activity; Coastal sediment; Dose assessment

References:

[1] G. Karahan, N. Öztürk, and A. Bayülken. *Water Research*, **34** (2000) 4367.
[2] O. Selçuk Zorer, H. Ceylan, and M. Dogru. *Environmental Monitoring and Assessment*. **148** (2009) 39.
[3] M.Y. Hanfi, I.V. Yarmoshenko, A.A. Seleznev et al., *Journal of Radioanalytical and Nuclear Chemistry*, **323** (2020) 1047.
[4] E.O. Agbalagba, S.U. Egarievwe, and E.A. Odesiri-Eruteyan et al., *Journal of Environmental Protection*, **12** (2021) 526.
[5] M.Y. Hanfi, I. Yarmoshenko, and A.A. Seleznev. *Atmosphere*, **12** (2021) 571.
[6] K.A.M. Erol, Z.Ü. Yümün and K.U.R.T. Dilek. *Journal of the Turkish Chemical Society Section A: Chemistry*, **4** (2017) 889.

Comparison of glass matrices used for containment of high level radioactivity by Raman spectroscopy

Amrita Dhara Prakash§, V. K. Mittal, T. P. Valsala, D. B. Sathe and R. B. Bhatt
[1] *Fuel Fabrication, Nuclear Recycle Board, BARC, Tarapur, Maharashtra, India*
§Email: amrita@barc.gov.in

Borosilicate glass is used for immobilization of High Level liquid Waste (HLW). This waste contains high level of α, β and γ radioactivity and immobilization in glass network helps in containment of activity. However the strength of glass network plays a vital role in determining how effectively the radioactivity can be contained without any release in the environment. The thermal, chemical and mechanical strength of the product glass widely depends on the additives present in the base glass. Two base glasses that are used for immobilization of HLW in India were chosen for this study. The composition of base glass is given in Table-1. Raman spectroscopy were performed to study how the presence of different kinds of modifiers are playing a role in glass network formation.

Fig. 1 shows the Raman spectra of both the samples. The band around 450cm^{-1} due to SiO_4 units with very few non bridging oxygen is more prominent in sample A and shifting of this band to lower wavenumber shows Ca and K modified SiO_4 units. The presence of a band around 960cm^{-1} in sample A and 895cm^{-1} in sample B is due to Q^3 units in sample A and Q^2 units in sample B (Q denotes central Si atom and n denotes the number of bridging oxygens around Si.). The band around 800cm^{-1} is characteristic to boroxol rings present in both the samples. However Sample A reveals tetraborate units also evident from band at 770cm^{-1} [1,2].

Table 1: Composition of base glass (mol %)

Oxide	Sample-A	Sample-B
SiO_2	57.43	62.03
B_2O_3	22.71	10.96
Na_2O	10.10	9.26
TiO_2	7.82	8.26
Fe_2O_3	1.94	0.86
CaO	-	7.54
K_2O	-	1.09

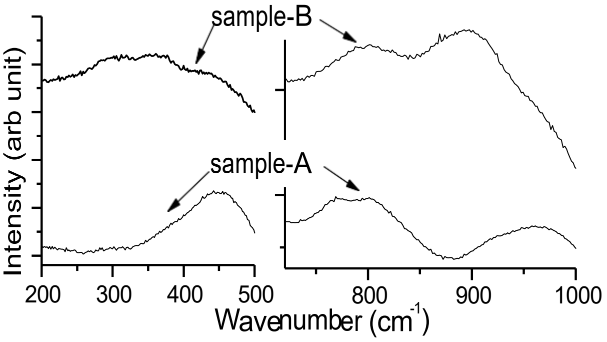

Fig. 1: Raman spectra of sample-A and B

Due to presence of larger number of network modifiers in sample B the silicate network shows more number of Q^2 units and relatively lesser number of Q^3 units revealing higher degree of deploymerization in sample B. However due to presence of divalent cations it offers more rigidity to the network in sample B compared to sample A. Study on different kinds of boron units in the sample will also provide information on strength of the network.

Authors wish to acknowledge Dr. Rekha Rao of Physics Group, BARC, for the Raman measurements.

§ Email: amrita@barc.gov.in

References:
[1] W.L. Konijnendijk and J.M. Stevels, *Journal of Non Crystalline Solids*, **20** (1976) 193.
[2] Ashutosh Goel et al., *Advances in Glass Science and Engineering*, **4** (2012) 42.

Study on the Natural Radionuclide (^{210}Po) Level in the Crustacean and Molluscan of Muthupet Mangrove Ecosystem, Tamil Nadu,India.

P.Raja[1,§], S. Ravikumar[1] ,P. Murugaiyan[1], R. Krishnamoorthy[2] and K. Barkavi[1]

[1]*P.G Research Department of Zoology, Rajah Serfoji Govt. College (A), Thanjavur – 613 005.*

[2] *PG. and Research Department of Zoology, Jamal Mohamed College,Tiruchirappalli-20.*
[§]Email: rajazoo75@yahoo.co.in

Muthupet is a town in Tiruvarur district lies adjacent to the Bay of Bengal and is in the southernmost part of the Cauvery delta and is bounded by Korayar and Bamaniyar rivers to the east and west respectively. The present study was carried out in Muthupet ecosystem to find out the distribution of ^{210}Po in abiotic and biotic samples. The levels of ^{210}Po in the water and sediment of the Muthupet Mangrove Ecosystem is 1.2mBq/l. and 6.8 Bq/kg respectively. The biological samples such as four species of crabs, prawns, gastropods, bivalves and two species of cephalopods were collected from the Muthupet Mangrove Ecosystem and subjected to the analysis of ^{210}Po activity in both hard and soft parts. ^{210}Po determinations were made by the standard technique of acid digestion, spontaneous deposition of ^{210}Po from an acid solution on to both sides of a polished silver disc and counting of the ^{210}Po alpha activity on the disc [1, 2]. The counting instruments used were an alpha counter with ZnS (Ag) detector with a background of 0.1 – 0.2 cpm and a counting efficiency of 30.3%.

The results of ^{210}Po activity in the above mentioned biological samples were presented in the figure 1. Among all the organisms tested soft tissue of *Meretrix meretrix* accumulated higher values of ^{210}Po activity where as*Penaeus indicus* accumulated higher values among the edible organisms. In general, molluscan species both soft tissue and shell displayed a high ^{210}Po activity when compared to crustaceans. The ability of aquatic organisms tested in the present study to concentrate radionuclides at a relatively higher level in different tissues and yet to survive and apparently to reproduce normally, indicates that they might have evolved control or tolerance mechanisms at cellular levels.

Keywords: MuthupetMangrove, ^{210}Po, Crustacean and Mollusca.

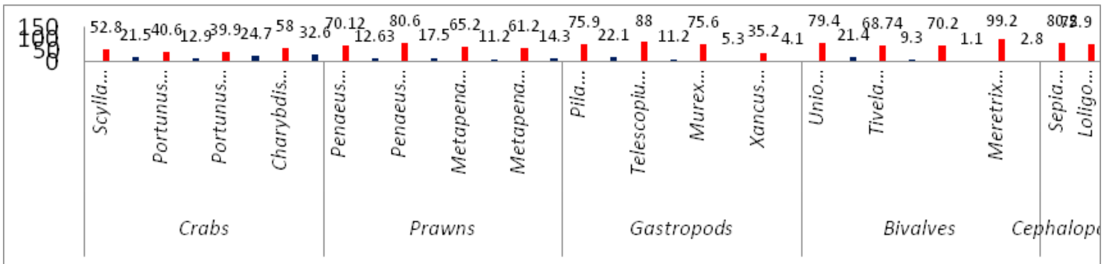

Fig. 1.The mean values of ^{210}Po activity in the Crabs,Prawns, Gastropods, Bivalves and Cephalopods of Muthupet Mangroves Ecosystem

Acknowledgements: Our sincere thanks are due to The Principal,Rajah Serfoji Government College (A), Thanjavur for constant encouragement, and The Principal, Jamal Mohamed College (A), Tiruchirappalli for extending their radiation counting facility.

Reference(s):

[1] W.W.Flynn, The determination of low levels of Polonium-210 in environmental materials. *Anal. Chim. Acta*. 43, (1968) 221-227.

[2] M.A.R.Iyengar, Studieson the distribution of natural radioactivity in marine organisms. Ph.D. Thesis, University of Bombay, (1983).

Synthesis and performance evaluation of copper-based hexacyanoferrate nanoparticles for the removal of cesium from aqueous streams

Krishan Kumar[1,§],Shrikant S. Padhy[1]and H. Seshadri[1]

[1]*Safety Research Institute, Atomic Energy Regulatory Board, Kalpakkam, Tamil Nadu, India,*
[§] Email: kgoyat55@igcar.gov.in

Prussian blue-based materialsare widely used in the form of thin films, ink-based solutions, and nanoparticles due to their ability to selectively remove cesium (Cs) from aqueous streams.Nanoparticles of Prussian blueanalogue, copper-based hexacyanoferrate (CuHCF) nanoparticles have recently gained a lot of attention for Cs removal. The removal efficacy is largely influenced by many factors, including the sorbent particle's active site, surface area, pH, dosage and reaction time, synthesis methodology etc [1,2]. The present study discussesthe synthesis of CuHCF nanoparticles using the co-precipitation method and an electrochemical route and compares its performance for the Cs removal from the aqueous streams.

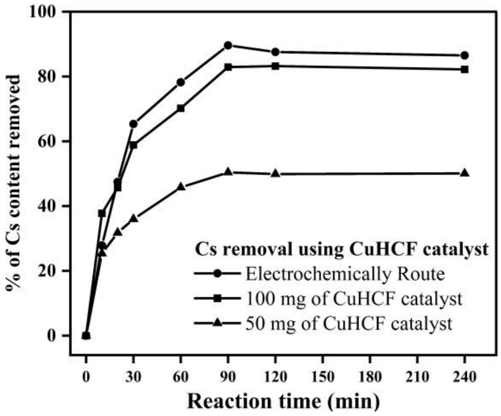

Fig. 1: Cs removal from aqueous stream using CuHCF catalyst

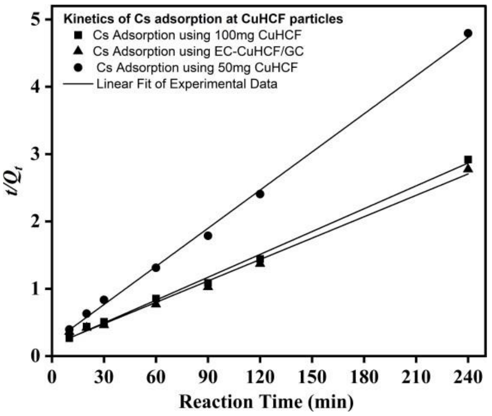

Fig. 2 Pseudo second-order kinetics model for Cs adsorption using CuHCFcatalyst

The removal efficiency for Cs (100mg/L) using CuHCF catalyst was investigated by conducting several experiments to understand the influence of experimental parameters such as pH, catalyst loading, initial concentration, reaction time, etc.The extent of Cs removal from aqueous was carried out using Atomic Absorption Spectrophotometer.Nearly 85% and 90% of Cs removal using CuHCF catalyst synthesised by the conventional and electrochemical method could be achieved in 90 min respectively (Fig.1). Studies reveal that the CuHCF particles synthesised using an electrochemical route has performed better than conventional co-precipitation synthesis method. The adsorption kinetics and isotherms fit well with a pseudo-second-order model and Langmuir isotherm, respectively (Fig.2). The study demonstrates that the synthesised CuHCFcatalyst is highly effective for the Cs removaland can be regenerated after use.Therefore, the adopted methodology has several advantages over the conventional method, including in-situ synthesis and catalyst recycling, making it highly cost-effective.

References:

[1] A. Nilchi, B. Malek, M.M. Ghanadi, A. Khanchi, *Journal of Radioanalytical andNuclear Chemistry*258 (2003) 457.
[2]Tingting Xia, Liangliang Yin, Yuhan Xie, Yanqin Ji, *Chemical Physics Letters*, 746 (2020) 137293.

Determination of ^{238}U, ^{232}Th, and ^{40}K and the associated radiation hazards along the north Chennai to Pondicherry coastal area, India

V. Sathish[1] and A. Chandrasekaran[1,§]

[1]*Department of Physics, Sri Sivasubramaniya Nadar College of Engineering Chennai, India*
[§] Email: chandrasekarana@ssn.edu.in

East coast zones of states in India especially Orissa, Tamil Nadu, and Kerala are known for their natural radioactivity caused by deposits of monazite-bearing sands. For that reason, the current investigation focused on radioactivity in coastal sediments because it might have a very large background level depending on the geology of the location. Hence the sediment samples are collected at 21 coastal areas from North Chennai to Pondicherry of India to determine the activity concentration of natural radionuclides (^{238}U, ^{232}Th, and ^{40}K) using a NaI (Tl) γ -ray detector. For efficiency calibration, the approved standard International Atomic Energy Agency (IAEA) sources of reference-grade materials such as RG-U (4940 ± 30 Bq kg^{-1}), RG-Th (3250 ± 90 Bq kg^{-1}), and RG-K (14000 ± 400 Bq kg^{-1}) were used [1]. The energy calibration was accomplished by inserting known-energy gamma sources, ^{137}Cs (662 keV) and ^{60}Co (1173-1332 keV), into the detector. The specific activity of ^{238}U, ^{232}Th, and ^{40}K is calculated by using the following Eq. (1),

$$A\,(\mathrm{Bq\ kg^{-1}}) = \frac{\mathrm{NCPS}}{\mathrm{W} \times \eta} \tag{1}$$

where NCPS – net counts per second, W – total mass of each sample in (kg). η – photo peak's efficiency as determined via efficiency calibration. Activity concentration ranges for ^{238}U, ^{232}Th, and ^{40}K are 12 ± 2 to 183 ± 3 Bq kg^{-1} with an average value of 60 Bq kg^{-1}, BDL – 495 ± 4 Bq kg^{-1} with an average value of 70 Bq kg^{-1}, 411 ± 10 to 853 ± 11 Bq kg^{-1} with an average value of 573 Bq kg^{-1} respectively. The mean activity concentrations of ^{238}U, ^{232}Th, and ^{40}K in the sediment samples are higher than the world average values [2]. Here, below detectable limit (BDL) of ^{238}U, ^{232}Th, and ^{40}K is 8, 8, and 30 Bq kg^{-1} respectively. The gamma absorbed dose rate (D_R) and outdoor annual effective dose equivalent (AEDE) are measured by using the following Eq. (2) and (3),

$$D_R = 0.462A_U + 0.604A_{Th} + 0.0417A_K \tag{2}$$

$$\mathrm{AEDE_{out}}\,(\mathrm{mSvy^{-1}}) = D_R\,(\mathrm{nGyh^{-1}}) \times 8760\ \mathrm{h\ y^{-1}} \times 0.2 \times 0.7\ \mathrm{SvGy^{-1}} \times 10^{-6} \tag{3}$$

The calculated mean value of D_R (94 nGyh^{-1}) is greater than the world average value of 59 nGyh^{-1} [2]. The computed AEDE indicates a mean value of 0.12 mSvy^{-1} for the samples which is greater than the world average value of 0.07 mSvy^{-1}.

References:
[1] N.Q. Hung, H.D. Chuong, T.T. Thanh et al., *Journal of Environmental Radioactivity*, **164** (2016) 197.
[2] UNSCEAR (2000) United Nations Scientific Committee on the Effect of Atomic Radiation. Sources and Effects of Ionizing Radiation. Report to General Assembly, with Scientific Annexes, United Nations, New York.

Natural Background Gamma Radiation Monitoring in Kashmir valley Using TLDs

M. Swarnkar[1], P.G. Shetty[1], R. A. Takale[1], S. K. Sahu*[1,2], V. Pulhani[1,2]

[1]Environmental Monitoring and Assessment Division, Bhabha Atomic Research Centre,
Trombay, Mumbai – 400085, India
[2]Homi Bhabha National Institute, Anushaktinagar, Mumbai – 400094, India
(Corresponding Author: Email: sksahu@barc.gov.in; Phone: +91-2225592375)

The Ambient environmental dose depends upon two factors natural radiation and manmade or artificially produced radiation. The natural radiation dose mainly arises from the cosmic radiation (galactic and solar) and from Earth‟s naturally occurring radionuclides material (NORM). These naturally occurring radionuclides are the major contributors to the total effective dose of ionizing radiation received by the population [1]. In current study measurement of gamma dose rate were done in ten districts of Kashmir. Very few data of gamma radiation dose levels is available of this region. Total 96 location were monitored on quarterly basis using TLDs and annual cumulative dose rate computed.

Thermoluminescence dosimeters (TLDs) were used for measurement of annual cumulative environmental gamma radiation dose rate. The advantages of passive TL dosimeters for environmental monitoring are that they are small, cheap and do not require power supply during monitoring [2]. The CaSO4 :(0.2 mole %) Dy Teflon TLD discs, specifically designed for environmental thermoluminescent dosimetric purpose were deployed at selected locations for the measurements. Monitoring area were divided into grids. TLD locations were selected based upon population density in these grids. TLDs, bearing an identification number were deployed at these sampling locations for a period of three months and were replaced by new TLDs of the next batch.

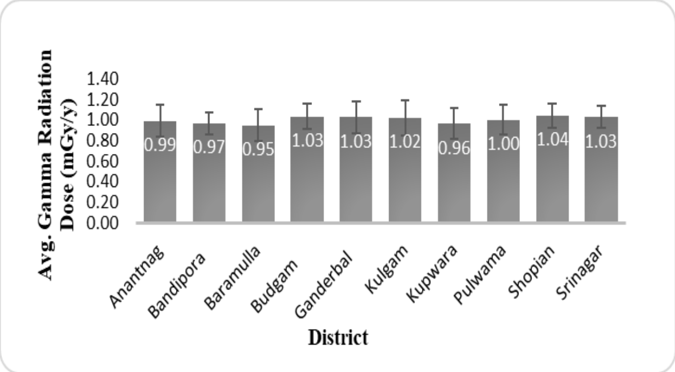

Fig. 1: External gamma radiation dose rates at various districts of Kashmir.

The minimum and maximum gamma doses measured at Lolab Valley, Kupwara district and Tral, Pulwama district were 0.53 mGy/y and 1.59 mGy/y, respectively. The average dose value in entire Kashmir region was around 1 mGy/y while the Indian national and world average value excluding High Background Radiation Areas (HBRAs) are 0.78 mGy/y [3] & 0.52 mGy/y [1], respectively. Height from mean sea level & NORM in soil are responsible for variation in dose rate, further study of these factors will be carried out for evaluation of spatial dose variation.

References:
[1] UNSCEAR: Sources, Effects and Risks of Ionizing Radiation, Report to General Assembly, United Nations, New York, (2000)
[2] Ranogajec-Komor, M., *Radiation Safety Management*, **2(1)** (2003), 2
[3] Nambi, K.S.V., et.al., *Radiation Protection Dosimetry*, **28(1)** (1987), 31

Estimation of effective radiation dose due to ^{222}Rn in groundwater to the population of Kodagu District, Karnataka State, India

S. N. Namitha, B. S. K. Lavanya, Mohammed Hidayath and M. S. Chandrashekara§

Department of Studies in Physics, Manasagangotri, University of Mysore, Mysuru 570006, India
§ Email: msc@physics.uni-mysore.ac.in

Radon a radioactive gas and its decay products in the atmosphere are the key contributors of human exposure to radiations from natural sources and pose a serious health risk [1]. The ingestion of radon through drinking water pathway gives rise to radiation exposure to the stomach and other organs of the body. Studies show a strong correlation between radiation exposure and health hazards among the population in a given environment [2].

In the present study, groundwater samples were collected from various locations of Kodagu District, Karnataka State, India to measure the ^{222}Rn activity concentration. The study area occupies 4102 km^2 and is comprised of rocks like granites, dykes, amphibolites and gneisses. As groundwater fulfils the major water demand of the population of study region it is necessary to estimate the concentration of ^{222}Rn in groundwater and to estimate the radiation dose to the public.

To analyse ^{222}Rn activity in groundwater, samples were collected from various locations of study area in air tight bottles of 200 ml volume. Proper care was taken such that no bubbles were formed inside the bottle during sampling. ^{222}Rn activity was measured immediately after sampling by emanometry technique employing Smart Radon Monitor (SRM) which was calibrated regularly using a standard source. 60 ml of the collected sample was transferred to the sample holder of SRM and air was bubbled through it using a specially designed pump. The dissolved radon gas thus released enters into a scintillation cell. Scintillations produced due to the alpha particles emitted by radon and its decay products were measured with the help of a photomultiplier tube which is coupled to counting electronics. Activity concentration of ^{222}Rn in water was calculated using the eqn. (1),

$$^{222}A_{Rn}\left(Bql^{-1}\right)=\frac{6.97\times10^{-2}\times D}{V\times E\times\left(e^{-\lambda T}\right)\times\left(1-e^{-\lambda t}\right)} \qquad (1)$$

Where, D = Sample counts – Background counts, V = Volume of water (60 ml), E = Efficiency of the scintillation cell (74 %), t = Counting duration (s), λ = decay constant for radon (2.098 x 10^{-6} s^{-1}), T = Counting delay after sampling (s).

^{222}Rn concentration in groundwater was observed to be in the range of 0.22±0.39 to 8.61±5.73 Bql^{-1} with an average value of 1.75±2.66 Bql^{-1}. The measured values are well below the recommended safety standards of 11.1 Bql^{-1} and 100 Bql^{-1} prescribed by USEPA and WHO respectively. Ingestion and inhalation doses due to ^{222}Rn in groundwater were calculated from the measured ^{222}Rn concentration. The total effective dose was found to vary from 0.77 to 29.84 μSvy^{-1}.

References:

[1] UNSCEAR, Annex B: Exposures from natural radiation sources, United Nations Scientific Committee on the Effects of Atomic Radiation, United States, (2000).

[2] BEIR Health risks from exposure to low levels of ionizing radiation, The National Academies report in brief, VII (2005).

^{226}Ra and ^{222}Rn concentration in groundwater samples of Chamarajanagar District, Karnataka State, India.

B.S.K. Lavanya[1], S.N. Namitha[1], K. S. Pruthvi Rani[2] and M.S. Chandrashekara[1§]

[1]*Department of studies in Physics, University of Mysore, Mysuru, 570006, India*
[2]*Department of Physics, Karnataka State Open University, Mysuru, 570006, India*
[§] Email: msc@physics.uni-mysore.ac.in

Exposure to natural radiation is an inevitable process to human being. Naturally occurring radionuclides have been present since the formation of the Earth. As ground water is in direct contact with these radionuclides, trace amounts of dissolved radioactive elements are present in it. When the ground water is used for drinking purposes, they cause serious health issues including cancer risks [1].

^{226}Ra, a naturally occurring radionuclide from the decay series of uranium has a very longer half-life. It decays into ^{222}Rn by emitting alpha particles that have enough energy to damage living cells. ^{226}Ra tends to accumulate in bones and teeth and is not metabolised by the body and only decays radiologically over time. ^{222}Rn decays by emitting alpha particle that pose inhalation and ingestion dose to the population. ^{226}Ra and ^{222}Rn in water cause multiple health hazards [2].

The study area Chamarajanagar district, of Karnataka State, India lies between latitudes 11°40'58" and 12°6'32"N and longitudes 76°24'14" and 77°64'55"E. The major rock types in the district are Granitic rocks and gneiss rock. People in the study area are mainly dependent on groundwater sources. Therefore, the distribution of radioactive elements in the groundwater and radiation dose to the public due to these radionuclides was studied.

For ^{226}Ra analysis emanometry method was employed. Water sample was pre-concentrated by co-precipitation and evaporation method. 70ml of solution was filled in a bubbler and kept undisturbed for 21 days. The air in the bubbler was transferred to the scintillation cell and counted for alpha activity using programmable counting system.

For ^{222}Rn measurements, water samples were collected in vials, from sampling stations. The measurements were done within 4-5 hours of sampling using Smart Radon Monitor [SRM] based on the detection of alpha particles emitted from radon and its decay products in the scintillation cell. 10% of the samples were analysed at other laboratory.

The concentration of ^{226}Ra in ground water samples, measured at 12 regions of Chamarajanagar district varied from 2.18 to 96.4mBql^{-1} with an average value of 31.38mBql^{-1}. These values lie well below the recommended limit of 1 Bql^{-1} by WHO [3]. The ^{222}Rn concentration varied from 1.2 to 11.65Bql^{-1} with an average value of 4.25Bql^{-1}, which is well below the recommended limit of 100 Bql^{-1} by WHO. The total ingestion dose due to ^{226}Ra and ^{222}Rn varied from 3.52 to 49.48 µSvy^{-1}. The values show that there is no significant health risk to general public from these radionuclides in water. A strong correlation between ^{226}Ra and ^{222}Rn concentrations are observed with adjusted R-Square value of 0.9 which indicate that they might be of same origin.

References:
[1] UNSCEAR, United Nations Scientific Committee on the Effects of Atomic Radiation, *Sources and effects of ionizing radiation*. New York: United Nations, (2008).
[2] C. R. Cothern, *Radon, radium, and uranium in drinking water*. CRC Press, (2014) .
[3] WHO, World Health Organization, *Guidelines for Drinking Water Quality-4th edition, Radiological aspects*: (2011), 203-217.

Transit time estimation of drying springs in Uttarakhand region using environmental tritium concentration

Sitangshu Chatterjee[1*], Vinod Khati[2], A. Jaryal[1], H. V. Mohokar[1], S. N. Kamble[1], U. K. Sinha[1], H. J. Pant[1]

[1]*Isotope and Radiation Application Division, BARC*
[2] *HESCO, Uttarakhand*
[§] Email: sitanshu@barc.gov.in

Springs are the main source of water for millions of people and their livestock in the Indian Himalaya Region (IHR). Erratic rainfall, seismic activity and ecological degradation associated with land use change for infrastructural development are impacting mountain aquifer systems. As a result, perennial springs in IHR region have either already dried up or become seasonal, resulting acute water shortages across thousands of Himalayan villages. Therefore, estimation of groundwater residence time is very vital as it indicates the renewal rate of the aquifers which has direct bearing on the future sustainability of the groundwater resources.

Environmental tritium is generally used to act as a qualitative indicator for the groundwater residence time (1). In most of the cases environmental tritium data suggests whether the groundwater recharge is modern or old or a mixture of both. Tritium measurements of the spring water samples were carried out both in pre-monsoon and post-monsoon seasons. Tritium values of the spring water samples clearly show the effect of seasonal variability. In post-monsoon tritium varies from 4.32 to 6.1 TU whereas in pre-monsoon tritium varies from 4.01 to 5.15 TU. In post monsoon sampling tritium value increases due to the input of fresh gulp of rainwater whereas in pre-monsoon time due to the higher residence time tritium value decreases. The seasonal variability in tritium values of the springs is shown in Fig. 1. Tritium concentration of the rainwater samples collected in the rain gauges varied from 5.23 TU to 5.80 TU having average value of 5.57 TU. By considering the rainwater tritium concertation as input value (C_{in}), the approximate transit time of the spring water is estimated using piston flow model equation:

$$C_{out}(t) = C_{in} \exp(-\lambda\tau_m) \qquad (1)$$

Using the above equation, the transit time of the spring water samples is found to vary between 6 months to 1.5 years. The lowest transit time (~ 6 month) is observed in case of V3SP8 sample whereas the highest transit time is estimated in V1SP1 spring water sample.

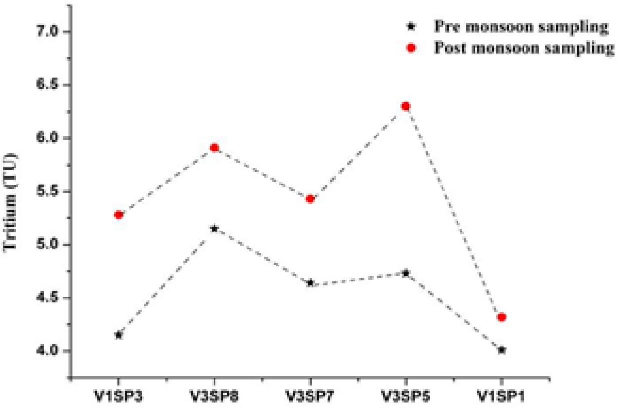

Fig. 1: Seasonal variability in tritium values of the spring water

Acknowledgements: The authors wish to acknowledge Dr. S. Kannan, GD, RC&IG for the support and encouragement during the study.

Reference:

Lindsey et al. (2000). Tritium as an Indicator of Modern, Mixed, and Premodern Groundwater Age, Scientific Investigations Report 2019–5090.

Synthesis of Phosphoramide Derivative Functionalized Fe_3O_4 Nanoparticles for Separation of Uranium

Pallavi Singhal[1§], Vandana Pulhani[1], Goutam Biswas[2]

[1]Environmental Monitoring and Assessment Division, Bhabha Atomic Research Centre,Mumbai 400085, India
[2]Department of Chemistry, Cooch Behar Panchanan Barma University, Cooch Behar, West Bengal, India 736101
[§]Email: psinghal@barc.gov.in,

Uranium is one of the most important elements for nuclear industry. It is also a well known nephrotoxic element with a maximum permissible contamination level of 30 ppb in drinking water[1]. Numerous methods have been developed to extract uranium[1]. However, most of the techniques are expensive, need pre-treatment of the sample, large contact time, non-selective and have low sorption capacity. Therefore, it is essential to design cost effective and environmentally friendly methods for uranium extraction. Earlier investigation[2] has shown that phosphoramide group binds effectively and selectively with uranium. Herein, this work has been extended and various derivatives of phosphoramide were synthesized . These derivatives are further coated onto Fe_3O_4 NPs. Different amount of ligand was added to Fe_3O_4 NPs and stirred for ~1 h. The coated particles were then characterized using XRD, FTIR, TEM, TG, Zeta potential. Uranium sorption studies were performed with these materials. It was observed that maximum sorption occurs at pH 6-7 region and equilibration reaches within 15 min of sonication. Sorption isotherm studies were performed to find out the maximum sorption capacity. The results were fitted in Langmuir isotherm and the maximum sorption capacity is in the range of 90-150 mg of uranium/g of sorbent. Further studies are underway. Recyclability of the material was checked and material can be used upto 10 cycles and >70% of uranium sorption was observed. Desorption was carried out with EDTA and it was found that >90% of the uranium gets separated from the material. The synthesized sorbent is selective and the mechanism of binding will be further understood by the XPS measurements.

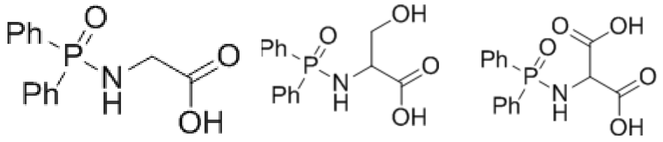

VS-10 **VS-11** **VS-12**

Fig. 1: Structure of various phosphoramide derivatives used for the study

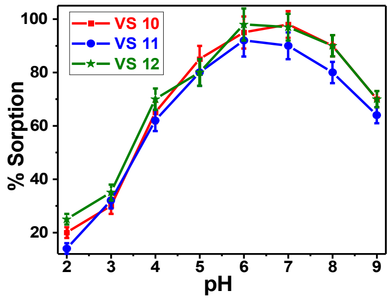

Fig. 2: pH dependent study of uranium with Fe_3O_4 coated phosphoramide derivatives.

Acknowledgements - The authors would like to acknowledge Dr. A. Vinod Kumar and Dr. D. K. Aswal of HS&EG for their continuous support.

References:
[1] P. Singhal et. al., *Journal of Industrial and Engineering Chemistry*, **90** (2020), 17.
[2] P. Singhal et. al., *Journal of hazardous materials,* **384** (2020) 121353.

Estimation of Uranium distribution coefficient in soils collected fromVisakhapatnam DAE campus and role of ground water chemistry

P. Sandeep, Sukanta Maity, Suchismita Mishra, C.B. Dusane, Dilip Kumar Chaudhary, R.K.Balaram,PadmaP.Savitri,AnilkumarS.Pillai, A.VinodKumar

EnvironmentalMonitoringandAssessmentDivision,
BhabhaAtomicResearchCentre,Mumbai-400085,India
*Email:deepu@barc.gov.in

UltimatefateofUraniumreleasedintothegeologicalenvironment,dependsonthedistribution coefficient (K_d). There exists a large uncertainty in the published literature for UK_d and hence site specific values are needed to estimate reliable impact assessment. Soil andwater chemistry play important role in the large variation of K_d values. Present study aims forthe estimation of $K_d$for U at DAE campus, Visakhapatnam and evaluation of the role ofgroundwaterchemistryonK_d.Soil (40nos)and groundwatersamples(15nos)were collected covering the entiresite (14 sq. km). Initially, sorption equilibrium and effect of solution pH on U sorption wasstudied by interacting the soil sample with U spiked groundwater. Results show that, only 3%of spiked U was sorbed on soil in 1hr and the value reached to maximum of 29% in 72 hrs.Variation of solution pH shows that U has maximum sorption on studied soils between pH 4-6,whereasalmostnosorptionwasobservedathigherpHi.e.,pH >8(Fig.1).K_d for U was estimated in all the collected soil samples and values are found to be inthe range of 0.1±0.007 L/kg to 245±14.5 L/kg with a median value of 49.7 L/kg, which iscomparativelyonalowerside[1].Allsoilsampleswerecharacterizedfordifferentparameters viz. Cation exchange capacity, Organic Matter, carbonate content 3a3nd pH. There was no significant correlationbetween soil parameters and K_d observed. Similarly, all collected groundwater samples werecharacterized for various anions (F^-, Cl^-, NO_3^-, SO_4^{2-} and HCO_3^-) to evaluate its influence onK_d.Ingroundwater,chloridewasfoundtohavethehighestconcentrationfollowedbybicarbonate and the least concentration was observed for F^- and NO_3^-. The generated anionicdata was used for correlation study and is presented in Table 1. A positive correlation (R^2 =0.7) was observed between NO_3^-, and K_d, whereas a negative correlation (R^2 = -0.6) wasobserved between HCO_3^- and K_d, which suggest that these anions are controlling the $K_d$of Uat this site. Although, NO_3^- has positive correlation, it has insignificant effect on U K_d due to its very low concentration in groundwater. In the present study, groundwater pH was found to be alkaline (pH 7.3-8.9) innature which favors the development of negative charge on soil surface and in this condition,with the presence of carbonate/bicarbonate in aqueous media, U is reported to form negativelychargedspeciessuchas($(UO_2)_2(OH)_3CO_3^-$,$UO_2(CO_3)_2^{2-}$,$UO_2(CO_3)_3^{4-}$)[2]whichexplainstheobservedlow$K_d$valuesforUatstudysite.

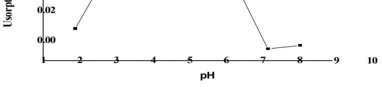

Figure1.Effect of solution pH onUsorptiononsoil

Table1CorrelationbetweenanionsingroundwaterandUK_d.

	F^-	Cl^-	NO_3^-	SO_4^{2-}	HCO_3^-	K_d
F-	1.0					
Cl-	0.0	1.0				
NO_3^-	-0.2	0.0	1.0			
SO_4^{2-}	0.0	1.0	0.0	1.0		
HCO_3^-	0.3	-0.3	-0.2	-0.3	1.0	
K_d	-0.4	0.3	0.7	0.2	-0.6	1.0

References

[1] S.Maity,S.Mishra,andG.G. Pandit.JRadioanalNuclChem295 (2013) 1581–1588.
[2] T.Watanabe and Y.Ikeda.EnergyProcedia,39(2013)81-95.

Investigation on the parameters influencing the activity estimation of the natural radionuclides in the environmental samples

M. Margret[1,2,§], S.Chandrasekaran[1,2], C.V.Srinivas[1,2] and B.Venkatraman[2]

[1] *Environmental Assessment Division, Safety, Quality and Resource Management Group*
[2] *Indira Gandhi Centre for Atomic Research, Kalpakkam-603102, Tamil Nadu, India*
[§] Email: mag@igcar.gov.in

Gamma-ray spectrometry yields excellent results for the samples of identical density enclosed within a specified geometry[1]. In a practical scenario, there may be a significant variation in density within a single sampling unit. In addition, different geometry must be accounted depending on the state of the sample to be studied, particularly in the case of low active samples. This work employs Monte Carlo (MC) modelling to look at the impact of density and geometry variations on the measured radionuclide activity.

The MC code is used to model the entire configurations (detector and sample) by considering the parameters as provided by the manufacturer with suitable modifications. The effect of densities is investigated by the simulated matrices with densities ranging from 1.31gm/cc to 1.51 gm/cc having same geometry. Simulations are also been carried out for different geometry(250ml, 500ml and 1000ml) with a constant density. The selected photo peaks of the gamma-ray energies are: 1764 keV from ^{214}Bi of the ^{238}U series, 2614 keV from ^{208}Tl for ^{232}Th and 1461 keV for ^{40}K. As shown in Fig 1, although the initial variation in AC is less than 0.3% at low density for all energies, it increases as much as up to 3% for higher densities. In fig 2, the matrices contained in the 250ml geometry display high AC values for all the radionuclides and vice versa; consequently, an appropriate correction[2] ought to be considered when computing AC for other geometries.

The results conclude that the density and geometry variations have an effect on the activity concentration estimations in the environmental radioactivity analysis.

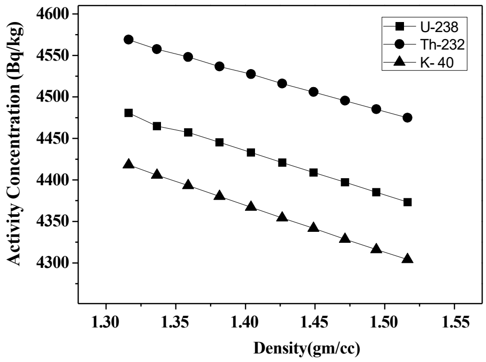

Fig 1. Variation of activity with

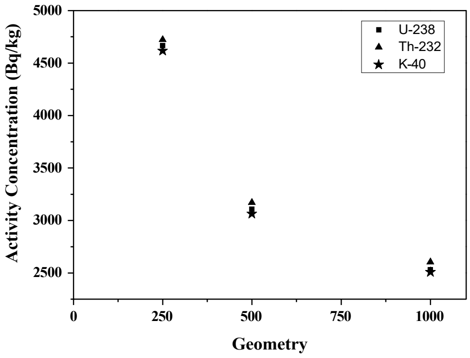

Fig 2. Variation of activity with

References:
1. G. Gilmore, Practical gamma-ray spectroscopy: John Wiley & Sons, 2011.
2. T. Boshkova and L. Minev, Applied Radiation Isotopes, 54 (2001), 777.

Distribution of Indoor radon, thoron and progeny levels at three coastal areas of Tamil Nadu, India

R.T. Asher Nebin[1], N. Chitra[2], S.N. Bramha[2], K S Briteena[2], S. Chandrasekaran[2], A. Yardily[1], S. Godwin Wesley[1], C.V. Srinivas[2] and B. Venkatraman[2]

[1]*Department of Chemistry, Scott Christian College, Nagercoil, Tamil Nādu, India*
[2]*Indira Gandhi Center for Atomic Research, Kalpakkam, Tamil Nādu, India*
Corresponding author email:snbramha@gmail.com

Radon (^{222}Rn) and Thoron (^{220}Rn), the radioactive gases from ^{238}U and ^{232}Th series, are the major cause for indoor radiation exposure. More than 52% of the total background radiation is considered to be due to inhalation of indoor ^{222} Rn Progeny (K.K. Narayan, D. N. Krishnan, et al., 1991). In this study, SSNTD-based (LR-115 Type II) single-entry pin-hole dosimeters and progeny badges: Direct Thoron Progeny Sensor (DTPS) and Direct Radon Progeny Sensor (DRPS) designed and developed by BARC are used for the passive measurement of indoor radon and thoron gas and progeny concentration in houses of SE coastal part of India. The study region includes three areas differing in their ambient natural gamma radiation levels viz., Kanyakumari (KNK): a high natural background radiation area (HNBRA), Kalpakkam (KPM): a medium natural background radiation area (MNBRA), and Parangipettai (PRP) a low natural background radiation area (LNBRA). This study aims to quantify the distribution of indoor radon, Thoron, and progeny concentrations in these three different areas.

The radon, thoron, and progeny concentration distribution in the three areas for the two phases are compared and depicted in fig. 1&2. Overall, the measured concentrations in Phase-1 were higher than in Phase-2 due to the seasonal effect. Phase-1 and Phase-2 are predominantly winter and summer, respectively. Concentrations in winter are higher due to closed conditions leading to poor ventilation. Area-wise comparison of concentration distribution shows that the radon, thoron, and progeny concentrations are lower for PRP than KPM and KNK. KNK and KPM show similar distribution pattern except for thoron concentration, where KNK exceeds KPM. This is because of the monazite deposits on the KNK coast. Based on radon and Thoron monitoring the radiation background in the areas cannot be quantified and compared. Indoor concentrations are largely governed by the building materials and ventilation conditions which act as the intervening factors Also, previous surveys provide strong evidence to conclude that the inhalation doses due to radon and Thoron gas and their decay products in the HBRAs are in the same range as observed in the NBRAs in India (Rosaline Mishra et.al. 2015).

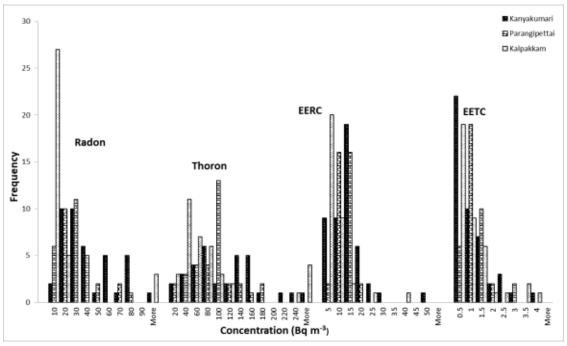

Fig. 1: Frequency distribution of radon/thoron and progeny (Phase-1)

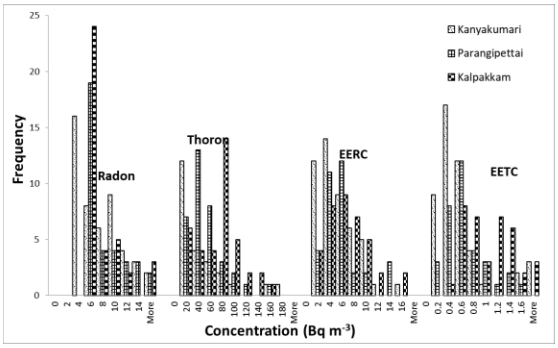

Fig. 2: Frequency distribution of radon/thoron and progeny (Phase-2)

References:

[1] K.K. Narayan, et al., Population exposures to Ionizing radiation in India; (1991), SRP (K) - BR -3.

[2] Mishra, R., et al., Journal of Environmental Radioactivity (2015), 147, 125-129.

Analysis of natural background gamma radiation levels in and around coastline districts of Tamil nadu, India

R. A. Takale[1], P.G. Shetty[1], M. Swarnkar[1], S. K. Sahu*[1,2], V. Pulhani[1,2]P.G. Shetty[1], M. Swarnkar[1], R. A. Takale[1], S. K. Sahu*[1,2], V. Pulhani[1,2]

[1]Environmental Monitoring and Assessment Division, Bhabha Atomic Research Centre, Trombay, Mumbai – 400085, India
[2]Homi Bhabha National Institute, Anushaktinagar, Mumbai – 400094, India
(Corresponding Author: Email: sksahu@barc.gov.in; Phone: +91-2225592375)

The coastline in the state of Tamil Nadu is the second largest coastline in India (1,076 km long) and is known as the coromandel coast. It is bounded by Utkal Plains in the north, Bay of Bengal in the east, Kaveri delta in the south and the Eastern Ghats in the West. There are 14 districts that share the coastline namely Thiruvallur, Chennai, Kancheepuram, Villupuram, Cuddalore, Mayildathurai, Nagapattinam, Tiruvarur, Thanjavur, Pudukottai, Ramanathapuram, Thoothukudi, Tirunelveli and Kanyakumari. In the aftermath of devastating tsunami, studies were undertaken to assess its impact on the environmental gamma radiation levels along the entire east coastal region of Tamil Nadu state.

An extensive environmental gamma radiation monitoring of fourteen coastal districts of Tamil Nadu state, was carried out using optimized Teflon embedded $CaSO_4$: Dy based environmental Thermo Luminescent Dosimeters (TLD). Ninety-three locations were identified and monitored on a quarterly basis. These quarterly dose values were converted into annual values and the analysis had been carried out. The district wise measured quarterly air dose rate values were converted into annual average air dose rates are presented in Table 1. Significant changes in gamma radiation dose rate due to seasonal variation were not observed in the present study. In general, the background gamma radiation levels at a given location are steady, typically within 20%. The external gamma radiation level ranges from 0.66 mGy/y at Mayildathurai to 1.51 mGy/y at Kanyakumari. It is important to note that tsunami waves removed huge quantities of surface deposits of monazite which reduces the mean activity level of thorium and uranium content to a very large extent (52% and 41%, respectively) in the beach sands of Tamil Nadu coast [1]. Earlier to tsunami predominantly at Kanyakumari the dose rate was 5.2 mGy/y [2] and now it is around 1.51 mGy/y. Overall annual average dose rate in coastline districts is 0.93 mGy/y while the Indian national background of Tamil Nadu state before tsunami was 0.96 mGy/y [2].

Name of District	Range (mGy/y)	Avg Air Dose-rate (mGy/y)
Thiruvallur	0.73 - 1.19	1.00
Chennai	0.79 - 1.14	0.92
Kancheepuram	0.73 - 0.83	0.78
Villupuram	0.74 - 1.01	0.89
Cuddalore	0.62 - 1.06	0.79
Mayildathurai	0.58 - 0.76	0.66
Nagpattinam	-	0.68
Thiruvarur	0.88 - 1.49	1.08
Thanjavur	0.58 - 0.86	0.76
Pudukottai	0.86 - 1.06	0.92
Ramanathapuram	0.70 - 1.07	0.90
Thootgukudi	0.75 -1.41	1.06
Thirunelveli	0.70 - 1.54	1.06
Kanyakumari	0.98 - 1.92	1.51
Average	**0.93 ± 0.22**	

Table 1: Range and Annual average gamma radiation levels in coastal districts of Tamil

References:

[1] KS Lakshmi, et.al., *Radiation Protection and Environment,* **42(1)** (2019), 22.

[2] Nambi, K.S.V., et.al., *Radiation Protection Dosimetry*, **28(1)** (1987), 31.

A decade (2011-2020) of Environmental monitoring of Tritium and its Committed Effective Dose assessment around Rawatbhata Rajasthan site

S. N. Tiwari[1,§] ,Rajpal Gill[1], A K Gocher[1], Tejpal Menaria[1], Mohit Sisodia[1], I V Saradhi[2] and A Vinodkumar[2]

[1]Environment Survey Laboratory, EMAD, BARC, Rawatbhata, Rajasthan 323307
[2]Environmnet Monitoring and Assessment Division, BARC, Trombay, Mumbai, 400085
[§]Email: sntiwari@npcil.co.in

Monitoring of anthropogenic tritium levels in the environment of Rawatbhata Rajasthan Site is carried out by Environmental Survey Laboratory up to 30 km radial distance to ensure that discharges and effective dose to public are within permissible limits due to operation of five pressurized heavy water reactors 220 MWe capacity.Released tritium from five operating NPP units (mostly in the form of HTO) are discharged to the atmospheric environment through 100m tall stacks and to aquatic environment to fresh water lake of Rana Pratap Sagar (RPS) as per technical specifications approved by AERB. Once released to the environment, undergoes dilution and diffusion and can give inhalation and ingestion dose to adult and infant population, via different pathways. In this study tritium concentration in environment (air and surface water) at various radial zones (1.6 km and beyond up to 30 km) and associated internal dose to representative person is presented for the period 2011-2020 during different seasons. Air sampling was carried out by moisture condensation method. 10 mL of collected air moisture and water samples are mixed with 10mL of DIN based counting cocktail in 20mL plastic vail and counted for 100min. in ultra-low-level liquid scintillation analyser (Perkin Elmer make. Minimum detectable level achieved is 0.1 Bq/m^3 and 5 Bq/L in air and water samples respectively.

Table: 1: H-3 concentration and CED at various radial zones

Rad. Zone	H-3 in Air (Bq/m3)				H-3 in Water (Bq/L)				CED to Public (µSv)			
	Range	Mean	SD	Median	Range	Mean	SD	Median	Range	Avg.	SD	Median
1.6	0.7-5.8	2.9	±1.5	2.3	6.0-25.0	12.2	±6.3	10.0	0.4-2.3	1.3	±0.6	1.1
1.6-5	0.3-2.1	1.0	±0.5	0.9	6.0-20.0	11.0	±6.3	9.0	0.2-1.0	0.6	±0.3	0.6
5-10	0.1-0.6	0.3	±0.2	0.2	6.0-17.0	10.0	±3.8	9.0	0.2-0.5	0.3	±0.1	0.3
10-15	0.1-0.5	0.2	±0.1	0.2	5.0-14.0	7.4	±2.3	6.0	0.2-0.5	0.2	±0.1	0.2
15-30	0.1-0.5	0.2	±0.1	0.1	5.0-11.0	6.3	±1.9	5.0	0.1-0.4	0.2	±0.1	0.2

It was observed that average tritium discharged to stack and aquatic body during the study period is 6.4 % and 0.8% respectively of the technical specification limits. Correlation study between tritium discharged through tall stack and its concentration at 1.6 km fence post was very good positively correlated (R^2=1.0). However, no such correlation observed between tritium discharged to RPS lake and its concentration at 1.6 km downstream of RPS lake. Maximum CED due to inhalation and ingestion of tritium at 1.6 km during the study period is 2.3 µSv with median value of 1.1 µSv which is much less than dose limit of 1mSv to representative person at this site.

References:

[1] Kamath SS and P M Ravi et.al., *Radiation Protection and Environment*, **Volume 41(1), Page 16**.

[2] Safety Guide No. AERB/NF/SG/S-5, Methodologies for environmental radiation assessment

Estimation of Atomic Concentration Ratio (^{137}Cs/K) of Cesium-137 and Potassium in Soil around Kaiga

Sanyam Jain[1§], R.M. Joshi[1], M.S.Vishnu[1], I.V. Saradhi[2]
[1]*Environmental Survey Laboratory, EMAD,BARC, Kaiga, 581400,*
[2]*Environmental Monitoring and Assessment Division, BARC, Mumbai, 400085*
[§]*Corresponding Author Email:* sanyam@barc.gov.in

The study presents the atomic concentration ratio [N(^{137}Cs)/N(K)] of^{137}Cs and total K in soils around the Kaiga site.Soil samples were collected from various locationsinthesurroundings of the Kaiga environment. The samples were processed and analyzed as per standard procedures [1]. The activity concentration of ^{137}Cs (i.e. A(^{137}Cs)) and ^{40}K(i.e. A(^{40}K)) in soil samples was determined using HPGe detector. ^{40}K, whichis aprimordial and naturally occurring radionuclide, having a long half-life of 1.28 billion years. The main source of ^{137}Cs in the environment isfallout that brings this radionuclide from the upper partsof the atmosphere to the ground. Fixation of ^{137}Cs in soilis known to be generally strong and most of it remains close tothe surface over a long time period [2]. Due to similar electronic structures, K and Cs havesimilar chemical propertiesand at insufficient concentrationsof K in soil, plants tend to take up chemically similarelements, including ^{137}Cs. Therefore, in assessing the hazard due to thepresence of ^{137}Cs in soil, it is desirable to not onlyquantify activity concentrations but to also determine the ratio of theatomic concentrations of ^{137}Cs and total K. The ratio (R) can be calculatedas[3],

$$R = \frac{N(Cs^{137})}{N(K)} = 2.82 \times 10^{-12} \frac{A(Cs^{137})}{A(K^{40})} \tag{1}$$

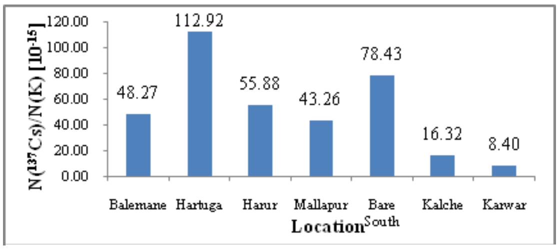

Fig.1 Atomic concentration ratio (R) of ^{137}Cs and K at various

The results of the ratio (R)around the Kaiga site areplotted in Fig.1. The ratio (R)was found to belowest for the Karwar location, which is a consequence of relatively high A(40K) and low spectrometry, the mean A(40K)in soil at Karwarlocation was observed to behighest (466±1.6 Bq.kg-1d.w.), whereas, it was found to be lowest for the Hartuga location (98±1.8 Bq.kg-1d.w.). The spatio-temporal variation in mean A(137Cs)was found to be varying from 1.4–4.7 (Bq.kg-1 d.w.) during the study period of 2015 to 2021. The mean A(137Cs) was observed to be higher in soil at Bare South (4.7±3.4 Bq.kg-1d.w.) and Harur (4.1±2.2 Bq.kg-1 d.w.) as compared to soil at Hartuga (3.9±2.7 Bq.kg-1d.w.) location. By looking only at the data, one couldconclude that soils at Bare South and Harur locations areless favorable concerning the plant uptake of137Cs,as compared to the Hartuga location. However, the data in Fig.1, indicates that the potential of137Cs entering into the food chain via uptake by plants for soil at Hartuga location is greater as compared to that ofBare South and Harur locations.Moreover, uptake of 137Cs by plantswill also depend upon thephysico-chemical properties of soil and the plant type. It is concluded that the ratio (R) is highest for soil atHartuga location and lowest for the Karwar location. The study will serve asa reference in case of accidentalradioactivity releases in the Kaiga environment.

References:

[1] A G Hegde et al, ERL Procedure Manual, HPD, BARC, 1998.
[2]Vosniakos F. K, Rad. Tran. in en.andfood. Berlin,Heidelberg: Springer-Verlag, 2012.
[3] Sostaric M et al, Archives of Industrial Hygiene and Toxicology, 72 (2021), 15-22.

Distribution study of Radium-226, Polonium-210 and Potassium-40 along with geochemical parameters in water samples of Chittorgarh, Rajasthan

Tejpal Menaria[1], D.S. Rathore[2], S.N. Tiwari[1], I.V. Saradhi[3], A. Vinod Kumar[3]

1. *Environmental Survey Laboratory, Rawatbhata, EMAD, BARC Mumbai-400085.*
2. *Mohan Lal Sukhadiya University Udaipur, Rajasthan 31300*
3. *Environmental Monitoring And Assessment Division, BARC, Mumbai-400085*

(Corresponding author e-mail: tejmenaria76@gmail.com)

Decay products of the ^{238}U series, ^{226}Ra and ^{210}Po are primarily alpha emitters while ^{40}K, a beta gamma emitter were analyzed and studied in well, hand pump, borewell, and surface water samples collected from study region. ^{210}Po was analyzed by auto deposition on a metal disc in a mild acidic medium using ascorbic acid under heating conditions (chemical recovery estimated byg ^{208}Po as tracer) and counted in the alpha counter (PLA make, efficiency, 21%). ^{226}Ra was chemically separated in 1:4 H_2SO_4 acid medium and EDTA at pH condition (4-4.4) by glacial acidic acid to co-precipitate $Ba(Ra)SO_4$ (yield was estimated using ^{138}Ba as carrier and simultaneously blank sample of ^{226}Ra as tracer) and was estimated as per standard procedure using Liquid Scintillation Analyzer [1]. Stable Potassium was estimated using flame photometry and using relation that 1 ppm of stable potassium contains 29.75 mBq/L of ^{40}K, activity concentration of K-40 in various samples were estimated. Various Geochemical parameters were measured using multi parameter analyzer. Hardness was determined by the EDTA complexometric method while alkalinity was evaluated by the H_2SO_4 titration method.

Concentrations of ^{226}Ra, ^{210}Po and ^{40}K in the water sample ranged from 1.0-12.6, 0.5-5.4 and 1.0-28.6 mBqL^{-1} while mean concentrations were 4.2±2.4, 2.1±1.0, and 8.4±4.8 mBqL^{-1}, respectively which are well below their recommended guideline values in drinking water. Single factor ANOVA analysis (α=0.05) for ^{226}Ra, ^{210}Po and ^{40}K concentration carried out on data (Table-1) which indicated significant variation of ^{226}Ra and ^{210}Po ($F_{c(critical)} < F_{s(statistical)}$) but insignificant variation for ^{40}K (F_c (2.83)>F_s (2.04)) in various water sources studied. The committed effective doses for adults from ^{226}Ra, ^{210}Po, and ^{40}K by ingestion are1.6, 0.7 and 0.07 µSvy^{-1}, respectively which are less than the prescribed individual limit of 100 µSvy^{-1}. Concentration of pH, conductivity, hardness, alkalinity total dissolved solid, chloride and fluoride ranged from 7.1-8.9, 226.0-2617.0 µS/cm, 135.0-935.0, 178.0-1272.0, 125.0-1384.0, 14.0-690.0 and 0.1-2.0 ppm respectively. These values are within BIS guideline values. No significant correlation between activity concentration of ^{226}Ra, ^{210}Po and ^{40}K and geochemical parameters was observed in the water samples in study region. The consumption of drinking water does not pose any unacceptable health effects on the population of this region w.r.t. the parameters studied.

Table –1: Single factor ANOVA for ^{226}Ra, ^{210}Po and ^{40}K concentration in different water sources

Water sources	N	**Mean**			**Std Dev.**			**Std Err**			**Variance**		
Radionuclides		^{226}Ra	^{210}Po	^{40}K	^{226}Ra	^{210}Po	^{40}K	^{226}Ra	^{210}Po	^{40}K	^{226}Ra	^{210}Po	^{40}K
Surface water	11	2.5	1.6	5.2	1.4	0.8	3.0	0.4	0.2	0.9	2.0	0.7	9.2
Hand pump	16	4.9	1.9	11.0	3.1	1.4	7.7	0.8	0.3	1.9	9.7	1.9	59.8
Well water	6	3.0	1.8	8.8	2.6	0.9	3.1	1.1	0.4	1.3	6.8	0.9	9.5
Bore well water	12	5.6	2.9	8.1	3.3	1.3	6.3	0.9	0.4	1.8	10.6	1.6	40.1
Validation	**Df**	**SS**			**MS**			**F stat**			**P value**		
Between group	3	72.0	12.4	221.0	24.0	4.1	73.7	3.11	2.91	2.04	0.04	0.12	0.12
Within group	41	316.7	58.2	1478	7.7	1.4	36.0				$F_{Critical}$(α=0.05) =2.83		
Total	44	388.7	70.6	1699									

References:

1. ERL procedure manual, 1998.

Evaluation of site-specific dry deposition velocity using ^{7}Be at Kakrapar Site, Gujarat

Shilpa Jain[1*], S.S. Wagh[1], A.K.Patra[1], I. V. Saradhi[2], A. Vinod Kumar[2]
*[1]ESL, Kakrapar Gujarat site-394651, [2]Environmental Monitoring and Assessment Division, BARC, Mumbai-400085(*Email ID: shilpajain@npcil.co.in)*

^{7}Be is a natural radionuclide of cosmogenic origin. It is produced in the atmosphere by spallation when cosmic rays hit nitrogen and oxygen atoms. Several studies show that ^{7}Be is one of the most important environmental radionuclide and can be used as a tracer of environmental processes such as cloud scavenging and precipitation or as a tracer for a transport and residence time of aerosols in the atmosphere [1]. This paper presents the results of studies carried out at Kakrapar Gujarat site during the period 2020-22 on the estimation of site-specific dry deposition velocities based on the concentrations of ^{7}Be in air and air deposits.

Air particulate samples were collected on Glass fibre filter paper using high volume sampler (1.2 m^{3} min^{-1}). Samples for dry deposition study were collected on polyethylene sheet (coated with grease, 1 m^{2} area) placed in a steel tray located on roof top of the laboratory. Samples were collected during the non-rainy season and measured in 100% RE p-type co-axial HPGe detector corresponding to the peak of 477.6 keV for ^{7}Be. Efficiency and energy calibration of the detector was carried out using certified reference material from IAEA. The deposited ^{7}Be activity (C, Bq) is estimated using the gamma spectrometry system. The dry deposition rate (activity deposited per unit area per day) is calculated using following equation:

$$(DR)_{dry} = C/(A \times D) \qquad (1)$$

where $(DR)_{dry}$ is the dry deposition rate of the activity (Bq m^{-2} d^{-1}), C is the total deposited activity due to dry deposition (Bq) for a period of D days and A is the area of exposure (m^{2}). The dry deposition velocity (m d^{-1}) is calculated using following equation:

$$V_d = (DR)_{dry}/C_a \qquad (2)$$

where C_a is the concentration of ^{7}Be in air (Bq m^{-3}).

Dry deposition rate and dry deposition velocity is calculated during the year 2020-22 is shown in Table 1. The overall mean site specific deposition rate during the year 2020-22 is observed to be 156 mBq m^{-2} d^{-1} which is comparable to reported value ranged 30.3-1090 mBq m^{-2} d^{-1} at Rajasthan Site [2] and 17-3556 mBq m^{-2} d^{-1} at Narora Site [1]. Dry Deposition Velocity at Kakrapar Gujarat site is observed to be in the range 1-105 m d^{-1} (Mean: 15 m d^{-1}) which is comparable to 25.9±10.4 at Kaiga Site [3], 136.4±25.3 m d^{-1} at Narora site [1]. Site specific deposition rate and deposition velocity is very useful for radiological impact assessment studies.

Table 1 : Dry deposition rate and dry deposition velocity at Kakrapar site using ^{7}Be

Year	Dry Deposition Rate (mBq m^{-2} d^{-1})	Dry Deposition Velocity			
		Range (m s^{-1})		Mean	
				m s^{-1}	m d^{-1}
2020	8-203	1.3E-05	4.1E-04	2.1E-04	18.5
2021	12 -588	1.2E-05	1.2E-03	3.9E-04	33.4
2022	101-1200	9.1E-05	1.8E-03	2.9E-04	24.8

References

[1] Gautam et. al., Radiation Protection Dosimetry, 198(16), (2022), 1258.
[2] Jain et al., 6th Asian and Oceanic Congress for Radiation Protection (AOCRP6), Abstract-61536, (2023), 349.
[3] James et. al., Radiation Protection Dosimetry, 141(3), (2010), 248.

Retention of Radionuclides on Vindhyan Clays

Aishwarya Soumitra Kar[1,2,§],Priyanka Balan[3], M. K. Das[1], S. Jeyakumarand R. K. Bajpai[2,4]

[1]*Radioanalytical Chemistry Division,*[4]*Technology Development Division,Bhabha Atomic Research Centre,Mumbai, India*
[2]*Homi Bhabha National Institute, Mumbai, India*
[3]*KJ Somaiya College, Mumbai, India*
[§] Email: aishj@barc.gov.in

Argillaceous clays are being considered as one of the suitable clay host rock for deep geological repository for disposal of nuclear high level waste worldwide. In Indian context, Vindhya argilliteis under evaluation for clay rock based repository.In the present study, the characterization of clay and sorption studies of Cs(I) and Am(III) has been carried out. The Vindhyan argillite have been characterized for mineralogical composition, elemental composition, morphology, functional groups and dissolved ions in addition to determination of ion exchange capacity (21 ± 1 mmoles/100g) and surface area (33 ± 2 m^2/g). Sorption equilibrium of Cs(I) and Am(III) was attained within ½ hour.The pH variation studies demonstrated that Cs(I) sorption was almost constant while that of Am(III) increased with pH (Fig. 1).Cs(I) sorption decreased with increase in ionic strength (pH 2-8) thereby confirming ion exchange mechanism of Cs(I) sorption (Fig. 2). However, the decrease was not as pronounced as observed in the case of typical ion exchange mechanism at lower Cs concentration (Fig 2(a)). Cs(I) adsorption isotherm studies showed two plateaus which in turn signifies Cs sorption via two kind of ion exchange sites (Fig. 3).Am(III) sorption decreased with increase in ionic strength in the lower pH range (pH 2, 4) while Am(III) sorption remains invariant in the higher pH range (pH 6, 8) (Fig. 4). This observation confirmed that ion exchange is dominant at lower pH range while surface complexation process dominates at higher pH for Am(III).Owing to higher sorption capacity, the Vindhyan argillite is suitable to retard the migration of radionuclides. However, further investigations such as Am(III) sorption isotherm, modeling ofsorption profiles of Cs(I) and Am(III) on Vindhyanargillite are in progress to get the detailed insight about the retention behaviour of these clays.

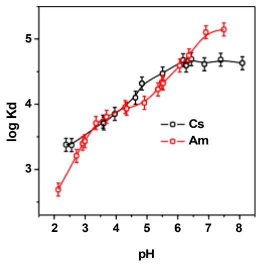

Fig. 1:Sorption of Cs (4.2E-10 M) & Am (6.7E-9 M) on Vindhyan Clay (2 g/L) at varying pH; Ionic strength = 0.1 M.

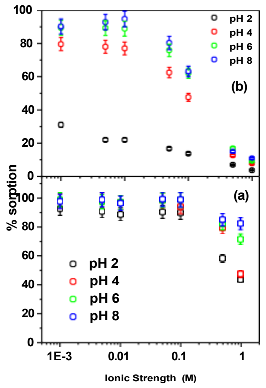

Fig. 2:Sorption of Cs (a. 4.2E-10M; b. 1E-5M) on Vindhyan Clay (2 g/L) at varying ionic strength.

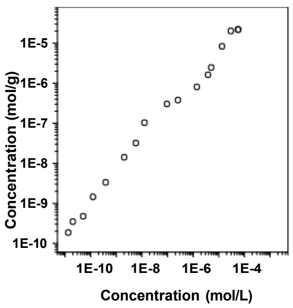

Fig. 3:Cs adsorption isotherm on Vindhyan Clay (2 g/L) at pH 5.2 ±0.2; Ionic strength =0.1 M

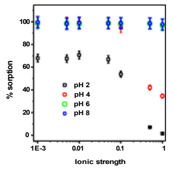

Fig. 4:Sorption of Am (6.7E-9M) on Vindhyan Clay (2 g/L) at varying ionic strength.

Role of Organic Matter on Sorption of U in Organic Rich Soil

Sukanta Maity§, C.B. Dusane, P. Sandeep, Suchismita Mishra, Dilip Kumar Chaudhary,
Anilkumar S. Pillai and A. Vinod Kumar
Environmental Monitoring and Assessment Division, Health Safety and Environment Group,
Bhabha Atomic Research Centre, Mumbai-400085, India
§Email: sukanta@barc.gov.in

Uranium (U) interacts with all components of the soil matrix such as clay minerals, aluminium and iron oxides, organic matter and micro-organisms. Organic matter both in soluble and insoluble form in soil play important role in sorption of uranium and its mobility. A study was initiated to understand the change in sorption behaviour of U with soil organic matter content and type. Soil samples (10 Nos.) were collected from deep forest area (having significant concentration of organic matter) and processed (dried, grinded, sieved and homogenized). Organic matter was estimated in soil samples through loss on ignition method. Sorption studies of U was carried out in the collected soil samples in three experimental sets. In Set 1, uranium sorption was conducted in collected soil sample where both soluble and insoluble organic matter were present. In Set 2, collected samples were thoroughly washed with distilled water to remove soluble organic matter. After washing the soil samples U sorption study was carried out where soluble organic matter was absent. In set 3, collected soil samples were heated at 450^0C to remove both soluble and insoluble organic matter. Later U sorption study was carried out. All the sorption studies were carried out using distilled water spiked with known U concentration in triplicates. U was analysed using LED Fluorimeter LF-2 (Quantalase). As mobility of uranium can be expressed in terms of distribution coefficient (K_d), these were calculated and are represented in figure 1.

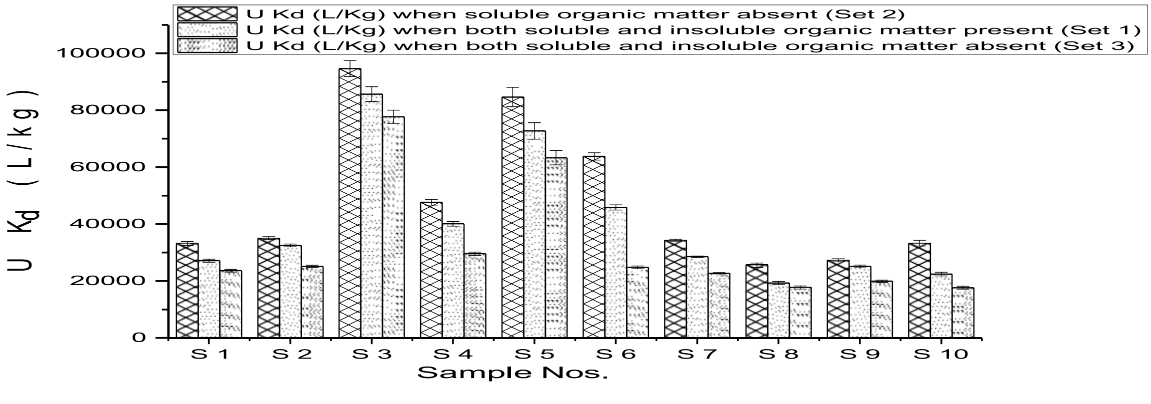

Figure 1: U K_d variation w.r.t. organic matter of soil.

Highest U K_d values were observed in all the studied samples where soluble organic matter was absent (Set 2), whereas lowest U K_d values were observed in all the studied samples (Set 3) where both soluble and insoluble organic matter were absent. Intermediate U K_d values were observed in all the studied samples where both soluble and insoluble organic matter were present. From this study it may be said soluble organic matter is helping uranium to mobilize in the environment whereas insoluble organic matter is helping uranium to sorb in the solid matrix which was compared with earlier published literature [1]. However, more detailed experimental study is required to get finer conclusion.

References:

1. P. Crançon and J. van der Lee, *Radiochim. Acta,* **91**, 673 (2003)

Study of Degree of Disequilibrium in deeper levels of Narwapahar Uranium mine, Singhbhum Shear Zone, Jharkhand, India.

Diwakar Gaur [1,§], *M.K.Sandilya*[2], *H.B. Shrivastava*[3].

[1]Uranium Corporation of India Ltd., Jaduguda Mines, East Singhbhum, Jharkhand- 832102.
[2]Atomic Minerals Directorate for Exploration and Research, Western Region, Jaipur.
[3]Atomic Minerals Directorate for Exploration and Research, Eastern Region, Jamshedpur
§ Email: diwakargaur@uraniumcorp.in

Abstract

Total reserve estimations, grade, width, leaching and host minerals associated, are some of the vital parameters for opening any uranium deposit for commercial mining and milling. Apart from these, there are other investigations necessary to make a deposit commercially mineable and that include study of secular equilibrium status of the uranium deposit. The presence of disequilibrium can affect the interpretation of gamma measurements and subsequent % eU_3O_8 estimates that result from gamma probes which in turn affects whole uranium production cycle. Apart from above, this study also becomes very much required during concurrent mining activities when doing day to day gamma ray log measurements for the estimation of % eU3O8 by the physicists of UCIL at different depths/levels/blast faces/secondary exploration of mine. Hence radioactive equilibrium-disequilibrium in any uranium deposit has a significant economic impact on uranium mining and its concentrate production. Looking the above concern, an intensive study has been performed on current productive levels of Narwapahar Uranium mine at a depth of 100 meter level (ML) to 275 meter level (ML) from surface level. Linear regression of U_3O_8 (Chemical) and Ra (eU_3O_8) data indicates that the equilibrium condition of the ore at all productive levels of mines is maintained. This supports the earlier studies which had been done on very limited number of samples during early stages of deposit exploration. This study indicates that the uranium deposit at Narwapahar mine represents a closed system with respect to mobilization of different elements of U-series. The results imply that the gamma ray probes in all applications will be suitable for exploring ore zones in underground as well as in all exploratory drills for quantifying mineral concentration.

Keywords: Narwapahar Uranium Mine, Equilibrium-disequilibrium, Gamma Ray Spectrometry, Jharkhand, Singhbhum Shear Zone (SSZ).

Separation methodology for bulk elemental impurities in U rich geological matrix using tri(2-ethylhexyl) phosphate

Aditi Singh[1], Sandeep P.[2], Suchismita Mishra[2*], Sukanta Maity[2], Anilkumar S. Pillai[2] and A. Vinod Kumar[2]
[1]*Christ University, Life-science department, Bengaluru, Karnataka*
[2]*Environmental Monitoring and Assessment Division, Bhabha Atomic Research Centre, Mumbai-400085, India*
*Email: suchim@barc.gov.in

Minerals of Uranium are complex in nature accompanied with many other bulk impurities like metals, anions, organic carbon etc. The accurate estimation of U and other elemental impurities concentration requires separation of U from its bulk matrix. Solvent extraction is a proven and versatile technique that was being used for separating U. Among different organic solvents, the phosphorous based functional groups received the most attention for the separation of uranium (VI) from other impurities. In the present study tri(2-ethylhexyl) phosphate (TEHP, >97% from Sigma Aldrich) was used for the separation of U from U-rich geological samples for bulk impurity analysis. For method optimization, aqueous feed (sample solution) molarity and organic-aqueous contact time were varied to find the most suitable condition for efficient separation and quantification of U and other elemental impurities. Mixed elemental standard solutions were prepared in 2M, 4M, 6M and 8M HNO_3 medium, whereas the organic phase was prepared by mixing the equal volumes of TEHP and n-heptane. Sample to solvent ratio was maintained at 1:2.5 and solvent extraction was carried out for 30 minutes using separator funnel shaker. The procedure was repeated twice to completely separate U from the aqueous feed solution. Each experiment was carried out in triplicate to statistically evaluate the results obtained at different molarities. In aqueous phase, elemental impurities (10 nos.) were analysed using ICP-AES (HORIBA Jobin Yvon, ULTIMA 2 model) and the estimated recovery (%) for bulk impurities are presented in Fig. 1 (a). U in organic phase was back extracted using deionized water and analysed using LED fluorimetry. Results show that, 88-98% of U was recovered from aqueous feed with HNO_3 molarity ranging from 2M to 8M shown in Fig.1(b). Efficient separation of bulk impurities from U (>95%) can be achieved at 4M nitric acid media. Further, U separation studies were carried out at different aqueous-organic contact time intervals (5, 15, and 30 minutes) and the results show that, even 5minute contact time is sufficient to separate the U from bulk impurities. The optimized methodology was applied on real U rich geological matrices for the separation of U from bulk matrix. Results show the optimized solvent extraction method is rapid and efficient in separating U from geological matrices.

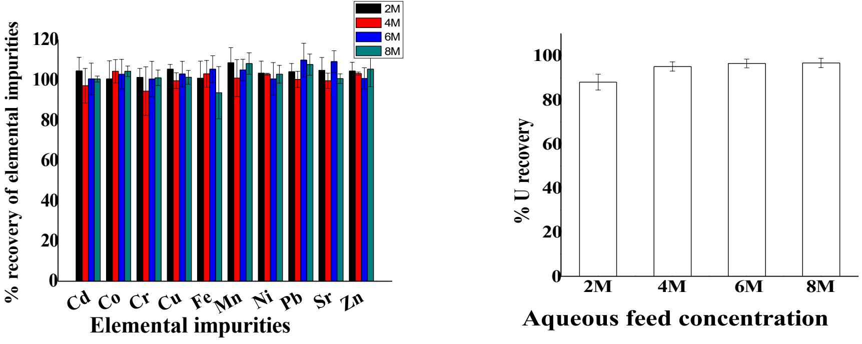

Figure 1. (a) Percentage recoveries of elemental impurities in aquous feed and (b) U recovery after solvent extraction

Reference :

1. A. Kuchkin, V. Stebelkov, K. Zhizhin, Ch Lierse von Gostomski, Ch Kardinal, A.H.J. Tan, B.K. Pong, et al., Radioanal. Nucl. Chem. **315** (2018) 435.

Assessment of few heavy metals in vegetables from Mumbai market

Sugandhi Suresh[1,§], Harshali S. Suryavanshi[2], Mahesh Tiwari[1] and
Vandana A. Pulhani[1]

[1] *Environmental Monitoring and Assessment Division, B.A.R.C., India*
[2] *The Institute of Science, Mumbai, India*
[§] Email: sugandhi@barc.gov.in

Vegetables are indispensable to the human health, and in particular provide the essential nutrients to maintain normal physiological functions. The more usage of fertilizers and pesticides has resulted in heavy metal accumulation in vegetable gardens. Exposure to heavy metals by the consumption of contaminated vegetables and its toxicity is a major concern as it may cause kidney, cardiovascular, nervous, and bone diseases in humans [1], congenital disabilities, low birth weight of babies and premature births [2]. The present study aimed to evaluate the concentration of Mn, Fe, Cu, Ni and Zn in legumes (green peas, beans), leafy vegetable(cabbage, cauliflower, spinach), stem (potato, ginger, garlic, turmeric),climber (tomato, okra),root(beetroot) and assess the associated health risk on human health due to consumption of it. The vegetables were purchased from Vashi APMC market, which receive vegetables from farming locations in the vicinity of Navi Mumbai. The edible parts of vegetables were cut into small pieces, dried and ground to fine powder. The powdered sample was homogenized with cellulose powder, made into a pellet and analysed for metal ion concentration using EDXRF. From the observed metal ion concentration, the health risk parameters like Estimated Daily Intake (EDI), Target Hazard Quotient (THQ) & Hazard Index (HI) were computed using the following equations.

$\boxed{EDI = (C_m * D_i) / B_{w.}}$ $\boxed{THQ = EDI / RfD}$ $\boxed{HI = \sum_{n=1}^{i} THQ_n ; n = 1,2,3...n}$ Where,
C_m = Metal conc. (mg/kg); D_i = Daily intake (kg/d); B_w =70kg; RfD=Oral ref. dose (mg/kg/d)

Table.1: Health risk due to ingestion of vegetables

Metal	**Legume**		**Leafy**		**Stem**		**Climber**		**Root**	
	EDI	**THQ**	**EDI**	**THQ**	**EDI**	**THQ**	**EDI**	**THQ**	**EDI**	**THQ**
Mn	0.02	0.14	0.005	0.25	0.01	0.07	0.004	0.05	0.003	0.02
Fe	0.13	0.19	0.03	0.04	0.03	0.04	0.06	0.08	0.07	0.10
Cu	0.004	0.09	0.001	0.02	0.001	0.02	0.001	0.07	0.001	0.02
Ni	0.003	0.13	0.001	0.03	0.001	0.03	0.001	0.09	0.001	0.03
Zn	0.01	0.04	0.002	0.01	0.002	0.01	0.004	0.02	0.002	0.01
HI	0.6		0.4		0.2		0.3		0.2	

It is observed from Table.1, that the EDIs of vegetables are lower than the maximum tolerable daily intake(mg/d) of each metal (Mn:4.1;Fe:15;Cu:2.5;Ni:0.1;Zn:15)[3]. The THQ for Mn, Fe, Cu, Ni & Zn in vegetables are found to be less than unity indicating no serious potential health risk to humans due to consumption of it. This is further supported by the computed HI parameter. Thus, the present study affirms that the vegetables are safe to consume. However, to understand the impact due to anthropogenic activity, the field(s)/area(s) that are prone to it are to be identified, surveyed and analysed for heavy metal ion concentration.

References:

1. Anwar, S. et. al., Environ. Monit. Assess. 188 (2016).
2. Taylor, C. et. al., 122,322-328, Int. J. Obstet. Gy (2015).
3. A.M.Basha et. A1, 505-512 Toxicology Reports (2014).

Assessment of Carbon-14 in wheat samples grown-up in the vicinity of NPP Site Narora

Y. P. Gautam[1§],Deepak Kumar[1], A. K. Sharma[1], Vineet Kumar[1], J. Kumar[1], I. V. Saradhi[2]
[1] *Environmental Survey Laboratory, Narora Atomic Power Station, Narora*
[2]*EMAD, Bhabha Atomic Research Centre, Trombay, Mumbai 400 085*
[§]*Email: ypgautam@npcil.co.in*

^{14}C ($T_{1/2}$=5730 y) is a pure beta emitter (with E_{max}=156 keV), occurs naturally due to its cosmogenic origin and is also produced in nuclear reactors due to neutron activation of ^{14}N, ^{15}N, ^{17}O, ^{16}O and ^{13}C. The released^{14}C in the form of $^{14}CO_2$ is quickly assimilated by plants through photosynthesis[1]. In order to estimate the impact, if any, on the environment around NAPS site due to release of ^{14}C, wheat samples were collected up to 30km radial distance from the plant site during the harvest season from the field. Since wheat is major crop being consumed locally in north India.

In this study 30 wheat samples were collected covering up to a 30 km radial distance around NAPS site and 5 no.s of wheat collected from clean area i.e. around under construction NPP site at GHAVP, Haryana during year 2020-21. The samples were combusted by thermal oxidation using Pyrolyser Trio-6 system, The samples are subjected to controlled oxidation at high temperature (600-900 C) to convert the carbon to carbon dioxide. Separated CO_2 was collected as dry ice in cryo-cooler system maintained at -106 C followed by passing through the pre-weighed mixture of 10ml each of carbon trap (CO_2 absorbent) and Carbon count (Scintillation Solution). By post weighing the mixture, amount of CO_2 trapped was quantified and counting the mixture in LSC (Quantulus 1220C Perkin Elmer, USA). The ^{14}C specific activity (Bq/kg of C) of wheat samples were estimated using following equation.

$$A\left(\frac{Bq}{Kg}C\right) = \frac{(C_g - C_b)\times 44.01}{(60\times E\times C)\times 12} \quad - (1)$$

Where C_g, C_b(gross and background count per min.), E (fractional Counting Efficiency) and C (Wt. of CO_2 kg)

Table-1 shows the ^{14}C specific activity in the wheat samples around NAPS site and clean area. The geometric mean of ^{14}C specific activity in wheat samples ranged from 225 to 249 Bq/kg C.The levels obtained in the current study beyond 10 km are compared to the level obtained in the samples of clean area (GHAVP site, Haryana). TCurrent preliminary study suggests that the ^{14}C level in wheat samples of nearby areas of NAPS site is insignificant compared to natural levels

Table-1: ^{14}C specific activity in wheat samples around site

Distance (km) from site	^{14}C specific activity (Bq/kg of C)		
	Around NAPS site		Clean area GHAVP site
	Range	GM	
1.6-5.0	236-268	249	224-228
5.0-10.0	223-255	233	
10.0-15.0	223-230	226	
15.0-30.0	223-229	225	

This study has been carried out to establish the analytical methodology for estimation of ^{14}C specific activity wheat samples. The change in ^{14}C levels at nearby areas is observed to be insignificant compared to natural levels.

Reference: [1] W.F. Libby, (1945), Atmospheric helium three and radiocarbon from cosmic radiation, Physical Review, **69**, 671-672.

Surface Complexation of Selenium Oxyanions at the Goethite – Water Interface: Validation through Spectral Signature of interfacial Water

Snigdha Srabanee[1], Anisha Bandyopadhyay[1], Sumit Kumar[§1,2], J. A. Mondal[1,3]

[1]*Homi Bhabha National Institute, Mumbai* [2]*Radioanalytical Chemistry Division,* [3]*Radiation and Photochemistry Division, Bhabha Atomic Research Centre, Mumbai, India*
[§] *Email: sumitk@barc.gov.in*

Environmental speciation and migration of radionuclides are controlled by the interaction of radionuclides with various components of the aquatic system. Solid surfaces, especially iron oxides, have been observed controlling localization of migrating radionuclides along the transport route, away from the nuclear waste sites or enhancing their transport when present in the colloidal form [1]. Governing process such as sorption at the solid sorbents, is found responsive to varying chemical conditions of the aquatic environmental system and, therefore, a predictive/mechanistic approach is needed to explain the sorption process of radionuclides. In the present study, surface complexation modeling was carried out for sorption characteristics of selenium oxyanions, selenate and selenite, on goethite surface under varying pH and the modeling result was validated using spectral signatures produced by Vibrational Sum Frequency Generation (SFG) spectroscopy for interfacial water in the studied systems.

Goethite (FeOOH) was synthesized in a hydrothermal process using hydrolysis of $FeCl_3.6H_2O$ and characterized for particle size, morphology, crystalline phase, and PZC (Zeta potential measurement).Selenate and Selenite sorption on goethite was investigated in a batch sorption mode under varying metal ion concentration (10^{-6}– 10^{-5} M), pH (3 – 10) and ionic strength (0.01 – 0.1 M NaCl). Typical anion sorption profile was seen in all the sorption studies - quantitative sorption of adsorbate till pH 5, subsequent gradual decrease in surface retention to zero percentage sorption by pH 10. Relatively stronger sorption was observed for selenite under varying metal ion concentration and unlike selenate, there was no ionic strength effect on sorption. Potentiometric titration of goethite suspension was carried out and modeled using a single surface site to determine the protonation-deprotonation constant. Using these constants and under the diffuse layer formulation for interfacial double layer, selenite was found binding in bidentate mononuclear inner sphere (IS) binding on goethite surface. Selanate surface speciation was found following outer-sphere mode binding along with a small contribution of monodentate mononuclear IS binding. In view of discordant EXAFS results for these systems, interfacial water structure was delineated for these systems to validate the modeling result. Fig.1 clearly presents the stronger disruption of Hydrogen-bonded water structure (3000 – 3600 cm^{-1}) near the goethite surface with increasing selenite concentration attesting stronger sorption of sorbing ion. Detailed analysis of these observations will be presented during the symposium.

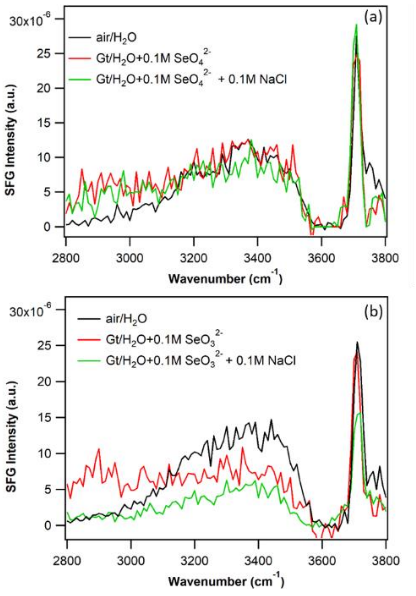

Fig. 1. SFG-intensity spectra in the OH stretch regions for the air/water, goethite/water + selenite and goethite/water + selenate interfaces.

References: [1] X. Zhang et. al., *J. Hazard. Mater.*, **424** (2022)127550.

Estimation of Natural Radioactivity in Soil Samples from Uranium Mining Zone of Sikar, Rajasthan, India.

Bhupesh Khyalia[1], Jyoti Yadav[1], Naresh Kumar[1], Balvinder Singh[1], Prikshit Gautam[2], Ranjeet Dalal[1§]

[1]*Centre of Radio Ecology & Department of Physics, Guru Jambheswar University of Science and Technology, Hisar, Haryana, India- 125001*
[2]*Department of Physics, Kirori mal college, Delhi University, Delhi, India - 110007*
[§] Email: ranjeet@gjust.org, bhupeshkhyalia11@gmail.com

Radionuclide‟s existence in the environment can have a hazardous impact on human health. Primordial radionuclides like uranium, thorium, and potassium lead to natural radioactivity in the soil. These radionuclides enter the body of human beings via ingestion or inhalation and long-term exposure to these radionuclides or to their progeny nuclei can cause serious health effects. AMD has discovered a significant amount of uranium deposits in the Sikar district of Rajasthan, India, and the mining activity may also begin there soon. Hence, the background radioactivity estimation in this region is of paramount importance. In the present study, we have estimated the presence of γ-emitting radio-nuclei in 47 soil samples collected from the above-mentioned region. Radioactivity in the soil is measured using Sodium Iodide NaI(Tl) scintillation detector gamma-ray spectroscopy techniques. The detector used is of the size of 2 × 2 inches with a multichannel analyser. The energy resolution of the detector is 7.1% at 662 KeV energy of ^{137}Cs. The concentration of ^{238}U, ^{232}Th, and ^{40}K radionuclides is estimated in soil samples. The spatial distribution map indicated only a few areas of high radioactivity as shown in figure 1. Radium equivalent activity, absorbed dose rate, age-dependent annual effective dose, and other hazard indices are also evaluated for the assessment of health risk to the public.

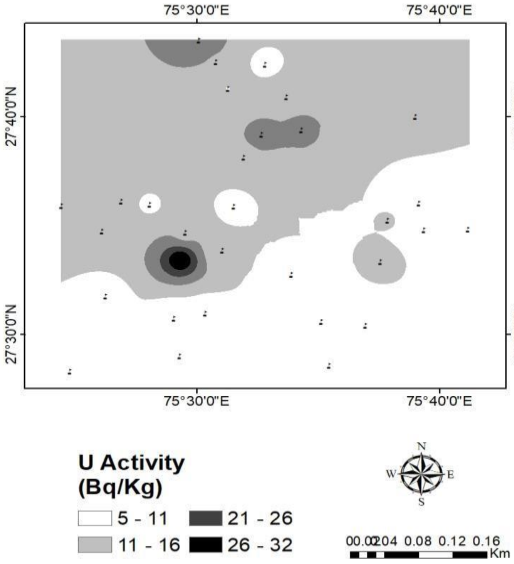

Fig. 1: Spatial distribution map of Uranium activity in the studied area.

Keywords: Radiation, uranium deposits, gamma-ray spectroscopy, hazard indices, radium equivalent activity.

Acknowledgments: The authors are thankful to University Grant Commission (UGC) for providing Junior Research Fellowship (JRF) which greatly supported our research work.

Soil to plant transfer factors (F_v) of ^{40}K for vegetables in the vicinity of IGCAR, Kalpakkam

R.U.K. Avaneesh[1], S. Chandrasekaran[2], S.N. Bramha[2], S.N. Panigrahi[2], C.V. Srinivas[2],
P.M. Ravi[1], N. Karunakara[1§]
[1]*Centre for Advanced Research in Environmental Radioactivity (CARER),*
Mangalore University, Mangalore-574199, India
[2] *RESG, Indira Gandhi Centre for Atomic Research, Kalpakkam-603102, India*
[§] Email: drkarunakara@gmail.com

The soil-to-plant transfer factors (F_v) values of radionuclides represent the extent of transfer of radionuclides from the soil to the plants. Studies on F_v are important to determine the potential exposure of human and animal populations to radioactive contaminants. The transfer factors can vary greatly depending on several factors such as the chemical form of the radionuclide in the soil, the type of plant, the soil conditions, and the growth stage of the plant [1]. While a large number of studies on F_v has been reported for temperate regions, such studies are very limited to tropical regions. In a previous study, we evaluated the F_v values for different plant species of the West Coast region of India [2]. Recently a detailed study on F_v values for different environmental transfer pathways involving soil, edible plants, grains, and grass systems has been initiated in the vicinity of Kalpakkam. In this paper, we present thethe soil-to-plant transfer factors for 04 Brinjal and 04 Bottle gourd samples, which were gathered from within the 0-15 km area of IGCAR, Kalpakkam.

The samples of different vegetables and soil in which they are grown were collected from the fields from different locations. The non-edible parts of the plant were discarded and the edible parts were processed, and the activity concentration of ^{40}K in the samples was determined using a 48% relative efficiency HPGe gamma spectrometer system. The$F_v$values were evaluated from the following equation:

$$F_v = \frac{Activity\ concentration\ of\ ^{40}K\ in\ vegetable(Bq\ kg^{-1}\ dry\ weight)}{Activity\ concentration\ of\ ^{40}K\ in\ soil(Bq\ kg^{-1}\ dry\ weight)}$$

The F_v thus evaluated varied in the range of 1.43-6.55 with a GM of 3.08. These values are similar to those reported by Rao et al. [2] for Kaiga region and the values tabulated in IAEA-TRS-472 [3].

Acknowledgement

The authors would like to thank Dr. B. Venkataraman, Director, Indira Gandhi Centre for Atomic Research (IGCAR), Kalpakkam for the suggestions and the IGCAR for funding the research programme.

References:

[1] Ehlken Sabine and K. Gerald, “Environmental processes affecting plant root uptake of radioactive trace elements and variability of transfer factor data: a review,” Journal of Environmental Radioactivity, (2002), **vol. 58,** pp. 97–112.

[2] Rao, Chetan., Prabhu, Ujwal., Karunakara, N., Somashekarappa, H.M., Nayak, P.D., & Ravi, P.M. Site-specific transfer factors of 226Ra, 228Ra, 40K, and 137Cs for vegetables in Kaiga region. *Radiation Protection and Environment*, (2008) **31(1-4)**, pp. 453-455.

[3] IAEA-TRS-472, “Handbook of parameter values for the prediction of radionuclide transfer in terrestrial and freshwater environments,” (2010), pp 69.

Dietary intake of natural and anthropogenic radionuclides from the plant based dietary items cultivated around under construction NPP (GHAVP) site at Gorakhpur, Haryana

Deepak Kumar[1] §, Y. P. Gautam[1], S. Kumar[1], A. K. Sharma[1], A. R. Tripathi[1], I. V. Saradhi[2]
[1] *Environmental Survey Laboratory, Narora Atomic Power Station, Narora*
[2]*EMAD, Bhabha Atomic Research Centre, Trombay, Mumbai 400 085*
§Email: deepak_kumar@npcil.co.in

Soil is formed by weathering of rocks and deposition of eroded matter. ^{232}Th, ^{235}U and ^{238}U decay series and singly occurring ^{40}K are major causes of natural radioactivity in soil. The man-made radionuclides like ^{137}Cs, ^{90}Sr etc. are released from nuclear fission and activation processes. Everyone is exposed to very small amounts of ^{137}Cs via ingestion (food and water) or inhalation and external exposure as a result of atmospheric fallout. These radioisotopes enter the human body primarily by ingestion of foods, while inhalation of these isotopes is limited (1). The study focused on the concentrations of ^{137}Cs, ^{40}K, ^{238}U and ^{232}Th in food crops cultivated in the fields around under construction GHAVP site, Haryana were determined. Different cereals, millets, pulses, vegetable and fruit samples were collected from various sampling locations within 30 km radial distances of the under construction nuclear power plant (GHAVP). Sample collection, preparation and analysis were carried using ERL protocol. Sealed containers with shed samples were stored for 30 days to reach secular equilibrium between ^{238}U its daughter products. Samples were analysed using coaxial P-type HPGe detector, 50% RE coupled to 16K MCA system. To evaluate ^{137}Cs, ^{40}K, ^{238}U and ^{232}Th using ^{137}Cs (661.66),^{40}K(1460 keV), ^{214}Bi(609 &1764 keV) and ^{228}Ac (338, & 911 keV) gamma peaks respectively. The efficiency calibration of the system was carried by using IAEA reference material. Table-1 gives the activity concentration of ^{137}Cs, ^{40}K, ^{238}U and ^{232}Th in the samples. The activity concentration is given for fresh weight/edible weight of food items. The activity concentration ^{40}K is high in all the samples compared to ^{238}U, ^{232}Th and ^{137}Cs. Pulses were observed to have highest ^{238}U activity concentration. Activity concentration of ^{238}U is higher as compared to ^{232}Th due densely farming activities and higher levels of Uranium in ground water compared to other parts of India. Intake of food material varies for different population groups mainly with age groups. Daily intake of radionuclide‟s was calculated based on mean value of activity concentration for different food categories and mean intake of the particular food category, the estimated mean daily intake of ^{226}Ra, ^{232}Th ,^{40}K and ^{137}Cs is 0.14, 0.03, 55.97 and 0.01 Bq per day respectively. Fig.-1 shows the intake of each radionuclide measured through the food categories studied.

Dietary items	Activity concentration (Bq/kg)							
	Cs-137		K-40		Th-232		U-238	
	Range	Mean	Range	Mean	Range	Mean	Range	Mean
Cereal	≤0.01 - 0.034	0.021	65.4 -148.4	114.7	0.06 - 0.29	0.04	0.06 - 0.42	0.19
Millet	0.022 - 0.043	0.032	227.9 -514.3	148.5	0.05 - 0.13	0.08	0.07 - 0.24	0.14
Pulses	0.025-0.054	0.032	320.4-389.6	159.5	0.09-0.44	0.25	1.32-2.89	2.51
Green Leafy	0.012 - 0.018	0.015	156.5 -198.2	75	0.08 - 0.13	0.07	0.13 - 0.19	0.16
Non leafy	≤0.02- 0.023	0.008	62.3 -245.7	96.9	≤0.01- 0.10	0.06	≤0.02 - 0.23	0.12
Roots & tuber	≤0.02	0.02	24.3 - 31.6	27.6	≤0.01	0.01	≤0.02 -0.04	0.03
Fruits	≤0.02	0.02	74.4-108.5	89.8	0.06-0.16	0.06	0.20-0.34	0.21

Table-1.Radionuclides in different dietary items.

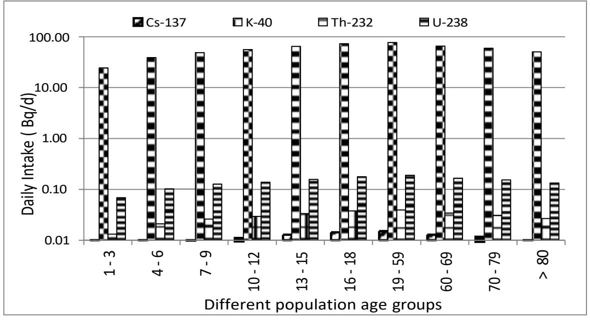

Fig.1 Intake of radionuclides for different age groups

This study will provide a baseline data of the natural radioactivity concentration in food items cultivate in the study area for further research.

References:

[1] UNSCEAR(2000), SOURCES AND EFFECTS OF IONIZING RADIATION, United Nations Scientific Committee on the effect of Atomic Radiation, United Nations, New York.

Gas chromatographic separation of Krypton from air mixtures using a long molecular sieve column

Krishnakumar P.[1§], Sureshkumar M. K.[1], Amit Bhatnagar[1], Kulkarni M. S.[1, 2]

[1]*Health Physics Division, Bhabha Atomic Research Centre, Mumbai, India*
[2]*Homi Bhabha National Institute (HBNI), Mumbai, India*
[§]*Email: krisp@barc.gov.in*

Introduction: Noble gas ^{85}Kr ($t_{1/2}$ = 10.76 year) is a fission product whose main source is the releases during reprocessing of nuclear fuel.Separation of Kr from air mixtures is a crucial requirement for sensitive measurement of ^{85}Kr concentrations in environmental air and also for preparation of ^{85}Kr enriched samples for industrial applications [1]. The usual procedure involves a multistep gas treatment using cryogenic methods to enrich Kr concentration in the mixture followed by a gas chromatographic separation of the individual components. In this work, the suitability of a long molecular sieve column for easy separation of Kr in the enriched sample from other minor gas components is described.

Material and Methods: An indigenously developed method using a gas chromatograph (GC 2010, CIC, Baroda) fitted with 8m long molecular sieve column (MS-5A 30/60 mesh 8m x 1/8" x 2mm ID) was used in this study. A synthetic mixture of composition, 85% Kr + 15% air was used as input to the GC. 100µL of the sample was injected and the separation was observed with a column temperature of 210°C.

Results and Discussion: Figure 1 gives the gas chromatogram for the studied sample. For the given conditions, it is observed that the retention time for O_2, N_2 and Kr are 9.413min, 20.898min and 22.213 min respectively (Table 1). A clear separation between Kr and N_2 is achieved in this preliminary effort itself and it is feasible to achieve further separation between N_2 and Kr by tweaking the column temperature alone [2]. The method being developed can be integrated to preparative and analytical requirements for Kr separation from air mixtures.

Table 1: Gas Chromatograph results upon injection of Kr sample

Element	Retention Time (mins)	Area	%	Height	%	Width
Oxygen	9.413	70.991	8.831	4.163	16.975	108.1
Nitrogen	20.898	266.060	33.098	8.023	32.714	94.1
Krypton	22.213	466.809	58.071	12.338	50.311	144.1

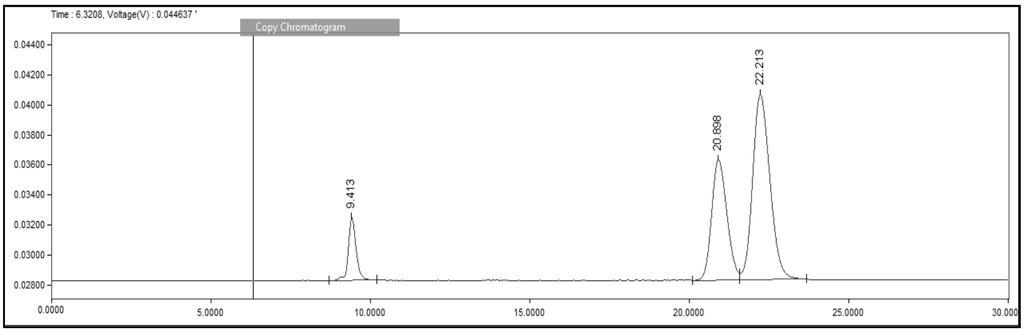

Fig. 1: GC spectrum observed after Kr gas injection.

References:

[1] Jao, Y, Cheng W L, Chen H J, Shaeh C C, Huang C C, Lin Y M; J. Radioanal. Nucl. Chem. 194(2) (1995) 411

[2] Momoshima N, Inoue F, Sugihara S, Shimada J, Taniguchi M; J. Environ. Radioact.101(2010) 615.

Appraising the factors favouring uranium mobilization in alluvial and hard rock aquifers of Rajasthan

Diksha Pant[1,2§], Tirumalesh Keesari[1,2], Annadasankar Roy[1,2], Uday Kumar Sinha[1] and Harish Jagat Pant[1]
[1] Isotope and Radiation application Division, Bhabha Atomic Research Centre*, Mumbai, India*
[2] *Homi Bhabha National Institute, Mumbai, India*
[§] Email: diksha@barc.gov.in

Increasing groundwater contamination in freshwater aquifers is one of the major concerns around the globe. Contamination in large parts of northern and north western aquifers of India has been reported in recent times by inorganic contaminants. Reports suggests that alluvial aquifers are prone to uranium contamination compared to others formations such as basalt, sandstone or gneiss type in India [1]. Many studies were undertaken to understand the source and mechanism of uranium mobilization in groundwater using hydrochemical techniques. However, the application of isotope techniques especially uranium isotopes has been very limited. Hence, with the objective to obtain deeper insights on the uranium mobilization in groundwaters of Jaipur district of Rajasthan, isotopes of uranium were applied (Fig. 1a).

Groundwater samples (1L) were collected from both alluvial and hard rock formations from depths ranging from 25 to 175 m bgl (Fig. 1b). Uranium isotopes were sequentially separated using DOWEX 1 X 8 column and measured using alpha spectrometer (ORTEC soloist). Results indicate that uranium activity ratio ($^{234}U/^{238}U$) (UAR) ranges from 1.44 to 2.85 with an average value of 2.04 in the alluvial formation and 1.38 to 2.97 with an average value of 2.05 in the hard rock formation. The spread in the UAR of both the formations is found to be similar, indicating common geochemical processes governing uranium mobilization in both the formations. Similar study was done in district of southwest Punjab and the UAR values indicated equilibrium condition [2].

From the depth profile (Fig. 1c), a larger spread was observed in UAR in the shallower zones i.e. 1.38 to 2.97 while for the deeper zones the spread is less i.e. 1.69 to 2.38. Less spread in the UAR data suggests longer interaction time leading to uniformity. From the plot of UAR vs U (Fig. 1d), it is observed that leaching of uranium from its mineral is the main process responsible for uranium mobilization in the study area. Based on the UAR systematics, it can be concluded that alpha recoil process is the main process for UAR > 1 and selective leaching of the ^{234}U is contributing to uranium concentration in groundwater of this region.

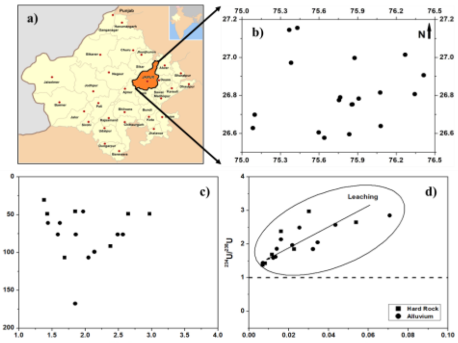

Fig. 1: a) Study area, b) sampling location, c) depth profile of $^{234}U/^{238}U$ and d) $^{234}U/^{238}U$ versus reciprocal U.

Acknowledgements: The authors would like to acknowledge the constant encouragement received from Dr. S. Kannan, Group director RC&IG and the team from Central Ground Water Board, Jaipur for their help in sampling.

References:

1. CGWB, 2019. National Compilation on Dynamic Ground Water Resources of India, 2017. Government of India Ministry of Jal Shakti Department of Water Resources, RD & GR Central Ground Water Board. http://cgwb.gov.in.
2. Diana A. Sharma et al, (2022) “Appraising the factors favouring uranium mobilization and associated health risk assessment in groundwaters of north-western India”, Ecotoxicology and Environmental Safety, 229, 113086, https://doi.org/10.1016/j.ecoenv.2021.113086.

Evaluating sustainability of Bhuj aquifer system, Western India using nuclear dating techniques

Annadasankar Roy[1,2], Uday Kumar Sinha[1], Bharatkumar G Hathi[3], Diksha Pant[1], Hemant Mohokar[1], Sitangshu Chatterjee[1,2], Harish Jagat Pant[1], Tirumalesh Keesari[1,2§]
[1]Isotope and Radiation Application Division, BARC, Mumbai, India
[2]Homi Bhabha National Institute, Mumbai-400 094, India
[3]Kachchh irrigation circle, Bhuj, India
[§]Email: tirumal@barc.gov.in

Increasing population, food demands in conjunction with climatic stressors are threatening groundwater sustainability of major regional aquifer systems in the world. Semi arid/arid regions are particularly vulnerable to groundwater overexploitation due to limited surface water resources and erratic/uncertain rainfall pattern. Bhuj Sandstone aquifer is one such fresh groundwater systems in Western India catering the domestic and irrigational needs for over 2.24 million population. Due to alarming level of groundwater depletion in past decade it is now important to protect and conserve the groundwater resources of this region for long term sustainability. Nuclear techniques using ^{3}H and ^{14}C can provide estimates of groundwater residence time which can help in planning sustainable groundwater management. In this study, five deep groundwater samples were collected and measured for stable (^{18}O, ^{2}H, ^{13}C) and environmental radioactive isotopes (^{3}H, ^{14}C) to evaluate the groundwater sustainability (Fig. 1). Isotope Ratio Mass Spectrometer (IRMS) and Liquid Scintillation Counters (LSC) were used for stable isotope and radioisotope measurements following standard methods. Results show that two samples have ^{3}H concentration less than 1 TU indicating groundwater recharge prior to 1950. The ^{14}C values varied from 26 to 73.6 pMC (percent modern carbon) with an average of 55.08 (±23.40) pMC. Residence time of the groundwater samples were calculated based on equation (1) which provide the uncorrected age of groundwater;

$$^{14}C_{age(uncorrected)} = 8267 \times \ln[(14C_{initial}/14C_{final})] \qquad (1)$$

Correction of the calculated groundwater ages are done to account for dilution and loss of active carbon by geochemical reactions both within the soil and along the flow path. Correction models applied in this study are; Pearson, Statistical Correction (STAT) and Chemical Mass Balance (CMB) models. Furthermore, inverse modelling was done using NETPATHXL to account for complex geochemical reactions modifying ^{14}C activity in aquifer. The groundwater ages obtained by different models are presented in Table 1. The overall results suggest that samples 1 and 3 have paleo-recharge components while rest of the samples appear to be modern. Based on the results it can be inferred that central part of the Bhuj aquifer hosts paleowater pockets. Very old groundwater ages and less modern recharge pose a pertinent concern on the groundwater sustainability of this region. Over-exploitation may further lower the groundwater levels and this would have long-term impact on the socio-economic development of whole Kutch region.

Table 1. Calculated residence time (in Years)

ID	Age (uncorrected)	Age (Pearson model)	Age (STAT model)	Age (CMB model)
1	11136	1171	10265	18798
2	3092	*Modern*	2221	9926
3	9066	2352	8195	11677
4	2534	*Modern*	1663	2534
5	2762	*Modern*	1891	4693

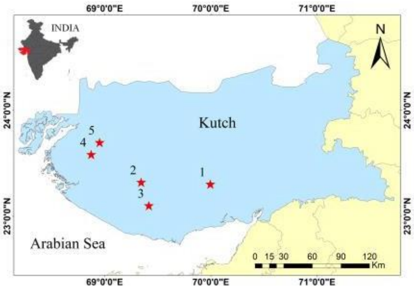

Fig. 1: Study area and sample location map

Estimation of Natural Radioactivity in Soil Samples from Punjab, India

R. C. Bhangare[1], M Tiwari[1], T. D. Rathod[1,2], M. Swarnkar[1], P. Y. Ajmal[1], R. H. Pillay[1], S. K. Sahu[§1,2], V. Pulhani[1,2]
[1]Environmental Monitoring and Assessment Division, Bhabha Atomic Research Centre, Trombay, Mumbai – 400085, India
[2]Homi Bhabha National Institute, Anushaktinagar, Mumbai – 400094, India
[§]Email: sksahu@barc.gov.in

Naturally occurring radionuclides (NORs) like ^{238}U, ^{232}Th, ^{226}Ra, ^{210}Pb and ^{40}K are ubiquitously distributed all over earth. NORs in soil are the most abundant source of radioactivity encountered by humans. Estimation of the NORs activities in soil is very important for determining the radiological status of a particular area. The natural background radiation data in soil can be used for various purposes like mineral profiling, risk assessment, the study of radioactivity input by anthropogenic activities, and the tracking of many environmental processes etc. In this study, surface soil samples collected from 22 districts of the state of Punjab, India were analysed for their Naturally occurring radionuclide content by gamma spectrometry (Using a BSI make, P type, 40% efficiency HPGe detector with Beryllium window) and the observed data was further used for calculating various dose parameters as discussed below.

Fig. 1 shows observed range of activity concentrations for the 5 radionuclides. In the figure, each legend mark represents a different district and the values at bottom of the column indicate the average soil radioactivity concentration for that radionuclide in entire state.

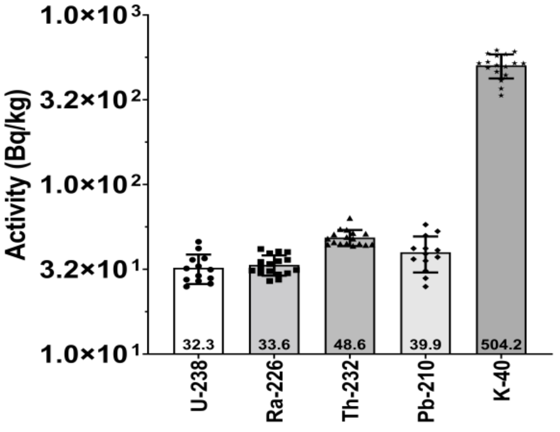

Fig. 1: Radioactivity levels in soil samples from different Punjab districts.

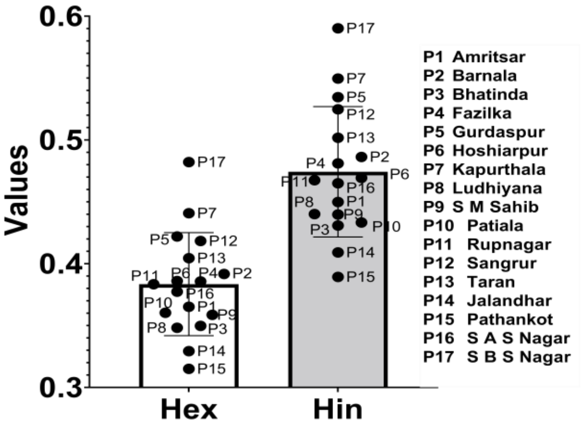

Fig. 2: External and Internal hazard indices for different Punjab districts.

The data was used to calculate radium equivalent activity (Raeq) in the soil along with absorbed dose (D), external (H_{ex}) and internal (H_{in}) hazard indices [1, 2]. The Ra_{eq} values ranged from 110 to 179 with average of 141 Bq/kg. The absorbed dose ranged from 51 to 83 with average value of 51 nGy/h. Fig. 2 shows the H_{ex} and H_{in} values for all studied districts. Soil from Shaheed Bhagat Singh nagar showed maximum value for both H_{ex} and H_{in} (0.48 and 0.59 respectively), which is due to highest ^{40}K activity, whereas Pathankot soil showed the minimum H_{ex} and H_{in} (0.3 and 0.37 respectively) values. Since both H_{ex} and H_{in} are below unity, radiological risk if any are not significant.

References:
[1] R. C. Bhangare et.al., *J Radioanal Nucl Chem* 300 (2014) 17
[2] K. M. Murthuza et al., *Materials Today: Proceedings* 65 (2022) 2606

Natural Radioactivity levels and resulting annual effective dose to public around Kudankulam due to terrestrial radiation

B.S.Selvi[1§], Thomas George[1], P.S.Rajan[1], B.Vijayakumar[1] and I.V.Sarathi[2]

[1] *Environmental Survey Laboratory, Kudankulam Nuclear Power project, Tamilnadu -627120*
[2] *Environmental monitoring and Assessment Division, BARC, Mumbai, India*
[§]Email: bsselvi78@gmail.com

Natural radiation is the largest contributor to the external dose of world population, the assessment of gamma radiation dose from natural sources is of particular importance (UNSCEAR 2000). Soil is the main source of continuous radiation exposure to soil habitants and human beings. The natural radioactivity levels (^{238}U, ^{232}Th and ^{40}K) in soils collected around Kudankulam Nuclear Power Plant (KKNPP) have been determined by gamma ray spectrometry. The absorbed gamma dose rate (D) in air 1 m above the ground surface and annual effective dose (H) were estimated as follows. (UNSCEAR 2000)

$$D = 0.0414A_K + 0.461A_U + 0.623A_{Th} \quad ---1$$

Where D (nGy h^{-1}) is the absorbed dose rate, A_K, A_U and A_{Th} are the activity concentrations for ^{40}K, ^{226}Ra and ^{232}Th respectively.

$$H(mSv\ y^{-1}) = D\ (nGy\ h^{-1}) * 8760 * T(h\ y^{-1}) * F(Sv\ Gy^{-1}) * 10^6) \quad ---2$$

T is the occupancy time, the indoor and outdoor occupancy factors are given as 0.8 and 0.2, respectively, and F is the conversion factor (0.7 Sv Gy^{-1}).

The activity content of ^{238}U, ^{232}Th and ^{40}K, resulting air absorbed dose rate and annual effective dose are evaluated and summarized in Table 1. South eastern coast of India having abundant deposits of monazite mineral, the activities due to ^{232}Th in soil along the coast are considerably higher. Due to high ^{232}Th content in soil, the air absorbed dose rate and annual effective dose are higher than the world average. However, these values are comparable with the high background radiation areas elsewhere in India and world.

Table 1: Natural Radioactivity, absorbed dose rate and annual effective dose around KKNPP

Year	No of samples	Activity (Bq/Kg dry wt)						Air Absorbed Dose rate	Annual Eff Dose		
		K-40		Th -232		U-238			In door	Out door	Total Dose
		GM	GSD	GM	GSD	GM	GSD	nGy/hr	mSv/year		
2012	16	290.1	1.50	114.0	1.50	24.3	1.40	94.23	0.46	0.12	0.58
2013	18	331.0	1.63	80.1	2.05	15.3	1.70	70.66	0.35	0.09	0.43
2014	18	202.8	5.50	201.5	3.30	29.1	2.60	147.35	0.72	0.18	0.90
2015	18	449.2	1.60	126.1	1.40	22.6	1.40	107.58	0.53	0.13	0.66
2016	18	305.0	2.10	181.8	2.00	29.5	1.60	139.49	0.68	0.17	0.86
2017	21	342.7	2.50	132.6	1.70	25.0	1.50	108.32	0.53	0.13	0.66
2018	18	326.6	2.70	128.4	1.40	21.3	1.40	103.33	0.51	0.13	0.63
2019	19	280.9	2.50	184.5	2.00	28.4	1.70	139.67	0.69	0.17	0.86
2020	22	301.4	2.20	184.8	2.30	28.2	2.20	140.61	0.69	0.17	0.86
2021	20	311.5	2.30	182.0	1.60	28.5	1.50	139.42	0.68	0.17	0.85
Average		**314.1**		**151.6**		**25.2**		**119.07**	**0.58**	**0.15**	**0.73**
World Average		**420**		**45**		**33**		**59**	**0.41**	**0.07**	**0.48**

References:
1. UNSCEAR (2000); Exposure from natural radiation sources, Annex-B. Sources and effects of ionizing radiation, United Nations, New York.

Risk assessment due to inhalation of radon in the environment of Madikeri taluk, Coorg District, Karnataka State

M. M. Prakash[1], Y. Narayana[1], C. S. Kaliprasad[2§], Beena Ullala Mata B. N.[3], Ganesh Prasad K.[2]
[1]*Department of Studies in Physics, Mangalore University, Mangalagangothri, India -574199*
[2]*Department of Physics, BMS college of Engineering, Bangalore, India-560019*
[3] *Department of Medical electronics, BMS college of Engineering, Bangalore, India-560019*
[§]Email*: kpkaliprasad23@gmail.com*

All living beings are under the exposure of terrestrial radiation inevitably. The global average annual radiation dose received by human beings is around 2.42 mSv y^{-1} [1]. Nearly 57% of the radiation dose is received due to inhalation of radon in indoor and outdoor environments. Radon is an inert radioactive gas formed by alpha decay of ^{226}Ra atoms, in various environmental matrices [2]. The radon exhalation depends on porosity of soil, which in turn depends on the physico chemical parameters of soil. The physico chemical parameters of soil is influenced by the climatic conditions of the region. Coorg district receives high annual rainfall, nearly 2500 mm [3]. The seasonal variation of indoor and outdoor radon was analysed, in the environment of Coorg [4]. The annual inhalation dose due to indoor and outdoor radon was estimated.

In Madikeri taluk, the average outdoor radon concentration in air in winter season was 8.64 Bq m^{-3}, whereas in summer season, it was 9.88 Bq m^{-3}. In monsoon the average was found to be 6.11 Bq m^{-3}, whereas in autumn season the average concentration was 7.04 Bq m^{-3}. The average annual inhalation dose due to outdoor radon is 0.077 mSv y^{-1}. In the winter season, the average indoor radon concentration was found to be 27.04 Bq m^{-3}, whereas the thoron concentration was found to be 5.72 Bq m^{-3}. The average indoor radon concentration was found to be 21.93 Bq m^{-3}during summer season, whereas the thoron concentration was found to be 4.30 Bq m^{-3}. In monsoon the average radon concentration was 29.07 Bq m^{-3}, but in case of thoron the average concentration was 6.55 Bq m^{-3}. In autumn season, the indoor radon concentration was found to be 24.10 Bq m^{-3}, whereas the average thoron concentration was 4.93 Bq m^{-3}. The average annual inhalation dose due to indoor radon was nearly 0.83 mSv $y^{-1.}$ The total annual inhalation dose due to indoor and outdoor radon was found to be 0.907 mSv y^{-1}.

References:

[1]. UNSCEAR (1993). United Nations Scientific Committee on the effects of Atomic Radiation. Sources and effects of ionizing radiation. Report to General Assembly, New York.
[2].Durrani SA, Illic R. Radon measurements by etched track detectors.(1997) World Scientific Publishing Co Pte Ltd, Singapore.
[3]. District Resource Map. Geological Survey of India.
[4]. M M Prakash, Kaliprasad CS, Narayana Y Risk assessment due to inhalation of Radon in Coorg district, Karnataka state. Journal of Radioanalytical and Nuclear chemistry. (2017). 314(3), 2057 – 2067.

Soil to Rice Transfer Factor of ^{210}Po in the local rice variety: a site-specific observation from the pot experiments

S. Panigrahi§, S. N. Bramha, S. Chandrasekaran, C. V. Srinivas, B. Venkatraman
Radiological and Environmental Safety Group
Indira Gandhi Centre for Atomic Research, Kalpakkam, TN, India, 603102
§ Email: snpanigrahi@igcar.gov.in

Primarily ^{210}Po comes from the ^{238}U decay series and is one of the most common contributors to the natural radiation dose to the population via food ingestion. Radionuclides present in the environment are transferred to the plants by uptake from soil through the roots. The critical pathways for radionuclides in tropical countries differ from those in temperate environment because the agricultural practices, soil type, rainfall and various other parameters and growth pattern. Hence site-specific information on transfer factor of various radionuclides is essential to calculate the dose. Rice (*Oryza sativa* L.), is the dominant staple food crop in humid tropical countries across the globe and almost 90% of the world‟s rice is produced and consumed in Asia (Karunakar et al., 2013).

In this study various pot experiments were conducted to understand the mobility of ^{210}Po in the soil-plant pathway at Kalpakkam site. The local rice variety (ADT-45) was grown in the experimental setups and samples of root, stem, early grains, mature grains, and soil were collected and analyzed for ^{210}Po in different growth stages. Standard methods of IAEA for radiochemical separation were followed and the plated samples were counted in an alpha spectrometer.

^{210}Po activity in the soil used for the experiments (Figure-1) varied between 8.2- 17.6 Bq/Kg (Geometric mean ± SD was 12.82±3.41). It enters the plat system through the root by the process of transpiration. Since the root is in direct contact with the soil it showed highest accumulation and the activity was found to be 8.56 – 15.25 Bq/Kg (11.47±2.91). Early grains had higher activity concentration as compared to the mature grains. ^{210}Po in early grain was 2.58 – 4.20 Bq/Kg (3.50±0.70) and that of mature grain was 1.67 – 2.80 Bq/Kg (2.26±0.47). Transfer factor of ^{210}Po in soil-rice pathway at Kalpakkam (Table-1) varied between 0.17 – 0.20 (0.18±0.01) which is lower than the TF values reported from Vietnam (Nguyen et al., 2021) and is comparable with the values presented in IAEA TRS-472. The mature grains have ^{210}Po activity within the safe limits. The roots of the rice plant have higher activity and TF as it is in close contact with the soil and has the capability of higher accumulation.

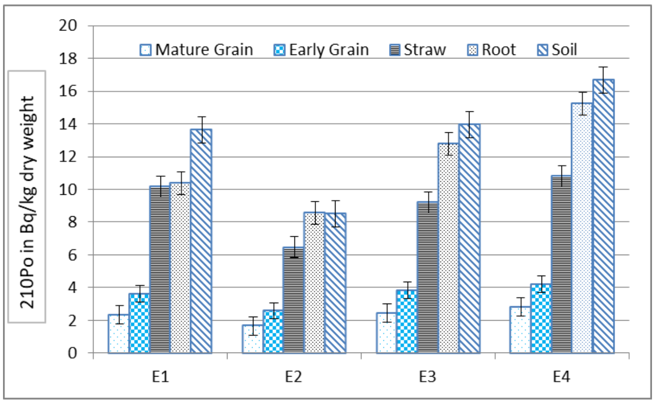

Fig. 1: Activity concentration of ^{210}Po in parts of rice plant experiments. E1 to E4 represents different experiments conducted

Table 1: Transfer factor values of ^{210}Po in different parts of the rice plant

Plant Part	^{210}Po Transfer Factor			
	E1	E2	E3	E4
Mature Grain	0.17	0.20	0.17	0.17
Early Grain	0.26	0.30	0.28	0.25
Straw	0.75	0.76	0.66	0.65
Root	0.76	1.01	0.92	0.91

References: [1] IAEA TRS-472, IAEA Technical Report Series No. 472. IAEA, Vienna. 2010.
[2] N. Karunakara, C Rao, P. Ujwal I. Yashodhara, S Kumara, P.M. Ravi, J. of Env Rad 118 (2013) 80-92
[3] Nguyen V T, Huynh N P T, Le C H. (2021), Sci. Tech. Dev. J.; 24(4):2177-2186.

Measurement and distribution of primordial radionuclides activities at three coastal areas of Tamil Nadu, India

R. T. Asher Nebin[1], S.N. Bramha[2§], N. Chitra[2], K S Briteena[2], S. Chandrasekaran[2], A. Yardily[1], S. Godwin Wesley[1], C.V. Srinivas[2] and B.Venkatraman[2]

[1]*Department of Chemistry, Scott Christian College, Nagercoil, Tamilnadu, India*
[2]*Indira Gandhi Center for Atomic Research, Kalpakkam, Tamilnadu, India*
[§]*Email:snbramha@gmail.com.*

The natural radioactivity in the environment is mainly due to the presence of radioactive isotopes, also known as radionuclides, that have been present in the Earth crust, since it was formed. These long-lived radionuclides are called primordial radionuclides. The primordial radionuclides such as ^{40}K,^{238}U, and ^{232}Th are the main source of contribution background radiation and its variation depends on factors such as; the region's geology and the presence of radon gas, and the composition of the local soil and rocks. In India, there are quite a few monazite-sand bearing placer deposits causing high background radiation along its long coastline (A. K. Ajithra, B. Venkatraman, et al., 2017). This study carried the activity concentrations of primordial radionuclides and ambient gamma in the foreshore beach sands of Kanyakumari: a high natural background radiation area (HNBRA), Kalpakkam: a medium natural background radiation area (MNBRA), and Parangipettai: a low natural background radiation area (LNBRA). The beach sand was collected as per IAEA protocol and brought to the laboratory; a hand-held GPS and ambient gamma monitoring system was used to collect the location and gamma data. The sand samples were dried and packed for 30 days to attend secular equilibrium and then counting are carried out by NaI (Tl) scintillator detector.

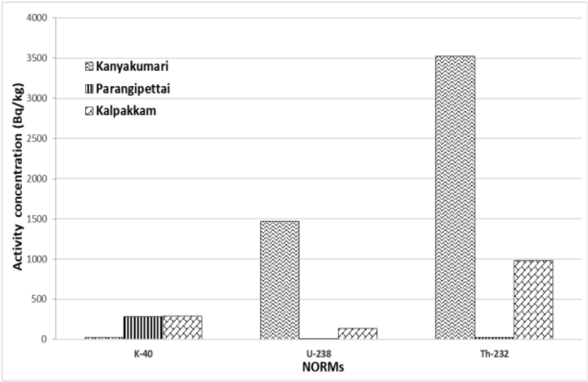

Fig. 1. Average activity concentration of the primordial radionuclides TN coast.

The natural ambient gamma dose rate (µSv/h) ranged from 0.03 to 6.72 at the Kanyakumari, from 0.01 to 0.11 at Parangipettai and from 0.05 to 3.71 at Kalpakkam coast. The activity concentration (Bq/kg) of the radionuclides ^{40}K, ^{238}U, ^{232}Th in the Kanyakumari samples ranged from 12.31±16 to 98.96±3, 3.53±1 to 6485.06±19 and 9.99±2 to 20544.5±51. In Parangipettai samples, the activity concentrations (Bq/kg) of radionuclides ranged from 112.87 ±1 to 374.99±6, 3.07±1 to 50.41±1, and 3.35 ± 1 to 244.67 ± 4. In Kalpakkam samples, the activity concentrations (Bq/kg) of radionuclides ranged from 8 ±0.3 to 401.82±12, 2.07±0.2 to 1882.01±11, and 3.5±1 to 11501.14±40. In this study the activity concentration of the radionuclides ^{40}K, ^{238}U, ^{232}Th from the beach sands of Kanyakumari district and Parangipettai are compared; Kanyakumari district is the High Background Natural Radiation Area due to monazite deposits at Vivekanandapuram, Manavalakurichi and some other sampling sites, whereas; Parangipettai is considered as Low Natural Background Radiation area due to lower level of Monazite deposit; when compared with Kanyakumari. It is also found that Kanyakumari beach sediments has lower potassium levels compared to Parangipettai and Kalpakkam samples.

References:

[1] A. K. Ajithra et al., Radiation Protection and Environment (2017), 40, 27 - 33.

Geopolymer and Cement as immobilization matrices in Near Surface Disposal Facility

Sonali Khurana[1,§], Ritu M Shrivastav[2, §], TK Pal[2], S Sen[3], VK Mittal[3], TP Valsala[3],
UV Deokar[1], G Ganesh[1], MS Kulkarni[1], R Sharma[3], RV Jayan[3], RK Bajpai[2],
YC Shivakumar[2], S Manohar[2]
[1]*Health, Safety & Environment Group,* [2]*Nuclear Recycle Group*, [3]*NuclearRecycle Board,*
Bhabha Atomic Research Centre
[§]Email: sonalikhurana@barc.gov.in; aritu@barc.gov.in

Radioactive waste, after treatment, is immobilized in a suitable matrix prior to disposal to ensure confinement. In India, radioactive sludge produced from chemical treatment of Low-Level Waste is fixed with cement-vermiculite matrix for storage into the underground concrete trenches. Cement-based materials, due to its inert binding capacity and stabilisation of radionuclides have been widely adopted for the encapsulation of low and intermediate level wastes. However, when the complexity of wastes increase or concentration of activity is increased, cements are unable to bind the radionuclides. As an alternative matrix, Geopolymers are reported to have a superior service life to cement owing to their low permeability to water and resistance to corrosion with respect to chloride and sulphates [1].

In the present study, leaching tests were performed on low level liquid waste with Ordinary Portland Cement (OPC) and fly-ash based geopolymer matrix employing IAEA Standard leaching procedure [2]. Fig 1 shows variation of Normalized Leach Rate (NLR, $g/cm^2/d$) of Cs-137 with leaching period from both matrices. Initially, the radionuclide release rate is much higher in OPC as compared to geopolymer. From the graph, it can be concluded that the geopolymer matrix exhibits much better radionuclide retention. Data available on service life of matrices evaluated from leach rate, also suggests the better durability of geopolymer as compared to cement.

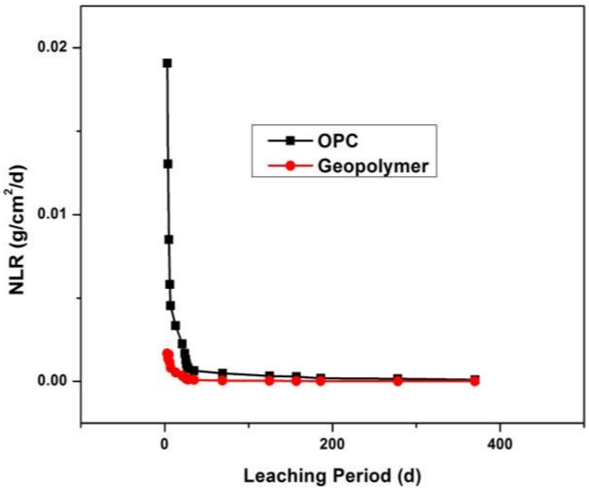

Fig 1. Comparative Leaching study of Cs-137

Even though several literature studies have shown the utilization of geopolymers on industrial scale, the performance of geopolymer as immobilization matrix for radioactive waste management still needs to be further investigated to predict the service life of immobilized waste product for its actual implementation on plant scale. Considering such vast number advantages over cement, such as high mechanical stability, lower environmental impact, better waste loading capacity and higher leachability index, geopolymer may offer a valuable alternative to Portland cement-based systems for radioactive waste management in future.

References:

1. Esther Phillip, Thye Foo Choo, et. al; “On the sustainable utilization of geopolymers for safe management of radioactive waste: a review”, Sustainability, 2023.
2. E. D. Hespe, “Leach testing of immobilised radioactive waste solids”, IAEA, 1970.

Assessment of Radioactivity Levels and Associated Radiological Hazards of Urban Soil from Mumbai

P. Kothai§, Sangeeta J. Sartandel, Vandana Pulhani

Environmental Monitoring and Assessment Division, Bhabha Atomic Research Centre, Mumbai – 400085, India
§Email: kothai@barc.gov.in

Radiation exposure to humankind involves diverse sources including natural and manmade origin. Where, natural sources include both cosmic and terrestrial radiation. In the present study, an attempt is made to study the radiation level and radiological hazard due to terrestrial radiation in Mumbai. 15 surface soil samples were collected around Trombay region in the vicinity of industries, traffic junctions and residential area. Samples were dried, sieved and the homogenized samples were then sealed in plastic and kept for a month to ensure the equilibrium between ^{226}Ra and their decay products. Activity concentrations were determined using a P-type HPGe detector of 50% efficiency, 2keV energy resolution for 1332keV ^{60}Co point source at 25cm height.

Activity concentrations of natural radionuclides such as ^{226}Ra, ^{210}Pb, ^{232}Th/^{228}Ra, ^{40}K and ^{137}Cs present in soil samples are depicted in Fig. 1. Results were ranged between 10.8-82.3 for ^{226}Ra, 70-341.4 for ^{210}Pb, 5.5-14.6 for ^{228}Ra, 51.9-188 for ^{40}K and 0.3-31.2 (Bq/Kg) for ^{137}Cs. Based on the activity concentrations of U, Th and ^{40}K, various parameters like Radium equivalent (Ra_{eq}), air absorbed dose rates due to terrestrial gamma rays at 1m above the ground level (in $nGyh^{-1}$), annual effective dose ($\mu SvYr^{-1}$), external hazard index, internal hazard index and gamma radiation representation level index were estimated and the box-whisker plot of all the parameters are presented in Fig 2. Equations and the conversion factors used for the estimation of various parameters are referred from [1] and [2].

In the present study Ra_{eq}, absorbed dose and the annual effective dose were found to be in the range of 27.4-67.4, 12.8-31.1 $nGyh^{-1}$, and 15.8-38.1 $\mu SvYr^{-1}$ respectively. Furthermore, the external and internal hazard index calculated for each sample varied from 0.07-0.18, 0.09-0.22 respectively. The gamma radiation representation level index ranged from 0.2-0.5.

Results of the study present normal levels of radioactivity due to natural as well as anthropogenic origin. The estimated preliminary values of Ra_{eq}, annual effective dose and radiation hazard index indicate risk due to radiation in the study area is insignificant.

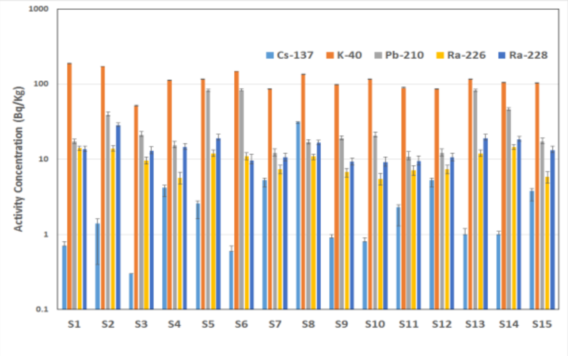

Fig.1: Activity concentrations (Bq/Kg) of radionuclides in soil samples

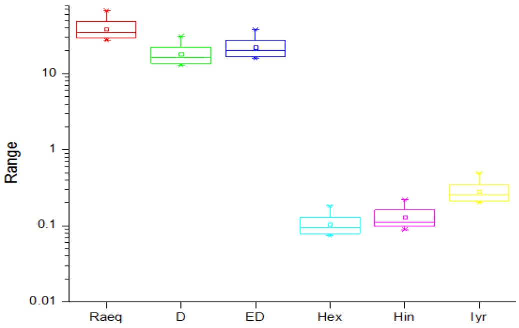

Fig.2: Box-Whisker plot of calculated parameters

References:
[1] A.H. Ahmed and D.T. Akrawy. Int. J. Recent Research and Review, 8(4) (2015) 48
[2] H.M. Diab, J Nuclear and Radiation Physics, 3(1) (2005) 53

Studies on uptake of tritium by fish conducted by simulated experiment in an aquarium.

M. K Jha§, A. K. Patra, C. P Joshi, V Sudheendran, A. Baburajan,
I.V Saradhi, A. Vinod Kumar
Environmental Monitoring and Assessment Division, BARC, Mumbai-400 085
§*E-mail:* mukeshjha@npcil.co.in

^{3}H in environment is incorporated into aquatic organism as tissue-free water tritium (TFWT) and partly it is converted into Organically-bound tritium (OBT). Organic tritium exists as exchangeable and non-exchangeable forms [1]. Exchangeable organic tritium is bound to hydrogen, nitrogen or sulphur in chemical groups that can dissociate and exchange rapidly with tritium in the HTO pool. The non-exchangeable tritium is bound to carbon in chemical groups that can"t dissociate and exchange rapidly. It has become increasingly recognized that OBT is the more significant tritium (^{3}H) fraction with respect to understanding ^{3}H behavior in the environment [2]. Keeping in view, an attempt was made to study the uptake of HTO by one of the most predominant aquatic fish species, *Notoporus-notoporous sp*. In order to quantify uptake of tritium, a controlled study was carried out in an aquarium by exposing the fish with 175 litre of water of with a specific activity of ^{3}H 880 Bq L^{-1}. Natural Evaporation loss in the aquarium is about 100 ml per day which is compensated with the buster pump used to aerate the aquarium. The change in ^{3}H activity is negligible due to the negligible evaporation loss. The experiment is planned to carry out the uptake process by considering one parameter at a time i.e ^{3}H activity in water. All the fish species are same with different body mass. The body mass of fishes were in the range of 20-140 gm. The TFWT and OBT activity was estimated in fish after different exposure periods. Tissue free water was extracted using freeze drier and Oxidiser system was used for extraction of bound tritium in fish. ^{3}H activity was measured using liquid scintillation spectrometer. TFWT and OBT activity was found to be in the range of 386-797 Bq L^{-1} and 120-206 Bq L^{-1} respectively. There is a variation of TFWT and OBT activity is observed. This may because the water is aerated with fresh air and might have diluted the tritium activity in aquarium. The initial reduction of OBT activity and then increase may be because of the uncertainty in analysis. TFWT to OBT ratio was observed to be 0.25-0.39 with an average value of 0.31. The OBT/TFWT ratio derived at Kakrapar can be used as site specific input parameter for the development of aquatic tritium models. However the present study indicate the requirement of an elaborate experimental study with large number of samples with more sample weight and lower minimum detectable level (MDL). However other experiments will be planned in future with varying parameters such as flow rate of tritiated stream, age of the fish, body mass etc. which may be suitable for dynamic condition.

Table 1. TFWT and OBT activity in Fish

Sr. No.	Exposure duration (day)	TFWT (Bq L^{-1})	OBT (Bq L^{-1})	OBT/TFWT
1	1	797±28	202±44	0.25
2	25	475±22	120±38	0.25
3	26	386±20	130±42	0.34
4	30	525±23	206±52	0.39

References:

[1] Diabate, S., Strack, S., Health Physics, 65, (1993), 698.
[2] IAEA TECDOC-1616, (2009).

Assessment of annual effective ingestion dose due to naturally occurring ^{40}K through dietary intake at Tarapur

Pratibha[1§], V. Sudheendran[1], R.H. Gaikwad[1], A. Baburajan[1], I.V. Saradhi[2], A. Vinod Kumar[2]

[1] *Environmental Survey Laboratory, Tarapur Atomic Power Station, EMAD, BARC, TAPP (P.O), Boisar, Palghar (Dt.), Maharashtra*
[2] *Environmental Monitoring and Assessment Division, BARC, Trombay, Mumbai*
[§] Email: pratibhachugh11295@)gmail.com

Radioactivity through dietary products is one of the important sources of internal exposure to the human population. Since potassium is present in the soil in abundance, ^{40}K, which constitutes 0.0117% of stable potassium, can reach the man through the dietary pathway. It is important to quantify the ^{40}K activity in these dietary items to compute the ingestion dose to the public at Tarapur. The paper discusses ^{40}K activity in the dietary products consumed by the local population collected during the period 2008-2022 (15 years). The details of samples collected and analyzed for ^{40}K are presented in Table 1. The samples were processed and subjected to gamma spectrometry using an HPGe detector and 1460 keV gamma line was used for the activity computation.

The geometric mean concentration of ^{40}K in each category of food sample during the study period along with respective site-specific dietary data (Patil et al., 2004), was used for the computation of ingestion dose (Hegde et al., 1998). Since different categories of food items constitute various species with varied ^{40}K activity, and also the consumption patterns among different categories of people like the fisherman, farmer, and general public are different; the 95th percentile activity was also computed and used for dose computation (Table 1). Among the different food items, the pulses were found to have the highest ^{40}K activity and also the dose contribution. The ingestion dose due to the geometric mean and 95th percentile of the activity was computed and was found to be 158.8 µSv and 303.3 µSv respectively. The annual mean ingestion dose due to ^{40}K computed for Tarapur site is found to be comparable with the global average value of 170 µSv y^{-1} as per UNSCEAR-2000.

Table 1 Population dose (µSv) due to ^{40}K (Bq kg^{-1}) in dietary products at Tarapur

Sample Category	Annual Intake (kg y^{-1})	No. of samples	G.M.(G.S.D) (Bq kg^{-1})	95th percentile (Bq kg^{-1})	Mean dose (µSv)	95th percentile (µSv)
Fish	20.0	910	56.3(2.1)	126	7.0	15.6
Cereals	151.0	130	41.9(1.4)	68.5	39.2	64.1
Meat	13.5	63	78.2(1.2)	102	6.5	8.5
Vegetable	42.0	352	76.5(1.9)	220	19.9	57.3
Fruits	9.9	32	73.5(1.5)	136	4.5	8.3
Egg	13.5	49	39.1(1.2)	53.0	3.3	4.4
Milk	42.2	177	27.0(1.5)	48.1	7.1	12.6
Pulses	32.5	22	347(1.8)	650	69.9	131
Salt	2.9	1	13.7 ± 1.0	13.7	0.2	0.2
Sugar	15.6	1	11.9 ± 0.5	11.9	1.2	1.2
	Total annual effective dose				**158.8**	**303.3**

G.M.: Geometric mean; G.S.D.: Geometric standard deviation

Reference(s):

1. Patil, S.S et al.," National Symposium on Environment -13, (2004), 206-211.
2. Hegde, A.G. et al., *"Environmental Radiological Laboratory Procedure Manual"*, Health Physics Division, Bhabha Atomic Research Centre, 1998.

Study on distribution coefficient (K_d) of ^{137}Cs in coastal sediment at Tarapur.

Sushant S. Dalvi[1,§], C.A. Shah[1,] , A.Baburajan[1], I.V. Saradhi[2] and A. Vinod Kumar[2]

[1] *Environmental Survey Laboratory, Tarapur Atomic Power Station, EMAD, BARC, TAPP (P.O), Boisar, Palghar (Dt.), Maharashtra*
[2] *Environmental Monitoring and Assessment Division, BARC, Trombay, Mumbai*
[§]Email: susdalvi@gmail.com

The low level liquid effluent generated during the operation of Nuclear Power Plants (NPP) and allied facilities at Tarapur is discharged to the Arabian Sea after treatment and adequate dilution and as per the discharge limit specified. ^{137}Cs is one of the major nuclides with a long half-life ($T_{½}$:30.2 y) found in the effluent discharge during normal operation and also in case of any emergency situation. The radionuclide released to the sea undergoes physical and chemical changes including bioaccumulation in the aquatic medium. The marine organisms prey on the suspended matter and shore-deposited sediment is an important pathway of ^{137}Cs activity reaching man. The study is focused on deriving the concentration ratio of ^{137}Cs in sediment to that in seawater, the distribution coefficient (K_d), which is an important model parameter for the aquatic transport of radionuclides. The shore-deposited sediment and coastal seawater samples collected from locations <1.6 km to 30 km distance from the main outfall (MOF) of nuclear facilities were processed, subjected to gamma spectrometry with HPGe and ^{137}Cs activity was estimated (Hegde, et al., 1998) for the period 2016-2022. The ^{137}Cs concentration in seawater from off-site locations was found to be 0.8 to 2.25 mBq L^{-1} and that in sediment it was 0.33 to 3.04 Bq kg^{-1}. The summary of the K_d value determined for coastal sediment at Tarapur during 2016-2022 is presented in Table 1.

Table 1 Summary of K_d (L kg^{-1}) value determined for coastal sediment at Tarapur

Sampling locations (km)	Geometric Mean (GM)	Median	Maximum	Minimum	1st quartile	3rd quartile	No. of samples
<1.6	1509	1582	9009	492	1000	2052	26
2.5	2379	2388	2596	2180	2284	2492	2
5.0	1499	2007	4459	416	1255	2148	9
8.0	674	684	1353	321	533	937	23
15.0	908	745	1592	630	688	1169	3
30.0	900	874	1427	653	773	938	5

The geometric mean K_d value varied from 674 to 2379 for different locations, with the lowest and highest value among the entire sample collected and assessed during the period was found to be 321 and 9009 respectively. The possible reasons for the 30-fold variation in the K_d at the controlled location, <1.6 km might be due to the enhance level in the discharge zone, the physical characteristics of the shore-deposited sediment, grain size and the clay/silt content of the sediment. Masashi, et al, 2019 has reported a higher K_d value in locations around Fukushima. Also from Table 1, the mean K_d value up to 5 km is found higher when compared to other locations, and reduces considerably beyond 5 km and is nearly uniform up to 30 km. This may be because the ^{137}Cs contributions from nuclear facilities are not found beyond 5 km and the observed concentrations mostly may be due to global fallout.

References:

[1] Hegde, A.G. et al., *"ERL Procedure Manual"*, HPD, BARC (1998).

[2] Masashi et al., JRNC, Published online https://doi.org/10.1007/s10967-019-06958-z (2019).

X-ray Photoelectron Spectroscopy study on borosilicate glass-ceramics for nuclear waste immobilisation

Ritu Kumari Pilania[1] and Charu Lata Dube[1, §]

[1]*School of Nano Sciences, Central University of Gujarat, Gandhinagar, Sector 30, 382030, India.*
[§]Email: charulata.dube@cug.ac.in

Abstract

The borosilicate glass-ceramics with varying loading percentages of SrO were synthesized with the melt-quench method for immobilization of Sr radionuclide (short-lived). it is aimed to immobilize the Sr radionuclide in the durable crystalline phase whereas other divalent alkalis such as Ca, Ba, etc. were taken to produce hindrance to the chemical durability of the matrix. The X-ray diffractograms confirmed the formation of glass ceramics. The XPS has been used to evidence the effect of SrO and TiO_2 addition, and crystallization in the glass phase. The lower binding energy (529.1 eV) and higher (531.5 eV) peaks of the O 1s signal are ascribed to non-bridging and bridging oxygen components, respectively. The O 1s peaks are shifted to higher binding energy with increasing content of SrO which indicates the increasing number of bridging oxygens. The binding energy at 102.3 eV of Si 2p signal corresponds to Si-O bonding which was almost identical for both samples with the loading of SrO (20 and 25 mol%). The Sr 3d and Ti 2p spectra also confirmed the formation of perovskite ($SrTiO_3$) phase in the glass samples. The Ti 2p spectra deconvoluted into two peaks which correspond to doublet ($2p_{3/2}$ and $2p_{1/2}$). The shift in the binding energy of cations (from loading of 20 to 25 mol%) was attributed to charge transfer. The detailed results will be presented at the conference.

Keywords: Glass-ceramics, XPS, NBOs and BOs.

Polonium-210 and lead-210 in Cigarette and Beedi used by Mangalore Population, Karnataka, India

C. S. Kaliprasad[1], Venunathan N.[2], M. M. Prakash[2], Y. Narayana[2], Beena Ullala Mata B. N.[3], Ganesh Prasad K.[1]
[1]*Department of Physics, BMS college of Engineering, Bangalore, India-560019*
[2]*Department of Studies in Physics, Mangalore University, Mangalagangothri, India -574199*
[3] *Department of Medical electronics, BMS college of Engineering, Bangalore, India-560019*
[§]*Email: kpkaliprasad23@gmail.com*

The activity concentration of radioactive ^{210}Po from ^{210}Pb in human consumption things is the greater interest due to the radiotoxicity of these two radionuclides. Polonium-210 is the daughter product of uranium-238 decay series, which is found in the air and soil. It is an alpha emitter with the decay of daughter product lead and its half-life of 138 days, which is present in trace level in the most of plants, food, human tissues. The accumulated polonium in the soil is transfers through the plants to food chain, to human body [1]. The tobacco is one of the most used natural products in the world through different types of by-products such as cigarette, Chew- see Smokeless Tobacco, Hookah, Kreteks and Pipe etc. The concentration of polonium in tobacco leaves varies from place to place, based on soil and its transport factors ratio. The Phosphate fertilizers are also one of the sources to accumulate polonium in plants [2]. The combustion temperature of the cigarette is 800 to 900 ºC which make the polonium to convert gases state and it moves to the lungs through smoke. The smoke contains the radioactive polonium which produces the health risk to the human population. Therefore, in the present investigation study the Polonium-210 in cigarette and Beedi used by the population of Mangalore.

In the present investigation, the activity concentration of ^{210}Po from ^{210}Pb was determined by using ZnS(Ag) alpha counter with an efficiency of 30% [3-4]. The wet-ashing method was employed for the chemical digestion [9]. About 20 g of dry sample was taken in a beaker and 50 ml of 4N HNO_3 was added followed by evaporation to dryness. The adding of 3:1 mixture of HNO_3 and $HClO_4$ destroys the organic matter, 1:1 HCl first and then with concentrated HCl. The activity of ^{210}Pb was estimated through ^{210}Po by allowing the ^{210}Po plated solution for a period of 14 months for build-up ^{210}Po from ^{210}Pb. The ^{210}Po activity in different brands of cigarette varies from 9.8 ± 1.71 Bq kg^{-1} to 15.7 ± 2.06 Bq kg^{-1}, with an average value of 10.74 ± 1.74 Bq kg^{-1}. The average polonium-210 activity in individual cigarette was found to be 7.03 mBq cig^{-1}. The ^{210}Pb activity in different brands of cigarette varies 9.8 ± 1.62 Bq kg^{-1} to 16.2 ± 2.09 Bq kg^{-1}, with an average value of 12.37 ± 1.88 Bq kg^{-1}. The average lead-210 activity in individual cigarette was found to be 8.12 mBq cig^{-1}. There are plenty of cigarette brands available in the market, out of that few of them selected based on the popularity by using. The sample code indicates from CG1, CG2, CG3, CG4 andCG5 is most popular to least popular brand as per usage and price per cigarette in increasing order. The sample CG3 shows high activity of 15.7 ± 2.06 Bq kg^{-1} and about 10.90 mBq cig^{-1}. The brand CG3 is one of the most favourite brands of youths.

References:

[1]. Carvalho, F.P., Polonium (^{210}Po) and lead (^{210}Pb) in marine organisms and their transfer in marine food chains. J. Environ. Radioact. 102, (2011) 462.

[2]. Bertil R.R. and Persson Elis Holm b., Polonium-210 and lead-210 in the terrestrial environment: a historical review, Journal of Environmental Radioactivity, 102, (2011) 420.

[3]. Kaliprasad C S and Narayana Y Distribution of ^{210}Po in Hemavathi riverine environment. Radiation Protection Dosimetry, 171(2016) 282.

[4]. ZagaV, Gattavecchia E. Polonium: the radioactive killer from tobacco smoke Pneumologia, 57 (2008) 249.

Radiation Protection during ^{46}Sc-Radiotracer Injection for Sediment Transport Study at Kolkata Port, India

Pratap Singh[1§], V. Shreenivas[1], Sunil G.[2], V. K. Sharma[2] and R. V. Kolekar[1]

[1] *Health Physics Division, Bhabha Atomic Research Centre, Mumbai, India*
[2] *Isotope & Radiation Application Division Bhabha Atomic Research Centre, Mumbai, India*
[§] Email: spratap@barc.gov.in

The shipping channels at port and harbours are commonly dredged to maintain navigable depth for smooth sailing of ships. The radiotracer technique is a practical method to assess the suitability of dumping locations for the dredged sediments (which must not return to the deepened out channel by tidal movement). In this method, ^{46}Sc-glass having physico-chemical characteristics similar to the sea-bed sand is injected at desired locations and its movement is monitored for sediment transport study [1]. For this purpose, radiotracer injections at two different locations have been carried out at Kolkata Port Trust (KoPT) Hooghly Estuary, Kolkata. Working with the challenges of prevailing high radiation levels and control of occupational exposure during handling of the radiotracer in a physically limited working space on a moving ship is summarized in this paper.

Table 1. Prevailing radiation levels data

Radiation dose rates (mGy.h^{-1})	
At Lead shielded Transport Container	0.15
At the Injection System	200-700
For Operators (Handling radiotracer)-Chest Level Background	2-50

In radiotracer injections, 148-230 GBq of ^{46}Sc ($T_{1/2}$:83.8d) was used and it was transported to the injection site in a 5.5 thick lead container. The working area on-board the ship was cordoned off; floor was covered with polythene and absorbent sheets to avoid floor contamination. Five trained and skilled radiation workers equipped with suitable personal protective equipments and radiation dosimeters were involved in each injection. Each step of the injection was planned and dummy trials were performed. Subsequently, the radiotracer was taken out from the transport container, mixed with local sand with the help of 1-3 meters Cee-Vee tongs and finally injected on to the sea-bed using pneumatically controlled injection system. Radiological monitoring was carried out at each stage using a teletector with a probe extendable up to 4m and a portable contamination monitor. Radiation dose rates of up to 700 mGy.h^{-1} were measured at the injection system during the experiments. Table 1 summarizes the prevailing radiation levels during handling of radiotracer. After injection of the radiotracer, no rise in radiation level at sea level was observed above the location of injection or its vicinity. Also, the deck area was found to be free from contamination. Water samples were collected from the sea surface level above the site of injection, subsequently analysed in High Purity Germanium (HPGe) spectrometer, these samples didn"t show ^{46}Sc contamination.

The radiotracer injections were conducted with utmost care and safety precautions. Meticulous mock trials and the involvement of skilled personnel in the experiment helped in minimizing the radiation exposure and ensured that there was neither any spillage of radiotracer nor any over exposure of any of the Personnel involved. Maximum individual exposure was reported as 1.1 mSv in a radiotracer injection. The collective dose was estimated to be 5.03 man-mSv in these radiotracer injections. Moreover, despite the limitations of space, manpower and instruments available on on-board the sea-faring vessel, radiation exposure could be controlled and minimized to achieve ALARA.

Acknowledgements: Authors would like to acknowledge constant encouragement of Dr. M S Kulkarni, Head, HPD; Dr. H J Pant, Head, IRAD and Shri RKB Yadav, RSSD, BARC.

References: [1] V. K. Sharma et. at., Radiotracer investigation for bed-load movement at New Mangalore Port, Mangalore, India *J. Marine Sciences Vol. 39(1), pp. 49-56 (2010).*

Solid solubility of MoO_3 in sodium borosilicate glasses for HLW Vitrification

Sourav Maity[1,2,§], J Selvakumar[1,2], S Srinivasan[2], Hrudananda Jena[1,3,§], N.R.Jawahar[2]

[1]*Homi Bhabha National Institute, Training School Complex, Anushakatinagar, Mumbai-400094, India*
[2]*Waste Immobilization Plant, Bhabha Atomic Research Centre, Kalpakkam-603102, India*
[3]*Materials Chemistry and Metal Fuel Cycle Group, Indira Gandhi Centre for Atomic Research, Kalpakkam-603102, India,* [§]Email: sourav@igcar.gov.in
[§]Email: hnje@igcar.gov.in, sourav@igcar.gov.in

Nuclear waste immobilization is a pivotal step for the environmental protection, public acceptability of nuclear energy. In this perspective various materials have been explored to immobilize the hazardous and radioactive waste in durable matrices. Currently, in India high level radioactive waste are vitrified in borosilicate glass matrix using Joule Heated Ceramic Melter (JHCM). A sodium borosilicate glass (NBS) comprising 5- components such as 48% SiO_2-26.3%B_2O_3-11.7%Na_2O-9.5%TiO_2-4.5%Fe_2O_3 has been chosen as the matrix. 76 wt. % of this glass was mixed with 24 wt % of the simulated high level waste (HLW) and ground well for thorough mixing, then the mixture was melted at 1000°C in air ambience by melt quench method. The waste composition varies with spent fuel origin and fuel reprocessing conditions; furthermore, HLW composition may change and higher fraction of transition elements like MoO_3 in HLW are expected which may pose problem as these element have lower solubility in NBS. These elements may form separate crystalline phases inside the vitrified waste glass. Separation of various phases in the final vitrified product may change the characteristic like leaching rate, mechanical strength etc. hence, it is necessary to understand the maximum solid solubility of MoO_3 in the chosen matrix as well as its effect on the solid solubility of other fission products present in the HLW.


1.1%Mo in HLW 1.3%Mo in HLW 1.6%Mo in HLW

Fig.1 Optical images of MoO_3 loaded glasses

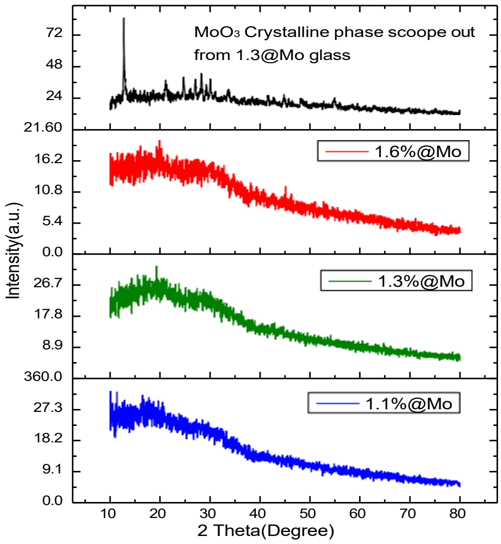

Fig.2 XRD patterns of MoO_3 loaded Glasses & precipitated crystalline MoO_3 Phase

In this study, varying compositions of Mo (Mo wt%: 0.3, 0.6, 0.8, 1.1%, 1.3%, 1.8%) in the form of MoO_3 are loaded into the NBS.The optical images of the waste loaded specimens are given in Fig.1. At higher oxide (above 1.3wt%) Mo is separated as yellow precipitate. The glass samples were characterized by X-ray diffraction (XRD) (Fig.2). It shows the glassy phase devoid of crystalline phases below 1.3 wt% of Mo (XRD patterns 1,2,3 from the bottom). But optical image shows the presence of crystalline yellow phase above 1.3 wt% of Mo loading. The XRD pattern (4th stack from the bottom) as shown in Fig.2 indicates the precipitation of excess MoO_3 in the glass matrix. Based on the observations it is found that Mo solubility is limited to < 1.3 wt.% in NBS.

Measurements of Indoor Radon and Thoron in dwellings of Kasimpur Thermal Power Plant Uttar Pradesh Using Twin Chamber Dosimeter Cups with SSNTDs

Ajay Kumar Mahur[1§], Roshan Lal Sharma[1] and Hargyan Singh[2]
[a]*Department of Applied Science, Vivekananda College of Technology and Management, Aligarh 202 001, U P, India*
[2]*Department of Physics, Sri T R Girls P G College, Aligarh 202 001, U P, India*
[§]E-mail:ajayapd1@gmail.com

The measurements of indoor radon are of importance because the radiation dose to human population due to inhalation of radon and its daughters contributes more than 50% of the total dose from natural sources and large scale studies have been carried out worldwide [1]. Thoron has only a 55.6 second half life compared to radon's 3.8 days. Thoron like radon is also a noble gas, in the thorium decay series, which means it is a free agent in the soil and can easily move out of the soil into our homes.

In Kasimpur a big coal fired thermal power plant is operational since long. Burning of coal which contains higher levels of uranium [2], the subsequent emission to the environment may cause enhancement in the ambient radiation levels. Measurements of radon and thoron levels were carried out in the dwellings around the thermal power plant. For comparison of ambient radon/thoron levels a similar study was also carried out at Aligarh which is a city near Kasimpur thermal power Plant.

Activity concentration of radon–thoron and their progeny levels in the dwellings under investigation were measured using the twin chamber Solid State Nuclear Track Detectors (SSNTDs) based dosimeters fitted with 12µm thick LR-115 type II pelicullable cellulose nitrate based SSNTDs manufactured by Kodak Pathe, France. Dosimeter cups fitted were placed in 30 rooms in different dwellings of Kasimpur and Aligarh city. From track density, Radon (C_R) and Thoron (C_T) activity concentrations were calculated using the relations and the sensitivity factor determined from the controlled experiments [3, 4]:

$$C_R(Bqm^{-3}) = \frac{T_m}{d \times S_m} \quad (1) \ \& \quad C_T(Bqm^{-3}) = \frac{(T_f - d \times C_R \times S_{rf})}{d \times S_{tf}} \quad (2)$$

Where C_R is the radon activity concentration, C_T is thoron activity concentration; T_m track density in membrane compartment; T_f track density in filter compartment, d exposure time.
Sensitivity factor for membrane compartment (S_m) = 0.019±0.003 Trc m^{-2} d^{-1}/Bq m^{-3} .
Sensitivity factor for radon in filter compartments (S_{rf}) = 0.020±0.004 Trc m^{-2} d^{-1}/Bq m^{-3}.
Sensitivity factor for thoron in filter compartment (S_{tf}) = 0.016±0.005 Trc m^{-2} d^{-1}/Bqm^{-3}

Radon activity concentrations vary from 8.4 Bq m^{-3} to 73.6 Bq m^{-3} whereas thoron activity concentrations vary from 4.1 Bq m^{-3} to 82.3 Bq m^{-3} and thus these values lie within the permissible safe limit 100 Bq m^{-3} [5].

References:

1. UNSCEAR (United Scientific Committee on the Effects of Atomic Radiation), Sources and effects of ionizing radiations, United Nations, New York, (2000)
2. Jojo, P.J., etal., *Nucl. Geophys*, 7 (1993) 445.
3. MayyaY.S., et al., *Radiat. Prot. Dosim.* 77(3) (1998) 177.
4. Sannapa, J.,et al.,s *Radiat. Meas*, 37 (2003) 55.
5. The World Health Organization WHO Handbook on indoor radon. *A public health perspective (Geneva -2009).*

EPR dosimetric properties of ‘Nd’ incorporated borate glasses: effect of sample composition

Seema Bhoir[1, §],Rajeswari B[1],Ritu Singh[1],Manoj Mohapatra[1,2]

[1]*Radiochemistry Division, Bhabha Atomic Research Centre, Trombay, Mumbai-400085*
[2]*Homi Bhabha National Institute, Anushakti Nagar, Mumbai-400094*
[§]Email: seemabhoir@barc.gov.in

Borate based glass-ceramics in pure form are rather unstable chemically because of their affinity towards moisture.This can be circumvented by the addition of suitable glass additives such as rare earths, transition metal ions etc**[1]**. As dosimetry is the backbone of radiation protection studies, there is a need for development of new dosimetric materials and processes for personal as well as industrial dose measurements. Among the various available dosimetric systems, IAEA recommends EPR (electron paramagnetic resonance) based dosimetry as the standard method for high dose measurements[2]. Often, the performance of EPR based dosimetric systems depend on the actual sample composition.

The present work deals with the EPR dosimetric properties of a novel borate based glass ceramic system doped with „Nd‟ from high dose dosimetry point of view.The borate glass-ceramic samples with varying „Nd‟content were prepared by melt-quenching technique. FTIR and EDXRF studies were done on the sample to ascertain the composition of the material. All the samples were irradiated at a constant gamma dose of 2.5kGy and the EPR experiments were carried out to know the effect of composition.

Figure 1showstheEPR spectra of the γ-irradiated sample. All the samples showed two set of signals at g=4.4374 and g=2.16. Among these, the first one is ascribed to Fe^{3+} ion present in a distorted geometry and the second one to radiation induced borate based radicals. Figure 2 shows the variation of peak intensity of the EPR signals as a function of „Nd‟ content. It can be seen from the figure that highest signal intensity was observed for the sample containing 0.5% of the rare earth ion. From the studies it can be inferred that this particular sample is best suited for radiation dosimetry in the observed dose region.

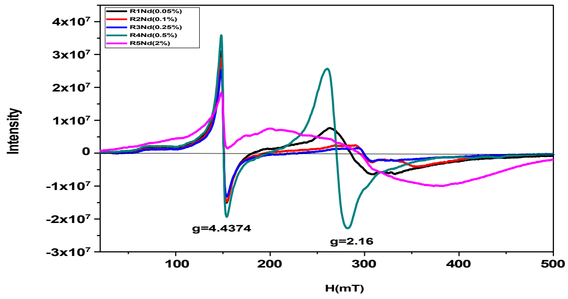

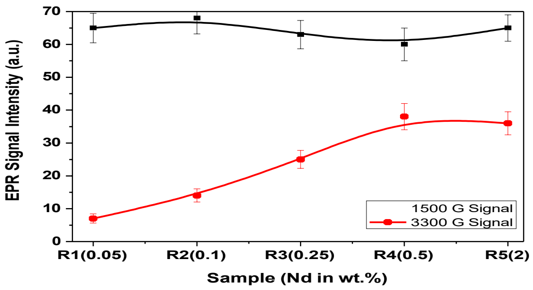

Fig1:-EPR spectra of the irradiated glass-ceramics   Fig2:-EPR Signal Intensity vsNd sample conc.

Acknowledgements-: The authors thankDr. P.K.Mohapatra, Head, RCD for his support and encouragement during the course of the work.

References:

1) M.I. Sayyed, A. Kumar, H.O. Tekin, R. Kaur, M. Singh, O. Agar, M.U. KhandakerProg. Nucl. Energy, 118 (2020) 103118
2) Kishor Mehta, Appl.Radiat.Isot. 47 (1996) 1155

Natural radioactivity levels of coal combustion residues produced in Indian thermal power plants

C. B. Dusane, Sandeep P.[§], Amar Pant, Sukanta Maity, D. K. Chaudhary, S. Mishra, Anilkumar S. Pillai and A. Vinod Kumar
Environmental Monitoring and Assessment Division, Bhabha Atomic Research Centre, Mumbai-400085, India
[§]Email*: deepu@barc.gov.in*

Abstract

Natural radiation background on the earth is mainly due to decay products of ^{238}U ($t_{1/2} = 4.5 \times 10^9$ years), ^{232}Th ($t_{1/2} = 1.4 \times 10^{10}$ years) and ^{40}K ($t_{1/2} = 1.3 \times 10^9$ years). Out of different daughter products, ^{222}Rn is the predominant contributor (50%) to the natural background radiation [1]. Phosphate fertilizers and coal combustion residue (CCR) from power plants are two by-products of human activity that can contribute to the natural background radiation locally. In the present study, CCR sampling was planned in such a way that it covers the majority of Indian coalmines. The CCR samples were collected directly from the electrostatic precipitator of thermal power plant from different states in India. CCR samples from 4 different thermal power plants were collected. These samples were placed in self-sealed polythene bags, and transported to the laboratory. In this study, high resolution gamma spectrometry system with p-type HPGe detector having a relative efficiency of 50% is used. HPGe detector was connected to 16k MCA (BOSON) through Gamma Pro spectrometry software. The CCR samples were sealed and kept for one month to establish the radioactive equilibrium between ^{226}Ra with its progenies.

The radioactivity of the samples was measured by counting the samples for 86400 seconds. The radioisotopes ^{214}Pb and ^{214}Bi that attained equilibrium in one month with their parent ^{226}Ra are considered for the measurement, whereas gamma lines of ^{228}Ac that are in equilibrium with ^{228}Ra are considered for the measurement. The gamma energy 1460.82 keV is used for the measurement of activity of ^{40}K. The activity of radioisotopes viz. ^{226}Ra, ^{228}Ra, ^{40}K estimated in CCRs collected from different states of India are presented in Table 1.

Table1. Activity in CCRs collected from different states of India.

Sample code	^{226}Ra (Bq/kg)	^{228}Ra (Bq/kg)	^{40}K (Bq/kg)
CCR-1	155.0±5.7	176.8±2.0	218.7±6.2
CCR-2	117.1±4.1	157.8±1.5	318.3±5.2
CCR-3	178.7±6.2	222.6±2.3	486.0±7.9
CCR-4	107.6±1.7	135.7±3.1	275.1±8.4

The activity levels in CCR samples are 4 to 5 times more as compared to that found in Indian coal samples. Worldwide reported natural radioactivity values in CCR samples are found to be 93-1028 Bq/kg for ^{226}Ra, 49-131 Bq/kg for ^{228}Ra, 348-1124 Bq/kg for ^{40}K. On comparing literature values with present study, it is found that natural radioactivity content in Indian CCRs are on lower side (except for ^{228}Ra) and hence, the Indian CCRs does not contribute significantly to natural background radioactivity [2].

References

[1] United Nations Scientific Committee on the Effects of Atomic Radiation, Sources and Effects of Ionizing Radiation. Report to General Assembly, AnnexB, UN, New York, 2008.
[2] A. K. Mahur, Rajesh Kumar, D. Sengupta, Rajendra Prasad. J Environ Radioact. 99 (2008) 1289–1293.

Study of Uranium and other Toxic Elements present in Coal from Coal Mines of Jharia Coalfield

A. Srivastava[1,§], N. Chauhan[1], N. Jaswal[1], N.Babbar[1], Amrit Pal Toor[2], M.Farasat[3], S. Goedert[3], Ulrich W. Scherer[3]and R.Bol[4]

[1] *Department of Chemistry, Panjab University Chandigarh, India*
[2] *Dr. SSB University Institute of Chemical Engineering & Technology, Panjab University, Chandigarh, India*
[3] *Institute for Physical Chemistry and Radiochemistry, Hochschule Mannheim, Germany*
[4]*Institute forBiosphere and Geosphere-3, Forschungzentrum Jülich, Jülich, Germany*
[§] E-mail: alok@pu.ac.in

The burning of coal is considered one of the significant sources of anthropologically driven pollution as it consists of several toxicants radiological/non-radiological which get released in the environment specially after being burned, the major pollutants being uranium, mercury and sulphur. Six samples of coal from different coal mines of Jharia Coalfield procured by the Lehra Mohabbat Thermal Power Plant in Punjab, India were collected and measured for their radiological/non-radiological toxicant content. Jharia coalfield is located in eastern part of India in the State of Jharkhand and has the largest coal reserves in India.

The measurement of concentration of radiological toxicant Uranium was carried out using the Low Level Gamma Ray Spectrometric Setup of the Institute of Physical and Radiochemistry of University of Applied Sciences, Mannheim, Germany whereas the measurement of concentration of non radiological toxicants was carried out using the ICP-MS Facility of Institute for Biosphere and Geosphere of Forschungzentrum Juelich, Juelich, Germany using standard protocol.

Table1: Concentrations of toxic elements found in the coalsamples compared with natural abundances.

Element (ppm)	JC 1 (mean)	JC 2 (mean)	JC 3 (mean)	JC 4 (mean)	JC 5 (mean)	JC 6 (mean)
As (1.5)	3.6	3.5	3.5	3.2	3.0	7.6
Hg (0.05)	0.41	0.36	0.30	0.35	0.32	0.31
Se (0.05)	15.9	11.0	14.0	10.4	13.0	11.5
Zn (4)	27.2	42.9	23.0	28.3	26.0	48.0
Mn (100)	111	68	86	193	331	700
Cd (0.20)	0.30	0.24	0.25	0.13	0.16	0.21
Cr (40)	32.0	31.4	30.6	38.6	32.0	35.0
Pb (130)	19.9	24.0	19.0	17.5	22.0	14.6
Cu (70)	26.2	30.0	24.9	29.8	33.8	36.8

It is observed that in Jharia coal U, As, Hg, Se, Zn, Mn and Cd are significantly enriched compared to their natural abundance. It is further observed that the concentration of the main pollutants namely uranium and mercury which could be determined in the present work is higher when compared to concentration value of 2 to 4.9 ppm for uranium and 0.14 to 0.18 ppm for mercury reported in literature (1-3).

Reference(s):

1. Jojo et al, *Nuclear Geophysics,***7** (1993) 445-448
2. Das et al, *Bulletin of Environmental Contamination and Toxicology*, **105**(2020) 502–512.
3. Das et al, *Journal of Environmental Science*, **100** (2021) 28-33.

Estimation of ^{14}C isoflux to the atmosphere: Impact on atmospheric $\Delta^{14}CO_2$

Sonali Yadav[1], Sabyasachi Rout[1§], Madav K. Murari[2], Rajveer Sharma[2], Amol. Chandrakar[1],
Vandana Pulhani[1], A. Vinod Kumar[1]
[1]Bhabha Atomic Research Centre, *Mumbai, India*
[2]Geochronology, Inter-University Accelerator Centre, *New Delhi, India*
§ Email: srout@barc.gov.in

^{14}C is a beta emitter of natural and anthropogenic origin with E_{max}=156.5 keV and $t_{1/2}$= 5730±40 years. ^{14}C is produced by various anthropogenic activities, including nuclear weapon testing, nuclear power plants, and the medical and research industries. As ^{14}C is chemically identical to ^{12}C it enters the carbon cycle easily and disturb the $^{14}C/^{12}C$ ratio. Hence, it is necessary to study the ^{14}C level in environmental matrices and assess its impact on atmospheric $\Delta^{14}CO_2$. The objective of this study is to measure the level of ^{14}C in different environmental matrices around the Mumbai and estimate the ^{14}C isoflux using equation (1) to see its impact on atmospheric $\Delta^{14}CO_2$.

$$\text{Isoflux} = \text{Flux (Carbon)} \times \Delta^{14}C_{DIS} \qquad (1)$$

Where, $\Delta^{14}C_{DIS}$ is the difference between reservoir and atmosphere (‰). This isoflux is used to calculate the changes in ^{14}C atmospheric budget as presented in equation 2.

$$\frac{dC_a\Delta_a}{dt} = F_r(\Delta_r - \Delta_a) + F_{oa}(\Delta_{oa} - \Delta_a) + F_{ff}\left(\Delta_{ff} - \Delta_a\right) + F_c\left(\Delta_c - \Delta_a\right) + F_n\left(\Delta_n - \Delta_a\right) \qquad (2)$$

Where, C_a is atmospheric CO_2 burden, F_r is CO_2 flux out of the terrestrial biosphere, F_{oa} is flux from ocean to atmosphere, F_{ff} is flux to the atmosphere from fossil fuel emissions, F_c is flux from natural cosmogenic production of ^{14}C and F_n flux due to atmospheric nuclear weapon testing and nuclear power plant industries and Δ is ^{14}C value of the denoted flux. For the study, samples such as air, sea water, vegetation (mangrove and mango leaves) were collected. The samples were processed and measured using Accelerator mass spectrometry (AMS) at IUAC, New Delhi, India. The isoflux values were calculated from the ^{14}C level in different environmental reservoir and are given in Table 1.

Table 1: Estimated ^{14}C isoflux and its impact on $\Delta^{14}CO_2$

Reservoir	Reported Flux F to atmosphere (Pg C y^{-1}) [1]	$\Delta^{14}C$ difference (‰)	Isoflux (Pg C ‰ y^{-1})	Impact on $\Delta^{14}CO_2$(‰ y^{-1})
Ocean (Ocean to atmosphere)	85±21	-55.405	-4709±1163.5	-5.25±1.296
Terrestrial Mangroves	52±11	24.089	1252±265	1.4±0.295
Terrestrial Mango leaves	52±11	6.077	316±66.8	0.35±0.074
Nuclear weapon Testing	8E-13	8.5E14	680	0.757
Cosmogenic Production	6.5±8E-13	8.5E14	5525±680	6.15±0.757
Fossil Fuels	6.4±0.6	-995	-6368±597	-7.1±0.665

The calculated values of isoflux were found lower than the earlier reported value of post bomb period (in 1995), which indicates a decreasing trend of difference between reservoir and atmosphere (‰) [1]. The impact of isoflux on atmospheric $^{14}CO_2$ is calculated assuming CO_2 mixing ratio of 421 ppm, preliminary inferred that, ^{14}C atmospheric budget trending towards pre bomb era. However more data is required to confirm this hypothesis.

References:

1. Turnbull, J.C., Graven, H., Krakauer, N.Y. (2016). Radiocarbon in the Atmosphere. In: Schuur, E., Druffel, E., Trumbore, S. (eds) Radiocarbon and Climate Change. Springer, Cham. https://doi.org/10.1007/978-3-319-25643-6_4

Activities of Primordial Radionuclides in the tobacco cultivated fields of Dindigul and Erode districts (Tamil Nadu, India)

M. Periyasamy[1§], S. Christobher[2], P. Athif[3], K. Jishnu[4], H.E. Syed Mohamed[5], A. Sadiq Bukhari[5]

[1]*Department of Zoology, Annai College of Arts and Scienc), Kumbakonam, Thanjavur District-612503, Tamil Nadu, India*

[2]*Department of Zoology, Nallamuthu Gounder Mahalingam College(Autonomous), Pollachi, Coimbatore District-642001, Tamilnadu, India*

[3]*Department of Zoology, M.E.S. Ponnani College, Ponnani, Malappuram District-679586, Kerala, India*

[4]*Department of Geology, Bharathidasan University, Khajamalai Campus, Tiruchirappalli - 620023, Tamil Nadu, India*

[5]*Environmental Research Laboratory, PG & Research Department of Zoology, Jamal Mohamed College (Autonomous), Tiruchirappalli-620020, Tamil Nadu, India*

[§]Email: periyasamyjrf@gamil.com

Present study has attempted to estimate the activities of primordial radionuclides such as 238U (Uranium-238), 232Th (Thorium-232) and 40K (Potassium-40) in the soil samples collected from tobacco plantations in Dindigul and Erode Districts. Rdioactivity concentrations of the collected soil samples were determined with the aid of a NaI gamma-ray detector, which ranged from BDL (2 Bqkg-1) to 20.3 Bqkg-1 for 238U, 5.1 to 156.5 Bqkg-1 for 232Th and 87.1 to 712.5 Bqkg-1 for 40K respectively with mean value of 6.41 Bqkg-1, 54.34 Bqkg-1 and 296.96 Bqkg-1 respectively. The results were also subjected to statistical analysis and found to be significant. The average activity concentrations of primordial radionuclides in the tobacco field soils of Dindigul and Erode Districts were compared with that of the reported world average values The activity concentration of 232Th in soil has found to be 6 times lower than the average world concentration (30 Bqkg-1) and the activity concentration of 40K has found to be 0.7 times lesser than the average world concentration (400 Bqkg-1) and for 238U is found to be 6 times lesser than the world average (35 Bqkg-1) which shows the levels of natural radiation in the tobacco fields are in low-levels.

Acknowledgements:

Authors were thankful to Dr. A.K. Khaja Nazeemudeen Sahib, Secretary and Correspondent, Dr. S. Ismail Mohideen, Principal and Dr. I. Joseph A. Jerald, Associate Professor and Head, Department of Zoology, Jamal Mohamed College, Tiruchirappalli for their constant support and guidance throughout the research work Period. Authors also thank UGC for funding the research project [F.No.41-96/2012(SR)]

Reference

[1] ICRP (2000) ICRP Publication 82: Protection of the public in situations of prolonged 168 radiation exposure. Annals of the ICRP Vol. 29, No. 1-2

Polymerization Kinetics and Rapid Nuclear Track Detection Properties of Novel Poly(disulfonyl diallyl carbonate) Materials

Abhijit D. Shetgaonkar[2], Diptesh G. Naik[1, §], Vinod K. Mandrekar[1], Adlete A. Mascarenhas[3], Vishnu S. Nadkarni[1]
[1] *School of Chemical Sciences, Goa University, Goa-403206, India.*
[2]*Dnyanprasarak Mandal's College and Research Centre, Assagao, Mapusa, Goa-403507, India.*
[3]*Goa College of Engineering, Farmagudi, Ponda, Goa-403401, India.*
[§] E-mail Corresponding Author: dipteshnaik@unigoa.ac.in

Incorporation of sulfur functionality (especially sulfonates and sulfones) in allyl based polymeric system have drastically changed the track detection properties of thermoset polymeric materials[1,2]. These materials have rapid track detection properties and high alpha sensitivity under chemical etching process[3]. Our recent work on developing novel poly(sulfone-carbonate) polymeric NTDs for rapid revelation of etched track have inspired us to further improvise and develop new class of sulfonyl-carbonate polymeric materials. A novel poly(disulfonyl-carbonate) copolymers for rapid detection of charged particle tracks via chemical etching has been developed. We have performed thekinetics of polymerization for 2, 2‟-Bis (2-allyl carbonate ethyl sulfonyl) diethyl ether (OESDAC) and allyl diglycol carbonate (ADC) (1:1 w/w) monomer composition. The kinetics of the polymerization reaction wasstudied by extending kinetics model developed by Dial *et. al.* for allylic monomers like ADC [4] to generate 12-hourconstant rate heating profile as shown in figure 1. To check the effectiveness of newly generated polymerization profile, correlation studieswereperformed, and the experimental results were found to be in agreement with linear correlation coefficient (R^2) of 0.9989, obtained from calculated yields (fig. 2).The polymeric detectorswereprepared by utilizing the 12 h heating profile and preliminary studies pertaining to alpha tracks/ fission fragments revelation are carried out (fig.3).

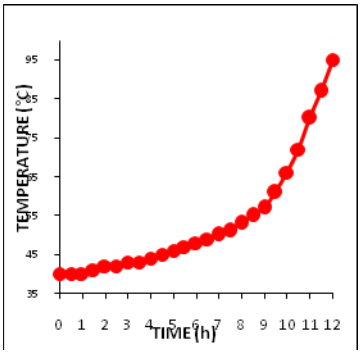

Fig.1: 12h constant rate heating profile for Poly (OESDAC-*co*-ADC) using 3% IPP.

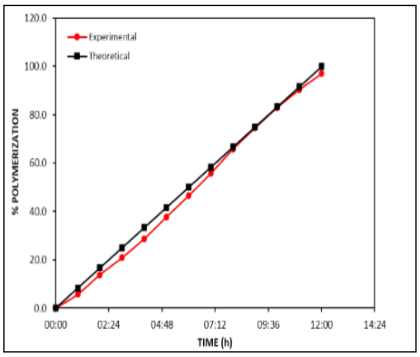

Fig.2: Verification of 12h constant rateheating profile for Poly (OESDAC-*co*-ADC) using 3% IPP.

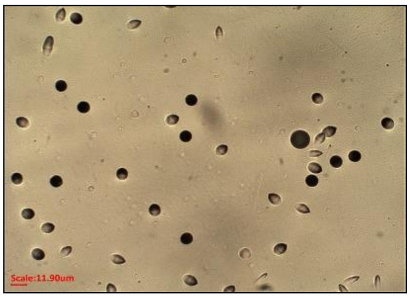

Fig.3:Alpha & fission fragments observed in poly (OESDAC-*co*-ADC) detector after 9 minutes of etching in 3N NaOH at 60°C (magnification: 40X), pre-exposed to ^{252}Cf source.

References:
[1] M. Fujii, R. Yokota, Y. Atarashi, *Int J Rad Appl Instrum D.***17** (1990), 19.
[2] V. K. Mandrekar, S. G. Tilve, V. S. Nadkarni, *Rad. Phy. & Chem*. **77**, (2008), 1027.
[3] D. G. Naik, V. S. Nadkarni, *Rad. Phy. & Chem*. **160**, (2019), 68.
[4] W. R.Dial, W.E. Bissinger, B.J.DeWitt, *et al.Ind. Eng. Chem*.**47**, (1955), 2447.
[5] V. S. Nadkarni, *Indian J. Phys*.**83**, (2009), 805.

Development of Analytical Methodology and Study of ^{14}C Release from gaseous effluents of KGS-3&4

G. S Salunke[1§], Veerendra. D[1], G.K Sunil[1], M.Seshaiah[1], B.Vinod Kumar[1]
Bharat. S[2], G.K. Nagaraja[3], N. Karunakara[4]
[1]*NPCIL KAIGA GENERATING STATION 3&4 Karnataka, 581 400*
[2,4]*Center for Advanced Research in Environmental Radioactivity (CARER), Mangalore University,* [3]*Department of Chemistry Mangalore University Mangalagangothri-574199 Karnataka, INDIA*
[§] Email: gssalunke@npcil.co.in

Introduction: This paper presents the analytical method developed for ^{14}C activity measurement from stack exhaust air using Liquid Scintillation Counting (LSC) Technique. The results obtained were compared with two different LSC Techniques. One with Traditional with two PMT (Perkin Elmer) and another with Hidex 600 SL with three PMTs which enables integration of Triple To Double co-incidence Ratio (TDCR) counting which enables automatic quench correction (colour & chemical).

Experimental setup: The cocktail used in the experiments is commercially available Gold Star (DIN (Di-isopropyl naphthalene isomer)) solvent. All samples were prepared in 20ml low potassium high performance borosilicate glass vials and counted in Perkin Elmer make Packard Tricarb 2900 TR LSAs (PELSA-1 and PELSA-2) and Hidex LSA (600 SL). In Perkin Elmer make LSAs, a quench curve was established with a set of unquenched ^{14}C standards. Transformed Spectral Index of External Standard (tSIE)is used as the quench indicating parameter. In Hidex LSA(600SL), TDCR method is used for quench correction. Background samples were prepared for sample to scintillation solution in the ratio of 1:5 and 3:15 of DM water and scintillation solution. Samples were prepared from stack exhaust air in the ration 1:5 and 3:15. Immediately after preparation, the samples were transferred to the sample chamber compartment of LSAs and allowed for one hour. Each sample was counted for one min. Background and efficiency were assessed for each LSA and Figure of Merit (FOM) was calculated. FOM was comparable in all the three LSAs. Results arrived with different sample to cocktail ratio and different LSAs is given in the following table.

LSA Make/ Ratio	^{14}C release(TBq GWe^{-1}a^{-1})	
	1:5 ratio	**3:15 ratio**
PELSA-1	0.149 to 0.365	0.083 to 0.381
PELSA-2	0.149 to 0.315	0.083 to 0.249
Hidex LSA	0.315 to 0.510	0.182 to 0.564

Conclusions: ^{14}C samples were analyzed in Perkin Elmer Make LSAs (PELSA-1 & PELSA-2) and Hidex make LSA (600 SL) with 1:5 and 3:15 ratio of sample to scintillation solution. Results arrived with different sample to cocktail ratio in different LSAs were in good agreement. Hence the ratio of 1:5 was adopted, which helps to reduce the consumption of scintillation solution. The releases measured this ratio at KGS-3&4 were in the range of 0.1 to 0.6 TBq GWe^{-1}a^{-1}. An inter comparison study of the results was carried out with **Center for Advanced Research in Environmental Radioactivity (CARER), Mangalore University** were in good agreement

References. [1]. Joshi et al. Measurement of ^{14}C emission rates from a pressurized heavy water reactor Health Physics 1986:5287-91

[2]. Optimisation of CO_2 absorption and Liquid Scintillation Counting method for Carbon-14 specific activity measurement in atmosphere Air. Applied Radiation and Isotopes 172(2021)109685. S. Bharat, N.Karunakara et al.

[3]. Carbon-14 emission from the pressurized heavy water reactor NPP at Kaiga India Journal of Environmental Radioactivity 255(2022) 107006 S. Bharat, N.Karunakara et al.

Activity Concentration of 210Po and 210Pb in Soil and Water samples of Tobacco Cultivated fields of Dindigul and Erode districts (Tamil Nadu, India)

S. Christobher[1§], M. Periyasamy[2], P. Athif[3], K. Jishnu[4], H.E. Syed Mohamed[5], A. Sadiq Bukhari[5]

[1]Department of Zoology, Nallamuthu Gounder Mahalingam College, Pollachi, (Autonomous)
Coimbatore District -642001, Tamilnadu, India
[2]Department of Zoology, Annai College of Arts and Science Kumbakonam, Thanjavur
District-612503, Tamil Nadu, India
[3]Department of Zoology, M.E.S. Ponnani College, Ponnani, Malappuram District-679586,
Kerala, India
[4]Department of Geology, Bharathidasan University, Khajamalai Campus, Tiruchirappalli -
620023, Tamil Nadu, India
[5]Environmental Research Laboratory, PG & Research Department of Zoology, Jamal
Mohamed College (Autonomous), Tiruchirappalli-620020, Tamil Nadu, India
[§]Email: christopherzoology@gmail.com

Present study has investigated the activity concentration of two radiochemicals ^{210}Po and ^{210}Pb in the water and soil samples collected from tobacco cultivated fields in Dindigul and Erode Districts. These radionuclides are all the natural radionuclides were vigorously studied because of their toxic nature and bio-accumulative property.Radioactivity concentrations of the collected soil and water samples were determined with the aid of a Alpha and Beta spectrometry probe detector. ^{210}Po in water ranged from 0.74 mBq L^{-1} to 1.26 mBq L^{-1} and ^{210}Pb in water ranged from 1.04 mBq L^{-1} to1.45 mBq L^{-1}, which revealed that the ^{210}Pb levels are higher than that of ^{210}Po in all the water samples. However the soil samples were recorded with higher level of ^{210}Po (0.86 Bq Kg^{-1} to 1.29 Bq Kg^{-1}) compared with that of ^{210}Pb (0.69 Bq Kg^{-1} to 0.92 Bq Kg^{-1}). The average activity concentrations of ^{210}Po and ^{210}Pb radionuclides in the tobacco field water and soils samples of Dindigul and Erode Districts were compared with that of the reported world average values. The radioactivity load in tobacco may depends on the activity concentration of radionuclides present in the environmental matrices.

Acknowledgements:

Authors were thankful to Dr. A.K. Khaja Nazeemudeen Sahib, Secretary and Correspondent, Dr. S. Ismail Mohideen, Principal and Dr. I. Joseph A. Jerald, Associate Professor and Head, Department of Zoology, Jamal Mohamed College, Tiruchirappalli for their constant support and guidance throughout the research work Period. Authors also thank UGC for funding the research project[F.No.41-96/2012(SR)]

References:

[1] UNSCEAR 2000. The United Nation Scientific Committee on the effects of Atomic 188 Radiation. Health Phys. 2000 Sep;79(3):314

Tight binding of Uranyl Ion in Rigid Coordination Environment in Non-Aqueous Medium

Deepa Bhardwaj[1], and Jai Deo Singh[2, §]

Department of Chemistry, Indian Institute of Technology Delhi (IITD), Hauz Khas, New Delhi 110 016, India[§]
[§]Email: jaideo@chemistry.iitd.ac.in

The chemistry of the uranyl ions forms the basis for fuel cycle, from mining uranium ores all the way to waste management and fuel reprocessing and in due course, decommissioning of power plants. Among all the actinides, the uranyl ion $(UO_2)^{2+}$ has received much attention because of its stability and is the prevalent form of natural uranium in the environment.[1] In a nuclear age and as an inorganic chemist‟s perception, the study of the uranyl ion is well defensible and cannot be limited to nuclear chemistry/ defense laboratories as it is a topic requiring deeper investigation and in particular, in academic research laboratories for new experimentation to resolve the mystifying behavior of uranyl ion. The uranyl (UO_2^{2+}) ion is classified as „*hard'* cationic species, prefers to bind „*hard'* donors like oxygen and nitrogen more strongly than the soft donors like phosphorus or sulfur.

Present investigation deals with the design and synthesis of acyclic organic species bearing (O– and N–) donor heteroatoms to examine their responsive behavior with UO_2^{2+} ion. The presence of multiple donor sites in acyclic and cyclic species bearing (O, N) donors in studies of UO_2^{2+} chemistry has largely been influenced because preferably such donor bases provide the demanding high coordination number to bind the uranyl ion with their hard O or N coordinating sites. It was reasoned that the donor species with some rigidity in the structure of the ligand backbone may display selectivity and different reaction behavior towards uranyl ion over other metal cations. Besides offering valuable experimental data for fundamental studies on the reactivity and coordination properties of the uranyl ion, the complexation chemistry of uranyl with Salophen–type donor bases has also been recognized for their potential as possible extractants and for developing uranium adsorbents and extractants in nuclear–fuel cycles.[2]

The preparation of acyclic organic species as achieved by the condensation of 1, 2–diaminobenzene and alkoxy–substituted hydroxy–benzaldehydes in ethanol under refluxing conditions. The responsive behavior of these organic donor species with uranyl ion in solution have been examined and the findings are presented herein. Under the experimental conditions, only (1:1) (M: L) complexes were obtained and the solvents (MeOH or Pyridine) used as reaction media and liberated (H_2O) molecule from uranyl salts were found to be coordinatively competitive in complexation process. For the sake of comparison, a Th(IV) complex was also isolated and its structure shows a different coordination environment compared to that with UO_2^{2+}.

References:

1. Chatelain, L.; Mougel, V.; Mazzanti, M. Ferrocene–Based Tetradentate Schiff Bases as Supporting Ligands in Uranium Chemistry. *Inorg. Chem.* **2015**, *54*, 5774–5783.

2. Leoni, L.; Cort, A. D. The Supramolecular Attitude of Metal–Salophen and Metal–Salen Complexes. *Inorganics.* **2018**, *6*, 1–17.

Estimation of radon-222 exhalation rate from soil surface in Purulia District, West Bengal, INDIA

Subhradeep Karmakar[1], Joydeep Mukherjee[1], Sushanta Sutradhar[1], Sayantan Mitra[1], Saheli Chowdhury[2], Chiranjib Barman[1] and Sonjoy Mondal[1,§]

[1]*Department of Physics, Sidho-Kanho-Birsha University, Purulia, India*
[2]*Jadavpur University, Kolkata, India*
[§] Email: sonjoymondal2009@gmail.com

The only radioactive noble gas that exists naturally in the crust of the planet is radon-222. Radon-222 is a colourless and odourless gas that permeates every part of our surroundings. Due to the uranium and radium decaying naturally, it may be found in rocks and soil. The amount of radon-222 released from soil and rock is influenced by a number of variables, including porosity, permeability, and the existence of geological faults and fractures. Moreover, the exhalation discharge of radon-222 gas from soil is greatly influenced by weather variables. The purpose of the current work is to investigate the effects of weather on radon in the area by estimating the exhalation rates of radon-222 for a 48-hour observation period from the soil surface at two different locations in Purulia district, West Bengal, in the easternmost part of the Chota Nagpur plateau region. It has been shown that the exhalation rate is favourably connected with relative humidity and negatively correlated with soil temperature. To determine the rate at which radon-222 is exhaled (E_{Rn}) from soil, we are utilising Eq. (1) [1] as

$$E_{Rn} = \frac{C_{Avg} \times V}{t_{acc} \times S} \qquad (1)$$

here, C_{Avg} = Average Radon concentration,
t_{acc} = Accumulation time
V = Volume of radon exhalation chamber (0.035 m^3)
S = Surface area covered by the chamber (0.211 m^2).

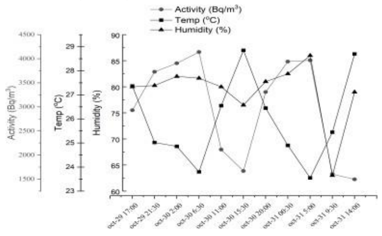

Fig. 1: Distribution of radon activity, temperature and humidity with time.

Result and Discussion:
48 hours observation and 3 hours intervals of radon exhalation in the soil from two different places (Sampling site-1 and Sampling site-2) at Purulia district, West Bengal, Indiaare calculated. The radon exhalation rate (E_{Rn}) of the Sampling site-1varies from 54.57 to 203.34 $Bqm^{-2}h^{-1}$ with a mean value 128.95 $Bqm^{-2}h^{-1}$ also the radon-222 activity of the studied area varies from 987.00 to 3677.50 Bqm^{-3} and the radon exhalation rate (E_{Rn}) of the Sampling site-2 varies from 82.66 to 219.51 $Bqm^{-2}h^{-1}$ with a mean value 151.08$Bqm^{-2}h^{-1}$ also the radon-222 activity of the studied area varies from 1495.00 to 3980.00 Bqm^{-3}.

Conclusion:

The variation of the radon exhalation rate depends significantly on local meteorological parameters. The radon exhalation appears to be negatively related with air temperature and positively related to air humidity. During this work there are no rainfall happened but dependence of soil radon exhalation on rainfall must be studied because moisture content of soil is known to affect significantly the radon emission rate from soil.

References:
[1] Vaupotic J, Gregoric A et.al., *Radon concentration in soil gas and radon exhalation rate at the Ravne Fault in NW Slovenia*, Nat Hazards Earth Syst Sci **10**(2010)895.

Study of Resuspension Factors of Radioactive Aerosols at Hotcell Facility

S.A. Yadav[1,§], P.T. Ghare[1,§] Bhaktivinayagam A[1], Vivek Kaushik[1], Atul Govalkar[1],
D.P. Rath[1], K.M.Pandit[2] Ashok Kumar P.[1] and M.S. Kulkarni[1]

[1] *Health Physics Division, BARC, Mumbai, India*
[2] *Post Irradiation Examination Division, Mumbai, India*
[§] Email: sunilk@barc.gov.in, ptghare@barc.gov.in

Hotcells of Post Irradiation Examination Division (PIED) deals with examination of different types of research as well as power reactor fuels and irradiated components. Radioactive aerosols may get airborne due to various hotcell operations. The migration of radionuclides across different environmental compartments can be studied by using Resuspension Factor (RSF). It is very useful in estimation of internal exposure from contaminated surfaces. RSF is site-specific and related to environmental parameters of the area. In this paper, RSF is estimated using ratio of airborne fraction to that of deposited contamination [1]. It holds great importance not only from the radiological protection point of view but also for environmental and radiological studies like particle size distribution, air quality measurement etc.

Hotcell isolation area was identified to study RSF due to its close proximity to the hotcells and accessibility. Air samplers with flow rate of 20 lpm, were installed at the elevation of human breathing zone [2]. Air borne activity and surface contamination monitoring was carried out in various sets considering two scenarios viz. occupied condition (during radioactive operations) and unoccupied condition (no personnel movement in the area). RSFs were evaluated using Eq. (1),

$$RSF = C_a/A \qquad (1)$$

Where C_a = Atmospheric concentration (Bq/m^3) and A = Surface concentration (Bq/m^2)

RSF values reported in literature are in the range of 10^{-4} - 10^{-8} m^{-1} for different environmental conditions[1]. The estimated resuspension factors are in the range of 10^{-5} - 10^{-7} m^{-1} (unoccupied condition) and 10^{-3} - 10^{-5} m^{-1} (occupied condition) with geometrical mean of 10^{-6} m^{-1} and 10^{-4} m^{-1} respectively (Fig. 1). It is observed that RSF values in occupied condition are higher by about two orders of magnitude to that of unoccupied condition. This work is helpful in planning and execution of radioactive operations for effective control of personnel exposure where air activity measurement is not possible or difficult to assess.

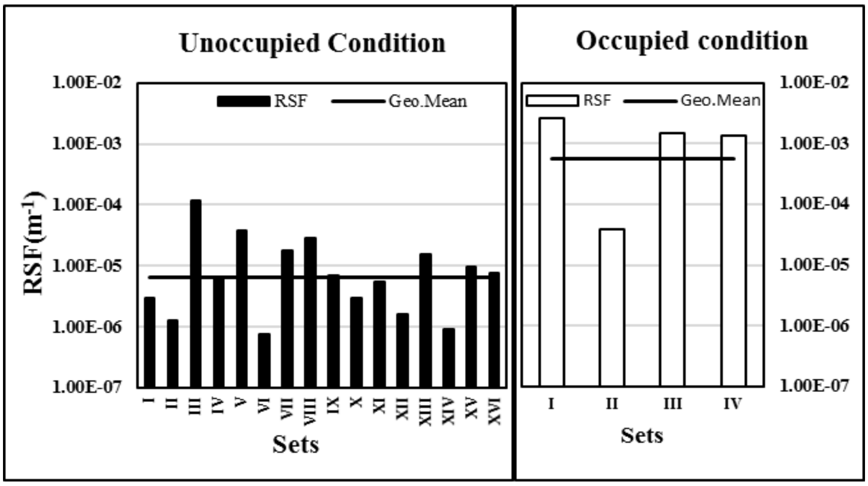

Fig. 1: RSF values of Unoccupied and Occupied Conditions

References:
[1] Herman Cember and T. E. Johnson, Introduction to Health Physics, Fourth Edition (2008).
[2] E. E. Hickey and G. A. Stoetzel, Air Sampling in the Workplace, NUREG-1400 (1993).

Radiation shielding efficacy and structural properties of Bi_2O_6W nanomaterial

B.M. Chandrika[1,2], M.R. Ambika[3§], H.C. Manjunatha[1§], L. Seenappa[1] and
A.J. Clement Lourduraj[2]

[1]*Department of Physics, Government College for Women, Kolar 563101, Karnataka, India*
[2]*Department of Physics, St. Joseph's College (Autonomous), Affiliated to Bharathidasan University, Tiruchirappalli 620002, Tamil Nadu, India*
[3]*Department of Physics, M.S. Ramaiah Institute of Technology, Bangalore 560054, India*
§ Email: mr.ambika01@gmail.com; manjunathhc@rediffmail.com

The living and nonliving systems are exposed to different radiations like X/Gamma rays, neutrons, bremsstrahlung radiations etc. in radiation environment. Exposure to high energy radiations like X/gamma rays and neutrons is of serious concern for radiation professionals as they result in several radiation hazards. Shielding plays a prominent role in reducing the radiation exposure. Attempts are being made by several researchers to explore a novel material which can effectively absorb high energy radiations and find a best substitute for lead which is known to be heavy and toxic. In the present study, authors have attempted to synthesize a novel material and investigate the radiation shielding ability and structural properties of Bi_2O_6W nanomaterial. Bi_2O_6W nanomaterial has been synthesized for the first time using green synthesis approach in order to have environmental friendly material. SEM, XRD & FTIR techniques were used to investigate the physical & chemical structure and gamma ray spectrometer to study the gamma shielding ability of the said material. Using the experimental data of material composition, neutron and bremsstrahlung shielding parameters have been estimated.

The XRD results reveal single crystal structure of the material. The mass attenuation coefficient was found to decrease with increase in photon energy due to the interaction of photons with the nanomaterial. The radiation protection efficiency is found to be high in lower energy range when compared to higher energy range of gamma photons. In addition to gamma shielding ability, the Bi_2O_6W nanomaterial is found to possess excellent neutron shielding ability and also absorbs the secondary radiations like bremsstrahlung radiations. Thus, the newly synthesized nanomaterial can be used for shielding of multiple radiations in the radiation environment thus proving its efficiency in low energy shielding applications.

Acknowledgements: The authors express their sincere gratitude to the management of M S Ramaiah Institute of Technology for funding a project through which the present study was carried out.

References:
[1] K. V. Sathish et.al., *Progress in Nuclear Energy*,**150** (2022) 104310.
[2] K. Mokhtari et.al., *Nuclear Engineering and Technology*, **53** (2021) 3051.
[3] N. Oliver et.al., *Nuclear Engineering and Technology*, **54** (2022) 3459.

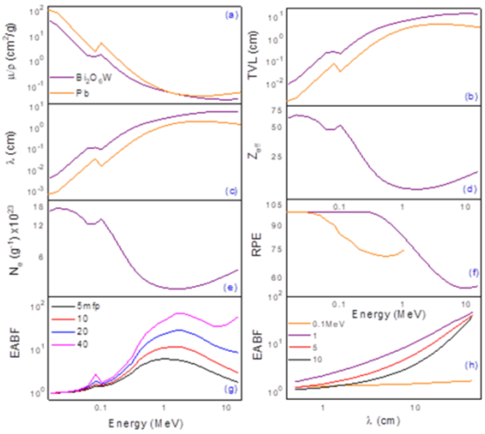

Fig.1: Radiation shielding parameters of Bi_2O_6W nanomaterial.

A Thin Film Nano-composite Scintillator for “in-field” Uranium Detection and Assay in Aqueous Samples

Sabyasachi Patra[1,§], Satyam Kumar[1], Amol Mhatre[1] and Rahul Tripathi[1,2]

[1] *Radiochemistry Division, Bhabha Atomic Research Centre, Mumbai – 400 085, India*
[2] *Homi Bhabha National Institute, Mumbai – 400 094, India*
[§] Email: spatra@barc.gov.in

Scintillators have been an important tool in the field of nuclear security, nonproliferation, and nuclear material accounting. Nanoparticle-polymer or glass composites based hybrid materials have emerged as low cost scintillators in recent years [1]. In the present work, optically transparent and water dispersible inorganic aluminosilicate nanotubes with methyl functionalized internal core (commonly known as Methyl Imogolite NTs) [2,3] have been used, for the first time, for one step sequestration and assay of uranium ions from dilute aqueous solution at ultratrace level. The NTs have been found to be efficient for capture of U(VI) ions from aqueous solutions at alkaline condition (pH = 8), which was then filtered through a microporous polyethersulphone (PES) membrane for on-top pre-concentration in the form of an ultrathin transparent film. Alpha particle tracks of uranium on a CR-39 detector confirmed the uniform spatial distribution of uranium loaded Imogolite NTs in the thin film. The thin film deposited PES membrane has been found to be self-scintillating and thus was subjected to photon counting at dark using a photomultiplier tube coupled to 1K multichannel analyzer. The recorded pulse height spectra at various U(VI) activity levels show well resolved peaks at higher pulse height due to the alpha particle scintillation compared to the background (see Fig. 1). The sample with ^{238}U activity as low as 1 mBq/mL (corresponding to U concentration in the ppb range) could be successfully assayed using the present sensor and has scope of further improving the detection limit. It is worthy to mention here that the characteristic pulse height spectrum with a well resolved peak at higher pulse height could only be obtained with the Imogolite-PES composite, but not with the individual components. This suggests the existence of an efficient alpha particle energy transfer mechanism between the different components in the composite sensor. The fast and efficient U(VI) capture using Imogolite NTs and its self-scintillating property in presence of PES membrane opens up possibilities for “in-field” detection and assay of fissile and other alpha emitting radioisotopes in aqueous samples with particular relevance to environmental remediation and nuclear forensic applications.

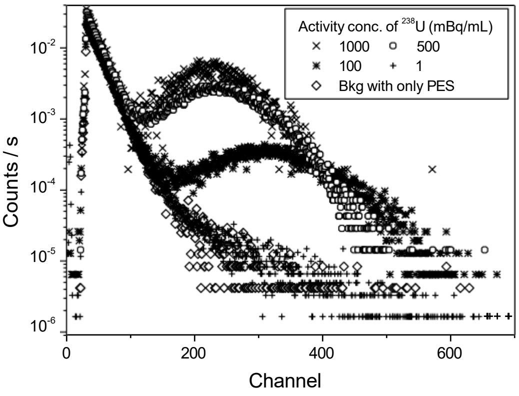

Fig. 1. Pulse height spectrum recorded in a photomultiplier tube coupled to 1K multichannel analyzer

References:

[1] Z. Kang, IEEE Nuclear Science Symposium and Medical Imaging Conference Record (NSS/MIC), 2012, DOI: 10.1109/NSSMIC.2012.6551399.

[2] D-Y. Kang, N.A. Brunelli, G.I. Yucelen, A. Venkatasubramanian, J. Zang, J. Leisen, Peter J. Hesketh, C.W. Jones, S. Nair, *Nat. Commun.*, **3342** (2014**)** 5.

[3] S. Patra, D. Schaming, P. Picot, M-C. Pignié, J-B. Brubach, L. Sicard, S. Le Caër, A. Thill, *Environ. Sci.: Nano*, **8** (2021) 2523.

GANDA: A Versatile Python Code for Non-destructive Nuclear Forensics and Assay of Sealed Radioactive Samples using γ-ray Spectrometry

Sabyasachi Patra[1,§], Satyam Kumar[1] and Rahul Tripathi[1,2]

[1] *Radiochemistry Division, Bhabha Atomic Research Centre, Mumbai – 400 085, India*
[2] *Homi Bhabha National Institute, Mumbai – 400 094, India*
[§] Email: spatra@barc.gov.in

High-resolution γ-ray spectrometry (HRGRS), due to its portability, is an important tool for in-field screening of fissile / radioactive materials in freights and personnel at borders and ports. However, its use for "in-field" absolute assay of radionuclides is limited majorly due to the unknown geometry and matrix density of the suspected seized samples and also the complexity of the HRGRS data analysis. Recently, we have proposed an iterative non-destructive assay (NDA) methodology for "on-site" assay of fissile and other radioactive materials in sealed packages, which expanded the scope of HRGRS beyond just screening and relative assay applications [1]. A quick absolute assay has been shown to be possible with reasonable accuracy in suspected packages that would help in making a quick on-site decision on the severity and the associated radiological threat of the diversion incidence. However, to use HRGRS as an "on-site" nuclear forensic tool for quick results, automation of the data analysis with minimum manual data handling is an absolute necessity. This would help in faster decision making while significantly reducing the analysis time, as well as reducing the associated risk of mishandling a large number of γ-ray measurement data.

A computer code has been developed at Radiochemistry Division, BARC with codename GANDA (**GA**mma based **N**on **D**estructive **A**ssay code) for NDA of fissile and other radioactive materials in sealed packages using HRGRS. The code is written in Python-3.8 using Numpy, SciPy and Pandas modules in Spyder environment. A supporting code has also been developed, which extracts the required measurements data at different gamma-ray energies of interest from the γ-ray peak report file (obtained from PHAST [2], a γ-ray peak fitting software developed at BARC), couple them with the respective decay data and finally save them in new data files, to be used as inputs in GANDA. The code is established based on an iterative point to extended source absolute efficiency transformation algorithm, discussed in detail in ref [1]. In order to simultaneously display and manipulate the data analysis, Pyplot in Matplotlib module has been used. The code allows the user to perform different operations necessary to analyze the HRGRS data which include construction of γ-ray energy dependent experimental and theoretical relative and absolute efficiency curves, transmission curves, as well as non-linear least square fitting of apparent mass data etc. The present code can provides both relative as well as absolute isotopic assay of U, Pu and any other γ-ray emitting radionuclide present in the sample with reasonable accuracy, without requiring the knowledge of sample geometry and the matrix. The code can also be used (or adopted easily) for more versatile applications, for example NDA of SNMs in nuclear fuel cycle, samples of environmental origin (example: contaminated soil) and others. With an aim to make the code more versatile as well as operator friendly, GANDA is in constant improvement.

References:
[1] S. Kumar, S. Patra, A. Mhatre, R. Tripathi, *Anal. Chem.*, **95** (2023) 3247.
[2] P.K. Mukhopadhya, 2001. Proceedings of symposium on intelligent nuclear instrumentation, Mumbai, p. 307.

In-house fabricated Gadolinium doped plastic scintillator for thermal neutron detection

S. Bhakta,[1] J. K. Ajish,[1§] M. Tyagi[2], Sonu[2], A. K. Chauhan[2], A. Kumar[1]

[1]*Radiation and Photochemistry Division,* [2]*Technical Physics Division*
Bhabha Atomic Research Centre,Trombay, Mumbai 400085
[§] Email: kuttan@barc.gov.in

Neutron detection and measurement is a crucial and challenging task in nuclear measurement. Its inert nature, energy dependent cross-section and complex energy spectrum makes neutron detection difficult. In nuclear industry, dose rate monitoring is crucial for workers in fuel fabrication facility, reprocessing plants, NPPs, spent fuel sites, etc [1]. Medical therapies, homeland security, material composition analysis, are some of the areas where neutron detection plays a key role. He-3 gas filled proportional counters are the most commonly used neutron detectors. They have a very small detection volume and also wide shortage of He-3 has sky-rocketed its price. Liquid scintillators are also widely used for neutron spectroscopy, but their high inflammability has restricted their field applications.

The current work is focused on synthesis of gadolinium loaded plastic scintillators (PS) for thermal neutron (n_{th}) detection. Gd has the largest n_{th} crossection than any naturally occurring element, which makes it a useful dopant in scintillators for detecting n_{th}.

$$n + Gd\text{-}155 \rightarrow Gd^{*}\text{-}156 \rightarrow Gd\text{-}156 + \gamma \text{ rays} + RX + CEe^{-} + Ae^{-} (8.536 \text{ MeV total}), \ (\sigma = 6.1 \text{x} 10^{4} \text{ b})$$

$$n + Gd\text{-}157 \rightarrow Gd^{*}\text{-}158 \rightarrow Gd\text{-}158 + \gamma \text{ rays} + RX + CEe^{-} + Ae^{-} (7.937 \text{ MeV total}). \ (\sigma = 2.6 \text{x} 10^{5} \text{ b})$$

The in house fabricated plastic scintillators were synthesized by thermal polymerization of styrene monomer using cell casting method. Commercially available styrene monomer after purification was added with suitable fluorophores and Gd salt and then polymerized at 120-140 °C. The temperature program for polymerization was designed after many trial and error experiments. The Gd doping in the PS was 0.3 wt%.

Whenever n_{th} interact with Gd, it gives low energy X-rays and conversion electrons along with continuum gamma. The low energy X-rays and conversion electrons effectively gives energy peaks around 34 keV and 77 keV. The peak about 77 keV includes about 50% interactions and integrating this peak may give about 50% detection efficiency. Therefore to get this peak, we need to calibrate the X-scale. The energy calibration was made using Cs-137 and Na-22 radioactive sources (fig. 1a). The n_{th} response was measured using 10 mCi Am-Be sources and moderated by 5 cm HDPE. The response by n_{th} was confirmed using Cd and borated rubber shielding. The gamma contribution around 77 keV can be easily stopped with Pb shielding and therefore the peak around this energy will appear only in case of n_{th} interactions. This is a preliminary study and further improvements in this system are under progress.

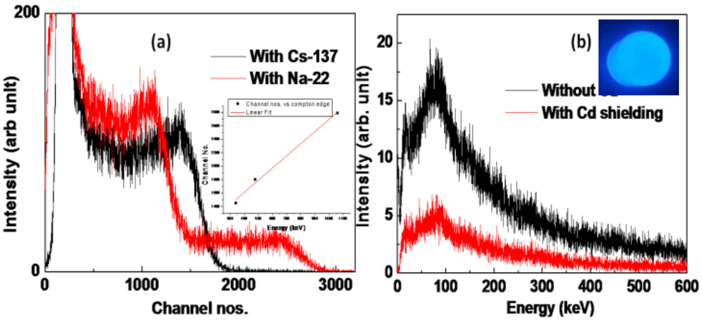

Figure 1: Pulse height spectra measured with (a) CS-137 and Na-22, (b) moderated Am-Be (Inset: Photograph of Gd doped PS)

References:
[1] J. Dumazert et. al., *Nuclear Inst. and Methods in Physics Research, A***882** (2018) 53.

Methodology for Non-destructive Assay of Heterogeneous Special Nuclear Material (SNM) Samples for Nuclear Forensic Applications

Sabyasachi Patra[1,§], Agnes M. Mani[1,2], Satyam Kumar[1] and Rahul Tripathi[1,2]

[1] *Radiochemistry Division, Bhabha Atomic Research Centre, Mumbai – 400 085, India*
[2] *Homi Bhabha National Institute, Mumbai – 400 094, India*
[§] Email: spatra@barc.gov.in

Several reports on nuclear smuggling during the past few decades have raised the need of a strong nuclear security infrastructure across the globe. This led to the rapid developments in the area of “nuclear forensics” [1]. In our recent study, we demonstrated that high resolution γ-ray spectrometry can play a key role in the “on-site” nuclear forensic investigations of suspected packages without altering their physical and chemical state [2]. Numerous challenges associated with absolute efficiency calibration and attenuation correction have been addressed by iterative way. This helps in a quick “on-site” decision making on the severity of the diversion and also the associated radiological threat.

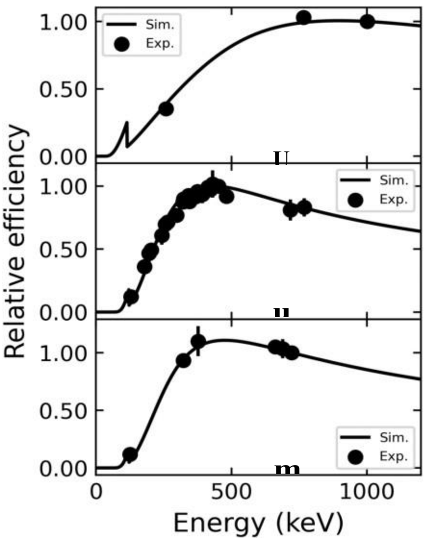

Fig. 1. Simulated and experimental relative efficiency curves for the isotopes ^{238}U, ^{239}Pu and ^{241}Am in a mock-up forensic sample.

In the present work, the methodology has been further extended for mixed actinide samples having heterogeneous distribution among different sub containments of varying density gradients. The methodology is based on an independent absolute efficiency calibration for different heterogeneously mixed actinides by an iterative “point” to “extended” source efficiency transfer approach. Geant-4 Monte Carlo simulations have been performed for point source efficiency calibration. Different mock-up nuclear forensic samples were prepared by randomly packing known standards of PuO_2 (~1 g), U-metal (~100 g) and AmO_2 (~20 mg), present in different sub-containments (SS tubes, polypropylene bag, thick Fe container etc.). The attenuation in the samples for different radionuclides has been independently solved by iterative variation of an effective SNM thickness for fitting the simulated relative efficiency curves (solid lines) to the experimental relative efficiency data (solid circles) (see Fig. 1). A few suitable forensic fingerprints have been identified using the characteristic photopeak count rate ratios to verify the heterogeneity of the samples and optimize sample-to-detector geometry. Different γ-ray emitting radionuclides in the mock-up samples were assayed using the proposed methodology without requiring the knowledge of sample geometry and the matrices. The present methodology is simple, fast and can provide reasonable estimate of actinides in complex heregeneously mixed samples, making it suitable for “on-site” nuclear forensics.

References:
[1] Z. Varga, M. Wallenius, M. Krachler, N. Rauff-Nisthar, L. Fongaro, A. Knott, A. Nicholl, K. Mayer, *TrAC Trends in Analytical Chemistry* **146** (2022) 116503.
[2] S. Kumar, S. Patra, A. Mhatre, R. Tripathi, *Anal. Chem.,* **95** (2023) 3247.

Non-destructive Assay of LEU-Pu Mixed Solutions using High-resolution γ-ray Spectrometry for Nuclear Forensic Applications

Sabyasachi Patra[1,§], Satyam Kumar[1] and Rahul Tripathi[1,2]

[1]*Radiochemistry Division, Bhabha Atomic Research Centre, Mumbai – 400 085, India*
[2]*Homi Bhabha National Institute, Mumbai – 400 094, India*
[§] Email: spatra@barc.gov.in

Uranium and plutonium are mixed in different ratios and chemical form to prepare fuels for today's nuclear reactors. U-Pu fuels of a wide variety of compositions and enrichment may be generated at different stages of fuel fabrication as well as during the reprocessing of spent fuels. In order to detect and deter diversion of those materials from regulatory control as well as to meet the requirement of "on-site" simultaneous assay of U and Pu in different stages of nuclear fuel cycle, development of suitable field-deployable non-destructive assay (NDA) methodologies are of utmost importance. Although, γ-ray spectrometry (GRS) is the most suitable NDA procedure for field application, the assay of U in presence of Pu by GRS is inherently challenging due to much lower specific activity of U compared to Pu.

In previous work, we demonstrated that Pu can be assayed in U-Pu mixed samples with reasonable accuracy using neutron multiplicity counting (NMC) and/or calorimetry, which can be used for absolute efficiency calibration of the γ-ray detector and subsequent assay of U [1]. However, in-field application of NMC and calorimetry is not preferred due to the need of bulk instrumentation and difficulty of transport. Moreover, as ^{239}Pu doesn't have detectable γ-rays above 769 keV, the efficiency calibration was not possible beyond this energy [1], making it difficult to use the most intense and interference free γ-ray of ^{238}U at 1001 keV. Recently, we developed an iterative methodology for absolute efficiency calibration over a wide γ-ray energy range (1-2500 keV) [2], which is expected to overcome the previous limitations due to its sole dependence on γ-ray spectrometry and an opportunity to use the 1001 keV γ-ray of ^{238}U.

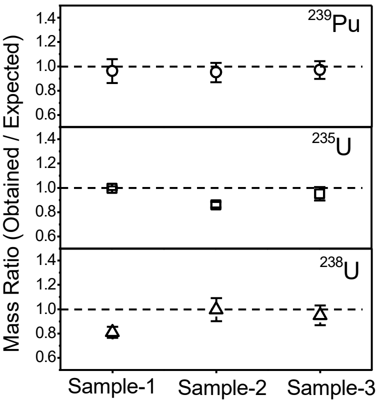

Fig. 1. Ratios of obtained to expected mass of ^{239}Pu, ^{235}U, and ^{238}U isotopes in the LEU-Pu mixed solutions.

In this work, the iterative methodology, demonstrated earlier for Pu samples of different reactor origins [2], has been extended further for the assay of LEU-Pu mixed solutions (^{235}U enrichment 15.6 %) at three different U-Pu compositions, such as 65 wt% U - 35 wt% Pu (Sample-1), 38 wt% U - 62 wt% Pu (Sample-2), and 25 wt% U - 75 wt% Pu (Sample-3). The Pu content in all the solutions was about 200 mg and the amount of U was varied. Fig. 1 gives the obtained to expected mass ratio of ^{239}Pu, ^{235}U and ^{238}U, demonstrating the capability of the present methodology to provide absolute assay with reasonable accuracy (reproduced within 10% except for ^{238}U in Sample 1, the highest attenuating sample). The ^{235}U enrichments have been found to be reproduced within 10-23%, showing its relevance for nuclear forensic applications.

References:
[1] S. Patra, R. Tripathi, P.K. Pujari, *Appl. Radiat. Isot.,* **176** (2021) 109891.
[2] S. Kumar, S. Patra, A. Mhatre, R. Tripathi, *Anal. Chem.,* **95** (2023) 3247.

Nondestructive Assay of Plutonium by Lanthanum Bromide Detector

Chhavi Agarwal[1,2§], Monica Gaur[2], Amol Mhatre[1] and Rahul Tripathi[1,2]

[1] *Radiochemistry Divison, Bhabha Atomic Research Centre, Trombay, Mumbai-400085*
[2] *Chemical Sciences, Homi Bhabha National Institute, Mumbai-400094*
[§] Email: cagarwal@barc.gov.in

The gamma ray based non-destructive assay of plutonium is used for safeguards, nuclear material accounting and for nuclear waste categorization and disposal. The gamma ray spectrum of Pu is very complex and with the age of the sample, the complexity in the spectrum increases due to the increase in ^{241}Am content in the sample. Due to this, generally HPGe based high resolution gamma ray spectrometry techniques are used for both the Pu isotopic determination and total content estimation. In the present work, the possibility to use low resolution lanthanum bromide ($LaBr_3$) detector for the assay of SNM such as Pu has been explored. The gamma ray spectra for research reactor (RR) and power reactor (PR) grade Pu samples have been acquired in $LaBr_3$ and HPGe detectors. It has been observed that due to the low resolution of this detector, a large number of gamma ray peaks of different isotopes of Pu and of ^{241}Am merge, and any distinct peak corresponding to these isotopes are not seen. The measured Pu gamma ray spectra in $LaBr_3$ detector have been used to identify useful peaks in different energy regions, and the contribution of different isotopes in these energy regions has been obtained using HPGe detector. This has been used to select three peak energy regions, namely 123-138 keV, 401-437 keV and 437-470 keV (represented as region 1, 2 and 3 respectively) with maximum ^{239}Pu contribution and absence of other Pu isotopes. The other contribution in these regions is due to ^{241}Am and hence the response in this region may change with the age of the sample. To study the effect of age on the responses in these energy regions, Pu spectra (both RR and PR grade) were simulated using GEANT4 toolkit with all the Pu and for ^{241}Am gamma ray energies given in the NNDC database [1]. It was observed that while the response of region 1 and 3 systematically varies with the age of the Pu (with variation as high as 60-70%), the region 2 response was practically constant (within 10%). This indicates that this region can be used for the assay of ^{239}Pu in sample of any age. Based on these studies, a linear response of region 2 with ^{239}Pu content could be achieved (fig.1), thereby showing the feasibility of using low resolution $LaBr_3$ detector for ^{239}Pu assay for samples of standard geometries with a maximum of 10% uncertainity/bias. This is important since ^{239}Pu is the major component in both RR and PR grade Pu sample and total Pu content can also be obtained if isotopic composition of the sample is pre-known. Further efforts will be made to take care of gamma-ray self-attenuation to assay samples with higher Pu content.

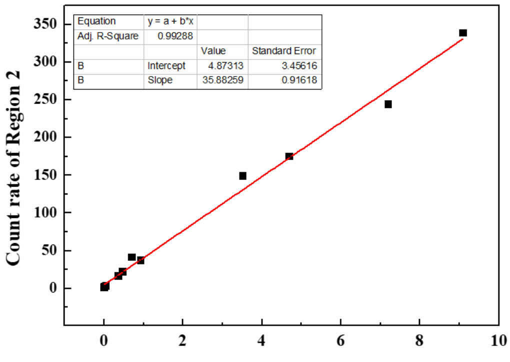

Fig. 1: Variation of count rate of peak energy region 2 (401-437 keV) as a function of Pu-239 amount.

References:

[1] National Nuclear Data Centre, Brookhaven National Laboratory retrieved from. https://www.nndc.bnl.gov/.

Machine Learning Based Approach for Identification of Significant Features for Nuclear Forensic Analysis

Shuchita Bahadur§, Jis Romal Jose and Mukesh Kumar Sharma

Radiation Safety Systems Division, BARC, Mumbai, India
§ Email: shuchita@barc.gov.in

The trafficking of nuclear and radioactive materials illicitly is a major concern for global security. Nuclear forensics has emerged as a scientific approach to identify the origin of intercepted materials involved in unauthorized events. Nuclear forensic analysis involves validating the signatures of the questioned material with reference materials, which is a multivariate analysis problem. Machine learning techniques are highly effective for such analysis, especially in scenarios involving large databases. To reduce the time required for experimentally extracting the signatures from the questioned material, it's often necessary to focus on a limited number of signatures. This paper proposes a machine learning-based approach to select the most important features (signatures) without compromising the accuracy of the analysis.

Feature selection was implemented using Extra Tree Classifier, an ensemble algorithm that seeds multiple tree models constructed randomly from the training dataset and sorts out the features that have been most voted for. The multivariate analysis of the questioned sample was implemented using a classification technique of machine learning called Multilayer Perceptron (MLP). The methodology was tested with an open literature dataset [1] of 22 mines around the world with total 565 samples on 36 minority element signatures. MLP was trained with 70% of the data and 30% of the data was used for validating the system. Extra Tree Classifiers, configured for 15 estimators, were used to enumerate relative importance score of each feature and topmost 12 of the most important features were listed. However, this method being statistical, the routine was iterated for multiple times to provide a consolidated group of selected features to be used effectively with original MLP classifier. These iterations resulted in a group of 13-19 distinct features which can be considered for analysis instead of entire feature space. Table 1 shows number of features and coressponding average prediction accuracy for that number of features. Figure 1 is one of the plots that represents all 36 signatures and the 19 red bars represent most prominent ones. The proposed approach identifies the most significant signatures for nuclear forensic analysis without compromising the prediction accuracy.

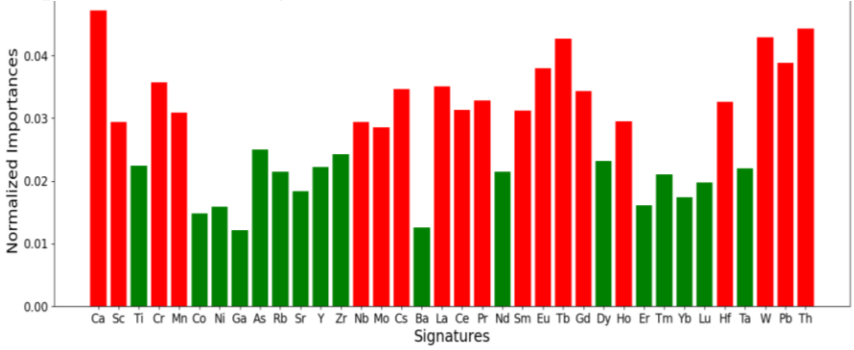

Figure 1. Normalized feature importances for the minor element signatures of mines

Number of signatures	Prediction accuracy
13	88.03%
14	90.19%
15	91.17%
16	91.54%
17	91.17%
18	91.91%
19	92.54%

Table 1. Prediction accuracy for top most signatures

Reference:
[1] https://www.mdpi.com/2075-163X/9/9/537/s1

Tellurite glass for high energy radiation shielding and effect of erbium on shielding properties

Rabina Goswami[1,§], Virendra Singh[2,*]

[1,2]*Department of physics, G.B Pant University of Agriculture & Technology,PantnagarIndia*
[§] Email: [§]rabinagoswami2001@gmail.com, [*]viren.pant@gmail.com

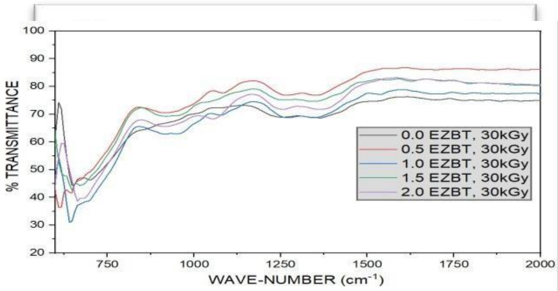

Fig: FTIR spectra of EZBT glass at 30 KGy dose

Lead and concrete are convectional gamma radiation on shielding materials. They have excellent shielding properties,however an alternative effective shielding material is required as the effect of concrete and lead are detrimentalon environment.In current study, Erbium-doped Zinc Boro-Tellurite (EZBT) glass samples of chemical composition (55-y)TeO2-25B2O3-20ZnO-yEr2O3, where value of y= 0, 0.5, 1.0, 1.5 and 2.0 mol.%, were synthesized and studied as potential gamma-radiation shielding material. Glass samples were exposed to dosages of 10 kGy, 20 kGy and 30 kGy using GC-5000 gamma irradiation chamber equipped with Co-60 source. XRD, FTIR, and UV-Vis spectroscopy were used to characterize glass samples before and after gamma irradiation. Theradiation-shieldingparameterswere also theoretically estimated using WinXCom software.The amorphous nature of the glasses was confirmed by the XRD spectra of all EZBT samples. FTIR results have revealed theminor changes in positions of bands, indicating glass matrix retains its structure and shows good corresponds to the conversion of TeO_4 into TeO_3 units which indicates the increase in Non-bridging oxygen(NBOs).Band above 1300 cm^{-1} show the conversion of BO_4 units to BO_3 units, after gamma irradiation and erbium inclusion, indicating the creation of more NBOs.IR absorption increases after gamma irradiation because samples become more polar after creation of NBOs. Density, a crucial shielding characteristic was foundincreasing with erbium doping and thedensity values were even greater than lead glasses and concrete.The impact of irradiation on the optical characteristics of glass samples was examined using the UV-Vis technique. Peaks at same wavelength were visible in the absorption spectra both before and after irradiation, however the intensity have been changed after gamma irradiation. This might be the result of creation of excess charge carriers created by ionizing radiation and thus absorbing more UV-Vis light. It was discovered that when erbium doping increased, the energy band gap shrank. Out of all fabricated samples, 2.0 EZBT was found to be the better shielding material, according to WinXCom results2.0 EZBT glass sample has a greater mass attenuation coefficient,smaller HVL, higher Z_{eff}than ordinary concrete and lead glasses. Sooourstudy shows that EZBT glass is a promising material for gamma radiation shielding.

Density of EZBT glasses

Samples	Density (g/cm^3)
0.0 EZBT	4.638
0.5 EZBT	5.021
1.0 EZBT	5.189
1.5 EZBT	5.351
2.0 EZBT	5.530

References:

Zulkefly SS, Kamari HM, Abdul Azis MNA, Wan Yusoff WMD**.** 2016. Influence of erbium doping on dielectric properties of zinc borotellurite glass system. *Materials Science Forum*. 846:161–71

Assay and identification of plutonium of different grades present in sub-Becquerel level by fission track technique

Amol Mhatre[1§], Chhavi Agarwal[1,2], and Rahul Tripathi[1,2]

[1] *Radiochemistry Division, Bhabha Atomic Research Centre, Trombay, Mumbai-400085*
[2] *Chemical Sciences, Homi Bhabha National Institute, Mumbai-400094*
[§] Email: amolm@barc.gov.in

Alpha activity estimation in sub-Becquerel level is required for environment and forensic applications. In our earlier work, scintillating polyethersulfone (PES) based polymer inclusion membrane was successfully tested for ~100 mBqmL^{-1} Pu estimation [1]. The detection limits were further lowered upto ~0.5 mBqml^{-1} by ion-imprinted polyethylene terepthalate (PET) sheet [2]. Along with the assay of total Pu present in low activity level, it is important to identify the grade of Pu which may help in obtaining information about its origin and history. In the present studies, an attempt has been made to use fission track technique in combination with the scintillation measurement, to get fission track to gross alpha activity ratio. The latter can be possibly treated as an indication of the grade of Pu in the sample if selective and quantitative extraction of Pu in presence of Am is achieved. In this work, the developed ion-imprinted PET substrates [2] were used for selectively quantifying total Pu in ~10-500 mBq activity range. These PET samples were loaded with Pu of both the research (RR) and power reactor (PR) grade and were quantified using alpha based scintillation counting. The PET samples along with Lexan SSNTD film, were then irradiated in Pneumatic Carrier Facility (PCF), Dhruva, BARC, Trombay. Along the Pu loaded samples, blank PET samples and a Ni foil were also irradiated. After irradiation, the fission tracks were revealed by etching the lexan fims in 6 molL^{-1} at 60ºC for 50 mins. The samples were randomly scanned to under 10x and 40x magnifications.

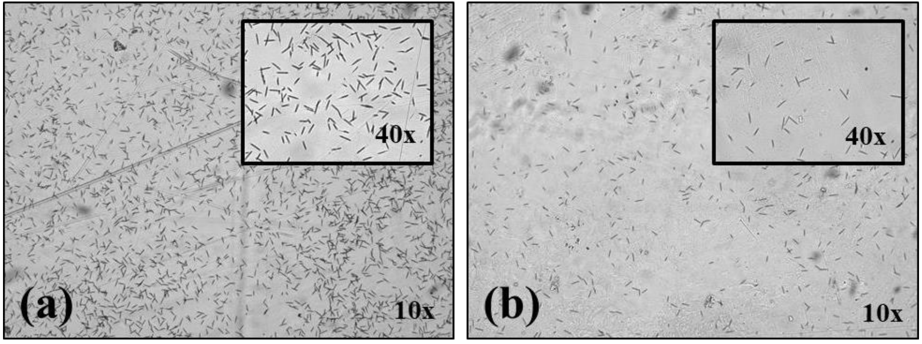

Fig. 1: Fission track images in lexan for (a) research and (b) power reactor grade Pu.

Fig. 1 shows the fission track images of the lexan film corresponding to the PET samples loaded with RR and PR grade Pu. As seen from the figure, the track density in RR grade sample is much higher than the PR grade sample. The fission tracks are a result of n-induced fission of ^{239}Pu mainly, which is higher in a RR grade Pu sample, and hence higher track density for equivalent total Pu content. Also, as seen from the 10x images of both the grade Pu samples, uniform distribution of tracks is observed.

References:
[1] A. Mhatre, C. Agarwal, R. Tripathi, poster G66, 15th Biennial DAE BRNS Symposium Nuclear and Radiochemistry (NUCAR-2021), Feb.22-26, 2022, BARC, Mumbai.
[2] A. Mhatre, C. Agarwal, R. Tripathi, Preparation of the imprinted PET sheet and its study in the low level alpha activity estimation, SESTEC.

Multifiller based polymer composites for shielding high energy ionising radiation

Sherry Shajan Kuttukaran[1], M. R. Ambika[1], N. Nagaiah[2§] and S. K. Shashi Kumar[2]

[1]*Department of Physics, M S Ramaiah Institute of Technology, Bengaluru-560054, India*
[2]*Department of Physics, Bangalore University, JB Campus, Bengaluru-560056, India*
[§] Email: nagaiahn@rediffmail.com

Radiation professionals working in the radiation environment have to follow principles of radiation protection, as the effects of high energy radiation would be severe over a long run. Hence, there is a serious concern towards minimising the radiation exposure. An efficient shielding material will rescue the personnels from this exposure. Attempts are being made by several researchers in fabricating a novel, light weight and effective gamma radiation shield. In the present study, the authors have attempted to fabricate multi-layered polymer composites with different filler in each layer. Polydimethyl silicone rubber was selected as matrix due to its potential property of being flexible moreover thermal and radiation resistant. High Z metals like Bismuth and molybdenum were selected as reinforcers as these are known to be excellent material in absorbing high energy ionising radiations like X/Gamma rays. Accordingly, 3 layered composites with PDMS+Bi+Mo were fabricated by simple open mold cast technique ie., 1MMB (10Mo+10Mo+10Bi in phr) & 2MMB (20Mo+20Mo+20Bi in phr) The structure of the composites was studied using XRD & FTIR technique. Gamma shielding parameters like attenuation coefficient, HVL thickness, relaxation length and other parameters like Z_{eff} & N_e were estimated for the said novel material.

The results reveal that, the linear attenuation coefficient (LAC) increases with addition of Bi & Mo and is found to be 0.653, 1.341 & 1.017, 1.793 & 0.102, 0.152 cm^{-1} for 1MMB & 2MMB polymer composites at 80keV, 356keV and 662keV gamma rays respectively. Since, the filler particles are of high dense & high Z materials, the probability of photons interacting with the material medium is high resulting in high attenuation coefficient. The HVL thickness of the materials is found to be 1.06, 0.51 & 0.68, 0.38 & 6.73, 4.532 cm for 1MMB & 2MMB at these energies respectively. The mass attenuation coefficient (MAC) of the novel composites 1MMB & 2MMB is found to be higher than the conventional materials like Lead and barite for 356 keV gamma rays. Inspite of adding high dense material, the material is found to be light weight and moreover flexible. Thus, the material can be molded into protective garments in the form of aprons, gloves etc. The novel, flexible, light weight and efficient material can be used for shielding of high energy ionising radiations like X/Gamma rays, thus being a substitute for the material Lead which is known to be heavy and toxic by nature.

Acknowledgements: One of the authors, Ambika M R, would like to express her gratitude for Ramaiah Institute of Technology for funding a project through which the present study has been carried out.

References:
[1] S. Alshahri, et al., *Polymers*, **13** (2021) 3081.
[2] M. R. Ambika and N. Nagaiah, *Chemistryselect*, **7** (2022) e202201214.

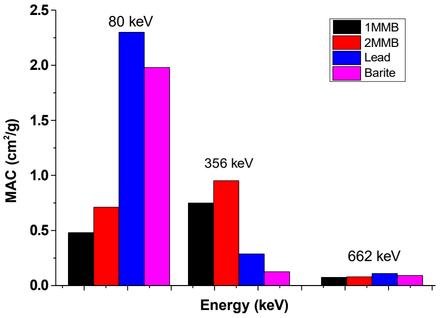

Figure1: Comparison of MAC

Simulation of scintillator shape and geometry for fast timing applications

K. Dhankar[1], K. R. Parthasarathi Hebbar[1], K. R. Sathya Krishna[1], Karthik Shastry[1], S. Mukherjee[2, §]

[1] *RV College of Engineering, Bengaluru, India*
[2] *Radiochemistry Division, BARC, Mumbai, India*
[§] Email: mukherjees@barc.gov.in

Development of next generation of ultra-fast scintillators is an active research area for its application in medical imaging [1], high energy physics [2] and astrophysics [3]. While various new and conventional candidates are proposed for eg MOF based scintillators [4], LaBr3(Ce), CeBr3, plastic scintillators etc, the effect of geometry on these new breed of scintillators has not been thoroughly studied. We have used FLUKA [5] simulation code to produce, transport and emit optical photons in various detector materials such as- plastic scintillator (EJ 228), BaF_2 and LaBr3(Ce). All the scintillators were stimulated by a point like source of gamma rays of energy ~ 1 MeV. The timing distribution of the optical photons from the „exit" surface was monitored by various FLUKA based user routines. The effect of – (a) optical photon reflection/absorption at various surfaces & (b) inelastic or elastic scattering was studied as a function of scintillator thickness and diameter for cylindrical geometry. For the next stage, we studied the effect of varying shapes such as truncated cone and cylinder on the timing properties. Effect of surface roughness or wrapping (Teflon, Tyvek) on the arrival time of optical photons was simulated. Our results will be beneficial for deriving optimum timing benefits from the new and emergent composite based scintillator materials [2, 6].

References:
[1] Lecoq, Paul. "Development of new scintillators for medical applications." Nuclear Instruments and Methods in Physics Research Section A: Accelerators, Spectrometers, Detectors and Associated Equipment 809 (2016): 130-139 ; Van Eijk, Carel WE. "Inorganic scintillators in medical imaging." Physics in medicine & biology 47, no. 8 (2002): R85
[2] Nikl, Martin, and Akira Yoshikawa. "Recent R&D trends in inorganic single-crystal scintillator materials for radiation detection." Advanced Optical Materials 3.4 (2015): 463-481. Hajagos, Tibor Jacob, et al. "High-Z sensitized plastic scintillators: a review." Advanced Materials 30.27 (2018): 1706956.
[3] Bloser, Peter F., et al. "Scintillators with silicon photomultiplier readouts for high-energy astrophysics and heliophysics." Space Telescopes and Instrumentation 2014: Ultraviolet to Gamma Ray. Vol. 9144. SPIE, 2014.
[4] J. Perego, I. Villa, A. Pedrini, E. Padovani, R. Crapanzano, et al.. Composite fast scintillators based on high-Z fluorescent metal–organic framework nanocrystals. Nature Photonics, 2021, 15, pp.393-400.
[5] Ahdida, C., et al. "New capabilities of the FLUKA multi-purpose code." Frontiers in Physics (2022): 705; Battistoni, Giuseppe, et al. "Overview of the FLUKA code." Annals of Nuclear Energy 82 (2015): 10-18; Vlachoudis, Vasilis. "FLAIR: a powerful but user friendly graphical interface for FLUKA." Proc. Int. Conf. on Mathematics, Computational Methods & Reactor Physics (M&C 2009), Saratoga Springs, New York. Vol. 176. 2009.
[6] Shevelev, V. S., et al. "Ultrafast hybrid nanocomposite scintillators: A review." Journal of Luminescence 242 (2022): 118534.

Fabrication of experimental setup for qualification of Pulsed Eddy Current sensor for creep measurement in molten metal environment.

T. V. Shyam[1,2,§], Archana Sharma[2], V. H. Patankar[2], Ankur Kaushik[3], K. K. Panda[3], A. Basak[3] , S.K. Apraj[1] and Nirupam Das[1]

[1] *Reactor Engineering Division, Bhabha Atomic Research Centre, Mumbai-400085, India*
[2] *Homi Bhabha National Institute, Mumbai-400094, India*
[3] *High Temperature Reactor Section, Bhabha Atomic Research Centre, Mumbai-400085, India*
[§] Email: tvshyam@barc.gov.in

A creep measurement sensor is designed and fabricated, based on pulsed eddy current testing technique, for its use in mechanical properties testing of metallic alloy test specimens to be used in future generation nuclear reactors. The signals of the pulsed eddy current sensors, which are kept opposite to the test specimen, are analyzed by deriving the slopes of the signals in the vicinity of Lift off point of Intersection (LOI) region for estimating the creep of test specimen indirectly. The paper describes about the design details of fabrication of the experimental test setup (as shown in Figure No.1) meant for qualifying the performance of pulsed eddy current creep sensor in molten metal coolant environment.

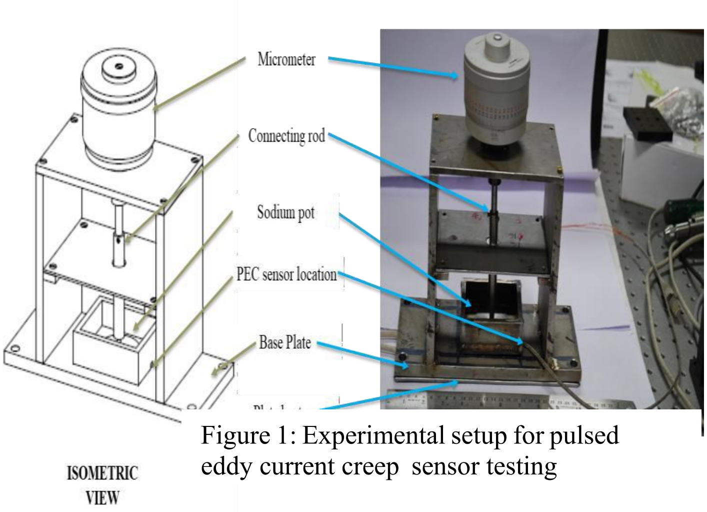

Figure 1: Experimental setup for pulsed eddy current creep sensor testing

The sensor, which can withstand up to 220 ̊C was embedded in the bottom face of tank. Initially testing was carried out without molten metal and checked for the performance of the sensor for predetermined gaps between sensor face and test specimen. The test setup was transferred to Glovebox having controlled moisture and oxygen environment. Further experiments were carried out with molten metal and feasibility of creep measurement of test specimens in molten metal medium with pulsed eddy current technique was established. The pulsed eddy current signals for varying gap of molten metal medium are shown in Figure No.2.

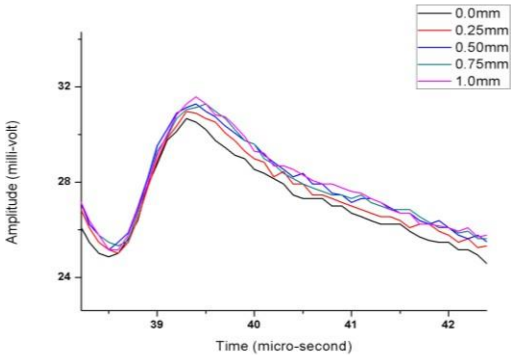

Figure 2: Pulsed Eddy current sensor signals for varying gap of molten metal

References:

[1] T V Shyam, A Sharma, V H Patankar, A Kaushik, S K Sinha and L Ferry, Experimental study of different innovative measurement methodologies applied to a canned pulsed eddy current testing probe suitable for dilation measurement of test specimens, Insight- Non Destructive testing and condition monitoring Journal, Volume 65, No.2, February 2023.

Development of liquid scintillation counter for alpha and beta counting

N.S.Tawade[1,§], S.C.Vishwasrao[2] and S.Sodaye[1]

[1]*Radiochemistry Division, Bhabha Atomic Research Centre,Mumbai, India*
[2]*Product Development Division, Bhabha Atomic Research Centre, Mumbai, India*
[§] Email: nstawade@barc.gov.in

Liquid scintillation counting is an analytical technique for quantitative measurement of α and β activity emitted from radioactive samples. A new low background liquid scintillation detector has been designed and developed. Additional features have been incorporated in this setup. A new safety interlock has been developed for protection of photomultiplier tube (PMT) to shutdown high voltage during sample changing and the bleeder circuit with negative bias operation mode to avoid DC blocking capacitor.

A perplex rod of coaxial shape with one end flat and other end semi-concaveis used as sample holder which is further couple to semi-convex shaped PMT with proper optical coupling for transferring scintillation light signal to PMT. The perplex rod has been coated with titanium (very small critical angle of reflection) to avoid leakage of scintillation energy from perplex rod. The entire assembly has been made light leakage proof by covering with light absorber black tape. This assembly has been covered in aluminum box which will cut low energy radiation entering inside this cavity (mainly lead x-rays coming from the shielding used to cover this entire assembly).

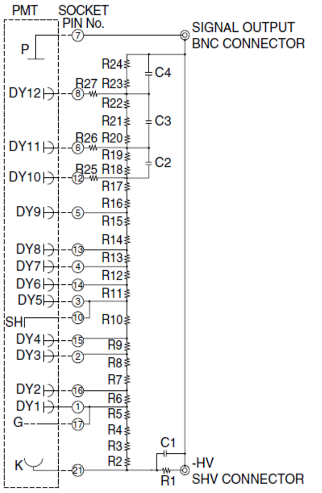

R1:10kΩ, R2-R6& R9-R13:220kΩ, R7-R8:154kΩ, R14-R21 & R23-R24:110kΩ, R25:51Ω, R26-R27:100 Ω, C1:470pF, C2-C3:10nF, C4:22nF

Figure.1:PMTBleeder circuit

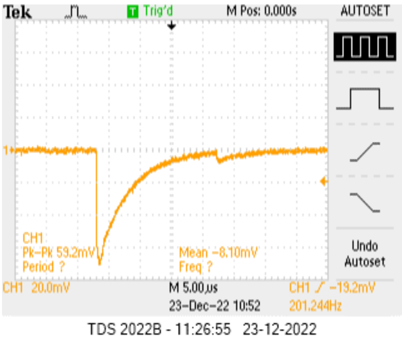

Figure.2:Preamp pulse

The PMT has 12 stage dynodes to obtain an electron multiplication of ~10^6. A high voltage bleeder circuit has been designed with chain of registers as shown in figure 1, which can sustain a bias voltage of 2000 V. The op-amp based preamplifier circuit has been developed to process the pulse signal obtained from PMT. The characteristic preamplifier pulse output is shown in figure 2. The output pulse has a pulse height 70 mV with 17 µs decay time for an alpha radiation emitted from ^{241}Am source. This preamplifier output pulse is converted into a TTL pulse using comparator circuit to count number of radiation events. This abstract discusses the instrumentation aspects of the development of the liquid scintillator.

Acknowledgements: Authors thank the workshop members of RC&IG for their support during fabrication of Perspexsample holder. Acknowledgements are due to Head, RCD for his keen interest and constant encouragement.

References:

[1] G. F. Knoll, *Radiation detection and measurement*,**3rd edition** (2009).
[2] Data sheet of Photomultiplier tube R331-05 Make: Hamamatsu Photonics (www.hamamatsu.com).

Development of Thermal Neutron Detector With Excellent n/γ Discrimination Capability Based on CsI:Tl Scintillator

Shiv Govind Singh[1,2,§], Durgesh Sisodiya[1,2], Giri Dhari Patra[1], Shreyas Pitale[1], Manoranjan Ghosh[1], Shashwati Sen[1,2], L. M. Pant[1,2]

[1] *Technical Physics Division, Bhabha Atomic Research Centre, Trombay, India*
[2] *HomiBhabha National Institute, Mumbai, India*
[§] Email: sgovind@barc.gov.in

Thermal neutron detection has importance in both neutron scattering experiments and homeland security [1]. Several isotopes are available for thermal neutron detection like ^{10}B, ^{6}Li,^{3}He and ^{157}Gdbecause of their high cross-section for low-energy neutron capture [2]. The availability and cost of ^{3}He and gamma transparency of other detectors is driving researchers to go for better and cost effective solutions for thermal neutron detection with n/γ discrimination capability. There are several inorganic scintillators containing^{6}Li like LiI:Eu, $LiCaAlF_6$:Ce, $LiAlO_2$, $LiGaO_2$, $LiBaF_3$:Ce, Cs_2LiYCl_6 and $Cs_2LiLa(Br,Cl)_6$etc that are being used for thermal neutron detection. However most of them are either hygroscopic or costly or lacks n/γ discrimination capability.

We have developed a composite type neutron detector which is cost effective, non-hygroscopic, scalable and have excellent neutron-gamma discrimination ability. CsI:Tl is used as the scintillating material in a particular configuration where a thin layer (50-100 micron) of neutron converting material (Li based like LiF, Li_2CO_3) is sandwiched between the CsI:Tl plates (0.5-1 mm thick). CsI:Tl has good pulse shape ability for gamma and alpha radiation (produced on ^{6}Li $(n,\alpha)^{3}$H reaction). We have used Li_2Co_3 and LiF as neutron sensitive material and performed the neutron detection at RSSD, BARC STAG facility using Am-Be neutron source. A figure of Merit of 2.9 has been achieved in n/γ separation and an efficiency up-to 8% (with natural Li) for thermal neutrons has been achieved. Efficiency may be further improved by optimizing the interlayer CsI:Tl thickness and the enrichment of Li. It is estimated that with 0.5mm CsI:Tl interlayer thickness and 90% ^{6}Li enrichment a detector efficiency of around 50% can be achieved for thermal neutrons.

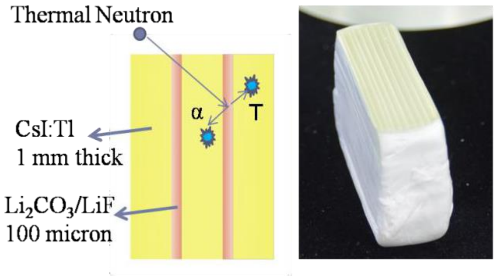

Fig1: CsI:Tl-LiF based neutron detector.

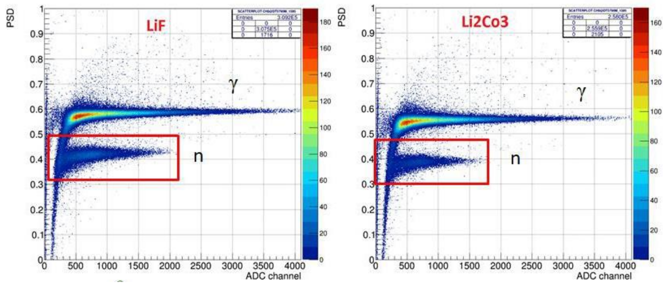

Fig.2 Pulse shape discriminnation ability of CsI:Tl for alpha and gamma.

References:

[1]. G van Eijk, C. W. (2004). Inorganic scintillators for thermal neutron detection. *Radiation Measurements*, *38*(4-6), 337-342.

[2]. Cieślak, Michał J., Kelum AA Gamage, and Robert Glover. "Critical review of scintillating crystals for neutron detection." *Crystals* 9.9 (2019): 480.

Calibration of alpha spectroscopy based Radon Progeny Monitor

R. P. Rout[1, §], R. Mishra[1,2], R. Prajith[1], A. T. Khan[1] and B. K. Sapra[1,2]

[1] *Radiological Physics and Advisory Division, Bhabha Atomic Research Centre, Mumbai - 400085, INDIA*
[2] *Homi Bhabha National Institute, Anushaktinagar, Mumbai 400094, INDIA*
[§] Email: rprout@barc.gov.in

Being radioactive and particulate in nature, inhalation of ^{222}Rn (Radon) progeny imposes carcinogenic risk and hence it is important to carryout precise measurement of its activity concentration [1]. We have designed an alpha spectroscopy based portable, low cost ^{222}Rn progeny monitor (RPM) using Si PIPS detector. The design, calibration and its comparison with other commercially available progeny monitors are described in the present study.

Design and calibration of the Radon Progeny Monitor (RPM)

The schematic diagram of the RPM consisting of a Si PIPS detector (10 mm x 10 mm) with a source holder and the detector electronics is shown Fig 1a.

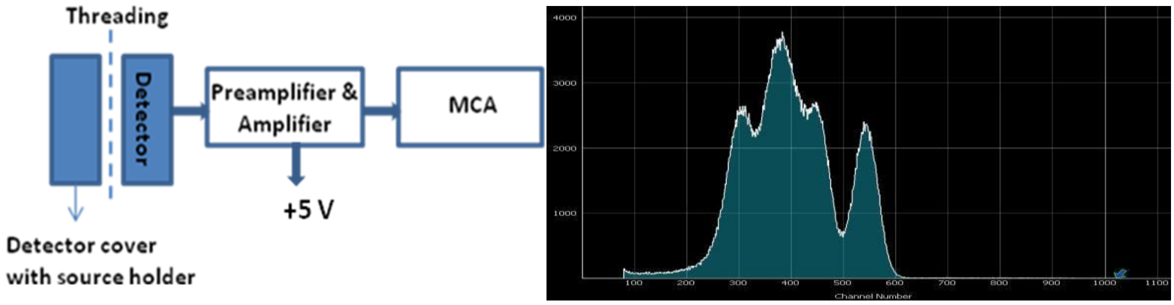

Fig 1 (a) Schematic diagram of RPM and b) ^{229}Th spectrum obtained using RPM

Energy calibration of the RPM was carried out from the spectrum (shown in Fig 1b) obtained using ^{229}Th disc source having multiple alpha energies of 5.8 MeV, 6.3 MeV, 7.1 MeV and 8.4 MeV. Efficiency of the detector was also determined from the obtained spectrum for 8.4 MeV alpha energy and was found to be 20.25 %.

Measurement of ^{222}Rn progeny activity concentration: An experiment was carried out in an 8 m^3 calibration chamber with radon source (Pylon make) in which sampling of airborne radionuclides was carried on a Filter Paper (FP) at a flow rate of 5 lpm. The progeny activity deposited on the FP was measured using RPM, ZnS alpha counter and Working Level monitor (WLM). The results are shown in Table 1 which shows a very good agreement.

Table 1. ^{222}Rn progeny concentration (C) measured using RPM, ZnS counter and WLM

	C (Bq/m^3)		
	RPM	ZnS alpha counter	WLM
Set-1	4796±10	4815±12	4780±9
Set-2	105±3	108±5	102±2

References

[1] WHO (2009), Handbook on indoor radon: a public health perspective

Single crystal growth of Tl doped Sodium Iodide (NaI:Tl) and in-house design, fabrication of gamma detector for field application

G.D. Patra[1], S.G. Singh[1,3], M. Sonawane[1], A. Gupta[2], J. Romal[2], M.K. Sharma[2,3], S. Sen[1,3, §]

[1]Technical Physics Division, Bhabha Atomic Research Centre, Mumbai-400085
[2]Radiation Safety Systems Division, Mumbai-400085
[3]Homi Bhabha National Institute, Anushakti Nagar, Mumbai-400094
[§] Email: shash@barc.gov.in

Thallium doped Sodium iodide (NaI:Tl) is the oldest [1] and most widely used scintillator materials to date. It is commercially available and is imported in huge numbers for application in DAE. Under the auspice of Atma Nirbhar Bharat it has been decided to develop gamma detectors using in-house grown NaI single crystals. Here we report the successful growth of 2 inch diameter single crystal of (NaI:Tl) and indigenous fabrication of full detector assembly by coupling the crystal with phtomultiplier tube (PMT), compatible preamplifier and hermetically sealing in an aluminum housing. The signal processing was done though Backpack Gamma Spectrometer System (BGSS) also developed in BARC [2]. NaI(Tl) crystal are grown using the Bridgman/Stockbarger crystal growth technique (Fig. 1(a)). The grown crystals are of 50 mm diameter and 70 mm in length. Due to hygroscopic nature of NaI, crystals were processed in a moisture controlled glove box. For hermetic sealing of the crystals with the PMT an aluminum casing was designed and fabricated locally. For signal processing a preamplifier board was also designed (Figure 1(b)). The full detector assembly consisting of the NaI crystal, PMT and preamplifier was housed inside the aluminum casing (Fig 1(C)). The detector assembly was connected to RSSD/BARC developed BGSS for gamma spectrometry (Fig 1(d)). These detectors have been tested inside the lab and in field condition with an energy resolution better than 7.5 % at 662 KeV which is comparable to commercial detectors (Fig 1(e)). Ten numbers of such detector assemblies have been successfully tested and will be employed for homeland security.

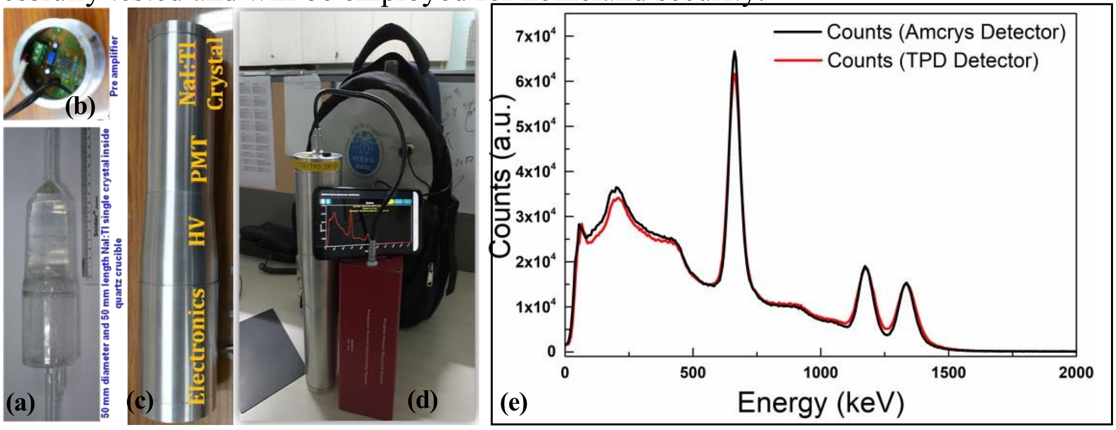

Fig 1: (a) Photographs of Grown Crystal, (b) Preamplifier board, (c) detector assembly and (d) Backpack Gamma Spectrometer System (BGSS) (e) Detector performance compared with the commercial detector.

References:
[1] Robert Hofstadter, Phys. Rev. 75, 796 Phys. Rev. 75 (1949) 1611
[2] A. Gupta, J. Romal, M.K. Sharma, J.P. Parmar, P. Chaudhury, M.S. Kulkarni, (Ed.). (2018). Design and development of FPGA based backpack gamma spectrometer. India: Indian Association for Radiation Protection.

Comparison of counting efficiencies of Shadow Shield Whole Body Monitor for PaediatricBOMAB and Reference Computational Phantoms

Rahul Roy§, H. K. Patni, P. K.Singh and P. D. Sawant

Internal Dosimetry Section, Radiation Safety Systems Division,
BARC,Trombay, 400085, India
§ Email: rroy@barc.gov.in

The Shadow Shield Whole Body Monitor (SSWBM) is a partially shielded system used for the assessment of internal dose to occupational workers due to high energy photon (E_γ>200 keV) emitters. The SSWBM installed at Health Physics Laboratory, BARC, Tarapur consists of a 12.7 cm diameter and 7.6 cm thick NaI(Tl) detector surrounded by 20.5 cm thick mild steel (MS) plates. This system has been calibrated using BOMAB and voxel phantoms, both having BARCreference dimensions [1]. Recently, ICRP has published reference paediatric computational (voxel) phantoms [2] for male and female representing various age groups of members of public. In the present study, 1-year (1Y) and 5-year (5Y) old voxel phantoms have been used to estimate the counting efficiency (CE) of SSWBM for ^{137}Cs and ^{60}Co and the results are compared with their BOMAB counterparts.

The system is experimentally calibrated using BOMAB phantoms with activity distributed in the axial cavities. SSWBM along with the 1Yand 5Yold voxel phantoms are numerically modelled in FLUKA code and the elemental composition of different materials was assigned using its advanced graphical user interface, FLAIR (Fig. 1). A user-written FORTRAN program was implemented to simulate uniform activity distribution in voxel phantom. Five batches of 10^9 primaries were used for simulation. The simulations have been carried out for the 662 keV and 1.17 & 1.33 MeV photons emitted by ^{137}Cs and ^{60}Co respectively. The scanning geometry of SSWBM is simulated by scoring energy deposition (DETECT card of FLUKA) at 15 different static detector locations. The final CE is calculated by averaging the detector responses at 15 locations and are listed in Table 1.

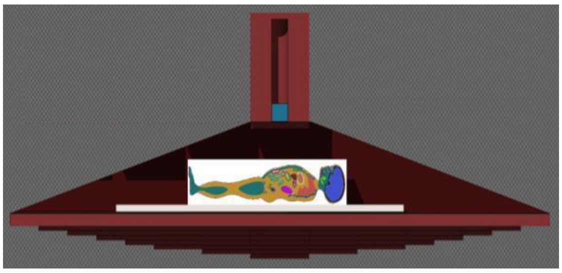

Fig. 1: Calibration of SSWBM using voxel phantom

Table 1. CEs of SSWBM using BOMAB and voxel phantoms

Age	Radio-nuclide	BOMAB	Voxel	Variation (%)
01Y	Cs-137	1.03E-03	7.86E-04	30.85
	Co-60	1.90E-03	1.33E-03	42.74
05Y	Cs-137	9.73E-04	8.20E-04	18.65
	Co-60	1.80E-03	1.40E-03	28.47

The results show that, for any age group CEs for BOMAB phantom are greater than voxel phantom. It is because of the localized axial source distribution in BOMAB phantoms, which imposes a relatively greater solid angle at detector face. Also, CEs for ^{137}Cs are lower than ^{60}Co because both peaks (1.17 & 1.33 MeV) are considered for the latter.

References:

[1] D.K. Akar, H. K. Patni and V. P. Ghare, *IARPIC* 209 (2018).

[2] ICRP- Paediatric reference computational phantoms. ICRP Publication 143. *Ann. ICRP* **49(1)** (2020).

Indigenous development of DC accelerator based compact sealed neutron generator

Prashant Singh[§], Mayank Shukla,Tushar Roy, Yogesh S. Kashyap, Shefali Shukla, Mahendra More, Baribaddala Ravi, L.M. Pant

Technical Physics Division,
Bhabha Atomic Research Center, Mumbai, India
[§] Email: prashants@barc.gov.in

Compact DC accelerator based sealed neutron generators with moderate neutron yield (10^6 to 10^7 n/s) has applications in mining exploration, oil well logging, coal analysis for power plants etc. Due to their compact size and controlled operation these generators are suitable for applications in areas such as detection of explosive detection [2],special nuclear materials[3], narcotics detection[4, 5] and material characterization. We present indigenous development of DC accelerator based 14MeV Deuterium(D)-Tritium(T) compact sealed neutron generator for laboratory and field applications. In these generators, a D-D (2.45 MeV) / D-T (14.1 MeV) fusion reaction occurs when an accelerated deuterium ion beam interacts with the target (D or T), producing mono energetic neutrons. The sealed tube consists of a cold cathode Penning Ion Source (PIS)[1], metallic D-gas reservoir, beam shaping & accelerating shroud and tritium target holder in-housed in an all metal-to-ceramic joints compact mechanical housing.Fig.(1) shows the assembled n-generator with HV connected at target side. D-gas from the reservoir in the ion source is released using a constant current DC power supply and a 3kV high voltage power supply ionizes the gas.The PIS is operated in pulsed mode with pulse duration ranging from of 100µs to 500µs and upto 1kHz repetition rate. To produce fusion neutrons, a deuterium ion beam is extracted through an aperture, accelerated to 90kV DC, and focused on a T-target. The ion source and DC acceleration are powered by micro-controlled indigenously built gate pulse generators and high voltage power supply that are remotely controlled using indigenous graphical user interface software through a remote PC. The generator gives a neutron yield of ~$8x10^6$ n/s at 80kV with 200µs pulse ON time and 500 Hz repetition rate. The neutron spectrum and neutron energy experiments were carried out using neutron spectrometer and liquid scintillator detector as shown in Fig.(2) and Fig.(3).

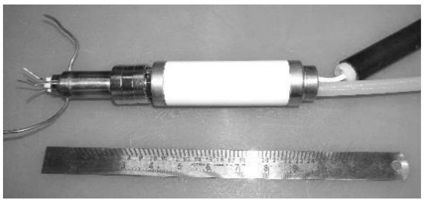

Fig. 1: Sealed Neutron Tube

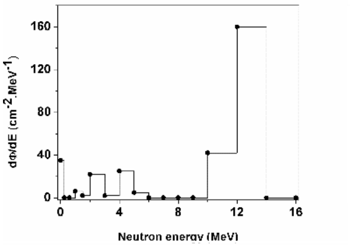

Fig. 2: Neutron Spectrum

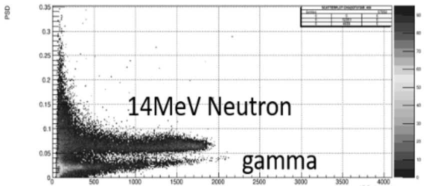

Fig. 3: Neutron Energy Measurement using liquid scintillator

References:
1. IAEA Radiation Technology Reports Series No. 1, 2012.
2. J. Reijonen, et al., Proc. Particle Accelerator Conference, Knoxville, Tennessee, 2005.
3. Alvarez, R. A. et al., J. Radioanal. Nucl. Chem. 1995, 192, 73–80.
4. P.C. Womble, et al., Nucl. Instrum. Methods Physics Res. B 1995, 99, pp 757–760
5. T. Gozani, D. Strellis, Nucl. Instrum. Methods Physics Res. B, 261 (2007), 1-2, pp.311-315

Track parameter of Alpha particles with different energies in LR115 Detector

Jalaluddin.S[1,§], Rosaline Mishra[1,2] ,R.P.Rout[1] and Rama Prajith[1]A.T.Khan[1] ,B.K.Sapra[1,2]

[1]*Radiological Physics and Advisory Division, Bhabha Atomic Research Centre, Mumbai 400094, India*
[2]*Homi Bhabha National Institute, Mumbai 400094, India*
§ Email: jalalph@barc.gov.in

LR115(cellulose nitrate) solid state nuclear track detector (SSNTD) is widely used in the measurement of Radon(Rn^{222}) and Thoron(Rn^{220}) gas and it's decay products. In the present study, the effect of incident alpha particles of different energies on the track diameter registered in LR 115 detector were analyzed. The exposure of LR115 detector to alpha particles incident leads to radiolytic scission of long polymer chains into shorter fragments and the production of reactive low molecular weight radiolytic products, which are more easily dissolved by etchant than the surrounding undamaged plastic during chemical analysis. This leads to a through and through etched track alongwith a slowly etching undamaged portion.

Experiment details

In the experiment ^{241}Am source having alpha particle energy of 5.48 MeV, has been used. LR115 detector is placed at different distances from the source to vary the incident energy. The range of alpha particle in air and the residual range after travelling a certain distance in air is given by Eqn (1) and (2).

$$Ra = 0.324E^{3/2} \quad (1)$$

$$Er = Eo\left(1 - \frac{L}{Ra}\right)^{2/3} \quad (2)$$

From equation (1), the range(R_a) of 5.48 MeV alpha particle in air is 4.16 cm. At specific distances Lbetween the LR115 film and the source, the residual energy is calculated by equation (2). The exposed LR115 detector at different distances from the source were chemically etched in 2.5N NaOH at 60°C for 90 minutes, to convert the latent tracks into optically visible tracks. The track counting was carried out by image analysis system.

Table1. Track diameter for different energy

Sr no	Distance (cm)	Residual energy(Er) MeV	Track diameter Range(μm)
1	1.03	4.53	No track
2	2.24	3.27	3-4
3	2.81	2.59	5-6
4	3.33	1.86	6-7
5	3.89	0.89	No track

Result and discussion

The distance from the source, the residual energy reaching the LR115 detector and the median track diameter is given in Table 1. It was observed that alpha particle with energy 4.53 MeV and 0.89 MeV was not able to register the track in LR115 since it has an energy window of 1.5 to 4 MeV.It was observed that as the residual energy incident on the LR115 detector decreases the corresponding track diameter increases.

References:
[1] R.L. Fleischer,P.B price , *Physical review*, **volume 156**(1967) number 2.

Tagged Neutron System (TNS) with multiple gamma detector

S. Bishnoi[1, §], R. Jilju[1], T. Patel[1], P.S. Sarkar[1] and L.M. Pant[1,2]

[1] *Technical Physics Division, Bhabha Atomic Research Center, Mumbai, India*
[2]*Homi Bhabha National Institute, Mumbai, India*
[§] Email: saroj@barc.gov.in

In recent years, fast neutron-based interrogation systems [1] have been used for the detection of the hidden explosives and contrabands in containers such as cargo, truck etc. It is due to their high penetration and ability to identify the material composition. One such technique is the Associated Particle Technique (APT), also known as Tagged Neutron Method. It is based on the inelastic scattering of fast neutrons (14 MeV) and registering the accompanied characteristic element specific gammas. However, the neutrons incident on the object are "tagged" in the sense that the direction (and emission time) of neutrons is known. The gamma rays are used to characterize carbon, oxygen and nitrogen, which are the major elements constituting explosives or narcotics. Discrimination between threat and commonly used material is consequently made by measuring relevant elemental ratios such as C/O, N/O, C/N etc. Moreover, the APT makes it possible to inspect a specific volume (voxel) inside the container, thus improving the selectivity of the method as well as signal-to-noise ratio.

An experimental Tagged Neutron System has been developed at Laboratory scale (Fig.1). Proof-of-Concept and system capability towards illicit material detection has been demonstrated with the use of a gamma detector [2, 3]. In next step of its development, an array of BGO gamma detectors with proper shielding was installed to improve the system performance in terms of statistic, sensitivity, acquisition time etc. Prior to that BGO‟s were characterized for their energy and time resolution in order to determine the suitability of the detectors for TNS. Pure element spectra of carbon acquired using test sample and data were analyzed with proper time window selection indicating successful implementation of the APT with TNS using multiple detectors. (Fig2.).

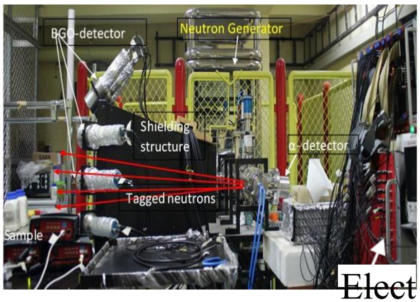

Fig1: Experimental TNS set up

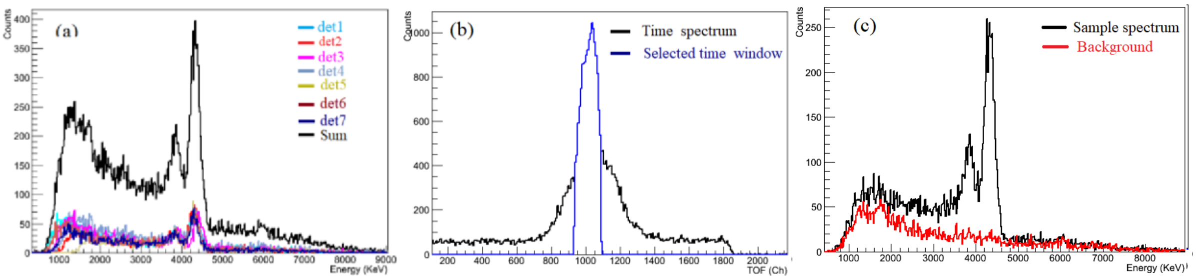

Fig 2:(a) Energy spectrum of carbon sample with individual BGO detector spectra (b) time spectrum with selected window (c) time co-related energy spectrum with background

This paper reports the development progress of the TNS incorporating multiple detectors and initial experimental results highlighting the analysis methodology of APT.

References:
[1]. M.Gierlik et. al., *Nucl. Inst. Meth. Phys. Res. A,* 834(2016)16.
[2]. S. Bishnoi et. al., *Eur Phys J Plus* (2020) 135:428
[3]. S. Bishnoi et. al. *Nucl. Inst. Meth. Phys. Res. A,* 923 (2019) 26.

Neutron spectrum unfolding: Effect of energy bin-width on the final solution spectrum and H*(10) values

S. P. Tripathy[1,2,§], Sabyasachi Paul[1], G. S. Sahoo[1] and M. S. Kulkarni[1,2]

[1] *Health Physics Division, Bhabha Atomic Research Centre, Mumbai, India*
[2] *Homi Bhabha National Institute, Mumbai, India*
[§] Email: tripathy@barc.gov.in

Neutron spectrum unfolding is an essential step involved in most of the methods used for neutron spectrometry and dosimentry. It involves the complex mathematical procedures to solve the Fredholm Integral Equation of first kind. Out of several unfolding algorithms, MAXED (Maximum Entropy Deconvoltion) was used in this work. This method is based on maximum entropy principle [1]. An experiment was performed to measure the neutrons produced from ^{9}Be(p,n) reactions (E_p=21 MeV), at 6 m facility of BARC-TIFR Pelletron Accelerator. A multi-shell single sphere neutron spectrometer, built in-house especially for the accelerator based neutron sources, was used for this purpose (Fig. 1) [2]. The system was found to be flexible and versatile to adapt any small size themal neutron detectors (e.g. OSL, TLD, Au foils, etc.). A total of 12 detectors could be used at different depths of the sphere. The response matrix of the spectrometer was constructed using FLUKA-Monte Carlo simulations. After irradiation, the detectors were analysed to obtain the netron-indced counts. These counts along with the response matrix of the spectrometer and a guess spectrum were fed as the inputs to the unfolding code.

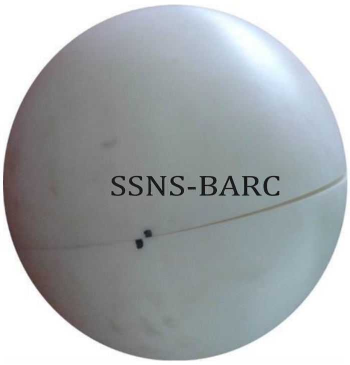

Fig. 1. Single Sphere Neutron Spectrometer (SSNS).

One of the prime objectives of this work was to study the effect of the energy binnings on the shape and peak height of the final solution spectrum. This is a crucial parameter as the neutron dose conversion coefficient varies drastically with energy and would affect the estimation of the dose values due to neutrons. A systematic study has been carried out with 4 different energy binnings (31, 51, 71, 121) of the unfolded neutron spectrum. Since the total energy range is from 0.1-19.1 MeV (total spreading of 19 MeV), the minimum binning suitable was fond to be 31. The unfolded unit spetra at different binnings is presented in Fig. 2. As can be seen, the peak height was found to be gradually reducing with the increase in energy binnings, even though the area under each spectrum is unit. The dose equivalent ($H^*(10)$) values as determined from the unit lethargy spectra for the same reaction were found to be 307.78, 314.57, 354.44, 382.89 pSv cm^{-2} for 31, 51, 71, 121 bin sizes respectively. To conclude, the 51 binnings is preferred, beyond which the tailings part at higher energies are almost overlapping.

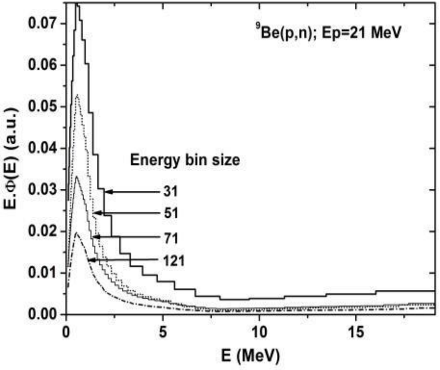

Fig. 2. Unfolded neutron spectra for ^{9}Be(p,n) reaction, in Lethargy scale.

References:

[1] M. Reginatto, et. al. EML-595, Environmental Measurements Laboratory, New York, USA (1998).

[2] S. P. Tripathy et. al., Radiation Measurements, **160** (2023) 106892.

Numerical Estimation of Efficiency of an over square LOAX HPGe detector for volume source

Ram Sharma[1, §], M. Manohari[2], S. Murugan[1], G. Ganesh[1], M.S. Kulkarani[1, 3]

[1]*Health Physics Division, Bhabha Atomic Research Centre, Mumbai, 400085.*
[2] *SQ&RMG, Indira Gandhi Centre for Atomic Research, Kalpakkam, 603102.*
[3]*Homi Bhabha National Institute, Mumbai, 400085*
Keywords: FLUKA, Efficiency, detector,
§ Email: sharmaram@barc.gov.in

Introduction: During the radioactive waste treatment, different number of non-standard geometric sample (protective wears, liquid sample, & metal scraps etc) is generated. For such cases standard reference source is not available. This difficulty is overcome using numerical simulation of the full energy peak efficiencies of a p-type LOAX (low energy coaxial) HPGe coaxial detector with 8.45 cm dia and 3.03 cm thickness with Be window of thickness 0.08 mm having 45% relative efficiency using FLUKA code. Efficiency curves were established for different geometries at different distances and were fitted using fifth-order polynomial logarithmic functions.

Materials and methods: The detector model was validated using experimental point source efficiency [1] and the experimental efficiency of IAEA reference standard volume source (^{137}Cs water source) of 6 cm diameter and 10 cm height with 7.94±0.0576 Bq activity kept at 3.8 cm from the detector. Efficiencies of volume source of different geometries with different density and composition were simulated for different energies using DETECT card in FLUKA.

Result and Discussion: Deviation between experimental and simulated efficiency was 6% validating the volume source sampling. Efficiency curve for cylindrical source with water and rubber medium and for cubical volume sources of steel are shown in Fig 1(a), Fig 1(b) and Fig 1(c) respectively. These efficiency curves were fitted in fifth-order polynomial logarithmic functions. The volume source efficiency was used to estimate the natural activity in the metallic plates used for the construction of steel room of lung monitor. The efficiency of cylindrical source was used to estimate the ^{137}Cs, ^{106}Ru activity in the LLW and the cuboidal source for the activity estimation in the solid waste.

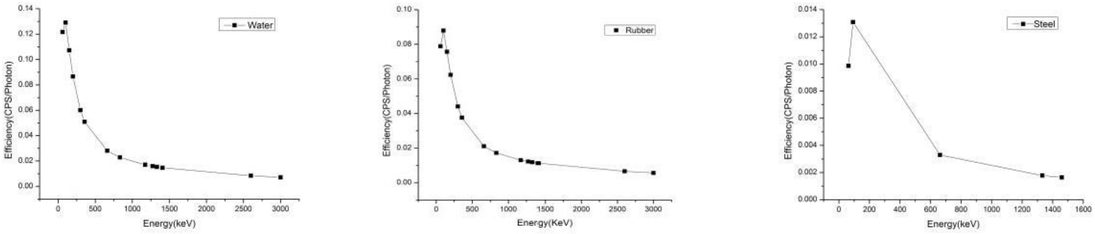

(a) (b) (c)

Fig.1 (a) cylindrical water source (b) cubical Rubber source (c) cubical steel source

Conclusion: Efficiencies was simulated for different shaped volume sources filled with different matrices (gloves, water etc.) and also for cubical steel. The efficiency curve obtained can be applied to quantify the activity of different radionuclides present in different volume samples.

References: 1. Ram Sharma et al., "Numerical response of an over-square LOAX HPGe detector for point source", (2023, February 7-11), AOCRP-6, Mumbai.

Application of two-dosimeter algorithms for dose estimation during hot cell refurbishment activities in a radiochemical plant

Krishnakumar P[1§], Jayan M P[1], Amit Bhatnagar[1], Sureshkumar M K [1]

[1]*Health Physics Division,*
Bhabha Atomic Research Centre, Mumbai, India
[§]Email: krisp@barc.gov.in

Introduction: Process hot cells in radiochemical plants have high radiation field, often highly inhomogeneous, where the single TLD on chest for personal exposure measurement may not be the most appropriate technique. In this study, four, two-dosimeter algorithms described in literature were employed to assess the individual dose during equipment refurbishment campaign in a process hot cell.

Material and Methods: 20 radiation workers were monitored with two TLDs, one worn at front and the other symmetrically back of their body. Both dosimeters were always used in parallel. Four two-dosimeter algorithms- two algorithms of the National Council on Radiation Protection (NCRP (70/30) and NCRP (55/50))[1], the algorithm of Electric Power Research Institute (EPRI (Xu et al.)[2] and that of Lakshmanan et al[3] were employed to estimate the whole body dose using the two sets of readings.

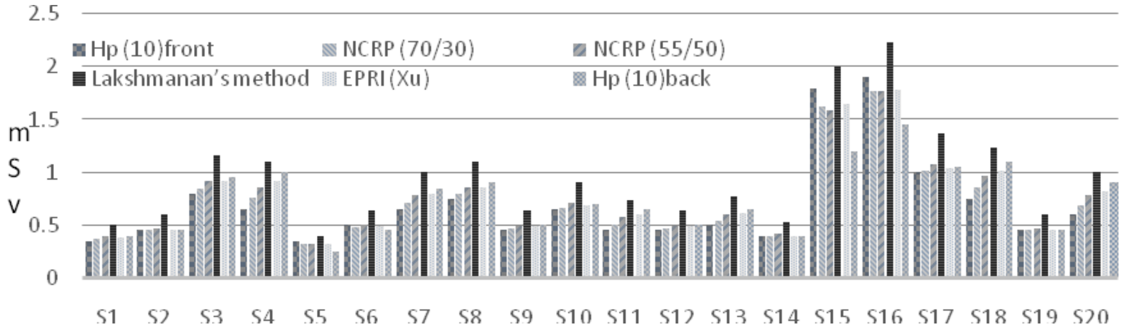

Fig. 1: Comparison of front and back TLD dose with 4 different 2 TLD algorithms.

Results and Discussion: The individual front and back TLD readings along with the resulted whole body dose from application of the four two-dosimeter algorithms are given in Fig.1.Difference between the front and back TLD readings shows that the radiation field at work place is inhomogeneous. In four of the twenty cases, the difference was more than 30% of the higher readings. Among the four algorithms, the EPRI method is found to produce results which is closer to the higher TLD readings and can be used as a practical tool. The method proposed by Lakshmanan et al always leads to overestimation, always higher than any of the two TLD readings. Among the two NCRP methods, the NCRP(55/50) method is found to be more suitable to avoid underestimation, when the back TLD readings are significantly higher than that of front TLD. Our results shows the requirement for more elaborate studies in future to fine tune personal dosimetry for workers engaged in inhomogeneous radiation field such as hot cells.

References:
[1] NCRP Report No. 122, (1995)
[2] United States Nuclear Regulatory Commission, Report No. RIS 2004-01,(2004).
[3] Lakshmanan, A. R., Kher, R. K., Supe, S. J., Radiation Protection Dosimetry. (1991), 35(4), 247.

EFFECTIVENESS OF LEAD APRON FOR EXPOSURE CONTROL IN MOX FUEL FABRICATION FACILITY

R. N. Dubla[1§], S Pattanayak[1], Kanhaiya Jee[1], S. K. Tibrewala[1], G. Ganesh[1], M.S.Kulkarni[1,2]

[1]*Health Physics Division, Bhabha Atomic Research Centre, Mumbai 400085, India*
[2]*Homi Bhabha National Institute*
[§] Email: rajendradubla@barc.gov.in

In mixed oxide (MOX) fuel fabrication facility, fuel pins are fabricated by powder metallurgy route which involves operations such as mixing, milling, compaction, sintering and grinding followed by loading of pellets in tubes, end plug welding etc. The MOX fuel consist of oxides of fissile & fertile radio-nuclides which involves handling of actinide which are alpha, gamma and neutron emitters, thus possess internal & external hazards. Therefore all the MOX fuel fabrication operations are being carried out in glove boxes (GBs). During normal operations, the internal hazard to the lab personnel is practically negligible and external exposure is mainly from gamma and neutron emitted by the actinides. To reduce the external exposure from gamma and x- ray emitted by different actinides and fission products present in the feed material, lead aprons are being used [1]. This apron is made of lead vinyl sheet (lead equivalence of 0.5 mm). In this study, gamma dose reduction due to implementation of lead apron is carried out for different MOX fuel fabrication process.

Table.1 Gamma dose reduction factor

Sr. No.	Process	Dose reduction factor (front side EPD dose Hp (10)/back side EPD dose Hp (10))
1.	MOX powder	3.00
2.	Pellet handling	3.01
3.	Pin fabrication	2.02
4.	Pin decont.	2.10
5.	Pin storage	2.34

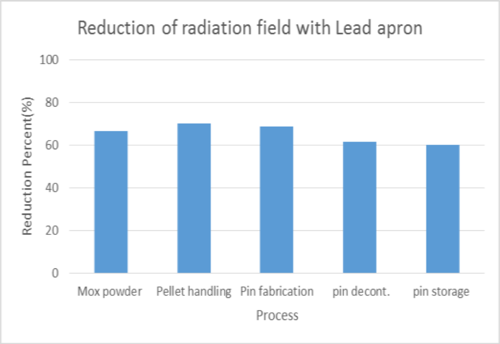

Figure.1 Reduction percent with lead apron

To study the effectiveness of lead apron, experiments were carried out to simulate different process of fuel fabrication. In this experiment, 5 kg of MOX powder and pellet containers are considered to simulate the powder and pellet handling process and 50 numbers of fuel pins are considered in a tray to simulate the pin handling process. Initially the radiation field is measured (Rad Eye G10 survey meter) with and without lead apron for different simulated process. The reduction percentage of radiation field is given in Figure 1. It is found that there is a reduction of 60-70 % of gamma dose rate with this apron. Later dose reduction factor is calculated by placing one EPD at front side and another EPD (Rad Eye make) at backside of the apron and exposed to different simulated process. The gamma dose reduction factor is given in the Table.1. It is observed that, the gamma dose reduction factor of 2-3 is achieved for different process. This variation of reduction factor may be due to influence of source geometry, gamma energy dependence and presence of other shielding material. Lead aprons were found to be very effective and is now being widely used in the facility.

Reference:

[1]A. Zimmer et.al., Journal of Nuclear Medicine May 2007, 48 (supplement 2) 470P.

Study of LET and etching effect in PADC (CR-39) using FTIR spectroscopic analysis

G.S. Sahoo[1,§], S.P. Tripathy[1,2], Sabyasachi Paul[1] and M.S. Kulkarni[1,2]

[1] *Health Physics Division, Bhabha Atomic Research Centre, Mumbai, India*
[2] *Homi Bhabha National Institute, Mumbai, India*
[§] Email: sahoo.gouri232@gmail.com

PADC (Polyallyl diglycol carbonate, known as CR-39) is a thermosetting polymer having chemical composition $C_{12}H_{18}O_7$ and is widely used in various fields of science and technology. The change in various physico-chemical properties of this polymer have been explored for its use as radiation detectors in different branches of science. In this work, we have studied the effect of heavy ions having different LET (linear energy transfer) values and the duration of chemical etching on the vibrational absorbance properties of PADC using FTIR technique. The PADC samples were irradiated to Li, C, O and F ions having different energies at Pelletron, IUAC, New Delhi. The beam energies were selected to have different LET in PADC (76 to 1002 keV/μm). The samples were then subjected to chemical etching with 6.25N NaOH at 70^0 C up to 8 hours in steps of 1 h along with the recording of FTIR spectrum after each step of etching.

Fig. 1 shows the typical FTIR spectrum of PADC in the range of 2100-600 cm^{-1}. Three prominent and high intense peaks (1735 cm^{-1}: ester C=O stretching, 1230 cm^{-1}: C–O–C aliphatic ester stretching and 785 cm^{-1}: =C–H bending) as well as other multiple low intense peaks were observed in the FTIR spectrum [1]. These peak intensities were found to be decreasing with the increase in LET of the ions as well as with the etching duration. Out of these peaks, intensities of 1735 cm^{-1} was considered and the variation of the absorbance with LET and etching time is presented as absorbance matrix in Fig. 2. The variation of absorbance of 1735 cm^{-1} with LET for 6 h etching is shown in Fig. 3. Since the observed decreasing behavior was not linear, the absorbance values were fitted with exponential decay equation with fixed parameter 0.72508 corresponds to the absorbance of un-irradiated and un-etched PADC. To conclude, the peak intensity of the functional group was found to be decreasing with the increase in LET as well as the etching time. Moreover, the decreasing behavior was observed to follow an exponential trend, instead of linear one.

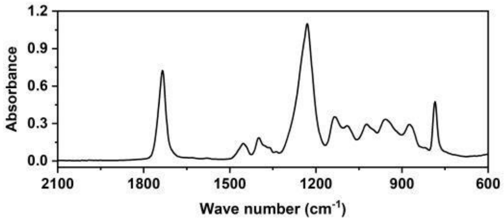

Fig. 1: FTIR spectrum of PADC.

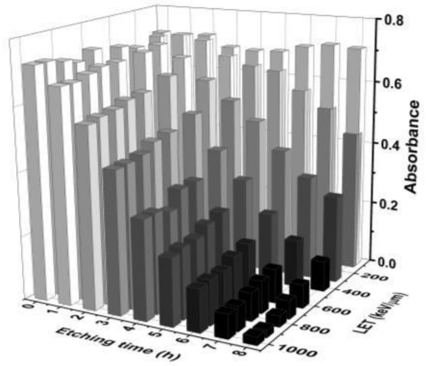

Fig. 2: Absorbance matrix for 1735 cm^{-1}.

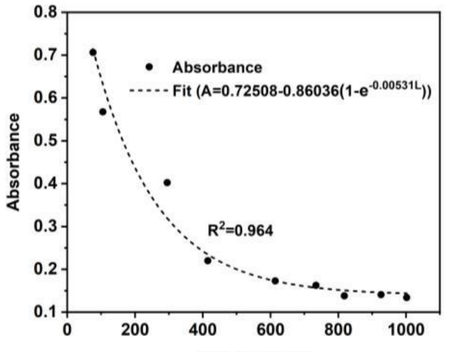

Fig. 3: Variation of absorbance of 1735 cm^{-1} of PADC with LET after 6 h etching.

Acknowledgements: Authors are sincerely thankful to Dr D K Avasthi and Dr Pankaj Kumar of IUAC for their help during experiment.

References:

[1] G.S. Sahoo et. al., *Nucl. Inst. Meth. Phys. Res. A*, **1041** (2022) 167331.

Augmentation of hot cell facility of MC&MFCG for pyro-processing

D. Bolasankar[1], T. Kalaiyarasu[1], R. Karunakaran[1], S. Rajeswari[1],
R. Padmanaban[2], Arul Kumar[2], Masanam[2], E. Mohanraj[2], N. Ravi[2]
P. Manoravi[1] and V. Jayaraman[1§]

[1]*Mini & Hot Cell Section, ACSD, FMCG*
[2]*Chemical Facilities Engineering Division, MFRG*
Materials Chemistry & Metal Fuel Cycle Group, IGCAR, Kalpakkam
[§] Email: vjram@igcar.gov.in

Hot cells with inert atmosphere are used for handling air sensitive, hygroscopic and radioactive materials like mixed carbide fuels and for pyro-processing of metallic fuels. Pyro-processing of spent metal fuels is based on electrochemical recovery of actinides in high temperature molten salts (LiCl-KCl eutectic with 58.5 mol.% LiCl). In order to demonstrate the remote operation feasibility of the electro-refining process of irradiated U-6Zr inside hot cells and also to study the process parameters, a laboratory scale (100g scale) pyro process facility was set-up in hot cells of MC&MFCG.

For this purpose, the existing hot cell facility was augmented with necessary modifications and customized to the experimental needs. Various systems such as a) Argon re-circulation system and b) Oil filled Radiation Shielding Window were refurbished completely. Various equipment such as a) HEPA Filter assembly, b) Furnace lifting mechanism, c) Pick and Place Radial Hoist Crane, d) Fuel pin cut section transfer vessel, e) Salt storage cum reaction vessel etc., were designed, fabricated and installed inside the containment box of the cell. Welding the outer vessel of the electro-refiner assembly inside the containment box with pre-mounted radiation glass viewing window was a challenge to be encountered and this job was accomplished by adopting stiffeners and cooling jackets during welding process. Inside this augmented hot cell facility, 100 g scale electro-refiner set-up was installed and commissioned.

Entire recirculation system was refurbished by replacing all QRC"s and two purification towers were designed, fabricated and installed in the loop to provide the required level of purity with regard to oxygen and moisture inside the containment box. Cut pin sections of irradiated fuel were transported from RML to RCL in a dedicated transfer vessel placed inside the la-chalhene container. A mechanical furnace lifting mechanism capable of lifting a load of 150 kg through a height of 400 mm and operable remotely from a distance of 2 meters from the isolation area has been designed fabricated and commissioned at the bottom of the cell. A radial hoist and positioning device has been designed and fabricated for loading, unloading and precise positioning operations of all in-cell equipment and installed in cell-2 of hot cell. A salt storage cum reaction vessel in to store the electrolyte under inert atmosphere after the process was designed, fabricated and installed inside the cell.

Using this facility, electro refining (ER) of FBTR irradiated U-6Zr(wt%) alloy fuel was successfully demonstrated by remote operation. This experiment is first of its kind in the field of pyro-process and has provided insight into the challenges that need to be encountered when performing ER process with irradiated fuel by remote operation.

Acknowledgements: The authors hereby acknowledge with thanks Dr. N.Sivaraman, Director, MC&MFCG, Dr. Kitheri Joseph, AD, MFRG, Shri.T.V.Prabhu, Head, CFED, for their participation and support rendered throughout the course of this work.

Author Index

A. Manivannan 70, 133
Achary S N 51
Acharya R 47, 88, 214, 215, 216, 230, 231, 234, 235, 240, 244, 251, 252
Adhikari Soumyakanti.. 279
Agarwal Chhavi 27, 377. 380
Agarwal Rahul 193
Agarwal Rohini 276, 286
Aggarwal Aarti 285
Aggarwal Sourabh 126
Aiswarya P M 68, 74
Ajish J K 374
Ajish Kumar K S 263, 292
Ajith D 65
Ajmal P Y 345
Alam Jane 1
Alam Md N 266, 267
Alangi Nagaraj 308
Alexander Rajath 55
Ali M 115
Ali Taslim 73
Alset Utkarsh 313
Ambika M R 371, 381
Amirdhanayagam Jeyachitra 275, 303
Amutha Suba M 200, 202, 221, 237, 256
Ananthanarayanan Arvind 289
Ananthasivan K 2, 75, 78, 122, 123, 125, 144, 147, 152, 156, 197, 199, 201, 208, 211, 220, 287, 294
Aneesh T 208
Annapoorani S 126, 157
Ansari S A 84, 93, 121
Anushree H S 167
Apraj S K 383
Apte Shree Kumar 4
Archana V 132
Arul A John 158, 174, 177, 182, 203
Arun B 169
Arunkumar V 66
Arya Ashok K 56
Ash S 266, 267
Ashokkumar P 101, 194, 370
Athif P 364, 367
Avaneesh R U K 340
Babbar N 362
Baburajan A 352, 353, 354
Badiger N M 245
Bahadur Shuchita 378
Bajpai R K 332, 350
Bakshi A K 207
Balaji Vadivelu 64
Balakrishnan S 69
Balamurugan M 78
Balan Priyanka 332
Balaram R K 324
Balhara Annu 50, 88, 111, 116
Bamal Sumit 264
Bandyopadhyay Anisha 49, 338
Banerjee Anannya 183, 184, 209
Banerjee Chayan 91
Banerjee Dayamoy 146, 150, 151, 207
Banerjee Piyali 84, 178
Banerjee Rumu Halder 55
Banerjee Sharmila 301
Bano Shehnaz 186
Bapuji T 212
Bar Tanmoy 170
Baribaddala Ravi 389
Barik Suvendu Kumar 69
Barkavi K 316
Barman Chiranjib 369
Barua L 266, 267
Basak A 383
Basak Dipali 170
Basu Chinmay 170
Basu Sandip 274
Bavya P 225
Beena Ullala Mata B. N. 347, 356
Begum Zahida 61
Bennal A S 245
Bera Santanu 63, 64, 79
Bhade Sonali P D 192

Author Index

Bhakta S	374
Bhaktivinayagam A	370
Bhandari Deep	180
Bhangare R C	223, 345
Bhanu Prasad CH.U	122, 220
Bharat S	366
Bhardwaj Deepa	368
Bhaskarapillai Anupkumar	309
Bhatkar P	272
Bhatnagar Amit	342, 394
Bhatt R B	84, 107, 140, 141, 142, 164, 178, 187, 236, 243, 315
Bhattacharya M	207
Bhattacharya S	65
Bhattacharyya Arunasis	103, 105, 109
Bhoir Seema	360
Bhoite Rahul	274
Bikash K N	124, 148
Bishnoi S	391
Bisht Ruchi	277
Biswal Jayashree	289, 290
Biswas Gautam	323
Bol R	362
Bola Sankar D	175, 202, 212, 217, 219, 397
Bootharajan M	106, 145
Bora Neetu	304
Borisova N E	109
Bramha S N	326, 340, 348, 349
Briteena K S	326, 349
Bukhari A Sadiq	364, 367
Chaitanya Vangala Sri Datta	99
Chakraborty Aparna	173
Chakraborty Avik	282, 292, 293, 301, 302, 306
Chakraborty Sudipta	282, 293, 306
Chakravarty Rubel	282, 293
Chand Satish	298
Chandra Nikesh	298
Chandrakar Amol	363
Chandramohan P	64
Chandran Neeraja	208
Chandran Sinu	63
Chandrasekaran A	311, 314, 318
Chandrasekaran S	325, 326, 340, 348, 349
Chandrashekara M S	320, 321
Chandrika B M	371
Chattaraj Saparya	101, 103, 194
Chatterjee Avika	273
Chatterjee Sitangshu	29, 322, 344
Chattopadhyay S	266, 267
Chaturvedi Shashank	6
Chaube R K	188
Chaudhary Dilip Kumar	324, 333
Chaudhary Nishant	55
Chaudhuri Punarbasu	159
Chaudhury Probal	43
Chaudhury S	121, 235
Chaudhury Sanhita	210
Chauhan A K	374
Chauhan N	362
Chavan S V	238
Chavan T A	162
Chindarkar A S	238
Chirayath Sunil S	7
Chitra N	326, 349
Chokkalingam R N	220
Chopra Manish	136
Choudhary Mahesh	259, 260, 264, 270, 271
Choudhary Manoj K	224
Choudhury Niharendu	136
Chowdhury Saheli	369
Christobher S	364, 367
Czerwinski Ken	9
Dadwal Vaishali	252
Dalal Ranjeet	339
Dalvi Sushant S	354
Damle Archana	272, 292
Dani Umesh	10
Danu L S	264
Das Debarati	49
Das M K	332
Das Nirupam	383
Das Pratik	135
Das S Saha	266, 267

Author Index

Das Satya Narayan 199
Das Tapas 227, 275, 303
Dasgupta Sandipan 170, 259, 270, 271
Datrik Chandra Shekhar 46, 87
Datta Arpita 234, 240
Datta Jagannath 170
Dawar Rimpi 68, 74, 137
De Sukanya 46, 264
De V 187
Deb A C 82, 129
Deep Shikha 252
Deo Kapil 180
Deokar U V 350
Desigan N 78, 119, 122, 144, 147, 152, 197, 220,
Devi K V Vrinda 185
Devi P S Remya 162
Devi S Sagunthala 208
Dhamodharan K 123, 197, 199, 201, 208, 211, 294
Dhanesh P R 220
Dhang P 266, 267
Dhankar K 382
Dhara Sangita 226
Dharashiokar A D 146
Dhibojini V 153
Divekar Sandesh Krishnakant 51
Dixit Rajashree 185
Dube Charu Lata 355
Dubey Nitin 270
Dubey Punit 181, 260, 270
Dubla R N 395
Dumpala Rama Mohana Rao 108, 107, 193
Durani Sameer 11
Dusane Chetan B 196, 324, 333, 361
Dutta Dhanadeep 30, 41
Dutta M 188
Egberink R J M 107
Elumalai M 241
Farasat M 362
G V S Ashok Kumar 124, 202, 229, 241, 248, 249, 250
Gaikwad R H 353
Gaikwad Revati 164, 236
Gamare Jayashree S 193
Gamre Naresh 251
Ganapathi A S 217
Gandhi A 259, 260, 264, 270, 271
Gandhi Shyamala 268
Ganesan R 153, 154, 155
Ganesh G 350, 393, 395
Ganesh Prasad K 347, 356
Ganesh S 60
Ganesh T 242
Garg Rohini 56
Gaur Diwakar 334
Gaur Monica 377
Gautam Prikshit 339
Gautam S 258
Gautam Y P 337, 341
Gayen J K 309, 310
Geetha N 310
George Reetta Sara 234, 240
George Thomas 346
Ghare P T 370
Ghodke T S 281
Gholve C S 257
Ghosh Abhijit 56
Ghosh Debojyoti 144, 152
Ghosh Manoranjan 385
Ghosh Sanchita 282
Gill Rajpal 328
Gireesan Prema 146
Gocher A K 328
Goedert S 362
Goel Shelly 136
Gopakumar Gopinadhanpillai 92, 102, 112, 120, 124
Gopalakrishnan Mary 91
Goswami Dibakar 54
Goswami Preeti 190, 191, 228
Goswami Rabina 379
Goswami Sunil 289
Govalkar Atul 370

Author Index

Goyal Priya	81
Guchhait S R	187
Gujar R B	93, 128, 291
Guleria Apurav	279, 282
Guleria Mohini	31, 275, 303
Gulnar A K	56
Gumber Nitin	82, 89
Gupta A	387
Gupta A K	251
Gupta Aashna	196
Gupta Ruma	45, 54, 206
Gupta S K	254
Gupta Santosh Kumar	49, 50, 67, 87, 88, 100, 111, 161, 282
Gupta Sonika	88, 214, 230, 231, 235, 251, 252, 255, 371
Hari Abina	279
Haria Hiral	80
Haridas Adish	158, 182
Hariharan Subramanian	63
Hathi Bharatkumar G	344
Hebbar K R Parthasarathi	382
Hemachandar V	101, 194
Hemalatha V	72
Hingu Akash	64
Huskens J	107
Jadhav Sachin	293
Jain Akanksha	297
Jain Ashish	44, 131
Jain Sanyam	329
Jain Shilpa	331
Jaison P G	190, 191, 228
Jalaluddin S	390
James Joshy P	222
Jang Harry	9
Jaryal A	322
Jassal Ravjit Singh	285
Jaswal N	362
Jawahar N R	114, 134, 309, 310, 358
Jayabun Sk	232
Jayachandran Kavitha	45
Jayachandran N	295, 296
Jayan M P	394
Jayan R V	350
Jayaraman V	72, 106, 157, 217, 219, 397
Jayashree R	44
Jaychandran N	238
Jebaraj Mahildoss D	208
Jena Hrudananda	69, 358
Jeyakumar S	71, 332
Jha Atanu	288
Jha M K	352
Jilju R	391
Jishnu K	364, 367
Jose Jis Romal	378, 387
Joseph Annie	151, 289
Joseph Kitheri	44, 70, 133
Joseph M	205
Joshi C P	352
Joshi Chandra Shekhar	283
Joshi Deepika P	304
Joshi Girish C	76, 277, 278, 283, 298
Joshi R M	222, 329
Kadwad V	281
Kailas S	12
Kakkum Perumal	217
Kalaiyarasu T	217, 219, 397
Kalgutkar D B	295, 296
Kaliprasad C S	347, 356
Kalmykov S N	109
Kamaldeep	274
Kamble S N	322
Kambli Manish S	50
Kanekar Avinash S	105
Kanhaiya Jee	395
Kannan Umasankari	180
Kanrar Buddhadev	129, 213
Kapoor K	23, 188
Kar Aishwarya Soumitra	332
Karak Ananda	107
Karki Kanchan	278
Karmakar Sanat	75
Karmakar Subhradeep	369

Author Index

Karthick R 197, 201, 294
Karthikayini S 311
Karunakara N 14, 246, 281, 340, 366
Karunakaran R 217, 219, 397
Kashyap Yogesh S 165, 176, 389
Kaur Gurjeet 285
Kaur Manpreet 247
Kaushik Ankur 383
Kaushik C P 99
Kaushik Vivek 370
Kavya S 174
Kelkar Anoop 164, 178, 187, 236, 243
Kerlin William 9
Keskar Meera 85
Khan A T 386, 390
Khan Bilal Hassan 163
Khati Vinod 322
Kholiya Deepak 283
Khurana Sonali 350
Khyalia Bhupesh 339
Kishan B 195
Kolekar R V 101, 194, 299, 357
Komal 283
Kothai P 351
Krishna Mohan T V 59, 63, 64, 79, 309
Krishnagopal Srinivas 16
Krishnakumar M 62
Krishnakumar P 342, 394
Krishnamoorthy R 316
Kuilya Subrata 59
Kulkarni Amit S 73, 77
Kulkarni Atul 313
Kulkarni M S 138, 207, 342, 350, 370, 392, 395, 396
Kulkarni S P 257
Kulkarni Savita 262
Kumar A 46, 115
Kumar Ajay 46, 173, 181, 264, 273
Kumar Amit 262
Kumar Arul 217, 397
Kumar Ashok 82, 129
Kumar Ashwani 48, 52, 210
Kumar Awadhesh 270
Kumar Chandan 269
Kumar Deepak 337, 341
Kumar Dheeraj 307
Kumar J 337
Kumar Krishan 143, 317
Kumar Manoj 268
Kumar Mukesh 123, 211
Kumar Namrata 164, 236
Kumar Naresh 339
Kumar Naveen 275
Kumar P V Nagendra 57, 58, 61, 160, 186
Kumar Pranaw 228, 235
Kumar Rajeev 180
Kumar S 95
Kumar S D 80
Kumar Sanjay 146, 150, 151
Kumar Satendra 131
Kumar Satyam 46, 48, 52, 372, 373, 375, 376
Kumar Shiny S 96, 104, 110
Kumar Sumit 338
Kumar Sunil 73, 77
Kumar U 266, 267
Kumar Vineet 337
Kumar Virendra 280
Kumaresan R 66, 217, 219
Kumari A Arul 239, 265, 300
Kumari Alpana 62
Kumari Anshul 309
Kumawat H 46
Kuttukaran Sherry Shajan 381
Kutty V K Madhavan 134
Lahiri Susanta 159
Lakshmipathy D V 189, 232
Lavanya B S K 320, 321
Layek Arkaprava 45
Lele Vikram 17
Liddle Stephen T 18
Lohar Sharad P 306
Louis-Jean James 9
Lourduraj A J Clement 371

Author Index

Madapu Kishore K 69
Madhavan Raja 66
Madhu S 255
Madhusmita 266, 267
Mahalakshmi V 157
Mahanty Bholanath 107, 109, 128, 218, 291
Mahesh D G 266, 267
Maheshwari N K 171
Mahur Ajay Kumar 259
Maiti Moumita 261
Maity Sukanta 324, 333, 335, 361
Maity U K 166, 175, 212, 225
Maji S 131
Maletha Pravind 274
Mallia Madhava B 292
Mallick Amod Kishore 180
Mandal B P 290
Mandrekar Vinod K 365
Mangamma G 99
Mani Agnes M 375
Manisha V 307
Manjunatha 245
Manjunatha H C 167, 168, 172, 179, 204, 242,
Manjunatha N 242
Manohar Smitha 146, 150, 151, 350,
Manohari M 393
Manoravi P 166, 175, 212, 217, 219, 225, 397
Margret M 325
Mariyappan S 217
Masanam M. 397
Mascarenhas Adlete A 365
Mathew K M 295, 296
Mathur Anupam 263, 307
Matta Phanindra Kumar 73, 77
Medhi Bikash 285
Meena D 254
Meena D L 243
Meena P 254
Menaka M 169
Menaria Tejpal 328, 330
Menon Sreeja Raj 301
Mestry Priya V 231, 251
Mhatre Amol 48, 372, 377, 380
Mishra Alok Kumar 156
Mishra G 46, 264
Mishra R 74, 386
Mishra R K 43, 146
Mishra Ratikanta 68
Mishra Rosaline 390
Mishra Satyabrata 119, 144, 152, 197
Mishra Suchismita 32, 196, 324, 333, 335, 361
Mishra Sudhir 19
Mishra Sujata 130
Mishra Utkarsha 181
Mishra V G 34
Misra Nilanjal 280
Misra U B 188
Mitra A 264
Mitra Arpit 301, 307
Mitra Sayantan 369
Mitra Sayantani 159
Mittal Bhagwant Rai 285
Mittal Sweety 292
Mittal V K 140, 141, 142, 315, 350
Modak Brindaban 94
Mohamed H E Syed 364, 367
Mohammed Hidayath 320
Mohan A 60
Mohan Anandhu 183, 184, 209
Mohanraj E 397
Mohapatra D K 86, 143
Mohapatra Manoj 67, 100, 101, 116, 194, 360
Mohapatra P K 20, 81, 84, 93, 105, 107, 109, 127, 128, 218, 291
Mohokar Hemant V 322, 344
Mondal J A 338
Mondal Sonjoy 369
Mor Jaideep 30, 41
More Mahendra R 165, 389
Muhammad Shafeeq 85, 90, 135
Mukherjee Archana 275, 302

Author Index

Mukherjee Joydeep 369
Mukherjee S 41, 264, 382
Mukherjee Saurabh 30
Mukhopadhyay Chandan 197, 201, 294
Mukhopadhyay S 185
Mula Soumyaditya 224
Muppalla Shobita R 258
Murari Madav K 363
Murugaiyan P 316
Murugan S 393
Murugesan P 60
Nadkarni Vishnu S 365
Nagaiah N 381
Nagar B K 73
Nagaraja G K 246, 366
Naik Diptesh G 365
Nair Akhilesh K 220
Nair Bhavya S 208
Nair Deepika 146
Namitha J 166, 205, 212
Namitha S N 320, 321
Nandi Chiranjit 65, 90
Narang Shubham 68, 74
Narayana Y 347, 356
Naskar Nabanita 159
Navita 76
Nayak A K 21
Nayak A R 195
Nayak Shrinibas 262
Nebin R T Asher 326, 349
Neelamegam M 229
Nelliyil Renjith B 42
Nishad Padala A 309
Nitin Yuva Raj 262
Osmani Mohammad Saif 132
P A Manojkumar 99
P Manikandan 70
P Philip Kumar 78
Padhy Shrikant S 143, 317
Padmanaban R 217
Padmanabhan R 248
Pai Rajesh V 82, 89, 129, 213
Paik Shrishma 53
Pakhui Gurudas 217, 219
Pal Asim 35
Pal Kuntal Kumar 75, 125, 287
Pal T K 350
Panda K K 383
Panda Pratyasha 130
Pandey Asish 164, 236, 243
Pandey Kanaklata 137, 198
Pandey Rakesh 164, 236
Pandey Usha 302, 307
Pandikumar G 158, 177, 182
Pandit K M 370
Panigrahi S 348
Panigrahi S N 340
Panja Suman 161
Pankaj 144
Pant Amar D 196, 361
Pant Diksha 343, 344
Pant Harish Jagat 276, 286, 288, 289, 290, 322, 343, 344
Pant L M 165, 176, 385, 389, 391
Parab Harshala J 80
Paradkar S N 281
Parayil Reshmi Thekke 67, 100, 101, 194
Parida S C 83, 97, 98, 135
Parvathy N 119
Patankar V H 383
Patel T 391
Pathak Nimai 43
Pathak Sachin S 117, 118
Patil Prashant A 117, 118
Patil S P 295, 296
Patil Sushil M 45, 54
Patkare Geeta 85
Patni H K 388
Patra A K 331, 352
Patra Chayan 144, 287
Patra Chita Ranjan 154
Patra Giri Dhari 67, 100, 111, 385, 387
Patra Kankan 141
Patra Sabyasachi 46, 48, 52, 210,

Author Index

	372, 373, 375, 376
Patra Sourav	282, 293
Patre Dinesh K	101, 194
Pattanayak S	395
Paul Sabyasachi	138, 392, 396
Paul Sumana	37, 190, 206
Periyasamy M	364, 367
Phadke M P	187
Phatak Rohan A	90
Pilania Ritu Kumari	355
Pillai Anilkumar S	196, 324, 333, 335, 361
Pillai Jisha S	121
Pillay R H	345
Pitale Shreyas	385
Pitchaiah K C	113
Poineau Frederic	9
Poswal H K	38
Prabhala Anupama	307
Prabhavathi P V	179
Pradhan Lopamudra	243
Pradhan M K	251
Prajith Rama	386, 390
Prakash Amrit	65, 185
Prakash Amrita Dhara	315
Prakash Babu D	172
Prakash M M	347, 356
Prasad Arvind	122, 147, 220
Prasad Sajin	264
Prasher Meenu	80
Prathibha T	119, 202
Pratibha	353
Premchander	60
Pugazhendi S	123, 211
Pujari Pradeep Kumar	46
Pulhani Vandana A	223, 312, 319, 323, 327, 336, 345, 351, 363
Raghunath T	229
Raghupathy S	158, 177, 182
Rahman M	175
Rai Abhishek Kumar	83
Rai Ratna	278
Raja P	316
Raja Sk Wasim	47, 216
Rajan P S	346
Rajani P	113, 114
Rajeev R	78
Rajendra B	188
Rajesh Puspalata	64, 152
Rajeswari A	293
Rajeswari B	360
Rajeswari S	202, 217, 219, 397
Rakshit Sutapa	257, 272, 302
Ramachandran K	48
Ramakrishna V	229
Ramakumar K L	22
Ramana J V	189, 232, 233
Ramanathan N	95, 200, 202, 221, 237, 256
Ramanjaneyulu P S	73, 77, 198
Rani K S Pruthvi	321
Ranjan Akash	243
Rao Ankita	96, 104, 110
Rao C V S Brahmananda	70, 92, 102, 106, 112, 113, 114, 120, 124, 145, 148, 149
Rao G S	114, 134
Rao J Prabhakar	217
Rao J S Brahmaji	124, 202, 229, 241, 248, 250
Rao Srinivasa G	99, 114, 134
Rao Y Balaji	23, 57 58, 61, 160, 186, 188
Rath D P	370
Rath Madhab C	279
Rathod T D	223, 345
Rathodre D S	330
Rathore N S	161
Raul Seema	164, 236
Raut D R	164, 236
Ravi Jammu	78
Ravi N	217, 397
Ravi P M	340
Ravikumar S	316
Ravisankar P	248
Ravisankar P	133

Author Index

Rawat Mandeep 278, 298
Rawat Neetika 108, 110, 115, 127
Rawat Swarnima 280
Ray Mukti Kanta 301
Ray Vinod K 160
Raychowdhury Shubhendu 276, 286, 288
Reddi Rani L 204
Reddy B R M 195
Reddy G L N 39, 189, 232
Reddy Ramakrishna 125
Reji T K 222
Rekha V 122, 211, 220
Reston M Joseph 60
Revathi P 134
Revathy K 126
Romal J 378, 387
Rout Alok 95, 202
Rout P C 251
Rout R P 386, 390
Rout Sabyasachi 363
Roy Annadasankar 343, 344
Roy Rahul 388
Roy S 266, 267
Roy Tushar 165, 176, 389
Rufus A L 309
S Jayalakshmi 92
S Nandakishore 62
Sachin Aditya Ramesh 92, 102, 112
Sagwal Malvika 261
Sah R K 140
Saha Debasish 72, 197, 239, 265, 300, 305
Saha Satyajit 96
Saha Sukhendu 170
Sahoo G S 392, 396
Sahoo Lalit Kumar 170
Sahoo Sarata Kumar 25
Sahu Ashok Kumar 141
Sahu Manjulata 137
Sahu R K 295
Sahu S K 223, 312, 319, 327, 345
Saini R 178
Saipriya G 114, 134
Saisubalakshmi D 248
Salunke G S 246, 366
Samanta Nibedita 131
Samanta Sudeep Kumar 214, 215, 227, 230, 231
Sampath M 156
Samui Pradeep 40
Samy Sowndharya R P 154
Sandeep P 324, 333, 335, 361
Sandilya M K 195, 334
Sane Surekha U 227
Sanil N 66
Sankhe A 187
Sankhla Rajesh 192
Santosh Kumar G 50, 67, 87, 88, 100, 111, 282
Sanyal Kaushik 213
Sapkal Jyotsna A 299
Sapra B K 386, 390
Saradhi I V 222, 328, 329, 330, 331, 337, 341,346. 352, 353, 354
Sarkar Arnab 183, 184, 209
Sarkar P S 391
Sarma Haldhar Dev 284, 302
Sarma M 162
Sartandel Sngeeta J 351
Sarvanan G 133
Sasi Bhushan K 190, 191, 228
Sathe D B 84, 107, 140, 141, 142, 164, 178, 187, 236, 243, 315,
Sathian V 43
Sathish V 314, 318
Sathya Krishna K R 382
Satpati Drishty 284, 297
Satpati S K 53
Saurabh Suman 123, 211
Savitri Padma P 324
Sawant D K 238
Sawant P D 388
Sawant Pramilla D 192
Saxena M K 73, 77, 137, 198

Author Index

Saxena S K 268
Scherer Ulrich W 362
Seenappa L 179, 255, 371
Selvakumar J 309, 310, 358
Selvan B Robert 200, 202, 221, 237, 256
Selvasundaravel R 60
Selvi B S 346
Selvi T 294
Sen Meghnath 43
Sen Nirvik 289
Sen Shashwati 385
Sen Soumya 142
Senapati Abhiram 69
Sengupta Arijit 81
Sengupta Pranesh 55, 80
Sengupta Somnath 120, 149
Senthilvadivu R 248, 249
Seshadri H 86, 143, 317
Seshaiah M 246, 366
Sethi Sanjay 307, 308
Shah C A 354
Shakila L 66
Shanbhag A A 138
Sharath Babu M 117, 118
Sharma A K 337, 341
Sharma Abhishek 97, 98
Sharma Abhishek K 238
Sharma Aman 173, 259, 260, 264, 270, 271, 273
Sharma Archana 383
Sharma B K 262
Sharma D B 218
Sharma Gopal 142
Sharma L K 195
Sharma M K 387
Sharma Manoj Kumar 83, 193
Sharma Mukesh Kumar 378
Sharma Rajveer 363
Sharma Ram 393
Sharma Ranjit 238
Sharma Roshan Lal 359
Sharma S C 138
Sharma S K 30, 41, 42, 195
Sharma Shikha 108, 115
Sharma V K 289, 290, 357
Sharma Vishal 234, 235, 240, 244, 252
Shashi Kumar S K 381
Shastry Karthik 382
Shekhar Kumar 139, 253
Shelkar Shubhangi A 280
Shenoy K B 281
Shete Yogita H 257, 272
Shetgaonkar Abhijit D 365
Shetty P G 312, 319, 327
Shetty Priyalata 293
Shivakumar Y C 350
Shravan Kumar D 208
Shreenivas V 357
Shrikala S B 149
Shrivastava H B 334
Shukla Jaya 285
Shukla Mayank 165, 176, 389
Shukla Rakesh 43
Shukla Shefali 165, 176, 389
Shyam Kumar S 153, 154, 155
Shyam T V 383
Singh Aditi 335
Singh Amandeep 247
Singh Amrit Pal 136
Singh Balender 238
Singh Balvinder 339
Singh D K 53
Singh Hargyan 359
Singh Jagat Pal 277
Singh Jai Deo 368
Singh K K 289
Singh M 243
Singh Manjeet 276
Singh Namrata 259, 260, 264, 270, 271
Singh Omveer 298
Singh P K 388
Singh Prashant 165, 176, 389
Singh Pratap 357
Singh Ritu 116, 360
Singh S G 387

Author Index

Singh S K	91, 226
Singh Sanjay	207
Singh Shiv Govind	385
Singh Sushant K	1
Singh V P	278
Singh Virendra	379
Singha S	266, 267
Singhal Pallavi	323
Sinha Pranay Kumar	156
Sinha U K	322
Sinha Uday Kumar	343, 344
Sinharoy Prithwish	150, 151
Sirvi Rahul	80
Sisodia Mohit	328
Sisodiya Durgesh	385
Sivakumar D	197, 199, 201, 211
Sivakumar Susheela	207
Sivaramakrishna B	114
Sivaraman N	113, 205
SNVMS Gupta	57, 58
Sodaye Suparna	313, 384
Sonawane M	387
Sonu	374
Sood Saurav	264
Sorate Pankaj	299
Sourav Maity	358
Sowmya N	167, 168, 172 ,179, 204, 242, 255
Srabanee Snigdha	338
Sreenivasulu Balija	102, 106, 112, 113, 114, 124, 148, 149
Sridhar K N	168
Srinivas C V	325, 326, 340, 348, 349
Srinivasan S	309, 310, 358
Sriram S	126, 157
Srivastav Ritu M	350
Srivastava A	128, 362
Srivastava Ashutosh	117, 118, 121, 127
Srivastava Dinesh	57, 58, 61, 160, 186
Srivastava R C	283
Srivastava Ranjan	298
Subba Rao R V	139
Subhrojit Bagchi	174, 203
Subramanian D V	158, 182
Subramanian V	169
Subramanian Veena	59, 63
Sudarshan Kathi	49, 50, 87
Sudeep Sahu	301
Sudha R	133
Sudheendran V	352, 353
Sugandhi Suresh	336
Suganthi S	126, 217
Suganyadevi C S	199
Sugilal Gopalakrishnan	91
Sukumar A A	189, 232
Sukumar S	60
Suman Shishu Kant	275, 302
Sundararajan K	106, 229, 239, 241, 248, 249, 250, 265, 300
Suneesh A S	148, 200, 202, 221, 237, 256
Sunil G K	246, 366
Sunil Kumar D	174, 203
Sunitha Y	189, 232, 233
Suranjan Bera	205
Suresh A	145
Suresh Kumar V	217
Suresh Sumathi	79
Sureshkumar M K	274, 342, 394
Suriyakumari K	217
Suryakumari K	126
Suryanarayana P	171
Suryavanshi Harshali S	336
Sushanthini G	148
Sutradhar Sushanta	369
Swain K K	162
Swarnkar M	312, 319, 327, 345,
Takale R A	312, 319, 327
Tawade Nilesh Subhash	46, 384
Tawate Megha	302
Tervankar Shriram	274
Thakare S V	251
Thamke Ajay	238
Thite A	288
Thomas Anitha Mary	62

Author Index

Thomas R G 46, 264
Thorat K 65
Tibrewala S K 395
Tirumalesh Keesari 343, 344
Tiwari M 223, 345
Tiwari Mahesh 336
Tiwari S N 328, 330
Toor Amrit Pal 362
Tripathi A R 341
Tripathi Rahul 46, 48, 52, 210, 372, 373, 375, 376, 377, 380
Tripathy S P 392, 396
Tyagi Avesh K 43, 257, 272
Tyagi M 374
Umamaheswari R 126
Upadhyay Mahima 259, 260, 264, 270, 271
Ushalakshmi K 72, 225
Utpalla Pranaw 30
Uvarani K 155
Valsala T P 84, 107, 140, 141, 142, 161, 164, 178, 187, 236, 243, 315, 350
Vasudha G S 172
Vats Bal Govind 110, 135
Vats Kusum 284
Veerendra D 246, 366
Velavendan P 75, 78, 125, 144, 156, 287
Venkata Sravani V 145
Venkatesan K A 75, 78, 119, 122, 123, 147, 152, 156, 197, 199, 201, 208, 211, 220, 287, 294
Venkatraman B 169, 325, 326, 348, 349
Venunathan N 356
Verboom W 84, 107, 128, 218, 291
Verma Mukesh K 308
Verma P K 109
Verma Poonam 71
Verma S K 278
Victor Jason 9
Vijayakumar B 346
Vijayalakshimi I 169
Vijayalakshmi S 72, 126, 157
Vijayan K S 122, 147, 220
Vimalnath K V 293, 306
Vinod A V 44
Vinod Kumar A 196, 324, 328, 331, 333, 335, 352, 353, 354, 361, 363
Vinod Kumar B 246, 366
Vinograd Victor 26
Vishnu M S 329
Vishwasrao S C 384
Viswanathan S 169
Vithya J 72, 239, 265, 300, 305
Wagh P J 187
Wagh S S 331
Wanage Gaurav 274
Wesley S Godwin 326, 349
Yadav Jyoti 339
Yadav S A 370
Yadav Sonali 363
Yadav Yugandhara Y 268
Yardily A 326, 349
Yashwantrao Gauravi 96
Yevale Pallavi 150

Dr. Bal Govind Vats joined BARC in 2011 through 54th batch of BARC training school after completing M.Sc. Chemistry from Gurukul Kangri Vishwavidyalay, Haridwar, Uttrakhand. He has received Homi Bhabha Award for securing first rank among all chemistry trainees of 54th batch. He has been actively involved in structural, complexation and spectroscopic studies of various actinide and lanthanide complexes and solid state chemistry related to work programme of DAE. He has received his PhD from HBNI in 2018. He has published more than 35 publications in various international peer reviewed journals.

Shri Pratik Das joined BARC in 2017 through 60th batch of OCES programme of BARC training school after completing M.Sc. Chemistry from University of Calcutta. He is actively engaged in structural, thermodynamic studies and transport properties of various highly corrosive and air sensitive fluoride salts mixture as a part of important developmental programme of DAE on molten salt reactors. He is also involved in structural, spectroscopic and thermodynamic studies of various crystalline ceramic materials for the purpose of nuclear waste immobilization. He has published 12 publications in international peer reviewed journals.

Dr. P.S. Ramanjaneyulu joined BARC in 2003 through BARC training school OCES-46 batch. He obtained his masters from Andhra University in 2002 and Ph.D., from HBNI in 2012. He has been involved in chemical quality assurance of various nuclear materials related FBTR, PRP and modified APSARA and other DAE programmes. Dr. Ramanjaneyulu involved in determination of H & D in pressure tube materials of IPHWRs for their life time management. He is very actively involved in indigenous development of various analytical instruments which are used for CQA of different materials w.r.to non metallics. He also involved in development of ion selective electrodes for various ions of interest in nuclear technology. He is recipient of several DAE group achievement awards. He is having about 25 publications in peer reviewed journals.

Dr. S.C. Parida joined B.A.R.C. in 1996, after graduating from 39th batch of the training school. He has obtained M.Sc. (Chemistry) from Utkal University, M.Sc. (Engineering) from Indian Institute of Science, Bangalore, Ph.D. from University of Mumbai and postdoctoral at The University of Alabama, USA. His field of research is thermodynamics and phase diagrams of materials of relevance to nuclear technology and development of storage materials for hydrogen isotopes. He has more than 80 international journal publications to his credit. He is a Ph.D. guide of Homi Bhabha National Institute, Mumbai. Dr. Parida is the recipient of IANCAS- Dr.Tarun Datta Memorial Award, TA Instruments-ITAS Young Scientist Award, Extraction & Processing Division Science Award (TMS, USA), Scientific & Technical Excellence Award (DAE), DAE-SRC Outstanding Research Investigator, ITAS-SETARAM Calorimetric Excellence Award. Currently, he is holding the position of Head, Product Development Division, BARC.

Dr. S. Kannan joined Fuel chemistry Division in 1986 after graduating from 29th batch of BARC Training School. At present he is a Director of Radiochemistry & Isotope Group. His research interest includes the complex chemistry of actinides and lanthanides and development of new ligands for actinide and lanthanide extraction. He is fellow of national academy of sciences and a senior professor and convener of board studies chemical sciences Homi Bhabha National Institute, Bombay. He is having around 120 journal papers to his credits.